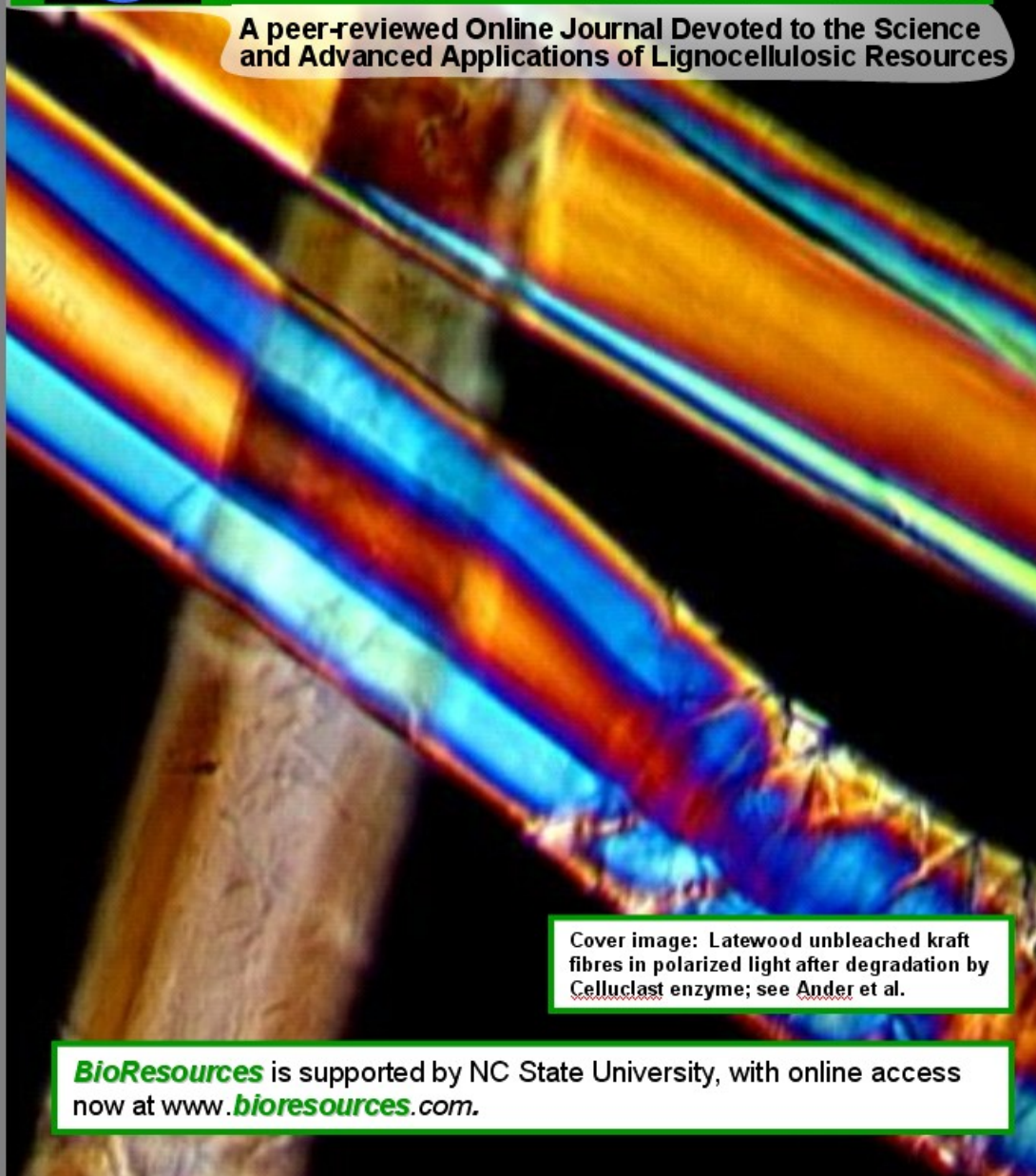


May 2008, Vol. 3, Issue 2



BioResources

A peer-reviewed Online Journal Devoted to the Science and Advanced Applications of Lignocellulosic Resources



Cover image: Latewood unbleached kraft fibres in polarized light after degradation by Celluclast enzyme; see [Ander et al.](#)

BioResources is supported by NC State University, with online access now at www.bioresources.com.



BioResources, a peer-reviewed journal
devoted to the science of lignocellulosic
materials, chemicals, and applications

NC STATE UNIVERSITY

College of Natural Resources
Department of Wood and Paper Science
Campus Box 8005
Raleigh, NC 27695-8005
919.515.7707/919.513.3022
919.515.6302 (fax)

BioResources

Contents: Vol. 3, Issue 1, February 2008

- Pawlak, J. J. (2008). **"A sustainable economy,"** *BioRes.* 3(1), 1-2.
- Wang, H., Li, B., and Shi, B. (2008). **"Preparation and surface acid-base properties of porous cellulose,"** *BioRes.* 3(1), 3-12.
- Malutan, T., Nicu, R., and Popa, V. I. (2008). **"Contribution to the study of hydroxymethylation reaction of alkali lignin,"** *BioRes.* 3(1), 13-20.
- Zoia, L., Canevali, C., Orlandi, M., Tolppa, E.-L., Sipila, J., and Morazzoni, F., **"Radical formation on TMP fibers and related lignin chemical changes,"** *BioRes.* 3(1), 21-33.
- Kontturi, E., Mitikka-Eklund, M., and Vuorinen, T. (2008). **"Strength enhancement of a fiber network by carboxymethyl cellulose during oxygen delignification of kraft pulp,"** *BioRes.* 3(1), 34-45.
- Nada, A.-A. M. A., Alkady, M. Y., and Fekry, H. M. (2008). **"Synthesis and characterization of grafted cellulose for use in water and metal ions sorption,"** *BioRes.* 3(1), 46-59.
- Ebringerová, A., Hromádková, Z., Košťálová, Z., and Sasinková, V. (2008). **"Chemical valorization of agricultural by-products: Isolation and characterization of xylan-based antioxidants from almond shell biomass,"** *BioRes.* 3(1), 60-70.
- Hromádková, Z., Malovíková, A., Mozeš, Š., Sroková, I., and Ebringerová, A. (2008). **"Hydrophobically modified pectates as novel functional polymers in food and non-food applications,"** *BioRes.* 3(1), 71-78.
- Heinze, T., Pfeifer, A., and Petzold, K. (2008). **"Functionalization pattern of tert-butyl-dimethyl-silyl cellulose evaluated by NMR spectroscopy,"** *BioRes.* 3(1), 79-90.
- Csóka, L., Lorincz, A., and Winkler, A. (2008). **"Sonochemically modified wheat straw for pulp and papermaking to increase its economical performance and reduce environmental issues,"** *BioRes.* 3(1), 91-97.
- Galgut, P. N. (2008). **"Radiographic observations on the use of two different regeneration materials in a single subject: Case study,"** *BioRes.* 3(1), 98-107.
- Talebniya, F., Pourbafrani, M., Lundin, M., and Taherzadeh, M. J. (2008). **"Optimization study of citrus wastes saccharification by dilute-acid hydrolysis,"** *BioRes.* 3(1), 108-122.
- Montoneri, E., Boffa, V., Quagliotto, P., Mendichi, R., Chierotti, M. R., Gobetto, R., and Medana, C. (2008). **"Humic acid-like matter isolated from green urban wastes. Part 1. Structure and surfactant properties,"** *BioRes.* 3(1), 123-141.
- Esteves, B. M., Domingos, I. J., and Pereira, H. M. (2008). **"Pine wood modification by heat treatment in air,"** *BioRes.* 3(1), 142-154.



BioResources, a peer-reviewed journal devoted to the science of lignocellulosic materials, chemicals, and applications

NC STATE UNIVERSITY

College of Natural Resources
Department of Wood and Paper Science
Campus Box 8005
Raleigh, NC 27695-8005
919.515.7707/919.513.3022
919.515.6302 (fax)

- Foulk, J. A., Akin, D. E., and Dodd, R. B. (2008). **"Influence of pectinolytic enzymes on retting effectiveness and resultant fiber properties,"** *BioRes.* 3(1), 155-169.
- Ioelovich, M., and Leykin, A. (2008). **"Structural investigations of various cotton fibers and cotton celluloses,"** *BioRes.* 3(1), 170-177.
- Mikkonen, K. S., Yadav, M. P., Cooke, P., Willför, S., Hicks, K. B., and Tenkanen, M. (2008). **"Films from spruce galactoglucomanan blended with poly(vinyl alcohol), corn arabinoxylan, and konjac glucomannan,"** *BioRes.* 3(1), 178-191.
- Subramanian, R., Kononov, A., Kang, T., Paltakari, J., and Paulapuro, H. (2008). **"Structure and properties of some natural cellulosic fibrils,"** *BioRes.* 3(1), 192-203.
- McSweeney, J. D., Rowell, R. M., Chen, G. C., Eberhardt, T. L., and Min, S.-H. (2008). **"Periodate and hypobromite modification of Southern Pine wood to improve sorption of copper ion,"** *BioRes.* 3(1), 204-216.
- Montoneri, E., Savarino, P., Bottigliengo, S., Musso, G., Boffa, V., Prevot, A. B., Fabri, D., and Pramauro, E. (2008). **"Humic acid-like matter isolated from green urban wastes. Part II: Performance in chemical and environmental technologies,"** *BioRes.* 3(1), 217-233.
- Soni, R., Nazir, A., Chadha, B. S., and Saini, H. S. (2008). **"Novel sources of fungal cellulases for efficient deinking of composite paper waste,"** *BioRes.* 3(1), 234-246.
- Chen, Y., Liu, Y.-F., and Tan, H.-M. (2008). **"Preparation of macroporous cellulose-based superabsorbent polymer through the precipitation method,"** *BioRes.* 3(1), 247-254.
- Gonzalez, R. W., Saloni, D., Dasmohapatra, S., and Cubbage, F. (2008). **"South America: Industrial roundwood supply potential,"** *BioRes.* 3(1), 255-269.
- Hu, G., Heitmann, J. A., and Rojas, O. J. (2008). **"Feedstock pretreatment strategies for producing ethanol from wood, bark, and forest residues,"** *BioRes.* (3(1), 270-294.

BioResources is a peer-reviewed scholarly journal devoted to the science of lignocellulosic materials, chemicals, and their applications. The journal is a service of North Carolina State University, College of Natural Resources (<http://cnr.ncsu.edu>). You can download PDF files without charge from <http://www.bioreources.com>, or <http://ncsu.edu/bioreources>, where you also can find **Author instructions**, journal policies, etc. Please direct correspondence to co-editors Martin A. Hubbe (hubbe@ncsu.edu, 919-513-3022) and Lucian A. Lucia (lucian.lucia@ncsu.edu, 919-515-7707).

A SUSTAINABLE ECONOMY

Joel J. Pawlak

There exists a direct correlation between improvements in standard of living and the consumption of resources. To be able to maintain the standard of living of a modern developed country, society must adapt to an economy based on sustainable processes, energy, and raw materials. The sustainable economy presents itself as a disruptive technology to the traditional economy, which is based largely on non-renewable resources. The issue seems to be more about when will we switch to a sustainable economy, rather than whether we will switch.

Keywords: Sustainable, Disruptive Technology, Environment, Economic Growth

Contact information: Department of Forest Biomaterials Science and Engineering, North Carolina State University, Raleigh, North Carolina 27695 USA; <mailto:jjpawlak@ncsu.edu>

The continuing evolution of the environmental movement, which originated in the 1960s and 1970s, is leading us to a new understanding of what it will mean to achieve environmental compatibility. The evolving paradigm is simply called sustainability. It is not really a new concept, but it is a concept which industry is now beginning to embrace. In this editorial, I will discuss why the environmentalist can support sustainability, why industry can support sustainability, and why sustainability is a necessary condition for developed economies. This issue is closely linked to our bioresources, as they constitute a valuable source of sustainable raw materials.

The idea of having a lower impact on the environment is an idea that nearly everyone can embrace. Conflicts embodied in the term “environmentalism” mainly arise when one finds that consumption needs to be curtailed to achieve environmental goals. In fact, nearly everything we consume ultimately becomes waste. On the planet Earth, for the most part, there is a constant amount of mass. We cannot create or destroy any significant amount of mass. Once a product is consumed, it will have a limited amount of “useful life” before it is rendered as waste. The “useful life” could just be a few short minutes, such as for a paper cup, or a few hundred years, as with a house. In the end, once something reaches the end of its useful days, it becomes waste. This means that as consumption increases, so does the amount of waste generated. While some elements in our society will reduce consumption for the sake of the environment, the vast majority of society constantly strives to improve its standard of living – *this can be read as increasing consumption*. In fact, the majority of the world strives to greatly elevate its standard of living. Thus, the simple solution to reducing environmental impact is to reduce consumption, which is not a realistic expectation.

To improve the environmental performance of society, there is only one realistic solution. This solution is sustainability. In an ideal sense, sustainability could be simply defined as zero waste. This would mean that as something is consumed, it becomes the raw material for something else. This concept is not novel, but it has subtlety that insures

that our need for raw materials is perpetually satisfied. At some point in time, our non-renewable resources will limit our ability to expand the economy, and a transition to a sustainable economy will happen. Chances are, the transition, as it happens, will not be perceivable to most people. In all likelihood, we will transition to a sustainable economy due to economic pressures and not societal demands.

The three phases of the traditional technology cycle are well known. Together, they constitute what is often called the technology S-curve. This description relates the performance of a technology as a function of the effort invested in the technology. Traditional technologies typically follow this kind of behavior - initial slow progress, followed by large gains in performance, and then an era of limited returns for efforts. I would suggest that sustainable technology is poised to be a disruptive technology. A disruptive technology is a technology that measures its value by a metric different than the existing technology. However, over time, the disruptive technology meets the performance of the existing technology, and then rapidly displaces the existing technology. Applying these concepts to traditional unsustainable technology, one can expect that when traditional technology's performance erodes due to limited resources and rising raw materials costs, sustainable technologies will rapidly replace the existing technology.

The threat of sustainable technology rapidly displacing existing technology is why industry should be interested in sustainability today. Often, the existing business cannot see the disruptive technology coming, because the disruptive technology does not yet perform at the level of the existing technology. The world of business is littered with companies cast aside by their best customers when disruptive technology is in play (Christensen 1997).

The question then simply becomes, when will sustainable technology become competitive with the existing technology? This question is yet to be answered. However, it is currently known that gasoline and other non-renewable fuels are at all-time high prices. It is also known that the pricing of many raw materials derived from non-renewable resources is increasing with no foreseeable reduction in price forthcoming. It is also known that Chinese economy has awakened. In the last few years, more than one billion people in Asia have gained access to the world economy, placing an even larger burden on the world's non-renewable resources. Taking these factors into account, it would seem that the traditional means for improving economic performance in industry by cutting raw material and process costs, may be coming to an end – that is to say, we are in the third phase of the technology S-curve for traditional industry. The time for the sustainable economy may be nearer than we think.

Reference Cited

Christensen, C. (1997). *The Innovator's Dilemma When Technologies Cause Great Firms to Fail*, Harvard Business School Press, Boston, Mass.

PREPARATION AND SURFACE ACID-BASE PROPERTIES OF POROUS CELLULOSE

Huanfeng Wang,^a Bin Li,^{a*} Baoli Shi,^b

Porous cellulose beads were prepared by solubilizing cellulose in sodium hydroxide/urea/sulfoarea aqueous solution and then solidifying liquid beads in hydrochloric acid. Scanning electron microscopy (SEM) was used to characterize the morphologies of surface, cross section, and wall structures of the porous cellulose beads, which are folded and porous. The surface acid-base properties of porous cellulose beads were characterized in detail by inverse gas chromatography (IGC). The Lewis basic number K_b was found to be 0.854, which is indicative of a Lewis basic polymeric material. With the discussion of the results of SEM and IGC, a conclusion can be drawn that the porous cellulose beads showed a good ability of adsorbing the smoking tar of cigarettes.

Keywords: Preparation; Characterization; Porous cellulose beads; Inverse gas chromatography; Scanning electron microscopy

Contact information: Heilongjiang Key Laboratory of Molecular Design and Preparation of Flame Retarded Materials, College of Science, Northeast Forestry University, P. O. Box 226, Hexing Road No 26, Harbin 150040, P. R. China. *Corresponding author: lbinzh62@163.com

INTRODUCTION

Cellulose and modified cellulose have recently been investigated (Siva et al. 2002) because of wide applications such as adsorbent materials, biodegradable materials, and so on. Especially they, as biodegradable adsorbent materials (Ronny et al. 2006), are widely used in wastewater treatment, absorbent industry, and medication adsorption. Cellulose can interact with adsorbates through hydrogen bonding, complexation, and other interactions. As an adsorbent (Stanley-wood et al. 1986; Liu et al. 2005), in general, cellulose is prepared to be spherical beads to enhance their surface area and adsorbing ability. Many methods have been used to prepare cellulose beads. For example, cellulose beads were prepared by using a solution of cellulose/NMMO/H₂O and sequential cooling, using a reversed-phase suspension technique (Liu et al. 2007).

Smoking tar is of great concern because of the toxic effect to the human beings (Kitamura et al. 2007). Smoking tar contains thousands of harmful substances, such as condensed ring aromatics, phenol, nitrogen-containing compounds and so on (Rustemeier et al. 2002). They could cause acute and even fatal effects when a large dosage is ingested. Evidence has shown that smoking tar is a human carcinogen and causes severe harm to the healthy. Many materials have been studied as adsorbents to remove tar from cigarette smoke, such as, activated carbon and molecular sieves. The investigation has focused on the preparation and characterization of cellulose beads (Liu et al. 2005; Zhou et al. 2005; Li et al. 2005) for adsorbing smoking tar (Bi et al. 2005; Singh et al. 2004).

Sorption measurements are very common in the characterization of solid/gas interfaces for various materials (Voelkel 2004; Sun and Berg 2003; Erika 2004). The intermolecular interactions can be classified into two categories, the Lifshitz–van der Waals (LW) interaction and the acid–base (AB) interactions. Since the magnitude of AB interactions is sometimes as much as an order of magnitude stronger than that of LW interactions, they sometimes play a dominant role in adsorption interface related phenomena (Adam 2004; Shi et al. 2007). Inverse gas chromatography is a powerful technique for investigating the acid-base properties of solid surfaces in porous form (Tayssir et al. 2002; Wu et al. 2004; Thielmann 2004; Frank et al. 2004; Narjès et al. 2007). It offers an alternative to the conventional gravimetric or volumetric methods for determining adsorption equilibrium isotherms, due to its simplicity, shorter measurement time, and a wider range of experimental possibilities. It has become widely utilized in recent years.

The Mechanism of Measuring Surface Acid-Base Properties by IGC

Inverse gas chromatography is a useful technique in evaluating the potential for interaction of different components of polymer blends, composites, and multicomponent polymeric systems (Sun et al. 2003; Prithu et al. 1995; Gutierrez, et al.1999; Jean. et al. 1991).

The direct data obtained from IGC is the net retention volume, V_n , given by:

$$V_n = (t_r - t_0)FCJ \quad (1)$$

Here, t_r is the retention time taken for the probe solvent, t_0 that for the non-interacting probe, F is the flow rate of carrier gas in ml/min, and J is the term correcting for the compressibility of the carrier gas, such that:

$$J = 1.5 \frac{(P_i / P_o)^2 - 1}{(P_i / P_o)^3 - 1} \quad (2)$$

In Eq. (2), P_i and P_o are the inlet and outlet pressure of carrier gas, respectively. C is a correction factor, allowing for the vapor pressure of water at the temperature of bubble flow meter used to determine the flow rate.

$$C = 1 - P_{H_2O} / P_o \quad (3)$$

where P_{H_2O} is the saturated vapor pressure of water at ambient temperature.

$$-\Delta G_a = RT \ln(V_n) \quad (4)$$

Here ΔG_a is the total free energy of adsorption of probe, R is the gas constant, T is the temperature of column, and V_n is the net retention volume.

The Lewis acid–base properties are calculated from ΔG_a , the contribution to the free energy of adsorption by Lewis acid–base (specific) interactions when polar (specific) solvents are injected into the chromatographic column. The expression is:

$$\Delta G_a = \Delta G_a^d + \Delta G_a^s \quad (5)$$

where ΔG_a^d is the dispersive contribution to the total free energy of adsorption, which is determined with *n*–alkanes, and ΔG_a^s is the contribution to the free energy of adsorption by Lewis acid–base (specific) interactions when polar (specific) solvents are injected into the chromatographic column.

From Eqs. (4) and (5), $-\Delta G_a^s$ may be defined as:

$$-\Delta G_a^s = RT \ln \left(\frac{V_n}{V_{n,ref}^d} \right) \quad (6)$$

where, V_n and $V_{n,ref}^d$ are the retention volumes of the polar probe and derived from the *n*-alkane reference line, i.e. ΔG_a^s results from the distance between the $RT \ln(V_n)$ value of polar solvent and the straight *n*-alkane line.

The enthalpy of specific interactions ΔH_a^s can be determined by studying the variation of ΔG_a^s with the temperature according to following equation (7):

$$\Delta G_a^s = \Delta H_a^s - T\Delta S_a^s \quad (7)$$

where ΔS_a^s is the specific entropy of adsorption. The results of ΔH_a^s were from the slope of the plot of $\Delta G_a^s/T$ vs. $1/T$. The Lewis acid number K_a and Lewis base number K_b are calculated according to Eq. (8):

$$-\Delta H_a^s = K_a \times DN + K_b \times AN^* \quad (8)$$

In this expression, DN and AN^* are the Gutmann's Donor and modified Acceptor numbers of probes, respectively. Plotting $-\Delta H_a^s/AN^*$ against DN/AN^* usually produces a linear correlation, the slope and intercept of which give K_a and K_b , respectively.

EXPERIMENTAL

Materials

Cellulose was purchased from Shandong Gaomi Chemical Fiber Corporation. The degree of polymerization (DP) was 500~600. Blowing Agent AC ($C_2H_4N_4O_2$) was purchased from Tianjing Yongchangsheng Chemical Corporation. Sodium hydroxide, urea, and sulphourea were analytical grade, which were purchased from Beijing Yili Chemical Regents Corporation. For the IGC analysis, the apolar *n*-alkanes probes were *n*-pentane (C_5), *n*-hexane (C_6), *n*-heptane (C_7), *n*-octane (C_8), *n*-nonane (C_9), and *n*-decane (C_{10}). The polar probes were trichloromethane (TCM), ethyl acetate (Acet.), diethyl ether (ether), and tetrahydrofuran (THF). *n*-pentane (C_5) was taken as the non-interacting probe in this experiment, because the retention time of it was the shortest among all the probes. They are analytical grade solvents and were purchased from Tianjin Kermel Chemical Reagents Development Centre, China. The characteristics of the probe solvents are listed in Table 1.

Table 1. The Characteristics of Probe Solvents

Probe	$\alpha(\text{\AA}^2)$	$r_1^d(\text{mJ}\cdot\text{m}^{-2})$	$\alpha(r_1^d)^{0.5}(\text{\AA}^2(\text{mJ}\cdot\text{m}^{-2})^{0.5})$	$AN^*(\text{kJ}\cdot\text{mol}^{-1})$	$DN(\text{kJ}\cdot\text{mol}^{-1})$
<i>n</i> - C_5	46.1	16.0	184	-	-
<i>n</i> - C_6	51.5	18.4	221	-	-
<i>n</i> - C_7	57.0	20.3	257	-	-
<i>n</i> - C_8	63.0	21.3	291	-	-
<i>n</i> - C_9	69.0	22.7	329	-	-
<i>n</i> - C_{10}	75.0	23.4	363	-	-
TCM	44.0	25.9	224	22.7	0.0
Acet.	48.0	16.5	195	6.3	71.8
Ether	47.0	15.0	182	5.8	80.6
THF	45.0	22.5	213	2.1	84.4

α is molecular area of probe; r_1^d is surface free energy of probe; AN^* and DN are the Gutmann's modified acceptor number and donor number of probe, respectively.

Preparation of the Porous Cellulose Beads

Cellulose material with 500-600 degree of polymerization was dispersed into an aqueous solution consisting of 8%~12% sodium hydroxide and 6~12% urea /sulphourea at $-10\text{ }^\circ\text{C}$ (Ruan et al. 2004; Miani et al. 2004). The above mixture was stirred to obtain a viscose, and then a small amount of blowing agent AC was added. The viscose containing bladders were injected into a centrifugal machine to prepare spherical drops, and the spherical drops were solidified in 5% hydrochloric acid aqueous solution to obtain shaggy beads, and then washed and dried at $105\text{ }^\circ\text{C}$ for 4 hours. Finally, we obtained porous cellulose beads with $210\sim 270\text{g}\cdot\text{L}^{-1}$ packing density and $280\sim 380\text{ }\mu\text{m}$ diameters.

Characterization Method

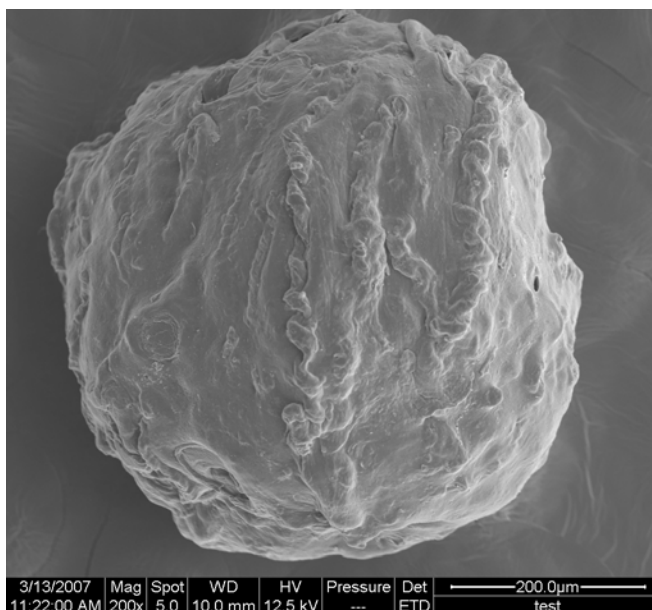
The IGC instrument was a GC-900A gas chromatograph (Shanghai TianPu Analytical Instrument Ltd., China) equipped with a flame ionization detector (FID). Nitrogen was used as the carrier gas. The flow rate was $14.39 \text{ mL}\cdot\text{min}^{-1}$, measured from the end of the column with a soap bubble flow meter. The injector and FID were heated to $140 \text{ }^\circ\text{C}$. The probe solvents were injected manually, using a $1.0 \text{ }\mu\text{L}$ Hamilton syringe. The injection volumes were $0.1 \text{ }\mu\text{L}$. The column was a stainless steel tube (0.5 m length, 2.56 mm i.d.). It was washed with acetone prior to use. The porous cellulose beads were aged at $100 \text{ }^\circ\text{C}$ for 8 h . A weighed amount of 1.0492 g ($120\text{--}140$ mesh) was packed into the column. The IGC experiments were performed at 50 , 60 , 70 , and $80 \text{ }^\circ\text{C}$.

The samples were coated with gold to prevent electrical charging and were observed by a QUANTA 200 Scanning Electron Microscope under vacuum at an acceleration of 20kV .

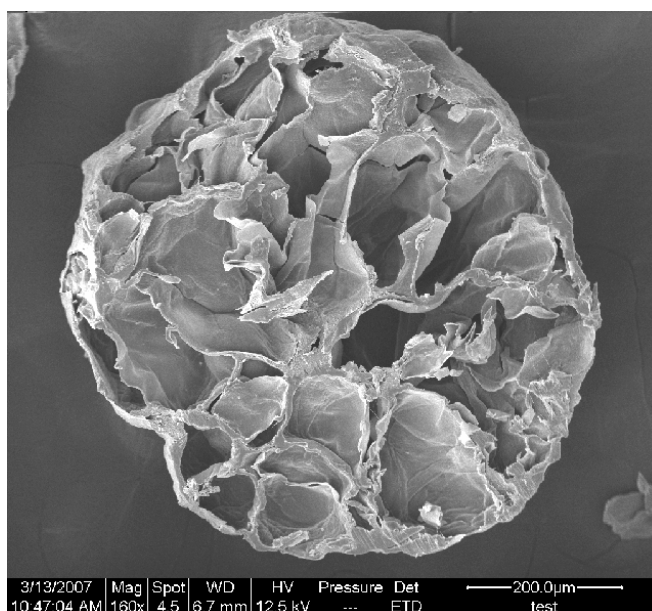
RESULTS AND DISCUSSION

SEM Characterization

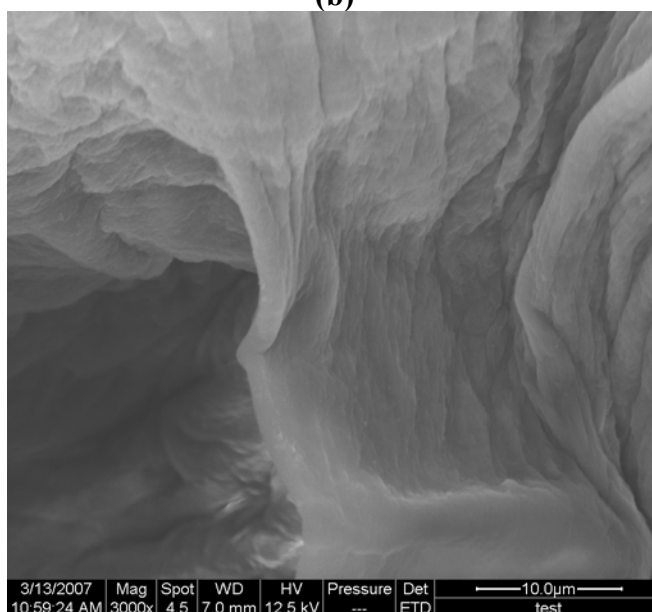
Figure 1, part (a) shows the apparent surface morphological structure of a porous cellulose bead. There are a lot of draped and porous structures on the surface. Part (b) shows the cross-section of a porous cellulose bead. Many cavities were distributed in the interiors of the beads. Draped and porous structures were formed by the blowing agent AC. These structures were considered to be beneficial to absorption properties of the porous cellulose beads. Part (c) shows the inner wall surface and cavities, which enlarge the surface area. The inter- and intra-structures allow the material to interact effectively with adsorbents.



(a)



(b)



(c)

Fig.1. Morphological structure of porous cellulose beads by SEM (a) SEM image of apparent surface morphological structure (b) SEM image of cross-section (c) SEM image of wall surface of cavities.

IGC Surface Characterization

Figure 2 shows a plot of $\ln(V_n)$ against $1000/T$ for *n*-alkanes and polar probes in an IGC experiment. Linear relationships of the plots were obtained. From the values of

net retention volumes of the probes, the surface properties of cellulose beads were determined.

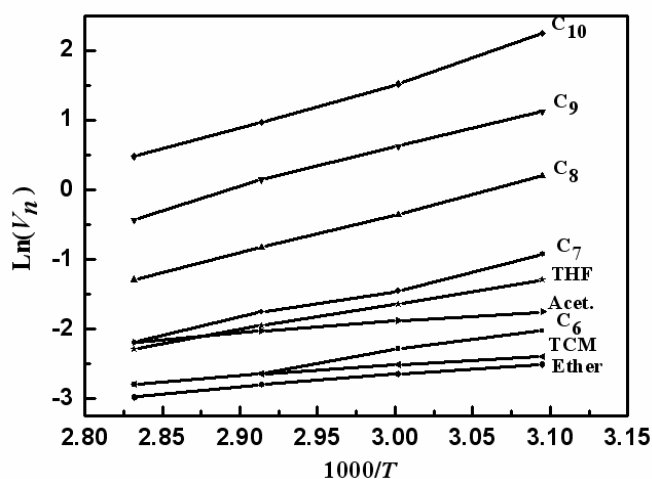


Fig.2. Plot of $\ln(V_n)$ against $1000/T$ for n -alkanes and polar probes

Figure 3 shows results of the free energy of adsorption by Lewis acid-base interactions ΔG_a^s for the polar probes adsorbed on porous cellulose beads at 323.15K. Table 2 lists the data for ΔG_a^s measured at the absolute temperatures shown.

Table 2. The Data of ΔG_a^s Measured at Various Absolute Temperatures

T (K)	323.15	333.15	343.15	353.15
TCM	-1.31	-0.55	0.50	1.22
Acet.	2.71	3.42	4.32	4.99
Ether	1.73	2.31	3.04	3.57

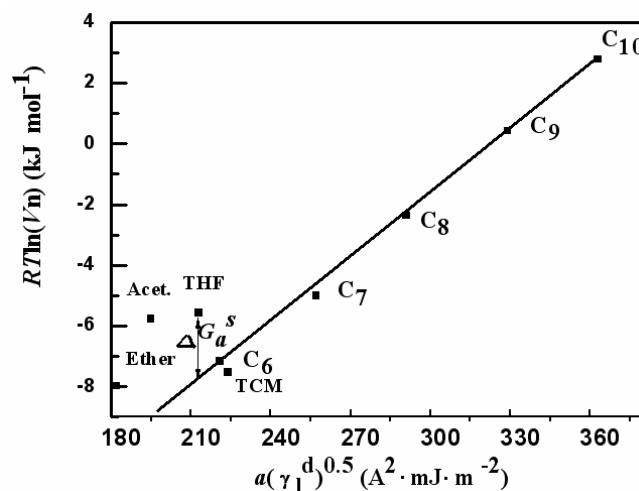


Fig.3. ΔG_a^s for the polar probes adsorbed on porous cellulose beads at 323.15K

According to Eq (7), the enthalpies of specific interaction ΔH_a^s of all polar probes were obtained from the free energy of specific interactions listed in Table 3. The results are listed in Table 3.

Table 3. The Enthalpies of Specific Interaction ΔH_a^s of all Polar Probes

Probe	TCM	Ethyl acetate	Ether
$-\Delta H_a^s$	18.76	13.10	9.89

Figure 4 shows a plot of $-\Delta H_a^s / AN^*$ against DN / AN^* for polar probes. A fine linear correlation was obtained for the three polar probes. The Lewis acidic number K_a was 0.081, obtained from the slope, and the basic number K_b was 0.854, obtained from the intercept. The result implies that the cellulose bead sample was a Lewis base polymer. This can be elucidated from cellulose molecular structure. The repeated segment of cellulose consists of glucose units, and each unit has hydroxyl groups. The lone electron pairs of oxygen atoms of hydroxyl groups must endow cellulose with a strong Lewis basic property. (Santos et al. 2002; Ceyda et al. 2007).

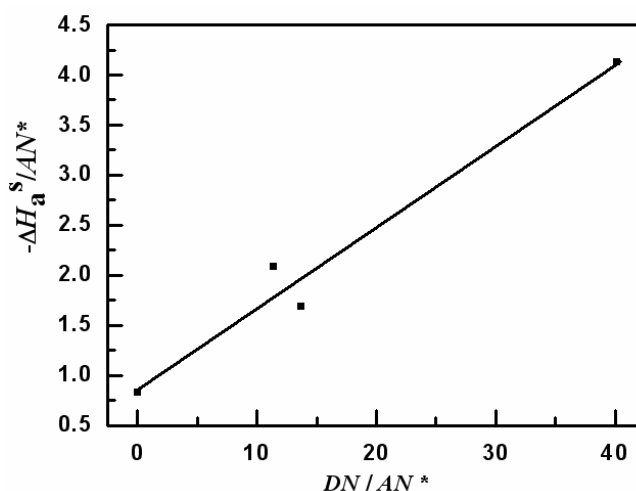


Fig.4. A plot of $-\Delta H_a^s / AN^*$ against DN / AN^* for polar probes

CONCLUSIONS

Porous cellulose beads were obtained by a basic solution–acid solidification method. The surface of the porous cellulose beads was rough, and the inner structures contained many cavities based on scanning electron microscopy. Surface properties of the beads, such as the Lewis acidic number K_a and basic number K_b , were measured by the inverse gas chromatography method. K_a and K_b were 0.081 and 0.854, respectively. The

results indicated that the porous cellulose beads were Lewis basic polymeric materials. On the other hand, inter- and intra-surface of the beads contained abundant hydroxyls, which can interact with condensed ring aromatics, phenol compounds by $p-\pi$ conjugation. These facts showed a good ability of adsorbing smoking tar of cigarettes, which has been proved by the cigarette company.

ACKNOWLEDGMENTS

The authors gratefully thank for the financial supports by Heilongjiang Science Fund for Distinguished Young Scholars (Grant no. JC04-06).

REFERENCES CITED

- Adam, V. (2004). "Inverse gas chromatography in characterization of surface," *Chemometr Intell Lab. 72*(2), 205-207.
- Bi, X. H, Sheng, G. Y., Feng, Y. L., Fu, J. M., and Xie, J. X. (2005). "Gas-and particulate-phase specific tracer and toxic organic compounds in environmental tobacco smoke," *Chemosphere* 61(10), 1512-1522.
- Ceyda, B., and Fatma, T. (2007). "Determination of the acid/base properties of MgY and NH₄Y molecular sieves by inverse gas chromatography," *J.Chromatogr. A* 1162(1), 83-89.
- Erika, F., János, M. and Béla, P. (2004). "Determination of the surface characteristics of particulate fillers by inverse gas chromatography at infinite dilution: a critical approach," *J.Colloid Interf. Sci.* 269(1), 143-152.
- Frank, T. (2004). "Introduction into the characterisation of porous materials by inverse gas chromatography," *J. Chromatogr A* 103 (1-2), 115-123.
- Gutierrez, M. C., Rubio, J., Rubio, F., Oteo, J. L. (1999). "Inverse gas chromatography: A new approach to the estimation of specific interactions," *J. Chromatogr. A* 845, 53-66.
- Jean, B. D., and Soo, J. P. (1991). "Surface characteristics of pitch-based carbon fibers by inverse gas chromatography method," *Carbon* 29(7), 955-961.
- Kitamura, M., and Kasai, A. (2007). "Cigarette smoke as a trigger for the dioxin receptor-mediated signaling pathway," *Cancer Lett.* 252(2), 184-194.
- Li, N., and Bai, R. B. (2005). "Copper adsorption on chitosan-cellulose hydrogel beads: Behaviors and mechanisms," *Sep Purif Technol.* 42(3), 237-247.
- Liu, M. H., Huang, J. H. and Deng, Y. (2007). "Adsorption behaviors of l-arginine from aqueous solutions on a spherical cellulose adsorbent containing the sulfonic group," *Bioresource Technol.* 9(5), 1144-1148.
- Liu, C. X., and Bai, R. B. (2005). "Preparation of chitosan/cellulose acetate blend hollow fibers for adsorptive performance," *J. Membrane Sci.* 267(1-2), 68-77.

- Narjès, R., Michel, N., Dréan, J.-Y., and Richard, F. (2007). "A study of the surface properties of cotton fibers by inverse gas chromatography," *J. Colloid Interf. Sci.* 31(2), 373-380.
- Prithu, M. I., and Schreiber, H. P. (1995). "Aspects of acid-base interactions and use of inverse gas," *Colloid surfac. A: Physicochemical and Engineering Aspects* 100, 47-71.
- Ronny, S., and Hans, R. (2006). "Molecularly smooth cellulose surfaces for adhesion studies," *J. Colloid Interf. Sci.* 301(2), 376-385.
- Ruan, D., Zhang, L. N., Mao, Y., Zeng, M., and Li, X. B. (2004). "Microporous membranes prepared from cellulose in NaOH/thiourea aqueous solution," *J. Membrane Sci.* 241(2), 265-274.
- Rustemeier, K., Stabbert, R., Haussmann, H. -J., Roemer, E., and Carmines, E. L. (2002). "Evaluation of the potential effects of ingredients added to cigarettes. Part 2: Chemical composition of mainstream smoke," *Food Chem Toxicol.* 40(1), 93-104.
- Santos, J. M. R. C. A., Fagelman, K., and Guthrie, J. T. (2002). "Characterisation of the surface Lewis acid–base properties of poly(butylene terephthalate) by inverse gas chromatography," *J. Chromatogr. A* 969(1-2), 111-118.
- Siva, V., and Mansoor, A. K. (2002). "Optimization and characterization of controlled release multi-particulate beads formulated with a customized cellulose acetate butyrate dispersion," *Int J Pharm.* 234(1-2), 179-193.
- Singh, G. S., Darshan, L., and Tripathi, V. S. (2004). "Study of microporosity of active carbon spheres using inverse gas chromatographic and static adsorption techniques," *J. Chromatogr. A.* 1036(2), 189-195.
- Shi, B. L., Zhang, Q. R., Jia, L. N., Liu, Y., and Li, B. (2007). "Surface Lewis acid–base properties of polymers measured by inverse gas chromatography," *J. Chromatogr. A* 1149(2), 390-393.
- Stanley-Wood, N. G., Sadeghnejad, G. R., and York, P. (1986). "Adsorption potential characterisation of modified celluloses," *Powder Technol.* 46(2-3), 195-199.
- Sun, C. H., and Berg, J. C. (2003). "A review of the different techniques for solid surface acid–base characterization," *Adv. Colloid Interfa.* 105(1-3), 151-175.
- Tayssir, H., and Jacques, S. (2002). "New approach to characterise physicochemical properties of solid substrates by inverse gas chromatography at infinite dilution: I. Some new methods to determine the surface areas of some molecules adsorbed on solid surfaces," *J. Chromatogr. A.* 969(1-2), 17-25.
- Thielmann, F., Butler, D. A., and Williams, D. R. (2001). "Characterization of porous materials by finite concentration inverse gas chromatography," *Colloids Surfaces A: Physicochemical and Engineering Aspects* 187-188, 267-272.
- Wu, Y. W., Li, Z., and Xi, H. X. (2004). "Influence of the microporosity and surface chemistry of polymeric resins on adsorptive properties toward phenol," *J. Hazard Mater.* 113(1-3), 131-135.
- Zhou, D., Zhang L. N., and Guo, S. L. (2005). "Mechanisms of lead biosorption on cellulose/chitin beads," *Water Res.* 39(16), 3755-3762.

Article submitted: Sept. 12, 2007; First round of peer-review completed: Oct. 29, 2007;
Revised version received and accepted: Nov. 5, 2007; Publication: Nov. 5, 2007.

CONTRIBUTION TO THE STUDY OF HYDROXYMETYLATION REACTION OF ALKALI LIGNIN

Theodor Malutan,^{*} Raluca Nicu, and Valentin I. Popa

The hydroxymethylation of alkali lignin with formaldehyde in alkaline solution was studied. The influence of reaction conditions of the hydroxymethylation of alkali lignin was followed by modifying the temperature, time, and the ratios of NaOH to lignin and CH₂O to lignin. Three different types of alkali lignin were utilized. The reaction was followed by total consumption of formaldehyde, and the resulting products were characterized through FTIR-spectra, thermogravimetry analysis, ash and moisture contents, as well as by the amounts of OH groups.

Keywords: Lignin, Hydroxymethylation, FTIR, Thermogravimetry

Contact information: Faculty of Chemical Engineering, P.O.Box 10, postal code 700050, Bd. D. Mangeron, no. 71 A, Romania, ^{*}Corresponding author: thmalu@ch.tuiasi.ro

INTRODUCTION

Lignin is a macromolecular compound much more reactive than cellulose or other natural polymers from chemical point of view, because of its functional groups. The reactivity of lignin is determined both by its particular structure with specific functional groups and by its structural modifications induced by separation methods used for different raw materials (Popa 1983). The presence of the hydroxylic groups, both phenolic and aliphatic, in lignin has enabled its utilisation as a partial substitute for phenol in the synthesis of products with a lot of applications (Popa et al. 2003).

The substitution of phenol, particularly with kraft lignin, in the synthesis of phenol - formaldehyde (PF) resins is the most studied use of lignin (Conner 2001). Phenol-formaldehyde resins are the major adhesives used for bonding wood panels for outdoor applications. The PF adhesive resins are used primarily as a binder (Çetin 2003) in the production of softwood plywood, oriented strandboard, and waferboard. The PF resins are synthesized by the reaction of phenol with formaldehyde. By varying the reaction time, reaction temperature, catalyst type, and the ratio of formaldehyde to phenol, a number of adhesive systems with different characteristics can be produced. For the resins used in the wood industry, sodium hydroxide is the most important catalyst, although other basic catalysts such as sodium carbonate, alkaline oxides and hydroxides, and ammonia can also be used. Resole resins are formed by heating the reactive ingredients in aqueous solution at about 80-100 °C. Initially, mono-, di-, and trihydroxymethyl derivatives of phenol are formed. Further, the reaction leads to condensation of the hydroxymethyl derivatives, giving methylene or ether linkages between phenol moieties (Conner 2001)

The partial substitution of phenol by a natural polymer such as lignin, the main by-product of the pulp industry, has presented an attractive alternative (Alonso et al. 2001, Lora and Wu 2007). Lignin also represents a product obtained from renewable resources and has an aromatic and highly cross-linked structure, similar to the network of PF resins (Fig. 1) (Benar et al. 1999).

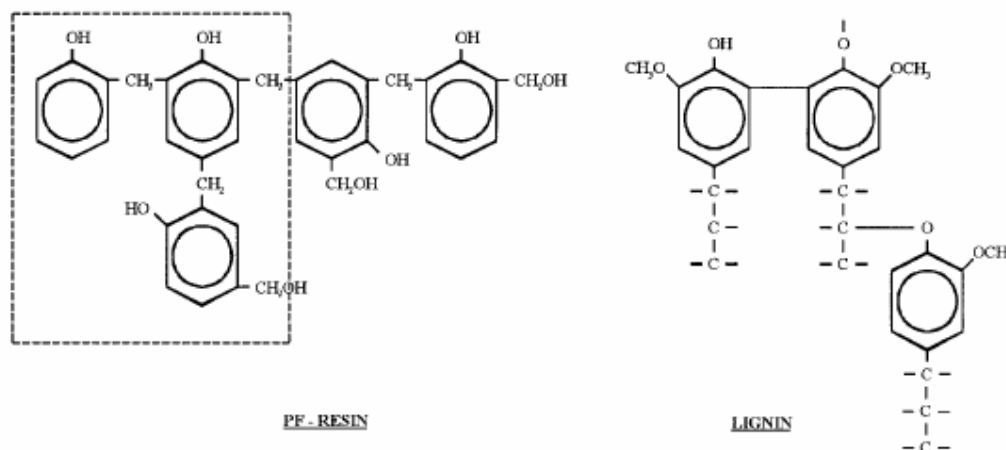


Fig. 1. Structure of PF resins and lignin

In the earlier studies, lignin has been incorporated into phenolic resins used as wood adhesives, but the current trend is to modify their chemical structure in order to increase the reactivity towards formaldehyde. The modification can be accomplished by different methods: methylation, phenolation, demethylation, and fractionation. During the methylation process, formaldehyde is added to the lignin in alkaline medium (Alonso et al. 2001).

The reactivity of lignin in hydroxymethylation depends on their sources (softwoods, hardwoods, or grass), on pulping conditions (pH, temperature, pressure), and on other reaction conditions (Peng et al. 1993). That is why the objective of this research was to study the hydroxymethylation reaction of annual plants alkali lignin (*Wheat straw* and *Sarkanda grass*) by condensation with formaldehyde in alkaline solution in order to establish optimum conditions and to characterize the resulting hydroxymethylated derivatives.

In order to prove the mechanism of interaction between lignin and formaldehyde, the modified products have been characterized by functional analysis; the amount of hydroxyl groups have been determined through a chemical method with acetic anhydride in pyridine medium (Faix et al. 1994) and by FTIR-spectra (Nada et al. 1998). Any increase in the hydroxyl content of hydroxymethylated lignin as compared to that of lignin is assumed to be due to a number of hydroxymethyl groups introduced into the lignin molecule by reaction.

The thermal stability of modified and unmodified lignin was studied by TGA.

EXPERIMENTAL

Lignin Hydroxymethylation

The experiments were carried out with different alkali lignin (offered by Granit Co.) as raw materials: L₁ (from *Wheat straw* 100-W-A), L₂ (from *Sarkanda grass* 100-S-A) and Protobind 1000 with characteristics presented in Table 1. The modification of lignin through the hydroxymethylation reaction was performed with formaldehyde - 37% solution, in alkaline medium, using NaOH solution at 3 % (w/w) concentration.

Thus, the lignin samples were dissolved in 100 mL NaOH solutions 3% (w/w) corresponding to a ratio of NaOH/L equal to 0.08 (w/w). The temperature of the lignin solution was 25 °C and the pH 9.7-9.9. The hydroxymethylation of the ionized lignin was performed by the addition of a formaldehyde 37% solution ($\rho = 1.08 \text{ g/cm}^3$) using a ratio 0.258 (w/w) of CH₂O/L, at room temperature. After that, the temperature was raised to 50 °C and subsequently to 90 °C. The total time of reaction was 3 h. The concentration of dissolved lignin in the reaction medium was nearly 280 g/L.

In parallel with the hydroxymethylated lignin a reference sample was obtained, using the same treatment without formaldehyde solution (it was replaced by distilled water). The parallel sample was analyzed using the same methods.

Precipitation of modified lignin was carried out through lowering of the solution pH value to an acid pH (1.5 - 2), using hydrochloric acid 1N solution. The obtained precipitate was centrifuged at 2500 rpm for 10 minutes, washed three times with distilled water to remove the undesired inorganic salts, unreacted aldehyde and any other residual reactants therefrom, and then dried in a vacuum oven overnight at 40 °C (Molin and Kuo 1987; Lin 1980; Marton et al. 1966).

Table 1. The Characteristics of Raw Lignin Samples

Characteristics	L1 (100-W-A)	L2 (100-S-A)	Protobind 1000
Acid insoluble lignin, %	90	87	-
Acid soluble lignin, %	1	2	-
COOH, mmole/g	3.8	3.3	2.1 – 2.3
Aromatic OH, mmole/g	1.7-1.8	1.8-1.9	1.9-2.1
OH/C9 groups chemical method	1.02	1.07	1.05
pH (10 % dispersion)	2.7	3.2	~ 3.5
Mw	3510	4310	1160
T softening, °C	170	163	200
Solubility in furfuryl alcohol, %	88.5	84	98.5
Solubility in aqueous alkali, pH 12, %	98.5	98.5	94
Ash, %	2.5	4.1	1.4-1.8

L1 – wheat straw lignin; L2-Sarkanda grass lignin.

FTIR Spectroscopy

Infrared (FTIR) spectra of the modified and unmodified lignin, pellet formed with KBr, were recorded on a Digilab FTS 2000 Fourier transform spectrometer, domain: 4000-400 cm⁻¹, resolution 4 cm⁻¹, 32 scans.

Termogravimetry Analysis

Thermal stability was studied via thermogravimetric analysis (TGA) on a METTLER TOLEDO instrument. Temperature ramps between 25 and 900°C at 15°C/min under nitrogen were performed to determine the mass loss of material as a function of temperature.

Gel Permeation Chromatography (GPC)

The molecular mass was determined by GPC (stationary phase: Sephadex LH20, mobile phase: 0.3 mL/min NaOH 0.1 N, 280 nm).

Determination of Total Hydroxyl Groups

The total OH groups content was determined by chemical method with acetic anhydride in pyridine medium (Faix 1994) and from FTIR spectral analysis (Nada et. al. 1998). The Ar-OH groups content was determined by a UV-Vis method (Gärtner et al. 1999).

RESULTS AND DISCUSSIONS

Determination of Unreacted Formaldehyde

During the lignin methylation, hydroxymethyl groups are introduced in the reactive positions of lignin, mainly in *ortho* positions (in relation to phenolic OH groups) of aromatic rings. Increasing the temperature, hydroxymethyl groups react at free positions of other lignin units or phenol to form methylene bonds (Benar et al. 1999). Under these conditions three

reactions can take place. The main one is the Lederer-Manasse reaction, where hydroxymethyl groups are incorporated in the aromatic rings of lignin, increasing the reactivity of the molecule (Fig. 2). Undesirable side reactions are the Cannizzaro reaction, in which the formaldehyde reacts with itself, and the Tollens reaction (Ayla and Nimz 1984) in which the lignin side chains are substituted by aliphatic methylol groups (Alonso et al. 2001; Zhao et al. 1994; Chen and Wu 1994).

The unreacted formaldehyde was determined during the methylation reaction through the sodium sulfite method (Walker 1975). To determine the quantity of formaldehyde which reacts with itself, a blank sample without lignin was exposed to the same conditions as those applied to the lignin. A preliminary experimental series for determination of formaldehyde consumption in secondary reactions was carried out. Finally, the values of consumption were corrected. The consumption of formaldehyde, comparing the hydroxymethylation and Cannizzaro reactions in the case of *Sarkanda grass* lignin (L_2), is presented in Table 2.

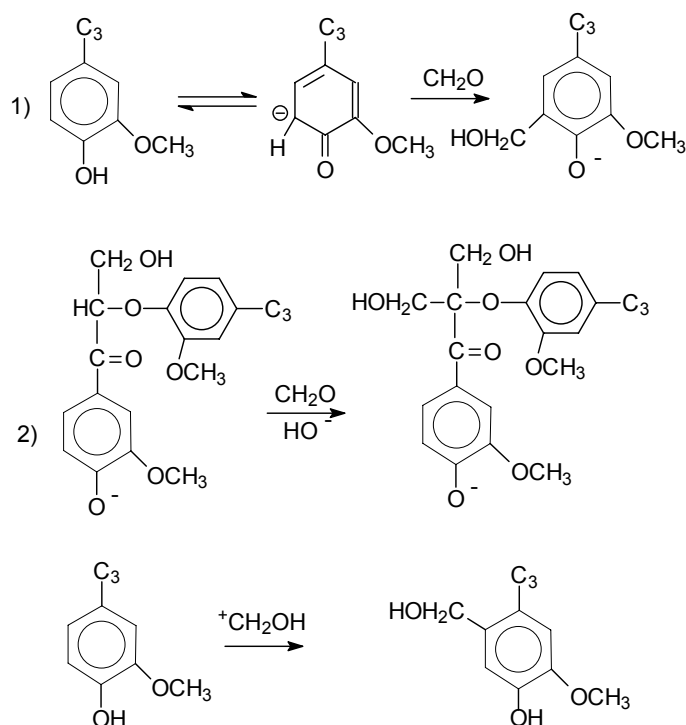


Fig. 2. Hydroxymethylation of phenolic ring of lignin units

The data presented in Table 2, show that an increase of the NaOH/L ratio from 0.04 to 0.16 (w/w) resulted in an increase in CH_2O total consumption, as well as an increase in Cannizzaro reactions. The optimal NaOH/L ratio was 0.08 (w/w). The alkali medium ensures ionization of the phenolic group of the lignin.

Table 2. The Variation of Formaldehyde Consumption in Hydroxymethylation of *Sarkanda grass* Lignin (L_2)

NaOH/L ratio, w/w	CH_2O consumption, mole	
	Total	Cannizzaro reaction
0.04	0.38	0.22
0.08	0.71	0.42
0.16	0.78	0.73

The reaction conditions were: temperature 90°C , time 180 min, $\text{CH}_2\text{O}/\text{L}$ ratio = 0.25 (w/w)

The results obtained under these conditions for hydroxymethylation of all lignin samples are presented in Table 3.

Table 3. The Formaldehyde Consumption in Hydroxymethylation of Lignin Samples

Sample	T, °C	pH	¹ Moles CH ₂ O reacted / 100 g lignin	OH/C ₉ groups chemical method	Ar-OH, mmole/ g lignin	OH/C ₉ groups FTIR	Mw
L1 (100-W-A)	initial		-	1.02	1.7-1.8	1.06	3510
	90	12.0	0.51	1.17	1.29	1.17	-
	90	10.5	0.20	1.17	1.76	1.16	-
	50	12.0	0.31	0.85	1.49	1.16	-
	50	10.5	0.20	1.03	1.66	1.24	990
L2 (100-S-A)	initial		-	1.07	1.8-1.9	1.05	4310
	90	12.0	0.35	1.64	1.53	1.19	-
	90	10.5	0.17	1.18	1.32	1.34	-
	50	12.0	0.46	1.01	1.78	1.20	-
	50	10.5	0.14	0.94	1.75	1.34	1205
Protobind 1000	initial		-	1.05	1.9-2.1	1.10	1160
	90	12.0	0.14	1.17	1.58	1.23	1325
	90	10.5	0.20	1.07	1.63	1.15	1270
	50	10.5	0.10	1.04	1.14	1.14	1080

The CH₂O/L ratio was 0.25 (w/w).

¹) The values corrected without the CH₂O consumption in Cannizzaro reactions.

The molecular mass determinations indicated a decrease of Mw during formaldehyde treatment (from 3510 to 990 for L₁, 4310 to 1205 for L₂).

By increasing the reaction temperature, the hydroxymethyl groups can react with free positions of other lignin units to form methylene bridges. Thus, in case of Protobind 1000 at temperature 90°C, the gravimetric mass increased from 1160 to 1325 (pH 12) and to 1270 (pH 10.5).

From Table 3 it can be observed that the reaction pH played an important role. At pH 12 the total formaldehyde consumption was high, and the Cannizzaro reactions were intensified. In these conditions, the lowest formaldehyde reactivity of lignin samples was observed in the case of Protobind 1000, whereas *Wheat Straw* (L₁) and *Sarkanda grass* (L₂) lignin were more reactive. This increasing of aliphatic OH is based on taking into account the methylation reaction of lignin through the Lederer-Manasse reaction.

Functional Analysis by FTIR Spectra

The FTIR spectra obtained were characterized by a broad O-H band at 3400 cm⁻¹, an intense C-H band at 2927 cm⁻¹, and another at 2854 cm⁻¹, which are typical of methoxyl groups. The aromatic skeletal vibrations occur at 1600 cm⁻¹ and 1500 cm⁻¹. These bands were used for normalization and their intensity was always set to 1.00. The C-H deformations band of asymmetric methyl and methylene appeared at 1470–1460 cm⁻¹, and carbon–oxygen ether bands at 1400–1000 cm⁻¹. The following ratios of the relative absorbance for different groups were defined:

$$\text{Mean value of OH groups} = \text{average} (A_{3430}, A_{1370}, A_{1165}, A_{1043}) / A_{1510(1600)}$$

$$\text{Mean value of phenolic OH groups} = A_{1370} / A_{1510(1600)}$$

$$\text{Mean value of OCH}_3 \text{ groups} = \text{average} (A_{2890}, A_{1460}, A_{1420}) / A_{1510(1600)}$$

$$\text{Mean value of C=O groups} = A_{1720} / A_{1510(1600)}$$

$$\text{Mean value of aromatic ring} = \text{average} (A_{1510}, A_{1600}, A_{844})$$

$$\text{Ratio of aliphatic to aromatic signals} = A_{2936} / A_{1510(1600)}$$

$$\text{S/G ratio} = A_{1330} / A_{1269}$$

The results obtained for functional groups are presented in Table 4. The ratios of absorbance of aliphatic OH and aliphatic (Ak) groups to aromatic groups can take into account the methylation reaction of lignin through the Lederer-Manasse reaction. In case of hydroxymethylation of *Sarkanda grass* lignin (L2), high values for these ratios were obtained in comparison with those of *Wheat straw* lignin (L1) or Protobind 1000. Under these reaction conditions the hydroxymethylation of Protobind 1000 lignin occurred without an important increases of the content of OH total groups and Ak/Ar ratios.

The content of Ar-OH groups was modified during the hydroxymethylation, probably because secondary reactions of condensation which can take place. The ratio of signals of phenolic OH groups indicates that during hydroxymethylation, lignin can be activated for side reaction, but these effects were very small.

A significant ratio of A_{1330}/A_{1269} (S/G) was observed, which means that there were the possibilities for substitution in 5 or 6 position due to the presence of guaiacyl or syringyl moieties in lignin structure.

Table 4. The Functional Groups of Hydroxymethylated Lignin

Sample	T, °C	pH	OH total groups	Ar-OH groups	OCH ₃ groups	Ak/Ar ratio	C=O groups	S/G ratio
L1 (100-W-A)	-	-	1.06	0.93	0.94	0.72	0.80	0.82
	90	12.0	1.17	0.92	1.14	1.08	0.83	0.97
	90	10.5	1.16	0.98	1.13	1.20	0.93	0.97
	50	12.0	1.16	0.99	1.09	1.08	0.89	0.93
	50	10.5	1.24	0.95	1.11	1.05	0.86	0.86
L2 (100-S-A)	-	-	1.05	0.91	0.96	0.88	0.88	0.82
	90	12.0	1.19	0.95	1.16	1.40	1.00	0.89
	90	10.5	1.14	0.95	1.10	1.11	0.92	0.85
	50	12.0	1.20	0.96	1.11	1.19	0.94	0.91
	50	10.5	1.34	0.78	1.18	3.20	0.77	0.57
Protobind 1000	-	-	1.11	0.89	1.05	1.17	0.89	0.83
	90	12.0	1.23	0.98	1.15	1.27	0.95	0.96
	90	10.5	1.15	0.98	1.13	1.20	0.91	0.96
	50	10.5	1.14	0.98	1.12	1.22	0.95	0.96

Thermogravimetric Analysis

Thermogravimetric curves reveal the mass loss of substances in relation to the temperature of thermal degradation, while the first derivative of that curve (DTG) shows the corresponding rate of mass loss. The peak of this curve (DTG_{max}) may be expressed as a single thermal decomposition temperature and can be used to compare thermal stability characteristics of different materials.

Thermal characteristics of hydroxymethylated and unmodified lignin are presented in Table 5.

The DTG_{max} (T_m, peak 2) appeared between 370 and 381 °C, and the loss of mass was between 35 % and 52 % for all lignin samples analysed. Hydroxymethylated lignin, when subjected to thermal cure, becomes insoluble in alkali. If we compare DTA curves of alkali lignin and methylolated alkali lignin, it can be observed that in the latter case a highly exothermic reaction started around 125°C, the material became stabilized over 190°C, and it did not melt up to 190°C, where it started to soften. The endotherm change around 110°C indicates a probable loss of water, absorbed or structural. The thermal cure of methylolated lignin is a further proof of the presence of phenol alcohol structure.

Table 5. Thermogravimetry Data for Hydroxymethylated and Unmodified Lignin

Sample	Peak 1				Peak 2			
	T _{onset} , °C	T _m , °C	T _{offset} , °C	Mass loss, %	T _{onset} , °C	T _m , °C	T _{offset} , °C	Mass loss, %
L ₁	65.4	82.3	147.7	4.75	297.5	381	504.7	36.48
L ₁ H50pH10	68.0	81.7	140.0	6.64	303.2	373.4	512.8	43.74
L ₁ H50pH12	65.5	81.6	147.7	6.21	164	372.8	642	45.9
L ₁ H90pH10	58.0	79.3	126.6	5.54	220.3	371.9	688.8	48.35
L ₁ H90pH12	58.0	79.9	107.6	5.51	245.1	368.8	534.5	48.51
L ₂	58.6	82.5	140.3	4.58	290.8	373.6	489	35.16
L ₂ H50pH10	59.0	89.9	115.8	4.68	235.7	369.9	587.1	49.05
L ₂ H50pH12	58.0	78.9	108.2	6.66	248.1	372.4	557.6	48.46
L ₂ H90pH10	58.0	81.7	124.7	7.85	310.03	376.5	642.2	52.16
L ₂ H90pH12	52.0	72.4	104.1	5.37	231.6	363.1	552.24	47.63
P 1000	57.4	81.6	131	3.08	297.4	380.8	504.3	35.13
P1000H50pH10	56.8	77.4	109.2	5.05	227.1	376.7	656	52.01
P1000H90pH10	50.0	75.5	123.9	3.71	226.1	378.9	646.47	49.17
P1000H90pH12	56.0	64.8	102.6	4.95	221.9	377.5	595.2	49.12

*) Heat rate : 15 °C/min; Final temperature = 800 °C;

CONCLUSIONS

The reactivity of different kinds of lignin was studied relative to formaldehyde addition under alkaline conditions at two temperature (50°C and 90°C) and pH 10.5 and 12. The optimum conditions for methylation (reaction temperature was 50°C and pH 10.5 for lignin L₁ and L₂) depend of kind and structure of lignin. Under these conditions, the extent of the Cannizzarro reaction is low, and a substantial increase in the lignin hydroxymethyl groups is attained. The best reactivity was found for the *Sarkanda grass* lignin, in comparison with *Wheat straw* and *Protobind 1000* lignin. The aim of chemical transformation of lignin is both to enlarge its applications and to improve its product performance.

ACKNOWLEDGMENTS

The authors are grateful for the support of the CE - FP6 Program “ECOBINDERS”.

REFERENCES CITED

- Alonso, M. V., Rodríguez, J. J., Oliet, M., Rodríguez, F., Garcia, J., Gilarranz, M.A. (2001). “Characterization and structural modification of ammoniac lignosulfonate by methylation,” *Journal of Applied Polymer Science* 82, 2661-2668.
- Ayla, C., and Nimz, H. H. (1984). “Die Verwendung von Ablaugen-. lignin bei der Herstellung von Holzwerkstoffen,” *Holz Roh- Werkst.* 42, 415-419.
- Benar, P., Gonçalves, A. R., Mandelli, D., and Schuchard, U. (1999). “Eucalyptus organosolv lignins: Study of the hydroxymethylation and use in resols,” *Bioresource Technology* 68, 11-16.
- Çetin, N. S., and Özmen, N. (2003). “Studies on lignin-based adhesives for particleboard panels,” *Turk. J. Agric. For* 27, 183-189.
- Conner, A. H. (2001). “Wood: Adhesives,” *Encyclopedia of Materials: Science and Technology*, Amsterdam, New York, Elsevier Science, Ltd.
- Chen, R., and Wu, Q. (1994). “Modified lignosulfonate as adhesive,” *Journal of Applied*
- Malutan et. al. (2008). “Hydroxymethylation of alkali lignin,” *BioResources* 3(1), 13-20.

- Polymer Science* 52, 437-443.
- Faix, O., Argyropoulos, D. S., Robert, D., and Neirinch V. (1994). "Determination of hydroxyl groups in lignins," *Holzforschung*, 48 (5), 387-394.
- Gärtner, A., Gellerstedt, G., and Tamminen, T. (1999) "Determination of phenolic hydroxyl groups in residual lignin using a modified UV-method," *Nord. Pulp Pap. Res. J.* 14, 163-170.
- Lin, S. Y. (1982). "Method for polymerization of lignosulfonates," *United States Patent* 4,332,589.
- Lora, J. H., and Wu, Q. (2007) "Performance of two non-wood soda lignin derivatives in oriented strandboard powder phenolic adhesive," *Proceedings of the 8th ILI Forum Rome, May 10-12*, 213– 216.
- Marton, J., Marton, T., and Falkehag, S. I. (1966). "Alkali-catalyzed reactions of formaldehyde with lignins," *Adv. Chem. Series* 59, 125-144.
- Molin, K., Hse C.-Y, and Huang D.-H. (1991), "Alkali treated kraft lignin as a component in flakeboard resins," *Holzforschung*, 45, 47-54.
- Nada, A.-A. M. A., El-Sakhawy, M., and Kamel, S. M. (1998). "Infra-red spectroscopic study of lignins," *Polymer Degradation and Stability* 60, 247-251.
- Peng, W., Riedl, B., and Barry, A. O. (1993). "Study on the kinetics of lignin methylation," *Journal of Applied Polymer Science* 48, 1757-1763.
- Popa, V. I. (1983). *Technologies of lignin upgrading*, Polytechnic Institute Press, Iasi.
- Popa, V. I., Constantinescu, G., Lazar, N., and Popa, N. (2003). "Composites material based on lignin," *13th International symposium on Cellulose Chemistry and Technology, IVth Romanian-Italian on Pulp and Paper*, EPPIC Thematic Network - 3th Workshop, sept. 3-5, Iasi, Romania, 333.
- Rozmarin, Gh., Popa, V. I., Grovu-Ivanoiu, M., and Doniga, E. (1984). *Chemistry of Macromolecular Compounds. Chemistry of Wood - Applications*, Polytechnic Institute Press, Iasi.
- Sarghie, I., Tofan, L., Suteu, D., Bulgariu, L., and Rusu, G. (2004). Quantitative analysis - applications, Performantica Ed., Iasi.
- Zhao, L. W., Griggs, B. F., Chen, C.-L., Gratzl, J. S. and Hse, C.-Y. (1994). "Utilization of softwood kraft lignin as adhesive for the manufacture of reconstituted wood," *Journal of Wood Chemistry and Technology* 14(1), 127-145.
- Walker, J. F. (1975). *Formaldehyde 3rd ed.*, R. E. Krieger Publishers, Huntington, New York.

Article submitted: Sept. 4, 2007; First round of peer-reviewing completed: Oct. 25, 2007;
Revised version received and accepted: Nov. 12, 2007; Published: Nov. 13, 2007

RADICAL FORMATION ON TMP FIBERS AND RELATED LIGNIN CHEMICAL CHANGES

Luca Zoia,^a Carmen Canevali,^{b*} Marco Orlandi,^a Eeva-Liisa Tolppa,^a Jussi Sipila,^c and Franca Morazzoni^b

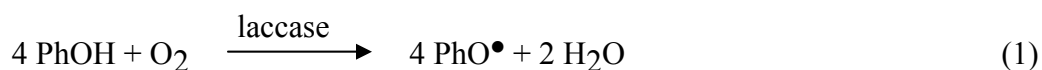
Oxidation of TMP fibers was compared at 298 K with molecular oxygen, in the presence of either [Co(salen)] in methanol or [Co(sulphosalen)] in water. Electron paramagnetic resonance (EPR) spectroscopy made it possible to reveal and quantify the formation of phenoxy cobalt radicals in the former case and of phenoxy radicals in the latter. These radicals reached the same concentration after 60 min from the onset of reaction. Fiber integrity was more preserved after oxidation in water than in methanol, as assessed by heteronuclear single quantum coherence - nuclear magnetic resonance (2D-HSQC-NMR) spectroscopy, nuclear magnetic resonance spectroscopy of carbon (¹³C-NMR), and Gel Permeation Chromatography (GPC). These results suggest that efficient radical formation on fibers can be achieved also with water-soluble catalysts. Thus, it is proposed that treatment with molecular oxygen in the presence of [Co(sulphosalen)] in water represents a promising way to approach an environmentally sustainable radicalization of fibers, without heavy modification of the lignin structure.

Keywords: Lignocellulosic fibers, Phenols, [Co(salen)], [Co(sulphosalen)], Radicals, EPR, NMR

Contact information: a: Dipartimento di Scienze dell'Ambiente e del Territorio, Università di Milano-Bicocca, Piazza della Scienza 1, 20126 Milano, Italy; b: Dipartimento di Scienza dei Materiali, Università di Milano-Bicocca, Via R. Cozzi 53, 20125 Milano, Italy; c: Laboratory of Organic Chemistry, University of Helsinki, P.O. Box 55 FIN-00014, Helsinki, Finland; *Corresponding author: carmen.canevali@unimib.it

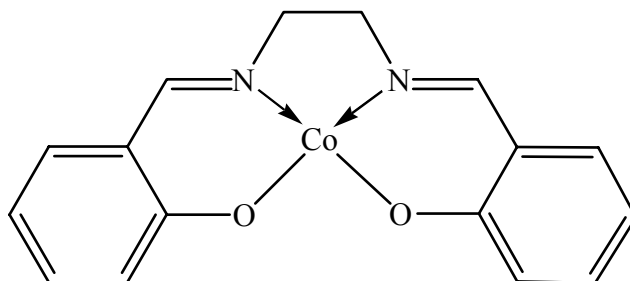
INTRODUCTION

In the field of packaging, materials with high barrier and mechanical properties are generally required. Wood fibers can achieve these properties, after proper modification. Attempts to modify fiber properties by grafting synthetic polymers onto the cellulose backbone started as early as the 1940's. Radical centers at the cellulose backbone behave as grafting initiators, and they can be generated by high-energy irradiation, by oxygen reaction in the presence of transition metal complexes, by decomposition of peroxides, or by radical transfer reaction (Bledzki et al. 1998). Alternatively, radical active centers can be produced on lignin at the fiber surface. As an example, the reaction of wood fibers obtained from thermomechanical pulp (TMP) with molecular oxygen and laccase as catalyst, was demonstrated to produce the radicalic activation of the surface lignin phenols through the formation of phenoxy radicals (Lund et al. 2003):



Under such treatment, glueless fiberboards were obtained, and the wet strength of paper was improved (Felby et al. 1997a; Lund and Felby 2001). The radical formation from surface lignin phenols can also improve other properties of interest for specific applications, such as hydrophobic or hydrophilic character (Buchert et al. 2005), as well as the improvement of paper strength properties (Chandra et al. 2004).

Besides by enzymatic treatment, phenoxy radicals on fibers can also be generated by reaction with molecular oxygen, using biomimic catalysts such as salen compounds. It was reported that molecular oxygen, in the presence of N,N'-ethylenebis(salicylideneiminato) cobalt(II), [Co(salen)] (Scheme 1), efficiently formed radicals on CTMP and TMP fibers in methanol (Canevali et al. 2005).



Scheme 1.

The characterization of the intermediate paramagnetic species by electron paramagnetic resonance (EPR) spectroscopy suggested that the radicalization mechanism was the same as that proposed for lignin model compounds in homogeneous phase (Bolzacchini et al. 1997; Canevali et al. 2002), occurring through the following three steps:



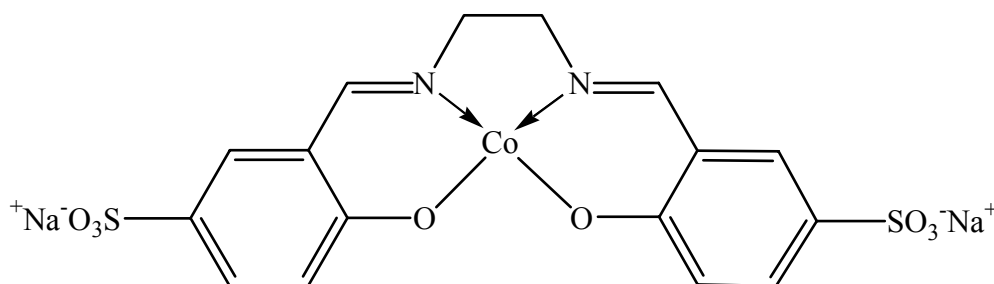
where ROH is the phenol unit and RO[•] the corresponding intermediate radical. In the first step of this mechanism, [Co(salen)] is co-ordinated by ROH and O₂, giving a superoxocobalt derivative, detected by EPR. In the second step, the superoxocobalt derivative reacts with another phenol ligand, giving an EPR active phenoxy cobalt radical, [Co^{III}(salen)(ROH)(RO[•])]. In the third step, the phenoxy cobalt radical is in equilibrium with a phenoxy-phenate cobalt radical; both were detected by EPR.

After treatment with molecular oxygen in methanol in the presence of [Co(salen)], TMP fibers formed a higher amount of radicals and in parallel underwent deeper structural and morphological changes than CTMP (Canevali et al. 2005). By using

[Co(salen)] as catalyst, the absolute amount of radicals in fibers reaches very high values, 10 times higher than those reported in the literature for the treatment with laccase and molecular oxygen of TMP (Felby et al. 1997b) and of milled wood lignin (Ferm et al. 1972). These results are probably due to the smaller molecular dimension of [Co(salen)] compared with laccase, which allows the biomimic catalyst to interact also with subsurface lignin phenol groups.

However, [Co(salen)] does not allow an environmentally sustainable radical formation on fibers and a water soluble catalyst should be used instead.

With the aim of developing an eco-friendly process for maximizing the radical amount, while preserving the fiber integrity, in the present paper the treatments of unbleached TMP fibers with molecular oxygen, in the presence of either [Co(salen)] in methanol or [Co(sulphosalen)] (Scheme 2) in water were compared.



Scheme 2.

The best conditions for radical formation on TMP fibers using salen catalysts were assessed in the proper solvent by varying the reaction time, under the experimental conditions which were found to maximize the formation of radicals in the presence of [Co(salen)] (Canevali et al. 2005).

The radicals formed on fibers during oxidation were identified and quantified by EPR spectroscopy. The radical formation data were correlated to the changes in lignin chemical structure, achieved by lignin units under oxidative treatments, as assessed by heteronuclear single quantum coherence - nuclear magnetic resonance (2D-HSQC-NMR) spectroscopy, nuclear magnetic resonance spectroscopy of carbon (¹³C-NMR) and Gel Permeation Chromatography (GPC).

EXPERIMENTAL

Materials

Pulps

The softwood unbleached thermomechanical pulp (TMP) was provided by Stora Enso Oyj. The amount of lignin in pulp was evaluated using the Klason method (Dence 1992) and resulted 27.1 %. The amount of extractives in pulp evaluated by Stora Enso, is reported in Table 1:

Table 1. Amounts of Extractive Components in TMP

Percentage of total extractives (w/w)	Fatty acids (mg/g)	Resin acids (mg/g)	Lignans and sterols (mg/g)	Sterylesters (mg/g)	Triglycerides (mg/g)
1.39	0.94	0.88	0.42	0.64	0.65

Reagents

N,N'-ethylenebis(salicylideneiminato) cobalt(II), [Co(salen)] (99%), was supplied by Aldrich. (Bis[(5-sulphonatosalicylaldehyde)ethylenediiminato] cobalt(II) disodium, [Co(sulphosalen)], was synthesized according to the literature (Sippola and Krause 2003). Methanol and deuterated DMSO-d₆ (Fluka) were used as received. Mill-Q water was used. Oxygen (99.99%) was supplied by Technogas.

Methods

Radical formation on fibers

Fibers and fines, hereafter named “fibers”, were obtained by suspending pulp in dichloromethane for 30 min, then in methanol for 60 min, under mechanical stirring, in order to eliminate extractives. Then, lignocellulosic fibers were recovered by filtration and dried in air at 353 K.

The best conditions for radical formation on TMP fibers using salen catalysts were assessed in the proper solvent by varying the reaction time, under the experimental conditions which were found to maximize the formation of radicals in the presence of [Co(salen)]: 298 K; fiber/[salen] ratio 10:1 w/w, corresponding to a molar ratio phenol/[salen] ~ 0.8; fiber concentration in the solvent 5.0 mg/ml; oxygen pressure 1 bar (Canevali et al. 2005). Thus, radicals were formed by suspending fibers (150 mg) in 30 ml of either methanol containing [Co(salen)] (15 mg) or water in the presence of [Co(sulphosalen)] (15 mg), then fibers were allowed to react for the required time with molecular oxygen (1 bar pressure) at 298 K.

After reaction, fibers were recovered by filtration, washed either three times with 30 ml of ethyl acetate and three times with 20 ml of acetone (after [Co(salen)] treatment) or three times with 20 ml of water (after [Co(sulphosalen)] treatment). The washed fibers were allowed to dry in air, then subjected to spectromagnetic and structural characterization.

Solvents and washing liquids were collected in order to check the presence of paramagnetic species by EPR spectroscopy. In all cases paramagnetic species were absent in these samples.

EPR measurements

Immediately after drying in air, fibers were inserted into the EPR tube and frozen at the liquid nitrogen temperature, in order to inhibit further reaction before the spectromagnetic investigation.

The EPR spectra were recorded at 123 K on a Bruker EMX spectrometer working at the X-band frequency, equipped with a variable temperature BVT 2000 unit (Bruker).

The g values were determined by standardization with α,α' -diphenyl- β -picryl hydrazyl (DPPH). The amount of paramagnetic species, expressed as area/mg, was calculated with a $\pm 10\%$ accuracy by double integration of the resonance lines and by accurately determining the weight of dry fibers filling 1 cm length of the EPR tube (sensitive part of the EPR cavity).

NMR analyses

NMR analyses were performed on lignin extracted from TMP fibers by a modification of the acidolysis method developed in the literature (Gellerstedt et al. 1994): dried fibers (5 g) were suspended in 175 ml of dioxane/water 82:18 v/v (0.1 M HCl) and refluxed under nitrogen for 3 h. The fibers were filtered and washed 3 times with 15 ml of dioxane/water 82:18 v/v, then with distilled water to reach a neutral pH. The filtrate was then evaporated under reduced pressure at 313 K until dioxane had been removed. The aqueous solution was kept overnight in a refrigerator to induce coagulation of lignin; the precipitate was collected by filtration through a fine porous glass filter and washed with distilled water. After drying in air at 353 K for 2 h, lignin was refluxed with hexane in a Soxhlet extractor for 8 h in order to remove low molecular weight compounds. The yield of lignin, evaluated as (extracted lignin) / (lignin in pulp) w:w %, was around 35-40%.

The extracted lignin was acetylated with acetic anhydride:pyridine 1:1 v/v and each sample, approximately 60 mg, dissolved in 0.75 ml DMSO- d_6 . The inverse detected ^1H - ^{13}C correlation (2D-HSQC-NMR) spectra were recorded on a Bruker 500 MHz instrument at 308 K. The spectral width was set 5 kHz in F2 and 25 kHz in F1. Altogether 128 transients in 256 time increments were collected. The polarization transfer delay was set at the assumed coupling of 140 Hz and a relaxation delay of 2 s was used. Spectra were processed using $\Pi/2$ shifted squared sinebell functions in both dimensions before Fourier transform. The ^1D - ^{13}C spectra were recorded using a Varian Mercury 400 MHz instrument at 308 K. The chemical shifts were referred to the solvent signal at 39.5 ppm. A relaxation delay of 10 s was used between the scans. Line broadening of 2-5 Hz was applied to FIDs before Fourier transform. For each spectrum, typically about 8000 scans were accumulated.

The number of primary, secondary and phenolic OH groups per aromatic ring was calculated (Cyr and Ritchie 1989; Faix et al. 1994; Robert and Brunow 1984; Landucci 1985) by multiplying the intensity of signals due to acetylic carboxyl groups divided by the intensity of signal due to methoxyl group, with the average number of methoxyl groups per aromatic ring in TMP lignins, this last number being evaluated by elemental and gas-chromatographic analyses (Girardin and Metche 1983).

GPC analyses

The investigation was carried out on acetylated lignin extracted from fibers. Before analysis, the acetylated lignin samples were dissolved in THF.

Analyses were performed using a Waters 600 E liquid chromatograph connected with an HP 1040 ultraviolet diode array (UV) detector set at 280 nm. The GP-column was an Agilent PL 3 μm MIXED gel E MW 220-400W. Polymer standards of poly(styrene) (PS) from Polymer Laboratories were used for calibration. The PS-

calibration curve was tested using acetylated dimeric, tetrameric, and hexameric lignin model compounds. Analysis were performed at a flow rate of 0.8 ml/min

The evaluation of both the number-average molecular weight (M_n) and the weight-average molecular weight (M_w) was performed following the methodology developed in the literature (Himmel et al. 1989).

RESULTS AND DISCUSSION

Radical Formation on Fibers

Radicals formed on TMP fibers after reaction at 298 K with molecular oxygen in the presence of either [Co(salen)] in methanol or [Co(sulphosalen)] in water, were identified and quantified by EPR spectroscopy at 123 K (see Experimental).

In water an isotropic signal ($g = 2.004$ $\Delta H_{pp} = 9$ G) was observed (Fig. 1), very similar to that formed on fibers after treatment with laccase (Hon 1992) and attributable to phenoxy radicals.

In methanol an eight-resonance line signal was detected (Fig. 2a), very similar in shape to that observed (Bolzacchini et al. 1997; Canevali et al. 2002) in frozen solution during the oxidative degradation of lignin model compounds (Fig. 2b), which is attributable to the phenoxy cobalt radical, [Co^{III}(salen)(ROH)(RO[•])].

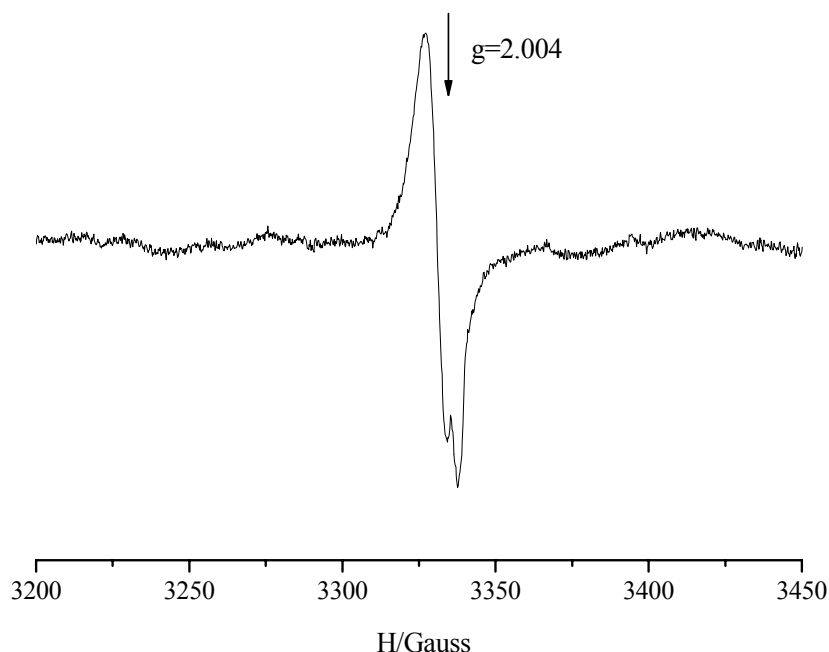


Fig. 1. X-band EPR spectrum recorded at 123 K on TMP fibers after oxidation in water in the presence of [Co(sulphosalen)] at 1 bar O₂ pressure for 60 min.

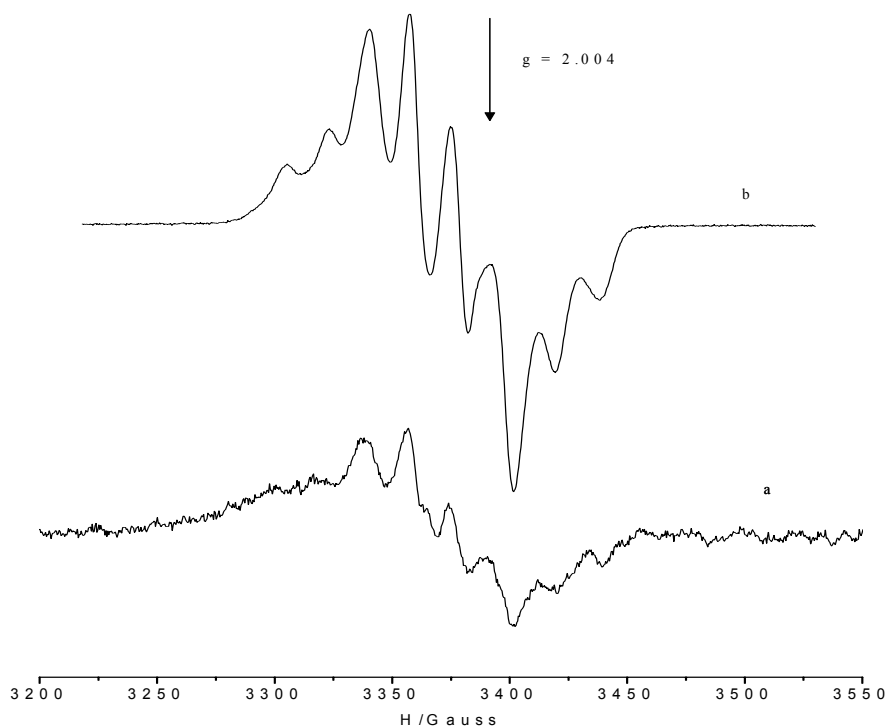


Fig. 2. X-band EPR spectra recorded at 123 K after oxidation in methanol in the presence of [Co(salen)] at 1 bar O₂ pressure for 30 min a) on TMP fibers and b) on E-methyl ferulate.

The radical signal formed by lignin model compounds in solution was deeply investigated in previous studies, both by X-band and high frequency (HF) EPR spectroscopy and showed axial magnetic anisotropy of g and A (⁵⁹Co) tensor components, with $g_{\perp} > g_{\parallel}$ and $A_{\parallel} > A_{\perp}$. The hyperfine coupling constant values vary with the ROH molecule (Canevali et al. 2002). In the case of lignocellulosic fibers, the observed signal is probably the envelope of several phenoxy cobalt radicals, which are [Co^{III}(salen)(ROH)(RO•)]-like, originated by the co-ordination of [Co(salen)] to different phenols present at the lignin surface. This causes a higher width of resonance lines with respect to the species containing a unique ROH ligand (Canevali et al. 2005).

The difference in the paramagnetic species formed during oxidation in the presence of [Co(salen)] and [Co(sulphosalen)] needs further investigation in order to be explained, which goes behind the scope of the present paper.

The best conditions for radical formation on TMP were assessed by evaluating the amount of paramagnetic species formed at different times of reaction (5, 15, 30, 60 min) in the presence of [Co(sulphosalen)] in water (Fig. 3a) or in the presence of [Co(salen)] in methanol (Fig. 3b).

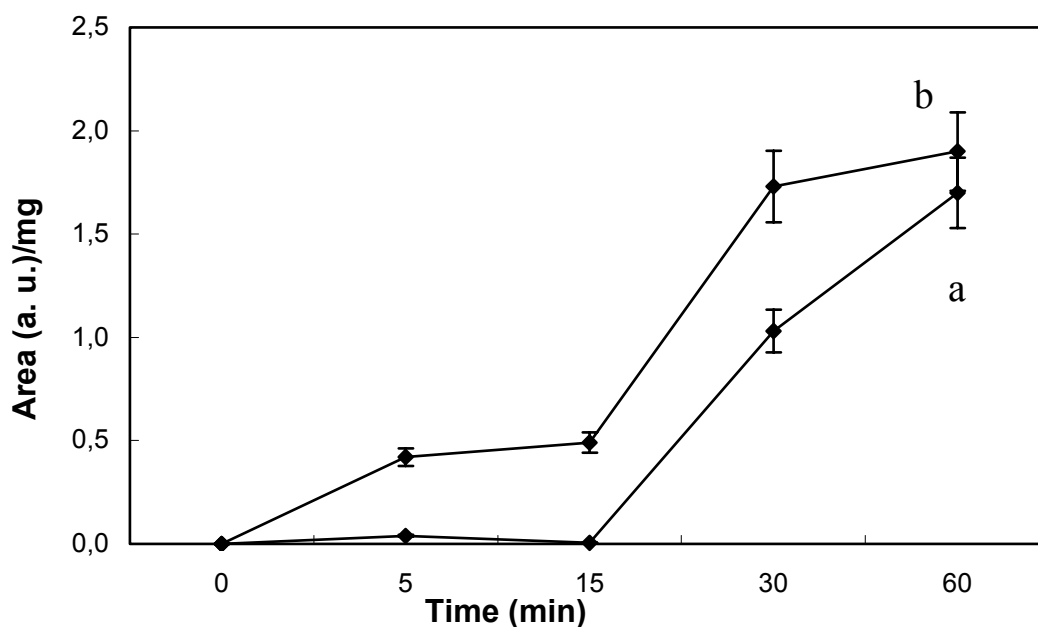


Fig. 3. Amounts of radicals, reported as area of EPR resonance lines (arbitrary units) per TMP fiber weight (mg), formed at different reaction times: a) phenoxo radicals formed in the presence of [Co(sulphosalen)] in water and b) phenoxo cobalt radicals formed in the presence of [Co(salen)] in methanol.

During both treatments, the amount of radicals gradually increased, [Co(salen)] in methanol being more reactive than [Co(sulphosalen)] in water at each time of reaction, except after 60 min of reaction, when the amounts of radicals formed in the two ways do not significantly differ.

Change in Lignin Structure

In order to evaluate changes in lignin chemical structure induced by catalytic oxidations in the presence of [Co(salen)] or [Co(sulphosalen)], lignins extracted by acid hydrolysis of fibers were characterized by 2D-HSQC-NMR spectroscopy, to identify the main intermonomeric units, and by ^{13}C -NMR spectroscopy, to quantify the principal intermonomeric units and the amount of alcoholic and phenolic groups. Spectra were run in DMSO- d_6 on the acetylated samples for the following three reasons: i) to avoid lignin fractionation before NMR analysis (Sipila 2002), ii) to increase the lignin solubility in DMSO- d_6 and iii) to enhance the chemical shift dispersion of the side chain units (Adler et al. 1987). As investigated lignins were obtained from both unreacted and oxidized fibers, the structure modifications due to the oxidative treatment were unequivocally distinguished from those due to the isolation method.

A preliminary evaluation by Klason method (Dence 1992) of the lignin amount in fibres after oxidation treatments and a preliminary evaluation of methoxyl content in

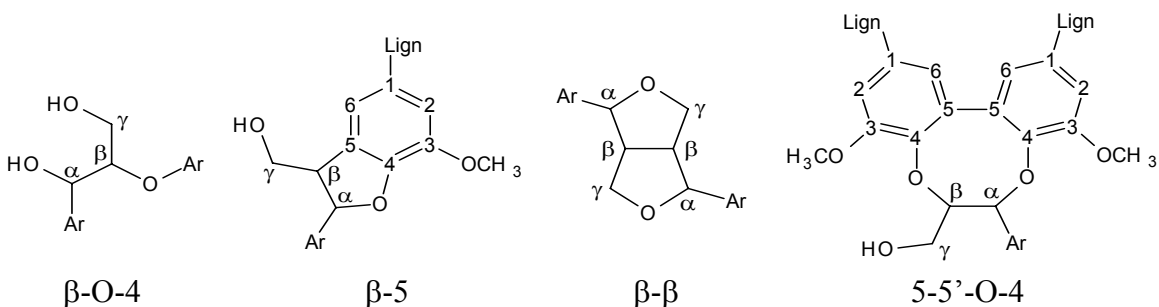
lignin by the Zeisel method (Girardin and Metche 1983) allowed us to exclude relevant delignification effects. The data are reported in Table 2.

Table 2. Lignin Amount in TMP Fibres Before and After Treatment with [Co(salen)] and [Co(sulphosalen)] and Amount of Methoxyl Content In Lignin Extracted from Fibres Before and After Treatment with [Co(salen)] and [Co(sulphosalen)].

Type of fibers	% lignin amount in fibers *	$\mu\text{mol OCH}_3 / \text{mg lignin}^{**}$
Untreated TMP	27,1	4,06
[Co(salen)]-treated TMP	27,0	4,05
Co(sulphosalen)]-treated TMP	27,1	4,07

*Klason method, ** Zeisel method

The assignment of predominant signals in 2D-HSQC-NMR spectra was based on the chemical shift data of lignin model compounds and of milled wood lignin (MWL), as reported in the literature (Drumond et al. 1989; Ralph 1996; Kilpelainen et al. 1994). The predominant intermonomeric units found in TMP lignins extracted from fibers are reported in Scheme 3: arylglycerol- β -aryl ether (β -O-4 unit), phenylcoumaran (β -5 unit), pinosresinol (β - β unit) and dibenzodioxocine (5-5'-O-4 unit).



Scheme 3.

The quantitative evaluation of the predominant intermonomeric units by ^{13}C -NMR showed that unreacted TMP lignin and TMP lignin treated with [Co(sulphosalen)] were rich in β -O-4 units and also contained significant amounts of β -5 units (Table 3). Instead, after [Co(salen)] treatment, the amount of β -O-4 and β -5 units in acetylated lignin approximately reduced to a half, with respect to untreated TMP. The amount of β - β units did not change after both treatments, while the 5-5'-O-4 units were not observed in lignin extracted from [Co(salen)]-treated TMP.

Table 3. Relative Amounts of the Predominant Intermonomeric Units in TMP Lignins Extracted from Fibres Before and After Treatment with [Co(salen)] and [Co(sulphosalen)].

Structural units	Untreated TMP	[Co(salen)]-treated TMP	[Co(sulphosalen)]-treated TMP
β -O-4	++++	++	+++
β -5	++	+	++
β - β	+	+	+
5-5'-O-4	+	traces	+

In addition to the elucidation of the structural changes in lignin intermonomeric composition, a quantitative evaluation of alcoholic and phenolic groups in TMP fibers, before and after the oxidative treatments, was also performed. It was shown that treatment in the presence of [Co(salen)] induced significant changes in the amount of alcoholic and phenolic groups per aromatic ring, while in the presence of [Co(sulphosalen)] the number of hydroxyl groups did not significantly change (Table 4). These results agree with the observed relative amounts of the predominant intermonomeric units, detected by ^{13}C -NMR and suggest that chemical lignin structure is better preserved after treatment with [Co(sulphosalen)] in water than with [Co(salen)] in methanol.

Table 4. Number of Primary, Secondary and Phenolic OH per Aromatic Ring in TMP Acetylated Lignins, Before and After Treatment with [Co(salen)] and [Co(sulphosalen)].

OH Type/ C_6H_6	δ/ppm	Untreated TMP	[Co(salen)]-treated TMP	[Co(sulphosalen)]-treated TMP
primary	169.9-171.0	0.52	0.36	0.52
secondary	169.5	0.28	0.24	0.29
phenolic	168.6	0.20	0.15	0.19

The effects of salen treatments on lignin structure were also elucidated by evaluating the molecular weight distribution changes in the extracted acetylated lignins. Results show that the changes in M_n , M_w and polydispersity (M_w/M_n) of acetylated lignins, after [Co(sulphosalen)] treatment, are not significant, whereas in the case of [Co(salen)] treatment a small increase for M_n (from 5600 to 7500) and for M_w (from 13600 to 18000) was observed (Table 5). These results agree with those obtained by NMR investigation.

Table 5. M_n , M_w and Polydispersity Ratio (M_w/M_n) Values of TMP Acetylated Lignins, Before and After Treatment with [Co(salen)] and [Co(sulphosalen)].

Molecular weight distribution	Untreated TMP	[Co(salen)]-treated TMP	[Co(sulphosalen)]-treated TMP
M_n	5600 ± 500	7500 ± 500	5800 ± 500
M_w	13600 ± 1000	18000 ± 1000	14100 ± 1000
M_w/M_n	2.43 ± 0.04	2.40 ± 0.04	2.43 ± 0.04

CONCLUSIONS

1. The results of EPR investigation showed that the oxidation of unbleached TMP fibers by molecular oxygen, catalyzed by [Co(sulphosalen)] in water, induced the formation of phenoxy radicals that were very similar to those reported in the literature for the treatment of the same fibers with molecular oxygen and laccase (Lund et al. 2003). By contrast, in the presence of [Co(salen)] in methanol, phenoxy cobalt radicals similar in structure to those formed during the oxidation of lignin model compounds (Bolzacchini et al. 1997; Canevali et al. 2002) were observed.
2. After 60 min of reaction, the amount of radicals formed on TMP fibers in the presence of either [Co(salen)] or [Co(sulphosalen)] did not significantly differ. This result suggests that that efficient radical formation on fibers can be achieved also with water-soluble catalysts
3. The modification of lignin chemical structure was lower after oxidation with [Co(sulphosalen)] in water than with [Co(salen)] in methanol, as assessed by 2D-HSQC-NMR, ¹³C-NMR and GPC.
4. The obtained results showed that the treatment with molecular oxygen in the presence of [Co(sulphosalen)] in water represents a promising way to approach an environmentally sustainable radical formation on fibers, without an heavy modification of the lignin structure.

ACKNOWLEDGMENTS

This contribution was an original presentation at the *ITALIC 4 Science & Technology of Biomass: Advances and Challenges* Conference that was held in Rome, Italy (May 8-10, 2007) and sponsored by Tor Vergata University. The authors gratefully acknowledge the efforts of the Conference Organizers, Prof. Claudia Crestini (Tor Vergata University, Rome, Italy), Chair, and Prof. Marco Orlandi (Biococca University, Milan, Italy), Co-Chair. Prof. Crestini also is Editor for the conference collection issue to be published in *BioResources*.

REFERENCES CITED

- Adler, E., Brunow, G., and Lundquist, K. (1987). "Investigation of the acid-catalyzed alkylation of lignins by means of NMR spectroscopic methods," *Holzforschung* 41(4), 199-207.
- Bledzki, A. K., Reihmane, S., and Gassan, J. (1998). "Thermoplastics reinforced with wood fillers: a literature review," *Polymer-Plastics Technology and Engineering* 37(4), 451-468, and references therein.
- Bolzacchini, E., Canevali, C., Morazzoni, F., Orlandi, M., Rindone, B., and Scotti, R. (1997). "Spectromagnetic investigation of the active species in the oxidation of propenoidic phenols catalysed by [*N,N'*-bis(salicylidene)-ethane-1,2-diaminato]-cobalt(II)," *J. Chem. Soc. Dalton Transactions* 4695-4699.

- Buchert, J., Grönqvist, S., Mikkonen, H., Oksanen, T., Peltonen, S., Suurnäkki, A., and Viikari, L. (2005). "Process for producing a fibrous product," *European Pat. 2005*, WO2005061790.
- Canevali, C., Orlandi, M., Pardi, L., Rindone, B., Scotti, R., Sipila, J., and Morazzoni, F. (2002). "Oxidative degradation of monomeric and dimeric phenylpropanoids: reactivity and mechanistic investigation," *J. Chem. Soc. Dalton Transactions* 15, 3007-3014.
- Canevali, C., Orlandi, M., Zoia, L., Scotti, R., Toppa, E.-L., Sibila, J., Agnoli, F., and Morazzoni, F. (2005). "Radicalization of lignocellulosic fibers, related structural and morphological changes," *Biomacromolecules* 6(3), 1592-1601.
- Chandra, R. P., Lehtonen, L. K., and Ragauskas, A. J. (2004). "Modification of high lignin content kraft pulps with laccase to improve paper strength properties. 1. Laccase treatment in the presence of gallic acid," *Biotechnol Prog* 20, 255-261.
- Cyr, N. and Ritchie, G. S. (1989). *Lignin Properties and Materials*, W. G. Glasser, S. Sarkanen eds.; American Chemical Society 28, 372-381.
- Dence, C. W. (1992). *Methods in Lignin Chemistry*, Y. Lin, C. W. Dence, eds.; Springer-Verlag, Berlin, 33.
- Drumond, M., Aoyama, M., Chen, C. L., and Robert, D. (1989). "Substituent effects on carbon-13 chemical shifts of aromatic carbons in biphenyl type lignin model compounds," *J. Wood Chem. Technol.* 9(4), 421-441.
- Faix, O., Argyropoulos, D. S., Robert, D., and Neirinck, V. (1994). "Determination of hydroxyl groups in lignins evaluation of ¹H-, ¹³C-, ³¹P-NMR, FTIR and wet chemical methods," *Holzforschung* 48, 387-394.
- Felby, C., Pedersen, L. S., and Nielsen, B. R. (1997a). "Enhanced auto-adhesion of wood fibers using phenol oxidases," *Holzforschung* 51(3), 281-286.
- Felby, C., Nielsen, B. R., Olesen, P. O., and Skibsted, L. H. (1997b). "Identification and quantification of radical reaction intermediates by electron spin resonance spectrometry of laccase-catalyzed oxidation of wood fibers from beech (*Fagus sylvatica*)," *Appl. Microbiol. Biotechnol.* 48(4), 459-464.
- Ferm, R., Kringstad, K. P., and Cowling, E. B. (1972). "Formation of free radicals in milled wood lignin and syringaldehyde by phenol-oxidizing enzymes," *Sven. Papperstidn.* 14, 859-865.
- Gellerstedt, G., Pranda, J., and Lindfors, E.-L. (1994). "Structural and molecular properties of residual birch kraft lignins," *J. Wood Chem. Technol.* 14(4), 467-482.
- Girardin, M., and Metche, M. (1983). "Rapid micro determination of alkoxy groups by gas chromatography. Application to lignin," *J. Chromatography* 264(1), 155-158.
- Himmel, M. E., Tatsumoto, K., Oh, K. K., Grohmann, K., Johnson, D. K., and Li Chum, H. (1989). *Lignin properties and materials*, W. G. Glasser, S. Sarkanen ed. American Chemical Society, chapter 6, 82.
- Hon, D. N. S. (1992). *Methods in Lignin Chemistry*, Y. Lin, C. W. Dence, ed. Springer-Verlag, Berlin, 274.
- Kilpelainen, I., Sipila, J., Brunow, G., Lundquist, K., and Ede, R. M. (1994). "Application of two-dimensional NMR spectroscopy to wood lignin structure determination and identification of some minor structural units of hard- and softwood lignins," *J. Agr. Food Chem.* 42(12), 2790-2794.

- Landucci, L. L. (1985). "Quantitative carbon-13 NMR characterization of lignin 1. A methodology for high precision," *Holzforschung* 39(6), 355-359.
- Lund, M., Eriksson, M., and Felby, C. (2003). "Reactivity of a fungal laccase towards lignin in softwood kraft pulp," *Holzforschung* 57, 21-26.
- Lund, M., and Felby, C. (2001). "Wet-strength improvement of unbleached kraft pulp through laccase-catalyzed oxidation," *Enzyme Microb. Technol.* 28(9-10), 760-765.
- Ralph, J. (1996). "An unusual lignin from Kenaf," *J. Natural. Prod.*, 59(4), 341-342.
- Robert, D., and Brunow, G. (1984). "Quantitative estimation of hydroxyl groups in milled wood lignin from spruce and in a dehydrogenation polymer from coniferyl alcohol using carbon-13 NMR spectroscopy," *Holzforschung* 38(2), 85-90.
- Sipila, J. (2002). *Proceedings of 7th European Workshop of Lignocellulosic and Pulp*, Turku 26-29 August, 67-70.
- Sippola, V. O., and Krause, A. O. I. (2003). "Oxidation activity and stability of homogeneous cobalt-sulphosalen catalyst. Studies with a phenolic and a non-phenolic lignin model compound in aqueous alkaline medium." *Journal of Molecular Catalysis A: Chemical* 194(1-2), 89-97.

Article submitted: Sept. 18, 2007; First round of peer review completed: Nov. 1, 2007;
Revised article received and approved: Nov. 26, 2007; Published, Nov. 27, 2007.

STRENGTH ENHANCEMENT OF A FIBER NETWORK BY CARBOXYMETHYL CELLULOSE DURING OXYGEN DELIGNIFICATION OF KRAFT PULP

Eero Kontturi,* Mia Mitikka-Eklund, and Tapani Vuorinen

Sorption of carboxymethyl cellulose (CMC) on the fiber surface was applied during oxygen delignification to enhance the strength properties of softwood kraft pulp. Unlike many previous efforts, the focus was not set on the improvement of selectivity of oxygen delignification, i.e. retaining stable viscosity vs. decreasing kappa number. Instead, without an improved selectivity, handsheets from CMC-treated fibers exhibited a 15% improvement in tensile index and 25% improvement in tear index after a full bleaching sequence in comparison to the untreated reference pulp. Since it is demonstrated that the CMC addition can be incorporated as an integral step in the fiberline process, the method offers an effortless and viable option to produce pulp resulting in stronger paper products.

Keywords: Carboxymethyl cellulose, Oxygen delignification, Selectivity, Tear strength, Tensile strength

Contact information: Laboratory of Forest Products Chemistry, Helsinki University of Technology, P.O.Box 6300, FIN-02015 TKK, Finland; *Corresponding author: eero.kontturi@tkk.fi

INTRODUCTION

At present, it is common to include an additional step between cooking and bleaching of kraft pulp: oxygen delignification. An environmentally agreeable choice, oxygen delignification is used to remove ca. 50% of the residual lignin before its selectivity towards lignin is lost (McDonough 1996). The reasons for the limit of lignin removal during oxygen delignification are still under debate (Gellerstedt and Heuts 1997; Moe and Ragauskas 1999; Argyropoulos and Liu 2000; Yang et al. 2003; Rööst et al. 2003; Kontturi et al. 2005; Shin et al. 2006), but the most explicit evidence suggests that covalent bonds between lignin and carbohydrates hinder the selective removal of lignin after a certain point (Chirat and Lachenal 1997; Fu and Lucia 2003; Axelsson et al. 2004). The purpose of this paper is to present a method which leads to a stronger fiber network after oxygen delignification of kraft cooked fibers without a drastic improvement in the selectivity towards lignin.

The chemistry of oxygen delignification has been resolved to a relatively high degree with model compound studies (for reviews, see Gierer 1997 and Gavrilescu 2005). The hydroxyl radical has been pointed out as the detrimental species, cleaving the glycosidic bonds of cellulose by a substitution reaction at the anomeric carbon (Guay et al. 2002), thus reducing the degree of polymerization of cellulose and, consequently, the fiber strength (Yang et al. 2003). Since its commercial introduction in the 1970s, improving the selectivity of oxygen delignification has been subject to repeated endeavors (Suchy and Argyropoulos 2002; Chen and Lucia 2002; Van Heiningen and

Violette 2003; Argyropoulos et al. 2004; Gaspar et al. 2004; Ruuttunen and Vuorinen 2005). So far, the only widespread procedure adapted by the industry is the addition of magnesium sulfate to impede the formation of hydroxyl radicals in the reaction mixture (Lidén and Öhman 1997).

Independent of developing a more efficient result from oxygen delignification, there is a vast area of research which focuses on improving the strength properties of paper products during the papermaking process. These methods function mainly by the addition of various polyelectrolytes – labeled dry strength agents - in the wet end of paper machine (Pelton 2004; Hubbe 2006). Recently, more refined tools, such as polyelectrolyte multilayers, have been applied in laboratory scale to yield substantial strength gains for paper (Wågberg et al. 2002; Eriksson et al. 2006). An additional interesting development in the field of enhancing the strength of a fiber network is the sorption of carboxymethyl cellulose (CMC) on the fiber surface, resulting in remarkably strong paper after the treatment (Mitikka-Eklund et al. 1999; Blomstedt and Vuorinen 2006; Laine et al. 2002, 2003a, 2003b; Ekevåg et al. 2004; Watanabe et al. 2004). CMC sorption is not subordinate to conventional strength agents: the mechanism of strengthening is very different to those of ordinary strength agents, and CMC has to be attached to the fiber in a separate step in the papermaking process. The strength gains by this method are considerably higher than when CMC has been used as a conventional dry strength agent, i.e., added to the wet-end of the paper machine (Beghella et al. 1997). Thus, CMC addition as a separate step has been termed “bipolar activation technology” (Laine et al. 2002, 2003a, 2003b) or “fiber engineering” (Mitikka-Eklund et al. 1999; Blomstedt and Vuorinen 2006), depending on the group involved with the research and on the technique applied to attach the CMC. It is noteworthy that the former technique employs high electrolyte concentration to screen the repulsion between the anionic fibers and anionic CMC, whereas the latter method relies on the low degree of substitution (DS), i.e. low charge density of the CMC, to enable the adsorption on the fibers. This latter method will be exploited in this work, since the highly alkaline conditions of oxygen delignification are optimal for properly dissolving the CMC with a low DS.

This paper intends to demonstrate how the CMC addition may be included in the oxygen delignification as an integral part of the chemical pulping process. Regrettably often in papermaking research, the pulping process and the paper machine are treated as isolated entities. Optimization of pulping parameters focuses on the preparation of strong, lignin-free fibers without considering the end product: a network of fibers. Optimization in the paper machine, on the other hand, focuses on the preparation of as strong a fiber network as possible without taking into account the effect of the raw material (pulp). Therefore, to combine the approach of strong fibers with the aim for strong fiber networks, we have tried to investigate the effect of CMC addition during oxygen delignification on the strength properties of the whole fiber network in the form of laboratory handsheets. Furthermore, the CMC-treated, oxygen delignified pulp will be subjected to subsequent bleaching stages to explore the full benefit of the strength improvement.

EXPERIMENTAL

Materials

Kraft cooked, unbleached spruce pulp was provided by a pulp mill in Eastern Finland. The CMC used for the sorption was Nymcel ZSB-10, F1226 (sodium salt) with a degree of substitution (DS) 0.2. NaOH, MgSO₄, phenol were all p.a. grade from Aldrich. Sulfuric acid was obtained as a 98 % (p.a.) solution from VWR.

Methods

Oxygen delignification with CMC sorption

Oxygen delignification was performed in an air bath digester in 10 % pulp consistency. The oxygen pressure applied was 8 bar, alkali charge 2.5 % NaOH on pulp, temperature 100°C. 1 % MgSO₄ on pulp was added as a stabilizer. The initial concentration of CMC in the suspension was 1 % on pulp. Prior to its addition, CMC was dissolved in 2 M NaOH solution and the amount of NaOH in that solution was taken into account when calculating the total alkali charge of the mixture. The high alkali charge during the delignification guaranteed that the CMC with a low DS (0.2) was properly dissolved throughout the procedure. The delignification was carried out for 60 minutes. Reference delignification stages were performed without the CMC addition.

Determining the extent of CMC sorption

The amount of attached CMC was quantified by analysing the carbohydrate content from the filtrates by phenol-sulfuric acid assay (Chaplin 1986) and assuming that the rest of the carbohydrates had adsorbed on the fibers. Since there is some carbohydrate detachment from the fiber during oxygen delignification, the phenol-sulfuric acid assay was prepared for the reference pulps, too. The amount of CMC that was not attached was then determined from the subtraction.

Table 1. The Bleaching Conditions for the Post Oxygen Delignification Stages (D₁ED₂).

Bleaching stage	Temperature [°C]	Time [min]	Consistency [%]	ClO ₂ [%, act. Cl ₂]	NaOH [%]	Final pH
OD ₁	50	60	10	3.0	0.6	5.0
OD ₁ E	60	60	10	-	1.8	12.4
OD ₁ ED ₂	60	180	10	1.5	0.5	6.4

Subsequent bleaching stages

After the oxygen stage, both the CMC treated pulp and the reference pulp were bleached by using the sequence D₁ED₂ (D for chlorine dioxide stage, E for alkaline extraction stage). Each stage was performed in a polyethylene bag with the conditions listed in Table 1.

Testing of pulps

The viscosity was determined according to the standard method SCAN-CM 15:88. The kappa number was determined according to SCAN-C 1:77.

Testing of laboratory handsheets

Handsheets were prepared according to the standard method SCAN-C 26:76 except for the wet pressing (490 kPa was applied) and drying (2h at 60°C in a drum drier was applied). Density was determined by ISO 534:1988. The strength properties were determined with the following standard procedures: tensile index (ISO 1924-2:1994), out-of-plane Elmendorf tear index (ISO 1974:1990), and bonding ability as Scott bond (TAPPI UM 403).

RESULTS AND DISCUSSION

Selectivity and Brightness

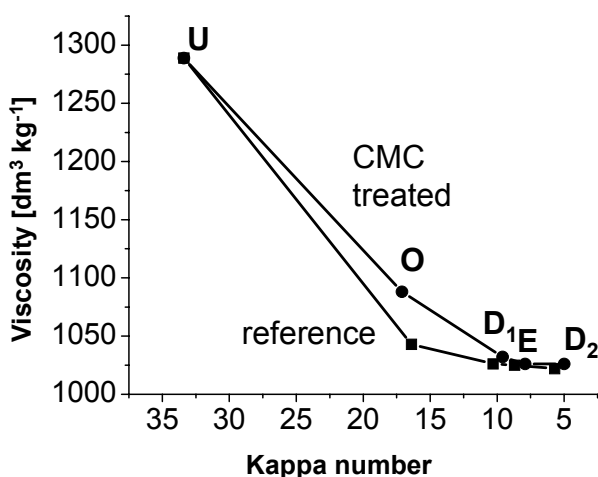


Fig. 1. Kappa number as a function of viscosity in the CMC-treated (●) and reference (□) pulps unbleached (U), after oxygen delignification (O), after first chlorine dioxide bleaching stage (D₁), after alkaline extraction (A), and after second chlorine dioxide bleaching stage (D₂).

The filtrate analysis after oxygen delignification revealed that 85 % of the CMC had been attached to the fiber, which is on the same order of magnitude that has been achieved with the CMC sorption during the kraft cook (Ekevåg et al. 2004). The selectivity of oxygen delignification and the subsequent bleaching stages for the CMC-treated and the reference pulps is expressed in Figure 1. Viscosity represents a measure of the degree of polymerization (DP) of cellulose in the fiber and the reduction in kappa number is a sound quantification of the delignification for softwood pulps. Figure 1 indicates a small improvement of selectivity for the CMC-treated pulp after the oxygen delignification stage and negligible deviations after the subsequent D₁E D₂ stages. It is noteworthy that the CMC sorption during oxygen delignification does not affect the delignification at all since the kappa numbers of the CMC-treated pulp and the reference

pulp are essentially similar. We can speculate that the larger viscosity of the CMC-treated fibers arises from the protective effect of the dissolved CMC which has not been adsorbed on the fibers: the detrimental hydroxyl radicals degrade the dissolved CMC rather than the cellulose within the fibers. Whatever the case, the small improvement in selectivity depicted in Fig. 1 has no industrial significance.

CMC sorption in the oxygen delignification stage does not affect the brightness development during oxygen delignification and the subsequent bleaching in any way (results not shown). This, together with the kappa number development, indirectly indicates that the removal of lignin and chromophoric structures is largely unaffected by the CMC addition. Moreover, the data suggest that additional consumption of bleaching chemicals by CMC is negligible.

Strength Properties

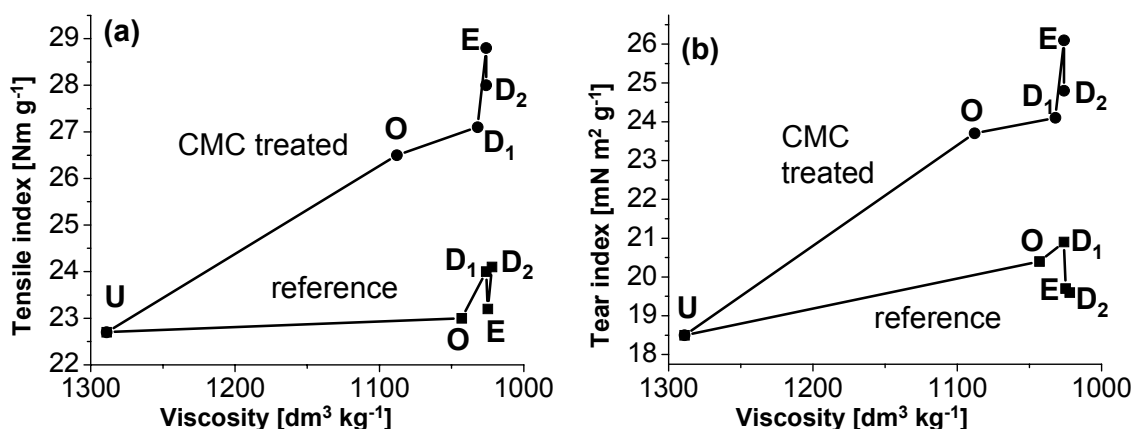


Fig. 2. (a) Tensile index as a function of viscosity, (b) tear index as a function of viscosity of the handsheets prepared from the CMC-treated (●) and reference (■) pulps unbleached (U), after oxygen delignification (O), after first chlorine dioxide bleaching stage (D₁), after alkaline extraction (A), and after second chlorine dioxide bleaching stage (D₂).

Figure 2a illustrates the development of the tensile index as a function of viscosity during oxygen delignification and the subsequent bleaching stages. The reference plot (without CMC sorption) indicates that although the viscosity drop during oxygen delignification was substantial, the tensile index stayed unaffected. This is a reported phenomenon, and sometimes the tensile index may even increase slightly after oxygen delignification (Yang et al. 2003). The same behavior was evident for tear index (Fig. 2b). In fact, the viscosity within the fiber needs to achieve a certain critical value before its decrease starts to affect the strength of the fiber network by decreasing tear and tensile indices (Rydholm 1965). Figures 2a and 2b, moreover, show that further bleaching by D₁E D₂ stages did not markedly influence the viscosity or the strength properties of the reference pulp.

However, when the pulp was subjected to CMC sorption during the oxygen delignification stage, both the tensile (Fig. 2a) and tear (Fig. 2b) indices increased considerably. After additional bleaching by D₁E D₂ stages, the strength improvement was

maintained, but to a smaller degree. The effect of CMC is emphasized in Fig. 3 in the more traditional tear-tensile graph. The strength gains by CMC addition were significant after the full D_1ED_2 bleaching: 25 % increase in tensile index and 35 % increase in tear index with respect to the values of the unbleached pulp. The reference pulp without the CMC sorption demonstrated a mere 5 % increase in both tear and tensile indices after oxygen delignification followed by D_1ED_2 bleaching. In other words, in comparison with the reference pulp without the added CMC, the CMC treated pulp possessed a 15 % improvement in tensile index and 25 % improvement in tear index after the full D_1ED_2 bleaching.

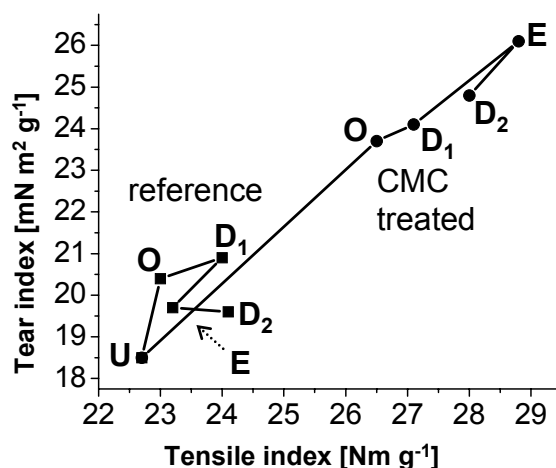


Fig. 3. Tear index as a function of tensile index of the handsheets prepared from the CMC-treated (●) and reference (■) pulps unbleached (U), after oxygen delignification (O), after first chlorine dioxide bleaching stage (D₁), after alkaline extraction (A), and after second chlorine dioxide bleaching stage (D₂).

In the previous research, CMC sorption to an already fully bleached softwood kraft pulp has resulted in up to 200 % increase in the tensile index (Laine et al. 2003b). The quoted method of addition, however, requires a separate step in the pulp preparation process and with its requirements of high temperature (120°C) and high electrolyte concentration, it is somewhat cumbersome to insert into the fiberline. To overcome this, Ekevåg et al. (2004) made an effort to include the CMC addition in the kraft cook. In consequence, the authors managed to improve the tensile strength of unbleached softwood kraft pulp by 20 %. The work by Ekevåg et al. (2004) also features subsequent bleaching performed on the CMC treated pulp, which resulted in 10 % increase of tensile index compared with the reference stage. Therefore, the 15 % improvement in tensile index (Fig. 2a) is a competitive result. The tear index in the quoted study (Ekevåg et al. 2004), on the other hand, was decreased by 20 % upon CMC addition. This inverse tear-tensile relationship is common with softwood pulps after the tear strength has passed through a maximum (Page 1994) and, moreover, tear index is more susceptible to a decrease in viscosity than the tensile index (Rydholm 1965). Furthermore, the tear strength of softwood kraft pulp expresses a decline along an industrial bleaching sequence (MacLeod et al. 1995). A constant increase of tear index with a steady growth in tensile index has only been achieved before with oxygen delignification and

subsequent bleaching of hardwood pulps (Hunt and Hatton 1987; Tran 2001), which express altogether a very different behavior with respect to the tear and tensile indices (Van den Akker 1958). Furthermore, the conventional dry-strength additives do not increase the tear strength but usually decrease it slightly (Davison 1980). The unimproved tear strength appears even when CMC is applied as a conventional dry-strength additive in the wet-end of the paper machine (Beghelli et al. 1997). The increase in both tear and tensile indices (Figs. 2 and 3) is an unexpected and positive result.

Bonding and Bond Strength

As mentioned in the introduction, numerous methods to improve the selectivity of oxygen delignification have been presented (Suchy and Argyropoulos 2002; Chen and Lucia 2002; Van Heiningen and Violette 2003; Argyropoulos et al. 2004; Gaspar et al. 2004; Ruuttunen and Vuorinen 2005). The direct comparison of those results with this work, however, is complicated because they focus on the relationship between the kappa number and viscosity, i.e., the selectivity of oxygen delignification, not the direct enhancement of the strength properties of the subsequent paper. In fact, often the papermaking strength properties of the pulps have not been presented in the pertinent publications. Indeed, there are several factors that dictate the strength properties of a fiber network and the degree of polymerization (DP) of the cellulose in the fibers, represented by viscosity, is only one of them. As mentioned above, the cellulose DP affects the paper strength after it decreases past a certain threshold value (Rydholm 1965). This threshold, however, is not usually reached under industrial pulping conditions.

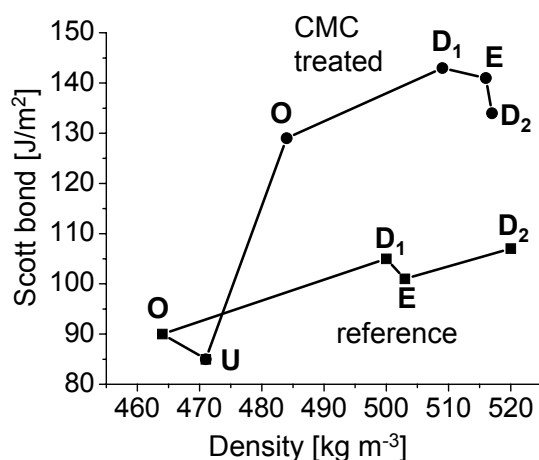


Fig. 4. Scott bond as a function of density of the handsheets prepared from the CMC-treated (•) and reference (■) pulps unbleached (U), after oxygen delignification (O), after first chlorine dioxide bleaching stage (D₁), after alkaline extraction (A), and after second chlorine dioxide bleaching stage (D₂).

The DP of cellulose affects the strength properties allegedly because it governs the strength of individual fibers to an extent (Gurnagul et al. 1992). Although the fiber strength is an important quality, the strength of a fiber network is also strongly influenced by the bonding between the fibers, namely by the extent of bonding and by the strength of the fiber-fiber bond. The extent of bonding and the internal bond strength of the fiber

network after oxygen delignification and the bleaching stages was examined by plotting the Scott bond (z-directional bond strength) as a function of density (extent of bonding) in Fig. 4. The increased Scott bond values due to CMC addition are in line with the improved strength properties of Fig. 2 but, interestingly, the density of the handsheets after oxygen delignification was hardly affected by the CMC addition. Although the two previously published basic methods of CMC addition both improve the strength properties of paper, they differ markedly in their influence on density. The method introduced by Laine et al. (2003b) has a minute effect on density, which raises speculation that the strength improvement comes mainly from the increased surface charge, which strengthens the fiber-fiber bond. In contrast, the method of Mitikka-Eklund et al. (1999) has an incremental impact on the sheet density, which led the authors to hypothesize that, in addition to the increased surface charge, the flexibility of the fibers increases and the CMC addition also positively influences the number of fiber-fiber bonds. We propose that this fundamental difference implies that also the mechanism of CMC addition is very different between these methods. Therefore, the reduced growth of density in Fig. 4 is surprising, since the method of addition applied here is essentially the one introduced by Mitikka-Eklund et al. (1999). It is evident that the prevalent conditions in oxygen delignification affect the CMC adsorption. It is probable that the presence of magnesium sulfate, although small in concentration (ca. 8 mmol dm⁻³), renders the sorption different. The high temperature and pressure (100°C, 8 bar) also contribute to the speculation that the adsorption mechanism here may well be akin to the one presented by Laine et al. (2003b). Since this method allegedly functions mainly by adding more charge on the fiber surface to improve the strength of the fiber-fiber bond, an interesting experiment for future research would be to see whether any CMC with a higher degree of substitution can be attached in the conditions of oxygen delignification.

As mentioned in the previous, the surface charge of the fibers has been acknowledged as an important factor in the strength of the fiber-fiber bond (Barzyk et al. 1997), which is indeed a major contributor to the strength gains achieved by the highly charged CMC species (Laine et al. 2003a, 2003b) as well as polyelectrolyte multilayers (Wågberg et al. 2002; Eriksson et al. 2006). In a recent work, Zhang et al. (2005) made an attempt to optimize the amount of charged groups in the fiber by tuning the conditions of oxygen delignification. As a result, the authors presented a 20 % increase in tensile index when the charge of the fibers was increased by 60 % during oxygen delignification. Regrettably, no other strength properties were tested and the authors did not investigate how the tensile strength would behave as a function of further bleaching stages. Unfortunately, we do not possess data on the charge properties of our pulps, because they are outside the scope of this descriptive introductory paper. It would be interesting to investigate, for instance, how the CMC attachment presented in this paper affects the strength properties when the charge of the fibers has been optimized according to Zhang et al. (2005). However, when delignification is concerned, other factors affecting the fiber-fiber bond should also be considered, such as the amount of surface lignin (Shao and Li 2006) or the DP of cellulose on the fiber surface (Kontturi and Vuorinen 2006). In the industrial conditions, moreover, the strength losses to fibers and the fiber network by mechanical damage have to be taken into account. For instance, concerning oxygen delignification, Allison et al. have suggested that most of the strength losses are induced

by mechanical changes, such as fiber deformations (Allison et al. 1998). This view has also been put forward as a generalization (MacLeod et al. 1987; Molin et al. 1996). More fundamental research on the origin of these different contributions to paper strength is required for better understanding the factors that affect the strength of a fiber network.

Impacts on the Fiberline Process

There is admittedly a drastic difference in the strength improvement of the fiber network depending on whether the CMC addition has been performed as a separate step or integrated in the process like in this work. We can speculate that probably the CMC is degraded to a lower molecular weight during oxygen delignification, thus enabling the penetration of CMC inside the fiber matrix. When the surface-specificity of the attached CMC is lost, the strength gains are also lost to a considerable degree (Laine et al. 2002). However, the method presented here offers a viable, realistic option with genuine strength improvements to include the CMC addition in the pulping and the subsequent papermaking process. The industrial applicability is something that still remains an unresolved problem with, for instance, polyelectrolyte multilayer deposition on fibers, in spite of the huge strength gains by that technique (Wågberg et al. 2002; Eriksson et al. 2006).

A further advantage is provided by the chemical nature of CMC. The inorganic catalysts designed to improve the selectivity of oxygen delignification (Suchy and Argyropoulos 2002) always raise questions about the toxicity, although the authors are sometimes prudent with the environmental implications (Gaspar et al. 2004). As a non-toxic cellulose derivative, CMC causes no environmental concerns.

It is clear that many factors affect the strength of a fiber network during the pulping process: the DP of cellulose in the fiber, the charge density on the fiber surface, the amount of lignin and extractives on the fiber surface, the flexibility of the fibers, etc. This introductory report does not intend to assess the contributions of these qualities. Rather, it serves as an example that simple treatments without the insertion of additional steps in the fiberline process have potential to positively influence the properties of the end product.

CONCLUSIONS

1. CMC sorption has been successfully included in the oxygen delignification of softwood kraft pulp with strength gains in both tear (+35%) and tensile (+25%) indices of the handsheets prepared from fully (D₁ED₂) bleached pulp. Formerly, CMC sorption has required a separate step of addition in the papermaking process.
2. Upon CMC sorption, the fiber-fiber bond was strengthened, as demonstrated by the increase in Scott bond, whereas the amount of bonds was largely unaffected, as witnessed by the relatively stable density of the handsheets.
3. The strength gains on the handsheets were achieved without an improvement in the selectivity of oxygen delignification.

ACKNOWLEDGMENTS

Sustainpack project is acknowledged for the financial support.

REFERENCES CITED

- Allison, R. W., Ellis, M. J., and Wrathall, S. H. (1998). "Interaction of mechanical and chemical treatments on pulp strength during kraft pulp bleaching," *Appita J.* 51(2), 107-113.
- Argyropoulos, D. S., Suchy, M., and Akim, L. (2004). "Nitrogen-centered activator of peroxide-reinforced oxygen delignification," *Ind. Eng. Chem. Res.* 43(5), 1200-1205.
- Argyropoulos, D. S., and Liu, Y. (2000). "The role and fate of lignin's condensed structures during oxygen delignification," *J. Pulp Paper Sci.* 26(3), 107-113.
- Axelsson, P., Gellerstedt, G., and Lindström, M. E. (2004). "Condensation reactions of lignin during birch kraft pulping as studied by thioacidolysis," *J. Pulp Paper Sci.* 30(12), 317-322.
- Barzyk, D., Page, D.H., and Ragauskas, A. (1997). "Acidic group topochemistry and fibre-to-fibre specific bond strength," *J. Pulp Paper Sci.* 23(2), J59-J61.
- Beghello, L., Long, L.-Y., and Eklund, D. (1997). "Laboratory study on carboxymethyl cellulose as a wet-end additive in paperboard making," *Paperi Puu* 79(1), 55-57.
- Blomstedt, M., and Vuorinen, T. (2006). "Fractionation of CMC-modified hardwood pulp," *Appita J.* 59(1), 44-49.
- Chaplin, M. F. (1986). *Carbohydrate Analysis: A Practical Approach*, M. F. Chaplin, and J. F. Kennedy, eds., IRL Press Limited, Oxford, pp. 1-36.
- Chen, S.-L., and Lucia, L. A. (2003). "Fundamental insight into the mechanism of oxygen delignification of kraft pulps: The influence of a novel carbohydrate protective system," *Cellulose Chem. Technol.* 36(3-4), 339-351.
- Chirat, C., and Lachenal, D. (1998) *1998 Tappi Pulping Conference*, Tappi Press, Atlanta, GA, pp. 619-624.
- Davison, R.W. (1980). In *Dry Strength Additives*, W.F. Reynolds (ed.), Tappi Press, Atlanta, pp. 1-31.
- Ekevåg, P., Lindström, T., Gellerstedt, G., and Lindström, M.E. (2004). "Addition of carboxymethylcellulose to the kraft cook," *Nordic Pulp Paper Res. J.* 19(2), 200-207.
- Eriksson, M., Torgnysdotter, A., and Wågberg, L. (2006). "Surface modification of wood fibers by using the polyelectrolyte multilayer technique: Effects on fiber joint and paper strength properties," *Ind. Eng. Chem. Res.* 45(15), 5279-5286.
- Fu, S., and Lucia, L. (2003). "Investigation of the chemical basis for inefficient lignin removal in softwood kraft pulp during oxygen delignification," *Ind. Eng. Chem. Res.* 42(19), 4269-4276.
- Gaspar, A. R., Evtuguin, D. V., and Pascoal Neto, C. (2004). "Polyoxometalate-catalyzed oxygen delignification of kraft pulp: a pilot plant experience," *Ind. Eng. Chem. Res.* 43(24), 7754-7761.
- Gavrilescu, D. (2005). "On the importance of radical formation in pulp bleaching," *Cellulose Chem. Technol.* 39(5-6), 531-549.

- Gellerstedt, G., and Heuts, L. (1997). "Changes in the lignin structure during a totally chlorine free bleaching sequence," *J. Pulp Paper Sci.* 23(7), J335-J340.
- Gierer, J. (1997). "Formation and involvement of superoxide and hydroxyl radicals in TCF bleaching processes: a review," *Holzforschung* 51(1), 34-46.
- Guay, D. F., Cole, B. J. W., Fort, R.C. Jr., Hausman, M. C., Genco, J. M., and Elder, T. J. (2002). "Mechanisms of oxidative degradation of carbohydrates during oxygen delignification. Part III: Reaction of photochemically generated hydroxyl radicals with 1,5-anhydrocellobitol and cellulose," *J. Pulp Paper Sci.* 28(7), 217-221.
- Gurnagul, N., Page, D. H., and Paice, M. G. (1992). "The effect of cellulose degradation on the strength of wood pulp fibres," *Nordic Pulp Paper Res. J.* 7(3), 152-154.
- Hubbe, M. A. (2006). "Bonding between cellulosic fibers in the absence and presence of dry-strength agents – a review," *BioResources* (<http://www.bioresourcesjournal.com/>) 1(2), 281-318.
- Hunt, K., and Hatton, J.V. (1987). "The effect of oxygen-delignification on the mechanical properties of white birch kraft pulps," *J. Pulp Paper Sci.* 13(2), J73-J74.
- Kontturi, E., Henricson, K., Vehmaa, J., and Vuorinen, T. (2005). "Quantification method for hydrogen peroxide formation during oxygen delignification of kraft pulp," *Nordic Pulp Paper Res. J.* 20(4), 490-495.
- Kontturi, E., and Vuorinen, T. (2006). "Fibre surface and strength of a fibre network," *Holzforschung* 60(6), 691-693.
- Laine, J., Lindström, T., Glad Nordmark, G., and Risinger, G. (2002). "Studies on topochemical modification of cellulosic fibres. Part 2. The effect of carboxymethyl cellulose attachment on fibre swelling and paper strength," *Nordic Pulp Paper Res. J.* 17(1), 50-56.
- Laine, J., Lindström, T., Bremberg, C., and Glad Nordmark, G. (2003a). "Studies on topochemical modification of cellulosic fibres. Part 4. Toposelectivity of carboxymethylation and its effects on the swelling of fibres," *Nordic Pulp Paper Res. J.* 18(3), 316-324.
- Laine, J., Lindström, T., Bremberg, C., and Glad Nordmark, G. (2003). "Studies on topochemical modification of cellulosic fibres. Part 5. Comparison of the effects of surface and bulk chemical modification and beating of pulp on paper properties," *Nordic Pulp Paper Res. J.* 18(3), 325-332.
- Lidén, J., and Öhman, L.O. (1997). "Redox stabilization of iron and manganese in the +II oxidation state by magnesium precipitates and some anionic polymers. Implications for the use of oxygen-based bleaching chemicals," *J. Pulp Paper Sci.* 23(5), J193-J199.
- MacLeod, J. M., Cyr, M., Embley, D., and Savage, P. (1987). "Where strength is lost in kraft pulping of softwood," *J. Pulp Paper Sci.* 13(3), J87-J92.
- MacLeod, J. M., McPhee, F. J., Kingsland, K. A., Tristram, R. W., O'Hagan, T. J., Kowalska, R. E., and Thomas, B. C. (1995). "Pulp strength delivery along complete kraft mill fiber lines," *Tappi J.* 78(8), 153-160.
- McDonough, T. J. (1996). *Pulp Bleaching – Principles and Practice*; C. W. Dence, and D. W. Reeve (eds.); Tappi Press, Atlanta, GA, pp. 213-239.
- Mitikka-Eklund, M., Halttunen, M., Melander, M., Ruuttunen, K., and Vuorinen, T.

- (1999). *10th International Symposium on Wood and Pulping Chemistry*, Yokohama, Japan, Vol. 1, pp. 432-439.
- Moe, S. T., and Ragauskas, A. J. (1999) "Oxygen delignification of high-yield kraft pulp," *Holzforschung* 53(4), 416-422.
- Molin, U.-B., Dahlbom, J., and Hornatowska, J. (1996). "Fiber deformation and sheet strength," *Tappi J.* 79(6), 105-111.
- Page, D. H. (1994). "A note on the mechanism of tearing strength," *Tappi J.* 77(3), 201-203.
- Pelton, R. (2004). "On the design of polymers for increased paper dry strength – a review," *Appita J.* 57(3), 181-190.
- Rööst, C., Lawoko, M., and Gellerstedt, G. (2003). "Structural changes in residual kraft pulp lignins. Effects of kappa number and degree of oxygen delignification," *Nordic Pulp Paper Res. J.* 18(4), 395-399.
- Ruuttunen, K., and Vuorinen, T. (2005). "Developing catalytic oxygen delignification for kraft pulp: Kinetic study of lignin oxidation with polyoxometalate anions," *Ind. Eng. Chem. Res.* 44(12), 4284-4291.
- Rydholm, S. A. (1965). *Pulping Processes*, Interscience Publishers, New York, p. 1160.
- Shao, Z., and Li, K. (2006). "The effect of fiber surface lignin on interfiber bonding," *J. Wood Chem. Technol.* 26(3), 231-244.
- Shin, S.-J., Schroeder, L.R., and Lai, Y.-Z. (2006). "Understanding factors contributing to low oxygen delignification of hardwood kraft pulps," *J. Wood Chem. Technol.* 26(1), 5-20.
- Suchy, M., and Argyropoulos, D.S. (2002). "Catalysis and activation of oxygen and peroxide delignification of chemical pulps: A review," *Tappi J.* 1(2), 1-18 and the references therein.
- Tran, A.V. (2002). "Effect of pH on oxygen delignification of hardwood kraft pulp," *Paperi Puu* 83(5), 405-410.
- Van den Akker, J. A., Lathrop, A. L., Voelker, M. H., and Dearth, L. R. (1958). "Importance of fiber strength to sheet strength," *Tappi* 41(8), 416-425.
- Van Heiningen, A., and Violette, S. (2003). "Selectivity improvement during oxygen delignification by adsorption of a sugar-based polymer," *J. Pulp Paper Sci.* 29(2), 48-53.
- Wågberg, L., Forsberg, S., Johansson, A., and Juntti, P. (2002). "Engineering of fibre surface properties by application of the polyelectrolyte multilayer concept. Part I. Modification of paper strength," *J. Pulp Paper Sci.* 28(7), 222-228.
- Watanabe, M., Gondo, T., Kitao, O. (2004) "Advanced wet-end system with carboxymethylcellulose" *Tappi J.* 3(5), 15-19.
- Yang, R., Lucia, L., Ragauskas, A.J., and Jameel, H. (2003). "Oxygen delignification chemistry and its impact on pulp fibres," *J. Wood. Chem. Technol.* 23(1), 13-29.
- Zhang, D., Chai, X.-S., Hou, Q., and Ragauskas, A. (2005). "Characterization of fiber carboxylic acid development during one-stage oxygen delignification," *Ind. Eng. Chem. Res.* 44(24), 9279-9285.

Article submitted: May 25, 2007; Peer-review completed: Nov. 5, 2007; Revised version accepted: Nov. 16, 2007; Published: Dec. 2, 2007

SYNTHESIS AND CHARACTERIZATION OF GRAFTED CELLULOSE FOR USE IN WATER AND METAL IONS SORPTION

Abd-Alla M. A. Nada,^{a*} Mohamed Y. Alkady,^b and Hesham M. Fekry^c

Graft copolymerization of acrylamide monomer onto cellulose, using ceric ammonium nitrate as initiator, was investigated. Water and metal ions sorption by this grafted cellulose were estimated. The conditions of grafting, e.g. grafting time, dose of initiator, ratio of monomer to cellulose, acid concentration and liquor ratio, were evaluated. The different properties as graft and graft efficiency percentage, as well as polymerization percent, have been determined. Grafted cellulose has been characterized by FTIR and swelling studies. Sorption of different metal ions in the mixture, e.g. Cu, Cr, Ni, and Pb, by grafted cellulose was investigated. The effect of hydrolysis of grafted cellulose by using sodium hydroxide on its swelling properties and metal ions sorption was also investigated. Hydrolysis increases the sorption affinity of grafted cellulose toward water and metal ions.

Keywords: Grafting, Hydrolysis, Selectivity, Swelling, Metal ions uptake, FTIR

Contact information: a. Head of Cellulose & Paper Dept, NRC, Dokki, Cairo, Egypt, b. Faculty of Science, Ain Shams University, Cairo, Egypt, c. El-Nasr Co. for Intermediate Chemicals, Cairo, Egypt

*Corresponding author : amnada46@yahoo.com

INTRODUCTION

Cellulose is a non-branched polymer of (1→4) β-O-glucopyranose linkage between glucose units. The degree of polymerization of cellulose is affected by the type of treatments. Cellulose is renewable, and due to its abundance in nature it affords material for cost-effective technologies of ion exchange (Nada et al. 2006; Sokker et al. 2006) and hydrogel (Chauhan et al. 2005; Kawabara et al. 1996). Cellulose and its derivatives have been used in metal ion absorption (Murguttim et al. 2000; Nada et al. 2003). Grafting of monomer with hydrophobic and hydrophilic ionic moieties combines a high degree of permeability (Chauhan et al. 2003). Grafted cellulose products, when used as ion exchangers, have advantages over conventional ion exchangers due to chemical resistance, low cost of preparation, and they also offer considerable hydrophilic surface area. Acrylamide and acrylic acid monomers have been successively grafted onto a cellulose backbone (Gitisudhe et al. 2005; Nada et al. 1998). Grafting is a simple technique to incorporate desired active functional groups on the backbone of a polymer for absorption metal ions. Grafting copolymerization of monomers onto cellulose and other natural polymers, e.g. starch and chitosan, supports the metal ions absorption and enzyme immobilization (Chauhan and Lai 2003). Some of the copolymer prepared from cellulose grafting with acrylamide are used for metal ions sorption. Hydrolysis of this grafted cellulose increases its partition coefficient and retention capacity as hydrogel (Chauhan et al. 2003; Chauhan et al. 2005). Cellulose can be derivatized to possess a

number of different functional groups, such as carboxymethyl and amines, to which ions can bind either by chemical or physical adsorption (Nada and El-Wakeel 2006). Grafting copolymerization onto cellulose induces physical changes, since the introduction of side chains leads to different structural characteristics in raw material. Grafting of cellulose shows new properties, such as hydrophobic or hydrophilic character and resistance to chemical and biological agents (Flaquie et al. 2000). Grafting yield can be increased by improving the fiber accessibility to monomer by swelling the substrate before polymerization (Kundu et al. 1998).

The aim of this work is to optimize the graft copolymerization of acrylamide onto cellulose. The effect of hydrolysis of this grafted cellulose on metal ions sorption and swelling percent is investigated. The use of FTIR spectroscopy to follow the molecular structure of the grafted and hydrolyzed grafted cellulose is also investigated.

EXPERIMENTAL

Material

The raw material used in this study was wood pulp (remaining as a waste after manufacture of mesquite mats) at EL Nasr Co. for Intermediate Chemicals, Cairo, Egypt. This material has the following analysis: α -cellulose 86.4, hemicellulose 5.2, and ash content 1 %. The remaining percentage consists of short-chain carbohydrates that are dissolved in water and alkali solution, acrylamide monomer, ceric ammonium nitrate, nitric acid, sodium hydroxide, and a mixture of metal ion solution containing a 20 microgram of each metal (Ni, Cu, Cr, and Pb).

Methods

Graft copolymerization

Grafting was carried out by steeping 5 g of cellulose (w) in acrylamide solution for 5 minutes and then added the dissolved ceric ammonium nitrate in nitric acid at 20°C for 2 hours (total liquor ratio was 25:1, i.e. total quantity of grafting liquor was 125 ml). After grafting, the sample was filtered, washed with distilled water, and then air-dried (w_1). This dried sample was extracted with distilled water in a soxhlet device for 48 hours to dissolve the formed homopolymer. After extraction, the sample was washed with distilled water and then air-dried (w_2). The different variables of the grafted copolymerization of acrylamide onto cellulose were studied e.g. liquor ratio (15:1 – 50:1), nitric acid concentration (0.5 – 0.3 %), initiator concentration (0.075 – 0.225 % based on cellulose), ratio of monomer to cellulose (1:1-4:1), temperature (15–50 °C), and grafting time (0.5-4 hours).

$$\begin{aligned} \text{Polymerization \%} &= [(w_1 - w)/w] \times 100 \\ \text{Graft \%} &= [(w_2 - w)/w] \times 100 \\ \text{Graft efficiency \%} &= [(w_2 - w)/\text{weight of monomer}] \times 100 \end{aligned} \quad (1)$$

Hydrolysis

The grafted cellulose was refluxed with 1.5 % NaOH solution for 2 hours using

a 25:1 liquor ratio. After hydrolysis the sample washed with distilled water till neutralization

Infrared spectroscopy

The infrared spectroscopy was carried out using a KBr disc technique by JASCO FTIR 3006 (Fourier Transform Spectrophotometer). The concentration of each sample was 1 %, the resolution of FTIR instrument was ± 3 , and the baseline was made automatically by the instrument.

Swelling studies

A known weight of grafted cellulose (0.5 g) was swollen by immersion in 50 ml of distilled water at room temperature for 24 hours. The swollen hydrogel was removed, wiped off with tissue paper to remove any superficial water until any water was taken up by new filter paper from the swollen hydrogel, and weighed (w_3).

$$\% \text{ swelling} = [(w_3 - w)/w] \times 100 \quad (2)$$

In another trial different volumes of water (10 -50 ml) were added to constant weight of grafted cellulose, and the swelling percentage was calculated.

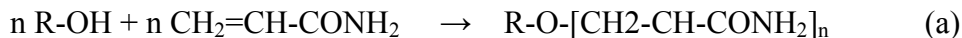
Metal ions sorption

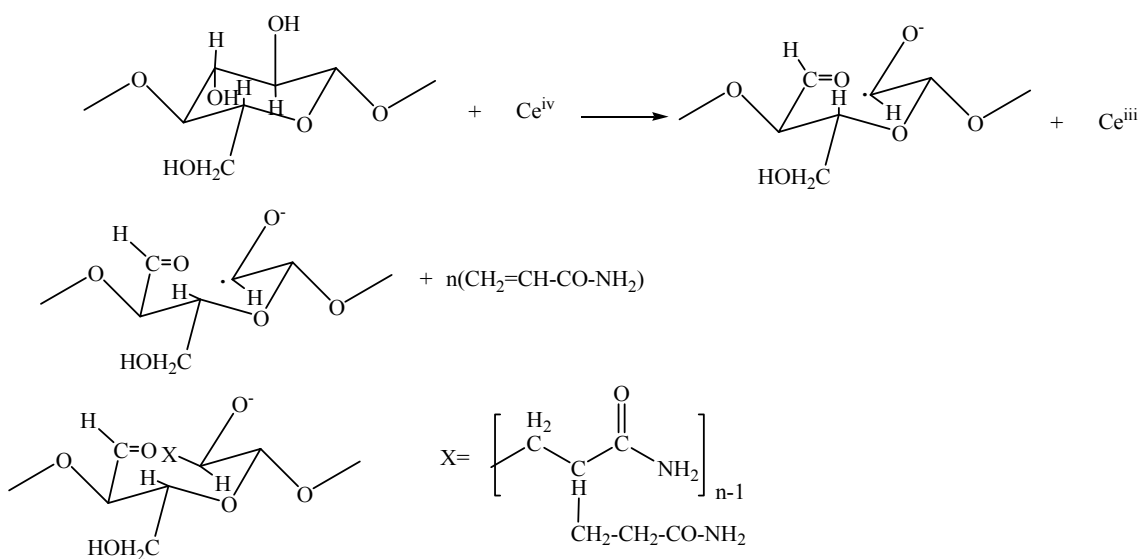
Adsorption of metals was determined by using Inductively Coupled Plasma Atomic Emission Spectrometry (ICP-AES). Sorption was carried out by stirring 0.1 g of grafted or hydrolyzed grafted cellulose for 30 minutes in 25 ml solution containing $20 \mu\text{g ml}^{-1}$ ions of (Ni, Cu, Cr and Pb). After filtraton, the remaining metal ions in the filtrate were determined using the ICP spectrometer.

RESULTS AND DISCUSSION

Infrared Spectra

Infrared spectra of cellulose, grafted cellulose and hydrolyzed grafted cellulose are shown in Fig. 1. Relative absorbance (ratio of any band intensity / band intensity at 1325 cm^{-1} , which corresponds to CH rocking for cellulose ring) (Yu Levdek et al. 1967) of the OH band at 3420 cm^{-1} was decreased by grafting due to the reaction of acrylamide monomer with the OH of cellulose.





By hydrolysis, the relative absorbance of this band (OH) increased due to the formation of carboxylic groups.

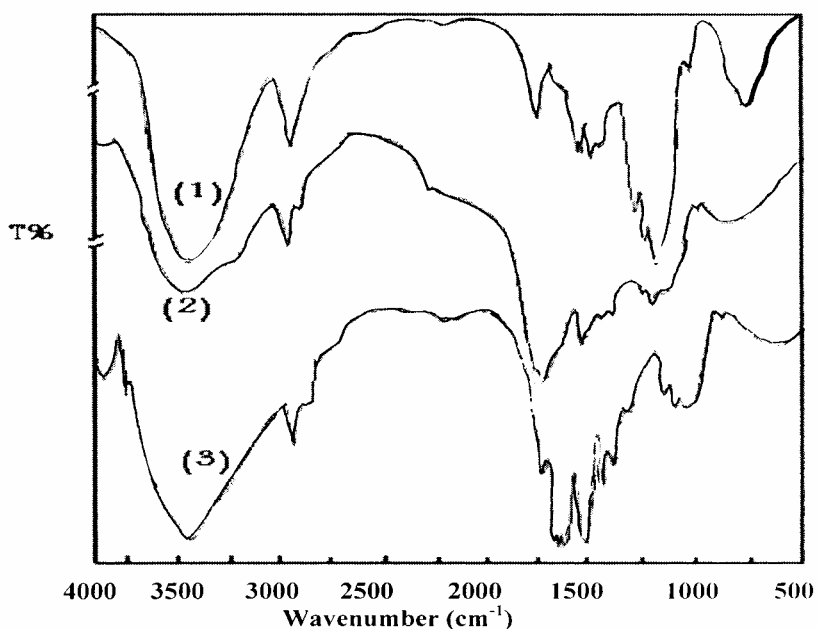
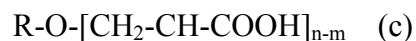
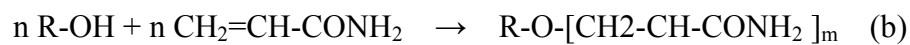


Fig. 1 Infrared spectra of (1) ungrafted, (2) grafted and (3) hydrolyzed grafted wood pulp.

Grafting increased the relative absorbance of CH vibration of CH₂ at 2930 cm⁻¹, as mentioned from the previous equation (a). The ratio of this band intensity to band intensity of the OH group at 3420 cm⁻¹ had a higher value in grafted than that in case of ungrafted wood pulp (Table 1). The relative absorbance of the band at 1650 cm⁻¹, which is characteristic to C=O of the amide group, increased by grafting, and it decreased by hydrolysis due to the change of some CONH₂ groups to carboxylic groups, which appeared at 1715 cm⁻¹. The ratio of the band intensity at wavenumber 1650 cm⁻¹ to the band intensity at 1115 cm⁻¹ (ether linkage between glucose units in cellulose chains) increased by grafting due to the increase of incorporated CONH₂ group onto cellulose. On the other hand, the relative absorbance of C-O-C band at 1115 cm⁻¹ decreased by grafting and hydrolysis. This means that some degradation of cellulose occurred during grafting and hydrolysis. The crystallinity index (ratio of band intensity at 1425 cm⁻¹ / band intensity at 900 cm⁻¹) (Nelson et al 1964) of cellulose was decreased by grafting due to the incorporation of amide groups. By hydrolysis, this crystallinity index was decreased due to the swelling of crystalline regions

Table 1. The Relative Absorbance of Some Bands in Wood Pulp, Grafted and Hydrolyzed Grafted Wood Pulp

Wavenumber cm ⁻¹	Group	Relative absorbance		
		w.p.	Grafted w.p	Hydrolyzed-grafted w. p.
3419	OH	1.92	0.95	1.45
2920	CH ₂	1.02	1.27	1.20
2820	CH ₂	-----	0.72	0.091
1650	CONH ₂	0.82	2.38	1.39
1715	COOH	---	-----	1.48
1114	C-O-C	1.74	0.99	0.90
Ratio 1654 / 1120	CONH ₂ /C-O-C	0.38	1.38	1.19
Ratio 2920 / 3419	CH ₂ /OH	0.54	0.72	0.69
1425 / 900	Cr.l.	2.43	2.1	1.96

Effect of Different Variables on Grafting Process

Nitric acid concentration

Figure 2 shows the effect of nitric acid concentration on the grafting parameters (polymerization, graft and graft efficiency %). These parameters were increased by increasing acid concentration from 0.5 to 1 % (Fig. 2). Increasing the acid concentration more than 1 % decreased these parameters.

The explanation of such behavior is that nitric acid in the grafting medium assists the grafting by causing inter- and intra-crystalline swelling of cellulose and also acting as a catalyst in hydrolysis of cellulose, leading to an improvement in monomer accessibility. Also 1% acid concentration is sufficient to establish a balance between the suppression of the rate of the active species formation and the rate of primary radicals. On the other hand, the experiment showed that the homopolymer formation was also enhanced in the

presence of acid. A higher concentration of acid, however may cause a degradation of backbone chains of cellulose as well as graft chains. Moreover, high acid concentration causes an oxidation of the formed free radicals, which decrease the rate of initiation with an increase of the homopolymer.

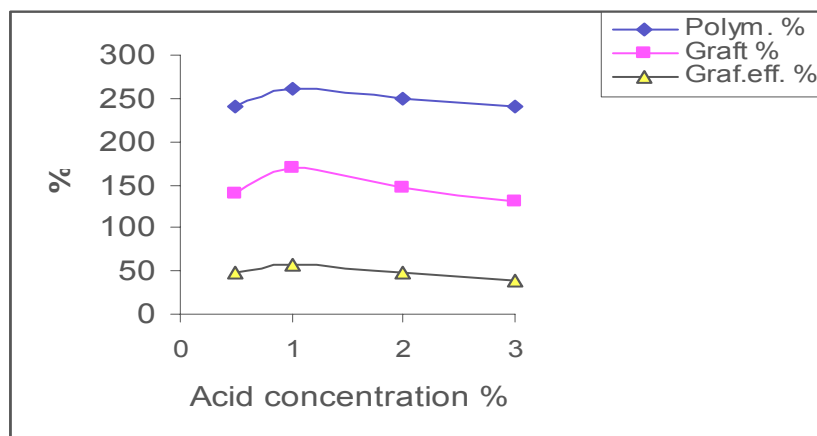


Fig. 2. Effect of acid concentration on the grafting parameters
L.R. 25:1, initiator conc. 0.15%, monomer to cellulose 3:1, Temp. 20°C for 2 hrs.

Ratio of monomer to cellulose

Figure 3 shows the effect of ratio of acrylamide to wood pulp on the different parameters of grafting. It is clear from the figure that the increase of ratio of monomer to cellulose increased the graft and graft efficiency %.

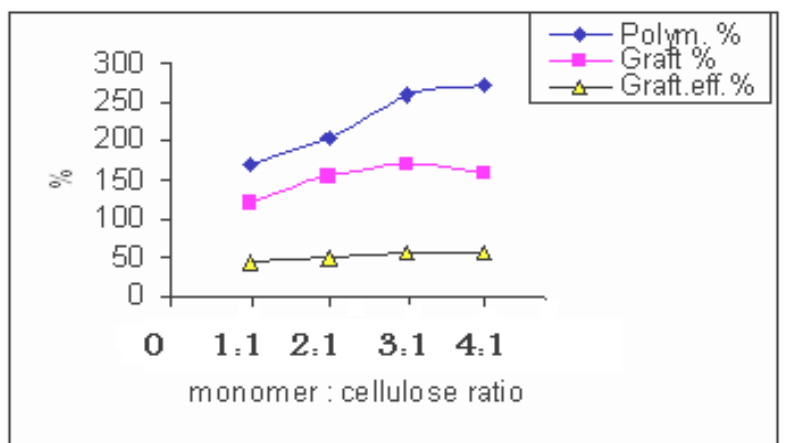


Fig. 3. Effect of monomer to cellulose ratio on the grafting parameters
L.R. 25:1, initiator conc. 0.15%, acid conc. 1 %, Temp. 20°C for 2 hrs

Enhancement in graft % can be attributed to the immobility of cellulose macroradicals. Hence, the availability of acrylamide molecule in the proximity of these radicals is a prerequisite for graft initiation and propagation. The enhancement can be due

to the formation of long graft chains. Increasing the ratio of monomer to cellulose more than 3:1 causes a slightly increase in graft % with increase the homopolymer formation due to the increase in the viscosity of grafting solution, which decreases the penetration rate of monomer solution through the cellulose chains, causing an increase of homopolymer formation.

Effect of initiator

The effect of initiator concentration on the grafting process is shown in Fig. 4. It can be observed that the graft and graft efficiency percentage were increased with increasing initiator concentration up to 0.15 %. This increase resulted due to the formation of a great number of grafting sites on the cellulose backbone, which, in presence of monomer, induced grafting. By increasing the initiator concentration more than 0.15 %, the graft and graft efficiency were slightly decreased, but the polymerization percentage was slightly increased. The increase of initiator more than 0.15 % caused a retardation of monomer diffusion through cellulose chains, accelerating the rate of termination. On the other hand, the increase in the initiator leads to initiation of many chains, which enhances the chance of mutual initiation of growing polymeric chains. These factors increase the formation of homopolymer and cause a fall in graft yield (Sikdar et al. 2003)

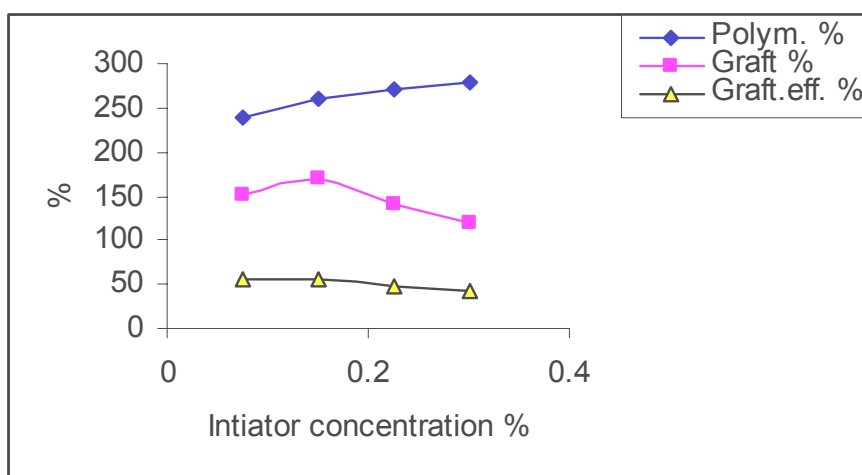


Fig. 4. Effect of initiator concentration on grafting parameters
L.R. 25:1, monomer to cellulose ratio 3 : 1, acid conc. 1 %, Temp. 20°C
for 2 hrs.

Effect of liquor ratio

It was found that an increase of liquor ratio up to 25:1 caused an increase in graft and polymerization percentage (Fig. 5). This can be explained by the increase of dispersion of cellulose in the grafting liquor, causing an increase in the contact between cellulose and monomer.

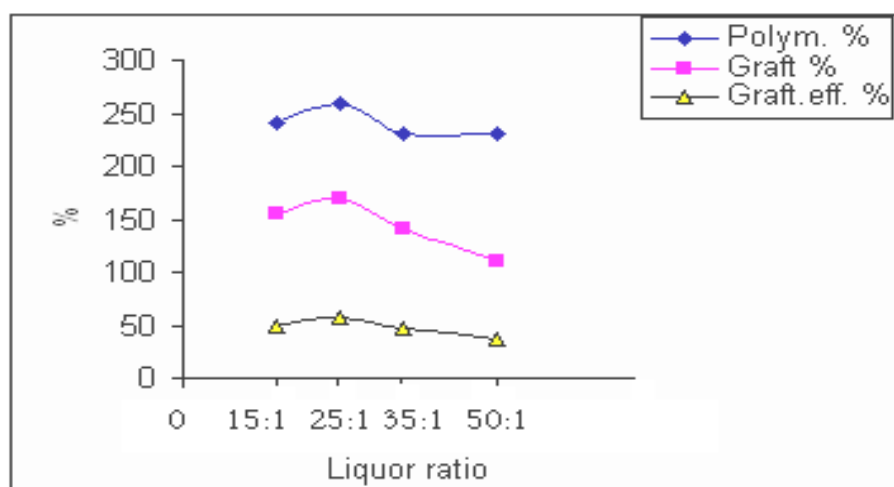


Fig. 5. Effect of liquor ratio on grafting parameters; Initiator concentration 0.15 %, monomer to cellulose ratio 3 : 1, acid conc. 1 %, temp. 20°C for 2 hrs.

Increasing the liquor ratio more than 25:1 decreased the graft and graft efficiency percentage, while a slight increase in the polymerization percentage was obtained. This can be due to the dilution of monomer and chemicals, which decreases from the contact between chemicals and cellulose.

Reaction time

Figure 6 shows the effect of reaction time on different grafting parameters. It can be seen from the figure that the increase of reaction time from 0.5 to 2 hours increased the grafting, graft efficiency, and polymerization percentage. Increasing the reaction time more than 2 hours caused the reaction rate to level off. This leveling off can be ascribed to the depletion in monomer and initiator, as well as the shortage of available grafting sites as the reaction proceeds. So, the graft and graft efficiency percentage increased with increasing reaction time to 2 hours. This increase in graft after particular time is considered to be a detrimental effect.

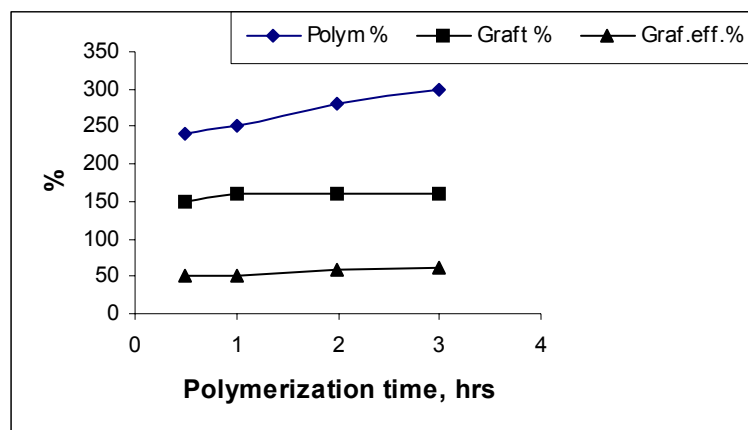


Fig. 6 Effect of time on the grafting parameters; Initiator concentration 0.15 %, monomer to cellulose ratio 3 : 1, Acid conc. 1 % Liquor ratio 25 : 1 Temp. 20°C

Reaction temperature

Graft copolymerization of acrylamide onto cellulose increased by increasing the reaction temperature from 15 to 20 °C, as shown in Fig. 7.

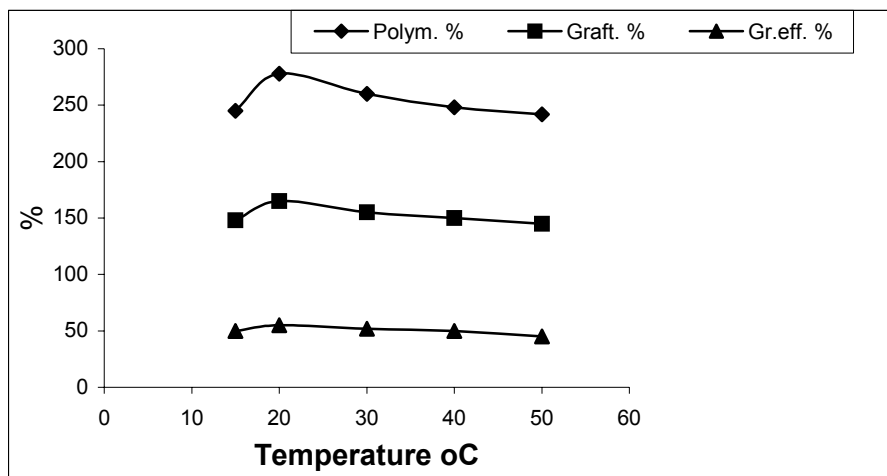


Fig. 7. Effect of reaction temperature on grafting parameters; Initiator concentration 0.15 %, monomer to cellulose ratio 3 : 1, acid conc. 1 % ,Liquor ratio 25 : 1 reaction time 2 hours

This effect is attributed to the increase of the rate of diffusion of monomers through cellulose chains, swelling of cellulose, as well as an increase of the rate of initiation and propagation of the grafting process (Nada and Youssef 1997). Increasing temperature more than 20 °C enhances the oxidation of free radicals, and mutual termination of growing macroradicals favors more homopolymer formation over the grafting reaction.

Treatment of Pulp

Before the grafting process, the wood pulp was treated with acid (sulphuric acid) at 1.5 % for 2 hours or with alkali soda at 3 % for 1 hour under reflux. Figure 8 shows the different grafting parameters of untreated, acid-, and alkali-treated wood pulp. The grafting of treated pulp with acid had higher grafting parameters than alkali- and untreated wood pulp. This can be attributed to the fact that acid treatment causes a decrease in the degree of polymerization (DP 580), and consequently the end groups of cellulose chains, causing an enhancement in the reactivity of the wood pulp toward grafting. On the other hand, the grafting of alkali-treated wood pulp (DP 910) was higher than that in case of untreated wood pulp (DP 890). This was due to the increase in the penetration rate of grafting chemicals through the cellulose chains because of the decrease in the crystalline parts of the alkali-treated wood pulp. The DP (degree of polymerization) of treated pulp with alkali is higher than untreated pulp due to the dissolving of small chains of cellulose during alkali treatment.

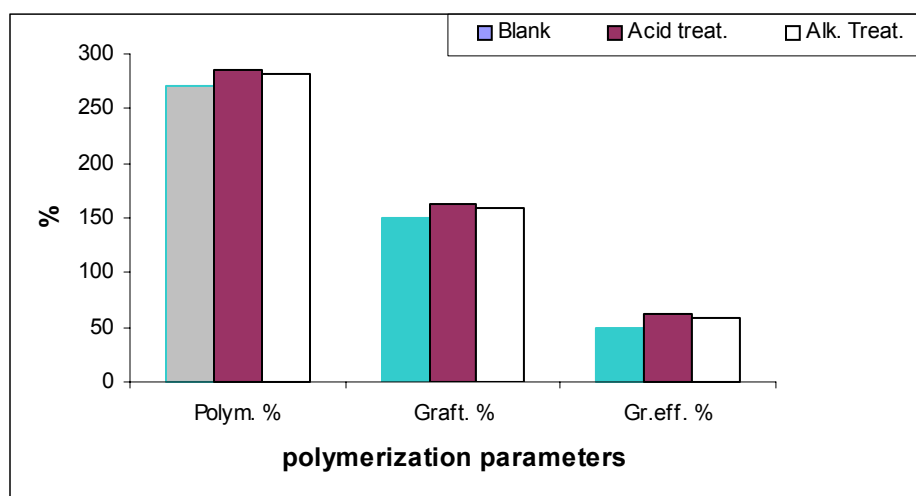


Fig. 8. Effect of different treatment of wood pulp on the Grafting parameters

Water Absorption

Table 2. Water Absorption (g/g) and Swelling (%) of Grafted and Hydrolyzed Grafted Wood Pulp

Samples	Graft %	Water uptake g/g		Swelling %	
		Graft.	Hydroly.	Graft.	Hydroly.
Ungrafted w. P.	0	1	1.8	61	104
Grafted untreated pulp	170	12.7	80.2	1080	7920
Grafted Acid. Treat. W.P.	190	11	54	1100	5000
Grafted alkal.treat.W.P.	180	11.8	85.2	1200	8600

Condition of grafting : L. R. 25 : 1, acid concentration 1 %, monomer : wood pulp ratio 3:1, initiator concentration 0.15 % (based on wood pulp), reaction temperature 20°C for 2 hours

The swelling percentage and water uptake were measured by steeping 0.5 g of sample in distilled water for 24 hours. The surface water on swollen samples (grafted and hydrolyzed grafted wood pulp) was removed by safely pressing between the folds of filter paper. Table 2 illustrates the swelling percentage and water uptake g/g. From the table it is clear that the grafted and hydrolyzed grafted acid-treated wood pulp had lower values of water uptake and swelling percentage than corresponding tests in case of untreated and alkali-treated wood pulp, although it had a higher graft percentage than the other pulps. This may be due to the higher proportion of crystalline regions of acid treated wood pulp (Table 1). This increase in the crystalline regions in the grafted, acid-treated wood pulp decreased the rate of diffusion of water through the grafted cellulose chains. On the other hand, water uptake and swelling percentage of the grafted wood pulp was higher than that in case of non-grafted wood pulp. This can be explained by the opening up of the matrix of wood pulp due to considerable loss of crystalline regions, which increased the diffusion of water through the grafted cellulose chains. Grafted alkali-treated wood pulp had a higher swelling percentage and water uptake than the grafted untreated pulp. This was due to the decrease in crystalline regions of grafted alkali treated wood pulp, which increased the diffusion of water through grafted cellulose

chains. Moreover, the hydrolyzed, grafted samples had a higher swelling percentage and water uptake than the grafted samples (Table 2). This is explained mainly by the change of some amide groups, which are incorporated in grafted samples to carboxylic groups.

So, the hydrolyzed grafted samples contained two different hydrophilic functional groups (-COOH, -CONH₂), which increased the swelling and water uptake for hydrolyzed samples. To show the effect of volume of water on swelling percentage and water uptake, known weights of hydrolyzed grafted samples (0.25 g) were steeped in different volumes of water for 24 hours (Table 3). It is seen from table that the swelling percentage increased with increasing the volume of added water to the hydrolyzed grafted wood pulp. This was due to the difficulty in dispersing the substrate in low volume of water, which decreased the diffusion rate of water through the substrate. Increasing the volume of added water enhanced the movement of substrate in water, and consequently the diffusion of water through cellulose chains increased.

Table 3. Effect of Volume of Water on the Swelling % and Water Uptake of Hydrolyzed Grafted Untreated, Acid and Alkali Treated Wood Pulp

Samples	Water added	10	20	30	40	50
		Swelling %				
Hydrolyzed grafted untreated w. p.		940	4700	6600	8000	8720
Hydrolyzed grafted acid treated w.p.		896	4400	6000	7630	8400
Hydrolyzed grafted alkali treated w.p.		903	4500	6050	7900	8500

Metal ions uptake

In this part, 0.1 g of the grafted or hydrolyzed grafted wood pulp was steeped with stirring in 25 ml of solution containing 20 µg ml⁻¹ of different metal ions (Cu, Cr, Ni, and Pb) for one hour. After steeping, the sample in solution was filtered, and the remaining metal ions in the filtrate were determined. Table 4 shows the metal ions uptake and retention capacity by grafted pulp.

Table 4. Metal ions Uptake and Retention Capacity of Grafted and Hydrolyzed Graftd Wood Pulp

Samples	Metal ions uptake %				Retention capacity			
	Cr	Pb	Mn	Ni	Cr	Pb	Mn	Ni
Grafted wood pulp	94.5	90	92.5	82	189	180	185	165
Hydrolyzed grafted wood pulp	97	92	95	90	194	185	190	180
Ungrafted wood pulp	8	4	3	1.5	16	8	6	3

$$\text{Metal ions uptake \%} = \frac{\text{amount of metal in polymer}}{\text{amount of the metal in the feed}} \times 100$$

$$\text{Retention capacity} = \frac{\text{amount of metal ions in polymer}}{\text{weight dry of polymer}}$$

Structural aspects of the polymeric backbone are important factors affecting metal ions sorption. The prepared grafted cellulose copolymers remove metal ions both by adsorption on N of amide groups and also by sorption in the bulk of grafted copolymer hydrogel. Therefore, the structure of a polymeric hydrogel affects the level of polymer interaction with water and the provision of active sites to absorb or coordinate metal ions. Hence, the sorption behavior and the quantity of metal ions taken up depend, in addition to the attributes of metal ions, also on different structural aspects of the polymer. It is clear from Table 3 that the metal ions uptake percentage and retention capacity of Cr were higher than for Mn, Cu, and Ni. This can be attributed to the fact that the Cr ion has a lower atomic radius than other metal ions and consequently its adsorption by polymer is high. In general, the amount of metal ions uptake by ion exchanger is affected by the electronegativity and hydrated values of metal ions. The sequence of metal ions sorption was as follows: Cr > Mn > Pb > Ni. Hydrolysis of the hydrogel affected the metal ions uptake percentage and retention capacity by activation of functional groups of grafting chains by opening up the hydrogel network and activating amide groups into more active groups, such as carboxyl groups, which have a stronger tendency to chelate and exchange ions (Couhan et al 2005). Partial hydrolysis of amide groups increased water uptake of hydrogel and increased the tendency of functionalized hydrogel, leading to enhanced metal ions sorption. So from Table 4 it is seen that the metal ions uptake percentage and retention capacity of hydrolyzed, grafted wood pulp was higher than for grafted wood pulp.

CONCLUSIONS

1. The optimum conditions of graft copolymerization of acrylamide onto wood pulp were liquor ratio 25:1, ratio of monomer to wood pulp 3:1, nitric acid concentration 1 %, and initiator concentration 0.15 % (based on wood pulp) at 20 °C for 2 hours.
2. Grafted acid-treated wood pulp had a higher graft and graft efficiency percentage, as well as polymerization percentage than grafted, untreated and alkali-treated wood pulp.
3. Water absorption and swelling percentage of the grafted, alkali-treated wood pulp were higher than corresponding results in case of grafted untreated and acid treated wood pulp.
4. Hydrolysis of grafted alkali treated wood pulp increased its affinity toward water absorption and swelling percentage. Also it improved its affinity toward metal ions, increasing the metal ion uptake and retention capacity.

REFERENCES CITED

Chauhan, G. S., Guleria, L., and Sharma, R. (2005). "Synthesis, characterization and metal sorption studies of graft copolymer of cellulose with glycidyl methacrylate and some comonomer," *Cellulose* 12, 97-110.

- Chauhan, G. S., Guleria, L., and Lai, H. (2003). "Synthesis of graft copolymer of acrylamide and comonomer onto cellulose. A study of the effect of comonomer on polymer yields, structure and properties," *Polymer, Polymer Composites* 11, 1-7.
- Chauhan, G. S., and Lai, H. (2003). "Novel grafted cellulose based hydrogel for water Technologies," *Desilination* 159, 131-138.
- Chauhan, G. S., Singh, B., and Kamar, S. (2005). "Synthesis and characteristics of N-vinyl pyrrolidone and cellulose based functional graft copolymer for use as metal ion and iodine sorbent," *Journal of Applied Polymer Science* 98, 373-383.
- Chauhan, G. S., Singh, B., Chauhan, S., Verma, M., and Mahajan, S. (2005). "Sorption of some metal ions on cellulose based hydrogel." *Desilination* 181, 217-224.
- Flaque, L., Rodrigo, L. C., and Ribes Gnes, A. (2000). "Biodegradation studies of cellulose and its vinyl copolymer by thermal analysis and mechanical spectroscopy," *Journal of Applied Polymer Science* 76, 326-335.
- Gitisudhe, G., Prufulla, K. S., and Samal, R. K. (2005). "Graft copolymerization onto wool fiber: Grafting of acrylamide onto fibers initiated by potassium monopersulfate/F(II) redox polymer," *Journal of Applied Polymer Science* 40, 471-480.
- Kawabara, S., and Kubota, H. (1996). "Water absorbing characteristics of acrylic acid-grafted carboxymethyl cellulose synthesized by photographing," *Journal of Applied Polymer Science* 60, 1965-1970.
- Kundu, S. K., Ray, D. K., Sen, S. K., and Bhadum, S. K. (1998). "Structure and physical properties of grafted jute fiber," *Cellulose Chemistry and Technology* 32, 173-183.
- Murguttim S., Vicini, S., Proiette, N., Capitani, D., Conio, G., Podomonte, E., and Segre, A. (2000). "Physical-chemical characterization of acrylic polymer grafted on cellulose," *Polymer* 43, 6183-6194.
- Nada, A. M. A., El-Wakeel, N., Hassan. M. L., and Abeer, M. A. (2006). "Differential adsorption of heavy metal ions by cotton stalks cation exchangers containing multiple functional groups," *Journal of Applied Polymer Science* 101, 4124-4132.
- Nada, A. M. A., Eid, M. A., Sabry, A., and Khalifa, M. N. (2003). Preparation and some application of phosphosulfonated bagasse and wood pulp cation exchanger," *Journal of Applied Polymer Science* 90, 97-104.
- Nada, A. M. A., Ibrahim, A. A., and Ahmed, M. A. (1989). "Water retention values of grafted cellulose with acrylamide," *Cellulose Chemistry and Technology* 23(5), 124-137.
- Nada, A. M. A., and El-Wakeel, N. (2006). "Molecular structure and ion exchange of amidoximated celulosic materials," *Journal of Applied Polymer Science* 102, 303-311.
- Nada, A. M. A., and Youssef, M. A. (1997). "Grafting of cellulose," in *Handbook of Engineering Polymeric Materials*, J. Stubenrauch (ed.), New York, Ch. 34, 529-539.
- Nelson, M. L., and Connor, R. T. (1964). "Relation of certain infrared bands to cellulose crystallinity and crystal lattice type, p. II A new infrared ratio estimation of crystallinity of cellulose I and II," *Journal Applied Polymer Science* 8, 1325-1332.
- Sokker, H. H., Abdel-Ghafar, A. M., and Nada, A. M. A. (2006). "Synthesis and characterization of radiation grafted copolymer for removal of nonionic organic contaminants," *Journal of Applied Polymer Science* 100, 3589-3595.

- Sikdar, B., Basak, R. K., and Mitra, B. C. (2003). "Studies on graft copolymerization of acrylonitrile onto jute fiber with permanganate ion initiation system in presence of air," *Journal of Applied Polymer Science* 55, 1673-1682.
- Yu Levdek, K. I., Inshakova, M. D., Miyurov, E. P., and Nikitin, N. V (1967). Trvses Nauch Issled Inst. *Tselyl Burn Prom.* 52, 109-115.

Article submitted: July 4, 2007; Peer-review first round completed: Oct. 10, 2007;
Revision received and accepted: Dec. 2, 2007; Published Dec. 4, 20007

CHEMICAL VALORIZATION OF AGRICULTURAL BY-PRODUCTS: ISOLATION AND CHARACTERIZATION OF XYLAN-BASED ANTIOXIDANTS FROM ALMOND SHELL BIOMASS

Anna Ebringerová,* Zdenka Hromádková, Zuzana Košťálová, and Vlasta Sasinková

The isolation of non-cellulosic polysaccharides from almond shells (AS) and their solid residue (ASR) after autohydrolysis was investigated using a two-step alkaline extraction without and in combination with short ultrasonic treatment. The obtained polysaccharide preparations were characterized by yield, chemical composition, and structural features, and the antioxidant activity of the water-soluble preparations tested. The results showed that the use of ultrasound at a reduced extraction time of 10 min as compared to 60 min of the classical procedure, with a 5% NaOH solution, resulted in the greatest yield of hemicelluloses. The AOA of their water-soluble portion ranged between 48 and 80%, indicating the antioxidant potential of these materials. The xylan polymers isolated from both AS and ASR might serve as biopolymer sources in native form or after targeted modification for production of value-added substances and polysaccharide-based antioxidants applicable in food, cosmetics, and other areas.

Keywords: Almond shells, Extraction, Ultrasound, Xylan, Pectic polysaccharides, Phenolics content, Antioxidant activity.

Contact information: Institute of Chemistry, Center for Glycomics, Slovak Academy of Sciences, SK-845 38 Bratislava, Slovakia; * *Corresponding author:* chemebri@savba.sk

INTRODUCTION

Commercial processing of grains and seeds yields low-value by-products such as hulls, husks, polish waste, etc. These agricultural by-products are rich in cellulose and non-cellulosic polysaccharides (hemicelluloses, pectin) as has been recently reviewed (Ebringerová et al. 2005; Popa and Volf 2006) as well as in antioxidants (Moure et al. 2001; Garrote et al., 2004), and may serve as potential raw materials for the production of high-value added substances, such as natural antioxidants, ‘super gel’ for wound dressing, biodegradable commodity plastics, drug carriers, xylo-oligosaccharide prebiotics, polymeric additives in functional foods, etc. In this context almond shells (AS), which may comprise from 35 to 75% of the total fruit weight and are available in large quantities, could be taken in account as a valuable agricultural by-product. Nearly one third of the AS biomass comprises xylan type- hemicelluloses (Nabarlatz et al. 2005), which are biopolymers with a broad application potential in natural form or after targeted modification, but not yet established industrial utilization (Ebringerová and Heinze 2000). AS are also rich in lignin and other phenolic compounds (Pinelo et al. 2004; Moure et al. 2006; Amarowicz et al. 2006), representing natural antioxidants, which exhibit promising biological capacities to protect the human body from free radicals,

retard the progression of many chronic diseases, and retard lipid oxidative rancidity in foods (Dizhbite et al. 2004; Vaya and Aviram 2001). Xylans containing phenolic compounds, such as free or bound phenolic acids and/or lignin, represent a very attractive group of natural antioxidants, because they combine antioxidant activity (AOA) of the phenolics with the physicochemical and functional properties of the polysaccharide moiety (Lu et al. 1998). Recently, feruloyl oligosaccharides prepared from wheat bran were shown to efficiently protect normal rat erythrocytes against free radical-induced hemolysis (Yuan et al 2005). As has been reported by Ohta et al. (1994), phenolic acids linked to carbohydrates exhibit a higher AOA than their free form.

In previous papers, the preparation and structural properties of xylo-oligosaccharides by autohydrolysis of AS (Nabarlatz et al. 2007a) and their immunostimulatory activity have been described (Nabarlatz et al. 2007b). However, the residual fiber biomass (ASR) resulting from the thermal treatment still contains ~ 15% xylan (Nabarlatz et al. 2007a). AS are harder and more rigid than wood, they have greater density and lower porosity, and their lignin content is similar to that of hardwoods (Nabarlatz et al 2007a). All these facts negatively affect the extractability of the xylan component.

The purpose of this paper is to investigate the extractability of the hemicellulose component of both AS and ASR materials using a two-step extraction method without and with application of ultrasonic treatment, the last aimed to increase the efficiency of the extraction process. Chemical and spectral methods are used to characterize the obtained hemicellulose preparations and their antioxidant capacity.

EXPERIMENTAL

Materials and Methods

Starting materials were air-dried almond shells (AS) purchased from MIMSA S.A. (Lleida, Spain) and milled to pass through a 1 mm screen and the fiber residue (ASR) obtained after autohydrolytic treatment of AS (Nabarlatz et al 2007a). The free radical 1,1-diphenyl-2-picryl-hydrazyl (DPPH[•]) was from Sigma-Aldrich (Germany), and gallic acid was from Merck (Germany).

The analytical methods used to characterize both materials (Table 1) are described in detail in the previous paper (Nabarlatz et al 2007a). The neutral sugar composition of the isolated preparations was determined after hydrolysis with 2M TFA by gas chromatography of the alditol trifluoroacetates and the acidic sugars qualitatively by paper chromatography as described by Kardošová et al. (2004). The uronic acid content was determined according to Ahmed and Labavitch (1977) using galacturonic acid as calibration standard, and the total phenolics content (TPC) by the Folin-Ciocalteu assay (Thaipong et al. 2006) using gallic acid as calibration standard. The radical scavenging activity was tested by the DPPH[•] method according to Rao and Muralikrishna (2006) using methanol/water as solvent. The scavenging effect is expressed as the concentration of the sample needed to decrease the initial DPPH[•] concentration by 50% (EC₅₀). Its inverse value was used to express the antioxidant activity (AOA).

FT-IR spectra of the samples (2 mg/200 mg KBr) were recorded on a NICOLET Magna 750 spectrometer with DTGS detector and OMNIC 3.2 software, using 128 scans

at a resolution of 4 cm⁻¹. ¹³C NMR spectra were recorded in D₂O or DMSO-*d*₆ at 25°C on a FT-NMR Advance DPX 300 spectrometer (at 75.46 MHz). Chemical shifts of signals were referenced to internal acetone (31.07 ppm). Ultrasonication was performed with the Ultragen system PERSON (20 kHz, at 200 W) for 10 min as described in more detail in a previous paper (Hromádková and Ebringerová 2003).

Extraction of Hemicelluloses

A two-step extraction procedure, schematically illustrated in Fig. 1, was used with varying conditions in the first step concerning the solvent (5% NaOH or 0.5% NaOH) and extraction time (without or with short application of ultrasonication), and with constant conditions (5% NaOH at room temperature for 1 h) in the second washing step. A more detailed description of the extraction procedure is described in a previous paper (Hromádková et al. 1999). In the experiments with AS the sample-liquid ratio used was 1:40 (g/ml) and in case of ASR it was 1:10 (g/ml). After separation of the extract (A) from the first step by filtration, the solid residue was immediately subjected to the washing step and the obtained extract (B) separated by filtration. The resulting fiber residue was successively washed with distilled water acidified with dilute HCl, distilled water and ethanol, and then air-dried. Its moisture content was determined by drying at 105 °C to constant weight. The hemicelluloses from the individual extracts A and B or the combined extracts (A+B) were precipitated by four volumes of ethanol. After overnight settlement of the precipitate, the pH of the dispersion was adjusted to 7.5 with acetic acid. Then the product was separated by filtration and exhaustively dialyzed against distilled water to reach a constant conductivity value. The insoluble precipitate (wis) eventually formed during dialysis was separated from the soluble (ws) one by centrifugation (10 min at 5000 g) and both fractions were recovered by lyophilisation.

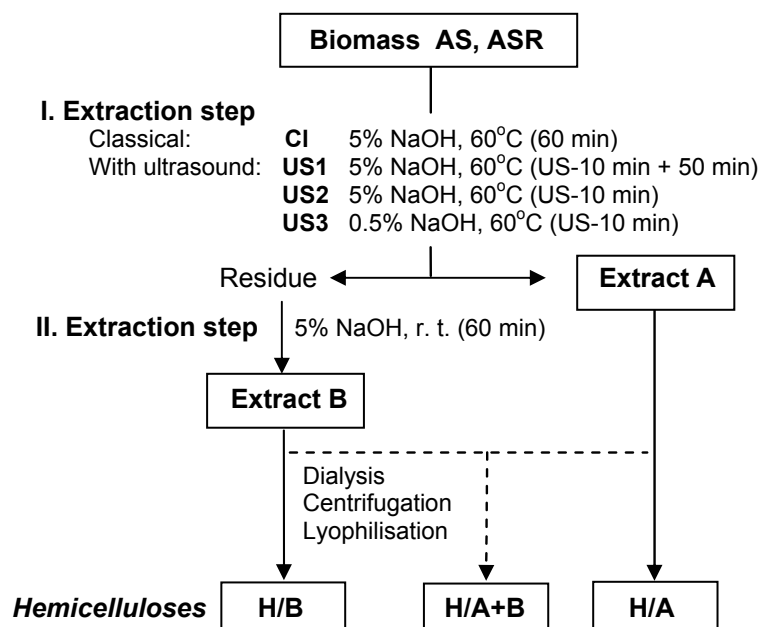


Fig. 1. Extraction scheme of the almond shell biomass (AS) and its fiber residue (ASR) after autohydrolysis.

RESULTS AND DISCUSSION

The analytical data in **Table 1** indicate that xylan and the arabinan component of pectic polymers were the most susceptible to hydrolysis during the hydrothermal treatment of almond shells (Nabarlatz et al. 2007a), which resulted in accumulation of cellulose, lignin and pectin, evidenced by the uronic acid content in the fiber residue (ASR). Chromatographic analysis of the acidic sugars in the hydrolyzates of AS and ASR indicated the presence of both 4-*O*-methylglucuronic and galacturonic acid, the last predominating in that of ASR.

Table 1. Chemical Composition Data of Almond Shell (AS) and its Fiber Residue (ASR) after Autohydrolysis

	Ash (%)	N (%)	Lignin ^a (%)	Xylan ^b (%)	UA ^c (%)	Neutral sugars (Rel. mol%)					
						Rha	Ara	Xyl	Man	Glc	Gal
AS	2.8	0.3	27.4	27.8	4.9	0.6	5.4	50.7	2.1	37.8	3.4
ASR	1.1	0	30.3	14.4	7.1	0	0.9	27.1	2.5	67.1	2.3

^{a)} Klason lignin; ^{b)} Expressed as xylose content (Nabarlatz et al. 2007a); ^{c)} Uronic acid content.

The extractability of the xylan component from AS and ASR was performed using a two-step alkaline extraction procedure (Fig. 1) with and without assistance of ultrasound in the first extraction step, which has been applied also for other lignocellulose materials (Hromádková et al. 1999; Hromádková and Ebringerová 2003).

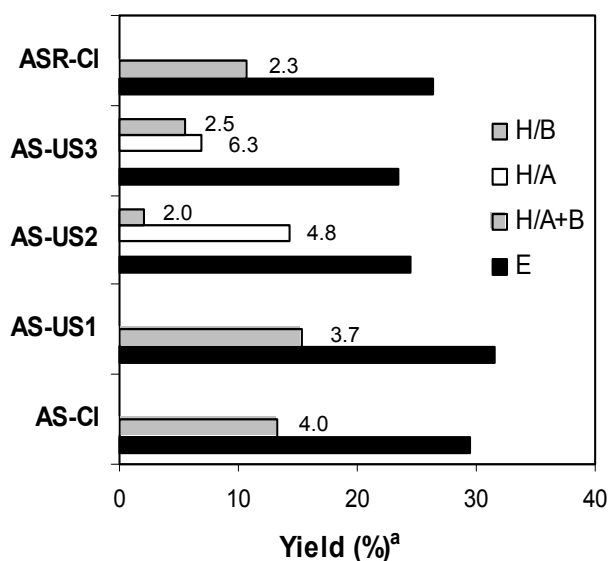


Fig. 2. Yield of the total extracted material (E) and of hemicellulose fractions (H) isolated from the individual extracts (A and B), and the combined extracts (A+B) according to the scheme in Fig. 1.

^{a)} All yields are calculated on the basis of the starting, oven dried materials and are averages from two experiments; The number inserted denotes the yield of the water-soluble portion of the hemicellulose fraction.

As illustrated in Fig. 2, the classical extraction of AS with 5% NaOH yielded 13.2% hemicelluloses, comprising 45% of the extracted material. A short application of

ultrasound (10 min) at the beginning of the first extraction step, lasting 60 min (AS-US1), increased the yield of both the extract and the isolated hemicelluloses due to a higher amount of the wis-fraction. By performing the extraction only with 10 min ultrasonication (AS-US2), the yield of the extracted material decreased in comparison to the former experiment. However, the amount of the hemicelluloses isolated predominately in the first extraction step increased and comprised about 67% of the extract, which is higher than what is obtained in the classical and former ultrasound-assisted extraction.

The sonication effect on the extractability of plant extractives (Mason et al. 1996) and polysaccharides (Hromádková et al. 1999) is known to depend also on the type of the extractant. Therefore, the extraction under sonication was performed in 0.5% NaOH (AS-US3). The yield of the extracted material was similar as in the former experiment, but the yield of the separated hemicelluloses was lower and comprised about 54% of the extract. This can be explained by the fact that in spite of the sonomechanical effect (Mason et al. 1996), the very low NaOH concentration hinders the release of the hemicelluloses from the attacked cell matrix due to their low solubility in this extractant.

Table 2. Chemical Composition Data of Hemicellulosic Fractions Isolated from AS and ASR

Sample	Fraction	TPC ^a (%)	UA ^b (%)	Neutral sugar composition (Rel. mol%)						
				Rha	Fuc	Ara	Xyl	Man	Glc	Gal
AS-CI	A,B/ws	8.9	9.1	-	4.4	23.2	56.6	4.9	6.1	4.8
	A,B/wis		8.6	-	-	6.5	86.7	-	2.1	4.7
AS-US1	A,B/ws	7.5	7.1	1.3	3.6	28.0	52.1	1.2	3.7	10.1
	A,B/wis		12.0	-	-	2.5	89.5	0.6	2.3	5.1
AS-US2	A/ws	10.1	11.1	1.1	1.0	35.5	41.4	5.4	3.5	12.1
	A/wis		8.9	-	-	1.5	97.7	-	0.2	0.6
	B/ws		10.6	8.6	1.1	-	39.5	43.4	2.0	3.7
AS-US3	A/ws	13.3	10.1	1.0	2.6	31.0	47.1	4.0	4.4	9.9
	A/wis		-	0.5	-	40.1	42.0	-	7.2	10.2
	B/ws	8.0	4.1	Tr	-	25.1	68.8	0.5	1.1	4.5
	B/wis		8.0	-	-	Tr	94.7	-	0.2	5.1
ASR-CI	A,B/ws	6.5	-	-	-	27.2	55.3	4.8	6.0	6.8
	A,B/wis		-	-	-	5.8	87.8	-	3.0	3.4

^{a)} Total phenolics content expressed as gallic acid equivalents; ^{b)} Uronic acid content; The values of TPC and UA are averages from at least four experiments and that of the neutral sugar composition from two experiments; Tr, Traces.

As expected, the yield of the hemicelluloses obtained from ASR in comparison to AS was lower (Fig. 2), because most of the extractible polysaccharides were isolated during autohydrolysis of AS in form of oligosaccharides (Nabarlatz et al. 2007a). But interestingly, according to the analytical data of both preparations (Table 2), the corresponding ws- and wis-fractions showed a very similar neutral sugar composition with xylose as the main component, particularly of the wis-fractions. These results indicate that the hydrothermal treatment of AS (Nabarlatz et al. 2007a) attacked a very susceptible and accessible portion of the xylan cell wall component (Hromádková et al.

1996), whereas a part of xylan integrated into the cell wall matrix was still preserved and extractable under the studied alkaline conditions at elevated temperature.

The sugar composition of the hemicellulose preparations and their ws- and wis fractions is listed in Table 2. The results indicate that xylan is predominating and accompanied by varying amounts of pectic polysaccharides, which is evidenced by the presence of galacturonic acid, rhamnose, fucose as well as galactose and particularly arabinose, both sugars typical of the arabinan and arabinogalactan components of the pectin network (Voragen et al. 1995). In the experiments with 5% NaOH the cell wall matrix was much more attacked and split by the alkaline reagent, and both xylan and pectin polymers were released, solubilized, and accumulated in the ws-fractions. The wis-fractions represent xylns with very low pectin contamination. On the contrary, the sonochemical attack using 0.5% NaOH is milder and the wis-fraction of the isolated hemicelluloses (US3-A/wis) contained both xylan and pectic polysaccharides in about equal amounts.

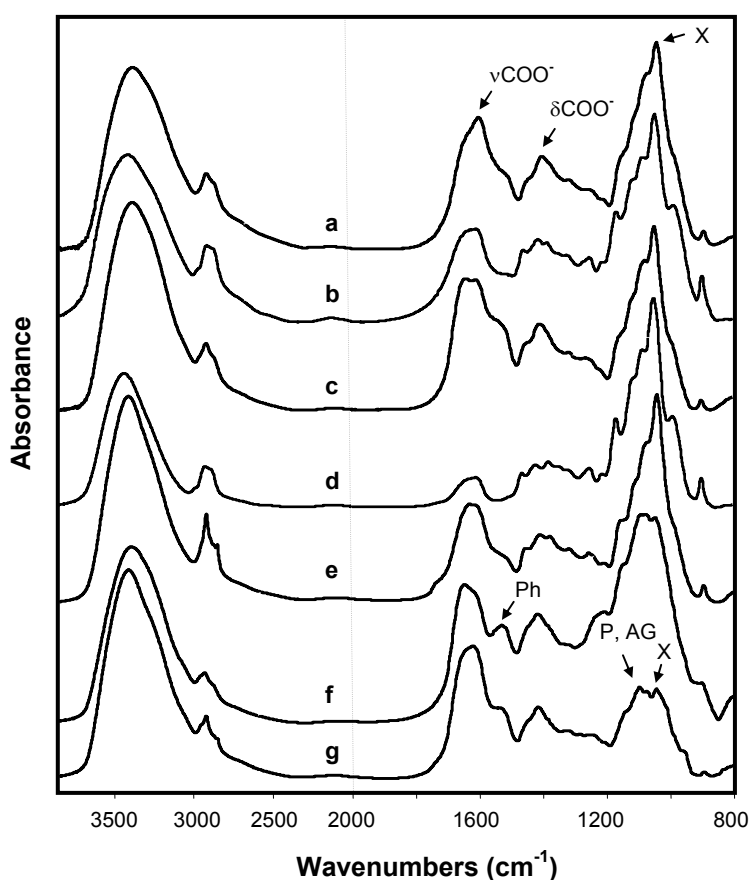


Fig. 3. FT-IR spectra of hemicellulose fractions (a) AS-CI-A,B/ws, (b) AS-US2-A/wis, (c) ASR-CI-A,B/ws, (d) AS-US3-B/wis, (e) AS-US3-B/ws, (f) AS-US3-A/wis, and (g) AS-US3-A/wis; Ph (aromatic ring of phenolics); P, pectin; AG, arabinogalactan; X, xylan.

The FT-IR spectra (Fig. 3) supported the suggestions about the presence of both xylan and pectic polysaccharides. The spectra show differences of the spectral patterns in the 1200-1000 cm^{-1} region with absorption bands typical for xylan, pectin and

arabinogalactans, and (ν_{asCOO^-}) and (ν_{sCOO^-}) bands of the carboxylic group of uronic acids at 1614 cm^{-1} and 1414 cm^{-1} , respectively (Kačuráková et al. 2000).

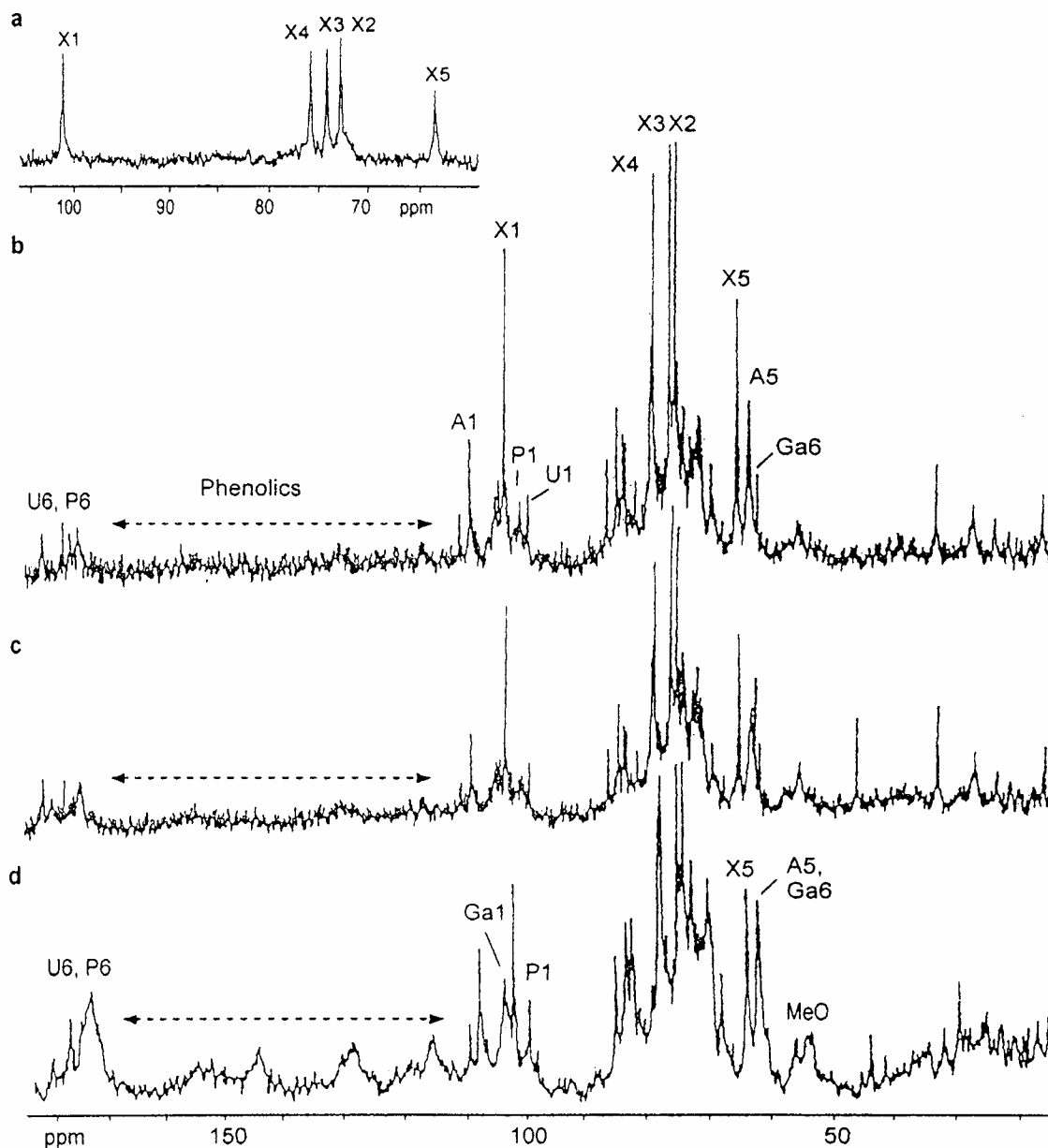


Fig. 4. ^{13}C NMR spectra of hemicellulose fractions (a) US2-A/wis in $\text{DMSO-}d_6$, and (b) CI-A,B/ws, (c) US1-A/ws and (d) US3-A/ws in D_2O .

As illustrated in Fig. 4, the ^{13}C NMR spectra of some of the obtained hemicellulose fractions confirmed the presence and various proportions of xylan and pectic polysaccharides, indicated by the sugar analysis. In the spectrum of US2-A/wis the resonances of the 4-linked β -D-xylopyranosyl residues (X1–X5) are dominating

(Ebringerová et al. 1995). In contrast, the spectra of the ws-fractions Cl-A,B/ws, US1-A/ws and US3-A/ws showed, except for the resonances at δ 103.2, 98.1, 83.2, 76.8, 75.8, 74.0, 64.1, and 60.5 ppm, characteristic of 4-*O*-methyl-glucuronoxylan (Ebringerová et al. 1995), the signals at δ 101–99, 110–107, and \sim 105, assigned to the anomeric carbons of α -D-galacturonic acid, α -L-arabinofuranose and β -D-galactopyranose residues, respectively, which are typical of pectic acid and arabinogalactans (Keenan et al. 1985; Kardošová et al. 2004). The varying pattern of signals at δ \sim 180–170 related to the C6 of uronic acids indicated the different proportion of galacturonic and 4-*O*-methyl-glucuronic acid constituents, i.e. reflecting the pectin/xylan proportion. Some of carboxyl group signals might originate from contaminating phenolics, indicated by the presence of bands at \sim 1505-1515 cm^{-1} of the aromatic ring vibrations in the FTIR spectra (Fig. 3) and by the total phenolics content (TPC) of the ws-fractions, ranging between 6.5–13.3 % (Table 2).

The ws-fractions were tested for antioxidant activity based on the radical scavenging effect in the DPPH \cdot assay (Rao and Muralikrishna 2006). This effect was quantified in terms of the sample concentration needed to decrease the initial DPPH \cdot concentration by 50% (EC_{50}). Its inverse value was used to express the antioxidant activity (AOA). As shown in Table 3, the AOA of the ws-fractions varied between 48-80% and it seems that the AOA activity correlates with the phenolics content ($R^2=0.701$), except of that from fraction AS-US1/A,B. The found AOA corresponds to the lower DPPH radical scavenging activity observed by Pinelo et al. (2004) for almond shell extracts obtained by water than by organic solvents, which is in accord with the different TPC and phenolics composition of these extracts.

Table 3. Total Phenolics Content (TPC) and Antioxidant Activity (AOA) of Water-Soluble Hemicellulose Fractions Isolated from Almond Shells

	AS-Cl/A,B	AS-US1/A,B	AS-US2/A	AS-US3/A	AS-US3/B
TPC (%)	8.9	7.5	10.1	13.3	8.0
EC_{50} (mg/mg) ^a	1.55	1.25	1.45	1.35	2.10
AOA (%) ^b	64	80	69	74	48

^{a)} sample/DPPH \cdot ; ^{b)} AOA = $1/\text{EC}_{50} \times 100$; The values are averages from at least two experiments.

However, it has to be mentioned that there are congruent reports on the relation between AOA and phenolics content (Kähkönen et al. 1999). Moreover, TPC does not reflect the composition of the present phenolics, which might be affected by the used extraction conditions. In case of sample AS-US1-A,B/ws, the alkaline extraction at 60 °C continued after the short ultrasonic irradiation by 50 min, thus enabling reactions of the formed radicals generated from the lignin as well as polysaccharides components resulting in production of other phenolics. Nevertheless, the presented results indicate that the water-soluble polysaccharide-phenolic complexes isolated from AS have the potential to be used as polymeric antioxidants.

CONCLUSIONS

1. Hemicellulose preparations composed of 4-O-methylglucuronoxylan, pectic polysaccharides, and phenolics can be isolated from both AS and ASR with dilute alkali extraction using a two-step extraction procedure. By a short application of ultrasound in the I. extraction step with 5% NaOH, not only the yield of hemicelluloses, but also the extraction time and hereby the heating time can be significantly shortened (from 60 min to 10 min), which is important from the technological point of view. The yields of the hemicelluloses ranged between 12.5-16.3% of AS and 10.7% of ASR. The recovered hemicelluloses comprised 41-67% of the extracted material, indicating losses of aqueous ethanol soluble substances (native phenolics, lignin and degradation products of lignin, and polysaccharides).
2. The water-soluble portion of the hemicellulose fractions from AS exhibited antioxidant activities in the DPPH radical scavenging test (ranging between 48-80% at doses 1.25-2.10 mg sample/mg DPPH[•]) indicating their potential application as polysaccharide-based antioxidants in food, pharmacy and cosmetics. This is substantiated by the fact that almond shells were not reported to contain toxic or otherwise harmful components, and the formation of novel ones are not expected under the described extraction conditions.
3. Using as extractant 5% NaOH in the I. step, the xylan component predominates in fractions of the classical as well as ultrasound-assisted extractions, and is accumulated mainly in the water-insoluble portions. The use of 0.5% NaOH in this step makes it possible to separate ws-hemicelluloses with different proportions of xylan and pectic polymers, and a very pure wis-xylan fraction in the II. step.
4. The isolated xylan-phenolics complexes from both AS and ASR are applicable wherever antioxidant activity combined with the functional properties of the polysaccharide components can be utilized. In general, the isolated hemicellulose fractions from both AS and ASR might serve as biopolymer source in its native form or after targeted modification for the production of value-added polymeric substances utilizable in various technical and non-technical areas.

ACKNOWLEDGEMENTS

The authors are grateful for the support of the Slovak Grant Agency VEGA (grant No. 2/6131/06), the APVV agency (project COST-0036-06), and the SAS-COSTD29 action.

This contribution was an original presentation at the *ITALIC 4 Science & Technology of Biomass: Advances and Challenges* Conference that was held in Rome, Italy (May 8-10, 2007) and sponsored by Tor Vergata University. The authors gratefully acknowledge the efforts of the Conference Organizers, Prof. Claudia Crestini (Tor Vergata University, Rome, Italy), Chair, and Prof. Marco Orlandi (Biococca University, Milan, Italy), Co-Chair. Prof. Crestini also is Editor for the conference collection issue to be published in *BioResources*.

REFERENCES CITED

- Ahmed, A. R., and Labavitch, J. M. (1977). "A simplified method for accurate determination of cell wall uronide content. *J. Food Biochem.* 1(4) 361-365.
- Amarowicz, R., and Shahidi, F. (2006). "Antioxidant activity of almonds and their by-products in food model systems," *J. Am. Oil Chem. Soc.* 83(3), 223-230.
- Dizhbite, T., Telysheva, G., Jurkjane, V., and Viesturs, U. (2004). "Characterization of the radical scavenging activity of lignins—natural antioxidants," *Bioresource Technol.* 95(3) 309–317.
- Ebringerová A., and Heinze T. (2000). "Xylan and xylan derivatives - biopolymers with valuable properties 1. Naturally occurring xylans, structures, isolation procedures and properties," *Macromol. Rapid Comm.* 21(9), 542-556.
- Ebringerová, A., Hromádková, Z., and Heinze, Th. (2005). "Hemicellulose," *Adv. Polym. Sci.* 128, 1-68.
- Garrote, G., Cruz, J. M., Moure, A., Domínguez, H., and Parajó, J. C. (2004). "Antioxidant activity of byproducts from the hydrolytic processing of selected lignocellulosic materials," *Trends Food. Sci. Tech.* 15(3-4), 191-200.
- Hromádková, Z., Ebringerová, A., Kačuráková, M., and Alföldi, J. (1996). "Interactions of the beechwood xylan component with other cell wall polymers," *J. Wood Chem. Technol.* 16(3), 221-234.
- Hromádková, Z. Kováčiková, J., and Ebringerová, A. (1999). "Study of the classical and ultrasound-assisted extraction of the corn cob xylan," *Ind. Crops Prod.* 9(2), 101-109.
- Hromádková, Z., and Ebringerová, A. (2003). "Ultrasonic extraction of plant materials – Investigation of hemicellulose release from buckwheat hulls," *Ultrason. Sonochem.* 10(3), 127-133.
- Kačuráková, M., Capek, P., Sasinková, V., Wellner, N., and Ebringerová A. (2000). "FT-IR study of plant cell wall model compounds: pectic polysaccharides and hemicelluloses," *Carbohydr. Polym.* 43(2), 195-203.
- Kähkönen, M. P., Hopia, A. I., Vuorela, H. J., Rauha, J.-P., Pijlaja, K., Kujala, T. S., and Heinonen, M. (1999). "Antioxidant activity of plant extracts containing phenolic compounds," *J. Agric. Food Chem.* 47(10), 3954-3962.
- Kardošová, A., Ebringerová, A., Alföldi, J., Nosál'ová, G., Matáková, T., and Hříbalová, V. (2004). "Structural features and biological activity of an acidic polysaccharide complex from *Mahonia aquifolium* (Pursh) Nutt.," *Carbohydr. Polym.* 57(2) 165-176.
- Keenan, M. H. J., Belton, P. S., Matthew, J. A., and Howson, S. J. (1985). "¹³C-NMR study of a sugar-beet pectin," *Carbohydr. Res.* 138(1), 168-170.
- Lu, F. J., Chu, L. H., and Gau, R. J. (1998). "Free radical-scavenging properties of lignin," *Nutr. Cancer*, 30(1), 31-38.
- Mason, T. J., Paniwnyk, L., and Lorimer, J. P. (1996). "The use of ultrasound in food technology," *Ultrason. Sonochem.* 3(3), S253-S260.
- Moure, A., Cruz, J. M., Franco, S. D., Dominguez, J. M., Sineiro, J., Dominguez, H., Nunez, M. J., and Parajo, J. C. (2001). "Natural antioxidants from residual sources," *Food Chem.* 72 (2), 145-171.

- Moure, A., Pazos, M., Medina, I., Dominguez, H., and Parajo, J. C. (2006). "Antioxidant activity of extracts produced by solvent extraction of almond shells acid hydrolyzates," *Food Chem.* 101(1), 193-201.
- Nabarlatz, D., Farriol, X., and Montané, D. (2005). "Autohydrolysis of almond shells from the production of xylo-oligosaccharides: product characteristics and reaction kinetics," *Ind. Eng. Chem. Res.* 44 (20), 7746-7755.
- Nabarlatz, D., Ebringerová, A., and Montané, D. (2007a). "Autohydrolysis of agricultural by-products for the production of xylo-oligosaccharides," *Carbohydr. Polym.* 69(1), 20-28.
- Nabarlatz, D., Montané, D., Kardošová, A., Bekešová, S., Hříbalová, V., and Ebringerová, A. (2007b). "O-Acetylated almond shell xylo-oligosaccharides exhibiting immunomodulatory activity," *Carbohydr. Res.* 342(8), 1122-1128.
- Ohta, T., Yamasaki, S., Egashira, Y., and Sanada, H. (1994). "Antioxidative activity of corn bran hemicellulose fragments," *J. Agric. Food Chem.* 42(3) , 653-656.
- Pinelo, M., Rubilar, M., Sineiro, J., and Núñez, M. J. (2004). "Extraction of antioxidant phenolics from almond hulls (*Prunus amygdalus*) and pine sawdust (*Pinus pinaster*)," *Food Chem.* 85 (2), 267-273.
- Popa, V. I. and Volf, I. (2006). "Green chemistry and sustainable development," *Environ. Eng. Management J.* 5(4), 545-558.
- Rao, R. S. P., and Muralikrishna, G. (2006). "Water-soluble feruloyl arabinoxylans from rice and ragi. Changes upon malting and their consequence on antioxidant activity," *Phytochemistry* 67(1), 91- 99.
- Thaipong, K., Boonprakob, U., Crosby, K., Cisneros-Zevallos, L., and Byrne, D. H. (2006). "Comparison of ABTS, DPPH, FRAP, and ORAC assays for estimating antioxidant activity from guava fruit extractives," *J. Food Comp. Anal.* 19(6-7), 669-675.
- Vaya, J., and Aviram, M. (2001). "Nutritional Antioxidants: Mechanisms of Action, Analyses of Activities and Medical Applications," *Curr. Med. Chem.–Imm., Endoc. & Metab. Agents.* 1(1), 99-117.
- Voragen, A. G. J., and Pilnik, W. (1995). "Pectins," In Stephen, A. M. (ed.) *Food Polysaccharides and their Applications*, Marcel Dekker Inc. New-York, 287-339.
- Yuan, X., Wang, J., and Yao, H. (2005). "Antioxidant activity of feruloylated oligosaccharides from wheat bran," *Food Chem.* 90(4), 759–764.
- Zhou, K., Laux, J. J., and Yu, L. (2004). "Comparison of swiss red grain and fractions for their antioxidant properties," *J. Agric. Food Chem.* 52(5), 1118-1123.

Article submitted: Sept. 19, 2007; First round of peer-review completed: Nov. 27, 2007;
Revised version received and approved: Dec. 4, 2007; Published: Dec. 6, 2007.

HYDROPHOBICALLY MODIFIED PECTATES AS NOVEL FUNCTIONAL POLYMERS IN FOOD AND NON-FOOD APPLICATIONS

Zdenka Hromádková,^a Anna Malovíková,^{a*} Štefan Možeš,^b Iva Sroková,^c and Anna Ebringerová^a

Butyl and hexyl amides of pectate with various amidation degrees were prepared from citrus pectin by means of alkylamidation of methyl-esterified pectins, followed by the total alkaline pectin methyl esters hydrolysis. These water soluble derivatives were characterized chemically as well as by elementary analysis and FT-IR spectroscopy. All prepared pectate amides exhibited the excellent emulsifying efficiency, and pectate hexyl amide also the ability to form stable foam. As the results of the study on the effect of pectin with DE 66% on the function of small intestine in pectin fed rats, the increase of specific activity of alkaline phosphatase, maltase, and aminopeptidase and the decrease of food utilization was demonstrated. The pectin derivatives might serve as emulsifiers and foaming additives in food production and other areas as well as nutraceuticals for obesity treatment.

Keywords: Pectin, Modification, Pectate alkylamides, Surface activity, Intestine enzymes, Obesity

Contact information: a: Institute of Chemistry, Center for Glycomics, Slovak Academy of Sciences, 845 38 Bratislava, Slovak Republic; b: Institute of Animal Physiology, Slovak Academy of Sciences, 040 01 Košice, Slovak Republic; c: Department of Chemistry and Technology of Rubber and Textile, Faculty of Industrial Technologies, Trenčín University of Alexander Dubček, 020 32 Púchov, Slovak Republic; * Corresponding author : chemmalo@savba.sk

INTRODUCTION

Pectin is one of the commercial polysaccharides produced from agricultural by-products- citrus peels and apple pomace. These pectins are complex acidic polysaccharides with a linear backbone of (1-4)- α -D-galacturonic acid units, which are partially methylesterified and bear as side chains neutral sugars of the arabinogalactan type (Thakur et al. 1997). There is a continuing interest in exploitation of the pectin component from other plant residues. The expanding uses of pectin within the food and pharmaceutical industries increases the demand for pectins and pectin-rich plant sources. Next to the citrus peels and apple pomace, various other agricultural by-products are available, such as sugar beet pulp (Michel et al. 1985), pumpkin peel (Jun et al. 2006), sunflower heads, grape and olive pomaces, etc. (Thakur et al. 1997).

Pectin is widely used in the food industry as a hydrocolloid additive with gelling, thickening and stabilizing properties, as well as recognized as a dietary fibre playing a significant role in reducing the risks of the high life style-related diseases - cardiovascular and gastrointestinal ones, obesity, diabetes, etc. (Prosky 2001). Among the many areas in obesity research, diet supplementation with pectin suggested as a fat-replacer, decreased

digestion and absorption of nutrients (Dvir et al. 2000; Drochner et al. 2004) and function of the small intestine (Chun et al. 1989). In relation to the prevention and treatment of obesity, there is a lack of knowledge on the effect of the structural features of pectin (such as the degree of methylesterification) as well as of partial hydrophobic modification, which are assumed to contribute to intermolecular interactions with the intestinal mucous membranes.

Hydrophobically modified pectins, such as alkyl esters of pectin and pectic acid (Klavons and Bennet 1995; Pappas et al. 2004) have been suggested as emulsifiers in cosmetic and pharmaceutical cream formulations, and as stabilizers or beverage clouding agents. Pectin amides (Reitsma et al. 1986; Anger and Dongowski 1988; Sinitsya et al. 2000) were reported to possess good gelling properties important in the low sugar diets, and useful as sorbents (Sinitsya et al. 2004). These pectin amides contain both methyl ester and amide groups. To our best knowledge, pectin amides without methyl ester groups (pectate amides) have not yet been studied.

The aims of the present paper were

- (i) to prepare a novel series of pectate derivatives with some carboxyl groups transformed into C₄- and C₆-alkylamides using the commercial citrus pectin as model pectin and characterize their structural and surface active properties, and
- (ii) to study the changes in the specific activity 'in vivo' of some enzymes of the small intestine and their possible role in the mechanisms that influence the rate of nutrient absorption under high fat diet feeding conditions using the model citrus pectinate.

EXPERIMENTAL

Materials

Commercial citrus pectin with degree of methylesterification DE = 66% (PE66) was from Danisco, Smiřice (Czech Republic). It contains 85% galacturonic acid and 15 % neutral sugars. The highly esterified pectin with DE 93% (PE93) was prepared from the commercial pectin at the Institute of Chemistry, Slovak Academy of Sciences (Bratislava, Slovakia) by esterification in acidic methanol. Both pectin preparations were used for the synthesis of amidated derivatives and physiological studies. The commercial citrus pectin amide (PE-NH₂) was kindly donated by Danisco (Smiřice, Czech Republic). The butyl and hexyl amines were from Merck (Germany). Alkaline phosphatase (AP) and aminopeptidase (AMP) were from Sigma-Aldrich (USA), and maltase was from Glycosynth (UK). High-fat (HF) diet was from Research Diet (USA).

Analytical Methods

DE was determined by precipitation of the insoluble copper pectates and pectinates (Tibenský et al. 1963). The degree of amidation (DA) was calculated using the following equation (Sinitsya et al. 2000):

$$\% \text{ DA} = \% \text{ N} / \% \text{ C} \times [6 + \text{DE}/100 + (\text{K}-1) \times \% \text{ N} / 14] \times 100, \quad (1)$$

where the % of carbon (C) and nitrogen (N) were determined by elementary analysis using analyser model 240 (Perkin-Elmer). Fourier-transform infrared (FT-IR) spectra of the samples (2 mg/200 mg KBr) were obtained on the NICOLET Magna 750 spectrometer with DTGS detector and OMNIC 3.2 software using 128 scans at a resolution of 4 cm^{-1} .

Synthesis of Pectate Alkyl Amides

The synthesis was carried out in two steps. In the first step the reaction was carried out with primary alkyl amines (butyl, hexyl) in a heterogeneous system using methanol at 5°C for 10–20 h according to Sinitsya et al. (2000). In a typical experiment, the pectin (15 g) was suspended in 150 ml dry methanol and hexylamine (90 ml) was added under stirring. The reaction proceeded at 5°C for 20 h. Then the products were washed with chloroform to remove the unreacted amine. The wet samples were treated with 0.1 M HCl in ethanol–water mixture (2:1, v/v) to convert carboxylates into their protonated form, washed with neutral ethanol, and air-dried yielding pectinic acid alkylamides. In the second step, these derivatives were further deesterified in alkaline medium in a suspension of 70% ethanol for 12 h, and the obtained pectate alkylamides were recovered by successive washing with ethanol and acetone, and drying on air.

Surface-Activity Testing

The emulsifying efficiency was tested on emulsions of the oil in water (O/W) type as described by Sroková et al. (2003). The emulsion was prepared by mixing a solution (0.05 g of the derivative in 9 ml water) and 1 ml of paraffin oil dyed with SUDAN IV in the laboratory mixer at 20,500 rpm for 1 min. The stability of the emulsion was estimated at three different time intervals after the emulsions had been prepared, i. e. 5 min (h_1), 1h (h_2) and 24h (h_3), and expressed in terms of the height (mm) of the oil and cream layers formed on the surface of the emulsion. The surface tension of aqueous polysaccharide solution in the concentration range $0.015\text{--}2.5\text{ g.l}^{-1}$ was determined at 25°C using the Du Nouy ring apparatus.

Enzyme Activity testing

Male Sprague-Dawley rats (30 day old) fed with high fat/high energy (HF) diet (4.04 kcal/g; 14.5% energy as protein, 30% as fat and 55.5% as carbohydrate) were divided into three groups: 1. control group (C), which was allowed free access to HF diet, 2. pectin group (P) receiving the same diet containing 15% (w/w) of the citrus pectin (PE66), 3. PF group, pair-fed to food intake of pectin fed group for 10 days. The activities of alkaline phosphatase (AP), maltase and aminopeptidase (AMP) were tested using a modified simultaneous azo-coupling method (Lojda et al. 1979, Nachlas et al.1960). Enzyme activity in a cryostat tissue sections ($8\text{ }\mu\text{m}$) was histochemically (cytophotometrically) analysed with a Vickers M85a microdensitometer. The measurements were performed using a x 40 objective, an effective scanning area of $28.3\text{ }\mu\text{m}^2$ and a scanning spot $0.5\text{ }\mu\text{m}$ in at least 30 brush border areas along the villus length in five sections of the jejunum. The integrated absorbance of enzyme activity was calculated as the absorbance values recorded by the instrument in min/mm^3 brush border \pm SE and these mean values were referred to one animal.

The measurements were performed using a x 40 objective, an effective scanning area of $28.3 \mu\text{m}^2$ and a scanning spot $0.5 \mu\text{m}$. The integrated absorbance of enzyme activity along the villus length of the jejunum was calculated as the absorbance values recorded by the instrument in $\text{min}/\text{mm}^{-3}$ brush border \pm SE.

RESULTS AND DISCUSSION

The alkylamidation of the model pectins was performed in two-steps by: (i) introduction of alkylamide groups yielding the intermediate derivative of pectinic acid alkylamide and (ii) removal of the methoxyl groups yielding the pectate alkyl amides. All derivatives were water-soluble. The derivatives were characterized by FT-IR spectra (Fig. 1a). The vibrations of the Amide I and Amide II at 1655 cm^{-1} and 1550 cm^{-1} , respectively, as well as the C=O stretching vibration of the ester and carboxylate groups at 1751 cm^{-1} and 1600 cm^{-1} , respectively, were differentiated using peak-fitting (Fig. 1b). The chemically determined degree of esterification (DE) and degree of amidation (DA) of both the intermediate and final products are summarized in Table 1. As seen in Table 1, the chemical modification of pectins was accompanied by depolymerization, indicated by the decrease of the intrinsic viscosity.

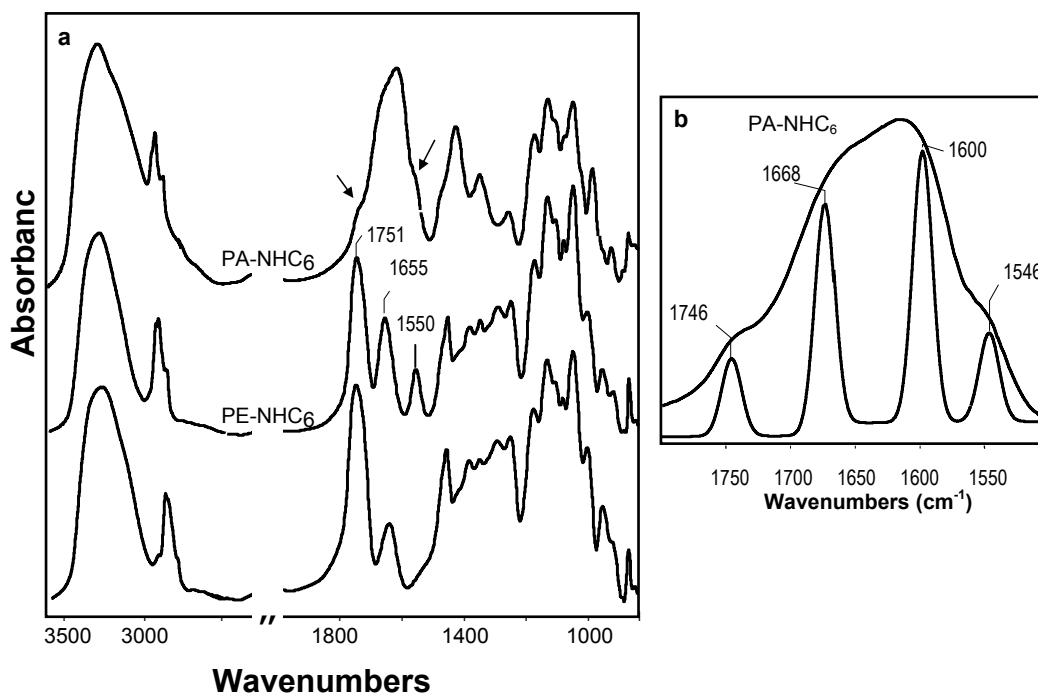


Fig. 1. FT-IR spectra in KBr of (a) the starting pectin (PE93), pectinic acid hexylamide (PE-NH₆) and pectate hexylamide (PA-NHC₆), and (b) the partial spectrum of PA-NHC₆ obtained by peak-fitting. The arrows indicate the Amide I and Amide II bands.

The surface activity of the original pectins, their butyl and hexyl amide intermediates and final pectate amides were tested for surface tension and emulsifying efficiency. All tested samples gave stable oil-in water emulsions.

The substitution of the methyl ester groups by alkyl amide groups resulted in very pronounced foaming, depending on the alkyl length and DA. With the hexyl derivatives the foam was stable after 24 h. Despite these properties, the surface-activity depressing effect of the derivatives was very low (69.7-59.8 mN.m⁻¹). Similar effects were observed with polymeric surfactants prepared from other polysaccharides such as from hydroxyethylcellulose (Sroková et al. 2003).

Table 1. Analytical Data and Surface Active Properties of Pectins and their Derivatives

Sample	DE %	DA %	[η] (ml.g ⁻¹)	Oil/Cream layers ^a (mm/mm)			γ_{\min} mN.m ⁻¹	c.m.c. g.l ⁻¹
				5 min	1h	24 h		
Original pectin								
PE66	66	0	434	0/0	0/0	0/12	nd	nd
PE93	93	0	132	0/8	0/11	0/11	nd	nd
Pectinate amide and alkyl amides								
PE-NH ₂	31	24	395	0/0*	0/0*	0/10*	59.8	1.08
PE-NHC4	85	13	92	0/0*	0/8*	0/11	69.7	1.37
PE-NHC6	nd	nd	176	0/0*	0/0*	0/7*	62.7	0.62
Pectate amide and alkyl amides								
PA-NH ₂	0	23	229	0/0	0/4	0/9	68.8	1.25
PA-NHC4	0	15	42	0/2	0/7	0/8	no	no
PA-NHC6	3	30	85	0/0*	0/10*	0/10	63.4	0.31
Tween 20				0/0	0/0	0/4		

^aOil/water emulsion: Height of oil and cream layers formed on the surface of the emulsion after 5 min, 1 h and 24 h; * Foaming; Tween 20, commercial synthetic emulsifier.

As a preliminary study of the effect of pectin and their derivatives on the function of the small intestine, the citrus pectin (PE66) was tested for changes in the activity of the small intestine enzymes AP, maltase and AMP in pectin fed rats. As illustrated in Table 2, the activity of these enzymes in the pectin group animals (P) significantly raised by 18%, 25%, and 23% respectively, in comparison with values of the control animals (C). These results are in accord with the reports about the increased activities of intestinal brush border bound enzymes using diet supplemented with pectin (Chun et al. 1989; Farness and Schneeman 1982).

The observed functional changes were also associated with significantly decreased food intake, food efficiency, as well as with significantly lowered epididymal plus retroperitoneal fat pad weight. These somatic changes were also associated with the alteration of the weight gain parameters (Control 48.0±2.1, Pectin 22.6±1.5*, PF±29.1*). Moreover, in the pectin fed animals (PF) as compared to C animals, the reduced intake of high fat (HF) diet did not change the intestinal enzyme and body fat parameters. This indicates that up-regulation of enzyme activities in P group is rather a consequence of specific effect of pectin than the decrease of luminal nutrition. Further studies with other pectins and pectin amide derivatives are in progress. The obtained results about the effect of pectin on the function of the small intestine can expand the knowledge on the

participation of the small intestine in the mechanisms that might play a key role on influence development of obesity and associated feeding and body fat disturbances.

Table 2. Effect of Citrus Pectin (PE66) on the Function of Small Intestine in Pectin-Fed Rats

Group	AP	Maltase	AMP	Body fat %	Food intake g/day	FE
Control	13.4±0.6	14.2±0.5	14.3±0.5	0.73±0.07	12.3±0.5	0.39±0.01
Pectin	15.8±0.2*	17.8±0.9*	17.6±0.9*	0.27±0.03*	9.6±0.8*	0.24±0.02*
PF	13.1±0.1 [#]	14.6±0.4 [#]	13.7±0.5 [#]	0.64±0.03 [#]	10.1±0.4*	0.30±0.01* [#]

Values are means ± SE (n = 8 animals/groups); Enzyme activity is given as a density values in jejunal enterocytes at wavelength of 520 nm; AP (Alkaline phosphatase), AMP (Aminopeptidase) and Maltase are intestinal enzymes; Body fat (%) represents epididymal plus retroperitoneal fat pads weight; FE (food efficiency) is given as the weight gain/food intake; * significantly different from C group; [#] significant differences between P and PF groups at P<0.05 by Tukey's test after ANOVA.

CONCLUSIONS

1. The results suggested that the novel butyl and hexyl amide pectates with DA ranging between 15-30% represent polymeric surfactants with excellent emulsifying efficiency, and in the case of the hexyl derivatives the ability to produce stable foams.
2. The derivatives are potential polysaccharide-based biodegradable surfactants useful in various technical applications and industrial processes.
3. The results of the effect of the pectin on the energy homeostasis of rats suggested that the enhanced activity of enzymes and decreased food utilization observed in pectin-fed rats might play an important role in prevention the development of obesity on high fat diet.

ACKNOWLEDGEMENTS

This work was financially supported by the Slovak Grant Agency VEGA (grant No. 2/6131/26 and 2/5141/25) and the agency APPV (project COST-0036-06).

This contribution was an original presentation at the *ITALIC 4 Science & Technology of Biomass: Advances and Challenges* Conference that was held in Rome, Italy (May 8-10, 2007) and sponsored by Tor Vergata University. The authors gratefully acknowledge the efforts of the Conference Organizers, Prof. Claudia Crestini (Tor Vergata University, Rome, Italy), Chair, and Prof. Marco Orlandi (Biococca University, Milan, Italy), Co-Chair. Prof. Crestini also is Editor for the conference collection issue to be published in *BioResources*.

REFERENCES CITED

- Anger, H., and Dongowski, G. (1988). "Amidated pectins—characterization and enzymatic degradation," *Food Hydrocolloids* 2(5), 371-379.
- Chun, W., Bamba, T., and Hosoda, S. (1989). "Effect of pectin a soluble dietary fiber on functional and morphological parameters of the small intestine in rats," *Digestion* 42(1), 22-29.
- Drochner, W., Kerler, A., and Zacharias, B. (2004). "Pectin in pig nutrition, a comparative review," *J. Anim. Physiol. Anim. Nut.* 88(11-12), 367-380.
- Dvir, I., Chayoth, R., Sod-Moriah, U., Shany, S., Nyska, A., Stark, A. H., Madar, Z., and Arad, S. M. (2000). "Soluble polysaccharide and biomass of red microalga *Porphyridium sp.* alter intestinal morphology and reduce serum cholesterol in rats," *Br. J. Nutr.* 84(4), 469-476.
- Farness, P. L., and Schneeman, B. O. (1982). "Effect of dietary cellulose, pectin and oat bran on the small intestine in the rat," *J. Nutr.* 112(7), 1315-1319.
- Jun, H. I., Lee, Ch.-H., Song, G.-S., and Kim, Z.-S. (2006). "Characterization of the pectic polysaccharides from pumpkin peel," *LWT-Food Sci. Technol.* 39(5), 554-561.
- Klavons, J. A., and Bennet, R. D. (1995). "Preparation of alkyl esters of pectin and pectic acid," *J. Food Sci.* 60(3), 513-515.
- Lojda, Z., Gossrau, R. and Schibler, T. H. (1979). "A laboratory manual," *Enzyme Histochemistry*, Springer-Verlag, Berlin.
- Michel, F., Thibault, J. F., Mercier, C., Heitz, F., and Pouillaude, F. (1985). "Extraction and characterization of pectins from sugar beet pulp," *J. Food Sci.* 50(5), 1499-1500.
- Nachlas, M. M., Monis, B., Rosenblatt, M. D., and Seligan, A. M. (1960). "Improvement in the histochemical localization of leucine aminopeptidase with a new substrate, L-leucyl-4-methoxy-2-naphthamide," *J. Biophys. Biochem. Cytol.* 7, 261-264.
- Pappas, CH. S., Malovíková, A., Hromádková, Z., Tarantilis, P. A., Ebringerová, A., and Polissiou, M. G. (2004). "Determination of the degree of esterification of pectinates with decyl and benzyl ester groups by diffuse reflectance infrared Fourier transform spectroscopy (DRIFTS) and curve-fitting deconvolution method," *Carbohydr. Polym.* 56(4), 465-469.
- Prosky, L. (2001). "Advanced Dietary Fiber Technology," Blackwell Science, Oxford 2001.
- Reitsma, J. C. E., Thibault, J. F., and Pilnik, W. (1986). "Properties of amidated pectins. I. Preparation and characterization of amidated pectins and amidated pectic acids," *Food Hydrocolloids* 1(2), 121-127.
- Sasinková, V., Hromádková, Z., Malovíková, A., Sroková, I., and Ebringerová, A. (2005). "Hydrophobically modified citrus pectin with pendant alkyl amine groups," *Book of Contribution, 4th Conference Structure and Stability of Biomacromolecules SSB 2005*, Košice, Slovakia, p. 95.
- Sinitsya, A., Čopíková, J., Prutyánov, V., Skoblyá, S., and Machovič, V. (2000). "Amidation of highly methoxylated citrus pectin with primary amines,"

- Carbohydr. Polym.* 42(4), 359-368.
- Sinitsya, A., Čopíková, J., Marounek, M., Mlčochová, P., Sihelníková, L., Skoblya, S., Havlátová, H., Matějka, P., Maryka, M., and Machovič, V. (2004). “N-octadecylpectinamide, a hydrophobic sorbent based on modification of highly methoxylated citrus pectin,” *Carbohydr. Polym.* 56(2), 169-176.
- Sroková, I., Miníková, S., Ebringerová, A., and Sasinková, V. (2003). “2-Hydroxyethyl)cellulose-based nonionic biosurfactants,” *Tenside Surf. Det.* 40(1), 73-76.
- Thakur, B. R., Singh, R. K., and Handa, A. K. (1997). “Chemistry and uses of pectin,” *Crit. Rev. Food Sci. Nutr.* 37(1), 47-73.
- Tibenský, V., Rosík, J. and Zitko, V. (1963). “Zur Bestimmung des Veresterungsgrades von Pektin,” *Nahrung* 7(4), 321-325.

Article submission received: Sept. 19, 2007; First round of peer-review completed: Nov. 27, 2007; Revision received and accepted: Dec. 6, 2007; Published: Dec. 8, 2007

FUNCTIONALIZATION PATTERN OF TERT-BUTYLDIMETHYLSILYL CELLULOSE EVALUATED BY NMR SPECTROSCOPY

Thomas Heinze,* Annett Pfeifer, and Katrin Petzold

Tert-butyldimethylsilyl cellulose with a degree of substitution (DS) of up to 2 could be obtained by homogeneous conversion of the biopolymer with tert-butyldimethylchlorosilane in *N,N*-dimethyl acetamide/LiCl in the presence of imidazole. The cellulose derivatives were characterized in detail by means of two-dimensional NMR spectroscopic techniques including subsequent derivatization of the original polymer by consecutive methylation-desilylation-acetylation. The very well resolved NMR spectra indicate that, dependent on the reaction temperature, 2,6-di-*O*-tert-butyldimethylsilyl moieties are the main repeating units. 3,6-di-*O*- and 6-mono-*O* functionalized repeating units were identified in very small amounts if the reaction is carried out at room temperature. Additionally, 2,3,6-tri-*O*-silylated functions appear if reaction is carried out at temperature of 100°C. Thus, a novel path for regioselective protection of position 2 and 6 for cellulose was established.

Keywords: Cellulose, Consecutive methylation-desilylation-acetylation, NMR, Protecting group technique, Regioselective functionalization, Tert-butyldimethylchlorosilane

Center of Excellence for Polysaccharide Research, Friedrich Schiller University of Jena, Humboldtstraße 10, D-07743 Jena, Germany, Fax +49-3641-948272, E-mail:* thomas.heinze@uni-jena.de
Member of the European Polysaccharide Network of Excellence (EPNOE), www.epnoe.eu

INTRODUCTION

The conversion of cellulose with reactive trialkylsilyl compounds yields organo-soluble cellulose derivatives that are interesting intermediates to form both fibres (Hermanutz et al. 2001) and ultrathin cellulose films, applying the Langmuir-Blodgett technique and subsequent desilylation (Schaub et al. 1993). Trialkylsilyl compounds with at least one bulky moiety are useful protecting groups in order to obtain products with a controlled functionalization pattern by the subsequent reaction of the remaining hydroxyl groups and deprotection. For example, the reaction of cellulose with thexyldimethylchlorosilane yields the 6-*O*-protected derivative, provided that heterogeneous reaction conditions are applied. Thus, 2,3-*O*-functionalized cellulose ethers and esters are available, on one hand (Klemm and Stein 1995). On the other, it was shown that the homogeneous silylation of the cellulose dissolved in *N,N*-dimethyl acetamide (DMA) in combination with LiCl leads to 2,6-di-*O*-thexyldimethylsilyl cellulose that is an appropriate intermediate for the preparation of 3-*O*-functionalized cellulose ethers (Koschella et al. 2006a; Petzold et al. 2004; Koschella et al. 2001). It clearly appeared that regioselectively substituted cellulose derivatives show different properties compared to the conventional products. Thus, regiochemistry is a helpful tool to design the properties.

In the context of protecting group technique with cellulose, our interest was focused on the tert-butyldimethylsilyl moiety. As early as 1987 Pawlowski et al. have found that the conversion of cellulose dissolved in DMA/LiCl with *N*-methyl-*N*-(tert-butyldimethylsilyl) trifluoroacetamide leads to the corresponding silyl cellulose with a degree of substitution (DS) of about 0.7 with a preferred functionalization at position 6 as revealed by solid state ^{13}C NMR spectroscopy (Pawlowski et al. 1987). Moreover, tert-butyldimethylsilyl cellulose with a DS of 0.96 prepared in DMA/LiCl possesses a selective modification of position 6 (Klemm et al. 1990). However, no information about the functionalization pattern of tert-butyldimethylsilyl cellulose with DS values above 1 is available. Consequently, the conversion with cellulose dissolved in DMA/LiCl with tert-butyldimethylchlorosilane was studied, and the products were characterized in detail applying two-dimensional NMR spectroscopic techniques including subsequent derivatization of the original polymer by consecutive methylation-desilylation-acetylation, which is very useful in order to get well resolved NMR spectra appropriate for the evaluation of the functionalization pattern.

EXPERIMENTAL

Materials

Cellulose (**1**) (Avicel, degree of polymerization, DP=250, Fluka) and LiCl (Merck) were dried at 100°C under vacuum prior to use. *N,N*-Dimethyl acetamide (DMA, Acros) was stored over molecular sieves. Tert-butyldimethylchlorosilane (TBS chloride, ABCR) was stored under argon atmosphere. Sodium hydride (Fluka, suspension in mineral oil) was washed with hexane and pentane, dried in vacuum at room temperature and stored under argon atmosphere. All other chemicals were used as received.

Methods

Tert-butyldimethylsilyl cellulose (9), general procedure

1.0 g (6.17 mmol) cellulose (**1**) was suspended in 30 mL DMA and stirred at 120°C for 2 h under exclusion of moisture. After cooling to 80°C, LiCl (1.8 g) was added and stirring was continued without heating until complete dissolution of the polymer occurred. Under vigorous stirring, imidazole (1.76 g, 25.91 mmol) was added. After dissolution of the imidazole, TBS chloride (3.25 g, 21.59 mmol) was added and stirring was continued for 24 h at room temperature (after about 1 h precipitation occurred). The mixture was added to 500 ml phosphate buffer (500 ml water, 3.57 g K_2HPO_4 , 1.77 g KH_2PO_4), the solid material was filtered off, washed with water (three times with 500 ml), two times with ethanol (300 ml) and dried in vacuum at 100°C.

Yield: 2.2 g; Degree of substitution (DS): 1.98 (determined by ^1H NMR spectroscopy after methylation, desilylation and peracetylation)

Tert-butyldimethylsilyl methylcellulose (9a), general procedure

To 1.6 g (4.09 mmol) 2,6-di-*O*-tert-butyldimethylsilyl cellulose (**9**) dissolved in 30 ml THF, 0.98 g (40.98 mmol) NaH (10 mol pro mol AGU) were added. The suspension obtained was stirred for 10 min and subsequently 2.56 ml (40.98 mmol)

iodomethane (10 mol pro mol AGU) was added. After stirring for 24 h at room temperature, the reaction mixture was allowed to react for additionally 48 h at 50°C. After cooling to room temperature, 5 ml 2-propanol and subsequently 5 ml water was carefully added. The mixture was put into 500 ml phosphate buffer (500 ml water, 3.57 g K_2HPO_4 , 1.77 g KH_2PO_4) and the precipitate was isolated by filtration. The precipitate was washed with 500 ml water four times and dried at 100°C under vacuum.

Yield: 1.44 g.

Desilylation of tert-butyldimethylsilyl methylcellulose (9b), general procedure

To 1.2 g (2.97 mmol) 2,6-di-*O*-tert-butyldimethylsilyl-3-mono-*O*-methylcellulose **9a** suspended in 20 ml THF, 3.75 g (11.88 mmol) TBAF \cdot 3H $_2$ O (4 mol pro mol AGU) were added and the mixture was allowed to react for 24 h at 50°C under stirring. After cooling to room temperature, the mixture was put into 100 ml methanol and the precipitated was isolated by filtration. The product (non-dried) was dissolved in DMSO and again treated with 1.5 g (4.76 mmol) TBAF \cdot 3H $_2$ O for 24 h at 50°C under stirring. The product was precipitated in 100 ml methanol. After filtration, washing with 50 ml methanol (four times) and drying at 100°C under vacuum product **9b** was obtained.

Yield: 0.48 g

Acetylmethyl cellulose (9c), general procedure

To 250 mg methylcellulose **9b** in 5 ml pyridine, 5 ml acetic anhydride and 25 mg DMAP were added. After a reaction time of 24 h at 80°C and cooling to room temperature, the mixture was put into 50 ml ethanol. The product was washed 5 times with 30 ml ethanol and dried at 100°C under vacuum.

Yield: 0.22 g

Measurement

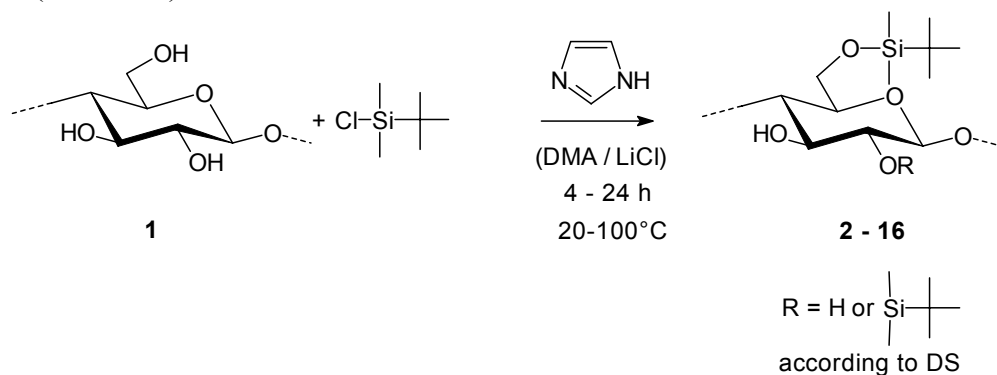
The FTIR spectra were recorded with a NICOLET AVATAR 370 DTGS spectrometer by using the KBr technique. The NMR spectra were acquired with a Bruker AVANCE 250 and AVANCE 400 in CDCl $_3$ (concentration of the sample: 5%) at a temperature of 30°C with the standard pulse sequences for 1H -, ^{13}C -, DEPT135-, and two-dimensional NMR spectroscopy. For the 1H NMR spectra 16 scans and for ^{13}C NMR spectra up to 55,000 scans were accumulated.

RESULTS AND DISCUSSION

Homogeneous silylation of cellulose with hexyldimethylchlorosilane is a valuable synthesis path to get cellulose derivatives that are modified at positions 2 and 6. In the context of studies on regiochemistry of polysaccharides, our interest was focused on tert-butyldimethylchlorosilane (TBS chloride) with less bulky tert-butyl moiety to study the reactivity of this silylating agent with regard to cellulose. Moreover, due to the fact that hexyldimethylchlorosilane is expensive and the removal of the protecting groups introduced after subsequent modification of the remaining OH groups is difficult,

alternative protecting groups are really needed. TBS chloride was not studied regarding a 2,6-di-*O*-protection of cellulose up to now.

Thus, conversions starting with cellulose dissolved in *N,N*-dimethyl acetamide (DMA) in combination with LiCl were studied, applying TBS chloride as reagent in the presence of imidazole at varying time, temperature, and molar ratio of cellulose to reagent (Scheme 1).



Scheme 1. Silylation of cellulose with tert-butyldimethylchlorosilane

After a usual work-up procedure, a product with a DS_{Si} of 1.85 (**2**) was obtained, applying a molar ratio of 1:3.0:3.6 (cellulose:TBS chloride:imidazole) and a reaction time of 2 h. An increase of the reaction time up to 24 h yields a slight increase of the DS_{Si} (Table 1, sample **4** and **12**).

Table 1. Conditions for and Results of the Conversion of Cellulose with Tert-butyldimethylchlorosilane in *N,N*-dimethyl acetamide/LiCl in the Presence of Imidazole.

Conditions			Product					
Molar ratio ^{a)}	Time (h)	Temp. (°C)	No.	DS	Solubility ^{c)}			
					THF	CHCl ₃	Toluene	Hexane
1:3.0:3.6	2	20/100	2	1.85	+	+	-(S)	-
1:3.5:4.2	2	20/100	3	1.92	+	+	-(S)	-
1:3.0:3.6	4	20/100	4	1.81	+	+	-(S)	-
1:3.5:4.2	4	20/100	5	1.87	+	+	+	-(S)
1:3.5:4.2	2	20	6	1.71	-S	-S	-	-
1:3.5:4.2	4	20	7	1.76	-(S)	-(S)	-(S)	-
1:3.5:4.2	6	20	8	1.85	+	+	+	-
1:3.5:4.2	24	20	9	1.98	+	+	+	-(S)+
1:3.5:4.2	24	100	10	2.04	-(S)	-(S)	+	+
1:3.5:4.2	24	100 ^{b)}	11	2.12	-(S)	-(S)	+	+
1:3.0:4.2	24	100	12	1.93	+	+	+	-(S)
1:3.0:4.2	24	100 ^{b)}	13	1.99	+	+	+	+
1:4.0:4.8	24	20	14	2.05	+	+	-(S)	-(S)
1:4.0:4.8	24	100	15	2.11	-(S)	-(S)	+	+
1:4.0:4.8	24	100 ^{b)}	16	2.09	-(S)	-(S)	+	+

^{a)} Molar ratio of cellulose:tert-butyldimethylchlorosilane:imidazole

^{b)} Reaction mixture contains additionally toluene

^{c)} + soluble, - insoluble, S swelling, THF tetrahydrofuran

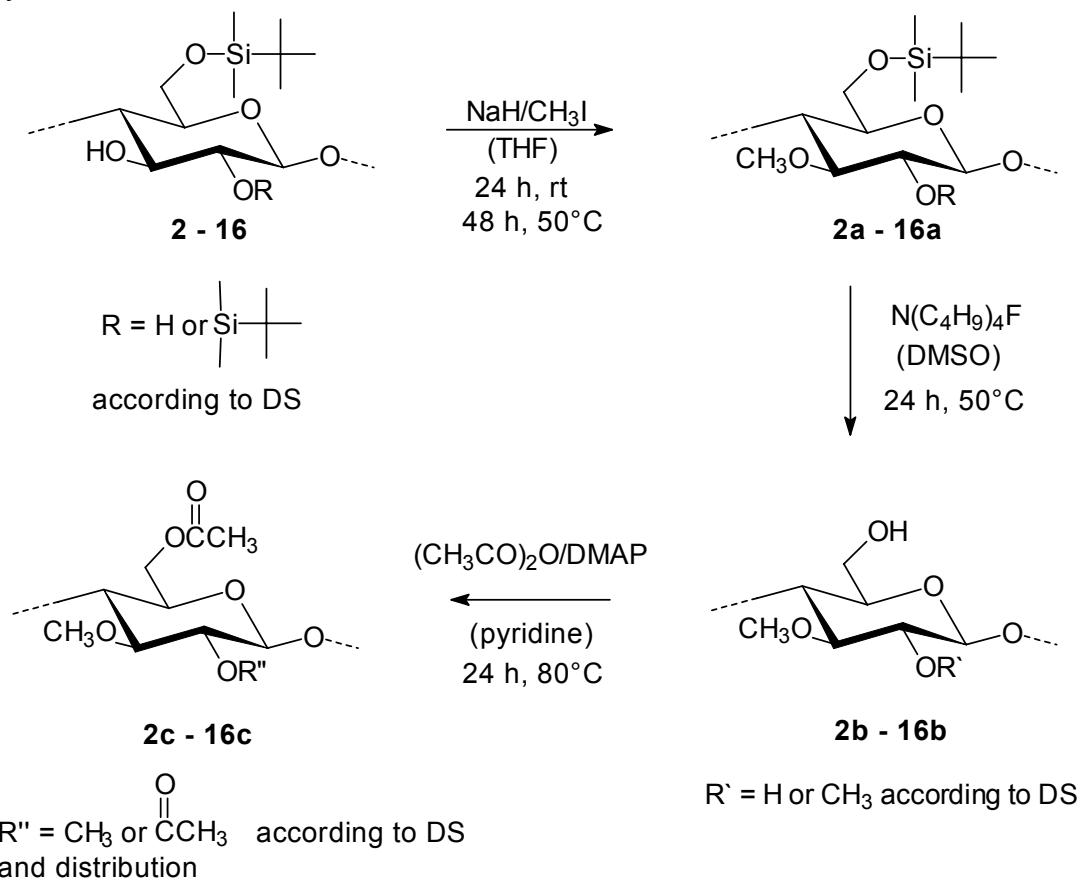
The increase of the molar ratio to 1:3.5:4.2 (cellulose:TBS chloride:imidazole) leads to samples with DS_{Si} values of about 2 after 24 h reaction time both at 20°C and 100°C (samples **9** and **10**).

Due to the fact that the TBS cellulose obtained forms a gel-like state during the reaction, toluene as co-solvent was added. However, no change in DS_{Si} appeared (compare samples **10** and **11**, **12** and **13**, **15** and **16**, Table 1). Even at higher molar ratio of 1:4.0:4.8, the total DS_{Si} does not exceed a value of about 2. Considering total DS_{Si} of the TBS cellulose, the results are comparable with those obtained by the reaction of cellulose with hexyldimethylchlorosilane in DMA/LiCl.

The TBS cellulose samples are well soluble in organic solvents (Table 1). It must be pointed out that slight difference in DS_{Si} may change the solubility significantly. Samples with a DS_{Si} of up to 2 are soluble in tetrahydrofuran and $CHCl_3$, while the solubility in these solvent does not occur at DS_{Si} of 2.1 (samples **11**, **15**, and **16**). On the contrary, samples of comparable high DS_{Si} dissolve even in hexane. From our results, no clear correlation between DS_{Si} and solubility of TBS cellulose in toluene appears. Moreover, slight changes in the functionalization pattern may vary the solubility. Thus, further detailed studies due to a completely structure characterization within AGU and along the biopolymer chain must be carried out. In any case, the samples are soluble in typical organic solvents and can be modified at the remaining hydroxyl groups; this is an important prerequisite to analyse the functionalization pattern because the resolution of NMR spectra of TBS cellulose is not sufficient. Moreover, further alternative analytical tools like GC-MS need subsequent derivatization steps. Thus, the subsequent modification of TBS cellulose is of general interest. According to our experiences in NMR spectroscopy of polysaccharides, it was decided to methylate the remaining hydroxyl groups. Subsequent desilylation and acetylation of hydroxyl groups yields samples that give very well resolved NMR spectra useful for the characterization of the functionalization pattern (Scheme 2, see e.g., Stein and Klemm 1995; Petzold et al. 2003; Heinze 2004; Koschella et al. 2006b). It is known from the consecutive methylation-desilylation-peracetylation of hexyldimethylsilyl celluloses that these reaction steps do not yield any displacement or splitting of the primary functional groups (Erler et al. 1992). Thus, it may be concluded that the chemical conversion used for analytical purpose is also suitable for tert-butyldimethylsilyl cellulose derivatives.

The 1H NMR spectra of samples **15c** and **16c** (Fig. 1) show the amazing result that the silylation of cellulose with TBS chloride under the conditions described yields a preferred functionalization of positions 2 and 6. Consequently, in the spectra the typical signals of 3-mono-*O*-methyl-2,6-di-*O*-acetyl cellulose (peak no. 1-6 in Fig. 1) are found. In addition, there are some signals of very low intensity that corresponds to repeating units with a 2,3-di-*O*-methyl-6-mono-*O*-acetyl- (peak no. 2' and 3') and 2-mono-*O*-methyl-3,6-di-*O*-acetyl- (peak. no. 2'' and 3'') substitution. After line fitting (MestRec) of the 1H NMR spectrum of sample **14**, it could be calculated that 3.9% of 2,3-di-*O*-methyl-6-mono-*O*-acetyl- and 4.2% of 2-mono-*O*-methyl-3,6-di-*O*-acetyl repeating units appear. It must be pointed out that the line fitting and calculation possess a large error; consequently another method like GC-MS should be developed to obtain reliable results regarding the quantitative determination of substructures. The 1H NMR spectra indicate that position 6 of all samples is completely silylated. An additional proof for the 6-*O*-

silylation gave the HSQC DEPT spectrum of the acetyl methyl cellulose obtained via the path shown in Scheme 2 starting from **9**, which possessed only negative signals for the acetylated position 6 as a consequence of the complete silylation of this position of polymer **9**.



Scheme 2. Synthesis path for subsequent methylation, desilylation and acetylation starting from tert-butyldimethylsilyl cellulose.

At a molar ratio of 1:3.5:4.2 (cellulose:TBS chloride:imidazole) a sample with a DS_{Si} of 1.76 (**7**) was obtained after 4 h reaction at 20°C. The ^{13}C NMR spectrum shows that 3-mono-*O*-methyl-2,6-di-*O*-acetyl cellulose is mainly formed (Fig. 2, peaks 1-11). As expected due to the $\text{DS}_{\text{Si}} < 2$, signals for a repeating unit with a functionalization pattern of 2,3-di-*O*-methyl-6-mono-*O*-acetyl moieties are found (Fig. 2; peaks numbered in red and marked with index ‘). The assignment of the peaks in ^1H - and ^{13}C NMR spectra is not only based on the two-dimensional spectroscopy (see following text) but also on the signal assignment carried out by Karakawa et al. (2002). In this work regioselectively functionalized methyl- and acetyl cellulose derivatives were prepared by ring-opening polymerization of α -D-glucopyranose 1,2,4-orthopivalate with a corresponding regioselective functionalization pattern regarding methyl moieties and subsequent acetylation.

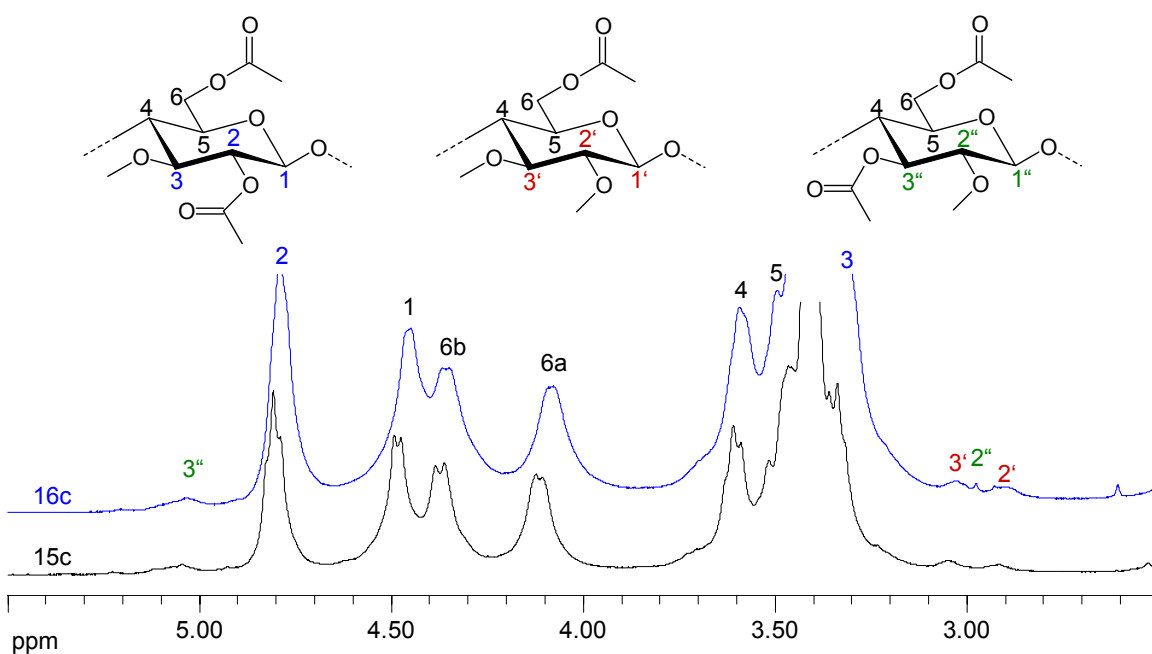


Fig. 1. ^1H NMR spectra of acetyl methyl cellulose **15c** and **16c** in CDCl_3 . Silylation conditions in DMA/LiCl : **15**: molar ratio 1:4.0:4.8 (cellulose:tert-butyldimethylchlorosilane:imidazole), 24 h, 100°C ; **16**: molar ratio 1:4.0:4.8 (cellulose:tert-butyldimethylchlorosilane:imidazole), 24 h, 100°C , addition of toluol.

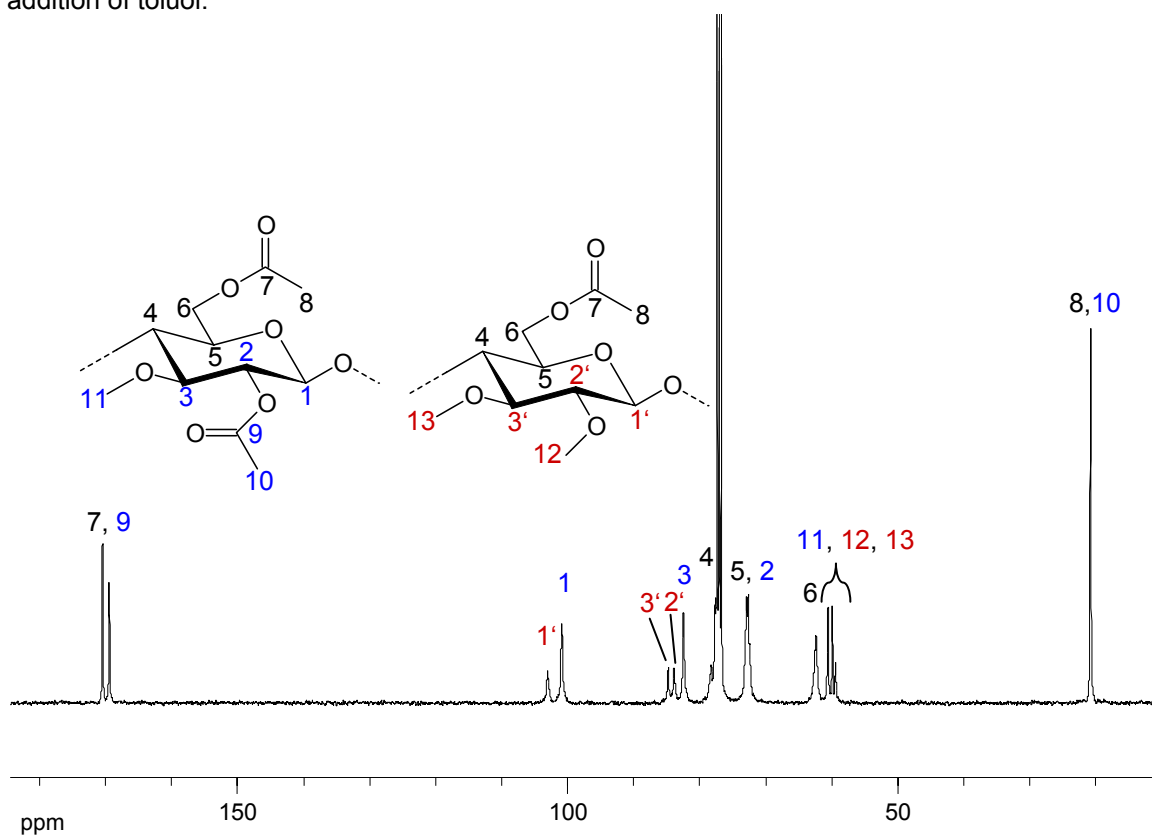


Fig. 2. ^{13}C NMR spectrum of acetyl methyl cellulose **7c** obtained from **7** (DS_{Si} 1.76) in CDCl_3 .

The $^1\text{H}, ^1\text{H}$ COSY NMR spectra of samples **9c** and **15c** additionally clearly indicate that 3-mono-*O*-methyl-2,6-di-*O*-acetyl moiety is the main repeating unit (Fig. 3, peak no. 1-3 in blue). All proton signals of this repeating unit could be identified by following the cross-peaks; beginning with the H-1 signal at 4.48-4.49 ppm, continuing by the H-2 signal at 4.78-4.80 ppm typical for an acetylation at this position and the H-3 signal at 3.32 ppm as a consequence of methylation.

The signals for the protons in position 6 were identified at 4.10 ppm for H-6a and at 4.35-4.37 ppm for H-6b as a result of the acetylation. The proton signals of position 4 (3.58-3.60 ppm) and 5 (3.46-3.47 ppm) could be detected independent of the substructure. Both, 2,3-di-*O*-methyl-6-mono-*O*-acetyl (peak no. 1', 2', and 3') and the 2-mono-*O*-methyl-3,6-di-*O*-acetyl substitution (peak no. 1'', 2'', and 3'') were identified by means of the cross-peaks although with very small amount independent of the reaction conditions. In the COSY NMR spectrum of **15c** (Fig. 3b), small amount of cellulose triacetate was found as revealed by typical peaks for H-1 (1*) at 4.33 ppm, H-2 (2*) at 4.76 ppm, and H-3 (3*) at 5.09 ppm (Heinze et al. 2006 and references herein). On the contrary, these signals could not found in the COSY spectrum of **9c**.

The triacetate structure is a result of trisilylated anhydroglucose units in the tert-butyldimethylsilyl cellulose. Trisilylation depends on the reaction conditions. Products obtained by reactions at room temperature did not contain a trisilylated moiety independent of the molar ratio although the same total DS could be realized as in the case of reactions at higher temperature.

No triacetate structures resulting from the trisilylation were found in the NMR spectra of **9c** (molar ratio 1:3.5:4.2, cellulose:TBS chloride:imidazole, Fig. 3a) as well as of **14c** (molar ratio 1:4.0:4.8, cellulose:TBS chloride:imidazole, data not shown).

However, a reaction at 100°C led to a complex structure of the silyl cellulose, i.e. the polymer contains 2,6-di-*O*-silyl units as the main component, in addition small amounts 6-mono-*O*-silyl, 3,6-di-*O*-silyl- and even 2,3,6-tri-*O*-silyl repeating units independent of the molar ratio. In the NMR spectra of the subsequent acetyl methyl celluloses, triacetate structures as a result of trisilylation were found independent of the molar ratio of the starting silylation reaction (**10**, 1:3.5:4.2, cellulose:TBS chloride:imidazole, data not shown, **15**, 1:4.0:4.8, cellulose:TBS chloride:imidazole, Fig. 3b, Fig. 4).

The assignment of the peaks in the COSY NMR spectra was additionally verified by hetero-nuclear two-dimensional methods. The HSQC DEPT spectrum of **15c** shows the main structure with 3-mono-*O*-methyl-2,6-di-*O*-acetyl moieties and all substructures, which were already identified by COSY NMR spectroscopy, as can be clearly concluded from the cross peaks (Fig. 4).

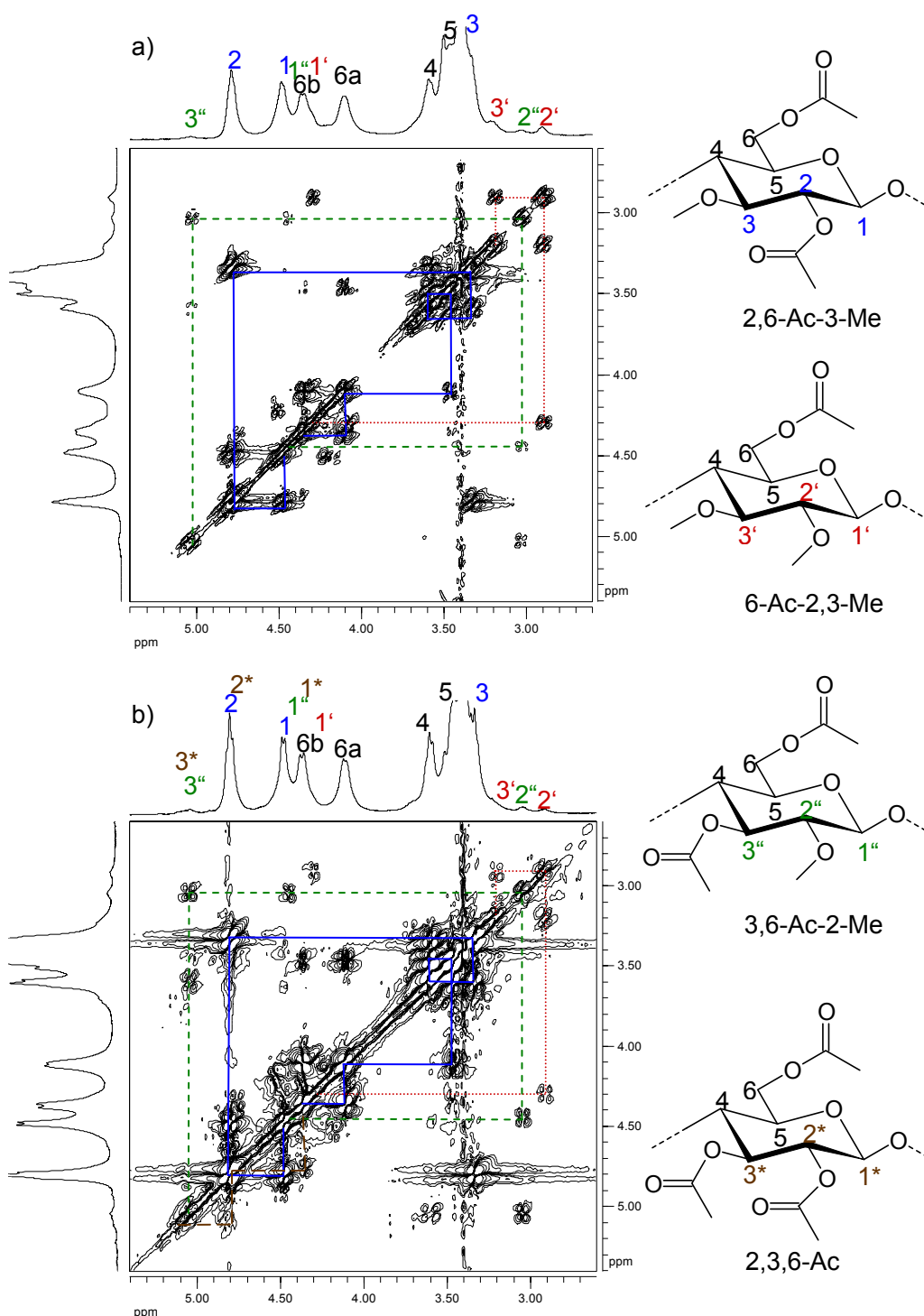


Fig. 3. ^1H , ^1H COSY NMR spectra of acetyl methyl cellulose **9c** (a) and **15c** (b) in CDCl_3 . Silylation conditions: **9** (DS_{Si} 1.98): molar ratio 1:3.5:4.2 (cellulose:TBS chloride:imidazole), 24 h, 20°C ; **15** (DS_{Si} 2.11): molar ratio 1:4.0:4.8 (cellulose:TBS chloride:imidazole), 24 h, 100°C ; assigned cross-peaks: — cross-peaks of the unit 2,6-di-O-acetyl-3-mono-O-methyl (2,6-Ac-3-Me); cross-peaks of the unit 6-mono-O-acetyl-2,3-di-O-methyl (6-Ac-2,3-Me), positions marked with ' , --- cross-peaks of the unit 3,6-di-O-acetyl-2-mono-O-methyl (3,6-Ac-2-Me), positions marked with " , ——— cross-peaks of the unit 2,3,6-tri-O-acetyl (2,3,6-Ac), positions marked with *.

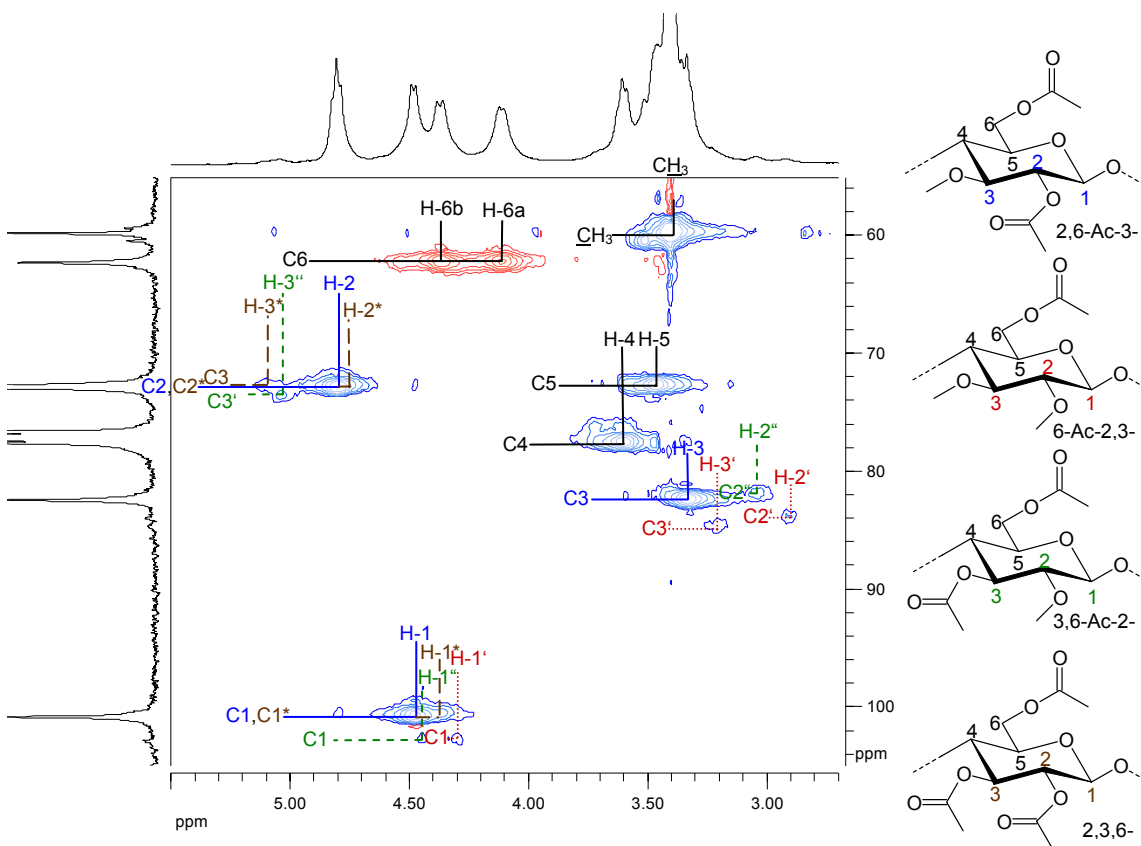


Fig.4. HSQC DEPT NMR spectrum of acetyl methyl cellulose **15c** in CDCl_3 . Silylation conditions: **15** (DS_{Si} 2.11): molar ratio 1:4.0:4.8 (cellulose:TBS chloride:imidazole), 24 h, 100°C ; assigned cross-peaks: — cross-peaks of the unit 2,6-di-*O*-acetyl-3-mono-*O*-methyl (2,6-Ac-3-Me); ... cross-peaks of the unit 6-mono-*O*-acetyl-2,3-di-*O*-methyl (6-Ac-2,3-Me), positions marked with ', --- cross-peaks of the unit 3,6-di-*O*-acetyl-2-mono-*O*-methyl (3,6-Ac-2-Me), positions marked with *, — cross-peaks of the unit 2,3,6-tri-*O*-acetyl (2,3,6-Ac), positions marked with *.

CONCLUSIONS

By silylation of cellulose with tert-butyldimethylchlorosilane in DMA/LiCl, regioselectively functionalized 2,6-di-*O*-protected biopolymer derivative is accessible for the first time. The silylation of cellulose with tert-butyldimethylchlorosilane in DMA/LiCl may show same regioselectivity as the silylation of the biopolymer with thexyldimethylchlorosilane. By means of subsequent methylation and acetylation procedures, it is possible to calculate the DS values and to identify the chemical structure of the repeating units in the polymer chain using one- and two-dimensional NMR techniques. The main structure is 2,6-di-*O*-silylated anhydroglucose. Moreover, it was even possible to analyze substructures including 3,6-di-*O*- and 6-mono-*O*-silyl repeating units, although in small amounts. 2,3,6-tri-*O*-silyl units were formed at high reaction temperatures independent of the molar ratio and the resulting DS. Thus, the results allow synthesizing products with controlled regioselectivity. Moreover, the results show again that NMR spectroscopy is a powerful tool to analyze cellulose derivatives, provided an

appropriate sample preparation is carried out, i.e., methylation, desilylation, and acetylation of the silyl cellulose.

ACKNOWLEDGMENTS

Th. Heinze gratefully acknowledges financial support of the “Fonds der Chemischen Industrie” of Germany.

REFERENCES CITED

- Erlar, U., Mischnick, P., Stein, A., and Klemm, D. (1992) “Determination of the substitution patterns of cellulose methyl ethers by HPLC and gas-liquid chromatography - comparison of methods,” *Polym. Bull.* 29(3-4), 349-356.
- Heinze, T. (2004). “Chemical functionalization of cellulose,” in *Polysaccharides: Structural Diversity and Functional Versatility*, S. Dumitriu (ed.), 2nd Ed., Marcel Dekker, New York, Basel, Hong Kong, Chapter 23, 551-590.
- Heinze, T., Liebert, T., and Koschella, A. (2006). *Esterification of Polysaccharides*, Springer Verlag, Heidelberg, pp. 151.
- Hermanutz, F., Gähr, F., Oppermann, W., Pirngadi, P., Stein, A., and Karstens, T. (2001). “Process for producing silylated cellulose for thermoplastic processing,” *Chemical Fibers Int.* 51, 271-272.
- Karakawa, M., Mikawa, Y., Kamitakahara, H., and Nakatsubo, F. (2002). “Preparation of regioselectively methylated cellulose acetates and their ^1H and ^{13}C NMR spectroscopic analyses,” *J. Polym. Sci. Part A: Polym. Chem.* 40, 4167-4179.
- Klemm, D., and Stein, A. (1995). “Silylated cellulose materials in design of supramolecular structures of ultrathin cellulose films,” *J. Macromol. Sci., Part A: Pure Appl. Chem.* A32, 899-904.
- Klemm, D., Schnabelrauch, M., Stein, A., Philipp, B., Wagenknecht, W., and Nehls, I. (1990). “New results for homogeneous esterification of cellulose by soluble intermediates,” *Papier* 44, 624-632.
- Koschella, A., Heinze, T., and Klemm, D. (2001). “First synthesis of 3-*O*-functionalized cellulose ethers via 2,6-di-*O*-protected silyl cellulose,” *Macromol. Biosci.* 1, 49-54.
- Koschella, A., Fenn, D., and Heinze, T. (2006a). “Water soluble 3-mono-*O*-ethyl cellulose: Synthesis and characterization,” *Polymer Bull.* 57, 33-41.
- Koschella, A., Fenn, D., Illy, N., and Heinze, T. (2006b). “Regioselectively Functionalized Cellulose Derivatives: A Mini Review,” *Macromol. Symp.* 244, 59-73.
- Pawlowski, W. P., Sankar, S. S., Gilbert, R. D., and Fornes, R. E. (1987). “Synthesis and solid state carbon-13 NMR studies of some cellulose derivatives,” *J. Polymer Sci., Part A, Polymer Chem.* 25(12), 3355-3362.
- Petzold, K., Koschella, A., Klemm, D., and Heublein, B. (2003). “Silylation of cellulose and starch - selectivity, structure analysis, and subsequent reactions,” *Cellulose* 10, 251-269.

- Petzold, K., Klemm, D., Heublein, B., Burchard, W., and Savin, G. (2004). "Investigations on structure of regioselectively functionalized celluloses in solution exemplified by using 3-*O*-alkyl ethers and light scattering," *Cellulose* 11; 177-193.
- Schaub, M., Wenz, G., Wegner, G., Stein, A., and Klemm, D. (1993). "Ultrathin films of cellulose on silicon wafers," *Adv. Mater.* 5, 919-922.
- Stein, A., and Klemm, D. (1995). "Selektive Cellulose Derivatisierung unter heterogenen Reaktionsbedingungen und Strukturaufklärung mit mehrdimensionaler NMR-Spektroskopie," *Papier* 49, 732-739.

Article submitted: Oct. 10, 2007; Peer-review completed: Nov. 27, 2007; Revised version received and accepted: Dec. 7, 2007; Published: Dec. 9, 2007.

SONOCHEMICALLY MODIFIED WHEAT STRAW FOR PULP AND PAPERMAKING TO INCREASE ITS ECONOMICAL PERFORMANCE AND REDUCE ENVIRONMENTAL ISSUES

Levente Csóka,^{a*} Attila Lorincz,^{b)} and Andras Winkler^{a)}

Wheat straw (an agricultural by-product) was pulped by an alkaline anthraquinone (AQ) process. Then the straw pulp was treated by high-power ultrasound under different noble-gas (argon, krypton, xenon) combinations. The pulps' degree of beating and acid-insoluble lignin content were measured. Handsheets were made from sonicated and control pulps and tested for paper tensile strength. In this study we explore which noble-gas combination with ultrasound may be more useable to reduce the lignin content and enhance fibrillation. We also describe the most effective ultrasound-assisted, modified alkaline pulping process. Overall, we found that in two steps ultrasonification decreased the residual lignin contents more than 75 %, the pulp fibrillation increased from 12 to 70 °SR within 20 min. of ultrasound irradiation, and the tensile index of the handsheets increased by 65%. For sustainable paper production, it is required to develop alternative paper resources. Paper made from alternate fiber resources with efficient technology will improve our living standards without sacrificing the environment, our habitat. High frequency ultrasound-based pulp processing offers significant improvements, and it reduces energy and chemical consumptions for pulp and paper production.

Keywords: *Sonochemistry, Ultrasound, Wheat straw, Alkaline pulping*

Contact information: a: Institute of Wood and Paper Technology, University of West Hungary, 9400 Sopron, Bajcsy Zs. E. u.4. Hungary b: Private entrepreneur, Mosonmagyaróvár, Magyar. u. 17. Hungary
**Corresponding author: lcsoka@fmk.nyime.hu*

INTRODUCTION

The chemical industry and large scale industrial technology for the manufacture of cellulosic pulp traditionally have relied to a large extent on the utilization of softwoods. Because paper production is increasing, pine forests have been more and more insufficient for this rapid growth, so that utilization of hardwoods has increased in the last decades. Most of these technologies developed for mass production of paper are based on the utilization of trees. Their theory and implementation have made it possible to increase the profitability of wood processing technologies. However harvesting and cutting of forest trees to obtain cellulose have reached the level of irreversible damage, and there can be serious environmental issues.

Agricultural residues such as wheat straw, which is the most frequently used annual plant in the pulp and paper industry, have been considered as fibrous raw materials for almost one hundred years. Wheat straw can yield about 4.0 t/a.ha amount of biomass annually from one hectare, compared to 1.0 t/a.ha for pine, because softwoods

need to grow for many years before cutting [Annus 1991]. Nearly 300 million tons of wheat straw are produced yearly in North America and Europe and only 8% of the world paper industry's total fibre consumption comes from wheat straw [Paper Technology 2006]. In the first half of the twentieth century, straw was still a significant raw material for the paper industry, yet its consumption in the industrial states has rapidly decreased since the 1940s [Rab 1993]. Wheat straw can be represented again as a significant fiber substitution opportunity for the next centuries. To date, straw pulps have been manufactured mainly by soda-anthraquinone and neutral or alkaline sulfite processes.

In cases of trees, only a certain part of it is utilizable or worth obtaining as papermaking fibrous material, while in the case of annual plants the whole plant – including leaves, nodes –, can be utilized for that purpose. Comparing the annual yields, we can assume that the biomass volume obtainable annually by photosynthesis in an arable unit is much higher in cases of annual plants than woods. The cellulose content of wheat straw stem is almost same as woods (35-40%), the hemi-celluloses content is higher (45-55%), while their lignin content is lower (15-20%).

Application of ultrasound techniques in the food industry result in more attention to the depolymerization of macromolecules, the preparation of emulsions, the disruption of biological cells, and the deflocculation of other solid materials that exist as flocs. It has been found that the extraction of organic compounds contained within the body of plants and seeds by a solvent are significantly improved by use of powerful ultrasound. The first direct extraction of lignin polymer by use of ultrasound has been reported in 2002 [Sun et. Al. 2002].

The aim of this study was to show how combinations of ultrasound in the presence of noble gas could be used for direct extraction of lignin molecules from alkali-anthraquinone pretreated wheat straw for papermaking. Ultrasound is a useful tool in nearly every case where a liquid and a solid must react. Furthermore, since ultrasound can radiate through large volumes of liquid, it is well suited for industrial applications. Liquid processing rates of 200 L/min are routinely accessible with acoustic power of 20 kW per unit [Suslick 2001].

EXPERIMENTAL

Materials

In manufacturing pulp from wheat straw (*triticum aestivum*), the whole wheat stem including leaves and knots were used. Wheat stems of suitable chopped size (20-40 mm) were pulped with alkaline anthraquinone (AQ) treatments.

Methods

Pulping procedures were carried out in a batch digester, rotating autoclave. The reaction temperature was 150°C, reaction time 20 min, and the reagents NaOH 15% and AQ 0.1% on o.d raw material. After washing the pulp, different ratios of pulp to water (2g in 140 ml, 2g in 210 ml and 2g in 280 ml distilled-water) and 2g in 210 ml distilled water under argon, krypton and xenon noble-gas compilations were irradiated by high-power ultrasound. The irradiation was carried using a TESLA sonication system

(20 kHz) provided with a transducer at sonic power of 150W/h and sonication time of 20 min in distilled water solution at room temperature, without cooling the reactor vessel. After the measurement of beating degree, the pulp was filtrated on a filter-paper and stored at 5°C until further chemical and mechanical testing, without blending or screening. Mineral acids were used to solubilize and hydrolyze carbohydrates in cell wall samples, leaving the lignin residue to be determined by gravimetric methods according to MSZ-EN 8234-87. The straw was burned at $575\pm 25^{\circ}\text{C}$ for 2 hours, and the residual minerals, i.e. the inorganic materials, were determined as ash content according to MSZ-ISO 1762.

RESULTS AND DISCUSSION

In this study six alkaline wheat straw pulp preparations were treated with application of ultrasound with and without noble-gas combinations. The anthraquinone-alkaline pulping procedure resulted in 55-65% yields of fibrous raw material at 17°SR degree of beating. The drainability of the pulps is summarized in Fig. 1.

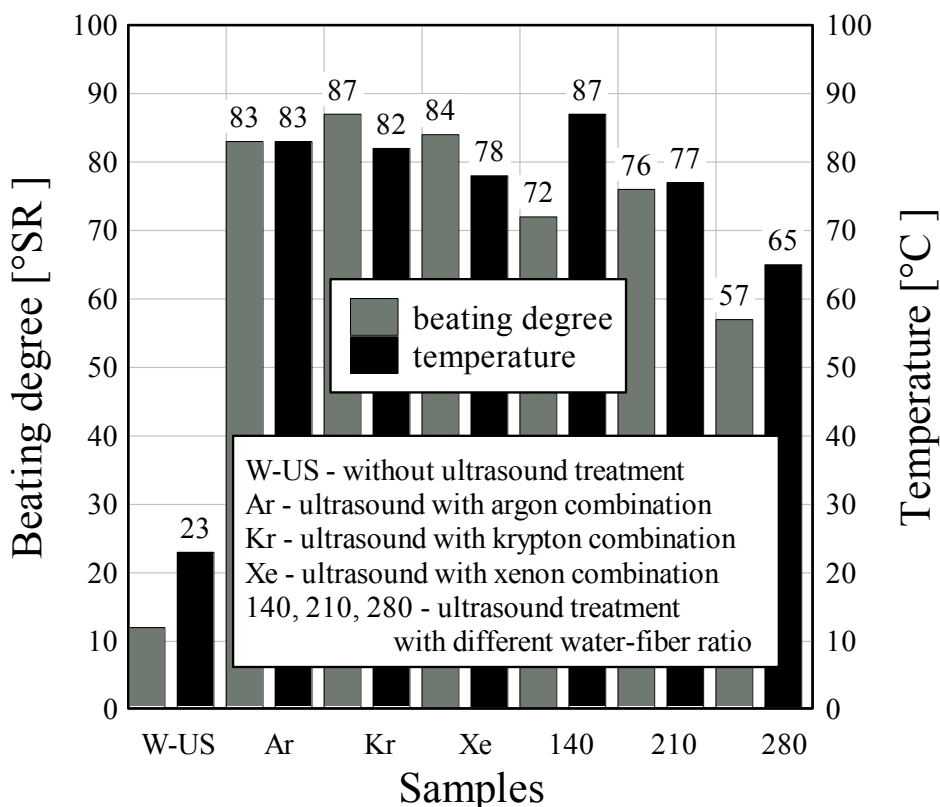


Fig. 1. Variation of beating degree under different ultrasound treatments

The ultrasonic treatment of the pulps resulted in increasing refining of the 140 and 210 samples, whereas there was a decrease in the case of the 280 sample. If the fiber-to-water ratio is lower, the mechanical effect of ultrasound on the cell walls is stronger,

resulting in an increased fibrillation. This helps also to dissolve the lignin components, and makes the cell wall structure accessible for further chemical reactions. All of the noble-gas and ultrasound combinations had the same result in terms of beating degree. In the present stage of the investigation it is not possible to ascertain which noble-gas has stronger influence on wheat straw pulp. Please note that the temperature changed during the sonication treatments. All of the results follow logically from the beating results; however the temperature rise did not have any physical consequences.

The acid-insoluble lignin fractions – reduced by ash – of the samples are shown in Fig. 2.

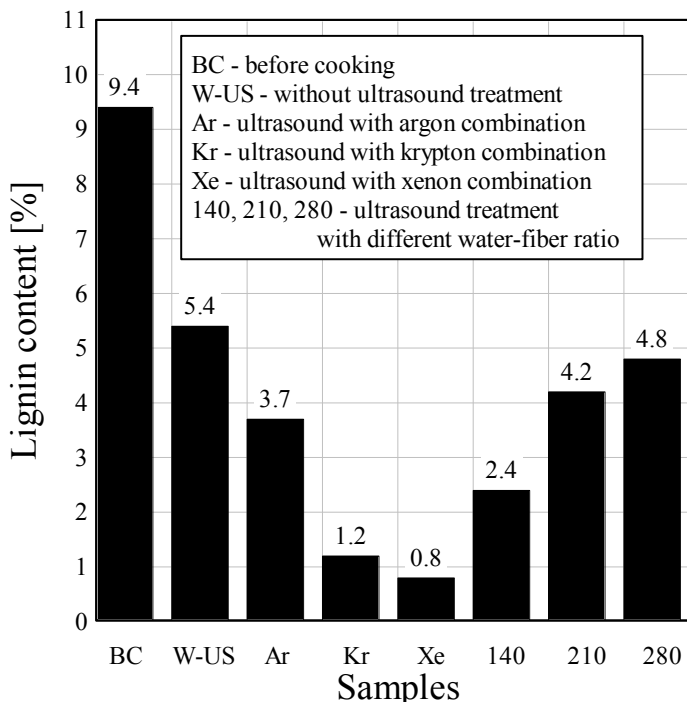


Fig. 2. Variation of lignin content of wheat straw and wheat straw pulp under different ultrasound treatments

The lignin content of the non-processed straw was 9.4%. After alkaline-athraquinone cooking treatment, the lignin content decreased to 5.4%. The ultrasonic irradiation resulted 2.4, 4.2 and 4.8% residual lignin in the experiments, in which 2g wheat straw pulp were suspended in 140, 210 and 280 ml distilled-water, respectively. The irradiation conditions were maintained constant; however the dissolution of lignin components from cell walls increased. During the irradiation of the densest water-fiber sample, more than half of the total lignin in the cooked pulp was released. The noble-gas combination resulted in raising lignin extractions from the fiber walls. The highest efficiency of the ultrasound-assisted lignin solubility was found when xenon gas was present during the treatment. It has been reported [Suslick 1989] that if xenon fills a cavity, the peak temperature reached during cavity implosion will be high, because xenon conducts heat poorly and retains the heat of the collapsing cavity – compared to argon, This is because xenon gas has the highest molecular weight among the noble gases considered. Consequently, the chemical effects of ultrasound do not arise from a direct

interaction with molecular species: No direct coupling of the acoustic field on a molecular level is responsible for sonochemistry or sonoluminescence. These derive from acoustic cavitation, which serves as an effective means of concentrating the diffuse energy of sound. However, as one would expect, the sonolysis of water produces both strong reductants and oxidants, which leads primary products H_2 and H_2O_2 of dissociation of water [Riesz 1985]. The latter may help the degradation and dissolution of lignin macromolecule through the well known bleaching reactions.

Using the obtained pulps we have produced standard laboratory hand sheets and measured their tensile strength. Results of the measurement are shown in Fig. 3.

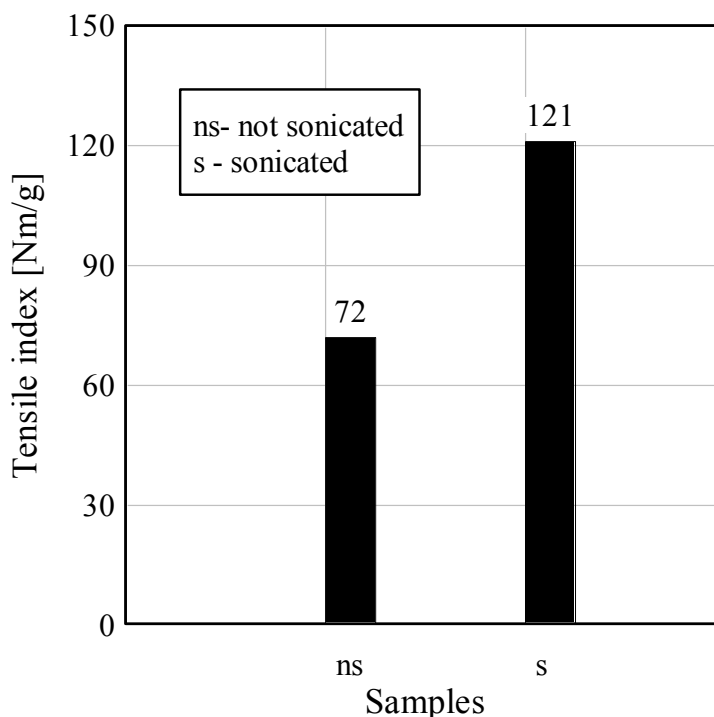


Fig. 3. Effect of sonication on the tensile index of paper test sheets from straw pulp

When analyzing the data it should be taken into account that freeness of the unbleached pulp made of wheat straw is only $17^{\circ}SR$, while that of sonically bleached and milled straw pulp is $45^{\circ}SR$. It has been previously reported (Hernadi 2006) that unbleached wheat straw kraft pulps have 74-76 Nm/g tensile strength at $35^{\circ}SR$ and bleached pulps have 65 Nm/g at $42^{\circ}SR$. Based on physical properties, it can be stated that the tensile strength of unbleached, alkaline cooked wheat straw pulp was 72 Nm/g, while that of sonically bleached and sonically milled straw pulp was 121 Nm/g. Without mechanical milling of straw pulps, almost a doubling of tensile strength could be achieved by using ultrasound.

Further on we compared the pulp samples by electron-microscopy. Figure 4 shows electron-microscopy photos of the pulps. Based on the photos it can be stated that sonication resulted in a strongly fibrillated structure, and there was no diameter difference between the two pulps.

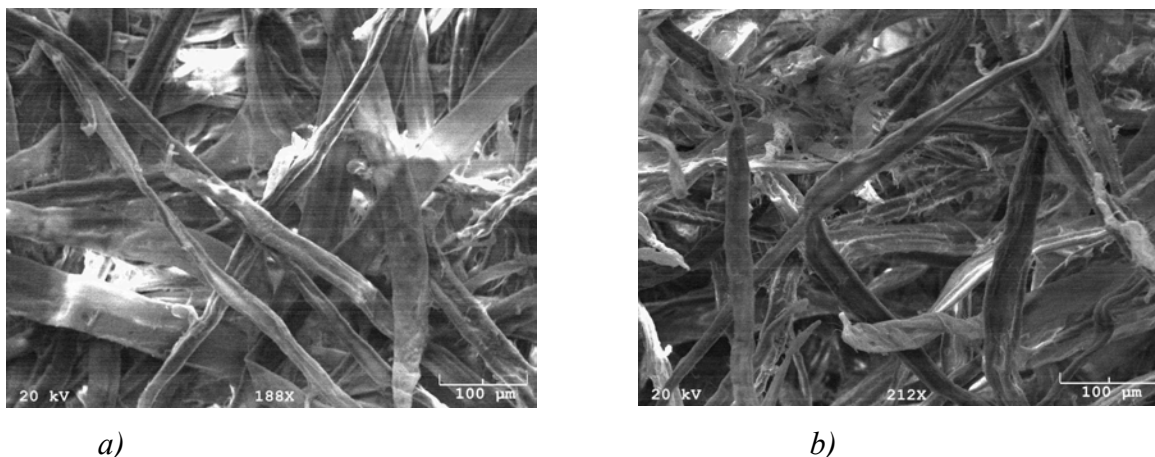


Fig. 4. Scanning electron microscopy images of a) non-sonicated and b) sonicated straw pulps

CONCLUSIONS

1. Ultrasound-irradiation of wheat straw pulp in the presence of inert gases, after alkaline AQ pre-treatment made possible the further dissolution of 31.5-85.2% of the lignin content.
2. SEM images showed that the increased fibrillation of fibers resulted in higher tensile strength of the sonicated straw paper.
3. Based on the results we would like to build a larger, pilot-scale high-power ultrasonic reactor to evaluate the industrial possibilities of sound-induced straw pulping.

ACKNOWLEDGMENTS

We are grateful for the financial support of this research from the ERFARET program of the Hungarian National Office for Research and Technology No. 200508-2.3.

REFERENCES CITED

- Annus, S. (1991). "Papiripari rostok fobb tulajdonsagai," *Papiripar*, 35(2), 188-192.
- Rab, A., and Szikla, Z. (1993). "Suitability of straw pulp for papermaking," in Roberts F. (ed.), *World Pulp and Paper Technology*, Sterling Publications Ltd, London, p: 59-63
- Riesz, P., Berdahl, D., and Christman, C. L. (1985). "Free radical generation by ultrasound in aqueous and nonaqueous solutions," *Environmental Health Perspectives* 64, 233-252
- Riddlestone, S. (2006). "Industry update: MiniMill trials show UK can make paper from straw," *Paper Technology* 47(6), 46-47.
- Sun, R. C., and Tomkinson, J. (2001). "Comparative study of lignins isolated by alkali and ultrasound-assisted alkali extractions from wheat straw," *Ultrasonics Sonochemistry* 9, 85-93.

- Suslick, K. S. (1989). "The chemical effects of ultrasound," *Scientific American* 260, 80-86.
- Suslick, K. S. (2001). "Sonoluminescence and sonochemistry" in *Encyclopedia of Physical Science and Technology*, 3rd Ed. R. A. Meyers (ed.); Academic Press, Inc.: San Diego.

Article submitted: Oct. 9, 2007; Peer review completed: Nov. 27, 2007; Revised version received and approved: Dec. 11, 2007; Published: Dec. 13, 2007.

RADIOGRAPHIC OBSERVATIONS ON THE USE OF TWO DIFFERENT REGENERATION MATERIALS IN A SINGLE SUBJECT: CASE STUDY

Peter N. Galgut, Ph.D., M.Phil., M.Sc., BDS., MRD.RCS.

Two infrabony defects (i.e. defects in tooth supporting bone that extend into the body of the bone) in different sites in the same individual were treated surgically. Tissue regeneration was incorporated into the surgical procedures using a different material in each site (oxidized cellulose mesh and bioglass). The post surgical radiographic appearance showed increasing calcification in both sites that was not complete even at 15 months after placement. The radiographic appearance of both sites was similar but calcification was observed above the crest of alveolar bone in the oxidized cellulose mesh site that was not present with bioglass site. As calcification did not appear to be complete by 15 months after placement and it did not resemble true bone in either site, it would appear that the regenerative process was not yet complete by this time. Bone regeneration may therefore progress slowly over a protracted period of time after placement. Some evidence is present that oxidized cellulose mesh may have enhanced regenerative capacity by comparison to other synthetic bone regeneration materials such as hydroxyapatite and bioglass. No conclusions could be drawn from this single case study and further work is necessary to confirm and investigate these observations more fully.

Keywords: Guided tissue regeneration, Hydroxyapatite, Bioglass, Oxidized cellulose, Tissue regeneration, Bone formation, Biomaterials

Contact information: Dr Peter Galgut, 26 Pembroke Hall, Mulberry Close, Hendon, London NW4 1QW, United Kingdom. E-mail: "Admin" <peter@periodontal.co.uk>

INTRODUCTION

Periodontal disease is a condition affecting the majority of the adult population to a greater or lesser degree. Essentially, accumulation of microbial dental plaque biofilm causes the release of toxic and irritant by-products, which causes inflammation of the gingival (i.e. gum) margins known as gingivitis. With time the inflammation becomes so established as to result in a conversion from superficial inflammation to deeper seated destructive change. This results in breakdown of the delicate seal between the gingival margins and the teeth, with formation of pockets of dental plaque infection below the gingival margins. This is known as periodontitis and is characterized by the formation of periodontal pockets. These periodontal pockets, contaminated by pathogenic plaque bacteria, cause more deep-seated inflammatory change. This results in more destruction of the attachment of the teeth to the underlying bone, but more importantly resorption of the supporting bone. As a result of increasing loss of bony support, the gingivae recede,

and the teeth start to become mobile and drift out of alignment. Ultimately abscess formation and tooth loss occur.

Management of this condition is aimed at eliminating and controlling the reinfection of pathogenic bacteria in dental plaque biofilm to arrest of the condition. While eliminating plaque biofilm from periodontal pockets is often successful, recontamination does occur, and retreatment may be necessary. As a result the condition can be arrested in most cases, but in some instances retreatment is necessary to maintain health.

The major problem in periodontics is that once bone loss has occurred, it will not spontaneously regrow. This is a well known problem in many medical situations in which bone is lost, and that while the remaining bone has the capacity for regrowth, the memory matrix for the missing bone is lost, and the osteoblasts are unable to regenerate the lost bone. Therefore, in the management of periodontitis, but also other medical conditions in which bone loss is a feature, achieving regeneration of the lost bone is a primary objective outcome that has eluded clinicians. Considerable research has been directed at achieving regeneration of bone in clinical situations.

Essentially there are two ways of achieving tissue regeneration in defects in bone caused by destructive periodontal diseases: grafting/infill techniques, and guided tissue regeneration (GTR).

Achieving bone regrowth using grafting/infill techniques by demineralised freeze-dried bone has been very popular, and good results have been reported. However increasing concerns in the general population and the profession about the use of tissue-derived products has resulted in an increasing use of synthetic alternatives. Many materials have been used for this purpose, and these have included plaster of Paris (Radentz and Collings 1965) and hydroxyapatite/tri-calcium phosphate materials (Galgut 1990, 1992, 1998). Plaster of Paris was used many years ago, with little apparent success, although there has been some revival in interest in this material more recently. The hydroxyapatites and tri-calcium phosphate materials are manufactured for dental use in many different forms, which include resorbable/non-resorbable, sintered/non-sintered, and different physical structures, all of which were claimed to give superior results. However, when used clinically, it has been reported that these materials do not live up to expectations (Galgut et al. 1992; Polson and Yukna 1994; Stahl and Froum 1987; Caranca et al. 1987), and therefore the use of these materials in clinical practice has waned with time. More recently bioglasses have been developed for use in infrabony defects to encourage bone regrowth. BioGlass® was developed by Professor Larry Hench in response to a request by the American Medical Corps to develop a material to help regenerate bone for Vietnam war veterans who had suffered extensive bone damage. As with all glass it is made up predominantly of silicon dioxide (SiO_2), but other substances include Na_2O , CaO , and P_2O_5 , but characteristically, in a high $\text{CaO}/\text{P}_2\text{O}_5$ ratio, which makes BioGlass® highly bioactive in aqueous media. Results of the use of these materials clinically have been encouraging (Wilson and Low 1992; Zamet et al. 1997).

Guided tissue regeneration has been used extensively to achieve regeneration of bone and periodontal structures. This technique employs barrier membranes, placed over bony defects to preferentially promote bone growth as opposed to scar tissue formation

from maturing granulation tissue. A number of different membrane materials have been used, and results of treatment using this technique have been good.

Cellulose based wound dressings were developed by Johnson & Johnson for medical use in the early 1980's, and a specific dressing to promote wound healing in dentistry called Surgicel (oxidized cellulose mesh) was produced as a post dental extraction dressing for use in the mouth. This material occluded and sealed the extraction socket wounds by absorbing blood from the wounds, which then clotted to form a semirigid blood-mesh conituum. The product, being extracted from seaweed contains high CaPO_4 concentrations which were claimed to provide the mineral basis for enhanced bone growth. In addition the material was claimed to be bacteriostatic. This material has been used to promote healing in dentistry for many years, and more recently in surgical applications (Sharma et al 2003) to control postoperative haemorrhage. Different forms of this material have also been used to aid in tissue regeneration of cartilage (Svensson et al 2005). Being licensed for use in the oral cavity, with the ability to form an infill and scaffold to support maturing granulation tissue, with natural biodegradable properties which potentially encouraged bone regeneration, and with bacteriostatic properties, oxidized cellulose mesh seemed to have ideal properties for consideration as a bone regeneration material in the treatment of periodontal defects in bone arising from the ravages of destructive periodontal diseases.

This author has published a number of case studies (Galgut 1990, 1990) utilising oxidized cellulose mesh to achieve enhanced regeneration of periodontal tissues using the GTR technique. In attempting to reduce the amount of postoperative attachment loss, a combination technique using hydroxyapatite as an infill material, followed by oxidized cellulose mesh used as a protective and exclusive membrane has been described (Galgut 1990). However, it was shown that the clinical benefit using this combination technique was limited. Subsequently, another variation of this technique has been described (Galgut 1994) in which the oxidized cellulose mesh was cut into small pieces and placed incrementally into a defect to act as a scaffold for maturing blood clot and granulation tissue, as well as over it to act as a protective membrane, using the material in a combined infill and GTR technique. A case report has been published (Galgut 1998), demonstrating that similar results can be achieved in clinical healing when using oxidized cellulose mesh in this way, as compared to bioglass. Although these case studies (Galgut 1994, 1998, 1990, 1990) have shown good results clinically, the question remains as to whether actual tissue regeneration using this material occurs, and how it compares to other materials used for this purpose.

AIM

The aim of this paper is to compare radiographically the amount of bone re-growth using oxidized cellulose mesh versus bioglass placed into two surgically exposed defects in the same patient.

MATERIALS AND METHODS

The subject for this case study was a 50 year old medically healthy Caucasian male who had been referred for periodontal treatment. On initial examination it was found that multiple periodontal pockets of infection were present, ranging from 4 to 8mm in depth, the plaque score was 75% (indicating very poor oral hygiene), and the gingival bleeding score was 16% (demonstrating the presence of high levels of active inflammation). Periapical radiographs using a paralleling technique were taken pre-operatively. The patient was referred to the practice hygienist for an initial phase of treatment, which included oral hygiene instruction, supra- and subgingival scaling, and root planing of the periodontal pockets. After completion of the initial phase of treatment, the patient was seen for further scaling and root planing of the residual pockets by the author. After four weeks the healing response was assessed, and very little reduction in probing depths had occurred in a number of pockets, predominantly tooth 23, and teeth 45, 46, and 47, although the plaque score and gingival bleeding scores had reduced to negligible levels. Surgery was therefore indicated and, as infrabony defects were present, it was decided to use a regeneration technique to promote infill of these defects. Replaced flap surgery was undertaken using local anaesthetic, taking care to preserve as much of the gingival tissue as possible. The surgical flaps were reflected, the root surfaces exposed, and residual accretions were removed. The surgical sites were then flushed with a weak solution of hydrogen peroxide to cleanse and disinfect them prior to placement of the regenerative materials. Oxidized cellulose mesh (Surgicel®, Johnson & Johnson Ltd., Slough, U.K.) was placed using an incremental technique in the defect in tooth 23, using a technique previously described (Galgut 1994), and bioglass (Perioglass®, US Biomaterials Corp., Florida, USA.) was placed in the defects on teeth 45, 46, and 47. The patient was instructed to brush the teeth at the surgical sites very lightly, taking care to avoid brushing the gingival margins, and to rely on the use of chlorhexidine mouthwash three times a day after meals during the initial healing period. The patient was seen one week later for removal of sutures, at which time healing was progressing satisfactory. The patient was seen three monthly thereafter for maintenance visits. As clinically observable gingival health had been achieved, with resolution of periodontal pocketing, no radiographs were taken until the fourth review appointment after surgery which was in fact 15 months after the initial preoperative radiographs.

RESULTS

The results of this case study are presented in the radiographs listed as Fig. 1 a,b (pre-operatively and 15 months postoperatively) and Fig. 2 a,b (pre-operatively and 15 months postoperatively) for infrabony defects between the teeth).

Figure 1a shows the defect in the bone surrounding the teeth pre-operatively. This was a "gutter" defect extending circumferentially around teeth, together with horizontal bone loss. This site received oxidized cellulose mesh, filling the "gutter" and covering the defect to a thickness of approximately 1.5mm above the alveolar crest. Figure 1b, a radiograph taken 15 months after placement, shows a band of partial radio-

opacity extending approximately 1 mm supra-crestally around teeth, with some increase in radio-opacity in between the teeth. The increase in radio-opacity in this infra-bony defect in between the teeth is difficult to discern, because a thick plate of cortical bone was present, which masked the extent of the defect on these radiographs. Nevertheless the supra-crestal radio-opacity is clearly visible, and it should be noted that this is not as radiodense as the original alveolar bone, indicating that the radiodensity of the calcified material filling the defect, presumably bone, was not equivalent to the original alveolar bone at this point in time.

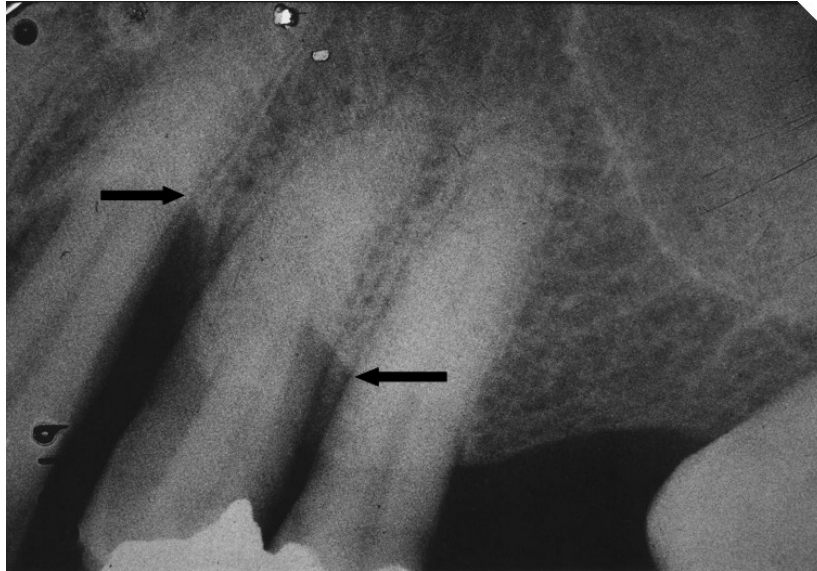


Figure 1a. Radiograph showing bone loss around several teeth with an infrabony defect between two teeth (see arrow).

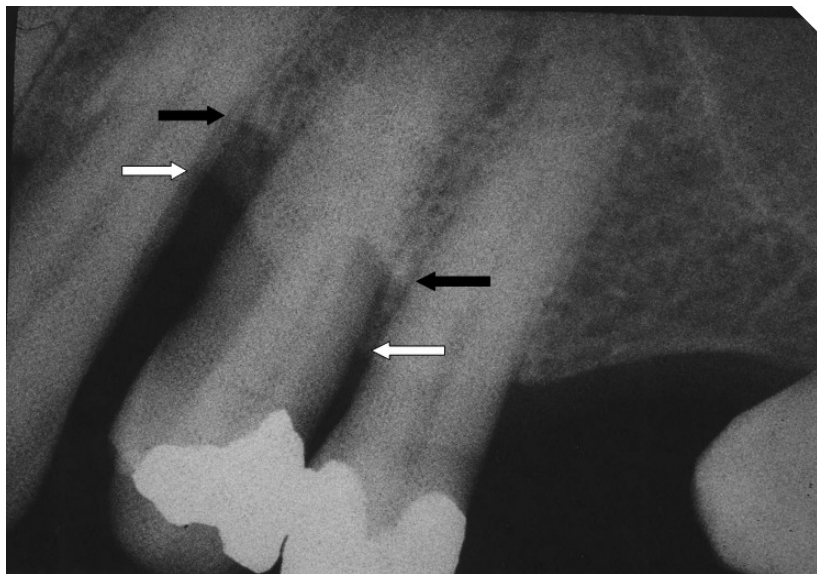


Figure 1b. Radiograph of the same site 15 months postoperatively showing infill of the infrabony defects (see arrows) and an increase in radiodensity supracrestally, which has not matured to form the radiographic characteristics of bone. (White arrows = change; black = baseline.)

Figure 2a shows other defects in a different site in the same patient pre-operatively. It can be seen that extensive horizontal and vertical bone loss had occurred.

At 15 months postoperatively (Fig. 2b) it can be seen that the defects had partially filled in. A diffuse partially radio-opaque material is visible interdentally and coronally to the bony margins of the original infrabony defect (see arrows).

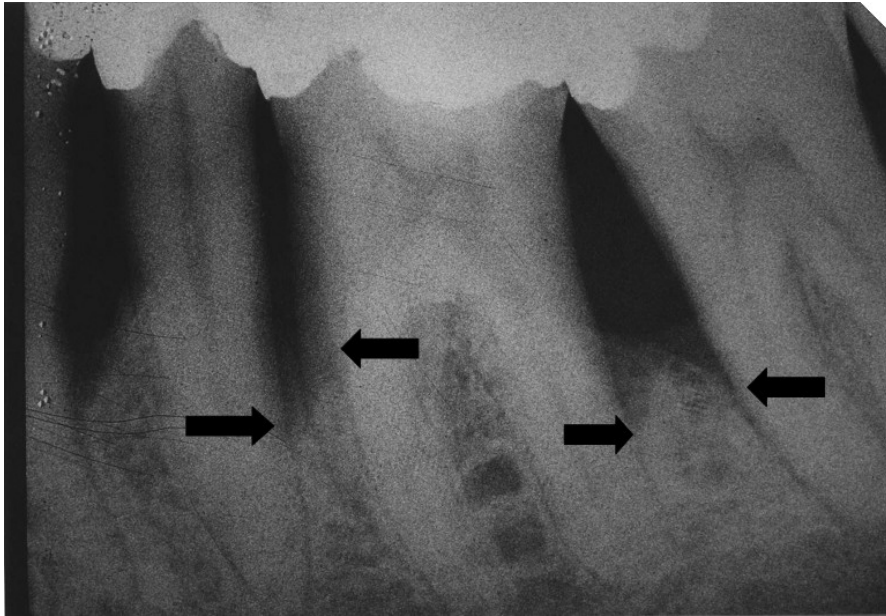


Figure 2a. Pretreatment radiograph showing bone loss and infrabony defects between several teeth.

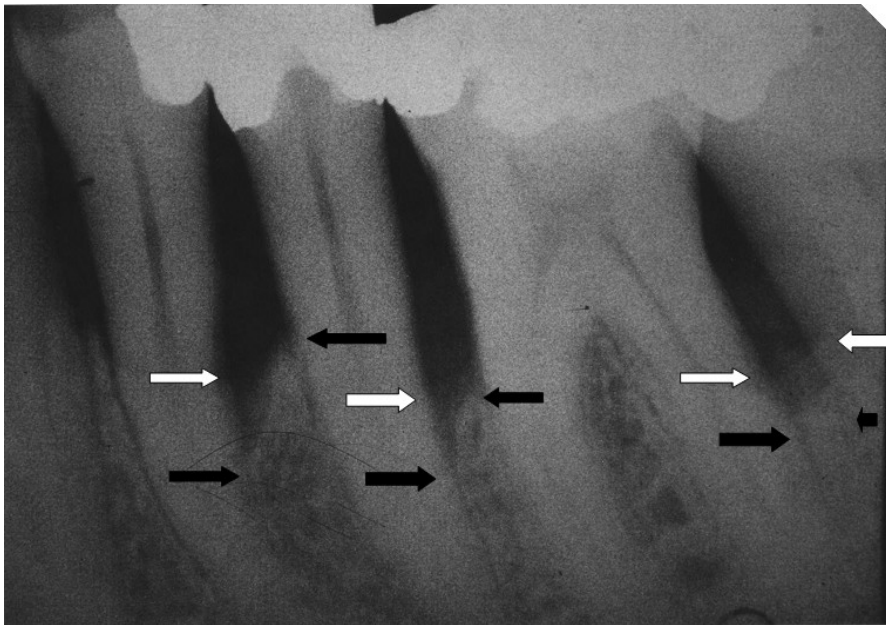


Figure 2b. Radiograph of the same site taken 15 months postoperatively showing an increase in radiodensity in the infrabony defects but only partial infill of the defects. The radiodense material is diffuse and without trabeculations indicating that it had not matured into bone. (White arrows indicate change; black arrows show baseline.)

The defect between the teeth illustrated in Figs. 2a and b show increased radio-opacity, which reduces from the bony surface of the original defect towards the coronal root surface. Furthermore, it should be noted that a clear demarcation line can be seen between the alveolar crest and the less radio-opaque material. Similarly it should be noted that no clear boundary can be determined at the coronal edge of the healing defects in the 15 monthly post-treatment radiograph. The absence of a clear edge to the partially radio-opaque material indicates an ongoing calcification process, presumably forming bone, which was not yet complete 15 months after placement. If these ill-defined areas of increased radio-opacity indicate a calcification process forming new bone, it seems as though this process was not completed by as long as 15 months after placement.

This characteristic of partial radio-opacity has been observed in both the site that received oxidized cellulose mesh and the site that received bioglass, possibly indicating that the calcification process and bone formation takes place over an extended period of time, exceeding 15 months after placement, irrespective of the material used.

DISCUSSION OF RESULTS

In this paper two sites in the same patient were treated using different defect infill materials to achieve tissue regeneration. The radiographic appearance 15 months after placement indicated some radio-opacity developing in both sites. It may be assumed that this radio-opacity is part of a calcification process that may eventually lead to bone formation. However the radiographic characteristics of neither of these materials resembled bone, as no trabeculations, lamina dura, or radiodense cortical surfaces, characteristic of true bone were visible in either of these sites. Therefore, if bone was forming, it had not completed the regenerative process in either of the treated sites by 15 months after placement.

As both sites were in the same patient, one may assume that the conditions for healing were similar, and the fact that the radiographic appearance of both sites was similar indicates that both infill materials had a similar effect of enhancing calcification, which may lead to the formation of true bone, but this process takes place over a protracted period of time.

A number of clinical studies have shown that very little difference is clinically observable in the amount of regeneration that can be achieved using either G. T. R. or graft/infill techniques (Polson 1994; Polson et al. 1994). The amount of tissue regeneration that can be achieved and the rate of tissue regeneration is dependent on a multitude of factors including postoperative contamination of the site, the cells that repopulate the wound during healing phase, the availability of nutrients, oxygen, and the appropriate cascade of growth factors within the healing wound, over which the clinician has no control (Nerem and Sambanis 1995).

Any conclusions from this case study of only two sites should be viewed with great caution, but the appearance of these sites in which two different materials were used was remarkably similar 15 months after placement both in a radiographic appearance, and the extent of the regenerative process. This observation is in agreement with other more substantial work that has concluded that calcification and bone formation occurs

over an extended period of time, which may be in excess of 12 months with little observable difference between sites treated with different materials (Moon et al. 1996; Polson 1994).

An interesting additional observation was that the site that received the oxidized cellulose mesh was actually showing increased radio-opacity supra-crestally, indicating that bone may have been regenerating above the most coronal margin of the alveolar crest. This was not occurring in the bioglass site, in which the defects were only partially filled and were showing some residual angulation of the crest, characteristic of reduced, but not completely filled infrabony defects. This is a well documented observation with hydroxyapatites, which characteristically achieve calcification/infill only in the deepest parts of infrabony defects, and partial infill coronally (Galgut 1990, 1992, 1998). Therefore, although the radiodensity of both sites was similar, indicating a similar degree of calcification taking place, it was observed that the site receiving the oxidized cellulose mesh not only achieved complete infill of the site, but also has the potential to encourage regeneration supra-crestally. This may be a major advantage of this material in comparison to other synthetic bone regenerative materials. Skoog (1967) highlighted the substantial regenerative capacity of oxidized cellulose mesh in cleft palate cases where it was used to induce new bone formation where no bone previously existed. More recent work demonstrating significant reparative and regenerative properties of oxidized cellulose in gynaecological and cartilage repair procedures support the findings of this case study (Sharma et al. 2003).

Therefore it may in fact be possible to achieve enhanced bone regrowth in periodontal (and other) defects using oxidized cellulose mesh. Whether this effect can be achieved predictably in clinical practice, or this observation is a chance finding, or whether this represents some erroneous interpretation of the radiographs cannot be determined from this single site. Therefore, more work needs to be done in order to confirm this observation.

CONCLUSIONS

No definitive conclusions can be drawn from the radiographic observation of two sites in a single individual. However the interesting observation that calcification, possibly leading to bone formation takes place over an extended period of time, and is not complete by 15 months after placement is supported by other work. In both materials used in this case the calcification process seemed to be similar, an observation also supported by other published work, albeit not using oxidized cellulose for this purpose.

However, the observations that with oxidized cellulose mesh not only was complete defect fill achieved, but some supra-crestal calcification was evident on the radiographs have not been reported previously, and the subject needs to be investigated more fully in more definitive controlled clinical trials.

REFERENCES CITED

- Caranca, F. A., Jr., Kenney, E. B., Lekovic, V., Talamante, E., Valencia, J., and Dimitrijevic, B. (1987). "Histologic study of healing of human periodontal defects after placement of porous hydroxyapatite implants," *J. Periodontol.* 58, 682-688.
- Galgut, P. N. (1994). "A technique for treatment of extensive periodontal defects: A case study," *J. O. Rehab.* 21, 27-32.
- Galgut P. N. (1998). "Occlusion of surgical wounds to improve postoperative healing of tissues in regenerative techniques: Two case reports," *Periodontal Insights*, Sept., 12-16.
- Galgut, P. N. (1990a). "Oxidized cellulose mesh used as a biodegradable barrier membrane in the technique of guided tissue regeneration: A case report," *J. Periodontol.* 61, 766-768.
- Galgut, P. N. (1990b). "Oxidized cellulose mesh: I. Biodegradable membrane in periodontal surgery," *Biomaterials* 11(Oct.), 561-564.
- Galgut, P. N. (1990c). "Oxidized cellulose mesh: II. Using hydroxyapatite bone grafting material in the treatment of infrabony defects," *Biomaterials* 11, 565-567.
- Galgut, P. N., Waite, I. M., Brookshaw, J. D., and Kingston, C. P. (1992). "A 4-year controlled study into the use of hydroxyapatite implant material for the treatment of periodontal bone defects," *J. Clin. Periodontol.* 19, 570-577.
- Galgut, P. N. (1998). "The limitations of tissue regeneration. Independent dentistry," (May), 72-78.
- Galgut, P. N. (1990d). "Variations in healing of infrabony defects treated with ceramic bone grafting material observed radiographically for a period of 3 years," *J. Oral Implantol.* XVI/3, 173-182.
- Moon, I. S., Chai, J. K., Cho, K. S., Wijestoo, U. M., and Kim, C. K. (1996). "Effects of polygalactin mesh combined with resorbable calcium carbonate or replaminiform hydroxyapatite on periodontal repair in dogs," *J. Clin. Periodontol.* 23, 945-951.
- Nerem, R. M., and Sambanis, A. (1995). "Tissue engineering: From biology to biological substitutes," *Tissue Engineering* 1(1), 3-13.
- Polson, A. M. (1994). "Synthetic Grafts and Regeneration," *Periodontal Regeneration: Current Status and Directions*. Quintessence books, Chapter 6: 111, Chapter 9: 164.
- Polson, A. M., Greenstein, G., and Caton, J. G. (1994a). "Resorbable barriers and regeneration," *Periodontal Regeneration: Current Status and Directions*, Quintessence books. Chapter 9, 151-164.
- Polson, A. M., and Yukna, R. A. (1994b), "Synthetic grafts and regeneration," *Periodontal Regeneration: Current Status and Directions*, Quintessence books, Chapter 6: 103-112.
- Radentz, W. H., and Collings, C. K. (1965). "The implantation of plaster of paris in the alveolar process of the dog," *J. Periodontol.* 36, 357-364.
- Sharma, J. B., Malhotra, M., and Pundir, P (2003). "Laparoscopic oxidised cellulose (Surgicel) for small uterine perforations," *Int. J. Gynaecol. Obstet.* 83, 271-275.
- Svensson, A., Nicklasson, E., Harrah, T., Panilaitis, B., Kaplan, D. L., Britberg, M., and Gatenholm, P. (2005). "Bacterial cellulose as a bacterial scaffold for tissue engineering of cartilage," *Biomaterials* 26, 419-431.

- Skoog, T. (1967). "The use of periostem and Surgicel R for bone restoration in congenital clefts of the maxilla," *Scand. J. Plast. Reconstr. Surg.* 1, 113-130.
- Stahl, S. S., and Froum, S. (1987). "Histologic and clinical responses to porous hydroxyapatite implants in human periodontal defects: 3 to 12 months post implantation," *J. Periodontol.* 56, 689-695.
- Wilson, J., and Low, S. B. (1992). "Bioactive ceramics for periodontal treatment: Comparative studies in the patas monkey," *J. Applied Biomat.* 3, 123-129.
- Zamet, J., Darbar, U. K., Griffiths, G. S., Bulman, J. S., Braggar, U., Burgin, W., and Newman, H. N. (1997). "Particulate bioglass as a grafting material in the treatment of periodontal intrabony defects," *J. Clin. Periodontol.* 24, 410-418.

Article submitted: Oct. 3, 2007; Peer-review completed: Nov. 15, 2007; Revised article received and approved: Dec. 16, 2007; Published Dec. 17, 2007.

OPTIMIZATION STUDY OF CITRUS WASTES SACCHARIFICATION BY DILUTE-ACID HYDROLYSIS

Farid Talebnia,^{a,b} Mohammad Pourbafrani,^{a,b*} Magnus Lundin,^a and Mohammad J. Taherzadeh^a

The effects of time, acid concentration, temperature and solid concentration on dilute-acid hydrolysis of orange peels were investigated. A central composite rotatable experimental design (CCRD) was applied to study the individual effects of these hydrolysis factors and also their inter-dependence effects. The enzymatic hydrolysis of the peels by cellulase, β -glucosidase, and pectinase enzymes resulted in 72% dissolution of the peels, including 18.7% galacturonic acid and 53.3% of a total of glucose, fructose, galactose, and arabinose. Dilute-acid hydrolysis up to 210°C was not able to hydrolyze pectin to galacturonic acid. However, the sugar polymers were hydrolyzed at relatively low temperature. The optimum results were obtained at 116°C, 0.5% sulfuric acid concentration, 6% solid fraction, and 12.9 min retention time. Under these conditions, the total sugars obtained at 41.8% dry peels and 2.6% of total hexose sugars were further degraded to hydroxymethylfurfural (HMF). No furfural was detected through these experiments from decomposition of pentoses.

Keywords: Orange peel, Dilute-acid hydrolysis, Experimental design, Sugar optimization

Contact information: a: School of Engineering, University of Borås, 501 90 Borås, Sweden.

b: Department of Chemical and Biological Engineering, Chalmers University of Technology, 412 96 Göteborg, Sweden. *Corresponding author: Mohammad.Pour_bafrani@hb.se

INTRODUCTION

Orange peel, a waste product from citrus processing factories, is partly used for cattle feed. However, the waste has about 66 million tons annual production (Pourbafrani et al. 2007) and a huge amount of it is still discarded to nature, causing several environmental problems (Tripodo et al. 2004). On the other hand, the peel contains various carbohydrate polymers, which make it an interesting choice for production of metabolites such as ethanol by appropriate microorganisms. An individual or combination of mechanical, chemical, and biological pretreatments, however, is required to break down cellulose, hemicellulose, and pectin polymers present in the cell walls of orange peels and convert them to their sugars' monomers (Grohmann et al. 1995; Grohmann and Baldwin 1992; Grohmann et al. 1994).

Enzymatic hydrolysis is an efficient method to release almost all carbohydrates present in the orange peels, but its application is hampered by the high cost of enzymes and the slow rate of the depolymerization reaction (Grohmann et al. 1995). Thus, development of a cost-effective method in which all or a high proportion of carbohydrates could be released will help to commercialize the processes using orange peels as raw materials. The advantages of dilute-acid hydrolysis for peel liquefaction and

releasing carbohydrates prior to enzymatic treatment have already been studied (Grohmann et al. 1995; Vaccarino et al. 1989a). There are different variables that might have impacts on the rate and extent of citrus peel hydrolysis by dilute-acid processes. Temperature, acid concentration (or pH), total solid fraction (TS), and time duration of the hydrolysis are the key variables in this process (Grohmann et al. 1995).

Statistical approaches in experimental design provide powerful tools to study and optimize several factors in a process simultaneously. Full factorial, partial factorial, and central composite rotatable designs (CCRD) are the most common techniques used for process analysis and modeling (Montgomery 2001). When the number of factors and responses increases, the last method (CCRD) is preferred, since it needs fewer tests than the other methods and gives almost as much information as other methods (Obeng et al. 2005). This method has already been applied for hydrolysis of a wide variety of materials to find the optimum conditions for corresponding processes (Canettieri et al. 2007; Rahman et al. 2007; Kunamneni and Singh 2005; Rodriguez-Nogales et al. 2007).

Factors that have previously been applied to investigate and optimize the hydrolysis of orange peels were limited to temperature and acid concentration, using one factor at a time rather than varying them simultaneously. This procedure does not allow studying the interaction between variables (if there is any), and thus the best condition that gives the highest yield of monomeric sugars and lowest yield of by-products cannot be achieved. Furthermore, decomposition of pentoses and hexoses produced to hydroxymethylfurfural (HMF) and furfural through the secondary hydrolysis reactions has not been studied.

The scope of the present work was to apply the central composite rotatable design to evaluate the variables that show significant effects in dilute-acid hydrolysis of orange peel. The main and interaction effects of variables on the yields of total liberated sugars and formation of HMF were studied. Based on the experimental design, a model was developed and the optimum conditions to attain the highest yield of carbohydrates and lowest yield of HMF were predicted and validated by an additional experiment. Furthermore, pectin resistance at high temperatures during acid hydrolysis was particularly investigated.

MATERIALS AND METHODS

Substrates and Enzymes

The orange peels used in this work were the residuals of Spanish orange obtained from Brämhults juice AB (Borås, Sweden) and stored frozen at -20 °C until use. The frozen peels were thawed and ground with a food homogenizer (ULTRA-TURAX, TP 18-20, Janke & Kunkel Ika-Labortechnik, Germany) to less than 2 mm in diameter. Total dry content of orange peel was determined by drying at 110 °C for 48 h. Three commercial enzymes, pectinase (Pectinex Ultra SP), cellulase (Celluclast 1.5 L) and β -glucosidase (Novozym 188), were provided by Novozymes A/S (Bagsvaerd, Denmark). Pectinase activity was measured by hydrolyzing 0.02% citrus pectin (P9135-Sigma) solution at 45 °C in 50 mM sodium acetate buffer at pH 4.8 (Wilkins et al. 2007). Cellulase activity was determined by hydrolyzing Whatman#1 filter paper in 50 mM

sodium acetate buffer at pH 4.8 and temperature of 45°C (Decker et al. 2003). The activities of pectinase and cellulase were measured as 283 international units (IU)/mg protein, and 0.12 filter paper units (FPU)/mg protein, respectively. The activity of β -glucosidase was reported as 2.6 IU/mg solid by the supplier.

Enzymatic and Acid Hydrolyses

Ground peels were added into 250 ml conical flasks containing 50 mM sodium acetate buffer at pH 4.8 to obtain 100 ml of peel/water slurry with solid fractions of 2, 4, 6, 8, and 10%. The slurries were then hydrolyzed by the enzymes at 45 °C and 140 rpm for 24 h in a shaker bath. For acid hydrolysis, ground peels were diluted with distilled water to obtain 100 ml of peel/water slurry with similar solid fractions as previously mentioned. Sulfuric acid (98%) was added to the slurries to reach final acid concentration of 0, 0.25, 0.5, 0.75, and 1% (v/v). Next, the slurries were heated in an autoclave at various temperatures of 100, 108, 116, 124, and 132 °C with different residence times of 5, 10, 15, 20, and 25 min according to the design of the experiment (Table 1). All samples were then cooled down to 85(±3) °C before removing them from the autoclave.

Acid Hydrolysis at High Temperature

A 10-L high-pressure reactor (Process & Industriteknik AB, Sweden) was used for acid hydrolysis. The reactor heated with direct injection of 60 bar pressure steam, which was provided from a power plant located in Borås, Sweden. The steam hydrolyzed the materials at desired temperature within the designed retention time. The materials were then explosively sent to an expansion tank to cool down for further processing and analyses. In these tests, two kilograms of orange peel/water slurry with solid concentration of 5-18% and acid concentration of 0-0.5% were loaded into the reactor and hydrolyzed for 10-30 min. at 140-210 °C.

Analytical Methods

An ion-exchange Aminex HPX-87P column (Bio-Rad, USA) was used at 85 °C for measuring glucose, galactose, arabinose, and fructose concentrations. Ultra-pure water was used as eluent at a flow rate of 0.6 ml/min. Concentrations of furfural, HMF and galacturonic acid were determined by an Aminex HPX-87H column (Bio-Rad, USA) at 60 °C using 5mM H₂SO₄ at a flow rate of 0.6 ml/min. A refractive index (RI) detector (Waters 2414, Milipore, Milford, USA) and UV absorbance detector at 210 nm (Waters 2487) were used in series. Furfural and HMF concentrations were analyzed from UV chromatograms, whereas the rest of the chemicals were quantified with a refractive index (RI) detector.

Statistical Analysis

The central composite rotatable experimental design method (CCRD) was chosen to determine the effect of four operating variables of the acid hydrolysis, including temperature (T), time, solid (TS), and acid concentration, and two response variables which were (a) yield of sugars defined as the sum of glucose, fructose, arabinose, and galactose produced per total peel dry mass, and (b) conversion of hexoses to HMF, hereafter called HMF yield. Selection of the factors and range of the variables were based

on the operating condition, which has a significant influence on the acid hydrolysis process according to previous works (Grohmann et al. 1995; Vaccarino et al. 1989b), as well as 40 preliminary experiments with 110-210 °C, 5-20%(w/w) solid concentration, 0-1%(v/v) acid concentration, and 5-30 min (data not shown).

Table 1: Coded (x_1 , x_2 , x_3 and x_4) and Respective Actual Levels (T, Solid%, Acid% and Time) in Experimental Design for Dilute-acid Hydrolysis of the Orange Peels by CCRD Method

Test no.	Coded level of variables				Actual level of variables			
	x_1	x_2	x_3	x_4	T(°C)	Solid(%)	Acid(%)	Time(min)
1	-1	-1	-1	-1	108	4	0.25	10
2	+1	-1	-1	-1	124	4	0.25	10
3	-1	+1	-1	-1	108	8	0.25	10
4	-1	-1	+1	-1	108	4	0.75	10
5	-1	-1	-1	+1	108	4	0.25	20
6	+1	+1	-1	-1	124	8	0.25	10
7	+1	-1	+1	-1	124	4	0.75	10
8	+1	-1	-1	+1	124	4	0.25	20
9	-1	+1	+1	-1	108	8	0.75	10
10	-1	+1	-1	+1	108	8	0.25	20
11	-1	-1	+1	+1	108	4	0.75	20
12	+1	+1	+1	-1	124	8	0.75	10
13	+1	+1	-1	+1	124	8	0.25	20
14	+1	-1	+1	+1	124	4	0.75	20
15	-1	+1	+1	+1	108	8	0.75	20
16	+1	+1	+1	+1	124	8	0.75	20
17	-2	0	0	0	100	6	0.5	15
18	+2	0	0	0	132	6	0.5	15
19	0	-2	0	0	116	2	0.5	15
20	0	+2	0	0	116	10	0.5	15
21	0	0	-2	0	116	6	0.0	15
22	0	0	+2	0	116	6	1.0	15
23	0	0	0	-2	116	6	0.5	5
24	0	0	0	+2	116	6	0.5	25
25	0	0	0	0	116	6	0.5	15
26	0	0	0	0	116	6	0.5	15
27	0	0	0	0	116	6	0.5	15
28	0	0	0	0	116	6	0.5	15
29	0	0	0	0	116	6	0.5	15
30	0	0	0	0	116	6	0.5	15

The number of tests required for CCRD is the sum of 2^k factorial runs with its origin at the center, $2k$ axial runs, and numbers of replicate tests at the center, where k is the number of the variables. In the current work, where the effects of four variables are to be evaluated, the recommended number of tests at the center point is six (Box and Hunter 1957), and therefore the total number of tests would be 30 as presented in Table 1. The values of the variables are coded to lie at ± 1 for factorial points, 0 for the center points and ± 2 for axial points (Obeng et al. 2005).

A software package called MINITAB[®] was used to evaluate and to fit the second-order model to these four independent variables according to the following equation:

$$Y = b_0 + \sum_{i=1}^k b_i x_i + \sum_{i=1}^k b_{ii} x_i^2 + \sum_{i < j} \sum_j b_{ij} x_i x_j + e \quad (1)$$

where Y is the dependent or response variable(s) to be modeled, x_i and x_j are the independent variables (factors), and b_i , b_{ii} and b_{ij} are the measures of the x_i , x_i^2 and $x_i x_j$ effects, respectively. The variable $x_i x_j$ represents the first-order interactions between x_i and x_j , and e is the error. When the response data are obtained from the test work, a regression analysis using the least-squares method is carried out to determine the coefficients of the response model, their standard errors, and significance. The effects were considered to be not statistically significant when the p -value was higher than 0.05 at the 95% confidence level (Obeng et al. 2005). The optimum values of the selected variables were obtained from the estimated variables in the model and by inspecting the response surface contour plots and MINITAB[®] optimizer.

RESULTS

Characterization of the Orange Peels

The dry matter content of the orange peels was measured at 20(±1.2)%. In order to find out the carbohydrate content of the peels, they were enzymatically hydrolyzed in shake flasks at 45 °C for 24 h. The respective loadings of pectinase, cellulase, and β-glucosidase were 1163 IU/g, 0.24 FPU/g, and 3.9 IU/g peel dry matter based on the optimized values previously reported (Wilkins et al. 2007). Yields of various sugars released in the enzymatic hydrolysis were not significantly influenced by increasing the concentration of peel solids. The average values of duplicate experiments are summarized in Table 2. The main carbohydrates after enzymatic hydrolysis were glucose, fructose, galactose, arabinose, and galacturonic acid (GA), accounting for 72% of the total solid content of the peels. These results are in agreement with those obtained from enzymatic hydrolysis of Argentina orange peel (Pourbafrani et al. 2007).

Table 2: Yields of the Sugars Released during Enzymatic Hydrolysis of the Orange Peels

Sugars	(%) of Total Solid
Glucose	27.1 ± 1.3
Fructose	14.1 ± 1.5
Galactose	5.0 ± 0.5
Arabinose	7.1 ± 0.6
Galacturonic acid	18.7 ± 1.5
Total	72

Dilute-acid Hydrolysis

Dilute-acid hydrolyses of the orange peels were performed according to the experimental design presented in Table 1. The results for yields of total sugars (Y_{TS}) and HMF (Y_{HMF}) are displayed in Table 3. The highest yield of sugars, 43.24%, was achieved in the 28th experiment at the center point of the experiments where 116 °C, 0.5% sulfuric

acid, 6% solid fraction and 15 min were applied. However, the more reliable value is the average of results of the 25th to 30th experiments, with a Y_{TS} value of 42.40 ± 0.53 %. Furfural, a decomposition product of pentoses, was not detected in any of the experiments, while HMF was the main by-product. The highest yield of HMF was obtained at 9.03% when temperature, time, acid concentration, and solid fraction were 124°C, 20 min, 0.75% and 4%, respectively.

Table 3: Actual Values and Predicted Values for Sugar and Hydroxymethyl Furfural (HMF) Yield

Test no.	Y_{TS}^a	Y_{TS}	Y_{HMF}^b	Y_{HMF}
	Actual	Predicted	Actual	Predicted
1	36.61	33.61	0.75	1.05
2	41.64	40.58	2.35	2.33
3	27.74	27.24	1.17	1.19
4	39.56	40.74	1.74	1.58
5	39.33	36.22	0.95	1.11
6	40.02	38.27	1.54	1.67
7	41.24	39.64	6.67	7.10
8	40.11	39.25	2.70	3.21
9	39.43	38.41	1.42	1.28
10	31.12	30.88	0.77	0.70
11	41.31	41.19	2.48	2.71
12	38.80	41.32	6.12	6.00
13	39.74	37.96	1.80	2.00
14	36.20	36.10	9.03	9.05
15	39.42	39.89	1.80	1.86
16	37.74	38.86	7.33	7.39
17	30.10	32.02	0.81	0.81
18	37.43	37.96	8.06	7.64
19	40.00	43.10	4.07	3.53
20	40.15	39.49	1.90	2.02
21	24.70	29.60	0.00	0.00
22	40.07	37.62	5.50	5.50
23	38.69	40.07	2.32	2.29
24	39.15	40.21	4.14	3.75
25	41.79	42.40	2.65	2.63
26	42.78	42.40	2.61	2.63
27	42.60	42.40	2.64	2.63
28	43.24	42.40	2.67	2.63
29	42.29	42.40	2.63	2.63
30	41.75	42.40	2.60	2.63

^a Gram of total sugars per 100 gram initial dry matter

^b As percentage of total hexoses converted to HMF

Dilute-acid Hydrolysis at High Temperature

Pectin was not hydrolyzed under the above hydrolysis conditions and no galacturonic acid was obtained in the hydrolyzates. Therefore, further experiments at higher temperature (140, 180, and 210 °C) for 10 and 30 min. and acid concentrations of zero, 0.05, and 0.5% and solid concentrations of 5, 6, 10, and 18% were carried out. However, no hydrolysis of pectin and no galacturonic acid in the hydrolyzates were

obtained. Furthermore, hydrolysis under these conditions did not improve Y_{TS} values than the results reported in Table 3.

Statistical Analysis of the Experimental Results

The results of statistical analysis including the estimated values of factors' coefficients, interactive terms, t from Student's t -test, and p -values are shown in Table 4. The larger magnitude of the t -value and the smaller magnitude of the p -value indicate more significance of the corresponding coefficient. Thus, temperature and acid concentration in linear and quadratic form were highly significant for the yield of total sugars ($p < 0.05$). Among the interactive terms, only interaction between temperature and acid concentration (X_{13}) was highly significant. For the second response variable (Y_{HMF}), temperature and acid concentration had the greatest effect on the formation of HMF, followed by total solid concentration and time. Temperature was the only significant quadratic term, but it showed interaction with all three other variables. Furthermore, there was an interaction between time and acid concentration regarding the yield of HMF (X_{34} in Table 4).

Table 4: Model Coefficients Estimated by Multiple Linear Regressions for Sugars and Hydroxymethyl Furfural (HMF) Yields

Factor	Yield of sugars			Yield of HMF		
	Coefficient	t-value	p-value	Coefficient	t-value	p-value
Intercept	42.41	42.70	0.000	2.63	19.95	0.000
X_1	1.48	2.99	0.009	1.70	25.86	0.000
X_2	-0.90	-1.82	0.089	-0.37	-5.72	0.000
X_3	2.00	4.04	0.001	1.48	22.45	0.000
X_4	0.03	0.07	0.944	0.36	5.51	0.000
X_1^2	-1.85	-3.99	0.001	0.39	6.45	0.000
X_2^2	-0.28	-0.59	0.560	0.03	0.58	0.569
X_3^2	-2.19	-4.73	0.000	-0.02	-0.37	0.717
X_4^2	-0.56	-1.21	0.242	0.09	1.57	0.136
X_{12}	1.01	1.66	0.116	-0.20	-2.47	0.026
X_{13}	-2.02	-3.33	0.005	1.06	13.11	0.000
X_{14}	-0.98	-1.61	0.126	0.20	2.52	0.024
X_{23}	1.00	1.66	0.118	-0.11	-1.37	0.189
X_{24}	0.26	0.42	0.677	-0.13	-1.70	0.110
X_{34}	-0.54	-0.88	0.388	0.26	3.31	0.005

* X_1 , X_2 , X_3 and X_4 are temperature, solid fraction, acid concentration and time, respectively. X_{ij} represents the first order interactions between X_i and X_j .

Regression analysis based on the coded variables on the experimental data was performed, and coefficients of the second-order models were calculated. Substitution of coefficients calculated and response variables in Eq. (1) resulted in the following empirical equations for yields of total sugars (Y_{TS}) and HMF (Y_{HMF}):

$$Y_{TS} = 42.41 + 1.48 X_1 - 0.90 X_2 + 2.00 X_3 + 0.03 X_4 - 1.85 X_1^2 - 0.28 X_2^2 - 2.19 X_3^2 - 0.56 X_4^2 + 1.01 X_1 X_2 - 2.02 X_1 X_3 - 0.98 X_1 X_4 + 1.00 X_2 X_3 + 0.26 X_2 X_4 - 0.54 X_3 X_4 \quad (2)$$

$$Y_{\text{HMF}} = 2.63 + 1.70 X_1 - 0.37 X_2 + 1.48 X_3 + 0.36 X_4 + 0.39 X_1^2 + 0.03 X_2^2 - 0.02 X_3^2 + 0.09 X_4^2 - 0.20 X_1 X_2 + 1.06 X_1 X_3 + 0.20 X_1 X_4 - 0.11 X_2 X_3 - 0.13 X_2 X_4 + 0.26 X_3 X_4 \quad (3)$$

The predicted values obtained from the model equations (Eqs. 2, 3) show good agreement with the actual values of both responses (Table 3). The regression for both responses was statistically significant at the 95% confidence level. The results of the second-order response surface model in the form of analysis of variance (ANOVA) for both responses are presented in Table 5. The suitability of the fitness can be checked by determination coefficients (R^2), which were 0.85 and 0.99 for the yields of total sugars and HMF, respectively. The R^2 statistic indicates the percentage of the variability of the optimization parameter that is explained by the model (Fannin et al. 1981) and, therefore, 15% and 1% of the total variations are not explained by the models developed for the corresponding yields of total sugars and HMF, respectively.

Table 5: Analysis of Variance (ANOVA) for Two Quadratic Models of the Total Sugar (TS) and HMF Yields

Responses	Source of Variation	Sum of squares	Degree of freedom	Mean square	F-value	Probability (p)
Y_{TS}	Regressions	489.67	14	34.97	5.91	0.001
	Residual	88.76	15	5.91		
	Total	578.43	29			
Y_{HMF}	Regressions	154.74	14	11.05	105.74	0.000
	Residual	1.56	15	0.10		
	Total	156.3	29			

Effects of Experimental Variables on Hydrolysis Results

The responses for yield of total sugars were depicted as three-dimensional surface plots of two factors, while the other factors were kept at center levels along with their corresponding contour plots in Figs. 1 and 2. The effects of temperature and acid concentration on the yield of sugars, when solid fraction and time were selected at their center points, are shown in Fig. 1a,b. At the lower levels of temperature, increase in acid concentration resulted in higher yield of sugars. Similarly, at low levels of acid concentration, increase in temperature had a positive effect on the sugar yield. However, at the higher levels of both temperature and acid concentration, the yield of sugars declined, certainly due to presence of the strong interaction between these two variables (Table 4). The maximum yield, 42.6%, was attainable only by conducting hydrolysis experiments in a limited region around 117 °C temperature and 0.6% acid concentration. Under these conditions, HMF yield was 3.4% (Fig. 1c). The effect of acid concentration at the lower levels of temperature on the formation of HMF was negligible, but the rate of sugar decomposition to HMF increased sharply with rising temperature as can be observed from closer counter lines at high temperature and acid concentration in Fig. 1c.

The effects of temperature and time on sugar yield are depicted in Fig. 1d,e. The maximum sugar yield, 42.6%, was obtained at 13 min and 120 °C, while the corresponding HMF yield was 3.4% (Fig. 1f). The minimum sugar yield of 27% was obtained when time and temperature were at the lowest levels, *i.e.* 5 min and 100 °C (Fig.

1e). There was an optimum level for time of hydrolysis where the highest yield of sugars could be obtained (Fig. 1,d,e).

The interdependence of temperature and total solid fraction is presented in Fig. 2a,b. In general, increase in total solid concentration led to a decreased yield of sugars. However, the extent of this reduction was lowered as the temperature was raised (Fig. 2a,b). Analysis of the effect of solid fraction and temperature on the second response variable (Y_{HMF}) showed that at the higher temperature, increase of the solid fraction resulted in a lower yield of HMF (Fig. 2c). The effect of variation of acid concentration and solid fraction is to a great extent similar to the effect of temperature and solid fraction, and therefore the same results can be inferred (data not shown). The highest yield of sugars, 43.1%, was achieved at 116 °C and 0.5% acid concentration with the lowest fraction of solid of 2% (Fig. 2b). The yield of HMF was around 3.5% under these conditions (Fig. 2c). Sugars' yield around 40% is attainable by precise adjustment of both temperature and acid concentration at 10% solid fraction (Fig. 2b).

Analysis of the effect of variation of acid concentration and time on sugar yield is presented in Fig. 2d,e. The surface plot for yield of carbohydrates reached a peak with increase in acid concentration and then declined with further increase in acid concentration. The optimum region that yielded maximum liberation of sugars (42.6%) corresponded to a time period of 15 min and acid concentration of 0.625%. The yield of HMF was around 3% in this region, and the rate of formation increased at higher acid concentration (Fig. 2f).

Based on the second-order models, numerical optimization was carried out to maximize the yield of carbohydrates and minimize yield of HMF, using the response optimizer in MINITAB[®]. The optimal values of test variables were calculated as 12.9 min, 116 °C, 0.5% v/v acid concentration, and 6% solid fraction, with the corresponding yields of 42.3% for carbohydrates and 2.5% for HMF. The validity of these results was confirmed through performing hydrolysis runs in triplicate under optimized conditions. The analyses show that the average yields of total sugars and HMF were 41.8% and 2.6%, respectively. These experimental findings were in close agreement with the model prediction. Sugars released by acid hydrolysis were equal to 79% of total sugars (excluding galacturonic acid) obtained by enzymatic hydrolysis (Table 2).

Analysis of concentration of various sugars released by carrying out hydrolysis under optimum conditions indicated that yields of glucose, fructose, galactose, and arabinose were 75%, 85%, 80%, and 80% of those from enzymatic hydrolysis, respectively. The major proportion of HMF formation resulted from decomposition of fructose, and there was a direct relationship between loss of fructose and formation of HMF when hydrolysis was performed at test variables higher than the optimum values. Thus, solid residue, which is mostly insoluble and crystalline cellulose, contains about 20% of the remaining, unhydrolyzed glucose and minor amounts of other sugars.

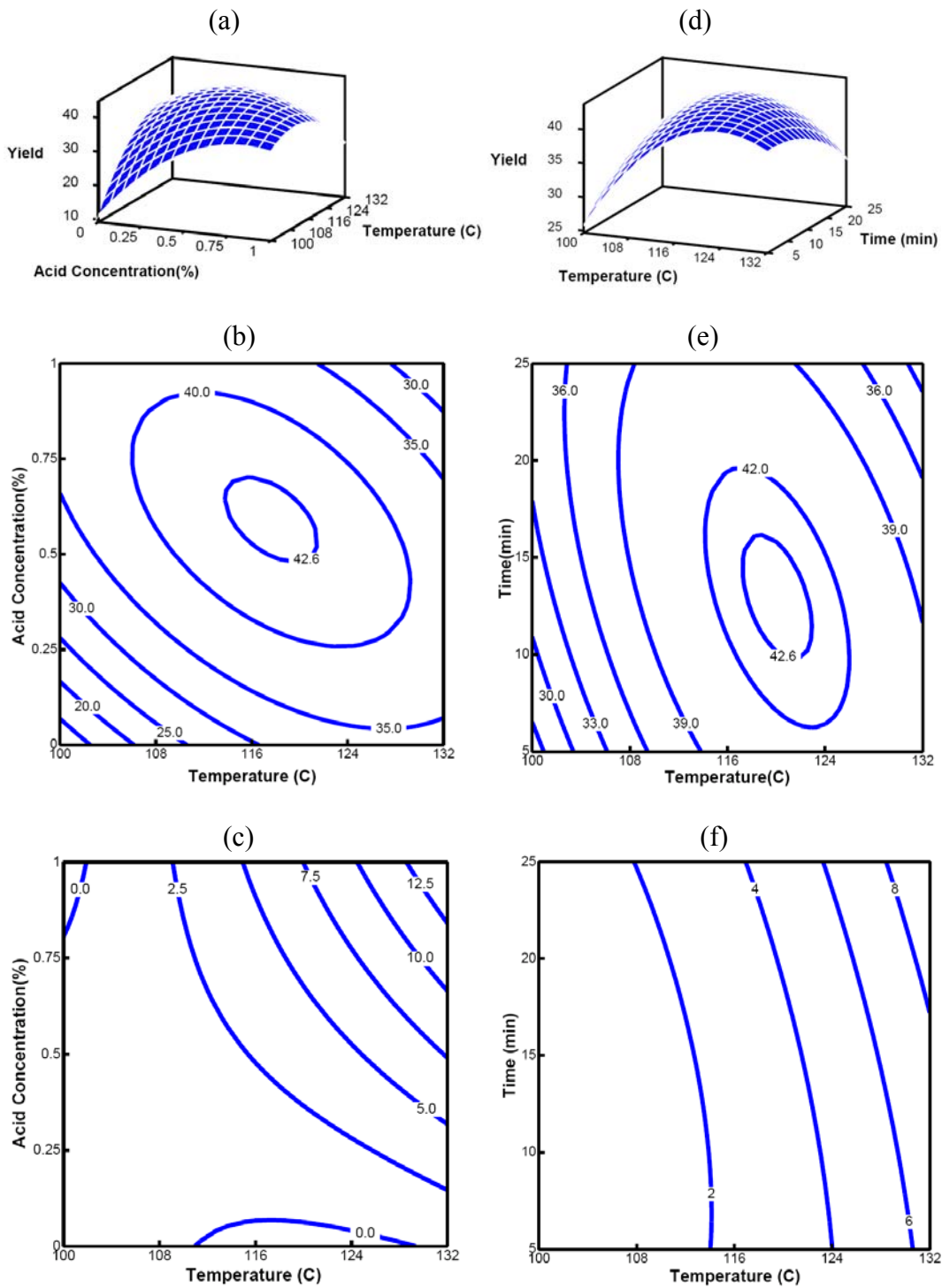


Fig. 1. Effect of temperature and acid concentration, time and temperature on the yield of total sugars (a,b,d,e) and HMF yield (c,f).

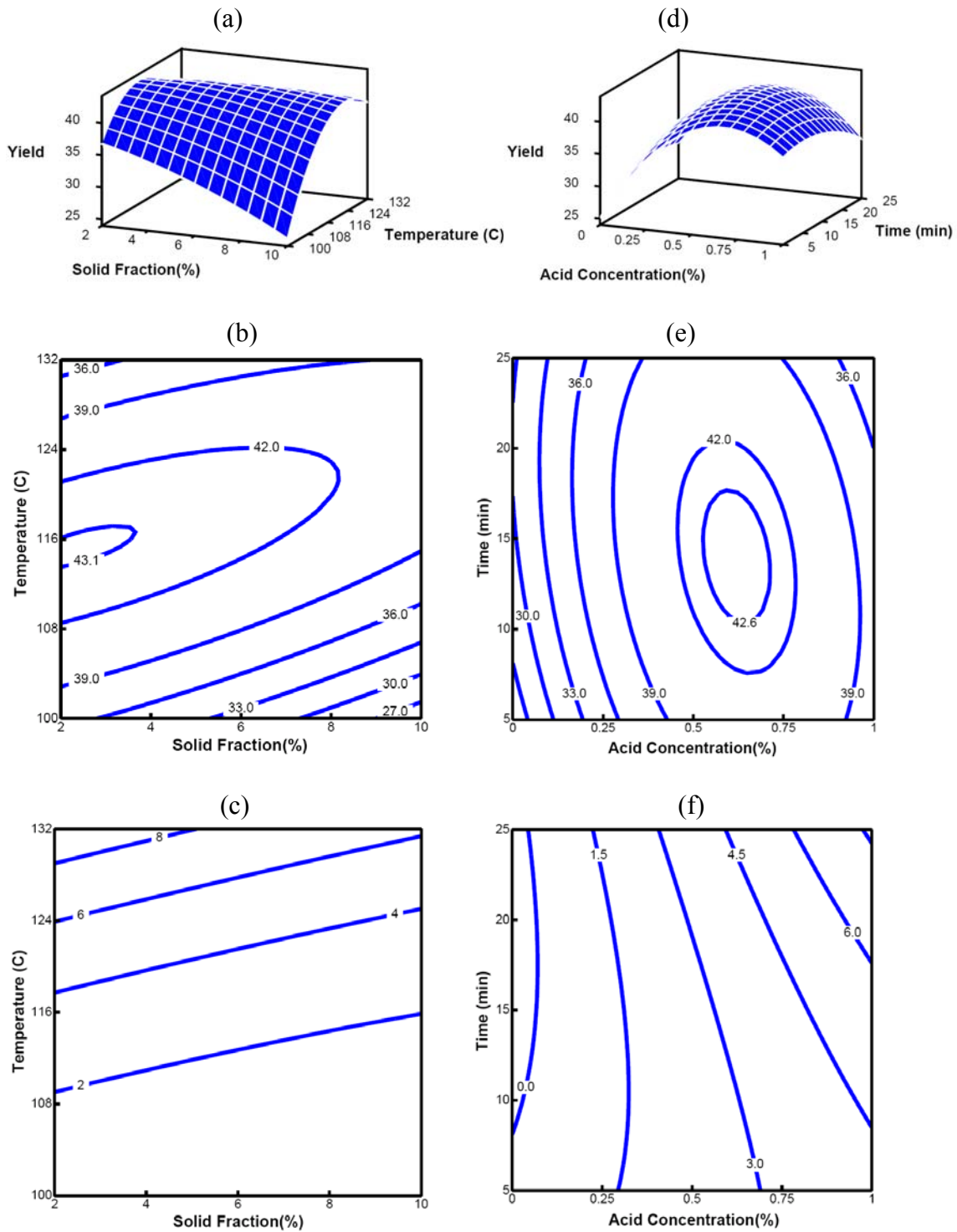


Fig. 2. Effect of temperature and solid fraction, time and acid concentration on the sugar yield (a,b,d,e) and HMF yield (c,f).

DISCUSSION

Dilute-acid hydrolysis of citrus peel is an effective treatment prior to enzymatic hydrolysis that allows solubilization of a large fraction of the solid. The remaining residue contains cellulose and solubilized pectin mixed with soluble mono- and oligosaccharides from the peel. The pectin can be either recovered as a product or further hydrolyzed to galacturonic acid and minor amounts of other sugars. A wider range of temperature can be applied in acid than in enzymatic hydrolysis, and the time required for acid hydrolysis is much lower than that for enzymatic reaction (Grohmann et al. 1995). However, acid hydrolysis suffers from the formation of inhibitors such as furfural and HMF due to decomposition of liberated sugars through the secondary reactions (Bienkowski et al. 1987; Taherzadeh et al. 2000; Azhar et al. 1981). Fructose is a soluble sugar in orange peel, which starts to decompose at 120°C, and its rate of decomposition is even faster at higher temperature (Grohmann et al. 1995). These facts suggest that the conditions for dilute-acid hydrolysis and the variables affecting this process should be carefully selected and optimized to yield the highest rate and extent of depolymerization of the carbohydrate polymers and maximum release of sugars, while the formation of inhibitory compounds is minimized.

The results of the current work indicate that furfural was not formed in the range of test variables applied. Furfural is a decomposition product of pentoses, and its formation is a first-order reaction, where the reaction constant is affected by both acid concentration and temperature. Arabinose is the only pentose sugar present in the peel hydrolyzate that is released gradually during hydrolysis. Among the various pentose sugars exposed to the acid for furfural formation, arabinose showed the lowest reactivity, with a small reaction constant (Garrett and Dvorchik 1969). Therefore, lack of furfural formation is most probably due to stability of arabinose and its low concentration in hydrolyzate under the applied conditions.

Formation of HMF during dilute-acid hydrolysis is a sequential reaction where cellulose and hemicellulose are first hydrolyzed to their hexose monomers, followed by decomposition of liberated hexoses to HMF. The kinetics of these two reactions were studied for lignocellulosic materials, and the results indicated that these hydrolysis and decomposition reactions are both first-order reactions and possess rates of similar magnitude (Saeman 1945). These two reaction rates are influenced by temperature and acid concentration. The higher ratio of the first reaction rate constant compared to the second one increases the yield of total liberating sugars. The profile of total liberated carbohydrates vs. time passes through a maximum, and hence there is an optimal time at which sugar production reaches a maximum. This time is a function of constant values of both reactions. Elapsing time of hydrolysis longer than the optimal value enhances the speed of the second reaction, leading to a decrease in net total sugar liberation (Saeman 1945). This fact can be interpreted in another way from results of statistical analysis in Table 4. Time represents no significant effect on the yield of sugars (Y_{TS}), while its effect on the HMF yield is significant and shows interaction with both temperature and acid concentration. Thus, time is an important factor for the overall hydrolysis process to achieve the highest yield of total carbohydrates.

The effect of total solid concentration is significant only for the yield of HMF. The major fraction of HMF is formed from decomposition of the soluble sugars (mainly

fructose) that are available in the early period of hydrolysis. Concentration of these soluble sugars is proportional to the solid fraction, and this is a possible reason for the significance of the total solid fraction for the second response variable. The positive impact of total solid fraction on the reduction of HMF yield might be attributed to the presence of temperature and acid concentration gradients at the higher levels of solid fractions, which decreases the decomposition rate of sugars to the HMF in the bulk medium.

Pectin was not hydrolyzed in this work, and therefore no galacturonic acid was detected through the analyses. Despite the soluble nature of released pectin fragments, the glycosidic bonds between galacturonic acid units are probably too resistant to acid hydrolysis due to a combination of inductive and conformational effects. However, because of the low rate of pectin depolymerization, a much longer time of hydrolysis is probably required for partial release of galacturonic acid (Grohmann et al. 1995; Timell et al. 1965).

CONCLUSION

Hydrolysis of citrus processing waste was carried out with dilute acid, and the optimum conditions as well as interaction between influencing factors were investigated by utilizing a central composite rotatable design (CCRD). Among the linear terms, temperature and acid concentration were the most significant variables for both yields of sugars and HMF, and the latter was also influenced by the solid fraction and time. Time of hydrolysis longer than its optimized value proved to have a negative effect on the yield of sugars, mainly due to formation of HMF. At the higher levels of both temperature and acid concentration, total solid fraction had no significant effect on sugar yield. The maximum yield of sugars and minimum yield of HMF can be obtained under the optimum conditions as 41.8% and 2.6%, respectively.

ACKNOWLEDGMENTS

The authors are grateful to the Foundation of Förenings sparbanken i Sjuhärad (Sweden) and Brämhults Juice AB for financial support of this work, and to Dr. Ilona Sarvari Horvath and Jonas Hanson for helping with the experimental work.

REFERENCES CITED

- Azhar, A. F., Bery, M. K., Colcord, A. R., Roberts, R. S., and Corbitt, G. V. (1981). "Factors affecting alcohol fermentation of wood acid hydrolysate," *Biotechnol. Bioeng. Symp* 11, 293-300.
- Bienkowski, P. R., Ladisch, M. R., Narayan, R., Tsao, G. T., and Eckert, R. (1987). "Correlation of glucose (dextrose) degradation at 90 to 190-degrees-C in 0.4 to 20-percent acid.," *Chem. Eng. Commun.* 51, 179-192.

- Box, G. E. P., and Hunter, J. S. (1957). "Multi-factor experimental-designs for exploring response surfaces," *Ann. Math. Stat.* 28, 195-241.
- Canettieri, E. V., Rocha, G., de Carvalho, J. A., and Silva, J. (2007). "Optimization of acid hydrolysis from the hemicellulosic fraction of Eucalyptus grandis residue using response surface methodology," *Bioresour. Technol.* 98, 422-428.
- Decker, S. R., Adney, W. S., Jennings, E., Vinzant, T. B., and Himmel, M. E. (2003). "Automated filter paper assay for determination of cellulase activity," *Appl. Biochem. Biotechnol.* 105, 689-703.
- Fannin, T. E., Marcus, M. D., Anderson, D. A., and Bergman, H. L. (1981). "Use of a fractional factorial design to evaluate interactions of environmental factors affecting biodegradation rates," *Appl. Environ. Microbiol.* 42, 936-943.
- Garrett, E. R., and Dvorchik, B. H. (1969). "Kinetics and mechanisms of the acid degradation of the aldopentoses of furfural," *J. Pharm. Sci.* 58, 813-820.
- Grohmann, K., and Baldwin, E. A. (1992). "Hydrolysis of orange peel with pectinase and cellulase enzymes," *Biotechnol. Lett.* 14, 1169-1174.
- Grohmann, K., Baldwin, E. A., and Buslig, B. S. (1994). "Production of ethanol from enzymatically hydrolyzed orange peel by the yeast *Saccharomyces-cerevisiae*," *Appl. Biochem. Biotechnol.* 45-6, 315-327.
- Grohmann, K., Cameron, R. G., and Buslig, B. S. (1995). "Fractionation and pretreatment of orange peel by dilute acid hydrolysis," *Bioresour. Technol.* 54, 129-141.
- Kunamneni, A., and Singh, S. (2005). "Response surface optimization of enzymatic hydrolysis of maize starch for higher glucose production," *Biochem. Eng. J.* 27, 179-190.
- Montgomery, D. C. (2001). *Design and Analysis of Experiments*, John Wiley and Sons, New York, 427-450.
- Obeng, D. P., Morrell S., and Napier-Munn, T. J. (2005). "Application of central composite rotatable design to modelling the effect of some operating variables on the performance of the three-product cyclone," *Int. J. Miner. Process.* 76, 181-192.
- Pourbafrani, M., Talebnia, F., Niklasson, C., and Taherzadeh, M. J. (2007). "Protective effect of encapsulation in fermentation of limonene-contained media and orange peel hydrolyzate," *Int. J. Mol. Sci.* 8, 777-787.
- Rahman, S. H. A., Choudhury, J. P., Ahmad, A. L., and Kmaruddin, A. H. (2007). "Optimization studies on acid hydrolysis of oil palm empty fruit bunch fiber for production of xylose," *Bioresour. Technol.* 98, 554-559.
- Rodriguez-Nogales, J. M., Ortega, N., Perez-Mateos, M., and Busto, M. D. (2007). "Experimental design and response surface modeling applied for the optimisation of pectin hydrolysis by enzymes from *A. niger* CECT 2088," *Food Chem.* 101, 634-642.
- Saeman, J. F. (1945). "Kinetics of wood saccharification – Hydrolysis of cellulose and decomposition of sugars in dilute acid at high temperature," *Ind. Eng. Chem.* 37, 43-52.
- Taherzadeh, M. J., Gustafsson, L., Niklasson, C., and Liden, G. (2000). "Physiological effects of 5-hydroxymethylfurfural on *Saccharomyces cerevisiae*," *Appl. Microbiol. Biotechnol.* 53, 701-708.
- Timell, T. E., Enterman, W., Spencer, F., and Soltes, E. J. (1965). "Acid hydrolysis of glycosides. 2. Effect of substituents at C-5," *Can. J. Chem.* 43, 2296-305.

- Tripodo, M. M., Lanuzza, F., Micali, G., Coppolino, R., and Nucita, F. (2004). "Citrus waste recovery: A new environmentally friendly procedure to obtain animal feed," *Bioresour. Technol.* 91, 111-115.
- Vaccarino, C., Locurto, R., Tripodo, M. M., Patane, R., Lagana, G. and Ragno, A. (1989). "SCP from orange peel by fermentation with fungi–acid-treated peel," *Biol. Wastes* 30, 1-10.
- Wilkins, M. R., Widmer, W. W., Grohmann, K., and Cameron, R. G. (2007). "Hydrolysis of grapefruit peel waste with cellulase and pectinase enzymes," *Bioresour. Technol.* 98, 1596-1601.

Article submitted: Sept. 30, 2007; Peer-review completed: Nov. 10, 2007; Revised version received and accepted: Dec. 17, 2007; Published: Dec. 18, 2007

HUMIC ACID-LIKE MATTER ISOLATED FROM GREEN URBAN WASTES. PART I: STRUCTURE AND SURFACTANT PROPERTIES

Enzo Montoneri,^{1*} Vittorio Boffa,¹ PierLuigi Quagliotto,¹ Raniero Mendichi,² Michele R. Chierotti,³ Roberto Gobetto,³ and Claudio Medana⁴

A humic acid-like substance (cHAL2) isolated from urban green wastes before composting was compared to a humic acid-like substance (cHAL) isolated from a mix of urban organic humid waste fraction and green residues composted for 15 days. cHAL2 was found to contain more aliphatic and O-alkyl C atoms relative to aromatic, phenol, and carboxyl C atoms, and to yield higher critical micellar concentration ($\text{cmc} = 0.97 \text{ g L}^{-1}$) and surface tension at the cmc ($\gamma_{\text{cmc}} = 37.8 \text{ mN/m}$) in water than cHAL ($\text{cmc} = 0.40 \text{ g L}^{-1}$; $\gamma_{\text{cmc}} = 36.1 \text{ mN/m}$). The results point out that biomass wastes may be an interesting source of biosurfactants with diversified properties that depend on the nature of waste and on its process of treatment.

Keywords: Urban refuse; Compost; Biosurfactants; Humic acids; Biomass.

Contact information: ¹Dipartimento di Chimica Generale ed Organica Applicata, Università di Torino, C. M. D'Azeglio 48, 10125 Torino, Italy; ²Istituto per lo Studio delle Macromolecole (CNR), Via E. Bassini 15, I-20133 Milano, Italy; ³Dipartimento di Chimica I.F.M., Università di Torino, Via P. Giuria 7, 10125 Torino, Italy; ⁴Dipartimento di Chimica Analitica, Università di Torino, Via Pietro Giuria 5, 10125 Torino, Italy; *Corresponding author: enzo.montoneri@unito.it

INTRODUCTION

Separate collection of urban food and green wastes and their compost products are interesting low entropy sources of organic C. They are available from confined spaces, and may have relatively low water (35-55 %) and high organic matter (26-50 %) contents (Quagliotto 2006; Ozores-Hampton and Obreza 2007). Recycling of the organic matter of these wastes for further uses is a worthwhile scope to be pursued for economic and environmental reasons. Composting is carried out nowadays in public and private facilities throughout the world (Kraft 2006; Newman 2006; Ozores-Hampton and Obreza 2007; Stoffella 1997) at a processing tipping fee of about 70 €/ton, while the compost product is proposed as fertilizer at a current market value which is not above 15 €/ton. Therefore, composting urban humid and vegetable residues has a net cost of about 55 €/ton. Very recently we have shown that compost is a rich source of biosurfactants and suggested that these materials may have a range of potential applications in the chemical industry. Indeed a humic acid-like compound isolated from compost was found to have quite remarkable surfactant properties (Quagliotto 2006) and good performance as a chemical auxiliary for dyeing nylon 6 (Savarino 2007). For the sake of simplicity, we

refer to this compound as cHAL. Composting, however, yields a wide range of different products, depending on the compost wastes mix and the composting time. As these compounds might in principle offer a range of properties from which to choose those tailored for specific needs, we wish to report herewith the structure and surfactant properties of a new compost isolated humic acid-like substance (here and after named cHAL2). Compared to cHAL, isolated from a mix of urban organic humid waste fraction and green residues composted for 15 days, cHAL2 was isolated from green urban wastes only before composting. Our long range purpose is to build a data inventory which at some point will make it possible not only to understand how the parameters characterizing the waste nature and the composting process influence the structure and surfactant properties of the isolated humic-like substances, but also to assess how much the source and structural difference of these substances affect their performance as auxiliaries for chemical technological uses.

EXPERIMENTAL

All reagents were Aldrich products, unless otherwise indicated. Ground urban green wastes, collected from the Amiat municipal plant in Torino, Italy were extracted according to a known procedure (Quagliotto 2006) to yield, in 12 % w/w yield relative to the starting dry waste, the humic acid-like material (cHAL2) investigated in this work. This material was found to contain 7.47 % water, 91.60 % volatile solids and 0.93 % ash by the weight losses measured after heating first at 105 and then at 800 °C. Further characterization for cHAL2 was performed by elemental analysis, solid state ^{13}C and solution ^1H NMR spectroscopy, IR spectroscopy, and surface tension measurements as previously reported (Quagliotto 2006). The determination of free phenol and carboxylic acid groups (Table 1) was accomplished by potentiometric titration according to a previous procedure (Brunelot 1989). Under our experimental conditions, deionized water was boiled under nitrogen atmosphere to remove dissolved CO_2 . This water was used to make the required sample and reagents solutions. The cHAL2 sample was dissolved at 1.87 g/L concentration in 0.015 N NaOH. The total alkali content in the solution was in excess relative to the total cHAL2 carboxyl and phenoxide content (Table 1) determined by ^{13}C NMR spectroscopy. This solution with pH about 12 was titrated with standardized 0.01 N aqueous HCl. Similar titration was performed on a blank solution containing the same amount of alkali as the above sample solution, but no cHAL2. The titrations were performed at 25 °C using an automatic Cryson Compact Titrator with a resolution of 1 μl of titrant in a thermostated glass cell under nitrogen blanketing to prevent dissolution of atmospheric carbon dioxide in the sample.

Under these experimental conditions, it was possible to obtain a potentiometric curve of satisfactory quality (Fig. 1). The elaboration of the experimental data (pH versus titrant volume in Fig. 1a) obtained under this condition is based on the linearization functions proposed by Gran (1952). According to the above method, from the linearized data plotted in Fig. 1b it was possible to extrapolate 3 equivalence points. Two of these points were obtained from the sample (cHAL2) titration curve and correspond to the added titrant volumes V_a and V_b . The third equivalence point, corresponding to the

added titrant volume V_c , indicates the endpoint of the titration of the blank alkali solution. This solution contained the same amount of added NaOH as the above titrated cHAL2 solution, but did not contain any cHAL2. In addition to these equivalence points, other two points, corresponding to the added titrant volumes V_{e1} and V_{e2} , were extrapolated from the first derivative of the cHAL2 titration curve in Fig. 1a. Based on the pH values measured at each of the above titrant volumes, the following assignments are given: i.e., V_b is considered the HCl volume necessary to titrate the excess NaOH over the sample total acidity, $V_b - V_{e1}$ is the HCl volume necessary to convert all ArONa groups to ArOH, and $V_{e2} - V_{e1}$, $V_a - V_{e2}$ and $V_c - V_a$ correspond to the volumes of HCl necessary to convert the sodium salts of carboxylic acids with increasing acidity strength to their free acid $-COOH$ forms.

Table 1. Data^a Found for cHAL^b, cHAL2^c and Peat Humic acid (PHA)^{d,e}

	C w/w %	Empirical Formula				
		C	H	N	O	S
cHAL	59.9 ^b	10	13.4	0.86	3.4	0.036
cHAL2	57.9 ^c	10	12.6	0.63	3.0	0.018
PHA	50.4-58.8 ^{d,e}	10	7.3-12.7	0.25-0.52	4.6-5.8	0.052

	pH	COX ^f meq/g	COOH meq/g	ArOY ^f meq/g	ArOH meq/g	MW
cHAL	4.00	5.71	1.10 ^g	3.38	1.90 ^g	15610
cHAL2	3.96	3.56	2.91 ^g	2.46	0.87 ^g	217630 ^h
PHA			2.76 ^e		3.28 ^e	17000 ^e

^aC content (w/w %) in ash free dry matter, elements atoms in empirical formula, pH of a water suspension (12 mg/30 mL) containing 0.01 N NaCl, free carboxylic (COOH) and phenol (ArOH) groups, weight(MW) and number-(MN) averaged molecular weights defined as previously reported (22).

^bIsolated in previous work (Quagliotto 2006).

^cIsolated in this work..

^dPeat (Montoneri 2003).

^ePeat (Terashima 2004).

^fTotal carboxyl (X = H or N) or phenoxide (Y = H, R, Ar) contents = $A/(1201.1 B)$, A = % band relative area from column 8 (carboxyl) or column 7 (phenoxide) in Table 2; B = 10^{-2} C w/w % from Table 1.

^gBy potentiometric titration.

^hData obtained in this work by SEC-MALS.

Dynamic light scattering (DLS) measurements were obtained with a ZetaSizer® (Malvern, UK), which has a detection window included between about 0.6 nm and 5 μ m. The measurements were carried at pH 7.0 and 25 C after filtering the cHAL2 sample solution on a cellulose acetate disk (Schleicher & Schuell) with a size cut-off of 0.8 μ m. The CONTIN method (Provencher 1976) was used to analyze the DLS data for calculating the hydrodynamic diameter (D_h) of the molecules or aggregates in solution.

Electrospray ionization measurements (ESI) were obtained using a LTQ Orbitrap high mass (M) resolving power ($R = M/\Delta M$) spectrometer (Thermo, Rodano, Italy), with electrospray interface and ion trap as mass analyzer. The flow injection effluent was delivered into the ion source using nitrogen as sheath and auxiliary gas (flow rate 10 $\mu\text{L}/\text{min}$). The source voltage was set at 4.0 kV in the negative ion mode. The heated capillary was maintained at 270°C. The tuning parameters adopted for the ESI source were the following: source current 100 μA , capillary voltage -9 V, tube lens -120 V. Mass spectra were collected in full scan negative mode in different ranges between 200 and 1500 mass to charge (m/z) ratio.

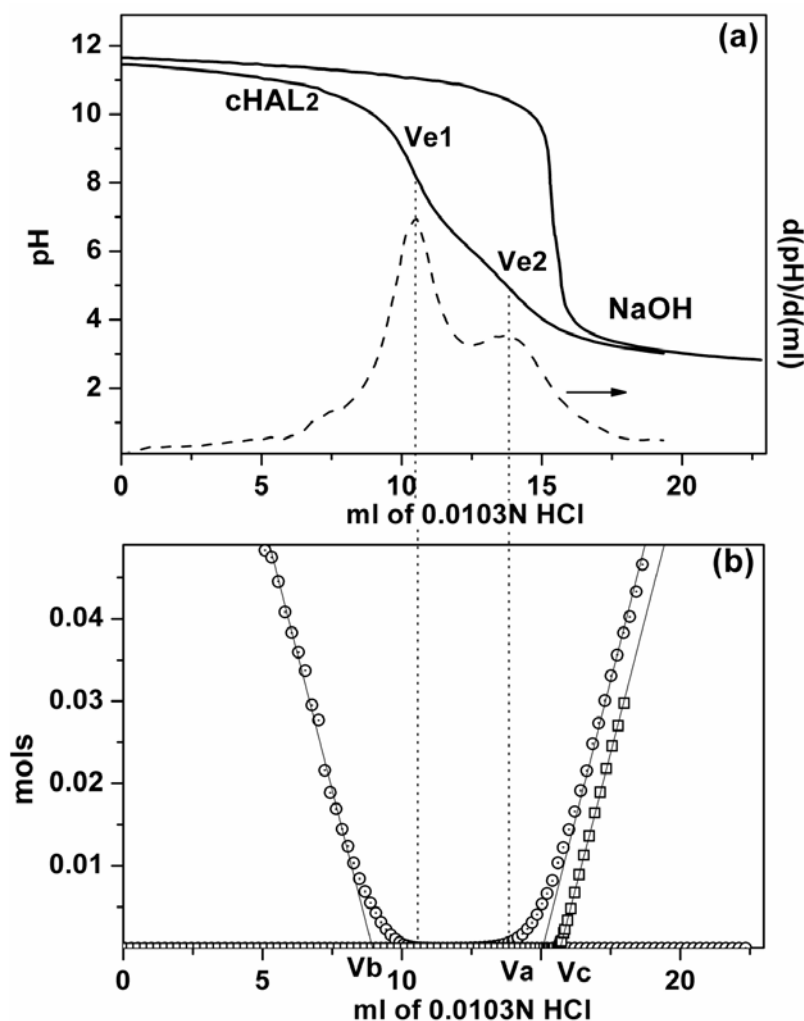


Fig. 1. Potentiometric titration of cHAL2. (a) Titration of 10 ml of a 0.0156 N NaOH solution dissolved in 30 ml of water and back-titration of 18.7 mg of cHAL2 dissolved in 10 ml of aqueous NaOH 0.0156 N and diluted in 30 ml of water. The dashed line indicates the first derivative (dpH/dml) of the cHAL2 back-titration. (b) Linearization of the NaOH titration curve (\square) and of the cHAL2 back-titration curve (\circ) according to the Gran method (Gran 1952).

Molecular investigation was performed also through fractionation and characterization by a multi-angle laser light scattering (MALS) detector on-line to a size exclusion chromatography (SEC) system. The SEC-MALS system consisted of an Alliance 2690 separation module, a 2414 differential refractometer (DRI) from Waters (Milford, MA, USA), and a MALS Dawn DSP-F photometer from Wyatt (Santa Barbara, CA, USA). This multi-detector SEC-MALS system was described in detail previously (Mendichi 2001). The wavelength of the MALS laser was 632.8 nm. The light scattering signal was detected simultaneously at fifteen scattering angles ranging from 14.5° to 151.3°. The calibration constant was calculated using toluene as standard, assuming a Rayleigh factor of $1.406 \cdot 10^{-5} \text{ cm}^{-1}$. The angular normalization was performed by measuring the scattering intensity of a concentrated solution of BSA globular protein in the mobile phase assumed to act as an isotropic scatterer. The refractive index increment, dn/dc , with respect to the solvent was measured by a KMX-16 differential refractometer from LDC Milton Roy (Riviera Beach, FL, USA). The dn/dc value for cHAL2 was 0.214 mL/g. The humic acid-like substance solubilization procedure and the SEC experimental conditions were quite similar to those previously reported (Kawahigashi 2005). The starting sample solution contained cHAL2 at 1 g L^{-1} concentration in 0.01M K_2HPO_4 -0.01M KH_2PO_4 aqueous buffer (pH 7.0) containing 10% methanol. The same solvent was used as SEC mobile phase under the following conditions: single aqueous Shodex OHpak KB805 column from Showa Denko (Tokyo, Japan), 35 °C temperature, 0.8 mL/min flow rate and 100 μL sample injection volume.

RESULTS AND DISCUSSION

To understand compositional and structural difference between materials isolated from composted wastes, one should first consider that composting is an aerobic biodegradation process of refuse biomass, leading to some mineralization of the original organic C and N and to chemical modifications of the remaining organic residue (Genevini 2002). Compared to the starting biomass waste, the composted waste is generally characterized by a lower content of polysaccharides, and by a relatively higher concentration of lignin-like material. Changes also involve chemical identities. Native lignin is modified to lignin-humus. The latter material, although not well defined, is usually characterized by its aliphatic/aromatic C ratio and by its content of carboxylic and phenolic functional groups. The humic acid-like organic fraction is separated (Montoneri 2003a) from the polysaccharide, protein, fats and other humic-like matter by extraction of the starting biomass with alkali and precipitation of the humic acid-like fraction at $\text{pH} < 1.5$. In our case, the humic acid-like material investigated in this work (cHAL2) was isolated from urban green wastes that were sampled right before composting. By comparison, our previously investigated (Quagliotto 2006) humic acid-like material (cHAL) was isolated from a 1:1 v/v mixture of food residues and public parks green wastes that had been composted for 15 days. To evidence the structural features of cHAL2, we like to refer to the above previous cHAL material for which the structure represented in Fig. 2 was proposed, based on the elemental analysis, acid groups

determination, and NMR data. Tables 1-3 report these characterization data for both cHAL and cHAL2.

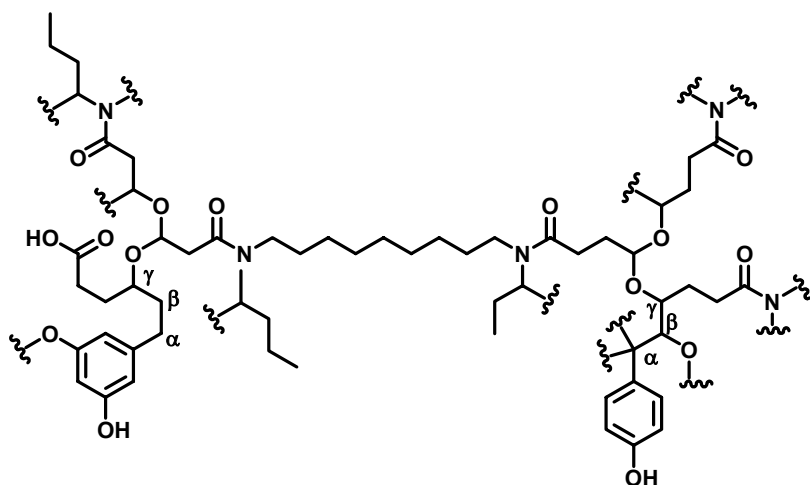


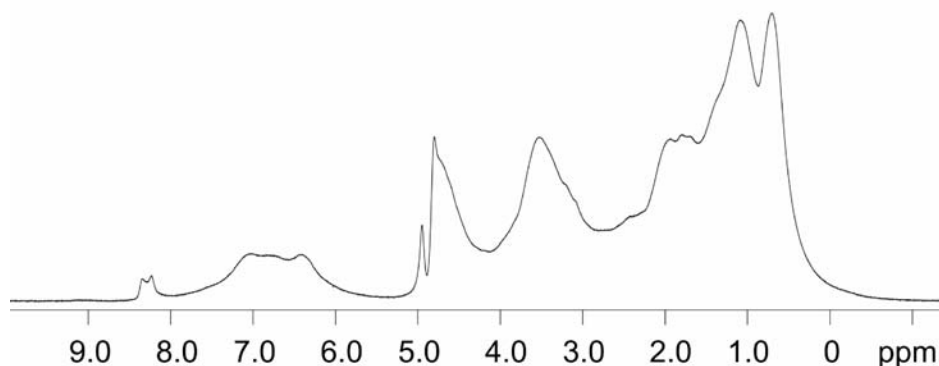
Fig. 2. Proposed molecular fragment for cHAL (Quagliotto 2006). H bonded to C omitted; sinusoidal bold lines indicate other fragments C, O, N atoms.

From Fig. 2 the cHAL structure may be visualized as an elongated hydrophobic portion made by a central 9 C long chain and by peripheral 2-3 C short chain aliphatic amide and di-O alkyl ether groups, to which two polar hydrophilic substituted propylphenol hydrocarbon residues are attached. The data obtained for cHAL2 (Tables 1-3) show that this material, compared to cHAL, is likely to have some significant structural differences: i.e., relative to the composition of the molecular fragment represented in Fig. 2 for cHAL, cHAL2 has 15 short chain aliphatic C, 5 O-alkyl C and 1 di-O-alkyl C more (Table 2). On an eq/g concentration basis, these features are accompanied by a relatively lower content of carboxyl and phenoxide functional groups (Table 1).

One aspect deserving particular attention in the characterization of humic acid-like substances is the determination of acid groups. It may be observed from the data in Table 1 that large fractions of the carboxyl and phenoxide groups consist of free carboxylic acids (-COOH) and phenolic (ArOH) groups. For the determination of these groups we have adopted the method suggested by Brunelot et al. (1989) for the potentiometric titration of humic and fulvic acids. As pointed out in the experimental section, these authors suggest that the potentiometric titration method may also yield the breakdown of carboxylic acids into functional groups with increasing acidity strength. We are convinced that this point would deserve deeper investigation in a specifically dedicated work. Within the more general issue addressed by our work, we are content with reporting the results in Table 1 as phenol (ArOH) and total carboxylic acid (COOH) groups. It may be observed that the values obtained for these groups by the above potentiometric titration method are consistent with the data obtained for total carboxyl

and total phenoxide groups by ^{13}C NMR spectroscopy (Fig. 3), inasmuch as the free acid groups turn out a fraction of the total phenoxide and carboxyl groups.

^1H NMR



^{13}C NMR

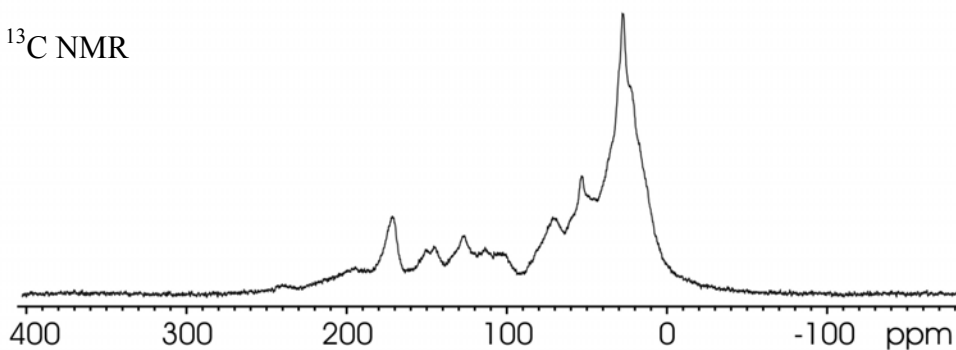


Fig. 3. Proton and carbon NMR spectra of cHAL2.

The IR spectra of the two humic acid-like compounds were also consistent with the presence of several functional groups and C bonds. IR peak absorbances were found at 1718 cm^{-1} for free carboxylic acid groups, at 1518 cm^{-1} for amide groups, at 1458 cm^{-1} for aromatic rings, at 1278 cm^{-1} for C-O bonds in phenol, phenyl ether, and COOH groups, in the $2000\text{-}3700\text{ cm}^{-1}$ range for O-H and/or N-H groups in COOH, phenol, amide groups, and carbohydrates, and at 2928 and 2855 cm^{-1} for protonated aliphatic C chains (Quagliotto 2006). In agreement with the NMR spectra the IR spectrum of cHAL2, compared to that of cHAL, showed higher intensity of the bands assigned to protonated aliphatic C chains and OH groups relatively to the bands assigned to C-O bonds in phenol, phenyl ether, and COOH groups. These features are likely to be memory of the main molecular constituents of the investigated green wastes such as polysaccharides, protein, lipids, and lignin. Particularly the higher content of O-alkyl and di-Oalkyl C in cHAL2, which is supported by the relatively higher intensities of both the ^{13}C NMR signals at $53\text{-}110\text{ ppm}$ (Table 2) and of the ^1H NMR signals at $2.5\text{-}4.2\text{ ppm}$ (Table 3), is equivalent to the presence of 1 carbohydrate hexose fragment per two aromatic rings.

Table 2. Assignments by Chemical Shift (δ , ppm) ranges and Relative Area of ^{13}C CPMAS NMR Bands, and C Distribution per Molecular Fragment Containing Two Aromatic Rings.

	Assignment band δ range (ppm)	1 Aliphatic C bonded to other aliphatic chain or to H		2	3	4	5	6	7	8	9	10
		Short chain 0-32	Long chain 32-53	Total aliphatic C 0-53	O-CH ₃ or N-alkyl C 53-63	O-alkyl C 63-95	di-O-alkyl C 95-110	Aro-matic C 110-140	Phenol or phenyl ether C 140-160	Carbox-yl C 160-185	Keto C 185-215	Other C 215-250
cHAL	band relative area (%)	32.3	12.9	45.2	8.4	9.2	3.5	14.8	6.8	11.5	0.6	-
	C distribution for two aromatic rings	17.9	7.2	25.1	4.7	5.1	1.9	8.2	3.8	6.4	0.33	-
cHAL2	band relative area (%)	36.0	13.6	49.5	6.5	11.5	3.6	9.1	5.1	7.4	4.6	2.6
	C distribution for two aromatic rings	30.4	9.5	39.9	5.5	9.7	3.0	7.7	4.3	6.2	3.9	2.2

Table 3. Assignments by Chemical Shift (δ , ppm) ranges and Relative Area of ^1H NMR Bands

	H in aliphatic C for hydrocarbon chains substituted at β or farther C, or in CH ₂ and CH ₃ bonded to aromatic C, or to carboxylic or amide groups		H in methine group bonded to aromatic C, or in aliphatic C bonded to O or to N	aromatic and olefinic H
band δ range (ppm)	0-1.2	1.2-2.9	2.9-4.3	5.9-8.1
cHAL2	23.6	39.0	26.5	10.9
cHAL	47.2	28.1	15.1	9.6

This molecular fragment is unlike to represent evidence of poly- or oligo-saccharide molecules simply mixed with the humic acid-like matter, since this material has been isolated by precipitation at $\text{pH} < 1.5$ (Montoneri 2003a). We rather favour the hypothesis that the above fragment was bonded covalently to the alkyl-phenoxy lignin-like part of the humic acid-like molecule. The higher content of fragments with carbohydrate structure in cHAL2 than in cHAL seems consistent with the different origin of these materials. Indeed, cHAL is a humic acid-like compound isolated from a refuse subjected to aerobic biodegradation for 15-d. Therefore, considering the longer biodegradation of cHAL relatively to cHAL2, a higher content of molecular fragments with carbohydrate structure is to be expected in the latter for thermodynamic and kinetic reasons (Montoneri 2003b). Also, it may be observed that the ^1H NMR spectra (Table 3) indicate a relatively higher content of aromatic H in cHAL2 than in cHAL. This fact, coupled with the relatively lower content of aromatic C indicated by the ^{13}C data (Table 2), suggests that the aromatic rings in cHAL2 are both fewer and less substituted. In turn, the lower substitution degree of the aromatic rings in cHAL2 seems consistent with the lower content of phenoxy groups reported in Table 1.

As most of the potential technological appeal of compost isolated humic acid-like substances have been inferred by us (Quagliotto 2006) to lie on their surface activity properties in solution, surface tension measurements constitute a basilar characterization for these compounds. Surfactants properties for cHAL2 were expected based on its structural analogies with cHAL and naturally occurring humic acids, i.e., presence of hydrophobic C chains and of polar groups. In principle, surfactants should give a surface tension (γ) versus concentration (C) plot where two clear linear regimes, premicellar and postmicellar, are evidenced. This is mostly found for simple surfactant molecules with one polar head. Oligomeric surfactants, such as the gemini surfactants (Quagliotto 2006) show a gradual transition between the two regimes, whose extension may be very large. These surfactants are made of molecules in which two or more polar groups are connected by lipophilic chains of variable length. Their oligomeric or polymeric nature is a key point in determining their capacity to micellize. The same could be expected for humic-like substance. When these materials are in solution as single molecules, these lie at the air-water interface to expose as the lowest possible hydrophobic surface to water. At higher concentration, when the air-water interface is saturated, the excess surfactant molecules aggregate forming micelles in the bulk water phase. In this form several molecules are held together by intermolecular forces to yield spherical or quasi-spherical clusters where hydrophobic surfaces stay in the inner micellar core and polar heads are directed toward the water phase. In a typical case, the premicellar and the postmicellar regimes are defined by two linear γ -C with different slopes. The intersection of the two

lines gives the cmc. For cHAL2, the results of our surface tension measurements against concentration are shown in Fig. 4. From the γ -C plot the slope change can easily be identified and the cHAL2 critical micellar concentration (cmc) and the surface tension at the cmc (γ_{cmc}) may be calculated 0.97 g L^{-1} and 37.8 mN/m . These values are higher than those reported for cHAL, i.e., $cmc = 0.40 \text{ g L}^{-1}$ and $\gamma_{cmc} = 36.1 \text{ mN/m}$ (Quagliotto 2006). Although the higher content of aliphatic C of cHAL2 usually would lead one to expect a lower cmc value than that of cHAL, the higher content of polar functional groups contributed by the O-alkyl and di-O-alkyl C in the former may introduce a higher degree of hydrophilicity that hinders micelles formation (Sulthana 2000). A similar effect has been reported for humic acids isolated from peat and soil upon increasing the relative content of carboxylic groups (Quagliotto 2006).

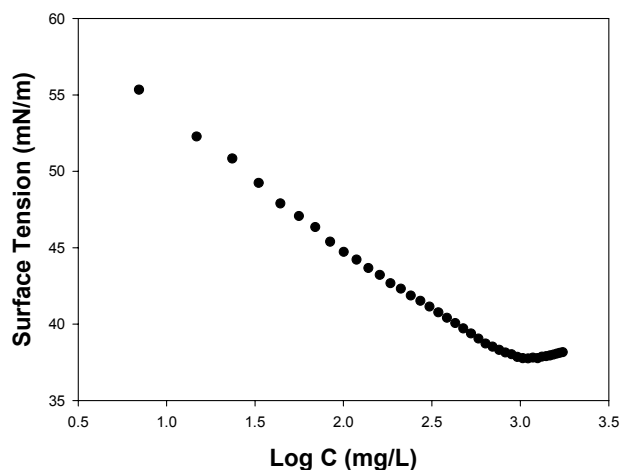


Fig. 4. Surface tension versus concentration (Log C) for cHAL2 water solution at pH 7

One structural feature of humic acid-like material which is currently a matter of dispute is their molecular weight (Sutton 2005). Measurements based on size exclusion chromatography (SEC) indicate values of the order of 10^4 - 10^5 D, whereas measurements performed by electrospray ionization (ESI) indicate values of the order of 10^3 Da. The ESI results, coupled with the fact that by gel permeation chromatography and high-pressure size-exclusion chromatography some workers have found that the apparent size of humic fragments changes drastically with addition of simple organic acids, has originated the belief that humic acid-like substances are aggregates of small molecules linked by hydrogen bonds and hydrophobic interactions, and not polymeric compounds containing covalent bonds only. The dispute over the molecular weight of humic acid-like substances is not only academic, but has relevance in relation to the performance of these materials as surfactants. With specific reference to our cHAL2 material, assessing the size of the molecules which give rise to the curve in Fig. 4 would make it possible to establish structure-properties relationships and then to use these in order to exploit the full potential of the material for specific technological applications. Thus, in this paper, we have address the molecular weight issue based on considerations and on experimental results which are described hereinafter.

In principle humic acid-like substances may yield two types of conformation in solution, which may be responsible for important interaction with other organic and inorganic species. These may be classified as micelles and pseudo-micelles (von

Wandruszka 2000). Whereas the former are aggregates of relatively small molecules held together by intermolecular forces, the latter may be visualized as macromolecules which, by virtue of the flexibility of the C chain, may fold and coil in a manner that directs hydrophilic (e.g. carboxy and hydroxy) groups outward and keeps more hydrophobic (e.g. hydrocarbon) moieties isolated in the center. This process produces an entity that is operationally similar to a conventional micelle, albeit more structurally constrained. Like a micelle, it has a hydrophobic interior and a more hydrophilic surface, giving it distinct solubilizing powers for nonpolar solutes. For our cHAL2 materials, we have carried out measurements of the molecular size and mass by three different techniques: i.e., ESI, SEC-MALS and DLS.

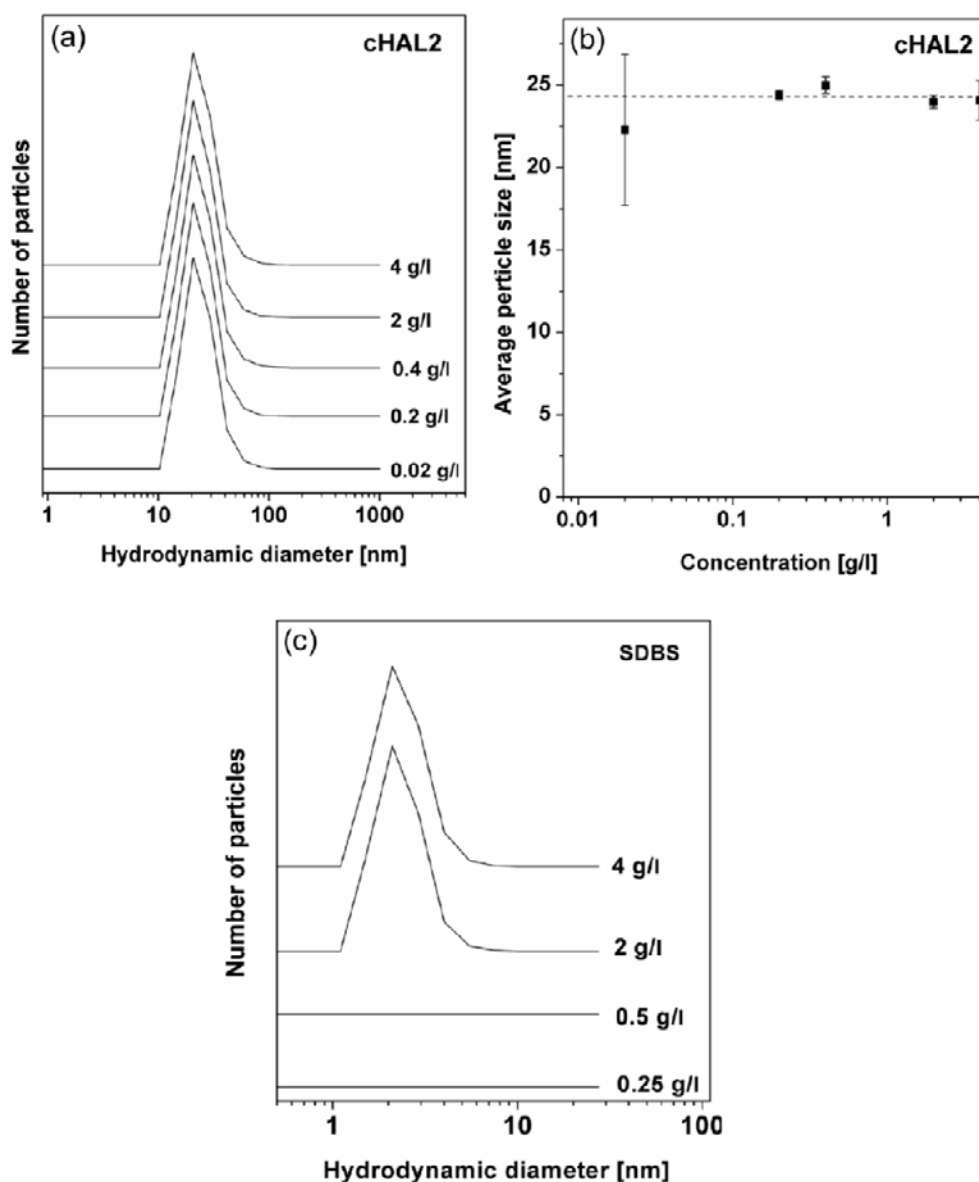


Fig. 5. Comparison between the particle size at different concentrations of cHAL2 (a and b) and the commercial additive SDBS (c). The particle size distribution of the two surfactants was measured at concentrations above and below the respective cmc values.

Dynamic light scattering (DLS) theory is a well established technique for measuring particle size over the 10^{-10} - 10^{-6} m range (Microtrac, Inc. 2007). DLS measures the velocity at which particles within a solvent diffuse due to Brownian motion. This is done by monitoring the fluctuation in intensity of the scattered light over the time. Indeed the scattered intensity due to the phase addition of the moving particles is constantly evolving, depending on the particle size. The Brownian diffusion velocity is inversely proportional to the particles size, expressed as hydrodynamic diameter (D_h). As this technique allows the determination of particle size distributions in solution at variable concentration, and therefore allows the calculation of the hydrodynamic diameter of the molecules or aggregates in solution, we performed DLS measurements at variable cHAL2 concentration (0.02-0.2 g L⁻¹). Based on our surface tension data (reported above) indicating formation of micelles for cHAL2 at 0.97 g L⁻¹, we expected by carrying DLS measurements below and above this concentration value to observe a change of D_h with cHAL2 concentration; i.e., a D_h increase above the 0.97 g L⁻¹ value due to the formation of molecular aggregates. Contrary to this expectation the plots in Fig. 5 do not show any significant change of D_h with concentration. The DLS measurements were repeated three times for each sample, and an average D_h value was calculated for every concentration. In Fig. 5b the average size, as calculated from three measurements, is reported as function of the concentration. The vertical bars indicate the standard deviation for every set of measurements. The data suggest that cHAL2 consists of particles with sizes included between 10 and 100 nm, and that this particle size distribution does not change upon changing the sample concentration. An average D_h of 24.4 nm was extrapolated from all the data here presented.

The same particle size was found by DLS measurements of a reference humic acid (HA) sample isolated from Suwannee River and supplied by the International Humic Substance Society (IHSS, St. Paul, USA) which was analyzed in solution at pH 7 and 0.04 g/L concentration (Baalousha 2006). The sizes measured for cHAL2 and the IHSS HA do not imply the absence of smaller particles. In fact, scattering intensity is inversely proportional to the sixth power of the radius for particles smaller than the wavelength of the laser; thus, larger particles scatter light more effectively than smaller ones. Therefore, large particles mask the presence of smaller ones in the sample. By comparison, we performed the same measurement on sodium dodecylbenzenesulfonate (SDBS). This well known synthetic commercial surfactant is reported to form micelles at 0.7-1.4 g L⁻¹ concentration in water and at pH 7 (Savarino 2007). With this molecule, our DLS measurements (Fig. 5c) showed signals at 2-4 g L⁻¹ concentration, whereas below the surfactant cmc value (0.25-0.50 g L⁻¹) the concentration the scattered intensity was extremely low and only the noise due to impurities bigger than 30 nm in the solution was detectable. In may be observed that the range of particle size for the SDBS small molecule is one order of magnitude lower than that observed for cHAL2. Also, contrary to the cHAL2 case, the data for SDBS indicate an increase of the particle size above the surfactant cmc value. The SDBS data therefore prove that DLS may show aggregate formation for small molecules, in the absence of large masking particles. By comparison, the lack of change of D_h with cHAL2 concentration, and therefore the absence of correlation between DLS and surface tension data, suggest that the large particles observed by DLS are not responsible for the surface tension dependence on concentration shown in Fig. 4, since their size seems unchanged over a very wide concentration range. Although the data do not make it possible to assess whether the large particles are aggregates or macromolecules, other small molecules must be present together with the larger particles. The small molecules would aggregate upon raising the cHAL2 concen-

tration and be responsible of the change of surface tension observed in Fig. 4. Evidence for the presence of both small molecules and large molecules was sought by the other two techniques, SEC-MALS and ESI.

In the SEC-MALS measurements the optimisation of the solubilization procedure and of the SEC experimental conditions for humic acid-like substances is not trivial. As reported in literature (Quagliotto 2006) and shown hereinafter, humic acid-like substances in aqueous solution are strongly aggregated and may yield micelles of various sizes. Furthermore, the aggregation extent may be significantly affected (Terashima 2004) by pH, ionic strength, and type of counterion of the used solvent. In addition to this, the SEC fractionation for these substances is a problem because column non-steric separation could occur. Often upon using non-optimized SEC conditions, multimodal and/or asymmetrical chromatograms with very long tails are obtained. With cHAL2 in the water- methanol solvent (see experimental), we have obtained a quasi-symmetrical chromatogram without a long tail, as opposed to asymmetrical long tail chromatograms obtained in the pure aqueous solvent. This fact suggested minimization of any presumable molecular aggregation due to the presence of methanol in the sample and elution solvent.

Figure 6 reports the experimental differential refractometer index (DRI) and light scattering (LS) signals, and the calculated molar mass (M) as a function of the elution volume (V). The $M=f(V)$ experimental function is the classical SEC calibration curve obtained directly from the on-line MALS detector. Using the $M=f(V)$ experimental function and the DRI curve, the molar mass distribution (MMD) for the cHAL2 sample reported in Fig. 7 was obtained. A summary of the molecular characterization of this sample is reported in Table 4. Basically, the cHAL2 sample shows an apparent molar mass centred around 150 kg/mol with a polydispersity of about 1.5-2.

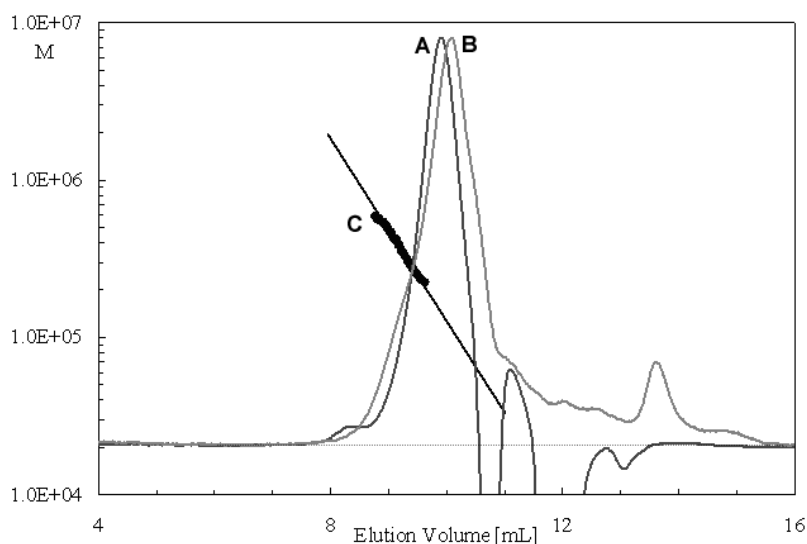


Fig. 6. Superimposition of concentration by DRI (curve A) and MALS with photodiode located at 90° (curve B) signals together with the calculated molar mass (M) as a function (line C) of the elution volume (V) for the cHAL2 sample.

Table 4. SEC-MALS Molecular Characterization^a of cHAL2.

M_p	M_n	M_w	M_z	M_w/M_n	M_z/M_w
g/mol	g/mol	g/mol	g/mol		
143,400	149,340	217,630	432,340	1.5	2.0

^aMolar mass of the chromatographic peak (M_p), number- (M_n), weight- (M_w) and z- (M_z) molar mass averages, and polydispersity indexes M_w/M_n and M_z/M_w .

The on-line MALS detector is also able to measure the molar mass (M) of the eluting fractions together with the dimension of the macromolecules, which is generally known as radius of gyration (R_g). This latter parameter is measured from the angular variation of the scattering intensity, when this is approximately higher than 8-10 nm. The $R_g = f(M)$ experimental function, (i.e., the conformation plot) of the cHAL2 sample is shown in Fig. 7. It is evident that the dimensional R_g parameter for the cHAL2 sample approximately ranges from 10 nm to 20 nm. Furthermore, from the estimated slope of the conformation plot (approximately 0.4) a compact quasi-spherical conformation of the cHAL2 aggregate or molecule could be inferred. The above 10-20 nm R_g value measured by SEC-MALS is consistent with the results obtained by DLS. By comparison, the molecular radius of naturally occurring humic acids has been reported to increase from 9.8 to 17.8 Å as the molecular weight increases from 5000 to 30000 (Tan 2003). Similarly to the DLS results, the SEC-MALS do not provide evidence of the presence of small molecules.

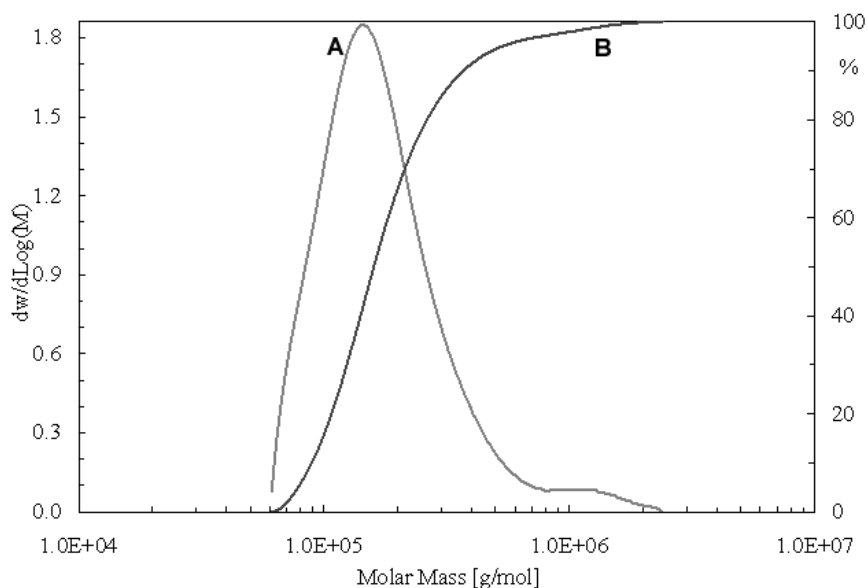


Fig. 7. Differential [$dw/d\text{Log}(M)$ for curve A] and cumulative (% for curve B) molar mass distribution (MMD) from SEC-MALS measurements for the cHAL2 sample.

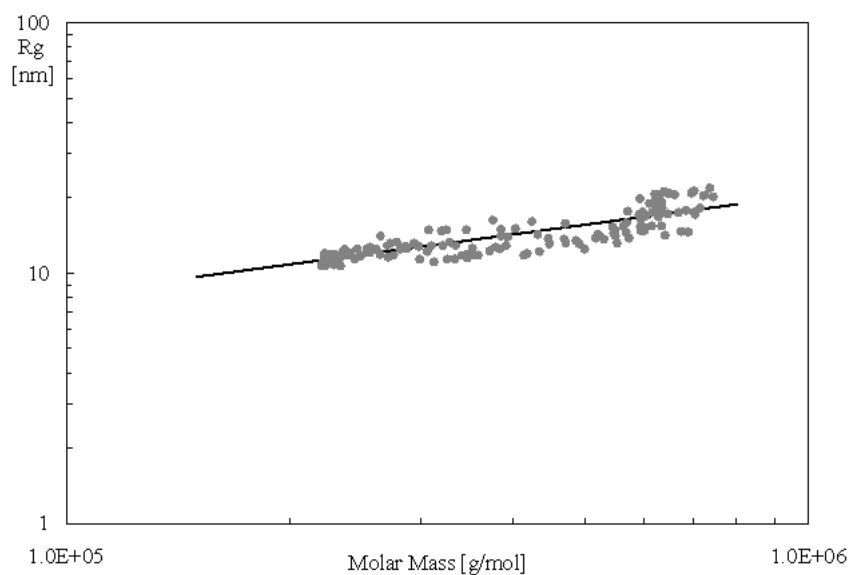


Fig. 8. Conformation plot from SEC-MALS of the cHAL2 sample; radius of gyration (Rg) as a function of molar mass.

Soft desorption ionization techniques, such as electrospray ionization (ESI), volatilize large ions for identification via mass spectrometry (MS), providing positive or negative ion mass/charge distributions that may represent the mass distribution of molecules within humic fractions (Sutton 2005). By this technique compounds may be analyzed from aqueous or aqueous/organic solutions at variable concentrations, similarly to the case of the above DSL measurements. As solvent evaporation occurs, the droplet shrinks until it reaches the point that the surface tension can no longer sustain the charge (the Rayleigh limit). At this point a "Coulombic explosion" occurs and the droplet is ripped apart. This event produces smaller droplets that can repeat the process as well as naked singly or multiply charged analyte molecules. High resolution mass spectrometry makes it possible to assign the charge value to an ESI signal originated by an ionized molecule through the examination of the signal isotopic peaks intensity.

Our ESI measurements were performed on cHAL2 and SDBS solutions at the same pH and sample concentrations as for the DLS measurements. The results of the ESI measurements for cHAL2 showed that below the surfactant sample cmc value the signals intensity was too low to allow any useful analysis of the recorded mass spectra. Above the cmc value, several significant signals were observed over the investigated 200-1500 m/z range (Fig.8). For the main signals falling in the 400-450 m/z range, z was proven equal to 1 by the distinctive isotopic pattern for singly charged ions which was observed in the spectra acquired at 60000 resolving power. Also, above the cHAL2 cmc value, the relative intensity of these signals was shown to increase linearly with the sample concentration. The same could not be assessed for the signals at m/z > 500. Although several signals at these m/z values are present in Fig. 9, their relative intensity did not change significantly with the sample concentration. These signals therefore were assigned to the measurements background noise and were not further analyzed for our scope. By comparison for the SDBS solutions in the 0.02 and 2 g L⁻¹ concentration range, which included the 0.7-1.4 g L⁻¹ values reported for the cmc of this compound (Savarino 2007), the signal of the C₁₂H₂₅(C₆H₄)SO₃⁻ anion at 325 m/z was well observed, together with

other two signals at 311 and 339 m/z which were likely to arise from $C_{11}H_{23}(C_6H_4)SO_3^-$ and $C_{13}H_{27}(C_6H_4)SO_3^-$ impurities. For this compound, the intensity of these signals increased linearly with concentration, but the same did not occur for the higher m/z signals, which were therefore assigned to the background noise. The results obtained for SDBS demonstrate that ESI is not able to assess the presence of molecular aggregates, as the weak interactions holding these species are broken during spray ionization. However, for the present work, the ESI results are highly important, inasmuch as they prove the presence of small molecules with molecular weights around 450 in the cHAL2 humic-like material, nearly half the weight of the fragment represented in Fig. 2. The enlarged spectra in the lower m/z region revealed repetitious peaks at discrete 14 Da. These suggest the presence of molecules with methylene chain of different lengths and are consistent with the above discussed NMR and IR spectroscopy findings. The ESI results also do not exclude the presence of larger molecules, as these might not volatilize under the analytical experimental conditions. Although the results obtained by the above three techniques together suggest the presence of small molecules together with large macromolecules, the real molecular mass distribution in the cHAL2 sample cannot be assessed.

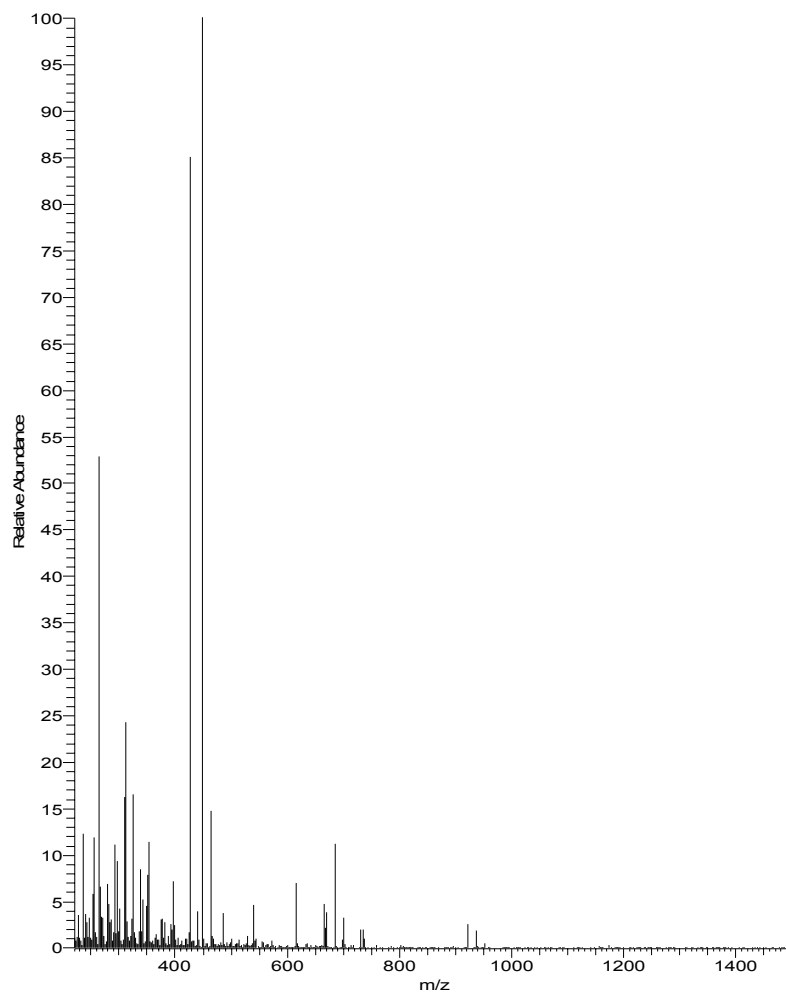


Fig. 9. Negative ion mode ESI spectrum acquired starting from 2.0g L^{-1} cHAL2 solution at pH7.

CONCLUSIONS

We have shown that two humic acid-like substances isolated from two different urban waste sources have different chemical structural features that significantly affect their surfactants properties. The results point out that biomass wastes may be an interesting source of biosurfactants with diversified properties that depend on the nature of waste and of its treatment process. Our structural investigation on cHAL2 suggests that, similarly to naturally occurring humic acids (HAs), it is likely to be a mixture of small molecules with molecular weight of the order of few thousands Da or less, and macromolecules with molecular weights of several hundred thousands. Whereas the size of the latter is not affected by their concentration in water, the small molecules probably can aggregate and be responsible for the surface tension versus concentration behaviour shown in Fig. 4. As to the potential performance of this humic acid-like substance in chemical technology, these materials could perform as classic surfactants due to their content of small molecules and capacity to yield micelles, and as dispersants due to their content of macromolecules (Showell 2006). In the next part of this work (Montoneri 2007, "Part 2") we will report the performance of cHAL2 as an auxiliary in a few important chemical technological applications and discuss the significance of the above structural features on performance rate.

ACKNOWLEDGMENTS

This work was carried out with Regione Piemonte Cipe 2004 funds for Cod. C 13 sustainable development program. This contribution was an original presentation at the *ITALIC 4 Science & Technology of Biomass: Advances and Challenges* Conference that was held in Rome, Italy (May 8-10, 2007) and sponsored by Tor Vergata University. The authors gratefully acknowledge the efforts of the Conference Organizers, Prof. Claudia Crestini (Tor Vergata University, Rome, Italy), Chair, and Prof. Marco Orlandi (Biococca University, Milan, Italy), Co-Chair. Prof. Crestini also is Editor for the conference collection issue to be published in *BioResources*.

REFERENCES CITED

- Baalousha, M., Motelica-Heino, M. and Le Coustumer, P. (2006). "Conformation and size of humic substances: Effects of major cation concentration and type, pH, salinity, and residence time," *Colloids and Surfaces A: Physicochem. Eng. Aspects* 272, 48–55.
- Brunelot, G., Adrian, P., Roullier, J., Guillet, B., and Andreoux, F. (1989). "Determination of dissociable acid groups of organic compounds extracted from soils, using automated potentiometric titration," *Chemosphere* 19, 1413-1419.
- Genevini, P. L., Adani, F., Veeken, A., Nierop, G. J., Scaglia, B., and Dijkema, C. (2002). "Qualitative modifications of humic acid-like and core-humic acid-like during high-rate composting of pig faeces amended with wheat straw," *Soil Sci. Plant Nutr.* 48, 143–150.
- Gran, G. (1952). "Determination of the equivalence point in potentionmetric titrations. Part II," *Analyst* 77, 661-671.

- Guetzloff, T. F., and Rice, J. A. (1994). "Does humic acid form a micelle?" *Sci. Total Environ.* 152, 31-35.
- Kawahigashi, M., Sumida, H., and Yamamoto, K. (2005). "Size and shape of soil humic acids estimated by viscosity and molecular weight," *J. Coll. Interf. Sci.* 284, 463–469.
- Kraft, E., Bidlingmaier, W., De Bertoldi, M., Diaz, L. F., and Barth, J. (Eds.) (2006). *Proceedings of the International Conference Orbit 2006 Biological Waste Management from Local to Global*. Weimar: verlag ORBIT e.V.; ISBN 3-935974-09-4.
- Mendichi, R., and Giacometti Schieron, A. (2001). "Use of a multi-detector size exclusion chromatography system for the characterization of complex polymers," *Current Trends in Polymer Science*, Pandalai S.G. Ed., Trans-World Research Network: Trivandrum India, Vol. 6, pp. 17-32.
- Montoneri, E., Savarino, P., Adani, F., Genevini, P. L., Ricca, G., Zanetti, F., and Paletti S. (2003a). "Polyalkylphenyl-sulphonic acid with acid groups of variable strength from compost," *Waste Management* 23(6), 523-535.
- Montoneri, E. (2003b). "Organic matter of compost" *Workshop Proceedings On the Role of Organic Matter in a Sustainable Agriculture*, Villa Marigola, Lerici, June 5-6, pages 84-88.
- Montoneri, E., Savarino, P., Bottigliengo, S., Musso, G., Bianco Prevot, A., Fabbri, D., and Pramauro, E. (2007). "Humic acid-like matter isolated from green urban wastes. Part II: Performance in chemical and environmental technologies," *Bioresources*, submitted for publication.
- Microtrac, Inc (2007). "Dynamic light scattering," available at <http://www.microtrac.com/dynamicscattering.cfm> [accessed August 2007].
- Newman, D. (2006). "Compostaggio in Italia, riflessioni sulle opportunità e prospettive future," paper presented at the meeting on *Recupero dei rifiuti industriali organici: conversione dei rifiuti in risorsa*, held at the University of Torino on December 13.
- Ozores-Hampton, M., and Obreza, T. (2007). "Beneficial uses of compost in Florida vegetables crops," *Compost facilities in Florida.pdf*, available at www.imok.ufl.edu/compost/pdf/Compost_Utilization.pdf [accessed April 13, 2007].
- Provencher, S. W. (1976). "A fourier method for the analysis of exponential decay curves," *Biophys. J.* 16, 27–41.
- Quagliotto, P. L., Montoneri, E., Tambone, F., Adani, F., Gobetto, R., and Viscardi, G. (2006). "Chemicals from wastes: Compost-derived humic acid-like matter as surfactant," *Environ. Sci. Technol.* 40, 1686-1692.
- Rosen, M. J. (Ed.) (1989). *Surfactants and Interfacial Phenomena*, 2nd edition, Wiley, New York. (forse eliminare)
- Savarino, P., Montoneri, E., Biasizzo, M., Quagliotto, P. L., Viscardi, G., and Boffa, V. (2007). "Upgrading biomass wastes in chemical technology. Humic acid-like matter isolated from compost as chemical auxiliary for textile dyeing," *J. Chem. Tech. Biotech.* in the press.
- Showell, M. S. (Ed.) (2006). *Handbook of Detergents. Part D: Formulation*, Taylor & Francis, Boca Raton, FL (USA).
- Stoffella, P. J., Li, Y., Roe, N. E., Ozores-Hampton, M., and Graetz, D. A. (1997). "Utilization of composted organic wastes in vegetable production systems," *Food & Fertilizer Technology Center Bulletin* 1997-12-01, available at <http://www.agnet.org/library/abstract/tb147.html> [accessed April 13, 2007].
- Sulthana, S. B., Bath, S. G. T., and Rakshit, A. K. (2000). "Solution properties of sodium

- dodecylbenzenesulfonate (SDBS): Effects of additives,” *Bull. Chem. Soc. Jpn.* 73, 281-287.
- Sutton, R., and Sposito, G. (2005). “Molecular structure in soil humic substances: The new view,” *Environ. Sci. Technol.* 39, 9009-9015.
- Tan, K. H., (ed.) (2003). *Humic Matter in Soil and Environment. Principles and Controversies*; Chapter 6; Marcel Dekker, Inc., New York.
- Terashima, M., Fukushima, M., and Tanaka, S. (2004). “Influence of pH on the surface activity of humic acid: Micelle-like aggregate formation and interfacial adsorption,” *Colloids and Surfaces A: Physicochem. Eng. Aspects* 247, 77-83.
- von Wandruszka, R. (2000). “Humic acids: Their detergent qualities and potential uses in pollution remediation,” *Geochem. Trans.* 1(2), 10-15.

Article submission received: Sept. 21, 2007; Peer-review completed, Dec. 15, 2007;
Revised version received and accepted: Dec. 17, 2007; Published Dec. 20, 2007.

PINE WOOD MODIFICATION BY HEAT TREATMENT IN AIR

Bruno M. Esteves,^{a*} Idalina J. Domingos,^a and Helena M. Pereira^b

Maritime pine (*Pinus pinaster*) wood has low dimensional stability and durability. Heat treatment was made in an oven using hot air during 2 to 24 h and at 170–200 °C. A comparison was made against steam heat treatment. The equilibrium moisture content and the dimensional stability (ASE) in radial and tangential directions were evaluated at 35%, 65%, and 85% relative humidity. MOE, bending strength and wettability were also determined. At the same mass loss, improvements of equilibrium moisture content and dimensional stability were higher for oven heat treatment, but the same was true for mechanical strength degradation. A 50% decrease in hemicellulose content led to a similar decrease in bending strength.

Keywords: Bending strength, Dimensional stability, Heat treatment, MOE, *Pinus pinaster*, Wettability

a: Centre of Studies in Education, Technologies and Health, School of Technology of Viseu, Polytechnic Institute of Viseu, Campus Politécnico Repeses, 3504-510, Viseu, Portugal *b:* Forest Research Centre, School of Agronomy, Technical University of Lisbon, Portugal; *Corresponding author: bruno@demad.estv.ipv.pt

INTRODUCTION

Heat treatment is a wood improvement and preservation process that is facing a recent surge of interest. Despite having started in 1946 with the work of Stamm et al., it was only in the last decade or so that it was systematically researched and industrially applied in some European countries. There are different commercial heat treatment processes: the Finish process (Thermowood) uses steam (Viitanen et al. 1994), the Dutch (Plato Wood) uses a combination of steam and heated air (Tjeerdsma et al. 1998b), the French (Rectification) an inert gas (Dirol and Guyonnet 1993) and the German (OHT) heated oil (Sailer et al. 2000).

The heat treatment increases the wood value by decreasing equilibrium moisture content (Jämsä and Viitaniemi 2001; Wang and Cooper 2005; Esteves et al. 2007a, b), improving dimensional stability (Viitaniemi et al. 1997; Yildiz 2002; Wang and Cooper 2005; Esteves et al. 2007 a, b) and durability (Dirol and Guyonnet 1993; Kamdem et al. 2002) along with a decrease of the heat transfer coefficient (Militz 2002). The heat treated woods also acquire a darker color similar to most tropical woods, which is an aesthetical advantage for some applications (Mitsui et al. 2001; Bekhta and Niemz 2003). The treatment is however detrimental to mechanical properties especially to static and dynamic bending strength (Yildiz 2002; Esteves et al. 2007 a, b), and also to compressive strength (Unsal and Ayrimis 2005).

When submitted to heating, wood changes its chemical composition through a thermal degradation that depends on temperature and time of exposure. For example, although wood presents a good thermal stability at 100 °C if the treatment time is long

enough some chemical bonds begin to break, even for lower temperatures (Shafizadeh and Chin 1976). The temperature at which thermal degradation begins depends also on the wood species. For example, Kollmann and Fengel (1965) concluded that there was only mass loss for temperatures higher than 100 °C for pinewood, and 130-150°C for oakwood. The temperature at which the degradation starts depends on the molecular mass and crystallinity of the wood components (Belville 1982).

Maritime pine (*Pinus pinaster*) is a low valued timber species because of the relatively poor dimensional stability and durability of pinewood and the difficult preservation which is only possible for small diameters. Additionally it has an unappealing yellowish color. Heat treatment could improve some of these aspects and be a possible alternative to environmentally doomed chemical preservation treatments. The French process has already been applied to treat *Pinus pinaster* wood.

This paper presents results on the treatment of pinewood describing the properties change along the treatment, the decrease in equilibrium moisture content and increase in dimensional stability, the decrease in wettability and the degradation of mechanical properties mainly of MOE and bending strength. The selected treatment was heating in hot air at temperatures 170-200°C and variable duration leading to different treatment severity. The improvement of properties was related to mass loss. A comparison is made between this treatment and the steam heat treatment reported by Esteves et al. (2007b) in the same conditions, therefore allowing analyzing the effect of an oxidative atmosphere which is likely to induce more intensive chemical changes on wood.

EXPERIMENTAL

Material and Wood Treatment

Pinewood samples were cut from the sapwood of a radial board of one maritime pine (*Pinus pinaster* Aiton.) tree from the Portuguese region of Águeda. Cubic samples with approximately 40 mm edge and samples with 360mmx20mmx20mm were cut with clear faces, kept in a conditioned room at 20°C and 50% relative humidity for 3 weeks and weighed afterwards. The equilibrium moisture content and the dry mass of the samples were determined. The heat treatment was made in an oven heated by electric coils located in the walls and with exhaustion of the heated gases by natural convection through an opening in the oven wall. The treatment was made for 2 to 24 h and at 170-200°C. The treatment started by putting the samples at ambient temperature in the oven, and the period to reach the treatment temperature was about 60 min. Four replicates were used for each combination of time/temperature of treatment and for each sample size. After treatment, the samples were cooled down in a dry environment and weighed. Mass loss was determined in relation to initial dry wood. Untreated samples were used as the control.

Wood Properties

Treated and untreated wood samples were kept in a controlled environment at 20°C and sequentially equilibrated at 35, 65, and 85% relative humidity for at least 4 weeks in each relative humidity and until the mass variation was less than 5% in two

consecutive days. Mass was determined and the equilibrium moisture content was calculated. The samples dimensions were measured in radial and tangential directions for all the relative humidity and dimensional stability of the heat treated samples was calculated as an Anti Swelling Efficiency (ASE). ASE gives the difference between the swelling coefficient of treated and untreated samples, from oven dry to 35% (ASE35), 65% (ASE65) and 85% (ASE85) relative humidity in percentage of the swelling values

$$\text{for the untreated samples. For example ASE}_{35} (\%) = \left(\frac{S_{nt} - S_t}{S_{nt}} \right) * 100$$

where S_{nt} and S_t represent the shrinking between 35% relative humidity and 0% relative humidity for untreated (nt) and treated (t) samples. The shrinking is determined in percent as

$$S(\%) = \left(\frac{L_{35\%} - L_{0\%}}{L_{35\%}} \right) * 100$$

with L representing the dimension of the sample.

Wettability was determined by the contact angle method in tangential and radial sections, with the contact angle measured 10 seconds after the contact of a 10 μ l water drop with the sample. Distilled water was used in this test.

The mechanical properties were determined with samples of 360x20x20 mm³ (axial x radial x tangential) by a three point bending device. MOE measurements were made using a constant velocity of 0.3 mm/min and for bending strength the velocity was estimated to cause rupture in about 3 min.

MOE and bending strength were determined according to the Portuguese standard NP-619 as:

$$\text{MOE(N/mm}^2) = \frac{\Delta F * L^3}{\Delta x * 4 * b * h^3}$$

$$\text{Bending strength (MPa)} = \frac{3 * F * L}{2 * b * h^{\frac{10}{6}}}$$

where F is the load on rupture measured in N/mm, $\frac{\Delta F}{\Delta x}$ is the slope of the elastic zone in N/mm, L is the arm length, h the height and b the width, all expressed in mm.

RESULTS AND DISCUSSION

Mass Loss

Figure 1 presents the mass loss with heat treatment for temperatures between 170-200°C along the treatment time.

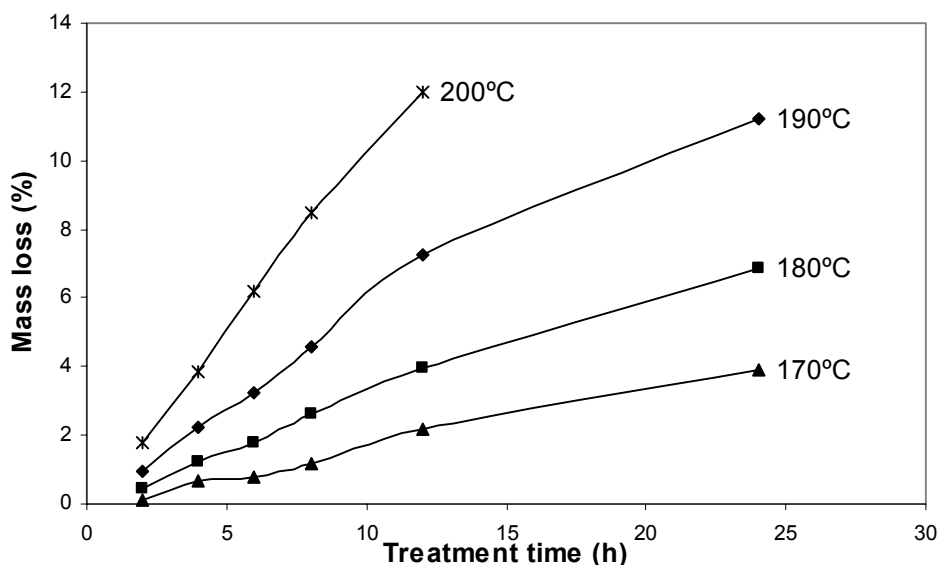


Fig. 1. Pinewood mass loss with heat treatment

Mass loss increased with the treatment time and with the temperature, and the same mass loss could be obtained with different temperatures, depending on the treatment time (Fig. 1). For example, a mass loss of 3% could be reached at 170°C in 17 h, at 180°C in 9 h, at 190°C in 5 h and at 200°C in only 3h. Similar results were reported by several authors. For instance, Zaman et al. (2000) treated *Pinus sylvestris* and *Betula pendula* at temperatures between 200°C and 230°C during 4-8 h and determined that the mass losses for pine varied between 5.7% (4h) to 7.0% (8h) at 205 °C, and between 11.1% (4h) and 15.2% (8h) at 230 °C and for birch 6.4% (4h) and 10.2% (8h) at 200 °C and 13.5% (4h) and 15.2% (8h) at 220 °C. Alén et al. (2002) studied the mass loss of heat treated spruce at temperatures between 180°C and 225°C during 4 to 8 hours and concluded that they were between 1.5% at 180 °C (4 h) and 12.5% at 225°C (6h). At higher temperatures mass losses are quite higher; Bourgois and Guyonnet (1988) attained a mass loss of 18.5% in just 15 min, reaching 30% for 1 hour for maritime pine wood at 260°C. Órfão et al. (1999) reported that *Pinus pinaster* wood starts to degrade at 140°C with or without the presence of oxygen.

The rate of mass loss was higher in the beginning of the treatment and decreasing for longer treatments. Since the mass loss showed an approximately linear variation with the treatment time until about 12 h, it was possible to adjust linear equations with statistically significant coefficients (R^2 between 0.972 and 0.998). The rate of mass loss (in h^{-1}) increased with the treatment temperature: 0.20 (170°C), 0.35 (180°C), 0.63 (190°C), 1.03 (200°C). The higher initial rate of mass loss was due to the thermal degradation of the more susceptible compounds, mainly hemicelluloses but also to the volatilization of some extractives as reported by Esteves et al. (2007c). For example in a treatment at 190°C during 6 h the hemicelluloses content decreases 17.2% in relation to the initial content and at the same time most of the original extractive compounds have disappeared (Esteves et al. 2007c). Similar results for the degradation rate were also reported for the heat treatment of other species like cedar (González-Peña et al. 2004).

Mass loss of oven heat treated pine wood was higher than for autoclave steam heat treated pine wood at the same conditions as reported by Esteves et al. (2007b). As an example, for a treatment at 200 °C during 6 h the mass loss for pine wood treated in the oven was 6.2%, while in the autoclave it was only 3.5% (Fig. 1). These results are in accordance with Stamm (1956), who reported that wood degrades more in the presence of air due to oxidation reactions. It is also known that the acetic acid produced in this process acts as a depolymerization catalyst, and it is possible that there is a higher content of acetic acid released on the oxidizing environment. Mazela et al. (2003) compared the mass losses with heat treatment in air or in an atmosphere with water vapor, using temperatures of 160°C, 190°C, and 220°C during 6-24h and reported that the mass losses in the presence of air and water vapor for a treatment during 6 hours were similar, but for 24h mass losses in air were much higher.

The extent of thermal decomposition is often measured by mass loss. In accordance to the Thermowood patent (Viitaniemi et al. 1997), a mass loss of 3% is needed to improve wood dimensional stability and at least 5% to improve durability.

Equilibrium Moisture Content

The equilibrium moisture content of pine wood decreased with heating even for very short treatment times.

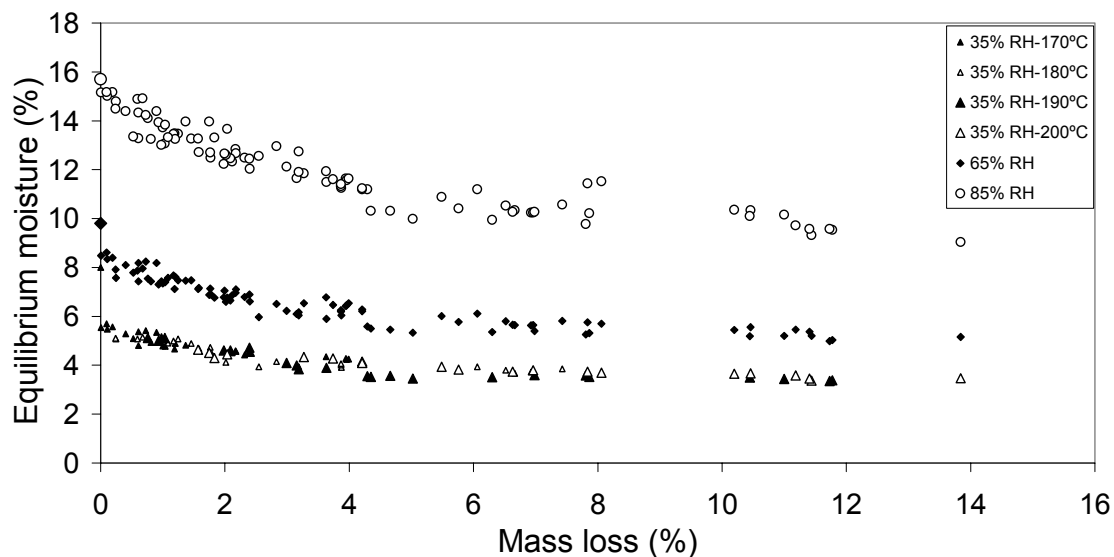


Fig. 2. Equilibrium moisture content of heat treated wood in relation to mass loss in different relative humidity environments.

Figure 2 presents the equilibrium moisture content at three different relative humidities (35%, 65% and 85%) as a function of mass loss. The equilibrium moisture content of heat treated pine wood decreased with the increase in treatment severity. The rate of decrease was higher for lower mass loss reaching a minimum value for about 4% mass loss. The behavior was similar for the three relative humidity environments. Although the net reduction of equilibrium moisture content was higher for 85% relative

humidity, the reduction in relation to untreated wood was higher for 35% relative humidity. These results are generally in agreement with Kamdem et al. (2002) for beech wood treated at temperatures between 200-260°C and conditioned at similar relative humidities (66% and 86%) and with Esteves et al. (2007a) for eucalypt wood.

A mass loss between 4-6% was enough to get the maximum reduction in equilibrium moisture and a higher treatment severity did not benefit the equilibrium moisture of wood (Fig. 2). Similar results were reported by Esteves et al. (2007b) with autoclave heat treated pine wood, but in this case the minimum equilibrium moisture content was obtained at about 6-8% mass loss. This means that for a treatment with steam it is necessary to attain a higher mass loss to have a similar reduction on equilibrium moisture. This is possibly due to the somewhat different degradation reactions with heat occurring in air and in steam environment. Viitaniemi et al. (1997) also reported identical results for spruce wood, with the minimum equilibrium moisture content being reached for about 6% mass loss.

The reduction on equilibrium moisture content is due to several factors. The degradation of hemicelluloses, which are the most hygroscopic structural compounds, plays an important role but the degradation of the amorphous regions of cellulose and the cross-linking reactions also contribute to the decrease on equilibrium moisture content as reported by several authors (Bhuiyan and Hirai 2005; Tjeerdma et al. 1998a; Tjeerdma and Militz 2005). Esteves et al. (2007c) reported that hemicelluloses content decreased 17.2% and 10.4% in relation to initial content at about 3% mass loss for a treatment in air and in steam environment, respectively. A higher mass loss is needed for the steam treatment to attain the same hemicelluloses reduction and consequently a similar effect on equilibrium moisture.

The reasons for the apparent stabilization of the equilibrium moisture content for higher mass losses are not clear, although Bhuiyan and Hirai (2005) refer that cellulose crystallinity decreases for more severe treatments which might increase the accessible hydroxyl groups.

Dimensional Stability

The heat treatment improved pine wood dimensional stability even for short time treatments, increasing with time and temperature of treatment. For example the radial ASE₃₅ of heat treated wood was 57% with 8 h at 170 °C, 4 h at 180 °C or 2 h at 190°C. The maximum values reached were between 63-73%. Similar results were reported by several authors, i.e. Yildiz (2002) with beech wood treated at 130-200°C during 2-10 hours.

The improvements on dimensional stability were higher for lower relative humidities (Fig. 3). For example at 65% RH, the tangential ASE ranged between 25 and 38% reaching a maximum of 62% while for 85% RH, the maximum tangential ASE was 44%. The increase in dimensional stability is mainly due to the decrease in equilibrium moisture content.

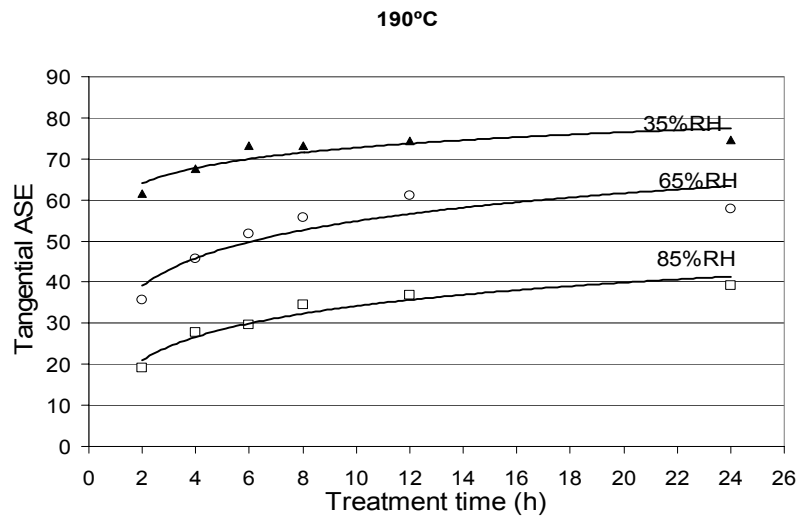


Fig. 3. Relationship between tangential ASE and treatment time for 35, 65 and 85% relative humidity. Each point is an average of 4 samples.

Figure 4 shows the variation of radial and tangential ASE with mass loss, at 35% relative humidity. The improvements were slightly higher in the tangential direction with ASE₃₅ ranging from 73 to 80% for treatments at 170-200°C. Although stability improved more in the tangential direction, the swelling of treated wood samples remained higher than in the radial direction. The behavior was similar for 65% and 85% RH. Analogous results were reported by Tjeerdsma et al. (1998a) with beech, birch, spruce, Scots pine and Monterey pine.

For outdoor furniture it is important to have similar radial and tangential swelling, that is to say, a low anisotropy; therefore the decrease in anisotropy with the heat treatment as given by the comparatively higher increase in tangential ASE is an advantage for this type of wood use.

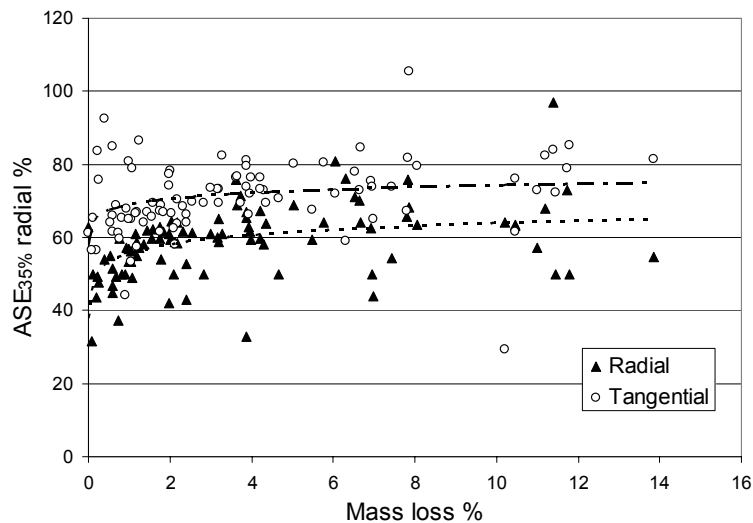


Fig. 4. Variation of radial and tangential ASE with mass loss at 35% relative humidity

The increase in dimensional stability was higher for smaller mass losses until about 4%. The results were similar for both directions but with slightly higher values in the tangential direction.

The maximum ASE values were obtained at a mass loss of about 4-6%, and only in a few cases a small increase of dimensional stability was observed for higher mass losses. These results are in accordance with those reported by several authors i.e. Viitaniemi et al. (1997) with spruce wood, in which the maximum ASE was obtained for mass loss between 5-6% and Esteves et al. (2007b) for autoclave heat treated pine and eucalypt wood for 6-8% mass loss.

Wettability

The surface wettability in relation to mass loss for radial and tangential sections is presented in Figure 5. The contact angle increased, and the wettability decreased, until about 3% mass loss for both sections, and after that stabilized for higher mass losses. Similar results were reported by Pecina and Paprzycki (1988) with Scots pine and Hakkou et al. (2003) with poplar, beech, spruce and Scots pine. The wettability decrease is due to the degradation of the most hygroscopic compounds, hemicelluloses, and amorphous cellulose, but also to dehydration reactions. The change of the extractive composition might also play an important role on wood wettability. At 3% mass loss according to Esteves et al. (2007c) most of the original pinewood extractives have disappeared and new ones have been formed. The new extractives formed are mainly some phenolic compounds and anhydrosugars.

An increase of wettability for higher mass losses is possible due to the degradation of macromolecular compounds as mentioned by Pecina and Paprzycki (1988). The differences in extractive chemical composition between 3% and higher mass losses, reported by Esteves et al. (2007c) could also contribute to a change of wood wettability.

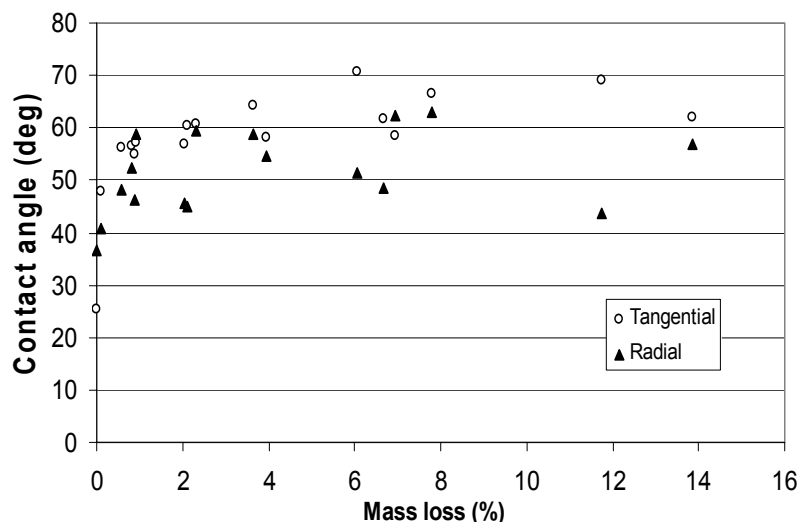


Fig. 5. Contact angle on tangential and radial sections in relation to mass loss during heat treatment .

Although wettability of untreated pine wood was higher for the tangential section, there were no significant differences between sections for heat treated wood.

Wettability influences gluing and finishing, mainly by increasing the absorption time of glues and varnishes; however, according to Vernois (2000) some varnishes can be adapted to this type of wood.

Mechanical Properties

MOE and bending strength decreased with heat treatment time and temperature. With 2 h of treatment, the MOE reduction was very small, with 2% (180°C), 0% (190°C), and 0% (200°C), and reached 6% (180°C), 12% (190°C), and 19% (200°C) with 12 h of treatment. The modulus of elasticity of pine wood decreased with mass loss during the heat treatment (Fig. 6). The decrease was less than 5% until about 4% mass loss, but increased subsequently and attained 16% for about 6% mass loss. Although the MOE decreased with heat treatment, at the mass loss necessary to obtain the maximum improvement on equilibrium moisture and dimensional stability (4-6%) the decrease was under 10% which is not significant. Yildiz et al. (2002) reported a decrease in MOE of about 45%, for beech wood treated at 130-200°C for 2-10 h but mass loss was not referred. Results reported by Esteves et al. (2007b) with steam heat treated pine wood showed a small increase until about 4% mass loss, followed by a decrease for higher mass losses. With the same treatment conditions, heating time and temperature, the reduction of MOE was higher for the treatment in air and the same happened when comparing at the same mass loss.

Bending strength of untreated pine wood was, on average 154 MPa, varying between 138-171 MPa and decreased in the heat treated pine wood samples more than the MOE. The relative decrease of bending strength was between 4- 38% with only 2 h of treatment at 180-200°C and 31% (180°C), 58% (190°C), and 58% (200°C) with 12 h of treatment.

The rate of bending strength decrease was higher for small mass losses, about 40% for 3% mass loss, decreasing afterwards, but reaching 60% for mass losses above 6% (Fig. 6). The reduction of bending strength was higher than the reported by Kim et al. (1988) for radiata pine treated at 180 °C during 2 h with a reduction of the modulus of rupture (MOR) of only 21% for dry wood and 27% for green wood. Bengtsson et al. (2002) obtained a similar reduction in bending strength of 50% for spruce wood and 47% for Scots pine wood treated at 220 °C. The reduction on bending strength is mainly due to the degradation of hemicelluloses. The close relationship between hemicellulose content and bending strength was also reported by several authors (Winandy and Morrell 1993; Winandy and Lebow 2001). For 7% mass loss only about 50% of hemicelluloses remained in wood which has a high impact on bending strength (Fig. 6).

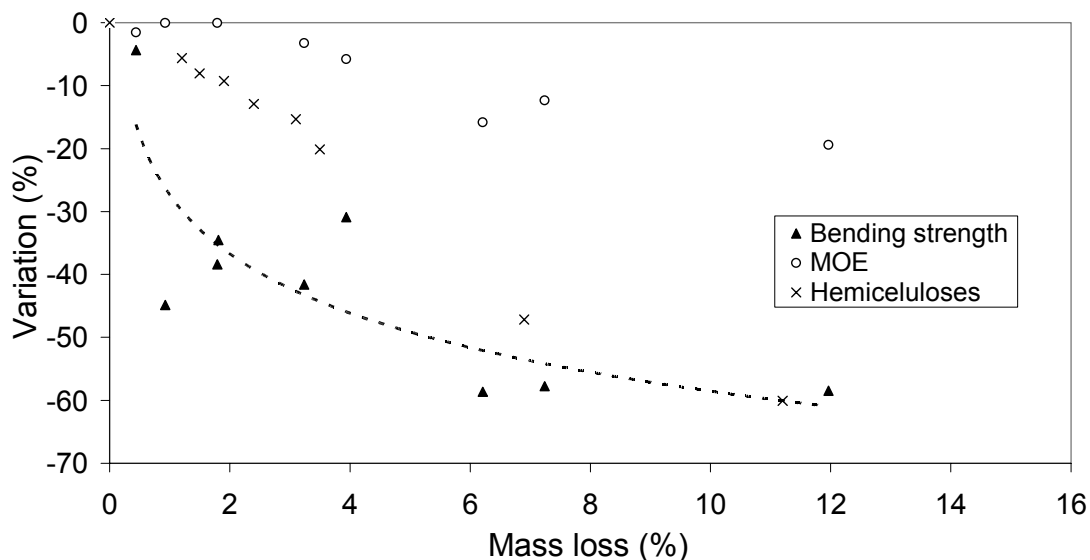


Fig. 6. Variation of bending strength, MOE and hemicelluloses content with mass loss during heat treatment. Each point is the average of 3 samples.

At about (4-6%) the reduction of bending strength would be about 40-60% higher than the reported by Esteves et al. (2007b) for steam heat treated pine wood (25%). It seems that a treatment with steam affects less the mechanical properties of wood with the same mass loss. Nevertheless, at the same mass loss the degradation of macromolecular compounds is different for wood treated with hot air or with steam. For example, at about 3% mass loss there is a decrease of hemicelluloses content of 17.2% and 10.4% for oven and autoclave treatment, respectively (Esteves et al. 2007c).

CONCLUSIONS

1. The heat treatment of pine wood improved some of its properties: equilibrium moisture content decreased, the dimensional stability increased, and the anisotropy and the surface wettability decreased. In relation to mechanical properties, MOE was little affected but bending strength decreased much more.
2. Mass loss of oven heat treated pine wood was higher than for steam heat treated pine wood under the same conditions.
3. At the same mass loss the equilibrium moisture content decreased more than for the steam treatment due to the higher degradation of hemicelluloses and amorphous cellulose.
4. The oven heat treatment improved more the dimensional stability but also affected more the mechanical properties of wood than steam heat treatment with the same mass loss, possibly due to the oxidation reactions and to the higher hemicellulose

degradation. A 50% decrease in hemicellulose content led to a similar decrease in bending strength.

REFERENCES CITED

- Alén, R., Kotilainen, R., and Zaman, A. (2002). "Thermochemical behavior of Norway spruce (*Picea abies*) at 180-225 °C," *Wood Sci. Technol.* 36, 163-171.
- Bekhta, P., and Niemz, P. (2003). "Effect of high temperature on the change in color, dimensional stability and mechanical properties of spruce wood," *Holzforschung* 57, 539-546.
- Belville, P. (1982). "Modélisation de la cinétique de pyrolyse de particules de bois de taille importante et du bilan matière de la gazéification à l'oxygène pur," *Thesis Université de Compiègne, France.*
- Bengtsson, C., Jermer, J., and Brem, F. (2002). "Bending strength of heat-treated spruce and pine timber," In: *International Research Group Wood Pre, Section 4-Processes, N° IRG/WP 02-40242.*
- Bhuiyan, T., and Hirai, N. (2005). "Study of crystalline behaviour of heat-treated wood cellulose during treatments in water," *J. Wood Sci.* 51, 42-47.
- Bourgeois, J., and Guyonnet, R. (1988). "Characterisation and analysis of torrefied wood," *Wood Sci. Technol.* 22: 143-155
- Dirol, D., and Guyonnet, R. (1993). "Durability by rectification process," In: *International Research Group Wood Pre, Section 4-Processes, N° IRG/WP 93-40015.*
- Esteves, B., and Pereira, H. (2007c). "Influence of heat treatments in pine wood extractives," *Submitted to Journal of Wood Chemistry and Technology.*
- Esteves, B., Domingos, I., and Pereira, H. (2007a). "Improvement of technological quality of eucalypt wood by heat treatment in air at 170-200°C," *For. Prod. J.* 57 (1/2), 47-52.
- Esteves, B., Velez Marques, A., Domingos, I., and Pereira, H. (2007b). "Influence of steam heating on the properties of pine (*Pinus pinaster*) and eucalypt (*Eucalyptus globulus*) wood," *Wood Sci. and Technol.* 41, 193-207. DOI : 10.1007/s00226-006-0099-0.
- González-Peña, M., Breese, M., and Hill, C. (2004). "Hygroscopicity in heat-treated wood: Effect of extractives," In: *International Conference on Environmentally Compatible Forest Products (ICECFOP)*. 22-24 September 2004. pp. 105-119.
- Hakkou, M., Pétrissans, M., El Bakali, I., Gérardin, P., and Zoulalian, A. (2003). "Evolution of wood hydrophobic properties during heat treatment," In: *Abstracts of the First European Conference on Wood Modification*, Ghent, Belgium.
- Jämsä, S., and Viitaniemi, P. (2001). "Heat treatment of wood – Better durability without chemicals," In: *Proceedings of special seminar held in Antibes, France.*
- Kamdern, D., Pizzi, A., and Jermannaud, A. (2002). "Durability of heat treated wood," *Holz Roh-Werkst* 60: 1-6.
- Kim, G., Yun, K., and Kim, J. (1998). "Effect of heat treatment on the decay resistance and the bending properties of radiata pine sapwood," *Material und Organismen* 32 (2), 101-108.

- Kollmann, F., and Fengel, D. (1965). "Changes in the chemical composition of wood by thermal treatment," *Holz Roh Werkst.* 12, 461-468.
- Mazela, B., Zakrzewski, R., Grzeskowiak, W., Cofta, G., and Bartkowiak, M. (2003). "Preliminary research on the biological resistance of thermally modified wood," In: *Abstracts of the First European Conference on Wood Modification*, Ghent, Belgium.
- Militz, H. (2002). "Thermal treatment of wood: European processes and their background," In: *International Research Group Wood Pre*, Section 4-Processes, N° IRG/WP 02-40241.
- Mitsui, K., Takada, H., Sugiyama, M., and Hasegawa, R. (2001) "Changes in the properties of light-irradiated wood with heat treatment: Part 1 Effect of treatment conditions on the change in color," *Holzforschung* 55, 601-605.
- NP 619 (1973)- "Ensaio de flexão estática de madeiras," In Portuguese.
- Órfão, J., Antunes, F., and Figueiredo, J. (1999). "Pyrolysis kinetics of lignocellulosic materials- Three independent reactions model," *Fuel* 78, 349-358.
- Pecina, H., and Paprzycki, O. (1988). "Wechselbeziehungen zwischen der Temperaturbehandlung des Holzes und seiner Benetzbarkeit," *Holzforsch. Holzverwert.* 40(1), 5-8.
- Sailer, M., Rapp, A., and Leithoff, H. (2000). "Improved resistance of Scots pine and spruce by application of an oil-heat treatment," In: *International Research Group Wood Pre*, Section 4-Processes, N° IRG/WP 00-40162.
- Shafizadeh, F., and Chin, P. (1976). "Thermal deterioration of wood," In: *Goldstein Wood Technology Chemical Aspects*. ACS Symposium Series, 57-81.
- Stamm, A. (1956). "Thermal degradation of wood and cellulose," *Ind. Eng. Chem.* 48, 413-417.
- Stamm, A., Burr, H., and Kline, A. (1946). "Stayb-wood-A heat stabilized wood," *Ind. Eng. Chem.* 38 (6), 630-634.
- Tjeerdsma, B., and Militz, H. (2005). "Chemical changes in hydrothermal wood: FTIR analysis of combined hydrothermal and dry heat-treated wood," *Holz. Roh Werkst.* 63, 102-111.
- Tjeerdsma, B., Boonstra, M., and Militz, H. (1998a). "Thermal modification of nondurable wood species: improved properties of thermally treated wood," In: *International Research Group Wood Pre*, document N° IRG/WP 98-40124.
- Tjeerdsma, B., Boonstra, M., Pizzi, A., Tekely, P., and Militz, H. (1998b). "Characterisation of thermally modified wood: molecular reasons for wood performance improvement," *Holz Roh-Werkst.* 56, 149-153.
- Unsal, O., and Ayrilmis, N. (2005). "Variations in compression strength and surface roughness of heat-treated Turkish river red gum," *J. Wood Sci.* 51, 405-409.
- Vernois, M. (2000). "Heat treatment of wood in France-State of the art," *Centre Technique du Bois et de l'Ameublement*, Paris, France.
- Viitanen, H., Jämsä, S., Paajanen, L., Nurmi, A., and Viitaniemi, P., (1994). "The effect of heat treatment on the properties of spruce document N° IRG/WP 94-40032, 4p.
- Viitaniemi, P., Jämsä, S., and Viitanen, H. (1997). "Method for improving biodegradation resistance and dimensional stability of cellulosic products," *United States Patent N° 5678324 (US005678324)*.

- Wang, J., and Cooper, P. (2005). "Effect of oil type, temperature and time on moisture properties of hot oil-treated wood," *Holz Roh-Werkst* 63, 417-422.
- Winandy, J., and Lebow, P. (2001). "Modeling strength loss in wood by chemical composition. Part I. An individual component model for southern pine," *Wood Fiber Sci.* 33 (2), 239-254.
- Winandy, J., and Morrell, J. (1993). "Relationship between incipient decay, strength, and chemical composition of Douglas-Fir heartwood," *Wood Fiber Sci.* 25 (3), 278-288.
- Yildiz, S. (2002). "Effects of heat treatment on water repellence and anti-swelling efficiency of beech wood," In: *International Research Group Wood Pre*, Section 4-Processes, N° IRG/WP 02-40223.
- Zaman, A., Alen, R., and Kotilainen, R. (2000). "Thermal behavior of *Pinus sylvestris* and *Betula pendula* at 200-230 °C," *Wood Fiber Sci.* 32 (2), 138-143.

Article submitted: July 17, 2007; Peer-review completed: Aug. 26, 2007; Revised version received and approved: Jan. 3, 2008; Published Jan. 5, 2008.

INFLUENCE OF PECTINOLYTIC ENZYMES ON RETTING EFFECTIVENESS AND RESULTANT FIBER PROPERTIES

[Jonn A. Foulk](#),^{a*} Danny E. Akin,^b and Roy B. Dodd^c

Enzymes have the potential to provide an improved method to ret flax for textile fibers. Retting is the separation or loosening of fiber bundles from the cuticularized epidermis and the woody core cells. New commercial pectinase products were evaluated both with and without ethylenediaminetetraacetic acid (EDTA) for retting efficiency. The Fried Test identified the most efficient enzymes and best retting conditions. All enzymes retted flax stems better in the presence of 18 mM EDTA. Pectinases that also contained cellulases reduced fiber strength, whereas those without cellulases effectively retted flax without substantial strength loss. Viscozyme, which has been used extensively in our enzyme-retting research, and several pectinolytic enzymes were compared in pilot plant scale tests. Texazym BFE and Bioprep 3000 L retted flax as well as Viscozyme in this system, and the fibers had higher tenacity. The monocomponent nature, commercial availability and price, and ability to ret flax in combination with EDTA at high pH indicated a potential advantage for Bioprep 3000 L in these tests. Retting with different enzymes and formulations resulted in fibers with different properties, thereby leading to protocols for tailored fiber characteristics.

Keywords: Flax; Fiber; Enzyme; Retting; Fiber quality

Contact information: a: Cotton Quality Research Station, ARS-USDA, Clemson, South Carolina 29633 USA; b: Russell Research Center, ARS-USDA, Athens, Georgia 30604 USA; c: Department of Agricultural and Biological Engineering, Clemson University, Clemson, SC, 29634 USA; *Corresponding author: jonn.foulk@ars.usda.gov

INTRODUCTION

Bast fibers, which form in the cortical regions of certain plants like flax, require retting in order to obtain commercial fibers for textile and other applications. Retting is the separation or loosening of fiber bundles from the cuticularized epidermis and the woody core cells and subdivision to smaller bundles and ultimate fibers. Microbial activity during retting causes a partial degradation of the components that bind tissues together, thereby separating the cellulosic fibers from non-fiber tissues. Earlier work has clearly indicated the requirement of pectinases in flax retting (Sharma 1987a; Van Sumere 1992). Two methods employed for retting flax at commercial levels using pectinolytic microorganisms are water- and dew-retting (Sharma and Van Sumere 1992). Water-retting traditionally depended upon anaerobic bacteria, such as *Clostridium spp.*, that live in lakes, rivers, ponds, and vats to produce pectinases and other enzymes to ret flax. The stench from anaerobic fermentation of the plants, extensive pollution of waterways, high drying costs, and putrid odor of resulting fibers resulted in a move away from anaerobic water-retting in the mid 20th century to dew-retting. Dew-retting is the

result of colonization and partial plant degradation by plant-degrading, aerobic fungi of flax stems, which are harvested and laid out in swaths in fields. The highest quality linen fibers are produced in Western Europe, which now uses dew-retting, but concern exists within this industry about low and inconsistent quality. Mainland China is currently expanding into flax production. Daenekindt (2004) reported that 80% of the fiber production in China is by warm water-retting and 20% is from “postponed” dew-retting; fiber yield is reported to be low and quality is moderate.

In the 1980’s, substantial research was undertaken to find an enzymatic replacement for dew-retting of flax for linen in Europe (Sharma and Van Sumere 1992). A wide range of commercially available enzyme mixtures containing polygalacturonases, pectin lyase, hemicellulases, and cellulases were screened for retting. Novozym 249 was found to be the most suitable for retting, with conditions of 55°C for 20 h and a straw:liquid ratio of 1:11. Flaxzyme, a product from Novo Nordisk, was developed from this work and was reported to produce fibers with good yield and quality (Van Sumere and Sharma 1991). The yield and hand of enzyme-retted fibers was as good or even better than those from high-quality water-retting. A disadvantage, however, was potential lower fiber strength due to the continued activity of the cellulases in the mixtures. Treatment with an oxidizing agent, such as sodium hypochlorite, or reagents giving a high pH that denatured the enzymes prevented the continuing cellulolytic activity. Research on enzyme-retting led to a series of patents and to a semi-industrial scale trial (Van Sumere 1992), but no commercial system was developed.

Interest has continued on use of enzymes for retting and bast fibers, including flax, with considerable interest at major international conferences (Gübitz and Cavaco-Paulo 2001; Hardin et al. 2002; Kozłowski et al. 2005). The Agricultural Research Service of US Department of Agriculture began a project on enzyme retting in the mid 1990’s towards improving flax fibers that could be used in short staple spinning systems for the US textile industry. The objective of this work was, therefore, not long line fiber for traditional linen, but instead short staple fibers for blending with cotton and other fibers. The requirements to maintain long fiber length and other restrictions necessary for traditional linen could be avoided, and new methods could be explored to produce a total fiber product from diverse sources of flax. Results from several studies have been reviewed (Akin et al. 2004). From available enzyme sources evaluated at the time, Viscozyme L appeared to be the most useful. This enzyme in combination with ethylenediaminetetraacetic acid (EDTA) was extensively evaluated, and a spray enzyme retting method was developed (Akin et al. 2000).

Fibers produced from various formulations and flax sources were evaluated and ranked in test yarns (Akin et al. 2001). Use of Viscozyme and EDTA became the basis on which other products and protocols were compared within our laboratory. Earlier work indicated that 0.05% to 0.3% of the commercial product Viscozyme L with about 18-25 mM EDTA, pH 5.0, 40°C for 24 h resulted in an appropriate retting formulation and method (Akin et al. 2002; Akin et al. 2001). Progressively higher levels or longer incubation times with Viscozyme weakened the fibers. While washing and drying by the methods used prevented continued action of cellulases (Akin et al. 2004), their presence initially in the mixture weakened fibers. Eliminating cellulases and strength loss from commercial retting enzymes became a goal.

Recent advances in enzyme technology have resulted in new products and processes for textiles (Akin and Hardin 2003), including enzymes with potential to improve retting of flax (Antonov et al. 2005; Kozłowski et al. 2005). Further work involving these and other pectinolytic enzyme products (Brühlmann et al. 2000) could improve current retting methods. The objective of research reported herein was to screen new pectinolytic enzymes for retting efficiency, using a series of tests. The more likely candidates were further evaluated by retting in larger amounts and processing in the USDA Flax Fiber pilot plant, using commercial type cleaning equipment. Fibers were assessed for fiber yield, fine fiber yield, and properties important for textile applications. Finally, chemical costs were compared based on available information.

MATERIALS AND METHODS

Enzymes tested for retting are listed in Table 1. The conditions used were those recommended by the suppliers for optimal pH and temperature, and in most cases the recommended levels were used. Cellulase (Sigma Cat. #C8546) at 20 U/ml, pH 5.0 and 37 °C was used as a positive control in weakening fibers in the study for microscopic analysis of fiber structure. While information from the sources often include amount of enzyme per weight of substrate, our percentages are v/v proportions for the solutions used in incubations of the flax substrate. Specific conditions are identified in experiments where pH, temperature, or enzyme formulations were varied. Other chemicals used in formulations included chelators and surfactants.

Table 1. Enzymes for Retting of Flax.

Product name	Source	Purpose / activity	Conditions		
			Required amounts	pH range	Temp. range
Texazym BFE	Inotex Ltd., Dvůr Královi, CZ	Elementarization of bast fibers. Degrades pectin layers binding elementary fibers.	2-10% owf	5-9	50-60°C
Texazym DLG	Inotex Ltd., Dvůr Královi, CZ	No impact on cellulase. Decomposition of hemicellulases & lignin partially in bast fiber. Elementarize bast fibers with BFE.	1-5% owf	4.5-5.5	60°C
Multifect Pectinase FE	Genencor Int., Rochester, NY	Concentrated pectinase complex containing pectinase, cellulase, hemicellulase, & arabinase activities.	0.01-0.1%	4.2-4.7	30-60°C
Multifect Xylanase	Genencor Int., Rochester, NY	Xylanase, typically used in animal feed. Low cellulase side activity.	25-75ppm	3.5-6.5	50-60°C
Viscozyme L	Novozymes North America, Franklinton, NC	Multienzyme complex for breakdown of cell walls in cereal/vegetable materials & the brewing industry. Contains cellulase, hemicellulase, arabinase & pectinase.	0.05-0.1%	3.3-5.5	25-55°C
Cellulase	Sigma-Aldrich, St. Louis, MO	From <i>Trichoderma reesei</i> for breakdown of cellulose	20U/ml	5.0	37°C
Bioprep	Novozymes North America, Inc.	Removes impurities & hydrophobic material from surface of cotton fibers. Alkaline pectate lyase.	0.1%	7-9	50-60°C

Information pertaining to these enzymes was obtained from product sheets of the sources.

EDTA (Fisher Scientific Co., Fair Lawn, NJ) was used at 18 mM concentration. Mayoquest 200, a commercial product with about 38% EDTA (Lynx Chemical Group, L.L.C., Dalton, Georgia) was used with various enzymes as a chelator. Barapon C-108, an amino polycarboxylic acid salt mixture, and Clavodene CIU, a mixture of surfactants (Dexter Chemical L.L.C., Bronx, NY), were used in formulations with Bioprep in some studies.

For Fried Tests, a sample of 'Jordan' flax was used in order to rank various enzyme formulations for the degree of fiber separation, and therefore retting efficiency (Henriksson et al. 1997). Jordan was grown as a winter flax crop near Plains, Georgia, during 2000-2001 and harvested for optimal fiber on April 25, 2001. Very thick or thin stems were removed to have a more uniform material. Twenty centimeter segments were excised from the mid section of over 100 stems, and each twenty centimeter segment was cut in half; the resulting 10 centimeter segments were mixed to provide a uniform substrate in all Fried Tests. Twelve stem segments were placed into each tube for enzyme-retting. Enzyme solutions were added to fill the tubes, which were placed in an incubator on a rotating wheel to continuously mix enzyme and substrate. Samples were prepared for the Fried Test as indicated (Henriksson et al. 1997). The liquid was decanted, the twelve stems were divided into 4 replicates of 3 stems per tube, 8 ml of boiling water was added to the tubes, tubes were aggressively mixed in a vortex mixer (Scientific Instruments Inc., model G-560) for 10 sec., and the tubes were manually shaken (4 up and down strokes). The degree of fiber separation from the stem core was judged independently by two laboratory workers experienced with this method. Fiber separation was scored from 0 (no separation) to 3 (extensive separation) using standard images.

To determine the effect of enzymes on fiber structure and potential degradation using microscopy, Jordan bast tissue from the stem centers was manually separated from core tissues and cut into 1 cm lengths. These bast sections (about 6 mg per tube) were incubated with enzyme formulations. Carded flax fiber tow (about 6 mg per tube of Grade 23, Danforth International Trade Associates, Point Pleasant, NJ) was also incubated in similar enzyme solutions. A portion of the flax tow was subjected to vortex mixing to add physical stress and facilitate observation of any fiber disruption due to enzymes. Enzyme levels for these tests were elevated over normal recommendations and used without chelators to assess any potential fiber breakdown due to enzyme. For microscopic analysis, enzyme-treated fibers were washed and mounted under glycerol on slides and examined under polarized illumination with a 2.5 X objective lens. Enzyme-treated fibers were compared with those incubated in buffer alone to identify criteria that could be used to judge enzymatic breakdown of fibers. Criteria used were: relative amounts of bends and breaks in fibers especially at fibernodes, visual assessment and location of short fibers broken at fibernodes, and presence of long fibers.

The cultivar 'Ariane', which is known for good fiber yield, was used in pilot plant scale enzyme-retting of fibers, which were subsequently processed and characterized for yield and properties. Ariane was grown to full seed maturity in the coastal plain of South Carolina and harvested in May, 1999. This material had been stored inside to prevent any weathering and has been a mainstay for our studies on enzyme retting (Akin et al. 2004). Seeds were removed and stems were crimped through fluted rollers to disrupt the

stem integrity and facilitate interaction of enzymes with tissues. For retting, 150 g samples of crimped straw were briefly soaked (2 min.) in enzyme solutions, drained for 30 sec., and incubated in conditions optimal for enzyme activity. After retting for a selected period of time (usually 24 h), flax straw was washed for 2 min. in water, and air dried. All treatments were carried out in triplicate.

Enzyme-retted, washed, and dried Ariane was processed through the USDA Flax Fiber Pilot Plant (Flax PP) (Akin et al. 2005) in the following order: 9-roller calender 1 X, top shaker 1 X, scutching wheel 1X, 5-roller calender 1 X, top shaker 2 X. After processing through the Flax PP, fiber samples were evaluated for shive content (ASTM D7076-05 2005), based on an NIR model (Sohn et al. 2004), and then conditioned (21 °C, 65% relative humidity) before passing through the Shirley Analyzer (SDL America, Charlottesville, NC). Shirley-cleaned fiber, i.e., fine fiber yield, was the basis for determining retting efficiency, as the finer fibers freed from shive and coarse bundles were collected. Shirley-cleaned fibers were subjected to a series of tests to judge quality. Shirley-cleaned fibers were assessed for shive content by the NIR method (ASTM D7076-05 2005). Strength in g/tex and elongation were determined for six trials each replicate using the Stelometer as in the cotton system (ASTM D1445-95 1999). Fineness was determined using airflow, based on a modified cotton micronaire method (Akin et al. 1999) using a standard method (ASTM D1448-97 1999), to give specific surface index (ASTM D7025-04a 2005) for three 5-g samples each treatment.

RESULTS COMBINED WITH DISCUSSION

The retting effectiveness by selected enzymes was initially assessed by the Fried Test for intact stem portions of flax. Texazym BFE alone effectively retted stems of Jordan flax, at 2, 5, and 10 % levels after 24 h; only 10% BFE retted flax at 7 h (Table 2). The addition of EDTA improved retting, showing effective fiber separation at 7 h for 5 % BFE. DLG was ineffective in fiber separation, even with EDTA, by this method.

The effect of retting was further evaluated using BFE, DLG, and Multifect Pectinase FE in several modifications of formulas and retting conditions (Table 3). Longer periods of time improved BFE retting effectiveness. While 1% BFE was effective at 24 h, the addition of EDTA facilitated enzyme retting with all levels of this enzyme. The 2% level appeared to be effective enough to warrant further study, and temperatures in the 50 to 60 °C range were more effective than lower temperatures. Incubation of stems with DLG at 5%, even with EDTA, did not result in fiber separation (Table 3). Multifect Pectinex FE was effective at 0.2% with EDTA, but not without the chelator (Table 3); lower levels were less effective even with EDTA.

Based on suppliers' recommendations, combinations of enzymes were tested and included BFE plus DLG and Multifect FE plus xylanase (Table 4). Addition of DLG as high as 0.5% did not improve retting efficiency of 1% BFE plus EDTA by the Fried Test. Similarly, addition of xylanase up to 0.15% to Multifect FE plus EDTA did not improve fiber separation.

Table 2. Enzyme-Retting of Flax by Texazym BFE and DLG using the Fried Test^a.

Enzyme	Amount	Presence of EDTA	Incubation time (h)	Fried Test Score ^c	
				#1	#2
BFE	2 %	-	7	2	1.5
	2 %	-	24	3	3
	5 %	-	7	2.6	1.8
	5 %	-	24	3	3
	10 %	-	7	3	2
	10 %	-	24	3	3
	5 %	+	7	3	3
	5 %	+	24	3	3
DLG	1 %	-	7	0	0
	1 %	-	24	0	0
	2 %	-	7	0	0
	2 %	-	24	0	0
	5 %	-	7	0	0
	5 %	-	24	0	0
	2 %	+	7	0.6	0.8
	2 %	+	24	1.4	0.8

^aTexazym BFE and DLG from INOTEX Ltd, Dvůr Královi, Czech Republic incubated at 60 °C with midsection stem lengths of Jordan flax at pH 7.0 and 5.0, respectively. BFE 2-10%, pH 7.0, 60 °C; DLG 1-5 %, pH 5.0, 60 °C.

^bEthylenediaminetetraacetic acid at 18 mM concentration.

^cTwo scorers independently ranked retted stems by standard images. Value is the average of 4 replicates having 3 stems each taken from a single incubation tube.

Table 3. Enzyme-Retting of Flax by Texazym DLG, Texazym BFE, and Pectinase FE using the Fried Test^a.

Enzyme amounts ^b	Incubation conditions	Fried Test Score ^c	
		#1	#2
DLG 3%	pH 5.0, 60 °C	1	1
DLG 5 %	pH 5.0, 60 °C	0.3	0.8
DLG 5 % (no EDTA)	pH 5.0, 60 °C	0	0
BFE 2 %	pH 7.5, 60 °C	2.5	3.0
BFE 2 %	pH 7.5, 50 °C	2.0	2.8
BFE 2 %	pH 7.5, 40 °C	1.5	2.0
BFE 2 %	pH 7.5, 23 °C	0.3	1.3
Pectinase FE 0.05 %	pH 3.9, 45 °C	1.0	2.0
Pectinase FE 0.1%	pH 3.9, 45 °C	1.5	2.4
Pectinase FE 0.2 %	pH 3.9, 45 °C	2.8	3.0
Pectinase FE 0.2 % (no EDTA)	pH 3.9, 45 °C	0.5	1.0

^aDLG and BFE are from INOTEX, Czech Republic. Multifect Pectinase FE is from Genencor International, Inc.

^bUnless indicated, EDTA was used with enzymes at 18mM.

^cTwo scorers independently ranked retted stems by standard images. Value is average of 4 replicates having 3 stems each taken from a single incubation tube.

Table 4. Enzyme-Retting by Pectinases Plus other Complementary Enzymes using the Fried Test.

Enzyme treatments ^a	Incubation time (h)	Fried Test score ^b	
		#1	#2
1 % BFE - no DLG	4	2	1.8
	8	3	2.8
1 % BFE + 0.5 % DLG	4	2.3	2.0
	8	3.0	3.0
1% BFE + 1.0 % DLG	4	2.3	2.0
	8	3.0	3.0
1 % BFE + 1.5% DLG	4	2.5	1.8
	8	2.8	2.3
0.5 % FE - no Xylanase	4	1.0	1.0
	8	2.0	1.5
0.5 % FE + 0.05 % Xylanase	4	1.0	0.3
	8	2.0	1.8
0.5 % FE + 0.1 % Xylanase	4	1.0	0.3
	8	1.5	1.3
0.5 % FE + 0.15 % Xylanase	4	1.3	1.0
	8	1.3	0.3

^aTexazym BFE and BFE + DLG incubated at pH 7.5, 60^oC + 18mM EDTA.

Multifect Pectinase FE and FE + Xylanase incubated at pH 3.9, 45^oC + 18mM EDTA.

^bTwo scorers independently ranked retted stems by standard images. Value is average of 4 replicates having 3 stems each taken from a single incubation tube.

The use of Bioprep 3000 L to ret flax was evaluated at various pH and with various additives (Table 5). Bioprep at 0.05% at pH 8 and 9 and with chelators effectively retted flax. Retting was slightly less effective at pH 7.

Table 5. Enzyme-Retting with Bioprep and Various Additives.

Enzyme treatments ^a		Fried Test score ^b	
		#1	#2
Bioprep 0.05%, pH 7.0	No additives	0.8	0.8
	+ 1.83% Mayoquest 200	2.8	1.8
	+ 1.83% Barapon	3.0	2.8
	+ 1.83% Barapon + 0.15% Clavodene	2.9	2.8
Bioprep 0.05%, pH 8.0	No additives	1.0	1.0
	+ 1.83% Mayoquest 200	3.0	2.8
	+ 1.83% Barapon	3.0	2.0
	+ 1.83% Barapon + 0.15% Clavodene	3.0	2.8
Bioprep 0.05%, pH 9.0	No additives	0.8	0.3
	+ 1.83% Mayoquest 200	3.0	2.8
	+ 1.83% Barapon	3.0	3.0
	+ 1.83% Barapon + 0.15% Clavodene	3.0	2.8

^a Incubated at 55^o C

^bTwo scorers independently ranked retted stems by standard images. Value is average of 4 replicates having 3 stems each taken from a single incubation tube.

Many of the enzyme mixtures tested contain multiple types of enzymes active against plant cell walls, including cellulases. Microscopic analysis of fibers after selected days of incubation shows clear signs of variation due to structural changes and breakdown of fibers (Table 6). Figure 1 shows examples from several treatments of fibers used to determine the degree of destruction. The pectinases Texazym BFE and Bioprep resulted in slight to no fiber destruction as indicated by microscopic assessment. In contrast, Texazym DLG and Sigma cellulase were very destructive to flax fibers (Table 6).

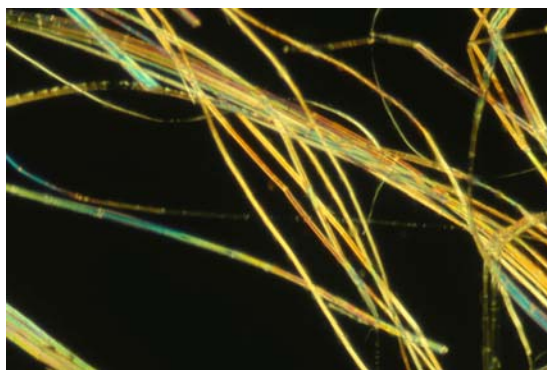


Figure 1 a

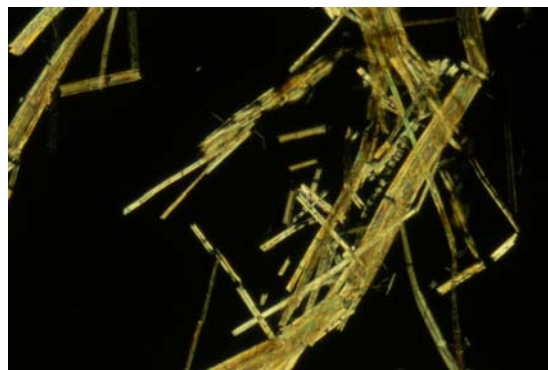


Figure 1 b

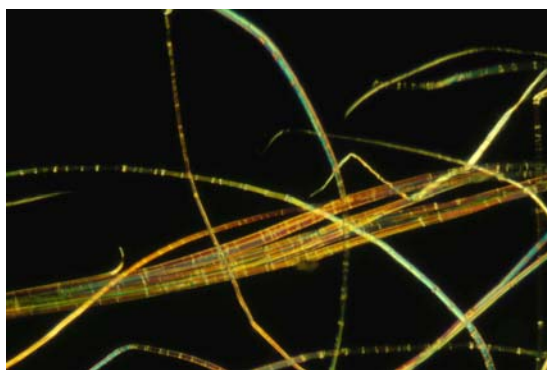


Figure 1 c

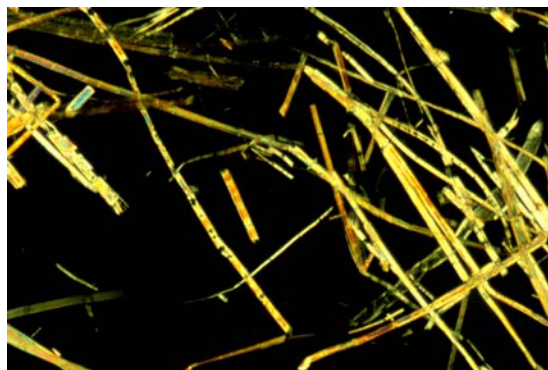


Figure 1 d

Figure 1. Polarized microscopic images showing structural modifications of Grade 23 tow flax fiber incubated with enzymes (2.5 lens for all images). a. Buffer pH 5.0 after 7 days resulting in intact long fibers and fiber bundles. b. Cellulase for 48 h with extensive short fragments due to breakdown at fibernodes. c. BFE 10% after 7 days showing intact long fibers and fiber bundles. d. Viscozyme 0.3% for 7 days showing numerous small fragments due to breakdown at fibernodes.

Further evaluation of the use of these enzymes for retting included the following: the amount of formulation uptake during brief (i.e., 2 min.) soaking, fine fiber yield, cleanliness, and relative cost based on enzyme uptake, fine fiber yield, and available cost information (Table 7). Uptake of the amount of formulation was similar among enzymes and was about 300 ml (ranging from 272 to 408 ml) for 150 g initial fiber weight, giving a liquid to fiber ratio of 2 - 2.7 to 1. Fine fiber yield, i.e., fiber cleaned by 1 pass through the Shirley Analyzer, was highest for Texazym BFE and Bioprep formulations but not significantly different from Viscozyme plus Mayoquest.

Table 6. Strength Loss of Flax Fiber Incubated with Various Enzymes.

Enzyme treatment	Fiber breakdown at day: ^a						
	-----1-----		-----2-----		-----7-----		
	Jordan	tow	Jordan	tow	Jordan	tow	tow (v)
10 % BFE - pH 7.5, 58 °C	0	0	1	1	0	0	0
5 % DLG - pH 7.5, 58 °C	1	1	2	2	2	2	2
5% DLG - pH 7.5, 58 °C	2	2	2	3	3	2	3
0.3 %Multifect pectinase - pH 3.9, 45 °C	0	0	1	1	2	2	2
0.3% Multifect Xylanase - pH 3.9, 45 °C	0	1	0	1	0	1	1
0.3% Multifect Xylanase - pH 5.0, 45 °C	0	1	1	1	1	1	1
0.3% Viscozyme - pH 5.0, 40 °C	1	2	1	1	2	3	3
20 U/ml cellulase - pH 5.0, 40 °C	2	2	2	2	3	3	3
2 % Bioprep - pH 9.0, 55 °C	ND ^b	ND	ND	ND	0	0	1
Buffer - pH 3.9, 45 °C	0	1	0	0	0	0	0
Buffer - pH 5.0, 45 °C	0	0	0	0	0	0	-

^aFiber breakdown was determined by microscopic observation of samples. Jordan bast, with shive manually removed, was excised from the center of the stem and cut into 1 cm pieces. Tow was a commercial tow fiber from Europe (Grade 23 supplied by Frank Riccio, Danforth International Trade Associates). A separate sample of tow was vortexed (Fisher Scientific, cat#12-812) for 30 sec at highest speed to add physical stress to fibers. A summary conclusion on breakdown was made from the following criteria: breaks and bends of fibers, amount and location of short fibers broken at nodes, presence of long fibers. Scores areas follows: 0, no breakdown; 1 slight evidence (not conclusive); 2, definite breakdown; 3 extensive breakdown.

^bNot determined

Shive content in fiber, as determined by the NIR model, showed that fiber that was subsequently Shirley-cleaned contained considerably less shive than that cleaned only by the Flax PP for all formulations. All enzyme-retted and Shirley-cleaned samples were cleaner than unretted fiber, and differences were not large among the enzyme treatments. Based on available information from suppliers, Bioprep and Bioprep plus Mayoquest gave the lowest cost per kg fiber. Since, one pass through the Shirley Analyzer fiber does not represent all the cottonized fiber that would be obtained, a relative cost rather than an absolute value was used to compare treatments. Bioprep only was the lowest cost, and a value of 1.0 was assigned and all other formulations were calculated as an increase over Bioprep (Table 7). Wide variations occurred for the enzyme formulations.

Properties important for application in textile and other industries are shown for fibers derived from the various enzyme-retting methods and cleaned by one pass through the Shirley Analyzer (Table 8). Retting with Texazym BFE and Bioprep, which

reportedly contain only pectinases, resulted in fibers with significantly higher strength than cellulase-containing mixtures, i.e., Multifect Pectinex FE and Viscozyme. Bioprep in all formulations resulted in higher elongation, although values were still small at 2.0 to 2.5%. Retting with Bioprep and Viscozyme produced fibers that tended to be finer than those from other treatments.

Table 7. Yield and Relative Cost for Flax Retted with Different Enzymes*.

Enzyme formulation ^a	Fiber Yield (% straw)		% Shive (NIR method)		Relative costs ^b Shirley-cleaned
	Pilot Plant	Shirley-cleaned (1 Pass)	Pilot Plant-cleaned fiber	Shirley-cleaned fiber	
2 % Texazym BFE + EDTA	36.2 ± 2.4abc	7.0 ± 1.2a	13.8 ± 2.0abc	2.7 ± 0.8bc	5.7
5 % Texazym BFE only	35.3 ± 2.5abc	7.2 ± 0.6a	10.5 ± 0.7c	3.3 ± 0.3b	10.2
0.1 % Pectinase + EDTA	32.9 ± 1.1bc	2.1 ± 0.5c	15.8 ± 1.0abc	3.2 ± 0.3bc	ND
0.2 % Pectinase + EDTA	32.2 ± 1.2c	2.2 ± 0.2c	13.5 ± 3.3bc	1.2 ± 0.7c	ND
0.1% Bioprep only	38.9 ± 0.9a	6.0 ± 1.1ab	19.8 ± 1.7a	4.1 ± 0.2b	1.0
0.1 % Bioprep + EDTA	36.7 ± 3.5ab	7.7 ± 1.4a	18.0 ± 3.5ab	3.7 ± 1.0b	1.4
0.1% Bioprep + B + C	34.3 ± 1.8bc	5.7 ± 1.3ab	14.5 ± 5.7abc	3.2 ± 1.1bc	3.5
0.05 % Viscozyme + EDTA	32.3 ± 2.7c	5.2 ± 2.3ab	14.3 ± 4.5abc	2.9 ± 2.1bc	3.4
Untreated	36.1 ± 4.5abc	3.2 ± 1.5bc	19.6 ± 3.8a	6.2 ± 1.0a	ND

* Values followed by different letters within columns are significantly different at P≤0.05.

^a Enzymes are listed in Table 1. Mayoquest 200 was added to provide 1.83 % EDTA. Incubations were at optimal conditions for specific enzyme.

^b Costs are provided to provide relative comparisons with Bioprep the lowest cost enzymatic application.

Table 8. Properties of fibers from flax ^a retted with different enzymes*.

Enzyme formulation ^b	Strength ^c (g/tex)	Elongation ^c (%)	Fineness ^d (SSI)
2.0% Texazyme BFE + Mayoquest 200	36.7 ± 1.5 ab	1.8 ± 0.1 bc	4.69 ± 0.10 ab
5.0% Texazyme BFE only	34.6 ± 2.0 b	1.6 ± 0.1 cd	4.27 ± 0.31 bcd
0.1% Multifect FE + Mayoquest 200	21.6 ± 3.7 d	1.3 ± 0 d	4.33 ± 0.1 bc
0.2% Multifect FE + Mayoquest 200	17.8 ± 2.2 d	0.5 ± 0.3 e	4.12 ± 0.05 bcde
0.1% Bioprep only	33.2 ± 2.4 bc	2.0 ± 0.3 abc	3.79 ± 0.05 cde
0.1% Bioprep + Mayoquest 200	34.9 ± 2.0 b	2.3 ± 0.3 ab	2.95 ± 0.63 f
0.1% Bioprep + Barapon + Clavodene	34.8 ± 4.8 b	2.5 ± 0.1a	3.55 ± 0.48 ef
0/05% Viscozyme + Mayoquest 200	27.6 ± 3.8 c	1.4 ± 0.5 cd	3.60 ± 0.69 def
Unretted	42.0 ± 5.5 a	1.9 ± 0.4 abc	5.20 ± 0 a

* Values followed by different letters within columns are significantly different at P≤0.05.

^a Ariane flax was grown to seed maturity in South Carolina as winter crop in 1998-1999.

^b Enzymes and chemicals are used as provided by suppliers under optimal conditions for activity. Mayoquest 200 was used at 18 mM EDTA based on a 38% EDTA content.

^c Fiber properties determined using a modified test method (ASTM D1445-95 1999a).

^d Airflow fineness determined using test method (ASTM D7025-04a 2005).

A chronological listing of research for enzyme-retting of flax beginning in 1932 has been reported by Van Sumere (1992). Enzymes screened for retting flax have typically been in mixtures from plant-degrading microorganisms (Sharma 1987a).

Because plant cell walls are complex structures of several components, consideration was given for a combination of polysaccharidases to release clean fibers (Sharma 1992). Residual cellulase activity, however, became problematic, and measures had to be taken to inactivate the enzymes after retting. Recently, we reported on the evaluation of several enzymes for fiber yield and quality, using small pilot plant samples (Akin et al. 2004). Products containing cellulases reduced fiber strength, with greater losses in strength with higher enzyme levels. Microscopic studies have shown that cellulases, and cellulase-containing enzyme mixtures preferentially attack the fibernodes or kink bands in fibers and fiber bundles (Khalili et al. 2002). Flax fibers are weakened by these preferential attacks at these sites, and tenacity is extensively reduced (Akin et al. 2001; Akin et al. 2004). Results also indicated polygalacturonase alone could effectively separate fibers, and the presence of other plant cell wall polysaccharidases may not be required (Akin et al. 2002; Akin et al. 2004; Evans et al. 2002). One objective of our work, therefore, was to find retting enzyme mixtures without cellulases. Until recently, these mixtures were not commercially available at reasonable costs.

The commercial enzymes used in the present study represented a mixture of polysaccharidases, e.g., cellulases and hemicellulases in some, as well as different types of pectinases. Polygalacturonase (PG) and pectate lyase (PL) are both depolymerizing enzymes for pectin; PG catalyzes random hydrolysis of α -1,4 polygalacturonic acid and PL carries out a nonhydrolytic breakdown of pectates and pectinates by a trans-elimination split of the pectic polymer (Sakai et al. 1993). PL is activated by Ca^{++} and usually is active at higher pHs (e.g., 8-10) than PG. Recent research has shown that alkaline pectinases such as pectate lyase are potentially important for retting bast plants (Antonov et al. 2005; Brühlmann et al. 2000).

The role of Ca^{++} chelators, such as EDTA, for improved retting is well known (Sharma 1988; Van Sumere 1992). Henriksson et al. (1997) showed that the addition of oxalic acid and EDTA facilitated the action of commercial enzyme mixtures, e.g., Flaxzyme. While the binding capacity for Ca^{++} of EDTA is greater at alkaline pH, Adamsen et al. (2002) showed that EDTA has substantial Ca^{++} binding activity even at pH 5, which explained the positive value of EDTA at lower pHs optimal for some enzymes.

The role for Ca^{++} chelators in flax retting likely arises from destabilizing bridges between Ca^{++} and polygalacturonic acid, thus leading to disruption of tissues. Flax reportedly absorbs considerable amount of calcium from the soil during growth (Sultana 1992), and analysis of Ariane flax using the inductive coupling plasma (ICP) method showed particularly high levels of calcium in the epidermal/cuticle regions compared to the fiber (300 versus 16 mmol/kg) (Akin et al. 2004). Other work (Jauneau et al. 1997; Rihouey et al. 1995) indicated higher levels of both non-methoxylated pectin and calcium levels in epidermal regions of flax compared to the fibers. This fact suggests that the cuticle/epidermal region of the stem is stabilized with the calcium bridges in addition to the waxy cuticle barrier. The application of EDTA with enzymes has been shown to improve retting, particularly in removing the epidermal/cuticle material from the fibers and fiber bundles (Akin et al. 2004; Akin et al. 1999). The use of EDTA alone has not given particularly good results. The inclusion of EDTA with enzymes, however, has

provided the best retting efficiencies in our protocol (Akin et al. 2004). Results in the present study confirmed this response with the new enzymes screened.

Several past studies in our laboratory have evaluated the effect of Viscozyme L plus EDTA for retting efficiency and for properties of flax fibers (Akin et al. 2000; Akin et al. 2004). Viscozyme L is not marketed for flax retting but is close in nature to Flaxzyme and worked well in our screening. A formulation was developed with 0.05 to 0.3% Viscozyme L plus about 18 -25 mM EDTA from Mayoquest 200. This product was our enzyme of choice for retting, but a characteristic of retting with Viscozyme is the progressive loss of fiber strength with increasing enzyme levels or incubation times. Multifect Pectinase FE, which is not listed for flax retting but for food and feed applications (product information from Genencor International, Rochester, NY), has substantial and progressive cellulolytic activity against flax fibers in our tests. Texazym BFE is reportedly a multi-component product without cellulase activity. Flax retting is one of the stated applications, and industry recommendations are to use it with DLG. Our data confirm the high retting efficiency of BFE with EDTA; the presence of DLG did not improve retting in our tests and alone reduced fiber strength substantially. Use of BFE at pH 7.5 might indicate significant activity by the PL, based on general knowledge of PG and PL enzymes (Sakai et al. 1993). The use of alkaline pectate lyases has been used for retting ramie (Brühlmann et al. 2000). Bioprep, a commercial pectate lyase, provides a potentially important enzyme for retting of flax due to its monocomponent nature, its commercial availability and price, and its ability to ret flax in combination with EDTA at high pH. Bioprep was developed as an environmentally friendly method to scour cotton, thereby replacing the heavy use of alkali. Its usefulness in scouring cotton has been proved (Durden et al. 2001; Eters et al. 2001). The mode of action is the detachment of the cotton fiber cuticle by degradation of the underlying pectin layer. Previous work with Bioprep (Akin et al. 2004) did not show successful retting, but enzyme levels were likely too low. The protocol used in the present study followed closely the experimental recommendation for cotton scouring (personal communication, S. Salmon, Novozymes North America Inc., Franklin, NC). An exception we used was the inclusion of EDTA with the enzyme in a retting formulation.

Of the enzymes tested in the present study, Bioprep plus EDTA provided good retting efficiency, high yields, strong fiber, and the best cost ratios with current economic information. Other conditions must be evaluated for optimization of the protocol. While the retted fiber is stronger with Bioprep than with Viscozyme, both enzymes appear to work well with EDTA in our pilot plant system, and fibers can be tailored with these enzymes for different properties. Sharma (1987b; 1987c) reported that enzymes other than those for retting may be important to remove components on dew-retted flax fibers and add value to low quality yarns. Similarly, fibers retted with Bioprep or Viscozyme might benefit from additional enzyme that remove non-cellulosic residues and improve utilization. Such work with increased enzyme levels remains to be done.

ACKNOWLEDGMENTS

We thank the following companies for providing products used in evaluations: Novozymes North America, Inc., Franklinton, NC; Inotex Ltd., Dvůr Královi, Czech Republic; Genencor International, Inc., Rochester, NY; Dexter LLC, Bronx, NY; and Lynx Chemical Group, LLC, Dalton, GA. We thank the following for excellent technical assistance: Nkaku Kisaalita and L.L. Rigsby, Russell Research Center, ARS-USDA, Athens, GA, and Brad Reed, Cotton Quality Research Station., ARS-USDA, Clemson, SC. Mention of trade names does not constitute an endorsement of one commercial product over another but is used only for identification purposes.

REFERENCES CITED

- Adamsen, A., Akin, D., and Rigsby, L. (2002). "Chelating agents and enzyme retting of flax," *Textile Res. J.* 72(4), 296-302.
- Akin, D., Dodd, R., and Foulk, J. (2005). "Pilot plant for processing flax fiber," *Ind. Crops and Prod.* 21(3), 369-378.
- Akin, D., Dodd, R., Perkins, W., Henriksson, G., and Eriksson, K. (2000). "Spray enzymatic retting: A new method for processing flax fibers," *Textile Res. J.* 70(6), 486-494.
- Akin, D., Foulk, J., and Dodd, R. (2002). "Influence on flax fibers of components in enzyme retting formulations," *Textile Res. J.* 72(6), 510-514.
- Akin, D., Foulk, J., Dodd, R., and McAlister, D. (2001). "Enzyme-retting of flax and characterization of processed fibers," *J. Biotechnol.* 89(2-3), 193-203.
- Akin, D., and Hardin, I. (2003). "The current state of the applications of biotechnology," in *Proceedings of the Annual International Conference & Exhibition*, American Association of Textile Chemists and Colorists, Research Triangle Park, NC, September 10-12, pp.189-195.
- Akin, D., Henriksson, G., Evans, J., Adamsen, A., Foulk, J., and Dodd, R. (2004). "Progress in enzyme-retting of flax," *J. Nat. Fibers* 1(1), 21-47 (2004).
- Akin, D., Rigsby, L., and Perkins, W. (1999). "Quality properties of flax fibers retted with enzymes," *Textile Res. J.* 69(10), 747-753.
- Akin, D., Slomczynski, D., Rigsby, L., and Eriksson, K. (2002). "Retting flax with endopolygalacturonase from *Rhizopus oryzae*," *Textile Res. J.* 72(1), 27-34.
- Antonov, V., Maixner, V., Vicenec, R., and Fishcer, H. (2005). "How do enzymes contribute to bast fibres industry?" in *Proceedings of the 11th Conference for Renewable Resources and Plant Biotechnology*, Institute of Natural Fibres, Poznan, Poland.
- ASTM D 1445-95. (1999). "Standard test method for breaking strength and elongation of cotton fibers (flat bundle method)," *Annual Book of Standards*, section 7, Textiles, ASTM, West Conshohocken, PA.
- ASTM D 1448-97. (1999). "Standard test method for micronaire reading of cotton fibers," *Annual Book of Standards*, section 7, Textiles, ASTM, West Conshohocken, PA.

- ASTM D 7025-04a. (2005). "Standard test method for assessing clean flax fiber fineness," *Annual Book of Standards*, section 7, Textiles, ASTM, West Conshohocken, PA.
- ASTM D 7076-05. (2005). "Standard test method for the measurement of shives in retted flax," *Annual Book of Standards*, section 7, Textiles, ASTM, West Conshohocken, PA.
- Brühlmann, F., Leupin, M., Erismann, K., and Fiechter, A. (2000). "Enzymatic degumming of ramie bast fibers," *J. Biotechnol.* 76(1), 43-50.
- Daenekindt, A., (2004). "Flax, hemp and allied fibres in the world," *Euroflax News* 21(1), 6-9.
- Durden, D. K., Ethers, J. N., Sarkar, A. K., Henderson, L. A., and Hill, J. E. (2001). "Advances in commercial biopreparation of cotton with alkaline pectinase," *AATCC Rev.* 1(8), 28-31.
- Ethers, J., Sarkar, A., Henderson, L., and Liu, J. (2001). "The influence of biopreparation of cotton with alkaline pectinase on dyeing properties," *AATCC Rev.* 1(5), 22-24.
- Evans, J., Akin, D., and Foulk, J. (2002). "Flax-retting by polygalacturonase-containing enzyme mixtures and effects on fiber properties," *J. Biotechnol.* 97(3), 223- 231.
- Gübitz, G., and Cavaco-Paulo, A. (eds.) (2001). "Biotechnology in the textile industry – Perspectives for the new millenium," *J. Biotechnol.* 89(2,3), 89-312.
- Hardin, I., Akin, D., and Wilson, S. (eds.) (2002). "Advances in biotechnology for textile processing," Department of Textiles, Mechandising and Interiors, University of Georgia, Athens, GA.
- Henriksson, G., Akin, D., Rigsby, L., Patel, N., and Eriksson, K. (1997). "Influence of chelating agents and mechanical pretreatment on enzymatic retting of flax," *Textile Res. J.* 67(11), 829-836.
- Jauneau, A., Quentin, M., and Driouich, A. (1997). "Micro-heterogeneity of pectins and calcium distribution in the epidermal and cortical parenchyma cell walls of flax hypocotyl," *Protoplasma* 198(1-2), 9-19.
- Khalili, S., Akin, D., Pettersson, B., and Henriksson, G. (2002). "Fibernodes in flax and other bast fibers," *J. Appl. Bot.* 76(5/6), 133-138.
- Kozłowski, R., Batog, J., Konczewicz, W., Mackiewicz-Talarczyk, M., Muzyczek, M., Sedelnik, N., and Tanska, B. (2005). "Latest state-of-art in bast fibers bioprocessing," in *Proceedings of the 11th Conference for Renewable Resources and Plant Biotechnology*, Institute of Natural Fibres, Poznan, Poland.
- Rihouey, C., Jauneau, A., Cabin-Flaman, A., Demarty, M., Lefebvre, F., and Morvan, C. (1995). "Calcium and acidic pectin distribution in flax cell walls: Evidence for different kinds of linkages in the cell junction and middle lamella of the cortical parenchyma of flax hypocotyl," *Plant Physiol. Biochem.* 33(4), 497-508.
- Sakai, T., Sakamoto, T., Hallaert, J., and Vandamme, E. (1993). "Pectin, pectinase, and protopectinase: Production, properties, and applications," in *Advances in Applied Microbiology*, vol. 39, S. Neidleman and A. Laskin (eds.), Academic Press, San Diego, pp. 213-294.
- Sharma, H. (1987a). "Screening of polysaccharide-degrading enzymes for retting flax stem," *Int. Biodeterioration* 23(3), 181-186 (1987a).

- Sharma, H. (1987b). "Studies on chemical and enzyme retting of flax on a semi-industrial scale and analysis of the effluents for their physico-chemical components," *Int. Biodeterioration* 23(6), 329-342.
- Sharma, H. (1987c). "Enzymatic degradation of residual non-cellulosic polysaccharides present on dew-retted flax fibres," *Appl. Microbiol. Biotechnol.* 26, 358-362.
- Sharma, H. (1988). "Chemical retting of flax using chelating agents," *Appl. Biol.* 113, 159-165.
- Sharma, H., and Van Sumere, C. (1992). "Enzyme treatment of flax," *Gen. Eng. Biotechnol.* 12, 19-23.
- Sohn, M., Barton, F., Morrison, W., and Akin, D. (2004). "Prediction of shive content in pilot plant processed flax by near infrared reflectance spectroscopy," *J. Near Infrared Spectros.* 12(4), 251-258.
- Sultana, C. (1992). "Growing and harvesting of flax," in *The Biology and Processing of Flax*, H. S. S. Sharma and C. F. Van Sumere (eds.), M Publications, Belfast, Northern Ireland, 1992, pp. 83-109.
- Van Sumere, C. (1992). "Retting of flax with special reference to enzyme-retting," in *The Biology and Processing of Flax*, H. S. S. Sharma and C. F. Van Sumere (eds.), M Publications, Belfast, Northern Ireland, pp.157-198.
- Van Sumere, C., and Sharma, H. (1991). "Analysis of fine flax fibre produced by enzymatic retting," *Aspects Appl. Biol.* 28, 15-20.

Article submitted: Nov. 25, 2007; Peer-review process completed: Dec. 31, 2007;
Revised article accepted: Jan. 3, 2008; Published: Jan. 5, 2008.

STRUCTURAL INVESTIGATIONS OF VARIOUS COTTON FIBERS AND COTTON CELLULOSES

Michael Ioelovich,* and Alex Leykin

Macro- and crystalline structure, as well as chemical composition of fibers related to various types and sorts of Israeli cottons, both white and naturally colored, were investigated. The differences in structural parameters and chemical compositions of the cotton fibers were evaluated. Samples of cotton of the "Pima"-type had long, thin and strong fibers with highly ordered supermolecular structure. Fibers of middle-long and hybrid cottons had some lower-ordered structural organization in comparison to long-length cotton, while fibers of naturally colored cotton were characterized with disordered supermolecular and crystalline structure. Dependence of tensile strength on orientation of nano-fibrils towards the fiber axis was found. Conditions of cellulose isolation from the different cotton fibers were studied. Structural characteristics of isolated cotton celluloses and obtained MCC are discussed.

Keywords: Cotton fibers, White cotton, Natural colored cotton, Cotton cellulose, Microcrystalline cellulose, Structure, Chemical composition

Contact information: Polymate Ltd, P.O.Box 73, Migdal HaEmek 23100, Israel;

*Corresponding author: bd895892@zahav.net.il

INTRODUCTION

Cotton is a vegetable fiber that comes from the seed capsules, or bolls, of an array of plants in the genus *Gossypium* of the family *Malvaceae* (Ioelovich et al. 1994). In modern times, cotton fibers remain as one of the most important types of fibers in the world, despite the high volume of wood cellulose and increasing number of synthetic fiber types available. Novel technologies of cultivation and treatment ensure widespread abundance of cotton and expand its application areas. Cotton fibers are the base material to produce a boundless range of products and commodities. These fibers historically are most popular for the textile industry due to softness, absorbency, strength and dyeability. Naturally colored cotton fibers are beyond comparison in the production of eco-textile goods, because such fiber types don't contain harmful synthetic dyes.

Currently cotton is the base raw material for a wide assortment of products, such as paper, chemicals, food additives, medical supplies, some cosmetic ingredients, tire cord, special reinforced plastics, and rubbers, etc. The major source of papermaking fibers is wood. However, also cotton fibers fill a significant place in papermaking. Cotton can be used for production high-quality and specialty paper types, such as tissue paper, technical papers, albums, drawing, and some printing papers, banknote and document papers, etc. (Cerchi and Tullio 2006). High-quality microcrystalline cellulose (MCC) produced from cotton cellulose can be used as an inactive excipient for tablets, gentle

filler cosmetic creams, and as an additive to dietary food (McGinley et al. 1993; Kleinebudde et al. 2000).

As is known, the chemical composition, macro-, and microstructure of cotton fibers have significant influence on the technological parameters and properties of the final cellulose products. Despite the existence of a high volume of scientific information, some specific features of different sorts and types of cotton fibers have not been sufficiently clarified. To select the optimal type of cotton as a raw-material required for the certain application area, versatile investigations of its structural characteristics should be carried out.

The main purpose of this paper is to provide a detailed structural analysis of various types of cotton fibers and isolated cotton celluloses using improved investigation methods.

EXPERIMENTAL

Materials

The various sorts of white middle-length (“Acala”) and long-length (“Pima”) cotton fibers, their hybrids, as well as fibers of natural colored cotton (“Acala” green and brown) cultivated in Israel have been studied. Soda cooking of the natural cotton fibers was carried out at 150 °C for 3 h using a cooking solution containing 1% NaOH, 0.5% H₂O₂ and 0.5% non-ionic surfactant Tergitol NP-9 (Nonylphenol Ethoxylate, M.W. 616).

Microcrystalline cellulose (MCC) was obtained from isolated cotton celluloses by treatment with boiled 2 N HCl for 30 min; then the acidic product was washed up to neutral pH, dispersed in water by Waring-blender, and spray-dried.

Methods

The investigations were carried out by methods of optical and electron microscopy, advanced X-ray diffraction, chemical analysis, and standard methods for determination characteristics of cotton fibers. Scanning electron micrographs were obtained with a Hitachi S-430 apparatus. Diffractometer Rigaku-Ultima Plus (CuK_α – radiation, $\lambda=0.15418$ nm) was used for X-ray investigations. The degree of cellulose crystallinity (X), corrected length (L) and lateral size of nano-crystallites (H), as well as orientation parameters of nano-fibrils were calculated according to improved methods (Ioelovich 1992; Ioelovich 1999).

RESULTS AND DISCUSSION

As can be seen from the microphotography, the cotton fibers had the appearance of twisted bands (Fig. 1). The fibers had lengths of 20-40 mm, widths of 10-30 μm , and thicknesses of the cell wall of 4-6 μm . A hollow, capillary-like lumen extends the length of the fiber. The wall of the natural cotton fibers is built from an external waxy layer - cuticle, primary P, and secondary S walls (Usmanov and Razikov 1974; Ioelovich and Leykin 2006). The thin cuticle and P-wall were observed to have nano-size thickness. The S-wall has thickness of 3-5 μm and is composed of three layers S1, S2 and S3. The dominating wall's

S2-layer of 2-4 μm contains lots of thin lamellas built from nano-fibrillar bundles, having different orientation towards the fiber axis. These bundles consist of elementary fibrils having lateral size 5-8 nm and form steep spirals orientated along the fiber axis.

Cotton fibers can be subdivided on two main types, middle-length and long-length fibers. The numerous sorts of the both cotton types and also hybrid sorts are selected, improved and cultivated in Israel. Besides, naturally colored cotton sorts are created in Israel using methods of selection and genetic engineering. We studied various sorts of long-length cotton of "Pima" type and middle-length cotton of "Acala" type. Besides some hybrid sorts and naturally colored (brown and green) cotton fibers were investigated too. The "Pima" sorts had the longest and the most uniform and strength fibers, while sorts of colored cotton contained shortest and weakest fibers (Table 1).

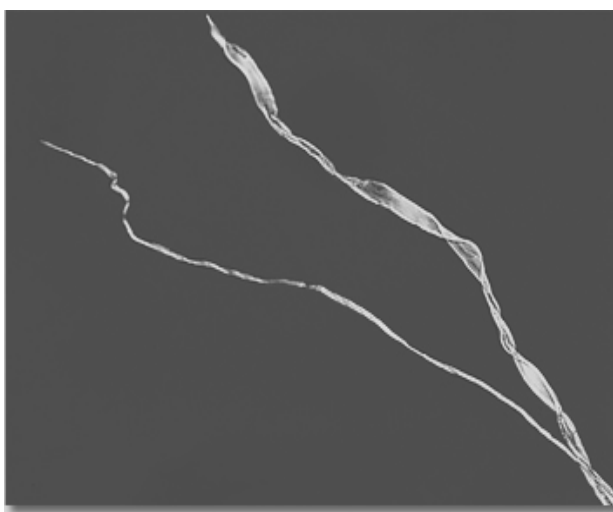


Fig. 1. Microphotograph of twisted middle-length cotton fibers of "Acala" type

Table 1. Main Characteristics of Cotton Fibers

Characteristics	Sorts "Pima"	Sorts "Acala"	Hybrid Sorts	Colored Cotton
Upper length, in	1.30-1.35	1.05-1.16	1.20-1.33	0.97-1.03
Length uniformity, %	85-87	80-82	82-86	78-80
Fineness, micronair	3.4-3.9	4.0-4.6	3.4-4.0	4.1-4.5
Tensile strength, g/tex	30-33	24-28	28-30	18-22

Fibers of white cotton of various types and sorts were found to have a high amount of α -cellulose (94-96%) and did not contain lignin. In contrast to white samples, the fibers of natural colored cotton contained lignin had decreased amount of α -cellulose and increased ash content (Table 2). Derivatives of lignin probably are responsible for the color of brown colored fibers and introduce a tint to green fibers. Green cotton is characterized by a high amount of extractive waxy component consisting mainly of suberin (Elesini et al. 2002).

Table 2. Chemical Composition of Dry Cotton Fibers

Component	Sorts "Pima"	Sorts "Acala"	Hybrid Sorts	Brown Cotton	Green Cotton
Cellulose, %	96.4	94.3	94.5	87.7	77.0
Pectin, %	0.8	2.2	1.6	2.3	2.5
Protein, %	1.2	1.4	1.5	1.3	1.4
Extractive, %	0.5	0.6	0.7	1.2	14.0
Ash, %	1.1	1.5	1.7	2.5	3.1
Lignin, %	0	0	0	5.0	2.0

Based on improved X-ray diffraction, a detailed analysis of nano-structure of cotton fibers was performed. As follows from the investigations (Table 3), fibers of "Pima" type cotton had the most ordered supermolecular structure, while fibers of natural colored cotton were characterized by decreased crystallinity, decreased crystallite sizes, and low orientated nano-fibrils.

Table 3. Structural characteristics of cotton fibers*

Characteristics	"Pima"	"Acala"	Hybrid Sorts	Brown Cotton	Green Cotton
X, %	68	66	67	65	63
H, nm	7	6	6	5	5
L, nm	120	100	110	90	83
K _{or}	0.96	0.88	0.94	0.85	0.79
a, nm	0.788	0.790	0.789	0.791	0.792
b, nm	0.818	0.819	0.818	0.820	0.820
c, nm	1.034	1.034	1.034	1.034	1.034
γ°	96.2	96.1	96.1	96.0	96.0
ρ _{cr} , g/cm ³	1.624	1.618	1.622	1.613	1.611
ρ _o , g/cm ³	1.57	1.56	1.57	1.55	1.55

* X-crystallinity degree; L-length and H-lateral sizes of nano-crystallites; a, b, c – parameters of C1-crystalline unit cell; γ - monoclinic angle; ρ_{cr}, ρ_o - specific weight of the C1-crystallites and the fiber; K_{or} - orientation coefficient of nano-fibrils towards the fiber axis

As follows from the investigations, the orientation coefficient of nano-fibrils directly influenced the tensile strength of the cotton fibers (Fig. 2). The correlation $TS = f(K_{or})$ can be expressed by a linear equation:

$$TS \text{ (g/tex)} = AK_{or} + B \quad (1)$$

where $A = 80$; $B = -44$.

The orientation coefficient is defined as:

$$K_{or} = 1 - 1.5 \sin^2 \varphi \quad (2)$$

where φ is the average disorientation angle of crystallite's "c"-axis or nano-fibrils towards the fiber axis.

With decreasing φ -angle, the orientation coefficient increased and the greater part of the strong covalent intra-fibrillar bonds were orientated along the fiber axis that contributes to strength of the cotton fibers.

Celluloses isolated from the white cotton fibers following soda cooking had high α -cellulose content (98.5-99.2%) and better-ordered crystalline structure (Tables 4, 5). Isolation of pure cellulose from naturally colored cotton fibers is a difficult process due to presence increased amounts of lignin, waxes, and mineral impurities. As a result, a lower yield of α -cellulose can be achieved from the colored cotton after soda cooking, e.g. only 90-92%.

Table 4. Chemical Composition of Isolated Cotton Cellulose in Dry State

Component	Sorts "Pima"	Sorts "Acala"	Hybrid Sorts	Brown Cotton	Green Cotton
α -Cellulose, %	99.2	98.5	99.0	92.0	90.0
β -Cellulose, %	0.6	1.2	0.8	7.5	9.4
Ash, %	0.1	0.2	0.2	0.5	0.6

Table 5. Crystalline Structure of Isolated Cotton Cellulose

Characteristics	"Pima"	"Acala"	Hybrid Sorts	Brown Cotton	Green Cotton
X, %	72	70	71	68	66
H, nm	9	7	8	6	6
L, nm	126	110	117	96	90
a, nm	0.785	0.788	0.787	0.789	0.790
b, nm	0.818	0.818	0.818	0.819	0.819
c, nm	1.034	1.034	1.034	1.034	1.034
γ°	96.3	96.2	96.2	96.0	96.0
ρ_{cr} , g/cm ³	1.631	1.625	1.627	1.620	1.618

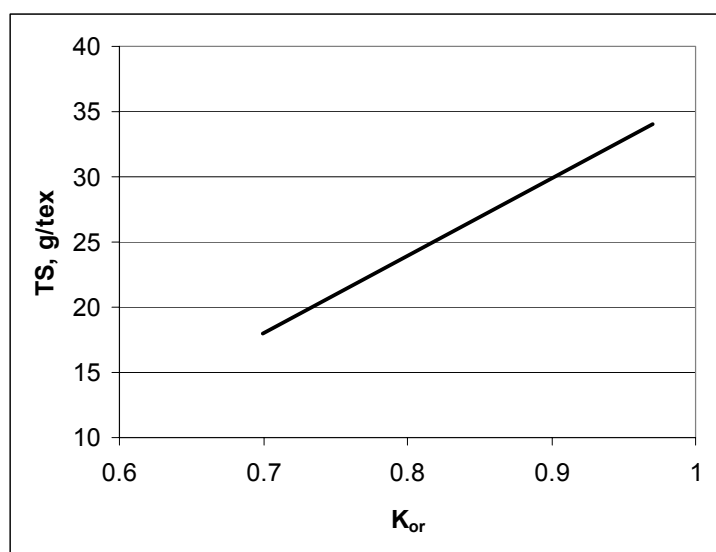


Fig. 2. Correlation between orientation coefficient (K_{or}) and tensile strength (TS) of various cotton fibers

Cotton cellulose having high degree of purity is a suitable starting material to produce cellulose derivatives and GRAS-grade microcrystalline cellulose (MCC), which are used in pharmaceuticals and/or the food industry. MCC obtained from white cotton

cellulose "Pima" and "Acala" with increased yield had a highly ordered crystalline structure and met the pharmacopeia's requirements for cellulose powders used as inactive medical excipients (Tables 6-8).

Table 6. Crystalline Structure of Cotton MCC

Characteristics	"Pima"	"Acala"	Hybrid Sorts	Brown Cotton	Green Cotton
X, %	85	80	81	76	72
H, nm	12	10	11	9	8
L, nm	126	110	117	96	90
a, nm	0.782	0.783	0.783	0.786	0.788
b, nm	0.817	0.817	0.817	0.817	0.817
c, nm	1.034	1.034	1.034	1.034	1.034
γ°	96.3	96.3	96.3	96.2	96.2
ρ_{cr} , g/cm ³	1.640	1.635	1.635	1.630	1.628

Table 7. Characteristics of MCC Samples

MCC-sample	Yield, %	DP*	Av. particle size, μm	Bulk density, g/cm ³	Tap density, g/cm ³
Pima -MCC	92	220	50	0.32	0.45
Acala-MCC	90	200	53	0.30	0.41
MCC of colored cotton	86	180	60	0.27	0.40

*DP – average degree of polymerization

Table 8. Microcrystalline Cellulose – Specification per USP 23/NF 18

Properties	Specification	MCC of Pima	MCC of Acala	MCC of colored cotton
Appearance	A fine, white odorless, crystalline powder	Passes	Passes	No-Passes due to a tint
pH of aqueous extract	5.0 – 7.0	6.0	6.0	6.0
Loss on drying	7% w/w max.	2% w/w	3% w/w	5% w/w
Water soluble substances	0.24% w/w	0.1% w/w	0.2% w/w	0.3% w/w (No-passes)
Starch	Absent	Absent	Absent	Absent
Residue on ignition	0.05% w/w	0.03% w/w	0.04% w/w	0.07% w/w (No-passes)
Heavy metals	<10 ppm	5 ppm	8 ppm	12 ppm (No-passes)
Ether soluble	0.05%	0.01%	0.01	0.1 (No-passes)
MICROBIAL LIMIT				
Total aerobic microbial count	100 per g max	Passes	Passes	Passes
Total combined molds yeast count	20 per g max	Passes	Passes	Passes
Staphylococcus Aureous	Absent	Absent	Absent	Absent
Pseudomonas	Absent	Absent	Absent	Absent

The long-length cotton cellulose “Pima” had an excellent purity degree, which makes it possible to obtain high-quality MCC having the most crystalline structure. Contrary to MCC from white cotton celluloses, microcrystal-line powders can be prepared from colored cotton celluloses with lower yield and had insufficiently ordered structure. Besides, MCC of colored cotton did not meet the requirements of USP 23/NF18 due to lower purity degree.

Cooking of the cotton fibers and partial hydrolysis of cellulose in the process of preparing MCC-obtaining led to ordering of the crystallite structure, which is observed as an increase in the degree of crystallinity, lateral size, and specific weight of crystallites. This is caused by a lateral co-crystallization process of initial nano-crystallites (Ioelovich et al. 1989; Ioelovich 1991). A linear dependence of specific weight on dispersity degree ($1/H$) of cellulose crystallites was observed (Fig. 3). The bigger crystallites had less distortion of the lattice, which promotes increasing their specific weight (Ioelovich 1999).

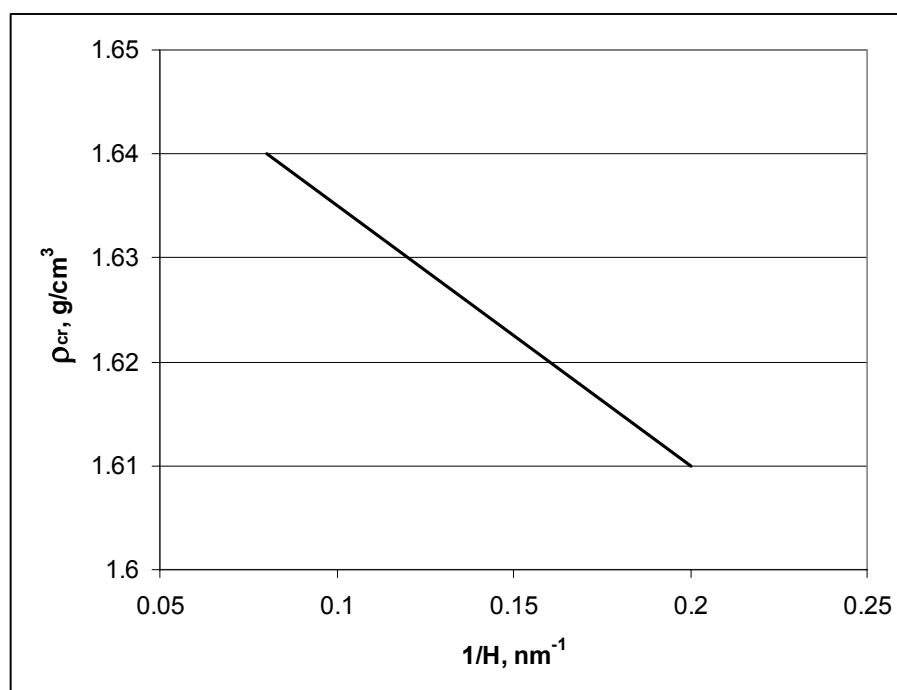


Fig. 3. Dependence of specific weight (ρ_{cr}) on lateral size (H) of cellulose crystallites

Based on ρ_{cr} and X values, the specific weight of the sample (ρ_o) can be calculated:

$$\rho_o = \rho_{am} + 0.01X (\rho_{cr} - \rho_{am}) \quad (3)$$

where $\rho_{am} = 1.45 \text{ g/cm}^3$ is average specific weight of amorphous (non-crystalline) domains of the cellulose nano-fibrils.

The calculated specific weight of the cotton fibers is close to experimental value (Table 3).

CONCLUSIONS

1. The structure and chemical composition of various types of cotton fibres: “Pima”, “Acala”, hybrid, and naturally colored cotton, were studied.
2. Samples of white cotton “Pima” had long, thin and strong fibers with high-ordered crystalline structure, while “Acala” and hybrid cotton have some lower-ordered structural organization.
3. In contrast to white cottons, the naturally colored cotton fibers were short and weak, contain lignin and increased amounts of waxes; moreover, they were characterized with a more disordered crystalline structure.
4. To obtain pure cellulose from white cotton fibers, milder cooking conditions are required than in the case of naturally colored cotton.
5. The cellulose isolated from long-length cotton “Pima” had an excellent purity degree that permits obtaining high-quality pharmaceutical-grade MCC.
6. The tensile strength of the cotton fibers was determined by orientation degree of nano-fibrils towards fiber axis.

REFERENCES CITED

- Cerchi, G., and Tullio, M., (2006). “Cellulose tissue paper including cotton fibers,” *European Patent*, No1676956.
- Elesini, U., Chuden, A., and Richards, A.F., (2002). “Study of the green cotton fibers,” *Acta Chim. Slov.*, 49, 815-833.
- Ioelovich, M., (1991). Study of cellulose cocrystallization process during its isolation from plants.” *Wood Chemistry*, 4, 27-33.
- Ioelovich, M., (1992). “For supermolecular structure of native and isolated celluloses,” *Acta Polymerica*. 43, 110-113.
- Ioelovich, M., (1999). “Concept of the native cellulose structural organization,” *J. SITA*, 1(1), 68-77.
- Ioelovich, M., and Leykin, A., (2006). “Microcrystalline Cellulose: Nano-Structure Formation,” *Cellulose Chem. Technol.* 40(5), 313-317.
- Ioelovich, M., Treimanis, A., Klevinska, V., and Veveris, G., (1989). “Changes of cellulose crystalline structure during its isolation from wood,” *Wood Chemistry* 5, 10-13.
- Ioelovich, M., Yucha, R., Gette, A., and Kenan-Katzelnik, A. (1994). “Evaluation of fiber from new cotton variety: interspecific hybrid,” *Israel Textile Journal*, 138, 6-8.
- Kleinebudde, P., Jumaa, M., and El Saleh, F., (2000). “Influence of degree of polymerization on behavior of cellulose during homogenization and extrusion/spheronization,” *AAPS PharmSci*, 2(3), 5-10.
- McGinley, E.J., et al., (1993). “Fat-like bulking agent for aqueous foods comprising MCC and galactomannan gum,” *US Patent*, No 5192569.
- Usmanov, H., and K. Razikov, K., (1974). *Light and electron spectroscopy of structural transformations of cotton fibers*, Fan, Tashkent.

Article submitted: Nov. 6, 2007; Peer-reviewing completed: Jan. 8, 2008; Revised version received and approved: Jan. 11, 2008; Published: Jan. 12, 2008.

FILMS FROM SPRUCE GALACTOGLUCOMANNAN BLENDED WITH POLY(VINYL ALCOHOL), CORN ARABINOXYLAN, AND KONJAC GLUCOMANNAN

Kirsi S. Mikkonen,^{a,b*} Madhav P. Yadav,^c Peter Cooke,^c Stefan Willför,^d Kevin B. Hicks,^c and Maija Tenkanen^a

The improvement of mechanical properties of spruce galactoglucomannan (GGM)-based films was sought by blending GGM with each of poly(vinyl alcohol) (PVOH), corn arabinoxylan (cAX), and konjac glucomannan (KGM). The blend ratios were 3:1, 1:1, and 1:3 (w/w), and in addition films were made from each of the polymers alone. Glycerol was used as plasticizer. Adding other polymers increased the elongation at break of GGM blend films. The tensile strength of films increased with increasing amount of PVOH and KGM, but the effect of cAX was the opposite. Dynamic mechanical analysis showed two separate loss modulus peaks for blends of GGM and PVOH, but a single peak for all other films. Optical and scanning electron microscopy confirmed good miscibility of GGM with cAX and KGM. In contrast, films blended from GGM and PVOH showed phase separation when examined by microscopy.

Keywords: Galactoglucomannan; Films; Blends; Mechanical properties; Dynamic Mechanical Analysis; Scanning Electron Microscopy

Contact information: a: Department of Applied Chemistry and Microbiology, University of Helsinki, P. O. Box 27, 00014 Helsinki, Finland; b: Department of Food Technology, University of Helsinki, P. O. Box 66, 00014 Helsinki, Finland; c: Eastern Regional Research Center, Agricultural Research Service, United States Department of Agriculture, 600 East Mermaid Lane, Wyndmoor, PA 19038 USA; d: Process Chemistry Centre, Åbo Akademi University, Porthansgatan 3, 20500 Åbo, Finland; *Corresponding author: kirsi.s.mikkonen@helsinki.fi

INTRODUCTION

Hemicelluloses are structural cell wall components that comprise 20–35% of the dry weight of wood and annual plants, and thus they are the most common plant polysaccharides other than cellulose (Sjöström 1993; Ebringerová and Heinze 2000). *O*-acetyl galactoglucomannans (GGM) are the main hemicelluloses in softwoods. They consist of backbones of β -1,4-D-mannopyranosyl and β -1,4-D-glucopyranosyl units carrying single α -D-galactopyranosyl residues that are 1,6-linked to mannose units, and acetyl substituents attached to C-2 or C-3 positions of mannose (Sjöström 1993). The ratio of mannose/glucose/galactose of water-soluble spruce GGM is approximately 4:1:0.5, and the degree of acetylation is about 30%. GGM with a molar mass of approximately 30–60 kDa can be recovered as a by-product from process water of mechanical pulping of spruce at a yield of 5 kg/ton pulp (Willför et al. 2003; Xu et al. 2007). GGM is a remarkable natural resource with great potential, but it is not currently isolated for industrial use (Willför et al. 2007). At the laboratory scale, GGM has been

tested for use as a raw material for biodegradable films. GGM-based films have the capacity for acting as oxygen barriers, but their tensile strength and elongation at break are rather low (Hartman et al. 2006a,b; Mikkonen et al. 2006).

Improved mechanical properties of films based on biopolymers have been sought by blending them with other natural or synthetic polymers. The toughness and elongation at break of e.g. pectin / starch-based films were increased by addition of poly(vinyl alcohol) (PVOH) (Coffin and Fishman 1996; Fishman et al. 2004; Fishman et al. 2006). PVOH is a water-soluble polymer produced by methanolysis of poly(vinyl acetate). The solubility of PVOH in water depends on its molar mass and the degree of ester hydrolysis (Hassan et al. 2002). PVOH has excellent film-forming properties and can be used as a barrier to oil, grease, organic solvents, and oxygen (Kirwan and Strawbridge 2003). The biodegradability of PVOH is arguable, as some micro-organisms produce PVOH-degrading enzymes, but the occurrence and overall number of those micro-organisms in nature is rather limited (Chiellini et al. 1999; Chen et al 2007).

Corn fiber, which is the main low-value by-product of the corn wet and/or dry milling process, contains large quantities of arabinoxylans (cAX) (Doner and Hicks 1997). The backbone of cAX consists of 1,4-linked β -D-xylopyranosyl units, to which short side chains of α -L-arabinofuranosyl units are connected by 1,3- and/or 1,2-glycosidic linkages. D-galactopyranosyl and D-xylopyranosyl residues are attached to the arabinofuranosyl branches. cAX also carries α -D-glucopyranosyluronic acid and feruloyl groups (Saulnier et al. 1995). Exploitation of cAX as a film former has been suggested (Fredon et al. 2002; Peroval et al. 2002; Zhang and Whistler 2004). Films have successfully been prepared also from other cereal arabinoxylans (Höije et al. 2005; Tenkanen et al. 2007).

Konjac glucomannan (KGM) occurs as a storage polysaccharide in tubers of *Amorphophallus konjac* (Takigami 2000). Its chemical composition resembles that of GGM, except that KGM does not contain galactose side groups, and it has significantly higher molar mass, approximately 1000 kDa (Li et al. 2006a). The mannose/glucose ratio of KGM is 1.6:1 and the degree of acetylation about 5%. KGM forms strong films by itself and as blends with various substances, including PVOH (Yue et al. 1995; Xiao et al. 2000a; Xiao et al. 2000b; Xiao et al. 2001a; Xiao et al. 2001b; Li and Xie 2004; Cheng et al. 2006; Li et al. 2006b; Ye et al. 2006; Cheng et al. 2007). The aim of the present study was to increase the tensile strength and elongation at break of GGM-based films by blending GGM with PVOH, cAX, and KGM. To study the homogeneity of the blend films, their thermal behavior was examined using dynamic mechanical analysis (DMA) and the film structure was viewed with optical and scanning electron microscopy (SEM).

EXPERIMENTAL

Materials

GGM was prepared from thermomechanical pulp of spruce according to Willför et al. (2003), with the exception that pulp taken after the second refiner in a two-stage refining system was used. The mannose content of the dried powder was determined by gas chromatography following methanolysis and trimethyl silylation (Sundberg et al.

1996). The GGM content was estimated from the mannose content and the mannose/glucose/galactose ratio of 4:1:0.5 to be 77 mole% of carbohydrates. The main non-GGM residual components were other polysaccharides, mainly pectic acids and arabinogalactans. Molar mass and the degree of acetylation of GGM were determined as described by Xu et al. (2007) to be approximately 50 kDa and 18%, respectively.

The cAX sample was isolated by alkali extraction from de-oiled and de-starched fiber fractions from commercial corn wet milling (ADM Research, USA). The method of isolation, as well as the characteristics of the obtained product (CFG-1), were described in detail by Yadav et al. (2007). PVOH (98–99% hydrolyzed, Mw 146,000–186,000 as reported by the supplier) and glycerol were from Sigma and KGM (BJ-C1) from Baoji, China.

Preparation of Films

The blend ratios of GGM with each of PVOH, cAX, and KGM were 1:0, 3:1, 1:1, 1:3, and 0:1 (w/w). Glycerol was used as plasticizer at 40% (w/w of the polymers). Polymers and glycerol were dissolved in de-ionized water at 95°C to produce a final polymer concentration of 10 g/L. Solutions containing cAX and a reference sample from pure GGM and glycerol were filtered through a steel sieve with 45 µm pore size to remove a small amount of insoluble particles. Air was removed by ultrasonication under vacuum for 5 min. Films with an average thickness of approximately 70 µm were prepared by casting 50 ml of solutions on polystyrene petri dishes (diameter 9 cm) and drying overnight at 60°C.

Mechanical Properties

An updated Instron 1122 mechanical property tester (Instron Corp., Norwood, MA, USA) with a 100 N load cell and TestWorks 4 data acquisition software (MTS Systems Corp., Minneapolis, MN, USA) was used to determine the tensile strength and elongation at break of films. The initial grip distance was 25 mm and the rate of grip separation 5 mm/min. The measurements were done at 21°C and 65% RH (in a climate room) and the films were stored at these conditions for at least three days before measurement. From those films that could be handled at this RH, two films of each type and five replicate specimens from each film were measured. The specimens were 5 mm wide and approximately 60 mm long. The thickness of the specimens was measured with a micrometer (Ames, Waltham, MA, USA, precision 1 µm) at three points and an average was calculated.

Dynamic Mechanical Analysis

Dynamic mechanical analysis was done on a Rheometrics RSA II solids analyzer (Piscataway, NJ, USA) using a film-testing fixture. Specimens of 7 mm × 38 mm were dried under vacuum for 30 min prior to testing. Specimen thickness was measured at three points with the micrometer and width at two points with a millimeter ruler, and averages were calculated. The gap between the jaws at the beginning of the test was 23.0 mm. A nominal strain of 0.1% was applied with a frequency of 10 rad/s (1.59 Hz). Storage modulus (E'), loss modulus (E''), and loss tangent ($\tan \delta$) were determined as a function of temperature from –100°C to 50°C at a heating rate of 10°C/min. The peak

temperature of E'' , determined by fitting a parabolic curve to E'' data with Origin 7.2 (OriginLab Corporation) software, was taken as glass transition temperature (T_g) (Kalichevsky and Blanshard 1993). All analyzes were done in triplicate.

Microscopy

Optical and fluorescence imaging of film surfaces was done with a model MZ FLIII stereofluorescence microscope equipped with a DC200 charge-coupled device camera (Leica Microsystems, Inc., Bannockburn, IL, USA) and oblique, transmitted illumination from a fiber optic bundle connected to a 150 W halogen lamp in an Intralux 5000-1 lamphouse (Volpi Manufacturing, Auburn, NY, USA). Matching epifluorescence images of sample areas were excited with violet light (~ 425 nm) from a 50 W Hg lamphouse and digital images of blue fluorescence (> 475 nm) were collected.

The cross-sections of the films were viewed with scanning electron microscopy (SEM). Rectangular strips of approximately $5 \text{ mm} \times 40 \text{ mm}$ were excised from the films with a razor blade and dehydrated by immersion in 10 ml of absolute ethanol. The samples were stored in sealed vials for three days, during which the ethanol was replaced twice. Film segments were quickly blotted dry, plunged into liquid nitrogen, and cooled for 5 min. The frozen film segments were fractured manually using tweezers by bending the strips against the surface of a brass block in liquid nitrogen. Fractured fragments were removed from the liquid nitrogen, thawed by immersion in ethanol, and subsequently critical point dried from liquid carbon dioxide. Dry fragments were trimmed and mounted on aluminium stubs using Duco Cement (ITW Performance Polymers, Riviera Beach, FL, USA) and colloidal silver adhesive (Electron Microscopy Sciences, Hatfield, PA, USA) and coated with a thin layer of gold by direct current sputtering. Images of oriented fracture faces were collected using a Quanta 200 scanning electron microscope (FEI Co., Hillsboro, OR, USA) operated in the high vacuum-secondary electron imaging mode.

RESULTS AND DISCUSSION

Mechanical Properties

Both the tensile strength and elongation at break of pure GGM-based films were low, as expected (Fig. 1). On average, the elongation at break was slightly higher and the tensile strength somewhat lower than when measured previously at lower RH (50% RH) with another instrument and different specimen dimensions (Mikkonen et al. 2006). Water has a plasticizing effect on biopolymer-based films (Talja et al. 2007), which is a probable explanation for the different results obtained at 65% RH in the present study. The mechanical testing of pure GGM-based films was repeated with each set of blend films (GGM / PVOH, GGM / cAX, and GGM / KGM) and some variation in the results was found. The tensile strength of pure GGM-based films was 3.5 ± 0.4 , 1.1 ± 0.3 and 0.85 ± 0.2 MPa when the films were prepared and measured together with its blends with PVOH, cAX, and KGM, respectively. The values of elongation at break of the corresponding films were $4.9 \pm 1\%$, $12.5 \pm 4\%$, and $10.9 \pm 4\%$.

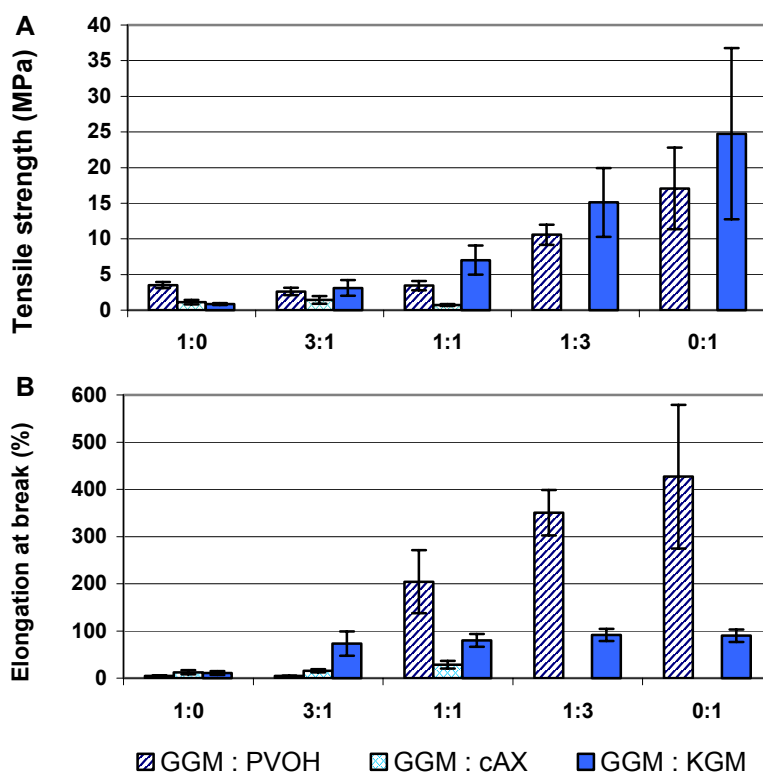


Fig. 1. (A) Tensile strength and (B) elongation at break of films from GGM blended with PVOH, cAX, and KGM at different ratios and plasticized with 40% (w/w of polymers) glycerol. Each average is based on $n = 10$ observations, and the error bars indicate standard deviations. GGM / cAX films with ratios of 1:3 and 0:1 could not be measured.

The tensile strength of films clearly increased when PVOH was used in GGM / PVOH at ratios of 1:3 and 0:1 (Fig. 1A). At lower PVOH levels, the differences in the tensile strength of GGM / PVOH blend films were small. The elongation at break of GGM / PVOH films increased almost linearly with increasing PVOH content from GGM : PVOH ratio of 3:1 to 0:1, but a small addition of PVOH did not have an effect as the elongation at break of GGM : PVOH 3:1 films was similar to that of films from pure GGM (Fig. 1B).

Adding cAX to GGM at a GGM : cAX ratio of 3:1 did not significantly affect the tensile strength of the films, but at the ratio of 1:1, the tensile strength decreased to almost zero (Fig. 1A). In contrast, the elongation at break of films increased slightly with increasing cAX content (Fig. 1B). The mechanical properties of GGM : cAX 1:3 and 0:1 films could not be measured, because cAX was very sensitive to changes in ambient RH, and these films were difficult to handle at 65% RH, which was used for tensile testing. cAX is more branched than the other studied polymers. It may absorb more water, which can lead to plasticization and softening of the films. We also tested pure cAX-based films using lower glycerol contents (25% and 10% w/w) and GGM / cAX blends using 25% glycerol, but even those films were too soft to measure at 65% RH. When prepared without added plasticizer, cAX films had a tensile strength of 4.2 ± 1.5 MPa and elongation at break of $21 \pm 9\%$. In the future, it can be worthwhile to test if cAX has

potential as a film forming and flexibility increasing component in blend films if treated as plasticizer, so that the amount of other plasticizers is decreased with increasing cAX content.

An increasing amount of KGM increased the tensile strength of the films (Fig. 1A). The increase was slow at low KGM contents, but escalated at high KGM contents. Even a small amount of KGM notably enhanced the elongation at break of films, which was high for all films containing KGM (Fig. 1B).

In a previous study, a moderate decrease in the degree of polymerization of guar gum galactomannan resulted in an increase of tensile strength and elongation at break of films (Mikkonen et al. 2007). Similarly, films from partially acid-hydrolyzed KGM showed higher tensile strength than native KGM-based films, when the acid treatment was relatively mild (Cheng et al. 2007). In both studies, however, a stronger hydrolysis of the polymeric chain led to decreased film mechanical properties. Suggested mechanisms of the initial improvement of tensile strength with decreasing molar mass were altered chain flexibility and mobility, and an optimal decrease of viscosity of the polysaccharide solution leading to better orientation of the film-forming polymers. GGM was found to decrease the viscosity of aqueous KGM solution (Xu et al. submitted) and therefore a small addition of GGM to KGM could have been expected to somewhat strengthen the films.

Several studies on KGM-based blend films have shown that there is an optimum polymer ratio that gives higher film tensile strength than either of the two polymers alone (Yue et al. 1995; Xiao et al. 2000a; Xiao et al. 2000b; Xiao et al. 2001a; Xiao et al. 2001b; Li and Xie 2004; Li et al. 2006b; Ye et al. 2006). For example, blends of KGM and PVOH reached a maximum tensile strength at 20% PVOH content (Xiao et al. 2000a), and also in the presence of glutaraldehyde, the tensile strength of KGM / PVOH blends was higher than that of films purely from either KGM or PVOH (Li and Xie 2004). Relatively similar or high molar masses of the both blended polymers could promote synergism. The molar mass of GGM is significantly lower than that of PVOH and KGM, and in the present study there was not an optimum blend ratio, as the films from pure PVOH and KGM had clearly higher tensile strength than any of the GGM / PVOH or GGM / KGM blends.

Dynamic Mechanical Analysis

The DMA tests of pure GGM-based films were also repeated with each set of blend films. The average T_g of pure GGM-based films measured at different times varied from -56 to -70°C (Table 1). The standard deviation between the replicate specimens was small each time. An attempt was made to control the plasticizing effect of water by vacuum-drying the film specimens before DMA testing. Despite that, the films probably absorbed some water from the air during attachment of the film strips in the instrument. The films from individual sets were generally analyzed within a few days, but the time between the analyses of the different sets was up to several weeks. Thus changes in the ambient RH might have affected the detected T_g values. This complicates the comparison of the T_g values of films from different sets, but most likely not of the films from the same set.

Table 1. Glass Transition Temperature (T_g) of Films from GGM Blended with PVOH, cAX, and KGM at Different Ratios and Plasticizer with 40% (w/w) of Glycerol (Mean Value \pm SD from Triplicate Analysis).

Ratio	GGM / PVOH*		GGM / cAX	GGM / KGM
	T_{g1} ($^{\circ}$ C)	T_{g2} ($^{\circ}$ C)	T_g ($^{\circ}$ C)	T_g ($^{\circ}$ C)
1:0	-70 ± 3	nd	-62 ± 0.9	-56 ± 1
3:1	-70 ± 0.9	-36 ± 3	-67 ± 2	-57 ± 1
1:1	-66 ± 0.1	-25 ± 1	-57 ± 0.05	-53 ± 2
1:3	-66 ± 0.8	-19 ± 7	-50 ± 2	-52 ± 2
0:1	-72 ± 2	nd	-65 ± 2	-53 ± 1

*Two glass transitions were detected for blends of GGM and PVOH. nd = not detected.

Figure 2 shows that there were two peaks in the E'' spectra of films containing both GGM and PVOH, indicated as T_{g1} and T_{g2} in Table 1. The second peak at approximately -20 to -30° C was more pronounced for GGM : PVOH 1:1 and 1:3 films than for films with the GGM : PVOH ratio of 3:1. The E'' curves of pure PVOH-based films had a single peak with a shoulder. Distinct glass transitions clearly indicate that GGM and PVOH were incompatible and that phase separation took place. Interestingly, the T_g values of the films from pure GGM and PVOH were close to each other and to the first detected T_g of the blends (T_{g1}), but the second T_g of the blends (T_{g2}) was clearly higher. It is possible that glycerol was unevenly distributed in the two separate phases, the GGM-rich and PVOH-rich phase. Plasticization decreases T_g , so the T_{g1} could have resulted from the phase containing more glycerol and T_{g2} from the phase with less glycerol.

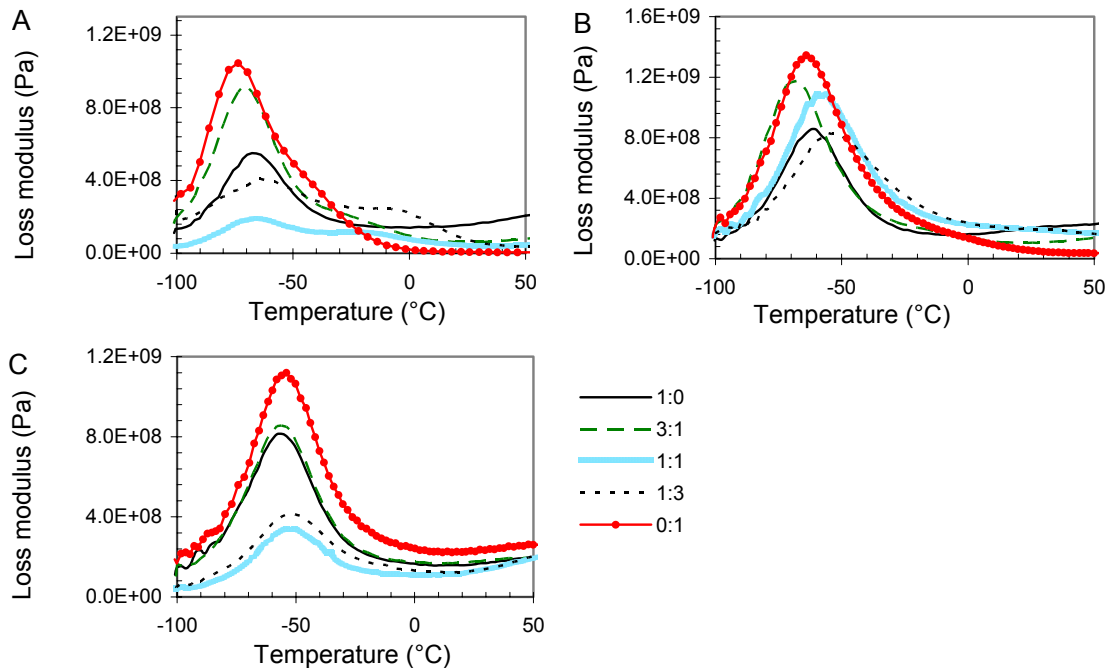


Fig. 2. Typical loss modulus spectra of films from GGM blended with (A) PVOH, (B) cAX, and (C) KGM at different ratios plasticized with 40% (w/w) of polymers glycerol.

All GGM / cAX and GGM / KGM films had a single glass transition (Fig. 2). The T_g of GGM / cAX blends increased with increasing cAX content, but the T_g of pure cAX-based films was lower and close to that of films based on pure GGM. The T_g of GGM / KGM films varied within only a narrow range. The E'' peak heights of all films varied notably, which was probably due to differences in the thickness of the films but is not expected to affect the peak temperature.

Microscopy

Optical microscopic imaging with visible light showed that pure GGM-based films had a slightly grainy surface (Fig. 3A). GGM contained a small amount of insoluble particles, some but not all of which were removed by filtration through the 45 μm sieve used in the preparation of GGM / cAX sample set. Those particles most probably formed the elevated spots seen by optical microscopy using visible light. The same spots autofluoresced, indicating that they could have contained residual aromatic structures originating from spruce wood. Because the aromatic substances are present in GGM only in trace amounts, reliable analytical data of their composition has not been obtained up to date. However, it is most likely that these structures arise from fragments of lignin-like moieties, possibly from so-called lignin-carbohydrate complexes.

Addition of PVOH resulted in increased unevenness of the film surfaces (Fig. 3). Films with GGM : PVOH ratios of 3:1 and 1:1 had a much rougher surface than the films from pure GGM. The films with GGM : PVOH ratio of 1:3 had a pattern of irregular minor shapes immersed in a continuous phase. In contrast, the surfaces of pure PVOH-based films were very smooth.

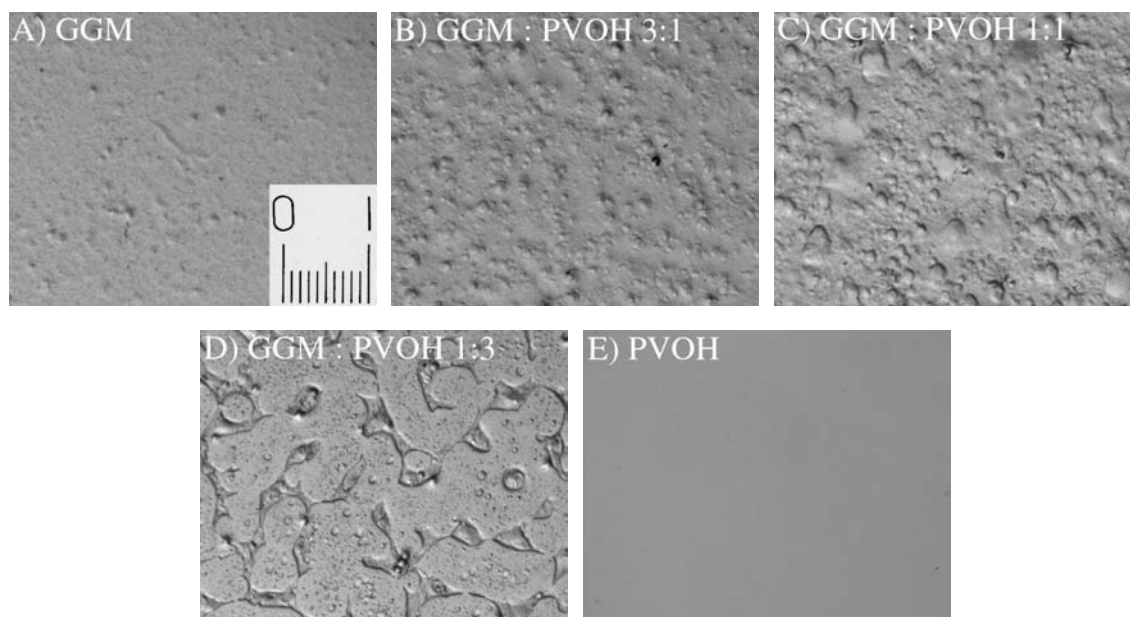


Fig. 3. Optical microscopic images of surfaces of films from (A) GGM; (B) GGM : PVOH 3:1; (C) GGM : PVOH 1:1; (D) GGM : PVOH 1:3 and (E) PVOH obtained using visible light. Scale bar = 1 mm. All images are at the same magnification.

The surfaces of GGM / cAX and GGM / KGM blend films looked much alike. Figure 4 presents images of films with GGM : cAX and GGM : KGM ratios of 1:1 and 0:1 as examples. Films containing GGM had a somewhat grainy surface, whereas those from pure cAX were smooth and those from pure KGM had some fiber-like formations. Films not containing GGM did not show significant fluorescence.

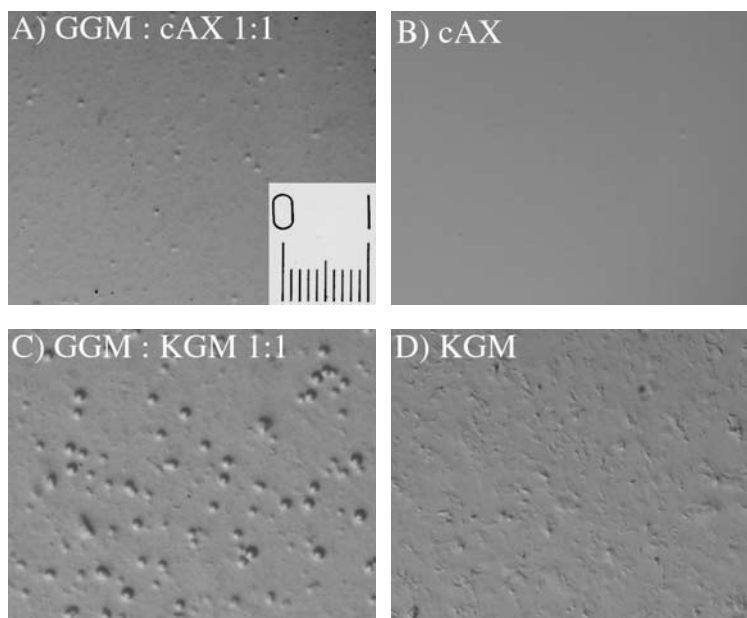


Fig. 4. Optical microscopic images of surfaces of films from (A) GGM : cAX 1:1; (B) cAX; (C) GGM : KGM 1:1 and (D) KGM obtained using visible light. Scale bar = 1 mm. All images are at the same magnification.

The cross-section of pure GGM-based film, viewed with SEM, was somewhat grainy with some dark and dense areas (Fig. 5A). There was a great contrast to images of blend films from GGM with PVOH, which clearly showed separation into two distinct phases. The film with GGM : PVOH ratio of 3:1 (Fig. 5 B) had spherical particles of different sizes in a continuous phase that resembled the cross-section of the film from pure GGM. When the ratio of GGM to PVOH was 1:1, the two phases were formed as layers on top of each other (Fig. 5C) and in some areas they had separated (Fig. 5D). At the GGM : PVOH ratio of 1:3 (Fig. 5E), the continuous phase looked similar to the cross-section of pure PVOH-based film (Fig. 5F), and there were small round and oval particles inside. The cross-sections of GGM / cAX and GGM / KGM blend films showed a homogeneous structure consisting of a single phase (Fig. 6).

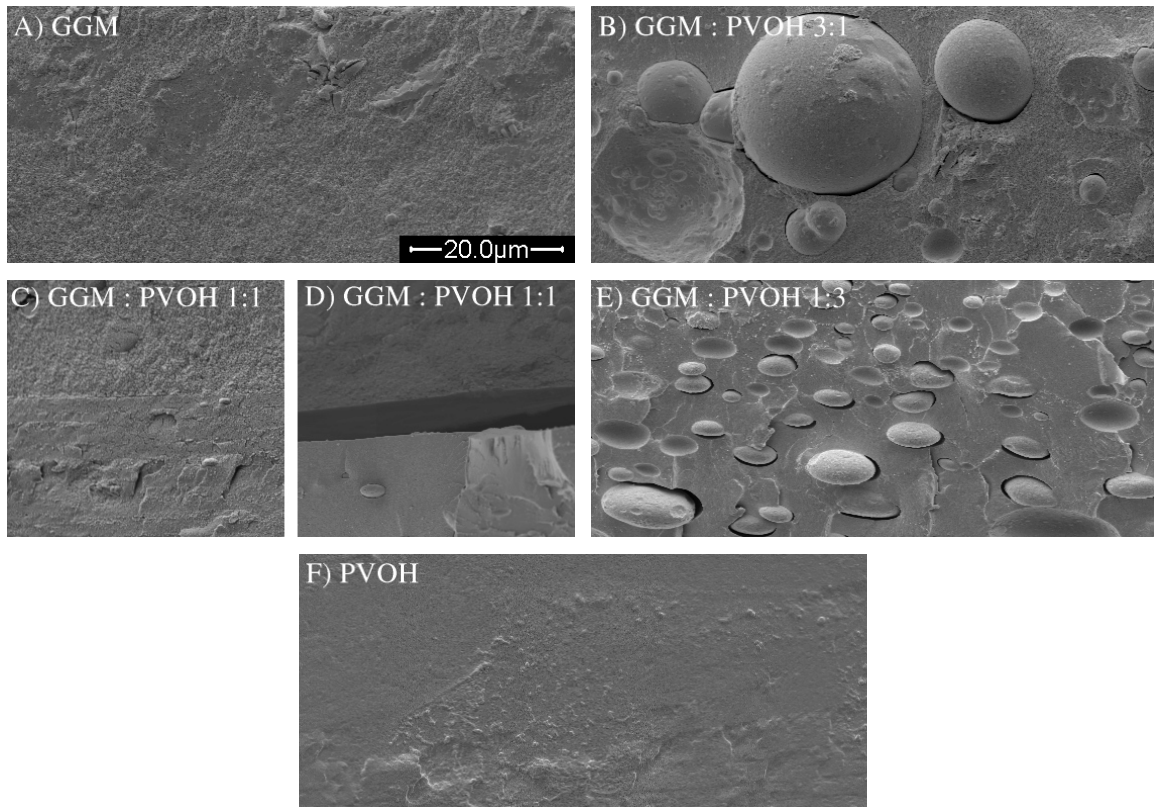


Fig. 5. Scanning electron micrographs of cross-sections of films from (A) GGM; (B) GGM : PVOH 3:1; (C and D) GGM : PVOH 1:1; (E) GGM : PVOH 1:3 and (F) PVOH. Scale bar = 20 μm. All images are at the same magnification.

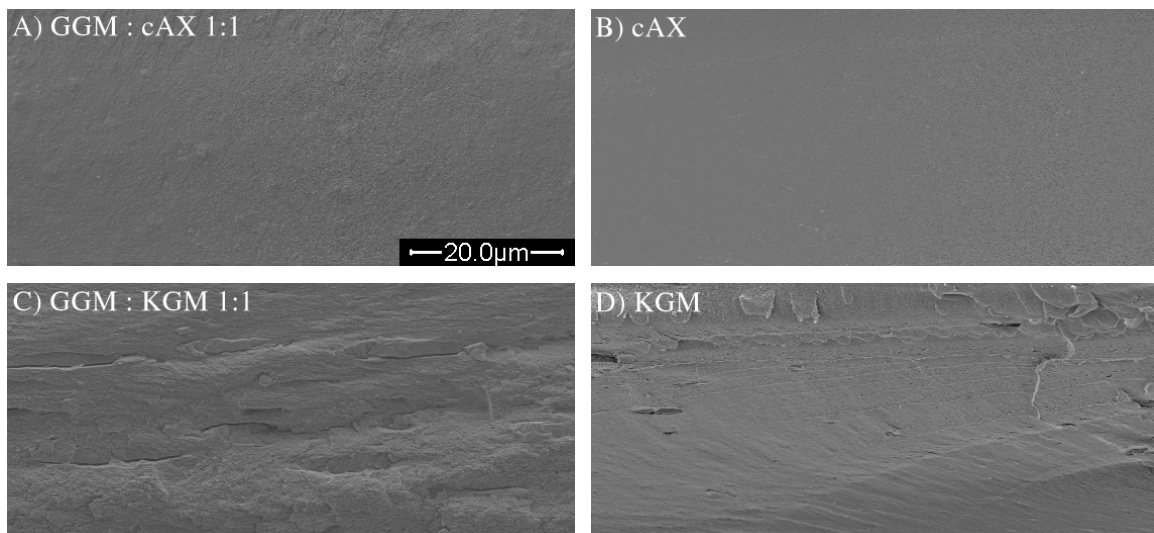


Fig. 6. Scanning electron micrographs of cross-sections of films from (A) GGM : cAX 1:1; (B) cAX; (C) GGM : KGM 1:1 and (D) KGM. Scale bar = 20 μm. All images are at the same magnification.

Microscopic studies by Xiao et al. (2000a) showed phase separation of PVOH and KGM, the latter of which has similar sugar composition to GGM. They found with IR spectroscopy that there was some hydrogen bonding between the two polymers, but not as much as between KGM and other polysaccharides. This could also explain the results of the present study. GGM might form strong hydrogen bonding and homogeneous mixtures with the other studied polysaccharides cAX and KGM, but not with PVOH, which has only one hydroxyl group attached to every second carbon atom of the polymeric chain. Based on SEM imaging, it can be reasoned that the mechanical properties of the GGM blend films were determined mainly by the properties of the continuous phase, which was formed of a homogeneous mixture of two polysaccharides in GGM / cAX and GGM / KGM blends, but of either GGM-rich or PVOH-rich phase in the films made from those two polymers.

Application Potential

Previously, Hartman et al. (2006a; 2006b) found that GGM can form films with low oxygen permeability. They showed decrease of storage modulus of plasticized GGM films with increasing ambient RH, but did not determine their tensile strength and elongation at break, which are important parameters concerning film applications. The present study proves that the tensile properties of GGM films were significantly enhanced by the addition of KGM or PVOH. Although the latter two polymers formed stronger and more flexible films alone than as blends with GGM, the estimated low cost of GGM makes it an interesting component of biodegradable films (Persson et al. 2007). To further evaluate the potential of GGM films in e.g. food packaging applications, water vapor barrier properties need to be studied.

CONCLUSIONS

1. GGM / KGM blend films were homogeneous and had higher tensile strength than the films from pure GGM. Even a small addition of KGM notably increased the elongation at break of GGM-based films. Blending GGM with KGM was found to be an effective way to improve the mechanical properties of GGM-based films.
2. Although the use of PVOH increased the mechanical properties of GGM / PVOH blend films, DMA and microscopic study showed that the two polymers were immiscible.
3. GGM and cAX formed homogeneous blend films, but they were very sensitive to high relative humidity.

ACKNOWLEDGMENTS

Chunlin Xu is acknowledged for the isolation of GGM and for the mannose content analysis, Guoping Bao for skillful technical assistance in SEM imaging of films, and David Coffin for assistance in DMA. Foundation for Research of Natural Resources in Finland, Finnish Funding Agency for Technology and Innovation (Tekes), and Academy of Finland are thanked for financial support.

REFERENCES CITED

- Chen, J., Zhang, Y., Du, G.-C., Hua, Z.-Z., and Zhu, Y. (2007). "Biodegradation of polyvinyl alcohol by a mixed microbial culture," *Enzyme Microb. Technol.* 40(7), 1686-1691.
- Cheng, L. H., Karim, A. A., and Seow, C. C. (2006). "Effects of water-glycerol and water-sorbitol interactions on the physical properties of konjac glucomannan films," *J. Food Sci.* 71(2), E62-E67.
- Cheng, L. H., Karim, A. A., and Seow, C. C. (2007). "Effects of acid modification on physical properties of konjac glucomannan (KGM) films," *Food Chem.* 103(3), 994-1002.
- Chiellini, E., Corti, A., Solaro, R. (1999). "Biodegradation of poly(vinyl alcohol) based blown films under different environmental conditions," *Polym. Degrad. Stab.* 64(2), 305-312.
- Coffin, D. R., Fishman, M. L., and Ly, T. V. (1996). "Thermomechanical properties of blends of pectin and poly(vinyl alcohol)," *J. Appl. Polym. Sci.* 61(1), 71-79.
- Doner, L. W., and Hicks, K. B. (1997). "Isolation of hemicellulose from corn fiber by alkaline hydrogen peroxide extraction," *Cereal Chem.* 74(2), 176-181.
- Eberingerová, A., and Heinze, T. (2000). "Xylan and xylan derivatives - biopolymers with valuable properties. 1. Naturally occurring xylans structures, isolation procedures and properties," *Macromol. Rapid Commun.* 21(9), 542-556.
- Fishman, M. L., Coffin, D. R., Onwulata, C. I., and Konstance, R.P. (2004). "Extrusion of pectin and glycerol with various combinations of orange albedo and starch," *Carbohydr. Polym.* 57(4), 401-413.
- Fishman, M. L., Coffin, D. R., Onwulata, C. I., and Willett, J. L. (2006). "Two stage extrusion of plasticized pectin/poly(vinyl alcohol) blends," *Carbohydr. Polym.* 65(4), 421-429.
- Fredon, E., Granet, R., Zerrouki, R., Krausz, P., Saulnier, L., Thibault, J. F., Rosier, J., and Petit, C. (2002). "Hydrophobic films from maize bran hemicelluloses," *Carbohydr. Polym.* 49(1), 1-12.
- Hartman, J., Albertsson, A.-C., Söderqvist Lindblad, M., and Sjöberg, J. (2006a). "Oxygen barrier materials from renewable sources: material properties of softwood hemicellulose-based films," *J. Appl. Polym. Sci.* 100(4), 2985-2991.
- Hartman, J., Albertsson, A.-C., and Sjöberg, J. (2006b). "Surface- and bulk-modified galactoglucomannan hemicellulose film and film laminates for versatile oxygen barriers," *Biomacromolecules* 7(6), 1983-1989.
- Hassan, C. M., Trakampan, P., and Peppas, N. A. (2002). *Water Soluble Polymers – Solution Properties and Applications*, Z. Amjad, ed., Kluwer Academic Publishers, New York.
- Höjje, A., Gröndahl, M., Tømmeraas, K., and Gatenholm, P. (2005). "Isolation and characterization of physicochemical and material properties of arabinoxylans from barley husks," *Carbohydr. Polym.* 61(3), 266-275.
- Kalichevsky, M. T., and Blanshard, J. M. V. (1993). "The effect of fructose and water on the glass transition of amylopectin," *Carbohydr. Polym.* 20(2), 107-113.

- Kirwan, M. J., and Strawbridge, J. W. (2003). *Food Packaging Technology*, R. Coles, D. McDowell, and M. J. Kirwan, eds., Blackwell Publishing, Oxford.
- Li, B., and Xie, B. (2004). "Synthesis and characterization of konjac glucomannan/poly(vinyl alcohol) interpenetrating polymer networks," *J. Appl. Polym. Sci.* 93(6), 2775-2780.
- Li, B., Kennedy, J. F., Jiang, Q. G., and Xie, B. J. (2006b). "Quick dissolvable, edible and heatsealable blend films based on konjac glucomannan - gelatin," *Food Res. Int.* 39(5), 544-549.
- Li, B., Xie, B., and Kennedy, J. F., (2006a). "Studies on the molecular chain morphology of konjac glucomannan," *Carbohydr. Polym.* 64(4), 510-515.
- Mikkonen, K., Helén, H., Talja, R., Willför, S., Holmbom, B., Hyvönen, L., and Tenkanen, M. (2006). "Biodegradable films from mannans," *Proceedings of the 9th European Workshop on Lignocellulosic and Pulp (EWLP), Vienna, Austria, 27-30 August 2006*, 130-133.
- Mikkonen, K. S., Rita, H., Helén, H., Talja, R. A., Hyvönen, L., and Tenkanen, M. (2007). "Effect of polysaccharide structure on mechanical and thermal properties of galactomannan-based films," *Biomacromolecules* 8(10), 3198-3205.
- Peroval, C., Debeaufort, F., Despre, D., and Voilley, A. (2002). "Edible arabinoxylan-based films. 1. Effects of lipid type on water vapor permeability, film structure, and other physical characteristics," *J. Agric. Food Chem.* 50(14), 3977-3983.
- Persson, T., Nordin, A.-K., Zacchi, G., and Jönsson, A.-S. (2007). "Economic evaluation of isolation of hemicelluloses from process streams from thermomechanical pulping of spruce," *Appl. Biochem. Biotechnol.* 136-140, 741-752.
- Saulnier, L., Marot, C., Chanliaud, E., and Thibault, J.-F. (1995). "Cell wall polysaccharide interactions in maize bran," *Carbohydr. Polym.* 26(4), 279-287.
- Sjöström, E. (1993). *Wood Chemistry Fundamentals and Applications*, Academic Press, Inc., San Diego, CA, USA.
- Sundberg, A., Sundberg, K., Lillandt, C., and Holmbom, B. (1996). "Determination of hemicelluloses and pectins in wood and pulp fibers by acid methanolysis and gas chromatography," *Nordic Pulp Paper Res. J.* 11(4), 216-219.
- Takigami, S. (2000). *Handbook of Hydrocolloids*, G. O. Phillips, P. A. Williams, eds., Woodhead Publishing, Cambridge, UK.
- Talja, R. A., Helén, H., Roos, Y. H., and Jouppila, K. (2007). "Effect of various polyols and polyol contents on physical and mechanical properties of potato starch-based films," *Carbohydr. Polym.* 67(3), 288-295.
- Thornton, J., Ekman, R., Holmbom, B., and Orsa, F. (1994). "Polysaccharides dissolved from Norway spruce in thermomechanical pulping and peroxide bleaching," *J. Wood Chem. Technol.* 14(2), 159-175.
- Tenkanen, M., Soovre, A., Heikkinen, S., Jouhtimäki, S., Talja, R., Helén, H., and Hyvönen L. (2007). "Production and properties of films from cereal arabinoxylans," *Proceedings of the Italic 4, Science and Technology of Biomasses – Advances and Challenges, Rome, Italy, 8-10 May 2007*, 70-73.
- Willför, S., Rehn, P., Sundberg, A., Sundberg, K., and Holmbom, B. (2003). "Recovery of water-soluble acetylgalactoglucomannans from mechanical pulp of spruce," *Tappi J.* 2(11), 27-32.

- Willför, S., Sundberg, K., Tenkanen, M., and Holmbom, B. (2007). "Spruce-derived mannans – a potential raw material for hydrocolloids and novel advanced materials," *Carbohydr. Polym.* doi: 10.1016/j.carbpol.2007.08.006.
- Xiao, C., Liu, H., Gao, S., and Zhang, L. (2000a) "Characterization of poly(vinyl alcohol)-konjac glucomannan blend films," *J. Macromol. Sci. Pure Appl. Chem.* 37(9), 1009-1021.
- Xiao, C., Gao, S., and Zhang, L. (2000b). "Blend films from konjac glucomannan and sodium alginate solutions and their preservative effect," *J. Appl. Polym. Sci.* 77(3), 617-626.
- Xiao, C., Lu, Y., Liu, H., and Zhang, L. (2001a). "Preparation and characterization of konjac glucomannan and sodium carboxymethylcellulose blend films," *J. Appl. Polym. Sci.* 80(1), 26-31.
- Xiao, C., Liu, H., Lu, Y., and Zhang, L. (2001b). "Characterization of poly(vinylpyrrolidone)-konjac glucomannan blend films," *J. Appl. Polym. Sci.* 81(5), 1049-1055.
- Xu, C., Willför, S., Sundberg, K., Pettersson, C., and Holmbom, B. (2007). "Physicochemical characterization of spruce galactoglucomannan solutions: stability, surface activity, and rheology," *Cellulose Chem. Technol.* 41(1), 57-65.
- Xu, C., Willför, S., and Holmbom, B. "Rheological properties of spruce galactoglucomannans. II. Blends with konjac glucomannan and other polysaccharides," submitted.
- Yadav, M. P., Johnston, D. B., Hotchkiss, A. T. Jr, and Hicks, K. B. (2007). "Corn fiber gum: a potential gum arabic replacer for beverage flavor emulsification," *Food Hydrocolloids* 21(7), 1022-1030.
- Ye, X., Kennedy, J. F., Li, B., and Xie, B. J. (2006). "Condensed state structure and biocompatibility of the konjac glucomannan/chitosan blend films," *Carbohydr. Polym.* 64(4), 532-538.
- Yue, C. L., Davé, V., Kaplan, D. L., and McCarthy, S. P. (1995). "Advanced materials from renewable resources: konjac/pullulan blends," *Polym. Prepr.* 36(1), 416-417.
- Zhang, P., and Whistler, R. L. (2004). "Mechanical properties and water vapor permeability of thin film from corn hull arabinoxylan," *J. Appl. Polym. Sci.* 93(6), 2896-2902.

Article submitted: November 2, 2007; Peer-review completed: Jan. 5, 2008; Revised version received and accepted: Jan. 17, 2008; Published: Jan. 19, 2008.

STRUCTURE AND PROPERTIES OF SOME NATURAL CELLULOSIC FIBRILS

Ramjee Subramanian,* Alexey Kononov, Taegeun Kang, Jouni Paltakari, and Hannu Paulapuro

This study examines the properties of cellulosic fibrillar fines manufactured from different pulp raw materials, bleached softwood kraft (BSWK), thermomechanical pulp (TMP), and non-wood sisal. Chemical characterisation showed that the carbohydrate and lignin contents of sisal were between those of BSWK and TMP. Sisal was found to contain about three times more calcium than BSWK and TMP. Measurements from the immobilization kinetics showed that the solids content after immobilization was highest for the sisal suspension, followed by TMP and BSWK. This indicates that the dewatering ability of the fines suspension increased in the order BSWK, TMP and sisal. The loss modulus (G'') was maximum with BSWK, indicating that the greatest viscous dissipation before immobilisation took place in the BSWK suspension. The strength properties of fines sheets decreased in the order BSWK, TMP and sisal. This is due to the highly fibrillated nature of BSWK fines, as illustrated by fibre saturation point (FSP), differential scanning calorimetric (DSC), and hydrodynamic specific volume (HSV) measurements.

Keywords: Microfibrils; Fines; Rheology; Immobilization; Dewatering; Strength; Chemical characterization

*Contact information: Department of Forest Products Technology, Helsinki University of Technology, P.O. Box: 6300, 02015 Espoo, Finland; *Corresponding author: rsubrama@cc.hut.fi.*

INTRODUCTION

There is currently renewed interest in engineering new cellulosic products from the structural elements of cellulosic fibres. Biodegradable, renewable, and ubiquitous, plant and wood fibres have a hierarchical structure consisting of smaller and mechanically stronger entities. An example of this structural hierarchy was illustrated by Frey-Wyssling (1957), who discussed the various scales of structure in cotton (Table 1).

Table 1. Structural Hierarchy in Cotton Fibres (after Frey-Wyssling 1957)

Scale	Area of cross section	Number of cellulosic chains on cross section
Cotton hair	314 000 000 nm ²	1*10 ⁹
Macro fibril	160 000 nm ²	5*10 ⁵
Micro fibril	625 nm ²	2*10 ³
Elementary fibril	30 nm ²	1*10 ²
Cellulose molecule	0.32 nm ²	1

Fibrillar fines obtained from cellulosic fibres are known for their unique structure, many useful characteristics, and large number of potential industrial, techno-logical, and commercial applications. It has been concluded earlier that the crystallinity of the fibrils and their accessibility to swelling or hydrolysis vary with the biological origin of the material and its pre-treatment (Berglund 2005).

Recently, several routes towards synthesizing fibrillar fines have been described in the literature. One industrial approach to produce cellulosic fibrils is based on the dissolution of cellulose in solvents, regeneration, and even potentially electrospinning (Liu and Hsieh 2002), where the dissolution process causes formation of structural elements of cellulose. Microcrystalline cellulose can be prepared by acid hydrolysis, eliminating the amorphous regions of cellulose (Dong et al. 1998). The cellulose microcrystals formed by this process, which randomly aggregate through hydrogen bonding, have diameters of 10-30nm. Formation of cellulosic microfibrils by a bacterial process has been studied by Tokoh et al. (1998). Production of microfibrils from non-wood resources, through separation of microfibrils from sugar beet and potato tuber cells, has been reported by Dufresne et al. (2000).

High-shear mechanical treatment to generate fibrillar fines have been described by Matsuda (2001). Formation and application of microfibrils from wood fibres has been studied by Taniguchi et al. (1998). Enzymatic hydrolysis combined with mechanical shearing and high-pressure homogenisation has been used for preparing cellulosic fibrils in gel form, as shown by Pääkkö et al. (2007).

Although various means of generating microfibrils have been tried in recent times, we have insufficient knowledge about the effect of the source, pulps of different origin, on the nature and characteristics of cellulosic microfibrils.

In this work, our preliminary aim was to examine pulps produced by two major pulping processes, chemical and mechanical pulps, as raw materials for cellulosic fibril production. On the other hand, initial tests with sisal pulp grinding showed that the sisal fines exhibited characteristics that were far different from those of chemical and mechanical pulp fines. Thus, we hypothesised that by using distinguished market pulps, composed of varying amounts of lignin - bleached softwood kraft (BSWK), thermomechanical (TMP), and non-wood sisal - it is possible to gain a better understanding of the effect of the raw material on the type of fibrillar fines produced with high-shear grinding. The pulps were degraded into fines by treating them in a high-shear Supermasscolloider[®]. The fines were analysed for chemical, rheological, water interactions, and strength properties. An optical microscope was used to study the structure of the fines. The information obtained from this study can be used for engineering new composite materials, and for process and product optimisations.

EXPERIMENTAL

Raw Materials

ECF-bleached softwood kraft pulp (non-dried pulp containing Scandinavian spruce and pine in equal amounts) was obtained from a Finnish pulp mill. TMP (made from Norway spruce), sampled from a reject line, was obtained from a Finnish pulp mill

at 30% consistency and stored in freezer to await experiments. Defrosted samples were disintegrated at 3% consistency and used for further grinding to produce fines. Commercial sisal pulp (obtained from Africa), cut into 5-cm pieces, was disintegrated and ground in the SuperMasscolloider[®] to produce fines.

Grinding

The grinding was carried out with an ultra-fine friction grinder (Super masscolloider^{®1}). The grinder reduces the fibres into fines by mechanical shearing (Matsuda et al. 2001). More details about operation of this grinder have been reported (Kang 2006). In this device, the grinding takes place between rotating and stationary abrasive stones made of silicon carbide (SiC). The gap between the stones with a grit class #46 (grit size 297-420 μm) was adjusted to 80 μm . The treated pulp was discharged by centrifugal force enhanced by rotor blades. The grinding degree was advanced by re-circulating the pulp suspension. Determination of energy consumption was somehow difficult, due to small operating gap. At this gap occasional contacts between stones have been reported.

Grinding was performed at room temperature with cooling of the stones by running water at the consistency of 3%. The BSWK and TMP pulps were re-circulated for 5 times and sisal pulp 4 times, respectively. The estimated maximum residence time in the gap for one path was in the order of 0.5 sec. The total time between grinding stones was in the range of 180 sec per path.

Sheet Forming and Mechanical Testing

Round sheets were formed from the fines in a dynamic drainage jar (DDJ) by filtering a stirred fines suspension onto a Whatman #604 filter paper with a diameter of 110 mm. The Whatman filter paper was removed from the DDJ, and the fines sheet was placed on a pressing plate. Old blotters were placed on the filter paper and couched by hand to remove the excess of water. Subsequently, filter paper was removed from the sheet. A new blotter was then placed over the sheet and gently pressed by hand to attach the blotter to the fines sheet. Finally, the sheets were air-dried using drying plates on a rack in a conditioning room (23°C, 50% RH).

Fines sheets strength properties were analysed according to ISO 1924-2:1994, except that the span length was 70 mm. Light scattering was measured according to ISO 9416-1998.

Fines Characterisation

The blend of fines was fractioned in a Bauer-McNett classifier, which segregates the fines suspension into different streams based on physical properties, such as fiber length and flexibility (Gooding and Oslon 2001). We slightly modified the standard, SCAN-M6:69, operating conditions by using 30g oven-dry pulp and 20 minutes of operating time. Progressively decreasing 100, 200, 300, 400 screen meshes were used in this study.

The immobilisation kinetics of the fines suspensions were measured with a Physica MCR 300 rheometer. Measurements were conducted with a plate-plate assembly

¹ Supermasscolloider[®] (Model MKZA 10-15J) is a trademark product of Masuko Sangyo Co. Ltd, Japan.

for the direct strain controlled oscillatory test (DSO) under constant conditions. Test conditions were as follows: temperature of 23°C, strain γ of 1%, angular frequency ω of 10 s⁻¹, and initial gap of 1 mm. Fines suspension at a consistency of 3% was applied onto the special polycarbonate filter with pore size of 0.22 μm . At consistency lower than 3% the test reproducibility was difficult to achieve. Vacuum of 300 mbar was applied after closing the gap and starting oscillation. The zero normal force between plate and sample was maintained by the decreasing gap during the process of dewatering. Immobilisation of the sample took place when solids content of pad reached the point where particles had established a spatial structure and could no longer move freely. The maximum of loss modulus G'' corresponded to this point (Wollny 2001).

Solute exclusion and thermoporosimetric measurements were performed to determine the fibre saturation point (FSP), the freezing bound water (FBW), and the non-freezing bound water (NFW) according to the methods described in the literature (Stone and Scallan 1968; Maloney and Paulapuro 2001). The hydrodynamic specific volume of pulp fines was determined as a fines sediment volume per solids after 24 hours of settling at a consistency of 1g/l under conditions described by Marton and Robie (1969).

Extractives, carbohydrates, free sugars, and cellulose were determined according to the test methods listed in Table 2.

Table 2. Chemical Analytical Methods Used for Analysing Organics and Inorganics in Fines

Components	Analytical Techniques
Cellulose	Tappi T249 cm-85
Extractives	Ekman, R. (1980), "Wood extractives of Norway spruce - A study of nonvolatile constituents and their effects on <i>Fomes annosus</i> ," PhD thesis, Laboratory of Forest Products Chemistry, Åbo Akademi University.
Lignin	Iiyama, K., and Wallis, A.F.A. (1988). "An improved acetyl bromide procedure for determining lignin in woods and wood pulps," <i>Wood Science and Technology</i> 22(3), 271-280.
Total carbohydrates	Bertaud, F., Sundberg, A., and Holmbom, B. (2002). "Evaluation of acid methanolysis for analysis of wood hemicelluloses and pectins," <i>Carbohydr. Polym.</i> 48(3), 319-324.
Free monomeric sugars	Pedro, F., and Holmbom, B. (1996). "Anionic groups in papermaking fibres: Origin, depth profile and surface distribution," <i>Nordic Pulp Paper Res. J.</i> 226(11), 216-219.
Metals	Mass spectrometry

Optical Microscopy Study

The structure of fines was studied qualitatively with a Leica DM LAM light microscope, equipped with a phase contrast optical system. Phase contrast microscopy is an optical technique that can be used to produce high contrast images of transparent specimens (Pluta 1989). In effect, phase contrast microscopy translates a phase shift of light waves into the differences in amplitude. This means that the samples can be examined in their natural state without staining. In particular, this is an advantageous for fines, as they are hard to detect even with stains.

RESULTS AND DISCUSSION

The fractional composition of the studied fines is shown in Fig. 1. It was found that the fines content (pass fraction, 200 mesh) was the highest for BSWK, followed by TMP and sisal fines. In addition, the BSWK fines contained the highest and sisal the lowest percentage of 400-pass fines. Optical microscopic observation of the BSWK fines passing the 200-mesh showed that a significant proportion of fines had dimensions which were larger than the size of apertures, i.e., above 76 μm . Hence, we infer that BSWK fines should be highly flexible in order to pass openings of smaller size.

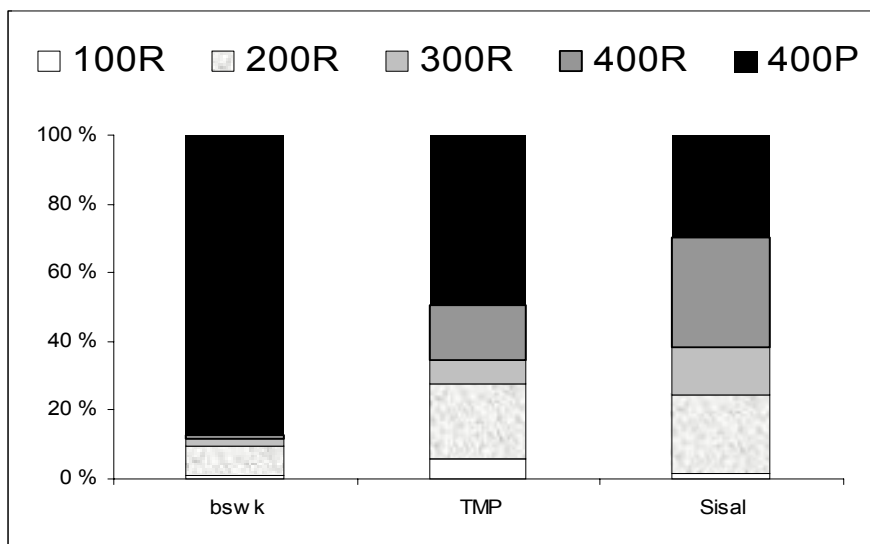


Figure 1. Bauer McNett fractions obtained for the three different fines materials. Abbreviations: R – Retained; P–Passed

The organic chemical constituents of the studied fines materials are shown in Fig. 2. It can be noted that sisal had a higher cellulosic content than TMP pulp fines. Also, the lignin content was the highest in TMP fines, followed by sisal and BSWK fines. TMP fines had a high content of free sugars, while sisal and BSWK fines contained minimal amounts of free sugars and extractives.

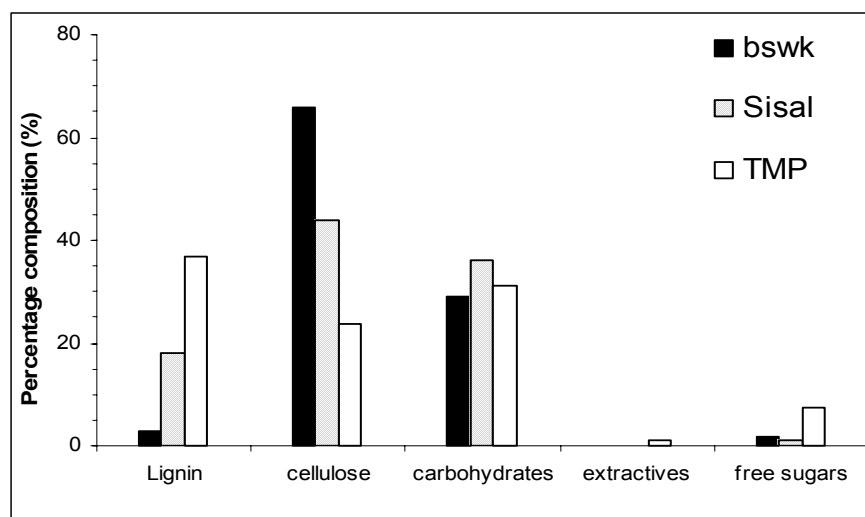


Figure 2. Organic composition of the three different pulp materials

Among the inorganic components found in the pulp fines (Fig. 3), sisal had the highest calcium content. Calcium is found as calcium oxalate in sisal pulp fines. Bleached softwood kraft pulp fines had the highest content of sodium in the structure. TMP pulp fines contained more manganese than the fines materials from the other two sources. The difference in the metal composition is attributed both to the raw material and the process. However, since the studied pulps are from the most common processes the information about metal composition is valuable.

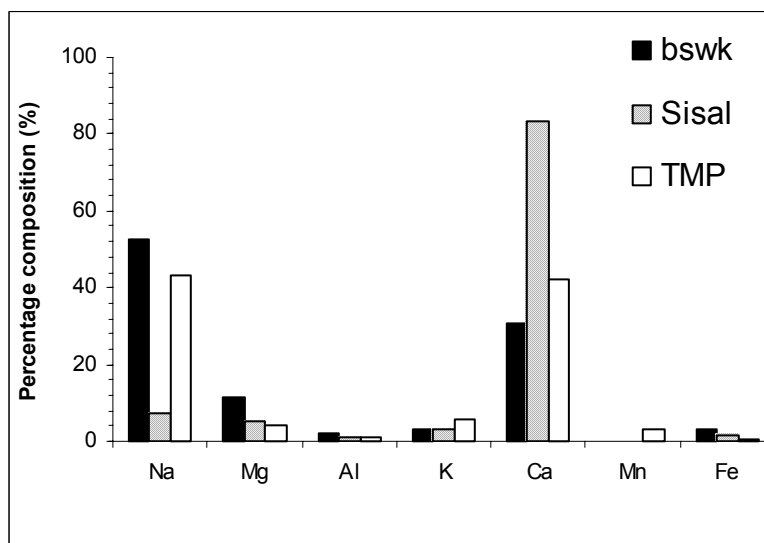


Figure 3. Metal composition of the three different pulp materials

Rheology is a powerful tool for characterising fines suspensions, as shown in Table 3. The rheological behaviour and dewatering process of the fines suspensions were examined using an immobilisation cell. The simultaneous measurement of dewatering

kinetics and the corresponding rheological properties reveals possible flow and dewatering behaviour of fines in forming or coating operations.

The ability of the material to store energy (and therefore, the structural strength, gel strength, and stiffness) is defined in terms of the storage modulus (G'). It was the highest for BSWK and practically the same for TMP and sisal suspensions. The loss modulus, G'' , is associated with the ability of the material to dissipate mechanical energy to heat in viscous flow. The mechanical loss factor, $\tan(\delta)$, which is a ratio of G''/G' , was smaller than 1 at immobilization point for all samples. Thus, the studied fines suspensions can be considered as gels (Almdal et al. 1993).

Table 3. Rheology of Different Pulp Fines Suspensions

Item	G'' @IMMO point (kPa)	Final bulk (cm ³ /g)	Final solids (%)	IMMO time (s)	Solids (mg)	$\tan(\delta)$ @ IMMO point	Consist. (g/l)
BSWK	29	5.49	8.5	15.3	63	0.33	20
TMP	13	2.73	11.2	29.8	115	0.41	38
Sisal	16	5.15	17.3	14.4	95	0.45	32

The loss modulus G'' at the immobilization point was highest for BSWK, which shows that the biggest energy dissipation to heat took place in the BSWK suspension, i.e., it had the highest viscosity just before immobilization. The energy dissipation in sisal and TMP fines was roughly similar and significantly lower than in BSWK. This observation is in agreement with the notion about high specific surface of the BSWK. The final bulk was lowest for TMP fines, showing that the structure of TMP fines was more compact than that of the other two fines materials.

The solids content obtained at the immobilisation point indicates the maximum possible dewatering from the mobile viscous fines suspension. The dewatering degree was highest for sisal fines, followed by TMP and BSWK fines. On the other hand, the immobilisation time varied for the fines suspensions, because of the different solids contents of the initial samples. With the BSWK samples, higher solids could not be reached, due to the developed internal surface, which able to hold more water.

The strength properties of the fines sheets are listed in Table 4. The basis weights of the fines sheets were not similar due to difficulties encountered in the forming process. It was difficult to dewater higher grammage BSWK sheets, while lower grammage TMP and sisal handsheets were too brittle to handle. According to our findings, the highly fibrillated BSWK fines formed structures with high density, tensile index, and stiffness. This is attributed to the increased specific surface area of the BSWK fines, resulting in an enhanced relative bonded area and tougher structure (Retulainen et al. 2002). In contrast, the stiff and the least conformable sisal fines particles gave the lowest tensile strength.

Table 4. Strength Properties of Sheets Composed of Fines

Sample	Basis weight (gsm)	Apparent density (kg/m ³)	Thickness (μm)	Tensile index (N*m/g)	TEA index (J/kg)	T. Stiff. index (MN*m/kg)	Light scattering (m ² /kg)
BSWK	86	1020	84	79	2839	6.7	3
TMP	138	586	226	28	198	3.0	49
Sisal	163	454	359	11	36	1.9	70

As expected, the light scattering was highest for the sisal fines and the lowest for the BSWK fine sheets. This is attributed to the bulkier structure of sisal handsheets and higher extension of solids-air interface. Furthermore, compared to TMP fines, sisal fines had higher brightness.

The higher fibrillation degree of BSWK has been confirmed by studies of fibril-water interaction, based on fibre saturation point (FSP) and differential scanning calorimetry (DSC) measurements. The measured FSP of the BSWK, TMP, and sisal samples was 4.43 g/g, 1.32 g/g, and 1.32 g/g, respectively. The total water held inside the fibrous material is classified in terms of bulk water (BW), freezing-bound water (FBW) and non-freezing bound water (NFW) (Fig. 4).

An increased degree of refining through fibre degradation leads to formation of fibrillar fines materials. In the case of BSWK, these fines particles form an intertwined, highly branched network structure. The highest amount of water, bulk water, was trapped in the inter-fibrillar space, corresponding to the macropores level. In addition, the amount of the intermediate pores, corresponding to FBW, was also higher for BSWK. On the other hand, bulk water was significantly lower in TMP and sisal fines due to their stiffer structure and higher hydrophobicity. Since the amount of non-freezing water, strongly associated with cell wall constituents, was similar for all the fines samples, their submolecular structure can be considered to be similar.

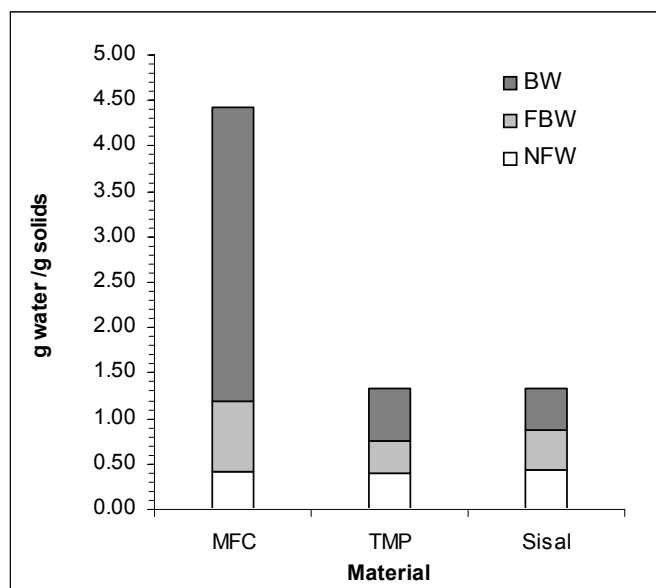


Figure 4. Water adsorption in the inter- and intra-fibrillar matrix, obtained with the differential scanning calorimetric technique and solute exclusion

The hydrodynamic specific volume (HSV) of the different fines, obtained from the sediment by settling of suspended materials, is shown in Table 5. According to the table, the BSWK had the highest HSV, showing that the fibrillar fines produced from bleached kraft pulp had the highest specific surface and occupied volume. On the other hand, sisal fines formed much denser sediment, showing that the fines were packed tighter and had the smallest specific surface area. However, higher density of sediment can be partly due to the higher acidity of sisal fines.

Table 5. Hydrodynamic Specific Volume of the Three Different Types of Fines Materials

Samples	Hydrodynamic specific volume (cm ³ /g)	pH
BSWK	778	6.7
TMP	180	6.0
Sisal	56	5.6

Optical Microscopic Study of Fines

Each particle of the BSWK fibrillar fines comprises a complex network, as shown in Fig. 5. The fibrils are flexible and capable of holding water in the inter-fibrillar space of their network structure. Thus, the high fibre saturation point (FSP) and free bound water (FBW), as shown in Fig. 4, can be attributed to the fibrillar networks. According to the micrographs, the fibrils have high aspect ratios. On the other hand, the network nature makes it difficult to apply conventional particle size measurements for determining the particle size distribution for these fines suspensions.

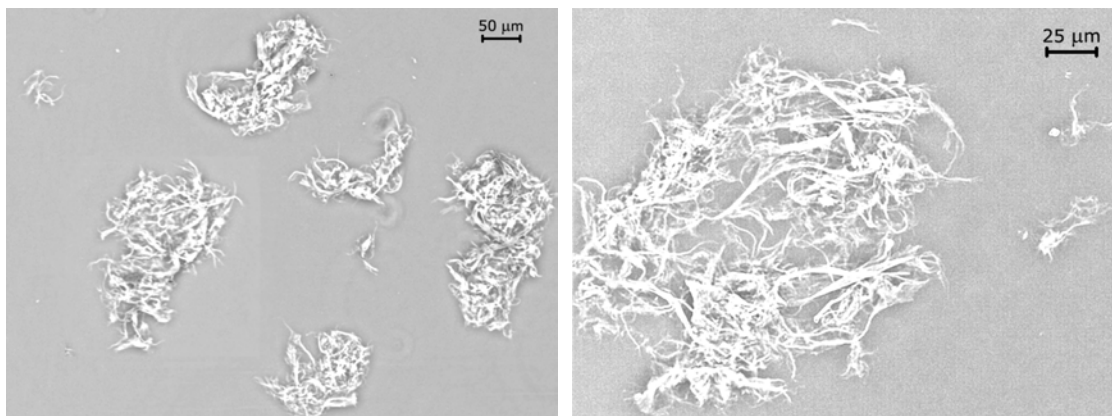


Figure 5. Negative phase contrast images of fibrillar fines obtained from bleached softwood kraft pulp; lower (left) and higher (right) magnification

TMP fines consisted of fibrillar and flake-like fines (Fig. 6). The TMP fibrillar fines were stiffer than BSWK fines. Sisal fines had the least flocculating tendency among the three types of fines (Fig. 6). Also, some of the fibrillar fines seemed to be longer and thicker.

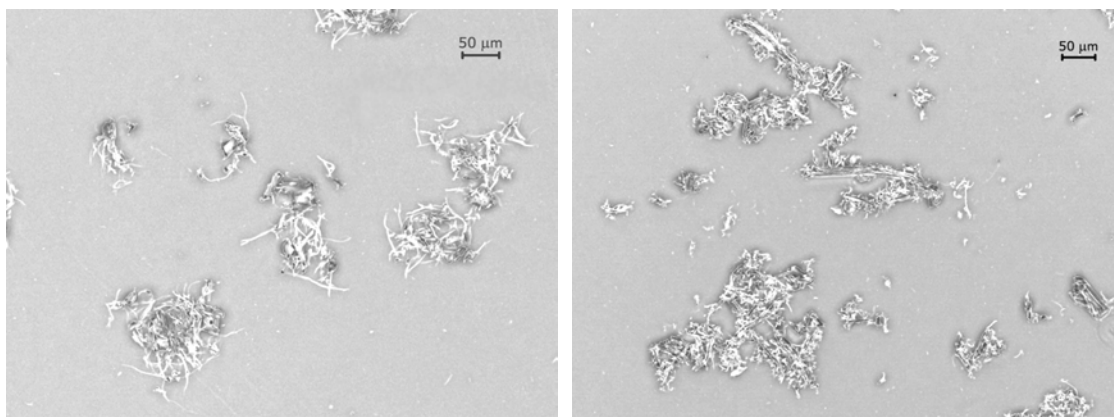


Figure 6. Negative phase contrast images of TMP fines (left) and sisal fines (right) obtained by pulp degradation in a Supermasscolloider®

CONCLUSIONS

In this study, fines material produced from two distinguished types of market pulps as well as from exotic sisal pulp were examined to determine their potential for use in various applications.

Chemical characterisation showed that the fines from typical sisal pulp contained significantly higher calcium ions, which may be a significant factor for some possible applications. Rheology studies showed that all the fines behaved viscoelastically, and that the dewatering degree was highest for sisal and lowest for BSWK pulps. The loss modulus was highest for BSWK, showing that the viscosity was greatest for these fines.

The highest and lowest density and tensile strength values were obtained for samples produced from BSWK and sisal fines, respectively. Highest strength and density of BSWK sheets were attributed to the augmented specific surface area, as indicated by fibril-water interaction and settling studies, of these fibrils.

Microscopic investigations confirmed that the BSWK fibrils form an intertwined extended network structure. On the other hand, TMP and sisal fibrils were stiffer and contained more flakes and coarser materials.

Fines material obtained from typical TMP and BSWK pulps, as well as from exotic sisal pulp, showed the range of properties that can be used to achieve different strength-dewatering combinations in paper or other composite products.

ACKNOWLEDGEMENTS

This work was presented in the 8th International Technical Conference on Pulp, Paper, Converting and Allied Industry, New Delhi, India. The publication of this manuscript has been approved by the conference organizers.

REFERENCES CITED

- Almdal, K., Dyre, J., and Hvidt, S. (1993). "Towards a phenomenological definition of the term 'gel'," *Polymer Gel & Networks* 1(1), 5-17.
- Berglund, L. (2005). "Cellulose based nanocomposites," in *Natural Fibers, Biopolymers and Biocomposites*, Mohanty, A. K., Mishra, M., and Drazal, L.T. (eds.), CRC press, 807-832.
- Chakraborty, A., Sain, N., and Kortschort, M. (2005). "Cellulose microfibrils: A novel method of preparation using high shear refining and cryocrushing," *Holzforschung* 59(1), 102-107.
- Dong, X. M., Revol, J-F., and Gray, D. G. (1998). "Effect of microcrystallite preparation conditions on the formation of colloid crystals of cellulose," *Cellulose* 5(1), 19-32.
- Dufresne, A., Dupeyre, D., and Vignon, M. R. (2000). "Cellulose microfibrils from potato tuber cells: Processing and characterization of starch-cellulose microfibril composites," *J. Applied Polymer Sci.* 76(14), 2080-2092.
- Frey-Wyssling, A. (1957). "A general structure of fibres," in *Proceedings of the Transactions of the First Fundamental Research Symposium*, BPBMA, Bolam, F. (ed.), Cambridge, 1-5.
- Gooding, R. W., and Olson, J. A. (2001). "Fractionation in a Bauer-McNett classifier," *J. Pulp and Paper Sci.* 27(12), 423-428.
- Holmbom, B., and Stenius, P. (2000). "Analytical methods," in *Papermaking Science and Technology* book series, Johan Gullichsen and Hannu Paulapuro (eds.), 4: *Forest Products Chemistry*, Per Stenius (ed.), Fapet Oy, 117-149.
- Kang, T., and Paulapuro, H. (2006). "New mechanical treatment for chemical pulp," *Proceedings of the Institution of Mechanical Engineers, Part E: Journal of Process Mechanical Engineering* 220(3), 161-166.
- Liu, H., and Hsieh, Y.-L. (2002). "Ultrafine fibrous cellulose membranes from electrospinning of cellulose acetate," *J. Polymer Sci. Part B. Polymer Physics* 40(18), 2119-2129.
- Maloney, T. C., and Paulapuro, H. (2001). "Thermoporosimetry of pulp fibres," in *The Science of Papermaking*, Proceedings of the 2001 Fundamental Research Symposium, BPBMA, Oxford, 897-926, 2001.
- Marton, R., and Robie, J. D. (1969). "Characterisation of mechanical pulps by a settling technique," *TAPPI J.* 52(12), 2400-2406.
- Matsuda, Y., Hirose, M., and Ueno, K. (2001). "Super microfibrillated cellulose, process for producing the same and coated paper and tinted paper using the same," *U.S. Pat.* 6,214,163 B1, Tokushu Paper Mfg. Co., Ltd (Matsuda et.al.), 18 pp.
- Pluta, M. *Advanced Light Microscopy, Specialized Methods*, vol. 2. Elsevier, Amsterdam, 1989.
- Pääkkö, M., Ankerfors, M., Kosonen, H., Nykänen, A., Ahola, S., Österberg, J., Ruokalainen, J., Laine, J., Larsson, P. T., Ikkala, O., and Lindström, T. (2007). "Enzymatic hydrolysis combined with mechanical shearing and high-pressure homogenization for nanoscale cellulose fibrils and strong gels," *Biomacromolecules* 8(6), 1934 -1941.

- Rånby, B. G. (1957). "The fine structure of cellulose fibrils," *Proceedings of the Transactions of the First Fundamental Research Symposium*, BPBMA, Bolam, F. (ed.), Cambridge, 55-82.
- Retulainen, E., Lukko, K., Fagerholm, K., Pere, J., Laine, J., and Paulapuro, H. (2002). "Papermaking quality of fines from different pulps - The effect of size, shape and chemical composition," *Appita J.* 50(6), 457-460.
- Stone, J. E., and Scallan, A. M. (1968). "A structural model for the cell wall of water-swollen wood pulp fibres based on their accessibility to macromolecules," *Cellulose Chemical Technology* 2(3), 343-358.
- Taniguchi, T., and Okamura, K. (1998). "New films produced from microfibrillated natural fibres," *Polymer International* 47(3), 291-294.
- Tokho, C., Takabe, K., Fujita, M., and Saiki, H. (1998). "Cellulose synthesized by *acetobacter xylinum* in the presence of acetyl glucomannan," *Cellulose* 5(4), 249-261.
- Wollny, K. (2001). "New rheological test method to determine the dewatering kinetics of suspensions," *Applied Rheology J.* 11(2), 197-202.

Article submitted: Dec. 12, 2007; Peer review completed: Jan. 9, 2008; Revised version received and accepted: Jan. 19, 2008; Published: Jan. 21, 2008.

PERIODATE AND HYPOBROMITE MODIFICATION OF SOUTHERN PINE WOOD TO IMPROVE SORPTION OF COPPER ION

James D. McSweeney,^a Roger M. Rowell,^a George C. Chen,^a Thomas L. Eberhardt,^b and Soo-Hong Min^c

Milled southern pine wood was modified with sequential treatments of sodium periodate and sodium hypobromite for the purpose of improving copper ion (Cu^{2+}) sorption capacity of the wood when tested in 24-h equilibrium batch tests. The modified wood provided additional carboxyl groups to those in the native wood and substantially increased Cu^{2+} uptake over that of unmodified wood. Sorption capacity (q_e) measured with an unbuffered standard solution increased to a maximum of 7.8 mg Cu^{2+} ion per gram of wood (treated) from 3.1 mg Cu^{2+} ion/g wood (untreated). Samples tested were first sodium ion exchanged to keep the pH of the standard solution from declining during the sorption test. The treatment necessary for maximum q_e was 3% (w/v) periodate for 24 h and 0.8% (w/v) bromine (as hypobromite) for 24 h; both treatments were at room temperature. These conditions corresponded to the maximum periodate concentration and treatment times tested. To further evaluate the efficacy of modification treatments, weight change after each treatment was determined. Weight loss after the periodate stage for any concentration and time used was minor, indicating the selective nature of this reaction. However, most of the weight loss was incurred after hypobromite treatment. Weight loss corresponding to the greatest increase in sorption capacity was 12.6% total from the combined periodate and hypobromite stages. The increase of carboxylate functional groups in the wood was monitored using FTIR/ATR spectroscopy.

Keywords: Periodate; Hypobromite; Selective oxidation; Copper ion sorption; Southern pine wood

Contact information: a: U.S. Department of Agriculture, Forest Service, Forest Products Laboratory, One Gifford Pinchot Drive, Madison, WI 53726; b: U.S. Department of Agriculture, Forest Service, Southern Research Station, Pineville, LA 71360; c: Samsung Corporation, Sungnam-si, Gyonggi-Do, Korea 463-824

INTRODUCTION

Carbohydrate chemists traditionally have used periodate compounds as an analytical tool for differentiation of ring sizes in sugars. The first documented use was the discovery by Malaprade (1928a,b) that periodic acid would readily cleave and oxidize the α -glycol groups on mannitol. Notably, Fleury and Lange (1932) reported that the periodate reaction was selective for hydroxyl groups attached to adjacent carbon atoms. These early and subsequent uses of periodates utilized the measurement of periodate consumed and formaldehyde and formic acid produced. The relative quantities of these assayed compounds can be useful in determining carbohydrate structure.

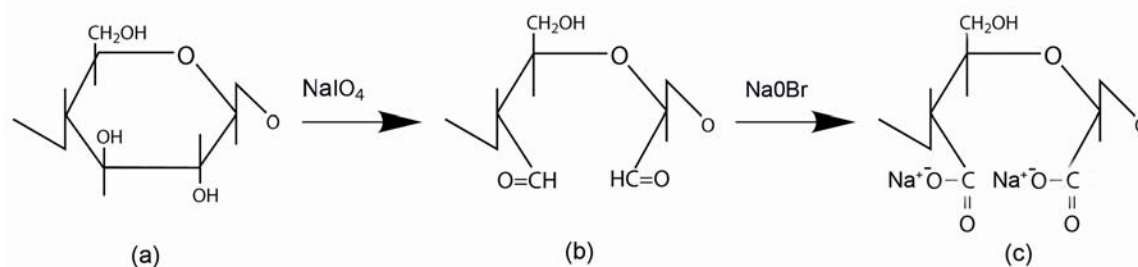


Fig. 1. Reaction of sodium periodate with cellulose glucose sugar unit (a) to produce dialdehyde (b). Sodium hypobromite oxidation of dialdehyde to dicarboxylate (c).

Because of the selective nature of the periodate reaction, we were intrigued by the prospect of employing it as part of a process to increase the carboxylic content of wood, thus improving wood's metal ion sorption capacity. Because polysaccharides constitute the largest fraction of the wood cell wall constituents and they contain a large number of hydroxyl groups, the potential for substantially increasing the number of carboxylate functional groups was expected to be high. Another interesting attribute of the periodate reaction was that it apparently will react with the crystalline as well as amorphous regions of the cellulose (Guthrie 1961). If crystalline regions were inaccessible, as might be expected, then the periodate reaction would be restricted to the amorphous fraction of cellulose, limiting its practical utility.

In addition to the abundance of modifiable functional groups in the wood polysaccharides, the selective nature of the periodate reaction is an important advantage. Glycosidic linkages between sugar units are unaffected by periodate oxidative reactions, avoiding a major decrease in degree of polymerization and loss of the wood substrate.

Periodate was also used as a reactant with the diols of wood polysaccharides by Chen and Rowell (1989). However, their purpose was to modify the wood to improve its resistance to attack by fungi and termites.

The treatment process in our study is a two-step oxidative process. The first step is periodate reacting with the carbohydrate polymers, resulting in ring scission and the formation of a dialdehyde within the monomeric units (Figure 1). The resulting aldehydes can then be oxidized to carboxylates in a second step with any number of oxidants; hypohalites are commonly used for this purpose. We are using hypobromite in the second oxidative step because it is a mild oxidant. Our intent is to avoid degradation of the modified wood that can result from an oxidant stronger than hypobromite.

Another study (Maekawa and Koshijima 1984) took a similar approach to ours, in this case using selective oxidation of cellulose powder to enhance its ability to bind with metal ions. In their study, periodate was used in the first oxidation step, and the second oxidation step utilized acid chlorite. They also studied the properties of these modified powders when combined with metal ions. Martin-Dupont et al. (2004) utilized periodic acid as part of a process to modify Douglas-fir bark to increase its binding capacity for

lead ion. Their process differed from ours in that they utilized a reductive amination in a second step to derivatize the dialdehydes with acid-containing groups.

This study is part of a larger research program by our laboratory that is seeking to improve the inherent metal ion sorption characteristics of wood and bark. Our objectives in this study were (1) to test the selective oxidation of southern pine wood and evaluate the results with respect to weight losses from the treatment steps and effect on metal ion sorption capacity as measured with a copper ion test protocol and (2) to monitor increases of carboxylate functional groups in the wood with Fourier transform infrared/attenuated total reflectance (FTIR/ATR) spectroscopy.

MATERIALS AND METHODS

Southern Pine Wood

One inch square by one-half inch thick pieces of wood were processed in a Wiley mill to pass through a 5-mm mesh size screen attached to the mill. The milled wood was sorted into size fractions by the use of 10-, 20-, 30-, and 40-mesh sieve screens in a shaker apparatus. The largest quantity fraction captured was between 10- and 20-mesh screen sizes and was the fraction used for testing. The 10- to 20-mesh wood fraction was oven dried for 4.5 h at 105°C, then stored in a desiccator containing anhydrous calcium sulfate.

Sodium Periodate

ACS reagent sodium periodate (99%) was prepared as an aqueous solution immediately before each use. A glass stirring rod was used to mix dry wood (25 g) in 500-mL periodate solution contained in a 1-L beaker. Separate experiments were conducted with three different concentrations of sodium periodate: 1%, 2%, and 3% (w/v) of reagent in de-ionized water (DI H₂O). Wood and reagent at each concentration level were reacted in separate timed experiments for periods of 6 and 24 h. These reactions were conducted at room temperature. The pH of the sample reaction mixture was checked periodically during each reaction period using a pH meter equipped with a double junction electrode. The target pH range was 3–5, and all samples remained in this range without the need for adjustment.

At the end of each reaction period, the mixture was filtered using vacuum and the filtrate set aside for analysis. Samples then were rinsed with a total of approximately 3 L of DI H₂O. The rinsed samples were placed in approximately 850 mL of DI H₂O and allowed to soak for 24 h to remove entrained periodate. After soaking, the filtered samples were rinsed with approximately 500 mL of DI H₂O and then air dried. Air-dried samples were dried for about 16 h in a 45°C vacuum oven, and then stored in a desiccator.

Sodium Hypobromite

ACS reagent bromine (99.5%) was used to prepare the sodium hypobromite solution immediately before each use. This was accomplished by dispensing with volumetric pipettes 3 mL of bromine in 50 mL Deionized (DI) H₂O containing 5 g

NaOH. From this solution, 5, 10, and 15 mL were transferred with pipettes to 10 g of the 1%, 2%, and 3% periodate-treated samples, respectively, in 300 mL DI H₂O contained in a 500 mL beaker. Samples and reagent were mixed with a glass stirring rod. The three levels of hypobromite (5, 10, and 15 mL) also were mixed with untreated wood to serve as periodate controls. During the reaction period, pH levels of the mixtures periodically were checked with the meter and small amounts of 2 N NaOH added to maintain a pH range of 10–11. Reactions were carried out 24 h at room temperature. At the end of each reaction period, the mixture was filtered using vacuum and the filtrate set aside for analysis. Samples were then rinsed with a total of approximately 3 L of DI H₂O. The rinsed samples were then placed in approximately 700 mL of DI H₂O and allowed to soak for 24 h, to remove entrained hypobromite. After soaking, the filtered samples were rinsed with about 500 mL of DI H₂O and then air dried. Air-dried samples were dried for approximately 16 h in a 45°C vacuum oven, and then stored in a desiccator.

Analysis of Oxidants

Consumption of periodate and hypobromite at the end of the reaction period was determined titrimetrically.

Periodate Consumption

A 5-mL volume of the filtrate from the filtered reaction mixture was added to 10 mL of 0.5 N KI and 20 mL of 1 N HCl in a beaker with magnetic stirring bar. The I₂ formed was titrated with 0.2 N Na₂S₂O₃·5H₂O until the endpoint marked by disappearance of the I₂ was visualized by the addition of soluble starch. The following equations from Lange (1961) described the reactions involved in the analysis (except for the periodate cation being K): KIO₄ + 7KI + 8HCl = 8KCl + 4I₂ + 4H₂O, therefore I = KIO₄/8; I₂ + 2Na₂S₂O₃·5H₂O = 2NaI + Na₂S₄O₆, therefore Na₂S₂O₃·5H₂O = KIO₄/8. A similar titration of 5 mL of the starting concentration of periodate also was performed to calculate the change in oxidant concentration. The following calculation was used:

Percent change =

$$[(\text{end mL Na}_2\text{S}_2\text{O}_3 \cdot 5\text{H}_2\text{O} - \text{start mL Na}_2\text{S}_2\text{O}_3 \cdot 5\text{H}_2\text{O}) / \text{start mL Na}_2\text{S}_2\text{O}_3 \cdot 5\text{H}_2\text{O}] \times 100$$

Hypobromite Consumption

Change in hypobromite concentration was determined as its bromine equivalent by acidification of the solution to be analyzed. The filtrate from the filtered reaction mixture was added to 10 mL of 0.5 N KI and 20 mL 1 N HCl in a beaker with magnetic stirring bar. Concentrated HCl was added to the solution until pH was about 0.5 as measured with a pH probe. This shifted the equilibrium of the predominantly hypobromite species in solution to bromine, which readily oxidizes KI to I₂. The I₂ formed was titrated with 0.2 N Na₂S₂O₃·5H₂O as in the periodate analysis. The following equations from Lange (1961) described the reactions involved in this analysis: Br₂ + 2KI = 2KBr + I₂; I₂ + 2Na₂S₂O₃·5H₂O = 2NaI + Na₂S₄O₆, therefore I = Na₂S₂O₃·5H₂O and Br = Na₂S₂O₃·5H₂O.

When calculating the percentage change in oxidant at the end of the reaction, the starting concentration of oxidant in the reaction mixture needs to be determined. First, a determination of milliequivalents per milliliter (meq/mL) of Br in the Br₂ stock solution is accomplished using the above titration method and calculating Br (meq/mL) = mL Na₂S₂O₃·5H₂O × 0.2 N/mL Br₂ titrated. Then the starting concentration of oxidant in NaOBr is calculated: NaOBr (meq/mL) = mL Br₂ × meq mL⁻¹/mL NaOBr. A measured volume of the NaOBr is added to the reaction mixture (wood + H₂O) and starting oxidant concentration is NaOBr (meq/mL) = mL NaOBr added × meq mL⁻¹/reaction mixture volume (mL). With the starting concentration of oxidant in each reaction mixture known, the following calculation is used to determine the change in oxidant concentration: %change = [(end meq/mL – start meq mL⁻¹)/start meq/mL] × 100.

Weight Loss

The selectivities of treatments were compared by measuring recovered weights of the treated samples after each treatment and rinsing, air-drying, and drying in a vacuum oven for 16 h at 45°C. The percentage change in weight was calculated with the following formula:

$$\text{Percent change} = [(\text{end weight} - \text{start weight})/\text{start weight}] \times 100$$

Sodium Ion Exchange

Samples that were not subject to a treatment under alkaline conditions (untreated and periodate-treated only) were sodium ion exchanged before Cu²⁺ ion sorption testing to prevent pH decline during the test. Samples (2.5 g) were placed in 150-mL beakers containing approximately 71 mL of DI H₂O and 4 mL of 0.05 M NaOH. The samples were mixed with a glass stirring rod and adjusted to about pH 11. During the 24-h reaction period at room temperature, sample pH was checked occasionally, and the pH was maintained at 10–11 with small additions of 0.05 M NaOH. After the 24-h reaction, samples were rinsed, air dried, and vacuum oven dried for 4.5 h at 45°C and stored in a desiccator until sorption testing.

Copper Ion Sorption

The efficacy of each modifying treatment was evaluated by testing sorption capacities of unmodified and modified wood with copper ion solutions. Each treatment regime tested (including periodate, hypobromite controls, and untreated) was triplicated. The copper ion standard acquired was 1000 mg/L atomic absorption standard solutions consisting of copper nitrate in 1% nitric acid. Before using in the sorption experiments, the standard solution was diluted to 50 mg/L and pH was adjusted with sodium hydroxide to pH 4.6. Samples were tested for sorption capacities in 24-h equilibrium experiments.

Approximately 100 mg of sample with weight recorded was placed in a 60-mL screw cap bottle, and 50 mL of the diluted standard was added. Bottles were shaken for 24 h at 150 revolutions per minute at room temperature on an oscillator. Shaking was alternated in both clockwise and counter-clockwise directions. After the shaking period, pH of the sample was checked with a pH meter equipped with a double junction electrode. To ensure a particle-free sample for copper ion analysis, 10 mL of the liquid

from the sample bottle was removed with a syringe and filtered through a 0.45- μm nylon syringe filter. Filtered samples were then analyzed for copper ion (Cu^{2+}) concentration with an inductively coupled plasma–atomic emission spectrometer instrument. Equilibrium sorption capacities were calculated by the following formula:

$$q_e = V(C_0 - C_e)/M$$

where V is volume of Cu^{2+} ion solution (L), M is mass of sample (g), C_0 is starting concentration of Cu^{2+} ion solution (mg/L), and C_e is end concentration of Cu^{2+} ion solution with wood sample after 24 h (mg/L), and q_e is Cu^{2+} sorption (mg/g sample).

FTIR Spectroscopy

Carboxylate functional groups in the wood samples were characterized using an FTIR spectrometer equipped with a single reflection attenuated total reflection (ATR) accessory. The carboxylate carbonyl band absorbance (approximately 1600 cm^{-1} band) depicted was normalized against the approximately 1320 cm^{-1} band associated with the cellulose C–H bending mode.

RESULTS AND DISCUSSION

Oxidative Treatment Effects on q_e and FTIR Spectra

Table 1 shows the effects of the oxidative treatments with regard to oxidant consumption, wood sample weight loss, and Cu^{2+} ion sorption (q_e). For periodate treatments only, smaller (than with second oxidation step) increases in q_e were apparent with increasing concentration of oxidant (samples 1–7). These reactions are expected to result in mainly the formation of aldehyde end groups from the scission of adjacent hydroxyl groups in sugar molecules. Without the subsequent hypobromite oxidation step to a carboxylic acid/carboxylate, the end group lacks the ability to exchange a metal ion for H^+/Na^+ . The q_e increase from periodate-only treatment could be partially due to the polar nature of the newly created aldehyde carbonyls chelating Cu^{2+} ions (in contrast to ion exchange). However, FTIR scans of the 24-h periodate-treated samples (Fig. 2) indicated that the absorbance bands in the approximately 1600 cm^{-1} region corresponding to carboxylate follow a pattern of increase with periodate level (similar to the increases of q_e), as compared with the untreated sample; the 6-h spectra are not shown but are very similar to the 24-h spectra. This would seem to indicate that some of the aldehyde groups have undergone oxidation to carboxylate groups. It is known that some aldehydes present in carbohydrates are capable of being oxidized to carboxyls by air oxidation. In fact, the aldehyde group is one of the most easily oxidized groups in carbohydrates (Green 1957).

Table 1. Oxidative Treatments on Milled Southern Pine Wood

Sample	Treatment ^{a,b,c}	Change in oxidant (%)	Weight change after treatment (%)	q_e^d (mg Cu ²⁺ per g sample)	2 x std. dev. of q_e
1	Untreated			3.1	0.6
Single-stage treatments					
2	1% periodate for 6 h	-20.3	-2.9	3.8	0.3
3	2% periodate for 6 h	-19.8	-2.8	4.0	0.2
4	3% periodate for 6 h	-22.6	-3.3	4.2	0.9
5	1% periodate for 24 h	-29.2	-1.9	3.7	0.3
6	2% periodate for 24 h	-29.2	-2.6	4.2	0.2
7	3% periodate for 24 h	-18.1	-2.5	4.2	0.8
8	0.3% Br ₂ for 24 h	-45.8	-2.1	3.7	0.2
9	0.6% Br ₂ for 24 h	-25.9	-1.4	4.0	0.4
10	0.8% Br ₂ for 24 h	-22.9	-0.9	4.1	0.3
Two-stage treatments					
11	1% periodate for 6 h, 0.3% Br ₂ for 24 h	-20.3, -90.9	-2.9, -2.8 Total: -5.7	4.5	0.7
12	2% periodate for 6 h, 0.6% Br ₂ for 24 h	-19.8, -89.8	-2.8, -5.9 Total: -8.7	5.9	0.1
13	3% periodate for 6 h, 0.8% Br ₂ for 24 h	-22.6, -89.1	-3.3, -14.0 Total: -17.3	6.9	0.3
14	1% periodate for 24 h, 0.3% Br ₂ for 24 h	-29.2, -82.6	-1.9, -3.4 Total: -5.3	4.7	0.6
15	2% periodate for 24 h, 0.6% Br ₂ for 24 h	-29.2, -85.3	-2.6, -5.6 Total: -8.2	7.0	0.7
16	3% periodate for 24 h, 0.8% Br ₂ for 24 h	-18.1, -87.7	-2.5, -10.1 Total: -12.6	7.8	0.5

^a Oxidant percentage is w/v.

^b Percentage Br₂ as sodium hypobromite.

^c Untreated and single-stage periodate-treated samples Na⁺ exchanged.

^d q_e sorption values an average of three replicates.

Similar to periodate-only, the hypobromite-only treated samples exhibited increases to q_e (samples 1, 8–10) and the FTIR 1600 cm⁻¹ region, indicative of the formation of new carboxyl groups (Fig. 3). It is known that hypobromite is capable of oxidation of the polysaccharide primary and secondary hydroxyl groups directly to carboxyl groups; however, the yield is low (Green 1957).

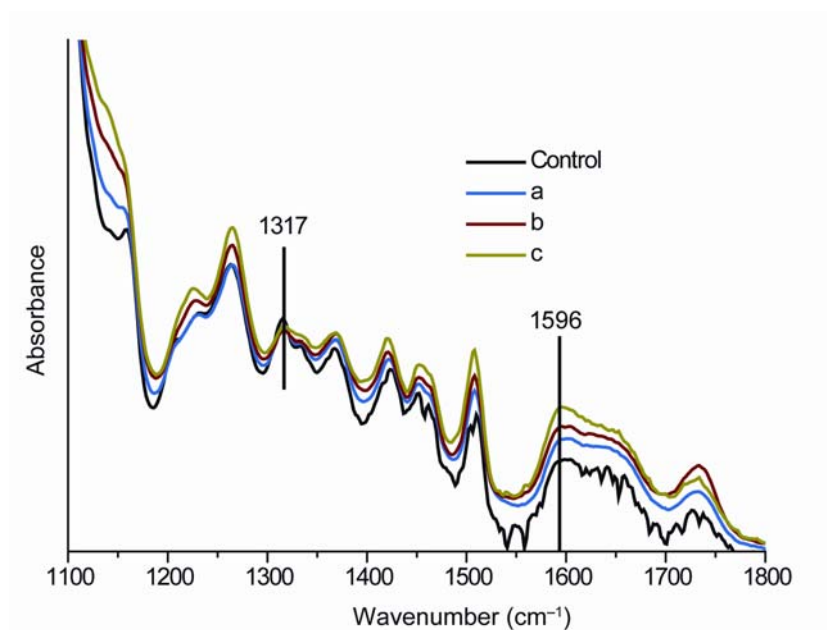


Fig. 2. FTIR scan of 24-h periodate-treated and Na-exchanged southern pine; Na⁺-exchanged untreated southern pine, showing carboxylate absorption region (1596 cm⁻¹). Baseline normalized at 1317 cm⁻¹. Control, untreated; a, 1% periodate for 24 h; b, 2% periodate for 24 h; c, 3% periodate for 24 h.

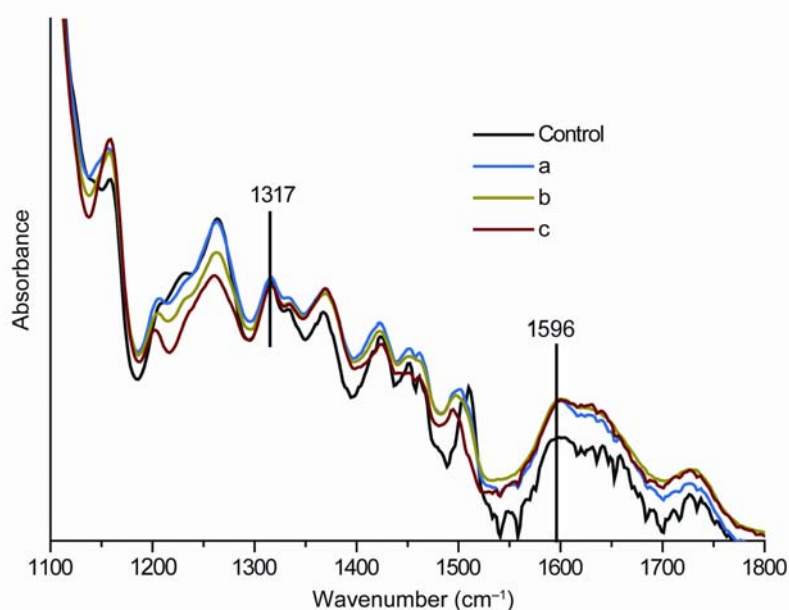


Fig. 3. FTIR scan of Br₂-treated (as sodium hypobromite) southern pine; Na⁺-exchanged untreated southern pine, showing carboxylate absorption region (1596 cm⁻¹). Baseline normalized at 1317 cm⁻¹. Control, untreated; a, 0.3% Br₂ for 24 h; b, 0.6% Br₂ for 24 h; c, 0.8% Br₂ for 24 h.

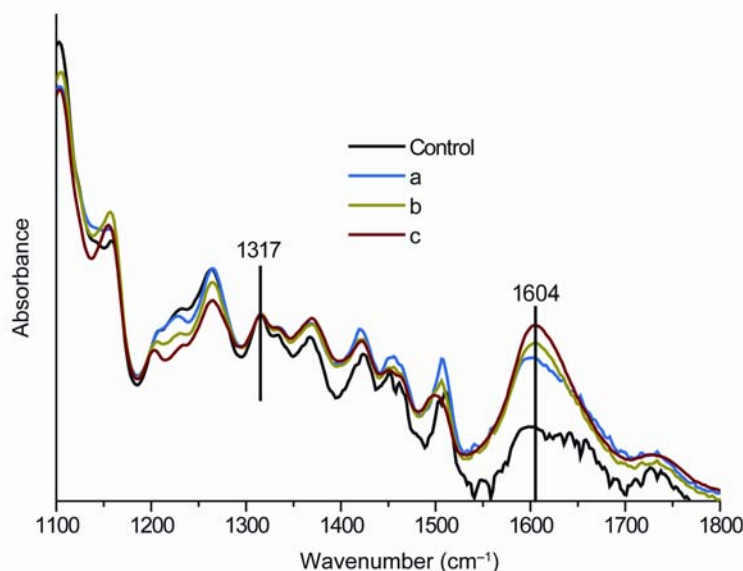


Fig. 4. FTIR scan of 6-h periodate-treated and Br₂-treated (as sodium hypobromite) southern pine; Na⁺-exchanged untreated southern pine, showing carboxylate absorption region (1604 cm⁻¹). Baseline normalized at 1317 cm⁻¹. Control, untreated; a, 1% periodate for 6 h, 0.3% Br₂ for 24 h; b, 2% periodate for 6 h, 0.6% Br₂ for 24 h; c, 3% periodate for 6 h, 0.8% Br₂ for 24 h.

The effect of a two-stage oxidative sequence (periodate and hypobromite) was apparent even at the lowest oxidant (1% periodate, 0.3% Br₂) level, and particularly at the two highest oxidant (2% and 3% periodate, 0.6% and 0.8% Br₂) levels. This effect is evident when viewing the q_e values (samples 1, 11–13) and the FTIR 1600 cm⁻¹ region absorbance (Fig. 4) for 6-h periodate treatment sequences, as compared with the periodate- or hypobromite-only treatments. The effect of time of the longer (24 h) periodate treatments is apparent (samples 1, 14–16; Fig. 5), yielding further increases to sorption values and the carboxylate functional groups of the modified wood. The FTIR scans for the 24-h periodate treatment sequence give perhaps the most sensitive indication of the differential effects of the three periodate levels used (1%, 2%, and 3%).

Weight Loss

The single-stage oxidation treatments had only minor weight losses of approximately 1% to 3% (samples 2–10). Weight losses began to increase noticeably after the second oxidative (hypobromite) stage, particularly at the 2% and 3% periodate levels. At these higher periodate levels, the shorter treatment time of 6 h did not appear to be a mitigating factor with respect to weight loss (samples 11–16; Figs. 6 and 7). However, the higher weight loss for sample 13 as compared to sample 16 seems anomalous and likely is an error. Clogging of the filter paper pores was a problem with sample 13 after the hypobromite stage, causing some sample loss. A switch in filter paper brand with sample 16 decreased the clogging problem.

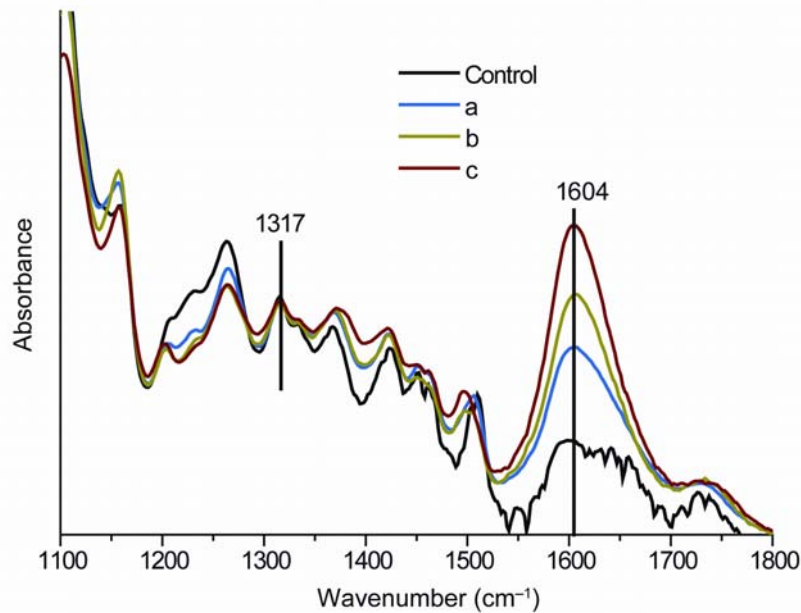


Fig. 5. FTIR scan of 24-h periodate-treated and Br₂-treated (as sodium hypobromite) southern pine; Na⁺-exchanged untreated southern pine, showing carboxylate absorption region (1604 cm⁻¹). Baseline normalized at 1317 cm⁻¹. Control, untreated; a, 1% periodate for 24 h, 0.3% Br₂ for 24 h; b, 2% periodate for 24 h, 0.6% Br₂ for 24 h; c, 3% periodate for 24 h, 0.8% Br₂ for 24 h.

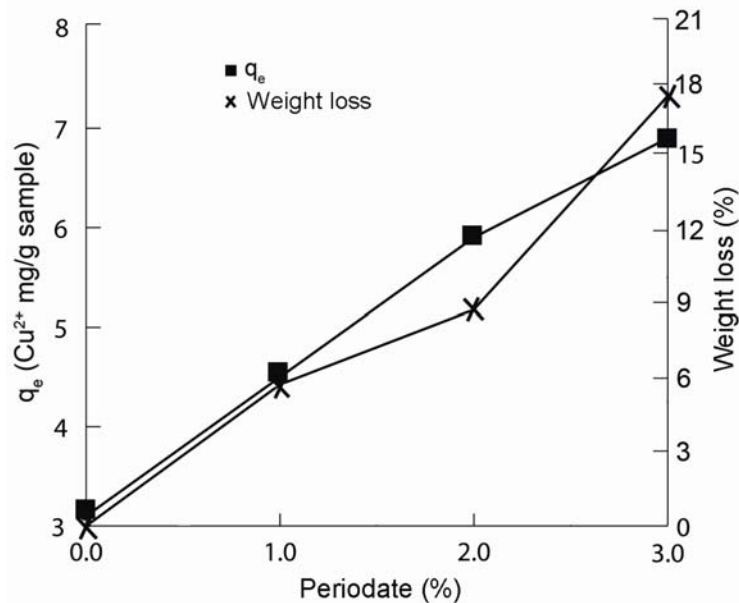


Fig. 6. Six-hour periodate and hypobromite treatments on southern pine wood showing effect of percentage periodate on Cu²⁺ sorption capacity and weight loss of sample. The point at 0% periodate and 0% weight loss is Na⁺-exchanged untreated wood.

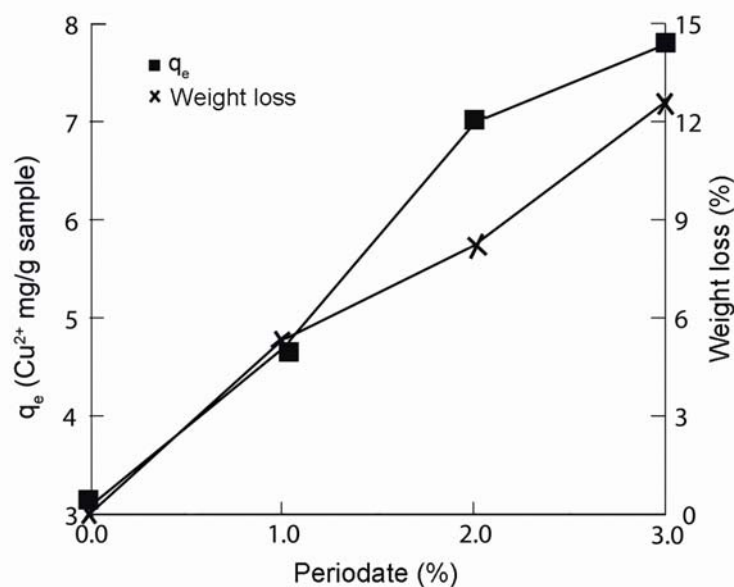


Fig. 7. Twenty-four-hour periodate and hypobromite treatments on southern pine wood showing effect of percentage periodate on Cu²⁺ sorption capacity and weight loss of sample. The point at 0% periodate and 0% weight loss is Na⁺-exchanged untreated wood.

It is reasonable to infer that these higher periodate levels began to show a loss of selectivity that has been described as “over-oxidation,” with cleavage of other types of carbohydrate bonds (Bobbitt 1956). This could occur when periodate levels are much greater than what is needed to react with just the available α -glycol groups. In Table 1, it can be seen that periodate consumed was only 20% to 30%, for either the 6- or 24-h reactions. It is interesting that the 2% and 3% periodate levels used in a single treatment stage did not result in similarly notable weight losses, as when combined with the second hypobromite stage. A possible explanation for this is that the alkaline pH conditions used in the hypobromite stage swell the fibers and allow washing out of the oxidative cleavage fragments. Because the weight loss was not observed in the hypobromite-only treatments (with alkaline pH), fragmentation must occur during the periodate stage.

Oxidation of lignin structures could be a minor contributor to weight loss of periodate-treated wood. However, we did not expect this reaction to be a major source of weight loss because periodate has been used to isolate lignin (retaining its polymeric structure) from the carbohydrate fraction of the wood. For example, Eisenbraun and Purves (1961) accomplished this by reacting a large quantity of sodium periodate (30% w/w) with spruce wood meal at pH 3.6 to 4.0 and then removing the carbohydrate fragments with a 0.1 N sodium hydroxide solution. This oxidation/extraction procedure was repeated four or five times.

It may be that a weight loss of more than 10% is a necessary trade off to produce a large number of new carboxyl groups from the modified wood. However, it may be

possible to attain higher yields of carboxyl groups while avoiding the effects of over-oxidation by increasing the reaction time at room temperature, while keeping the levels of periodate used less than 2%.

Another potential improvement in efficiency might be found by utilizing the solubilized oxidative fragments lost to the water rinse after treatment that may also contain some carboxyl groups. This might be done by treating the reaction mixture after each oxidation stage with a reducing compound to quench the excess oxidant; the excess base in the hypobromite stage could then be neutralized with acid. Finally, the excess water would need to be evaporated from the mixture.

An added benefit from recovery of the fragments is a reduction of organic compounds in waste water. This step reduces oxygen-consuming materials before they are added to the environment.

An alternative method to contain the filtration media would need to be used to avoid the loss of the smaller fragments when the modified materials are contained in a porous envelope or filter apparatus. This laboratory is currently testing a method to address the loss of fine media and avoid clogging of the filter apparatus by employing an extruder to make the wood or bark media into pellets. Very fine materials and those that are easily lost when contained within a porous envelope or filter mat can be utilized with this method.

CONCLUSIONS

1. Wood carbohydrates can be modified with room-temperature sequential oxidative treatments utilizing sodium periodate to convert α -glycol groups to dialdehydes, and sodium hypobromite to convert the dialdehydes to carboxylates, thereby substantially increasing the wood's Cu^{2+} ion sorption capacity and improving its utility as a heavy metal filter material.
2. The highest experimental treatment level of periodate (3% w/v followed by 0.8% Br_2 w/v as sodium hypobromite) increased the wood's Cu^{2+} ion sorption capacity by 148% and also resulted in a 12.6% weight loss from the water washing loss of soluble fragments.
3. To realize the full benefit of the selective nature of periodate oxidation, the level of periodate used may need to be adjusted close to a stoichiometric quantity for the number of glycol groups reacted.

REFERENCES CITED

- Bobbitt, J. M. (1956). "Periodate oxidation of carbohydrates," In: M. L. Wolfram (ed.), *Advances in Carbohydrate Chemistry, 11*. Academic Press, Inc., New York, pp. 1-41.
- Chen, G. C., and Rowell, R. M. (1989). "Fungal and termite resistance of wood reacted with periodic acid or sodium periodate," *Wood Fiber Sci.* 21, 163-168.
- Eisenbraun, E., and Purves, B. (1961). "Condensation of spruce periodate lignin with formaldehyde," *Can. J. Chem.* 39, 1518-1529.

- Fleury, P. F., and Lange, J. (1932). "The oxidation of acid alcohols and sugars by periodic acid," *Comptes Rendus*. 195, 1395-1397.
- Green, J. W. (1957). "Acids and oxidation products," In: Pigman, W. (ed.), *The Carbohydrates. Chemistry, Biochemistry, Physiology*. Academic Press, Inc., New York, pp. 299-366.
- Guthrie, R. D. (1961). "The 'dialdehydes' from the periodate oxidation of carbohydrates," In: Wolfrom, M. L. (ed.), *Advances in Carbohydrate Chemistry*, 16. Academic Press, Inc., New York and London, pp. 105-158.
- Lange, N.A. (ed.) (1961). *Handbook of Chemistry*, 10th edn. McGraw-Hill Book Company, Inc., New York, Toronto, London. 1969 pp.
- Maekawa, E., and Koshijima, T. (1984). "Properties of 2,3-dicarboxy cellulose combined with various metallic ions," *J. Appl. Polymer Sci.* 29, 2289-2297.
- Malaprade, L. (1928a). "Oxidation of some polyalcohols by periodic acid—applications," *Comptes Rendus*. 186, 382-384.
- Malaprade, L. (1928b). "Action of polyalcohols on periodic acid. Analytical application," *Bulletin de la Societe Chimique de France* 43, 683-696.
- Martin-Dupont, F., Gloaguen, V., Granet, R., Guilloton, M., and Krausz, P. (2004). "Chemical modifications of Douglas fir bark, a lignocellulosic by-product—enhancement of their lead (II) binding capacities." *Separation Sci. Technol.* 39(7), 1595-1610.

Article submitted: Nov. 9, 2007; Peer-review completed: Jan. 17, 2008; Revised version accepted: Jan. 27, 2008; Published: Jan. 31, 2008.

HUMIC ACID-LIKE MATTER ISOLATED FROM GREEN URBAN WASTES. PART II: PERFORMANCE IN CHEMICAL AND ENVIRONMENTAL TECHNOLOGIES

Enzo Montoneri,^{1*} Piero Savarino,¹ Stefano Bottigliengo,¹ Giorgia Musso,¹ Vittorio Boffa,¹ Alessandra Bianco Prevot,² Debora Fabbri,² and Edmondo Pramauro²

Novel uses of the organic fraction of municipal solid wastes for diversified technological applications are reported. A humic acid-like substance (cHAL2) isolated from green urban wastes was tested as a chemical auxiliary for fabric cleaning and dyeing, and as a catalyst for the photodegradation of dyes. The results illustrate the fact that biomass wastes can be an interesting source of products for the chemical market. Process and product development in this direction are likely to offer high economic and environmental benefits in a modern, more sustainable waste treatment strategy.

Keywords: Urban refuses; Compost; Biosurfactants; Detergents; Textile dyeing aids, Humic acids, Biomass; Biophotosensitizer; Photodegradation

Contact information: ¹Dipartimento di Chimica Generale ed Organica Applicata, Università di Torino, C. M. D'Azeglio 48, 10125 Torino, Italy; ²Dipartimento di Chimica Analitica, Università di Torino, Via Pietro Giuria 5, 10125 Torino, Italy; *Corresponding author: enzo.montoneri@unito.it

INTRODUCTION

Very recently we have shown that compost is a rich source of humic-like substances with excellent surfactant properties, and suggested for these materials a range of potential applications in the chemical industry (Quagliotto et al. 2006). This work focused primarily on upgrading biomass wastes in chemical technology (Savarino et al. 2007). To this purpose we plan in the long range to isolate from biomass wastes and to establish structure-properties relationships for products to be recycled to the market as chemical auxiliaries. Such results seem achievable by building a data inventory, which at some point will make it possible to understand how the parameters characterizing the waste nature and the composting process influenced the structure and chemical properties of the isolated humic-like substances, and also to assess how much the source and the structural differences of these substances affected their performance in the proposed chemical technologies.

In this context, our previous papers (Quagliotto et al. 2006; Savarino et al. 2007) have reported the chemical structure, surfactant properties and performance in textile dyeing of a humic acid-like compound (cHAL) isolated from a mix of municipal solid and green wastes mix composted for 15 days. We wish now to report on a new humic acid-like compound (cHAL2), which was isolated from a different source and under different conditions: i.e., from green urban wastes and before composting. The isolated cHAL2 material, compared to cHAL, has shown some significant differences in chemical

structure and surfactant properties which have been reported in Part I of this work (Montoneri et al. 2008): i.e., relative to cHAL, cHAL2 has a higher content of aliphatic and of O-alkyl C atoms relative to aromatic, phenoxy and carboxy C atoms; also, the values for the critical micellar concentration ($CMC = 0.97 \text{ g L}^{-1}$) and surface tension at the CMC ($\gamma = 37.8 \text{ mN/m}$) of cHAL2 were higher than those for cHAL ($CMC = 0.40 \text{ g L}^{-1}$ and $\gamma = 36.1 \text{ mN/m}$). Also cHAL, compared to the two major synthetic commercial surfactants sodium dodecylsulfate (SDS) and sodium dodecylbenzenesulfonate (SDBS), was found to have quite remarkable surfactant properties (Quagliotto et al. 2006) and to perform as a chemical auxiliary for dyeing nylon 6 (Savarino et al. 2007) as well and more conveniently, we wish now to report on how the new cHAL2 biosurfactant compares with SDBS and SDS for its technological performance. For this purpose, three potential applications for these materials have been chosen as ground for comparison. The range of potential applications of surfactants, however, is very wide and multidisciplinary (Research and Markets 2007; Houston 2007). We are also aware that high tech specialized knowledge is required nowadays for the development of new products from laboratory to commercial scale. We wish therefore to stress that the case studies chosen in this work are not meant as problems to be solved, but rather as grounds for assessing the value of the cHAL2 biosurfactant relative to major commercially synthetic surfactants. Our specific aims in this work were two. Firstly, we wished to demonstrate that cHAL2 might perform as well as or better than the established commercial surfactants under the same experimental conditions. Secondly, we wished to stimulate specialists in diversified technological applications to joint our efforts for assessing which level the organic fraction of municipal solid wastes could be a real alternative to synthetic commercial chemical auxiliaries and for developing new processes and products from renewable sources.

EXPERIMENTAL

The humic acid-like material (cHAL2) investigated in this work was isolated from ground urban green wastes, collected from the Amiat municipal plant in Torino, Italy. The wastes were treated 24 h at $65 \text{ }^\circ\text{C}$ under N_2 with aqueous $0.1 \text{ mol}\cdot\text{L}^{-1}$ NaOH and $0.1 \text{ mol}\cdot\text{L}^{-1}$ $\text{Na}_4\text{P}_2\text{O}_7$ at 1:50 w/v compost/solution ratio. The resulting suspension was cooled to room temperature and centrifuged at 6000 rpm for 20 minutes. The supernatant solution was separated. The solid residue was washed repeatedly with distilled water until the supernatant liquid phase was clear. All collected liquid fractions were mixed and acidified with 50 % sulfuric acid to $\text{pH} < 1.5$. The precipitated cHAL2 fraction was separated by centrifugation as above, washed with water until the final washing had neutral pH, vacuum dried at $60 \text{ }^\circ\text{C}$, and weighed. The extraction yield for the final product was 12 % of compost dry matter. This material was found to contain 7.47 % water, 91.60 % volatile solids, and 0.93 % ash by the weight losses measured after heating first at 105 and then at $800 \text{ }^\circ\text{C}$. Further characterization for cHAL2 was performed by elemental analysis, solid state ^{13}C and solution ^1H NMR spectroscopy, IR spectroscopy, molecular weight, and surface tension measurements. Analytical and instrumental details, as well as the results of these measurements, are reported in the

preceding Part I of this work (Montoneri et al. 2008). Textile dyeing (Savarino et al. 1999 and 2007), and fabric washing tests (EMPA 2006) were performed under the same experimental conditions reported in the cited references, unless otherwise indicated. For the dyeing tests the disperse dye, here called dye 1, was prepared as previously reported (Carpignano 1985). The dyeing bath had liquid to solid ratio (V/w) 5, pH 7 by 0.1 M tris buffer, and 1% dye related to the fiber weight. Dye dispersion was helped by bath sonication, using a Vibra-cell 120 W apparatus at 1.5-5 W for 10-15 min. Our indicators of dyeing efficiency were the color intensity (ΔE) and the color uniformity ($\sigma\Delta E$), which were determined by tristimulus colorimetry, using a Minolta CR200 instrument (Savarino et al. 1999). The ΔE parameter is the mean of five determinations of the color difference between the dyed and undyed fabric performed over five different sites comprised in a 2.5 cm² specimen area, while $\sigma\Delta E$ is the standard deviation around the mean ΔE value. Provided that each specimen had 10 x 10 cm² size, in most cases duplicate ΔE and $\sigma\Delta E$ values for the same specimen were obtained by repeating the set of five determinations on a different 2.5 cm² specimen area.

Similarly, the textile washing efficiency was evaluated according to published guidelines (EMPA 2006) on standard fabric EMPA 106 soiled with carbon black/mineral oil, which was purchased from Ausiliari Tessili Srl, Cornaredo, Mi. For our detergency tests, 10 x 10 cm (1.9-2.0 g) samples were cut and treated with 20 ml surfactant solution containing Na₂CO₃ at 2 g/L concentration in a tumble container at 90 °C for 20 min. Afterwards, the sample was withdrawn from the bath containing the surfactant solution, immersed in 100 ml deionized water at 30 °C for 20 min, withdrawn, and allowed to dry at room temperature. The washing efficiency was determined by measuring the ΔE parameter as above. In this case ΔE is the mean of eight measurements of the color difference between the standard soiled sample and the washed sample, which were performed across both faces of the specimen.

Dye photodegradation tests were performed by irradiating for three hours 5 mL aqueous solution of a sulfonated azodye (ethylorange, 5 mg L⁻¹) in a closed Pyrex[®] cell with a Xenon (1500W) lamp and a cut-off filter for wavelengths below 340 nm. The analysis of the ethylorange residue in solution after irradiation was done by HPLC, carried out according to a previously reported procedure (Bianco Prevot et al. 2004). Dye degradation kinetics was then studied in a cylindrical photochemical reactor (Helios-Italquartz, Milan), equipped with a 125 W medium pressure Hg lamp, under aerobic conditions by irradiating 500 mL of aqueous solutions containing 5-50 mgL⁻¹ of ethylorange and various amounts of cHAL2 in order to increase the cHAL2/EO ratio in the 0-200 w/w range. The system was kept under continuous stirring in order to avoid the formation of a concentration gradient, and air was bubbled to maintain the oxygen supply. Cold water circulating in the jacket surrounding the lamp kept the temperature within the reactor at 20°C; a Pyrex[®] glass jacket acting as a cut-off filter for wavelengths below 300 nm was employed, in order to avoid any possible contribution coming from direct dye photolysis.

RESULTS AND DISCUSSION

Our previous work (Quagliotto et al. 2006; Savarino et al. 2007; Montoneri et al. 2007) has indicated that the potential of humic acid-like substances isolated from compost to be recycled to the chemical market is connected to their surfactant properties. To rate these substances for their potential economic impact on the waste management industry, one should consider the current surfactant market. Recent estimates (Houston 2007) report a relatively large market size for performance surfactants (over 360,000 metric tons, worth € 738 million in Europe). These types of chemicals remain the formulators' best tool to fine tune and achieve special performance to differentiate new products. As industrial competition and environmental concern increase, performance surfactants must satisfy a number of requirements, such as high technology performance, low environmental impact, and low cost. Surfactants have a wide range of functional applications in which they can be used, and therefore are consumed in a number of end-user markets (Research and Markets 2007). Most of the surfactants are used up to make up detergents (Showell 2006). SDBS is the work-horse of this industry, and this justifies our approach to use it as reference material to evaluate the performance of our cHAL2 biosurfactant. Textile dyeing is another important application for surfactants, whose yearly global consumption in this industry is over 2×10^9 U.S. \$. The discovery that humic acid-like substances, in addition to their surfactants properties, could also catalyze the photodegradation of organic chemicals (Amine-Khodja 2006), prompted us to study also their effect on the photodegradation of dyes, as this seemed a very attracting perspective in connection with their application as chemical auxiliaries enhancing dyeing quality. We therefore chose the above three field of application for rating the technological potential of our cHAL2 compound, i.e., in fabric cleaning, fabric dyeing, and dye photodegradation.

Performance in Textile Dyeing

Rayon acetate (RA) fiber and the water insoluble dye 1 represented in Fig. 1 are a typical dyeing system (Savarino et al. 1995; Wang and Zhu 2006).

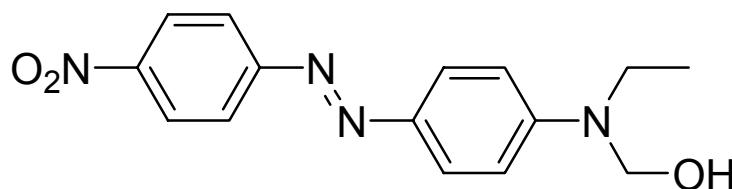


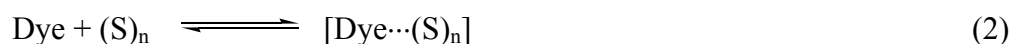
Fig. 1. Disperse dye 1.

Uptake of dyes having poor water solubility by the RA fiber may occur by hydrophobic and/or polar interaction between the fabric and the dye. However, the main problem is the dye solubility. Poor water solubility of the dye causes non-homogenous distribution of the dye throughout the fabric solid phase and the accumulation of the dye preferably on the fibre surfaces. Enhanced dye water solubility is achieved by addition of surfactants. These compounds are expected to perform based on the capacity of their

molecules (S) to aggregate and yield micelles in solution (Rosen 1989; Quagliotto et al. 2006):



Under this circumstance, diffusion of the dye into the surfactant's micellar core and formation of a complex by hydrophobic and /or polar interactions may occur:



The complexation equilibrium in reaction 2 would enhance the dye solubility in the dyeing bath, control the rate of release of the free dye concentration in solution, and, in turn, control the rate and yield of the dye uptake by the fiber.

Table 1. Color Intensity (ΔE)^a and Uniformity ($\sigma\Delta E$)^a of Rayon Acetate Fiber Dyed by the Disperse Dye 1 in the Presence cHAL2 at Variable Concentration (C, g·L⁻¹) under Bath Sonication at 4 W for 15 min.

C ^a	ΔE_1	$\sigma\Delta E_1$	ΔE_2	$\sigma\Delta E_2$	σ_{pool} ^b	d.f. ^c	ΔE_{avg} ^d
0.00	84.8	1.72	76.3	11.75			
0.28	81.8	6.85	81.7	6.93	6.89 c	8	81.7 a
0.45	85.9	0.41	83.9	1.70			
0.60	85.4	0.40	79.8	10.82			
0.60	85.8	0.65	83.0	4.19			
0.75	85.6	0.21	83.4	2.33			
0.90	84.8	0.35	84.2	0.44	0.40 a	8	84.5 a
1.20	85.3	0.30	83.0	2.58			
1.20	85.2	0.88	84.5	0.93			
1.50	84.3	2.56	83.0	2.53	2.54 b	8	83.7 a
2.00	86.0	0.27			0.33 a	12	86.0 b
2.00	86.1	0.37	86.1	0.35			

^aDuplicate values reported in the same line pertain to the same specimen (see experimental); results reported for the same C value, but in different lines, pertain to different specimen dyed at different time under the same conditions.

^bPooled standard deviation calculated from individual $\sigma\Delta E$ values for samples at the same C value, provided that the individual $\sigma\Delta E$ values were not statistically different by F test at 95 % confidence level (Natrella 1966); letters next to figures indicate variance inequalities by F test at 95 % confidence level: i.e., a < b < c.

^cDegrees of freedom of $\sigma(\text{pool})$.

^dAverage color intensity (ΔE_{avg}) calculated from individual ΔE values for samples at the same C value whose $\sigma\Delta E$ values were not significantly different by F test at 95 % confidence level; letters next to figures indicate ΔE_{avg} inequalities at 95 % confidence level (Natrella 1966): i.e., a < b.

Surfactants can also perform in textile dyeing for their dispersing power, which helps to achieve uniform and better dye penetration into the fiber. Dispersants do not necessarily need to micellize to achieve the desired performance. Polymers comprising carboxyl groups are well known to assist in particle suspension. Our chemical character-

ization of cHAL2 reported in Part I of this work (Montoneri et al. 2007) has shown that this humic acid-like substance consists of both small molecules with 400-450 Da molecular weight that can micellize, as well as macromolecules with 10^5 Da molecular weight. The latter ones by virtue of the flexibility of the C chain length may fold and coil to yield pseudo-micelles (von Wandruszka 2000), which have hydrophobic cavities to host small molecules and thus enhance their solubility.

Table 2. Color Intensity (ΔE)^a and Uniformity ($\sigma\Delta E$)^a of Rayon Acetate Fiber Dyed by the Disperse Dye 1 at 80 °C, 1 h Dyeing Time and 5 V/w Liquor/Solid Ratio in the Presence of cHAL2, SDS, and SDBS at 1-2 g L⁻¹ Surfactant Concentration (C) under Bath Sonication at 1.5 W for 10 min.

Surfactant	C ^a (g L ⁻¹)	ΔE_1	$\sigma\Delta E_1$	ΔE_2	$\sigma\Delta E_2$	σ_{pool} ^b	d.f. ^c	ΔE_{avg} ^d
none		74.9	13.61					
none		81.8	1.63					
SDBS	1.0	85.6	0.30	84.7	0.47	0.39 a	8	85.1a
SDBS	2.0	86.1	0.30	85.6	0.36	0.39 a	24	85.7c
SDBS	2.0	86.0	0.34	85.3	0.38			
SDBS	2.0	86.1	0.43	85.4	0.52			
SDS	1.0	84.4	1.28	84.1	1.50	1.39 b	8	84.3a
SDS	2.0	85.4	0.54	85.2	0.37	0.44 a	16	85.4b
SDS	2.0	85.7	0.45	85.2	0.37			
cHAL2	1.0	83.7	3.11	83.4	2.65	2.89 b	8	83.6 a
cHAL2	2.0	85.4	0.47	84.7	0.38	0.49 a	12	85.1a,b
cHAL2	2.0	85.1	0.59					

^aDuplicate values reported in the same line pertain to the same specimen (see experimental); results for one surfactant reported at the same C value, but in different lines, pertain to different specimen dyed at different time under the same conditions.

^bPooled standard deviation calculated from individual $\sigma\Delta E$ values for samples containing the same surfactant at the same C value, provided that the individual $\sigma\Delta E$ values were not statistically different by F test at 95 % confidence level (Natrella 1966); letters next to figures indicate variance inequalities by F test at 95 % confidence level: i.e., a < b

^cDegrees of freedom of σ (pool).

^dAverage color intensity. (ΔE_{avg}) calculated from individual ΔE values for samples containing the same surfactant at the same C value whose $\sigma\Delta E$ values were not significantly different by F test at 95 % confidence level; letters next to figures indicate ΔE_{avg} inequalities at 95 % confidence level (Natrella 1966): i.e., a < b < c.

In order to rate the performance of cHAL2 as a chemical auxiliary in textile dyeing, we have used the same approach that was previously reported for cHAL (Quagliotto et al. 2006). We therefore ran dyeing tests under the same conditions in the absence of additives and in the presence of each one of the following three additives used separately: i.e, cHAL2 and the two widely used commercial synthetic surfactants SDS and SDBS. The dyeing efficiency was rated by the measured values of the fabric color indicators defined in the experimental section: i.e., the color intensity (ΔE) and the color uniformity ($\sigma\Delta E$) parameters. As our previous work with cHAL, SDS, and SDBS (Quagliotto et al. 2006) in dyeing nylon 6 had indicated that for best performance the

additive concentration in the dyeing bath had to be above its CMC value, and that the order of surfactants performance seemed to follow the surfactant capability to micellize, we first wanted to confirm that this was true also for cHAL2. Thus, the dyeing efficiency against the cHAL2 concentration in the dyeing bath was first studied, and the data in Table 1 were collected. Afterwards, we obtained the data in Table 2, which compare cHAL2 and the other two synthetic surfactants at the concentration that was indicated best for cHAL2 by the results reported in Table 1.

Our data elaboration and interpretation was accomplished based on the following criteria. Provided that each specimen had $10 \times 10 \text{ cm}^2$ size, and that each ΔE value shown in Tables 1 and 2 is the average of five determinations taken across a randomly chosen 2.5 cm^2 specimen area, we ranked dyeing quality first by the equality, established via T and F tests at 95 % confidence level, between ΔE values, and between $\sigma\Delta E$ values respectively resulting from measurements performed across one specimen and/or over more than one specimen dyed under the same conditions. Secondly, we compared by the same T and F tests samples dyed at different additive concentration that passed the above ΔE and $\sigma\Delta E$ equality test. Samples not passing the variance equality tests were ranked last. For the samples passing the variance equality test, the pooled standard deviation values (σ_{pool}) were calculated, and the samples were ranked based on 95 % confidence level F test run over σ_{pool} values and on the average color intensity values (ΔE_{avg}) taken over measurements across one same specimen and/or different specimen dyed under the same conditions. The statistical ranking order of σ_{pool} and ΔE_{avg} values is indicated in Table 1 by the letters next to each numerical value. Based on these criteria, the data in Table 1 show that in the absence of cHAL2 the product quality was rather bad: i.e., large differences of color homogeneity and intensity across the specimen. This situation somehow improved already in the presence of low concentration of cHAL2 (0.28 g L^{-1}), but the best product quality seemed achievable at cHAL2 concentration above 1.5 g L^{-1} . The comparison of σ_{pool} values shows that, although at 0.9 g L^{-1} cHAL2 concentration a satisfactory color homogeneity across one specimen may result, the best product quality was attained at 2 g L^{-1} cHAL2 concentration for the following reasons. The samples dyed in the presence of 2 g L^{-1} cHAL2, compared to all other samples, showed no differences in color homogeneity and intensity both across the single specimen and between different specimens dyed under the same conditions. As indicated from the statistical comparison and rating of the reported σ_{pool} and ΔE_{avg} values, these specimens also exhibited the best values for the color indicators across the whole additive concentration range: i.e., lowest σ_{pool} value = 0.33 and highest average color intensity value (ΔE_{avg}) = 86.0. The results in Table 2 confirm the bad dyeing efficiency in the absence of surfactants by the wide color difference of both the dyeing indicators between the two specimens dyed with no added surfactant, and evidence also the better performance of cHAL2 at 2 g L^{-1} concentration than at 1 g L^{-1} . The former concentration value corresponds to nearly twice the surfactant CMC value and seems consistent with equilibrium 2 being shifted to the right upon increasing the number of the surfactant micelles in solution, and therefore with increasing the dye solubility in the dyeing bath. The statistical comparison of the σ_{pool} values for the three surfactants in Table 2 also suggests that at 2 g L^{-1} surfactant concentration no significant difference in color uniformity can be assessed between cHAL2 and the other two synthetic surfactants, although the color intensity at this surfactant concentration

seems slightly higher in the presence of SDBS ($\Delta E_{\text{avg}} = 85.7$) than in the presence of cHAL2 and SDS ($\Delta E_{\text{avg}} = 85.1-85.4$).

One last worthwhile comment on the performance of the above surfactants in textile dyeing pertains to the lowest additive concentration to achieve the best dyeing efficiency (C_{min}). Table 3 reports C_{min} values obtained in this work and in previous work next to the values obtained for the surfactant's CMC and for the measured color indicators in dyeing with two different fabric/dye systems. These data show that while the color intensity depended on the nature of the fabric/dye system, the color homogeneity indicator ($\sigma\Delta E$) was not significantly affected by the nature of the fabric and of the dye. For our scope, therefore, the results for C_{min} in Table 3 were defined as the lowest surfactant concentration that makes it possible to achieve the $0.28 \leq \sigma\Delta E \leq 0.44$ range of values. One may then readily observe that, while for both cHAL2 and SDS, C_{min} was definitely above 1 g L^{-1} , for SDBS C_{min} was not higher than 1 g L^{-1} . The SDS and SDBS C_{min} values found in this work for dyeing rayon acetate with dye 1 were similar to those previously reported (Quagliotto et al. 2006) for dyeing nylon 6 with the water insoluble dye 2. In the latter system we used, however, a humic acid-like surfactant (cHAL) with a rather low CMC value, and this exhibited accordingly a very low C_{min} (0.4 g L^{-1}), which corresponded to the CMC value. All together the data in Table 3 confirm that in dyeing with the two water insoluble azo-dyes 1 and 2, the surfactant C_{min} value to be used must be equal to or above the surfactant CMC value. Thus, although some contribution from cHAL2 macromolecules to the additive performance in assisting the fiber dyeing may not be excluded, a large part of the positive effect on the dyed product quality is apparently to be ascribed to the capacity of the additive low molecular weight components to micellize.

Table 3. Surfactants CMC and Minimum Surfactant Concentration (C_{min}) to Achieve Best Dyeing Efficiency (as measured by the ΔE and $\sigma\Delta E$ indicators defined in the experimental part) with Different Water Insoluble Dyes and Textile Fabrics at pH 7.

Surfactant	CMC (g L^{-1})	C_{min} (g L^{-1})	Textile Fabric/Dye	$\sigma\Delta E$	ΔE	d.f. ^b
cHAL	0.40	0.40	nylon 6/dye 2 ^a	0.28	46.5	8
cHAL2	0.97	2.00	rayon acetate/dye 1	0.42 ^c	85.6 ^d	24
SDBS	0.70-1.40	1.00	nylon 6/dye 2 ^a	0.39	47.7	8
SDBS	0.70-1.40	1.00	rayon acetate/dye 1	0.39	85.1	8
SDS	2.33	2.36	nylon 6/dye 2 ^a	0.32	49.0	8
SDS	2.33	2.00	rayon acetate/dye 1	0.44	85.4	16

^aData from previous work (Savarino et al. 2007); dye 2 as in Fig. 2.

^bDegrees of freedom of $\sigma\Delta E$ and ΔE .

^cPooled standard deviation calculated from individual $\sigma\Delta E$ values in Tables 1 and 2 for samples containing cHAL2 at 2 g L^{-1} concentration.

^dAverage value calculated from individual ΔE values in Tables 1 and 2 for samples containing cHAL2 at 2 g L^{-1} concentration.

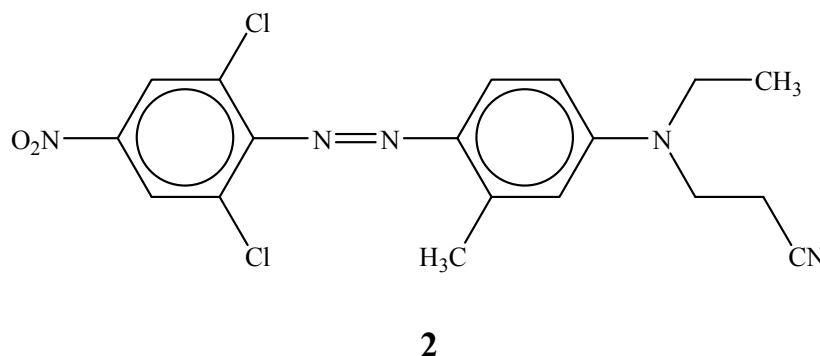


Fig. 2. Disperse dye 2.

Performance as Photosensitizer Agent.

In the textile industry more than three thousand dyes are used, and it is estimated that about 15% of the world dyes production is lost in the environment during the dyeing process (Zollinger 1991; Robinson et al. 2001). The environmental impact of dyes is not only related to their color, but also to their reduction producing carcinogenic aromatic amines (Gottlieb 2003). For these reasons they have to be efficiently removed from either industrial wastes or polluted natural water streams. Classical treatments such as physico-chemical, oxidative or, most commonly, active sludge biochemical processes have as a main drawback the production of secondary pollution due to the introduction of chemicals and/or to the possible accumulation of other bio-resistant species in the environment. As a possible innovative approach the use of advanced oxidation techniques has been proposed (Palmisano 2000), among which heterogeneous photocatalysis in the presence of TiO_2 suspensions has been shown to be convenient, since it works at ambient condition and uses a cheap and safe catalyst, atmospheric oxygen and solar (or simulated) light (Bahnmann 2004). Many papers have been published concerning the TiO_2 mediated degradation of azodyes in aqueous solutions (Konstantinou 2004). In this process, photosensitization (Kamat 1993) of the dye occurs upon excitation by visible light followed by electron transfer from the excited dye to TiO_2 , and reaction with water and dissolved oxygen to form highly reactive hydroxyl, superoxide, and perhydroxyl radicals. These species can then react with the cationic dye radical and lead to a complete mineralization of the organic substrate. It has been reported that also aquatic humic substances can undergo light excitation processes, which are able to produce reactive oxygenated species influencing the chemistry of dissolved organic compounds in natural waters (Hoigné et al. 1989; Canonica et al. 1995; Sakkas et al. 2002). Most recently, two papers have reported on the photosensitizing properties of humic-like substances (HLS) isolated from mixtures of yard trimmings, sewage sludge, and/or animal manure and grapes residues, which were collected after composting for 0-130 days. From the composted mixes, the humic-like substances were obtained either by simple water extraction (Amine-Khodja et al. 2006a) or by alkaline extraction followed by precipitation at acid pH (Amine-Khodja et al. 2006b). These substances have been found to enhance the photodegradation of organic pollutants in solar light, and their photodegrading activity has been found to increase between 0 and 70 days of composting and to remain quite constant between 70 and 130 days.

Provided that the ability of compost HLS to degrade organic pollutants under light excitation is of great importance from the environmental point of view, in connection to our research on compost isolated humic acid-like compounds, the above published results were particularly intriguing. Indeed, to qualify the potential of compost as source of chemicals for the industry, it was rather important to find out if cHAL2, in addition to enhancing the dyed product quality (as reported above), had potential for facilitating the disposal of the exhaust dye bath. We tested the performance of cHAL2 as a photosensitizer on ethylorange (EO) as the probe molecule. This azo-dye was chosen as a first model test dye because its high water solubility made it possible to use a relatively simple experimental procedure for our preliminary exploratory investigation. Figure 3 reports the dye percentage of degradation, calculated from the decrease of the starting EO concentration, as a function of the initial cHAL2/EO w/w ratio upon irradiation of each solution for three hours.

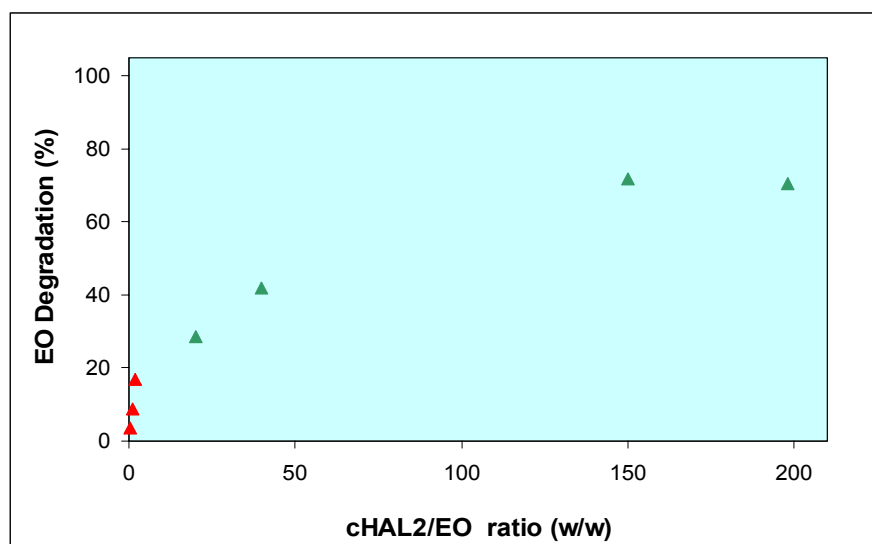


Fig. 3. Ethylorange (EO) degradation rate as a function of starting cHAL2/EO ratio in solution.

In these samples, the EO concentration was 50 mg L^{-1} for the cHAL2/EO w/w ratio below 10, and 5 mg L^{-1} for the cHAL2/EO w/w ratio ≥ 20 . A continuous increase of the degradation efficiency was observable up to a constant value of about 75 %, which was reached at ca. 150 cHAL2/EO w/w ratio where the cHAL2 concentration (0.75 g L^{-1}) approached its CMC value. These results offer scope for further investigation of humic acid-like substances isolated from different source wastes to use for the treatment of dye exhaust bath or dye-contaminated waters. Provided that the above high dye degradation rate allows easy removal of the color from the exhaust dye bath, we wished to find out if the dye degradation might result in the formation of uncolored toxic species. We chose to measure phytotoxicity to obtain a preliminary ready indication of the potential environmental impact of the above irradiated solutions. To this scope we measured the germination index of *Lepidium sativum* seeds according to a known procedure (Accotto

et al. 1998). Our tests showed no critical hindering of this plant germination rate either by the plain cHAL2 and by the cHAL2-EO solutions irradiated in the above experimental conditions. Work is currently in progress in order to assess the degradation mechanism and the ultimate fate of the dye and of the humic acid-like substance organic carbon. The photosensitizing effect of cHAL2 in the dye exhaust bath adds further potential credit to its use in dyeing technology, and should not be conflicting with the stability of the dyed fabric, provided that the additive was washed out of the dyed fabric upon completion of the dyeing process.

Performance in Fabric Detergency

Laundry detergents are expected to remove oily soil from fabric. This requires that soil transferred from the fabric to the detergent solution and dissolved into the latter. Surfactants by their capacity to lower the water surface tension and host oily soil particles into their hydrophobic micellar core provide the basis and bulwark of the cleaning power. However, in detergents formulations they are accompanied by a variety of other products (Watson 2006). Among these, polymers with carboxylic functional groups, poly(acrylic acid) for example, are used due to their dispersing power for soil particles. In this regard, fabric detergency and fabric dyeing may be considered to occur by similar mechanisms, but involving opposite processes: i.e., transfer of the soil particle from the fabric to the detergent solution in the former case, and of the dye from its solution bath to the fabric in the latter case. As reported above, cHAL2 containing small molecules and macromolecules with acid carboxylic groups seemed to have both of the above active principle types, i.e., the surfactant and the dispersing polymer. This humic acid-like substance seemed therefore very appealing to be tested in fabric detergency.

The results of our washing tests performed with cHAL2 are reported in Table 4 and Fig. 4. Our experimental plan involved washing the standard soiled fabric (see experimental section) with a water solution containing 2 g/L of Na_2CO_3 in the absence of any other additive, and in the presence of cHAL2 or of the synthetic commercial surfactants SDBS and SDS. To evaluate the data in Table 4 and Fig. 4, it should be understood that increasing values of the ΔE parameter (see experimental section) indicate increasing whiteness of the sample relative to the standard soiled sample, and therefore higher washing efficiency by the solution. The data in Table 4 show that relative to washing with the plain Na_2CO_3 solution, the degree of whiteness of the standard soiled fabric was significantly improved already at 0.4 g L^{-1} cHAL2, whereas the highest washing efficiency is reached with 1.2 g L^{-1} cHAL2, just above the additive CMC value, and at higher cHAL2 concentration no major or significant change of the washing efficiency ($6.40 \leq \Delta E \leq 8.61$) was observed.

The graphic representation in Fig. 4 allows a ready appreciation of the difference in the trend of performance (ΔE) versus surfactant concentration (C) for the biosurfactant cHAL2 and the commercial synthetic SDBS surfactant. Whereas at low concentration SDBS seemed to perform better than cHAL2, the ΔE difference between the two surfactants seemed to be attenuated at higher C values and certainly annulled at 2 g L^{-1} surfactant concentration. At this concentration, the second commercial surfactant (SDS) exhibited the lowest performance.

Table 4. Washing Efficiency (ΔE)^a of Standard Soiled Fabric by 2 g L⁻¹ Na₂CO₃ Solutions, with and without Added Humic Acid-like Substance Isolated from Compost (cHAL2) and Synthetic Commercial Surfactants at Variable Additive Concentration (C).

Surfactant	C ^b (g L ⁻¹)	ΔE^a	$\sigma\Delta E^a$
	0.00	1.93 a	1.20
SDBS	0.20	6.17c,d	0.98
SDBS	0.40	8.02 d	1.33
SDBS	0.60	7.98 d	1.40
SDBS	1.20	6.15 c,d	1.29
SDBS	2.00	7.75 d	1.12
SDBS	2.00	7.15 c,d	1.36
SDBS	2.00	6.35 c,d	1.20
SDBS	2.00	7.66 d	1.05
SDBS	2.00	6.55 c,d	1.59
SDBS	2.00	8.70 d	1.39
SDBS	2.25	8.30 d	1.45
SDBS	2.50	7.66 d	0.84
SDS	2.00	1.99 a	0.93
SDS	2.00	4.06 b	1.13
SDS	2.00	5.72 c	1.52
cHAL2	0.20	3.19 a	1.28
cHAL2	0.40	4.01 b	1.34
cHAL2	0.60	5.47 b	1.08
cHAL2	0.80	4.85 b	0.69
cHAL2	1.00	5.78 c	0.92
cHAL2	1.20	6.40 c,d	1.33
cHAL2	1.60	7.66 d	1.21
cHAL2	2.00	7.63 d	1.17
cHAL2	2.00	6.43 c,d	1.29
cHAL2	2.00	6.47 c,d	1.29
cHAL2	2.00	8.61 d	1.08

^aAs defined in experimental section; letters next to figures indicate ΔE inequalities by T test at 95 % confidence level (Natrella 1966): i.e., a < b < c < d

^bResults for one surfactant reported at the same C value, but in different lines, pertain to different specimen washed at different time.

It should however be pointed out that SDS at 2 g L⁻¹ is below its 2.33 g L⁻¹ CMC value (Savarino et al. 2007), whereas SDBS and cHAL2 are well above their CMC values. By comparison, the plot of ΔE vs. the CMC multiple (C/CMC) reported in Fig. 5 shows that the performance differences between surfactants at the same C/CMC value appear smaller than those shown at the same C value (Fig. 4). Although this fact may point out the importance of micelles formation for best performance, in real practice the additives are purchased on a weight basis and therefore it is more important to compare performances at the same additive weight, rather than at the same CMC multiple. The comparison of individual surfactants may yield hints regarding their performance potential. However, in real practice, mixtures of surfactants are used, as these may exhibit synergic effects. Our data show that cHAL2 may be an interesting candidate for use in detergents formulation.

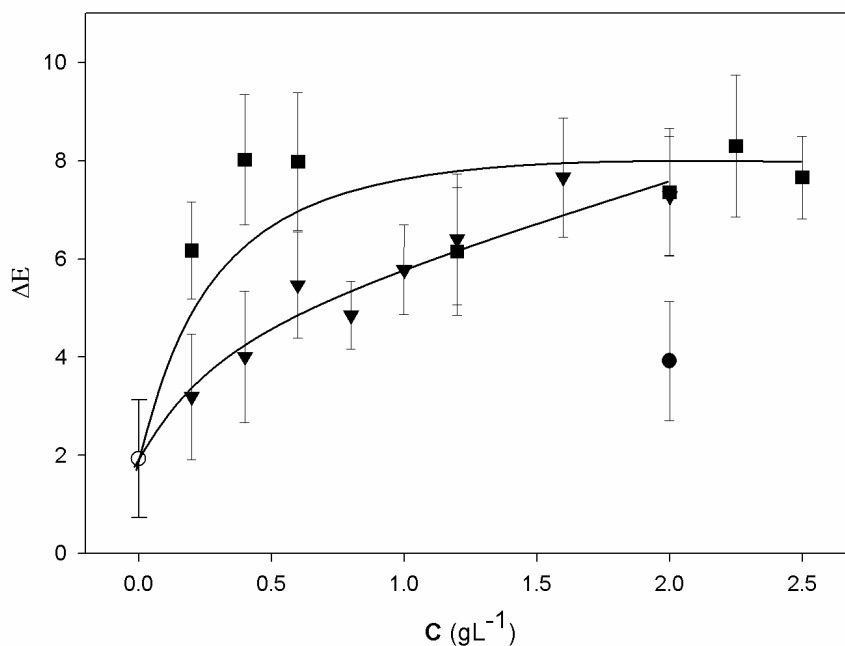


Fig. 4. Plot of ΔE vs. C data which are reported in Table 4 for plain sodium carbonate solution (\circ), SDBS (\blacksquare), SDS (\bullet) and cHAL2 (\blacktriangledown); ΔE values for SDS, SDBS, and cHAL2 at 2 g L^{-1} are averages taken over the replicate specimen shown in Table 4 for each surfactant. Error bars for the average ΔE values represent the pooled standard deviations calculated (Natrella 1966) from the single specimen standard values in Table 4.

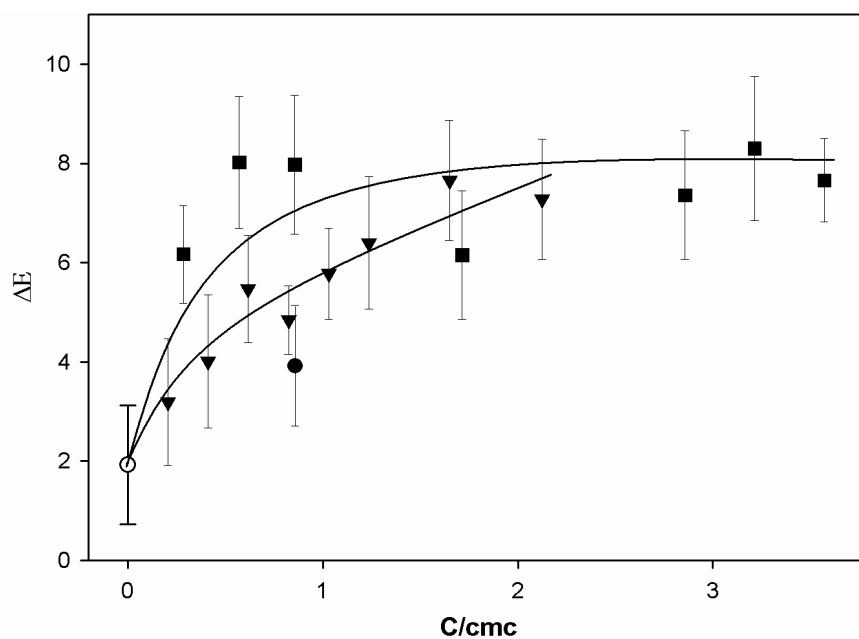


Fig. 5. Plot of ΔE vs. the CMC multiple (C/CMC): ΔE and C as in Fig. 4; CMC values (Savarino et al. 2007) = 2.33 g L^{-1} for SDS (\bullet), 0.97 g L^{-1} for cHAL2 (\blacktriangledown), 0.7 g L^{-1} for SDBS (\blacksquare).

CONCLUSIONS

1. We have shown that municipal solid wastes (MSW) contain valuable organic matter with surfactant properties, which can be recycled to the chemical market for several technological applications.
2. This fact, coupled with the expected friendly environmental impact of the above bio-surfactants, and with the large use of surfactants in modern life, allows us to expect promising economic returns on new biomass waste treatment processes that were specifically developed for recycling products to the chemical market. Indeed, assuming that the MSW isolated biosurfactants (MSWBS) were placed in the surfactant chemical market at the same price (Houston, 2007; Modler et al. 2007) as the commercial synthetic surfactants (CSS), the sales price of the former ones might run about 1-2 €/kg. Thus, using compost as source of bio-surfactants would raise the market value of this biomass waste from 15 €/ton (Newman 2006) to a few hundreds €/ton, deriving the value from bio-surfactant sales only. Such perspectives offer enough incentive to continue investigating the performance of wastes bio-surfactants in other applications, to assess product specifications and to optimize processes for their isolation. Particularly, as for materials of biological origin the source-product variability is mostly critical, further work on humic-like substances should be aimed to establish relationships between their source, structure, properties, and technological performance.
3. The advantages of demonstrating the potential for real commercialization of organics isolated from biomass residues would not be limited to the likely economic return of new waste management processes, but would also involve savings of oil consumption for manufacturing synthetic chemicals with similar properties and decrease of the related CO₂ emission to the atmosphere. To get a rough appreciation of the extent to which biosurfactants isolation and recycling may impact the current waste management practice, it should be considered that the oil world consumption for the manufacture of linear alkylated sulfonates, the major commercial synthetic anionic surfactants, is about 1 million tons/year (Modler et al. 2007) while the total biomass waste flow in the European Union alone is estimated to be a few billion tons/year (Piccinini 2005).
4. As the amount of available biomass wastes far exceeds the amount necessary to obtain enough biosurfactants to virtually replace all synthetic surfactants in the chemical market, the recovery of biosurfactants from biomass wastes cannot be used as the only means for an environmentally and economically efficient management of the wastes. However it may represent one good process to be integrated in biorefineries (Wang et al. 2004). Promotion of biorefineries producing multiple products, including higher-value chemicals as well as fuels and power, is indeed the most modern research trend on biomass treatment and is a priority topic in the current European Union (EU) calls for proposals (FP7 Energy 2007). Integration of the soluble organics extraction process with other biomass treatment technologies, such as those for biogas, bioethanol, or biodiesel production, is likely to affect the final plant products yield and quality and to increase the overall process economic return.

ACKNOWLEDGMENTS

This work was carried out with Regione Piemonte Cipe 2004 funds for Cod. C 13 sustainable development program. We are thankful to Prof. G. Piccone and Dr. C. Mozzetti of the Dipartimento di Valorizzazione e Protezione delle Risorse Agroforestali of the University of Torino for the phytotoxicity tests performed on the irradiated cHAL2/EO solutions.

This contribution was an original presentation at the *ITALIC 4 Science & Technology of Biomass: Advances and Challenges* Conference that was held in Rome, Italy (May 8-10, 2007) and sponsored by Tor Vergata University. The authors gratefully acknowledge the efforts of the Conference Organizers, Prof. Claudia Crestini (Tor Vergata University, Rome, Italy), Chair, and Prof. Marco Orlandi (Biococca University, Milan, Italy), Co-Chair. Prof. Crestini also is Editor for the conference collection issue to be published in *BioResources*.

REFERENCES CITED

- Accotto, E., Barberis, R., Belfiore, G., Nappi, P., Pantusa, S., Piccone, G., and Trombetta, A. (1998). "Metodi di analisi dei compost," *Collana Ambiente Regione Piemonte* 6. Regione Piemonte Assessorato Ambiente, Torino (I).
- Amine-Khodja, A., Richard, C., Lav'edrine, B., Guyot, G., Trubetskaya, O., and Trubetskoj, O. (2006a). "Water-soluble fractions of composts for the photodegradation of organic pollutants in solar light," *Environ Chem Lett* 3, 173–177.
- Amine-Khodja, A., Trubetskaya, O. and Trubetskoj, O., Cavani, L., Ciavatta, C., Guyot, G., and Richard, C. (2006b). "Humic-like substances extracted from composts can promote the photodegradation of Irgarol 1051 in solar light," *Chemosphere* 62, 1021-1027.
- Bahnemann, D. (2004). "Photocatalytic water treatment: solar energy applications," *Solar Energy* 77, 445-459.
- Bianco Prevot, A., Basso, A., Baiocchi, C., Pazzi, M., Marci, G., Augugliaro, V., Palmisano, L., and Pramauro, E. (2004). "Analytical control of photocatalytic treatments. Degradation of a sulfonated azo-dye," *Analytical and Bioanalytical Chemistry* 378(1), 214-220.
- Canonica, S., Jans, U., Stemmler, K., and Hoigné, J. (1995). "Transformation Kinetics of Phenols in Water: Photosensitization by Dissolved Natural Organic Material and Aromatic Ketones," *Environ Sci. Technol.* 29, 1822-1831.
- Carpignano, R., Savarino, P., Barni, E., Di Modica, G., and Papa, S. S. (1985). "Developments in the application of quantitative structure-property relationships of dyes," *J. Soc. Dyers and Col.* 101, 270-276.
- EMPA (2006). "Evaluation of detergents and washing processes with artificially soiled fabrics," *EMPA Test materials*, available at www.empa-testmaterials.ch [accessed April 13, 2007].

- FP7 Energy (2007). "Developing biorefinery concepts," EU calls for proposals, Theme 5, Energy.2007.3.3.3, available at http://cordis.europa.eu/fp7/cooperation/energy_en.html [accessed April 13, 2007].
- Gottlieb, A., Shaw, C, Smith, A., Wheatley, A., and Forsythe, S. (2003). "The toxicity of textile reactive azo dyes after hydrolysis and decolourisation," *J. Biotech.* 101, 49-56.
- Hoigné, J., Faust, B. C., Haag, W. R., Scully, F. E., and Zepp, R.G. (1989). "Aquatic humic substances as sources and sinks of photochemically produced transient reactants," *Adv. Chem. Ser.* 219, 363-381.
- Houston, C. A. & Associates, Inc. (2007). "Opportunities in performance surfactants in west europe," available by subscription at www.colin-houston.com [accessed April 13, 2007].
- Kamat, P. V. (1993). "Photochemistry on nonreactive and reactive (semiconductor) surfaces," *Chem. Rev.* 93, 267-300.
- Konstantinou, J. K., and Albanis, T. A. (2004). "TiO₂-assisted photocatalytic degradation of azo dyes in aqueous solution: kinetic and mechanistic investigations - A review," *Applied Catalysis B-Environmental* 49, 1-14 and references therein.
- Kraft, E., Bidlingmaier, W., De Bertoldi, M., Diaz, L. F., and Barth, J. (Eds.) (2006). *Proceedings of the International Conference Orbit 2006 Biological Waste Management from Local to Global*. Weimar: verlag ORBIT e.V.; ISBN 3-935974-09-4.
- Modler, R.F., Willhalm, R., and Yoshida, Y. (2007). "CEH marketing research report. Linear alkylate sulfonates," available at <http://www.sriconsulting.com/CEH/Public/Reports/Sample.pdf> [accessed April 13, 2007].
- Montoneri, E., Boffa, V., Quagliotto, P.L., Mendichi, R., Chierotti, M.R., Gobetto, R., and Medana, C. (2008). "Humic acid-like matter isolated from green urban wastes. Part I: structure and surfactant properties," *Bioresources* 3(1), 123-141.
- Natrella, M. G. (1966). *Experimental Statistics*, Besson, F. S. and Astin, A. V. (eds.), National Bureau of Standards Handbook 91, U.S. Government Printing Office, Washington, D.C.
- Newman, D. (2006). "Compostaggio in Italia, riflessioni sulle opportunità e prospettive future," paper presented at the meeting on *Recupero dei Rifiuti Industriali Organici: Conversione dei Rifiuti in Risorsa* held at the University of Torino on December 13.
- Palmisano, L. (ed.) (2000). *Processi e Metodologie per il Trattamento delle Acque*. Spiegel, Milano.
- Piccinini, S. 2005. "La digestione anaerobica e il compostaggio: L'integrazione operativa dei due sistemi," Milano, December 6, available at http://www.compost.it/biblio/2005_12_06_dig_anaer_comp/Piccinini-MI-6-12-05.pdf [accessed April 13, 2007].
- Quagliotto, P. L., Montoneri, E., Tambone, F., Adani, F., Gobetto, R., and Viscardi, G. (2006). "Chemicals from wastes: compost-derived humic acid-like matter as surfactant," *Environ. Sci. Technol.* 40, 1686-1692.
- Research and Markets (2007). "Surfactants industry: Global mergers and acquisitions," available from <http://www.researchandmarkets.com/reports/364485/> [accessed April 13, 2007].

- Robinson, T., McMullan, G., Marchant, R., and Nigam, P. (2001). "Remediation of dyes in textile effluent: A critical review on current treatment technologies with a proposed alternative," *Bioresource Technology* 77, 247-255.
- Rosen, M. J. (ed.) (1989). *Surfactants and Interfacial Phenomena*, 2nd edition, Wiley, New York.
- Savarino, P., Viscardi, G., Quagliotto, P., Montoneri, E., and Barni, E. (1995). "Developments in dyeing technology based on microemulsion technology," *J. Dispersion Science and Technology* 16, 51-68.
- Savarino, P., Viscardi, G., Quagliotto, P., Montoneri, E., and Barni, E. (1999). "Reactivity and effects of cyclodextrins in textile dyeing," *Dyes and Pigments* 42, 143-147.
- Savarino, P., Montoneri, E., Biasizzo, M., Quagliotto, P.L., Viscardi, G., and Boffa, V. (2007). "Upgrading biomass wastes in chemical technology. Humic acid-like matter isolated from compost as chemical auxiliary for textile dyeing," *J. Chem. Tech. Biotech.* 82, 939-948.
- Sakkas, V. A., Lambropoulou, D. A., and Albanis, T. A. (2002). "Photochemical degradation study of irgarol 1051 in natural waters: influence of humic and fulvic substances on the reaction," *Journal of Photochemistry and Photobiology A: Chemistry* 147, 135-141.
- Showell, M. S. (Ed.) (2006). *Handbook of Detergents. Part D: Formulation*, Taylor & Francis, Boca Raton, FL (USA).
- von Wandruszka, R. (2000). "Humic acids: Their detergent qualities and potential uses in pollution remediation," *Geochem. Trans.* 1(2), 10-15.
- Wang, J., and Zhu, Y. (2006). "Surfactants applications in textile processing," *Handbook of Detergents. Part D: Formulation* 9, 279-303. Showell, M.S. (ed.). Taylor & Francis, Boca Raton, FL (USA).
- Wang, M., Hess, R., Wright, C., Ibsen, K., Ruth, M., Jechura, J., Spath, M., Grahain, R., Sokhunsanj, S., Perlack, R., Werpy, T., and Jones, S. B. (2004). *Office of the biomass program. Multi-year Analysis Plan FY04-FY08*. U.S. Department of Energy, available at <http://www.osti.gov/bridge> [accessed April 13, 2007].
- Watson, R.A. (2006). "Laundry detergents formulations," *Handbook of Detergents. Part D: Formulation* 3, 51-104. Showell, M.S. (ed.). Taylor & Francis, Boca Raton, FL (USA).
- Zollinger, H. (ed.) (1991). *Colour Chemistry: Synthesis, Properties and Applications of Organic Dyes and Pigments*. VHS Publishers, New York.

Article submission received by journal: Sept. 21, 2007; Peer-review completed: Jan. 22, 2008; Revised version received and approved: Feb. 2, 2008; Published Feb. 3, 2008.

NOVEL SOURCES OF FUNGAL CELLULASES FOR EFFICIENT DEINKING OF COMPOSITE PAPER WASTE

Rohit Soni, Asiya Nazir, B. S. Chadha,* and H. S. Saini

Twenty thermophilic/thermotolerant fungal strains were isolated from composting soils and screened for production of different enzymes (Endoglucanases, β -glucosidase, Fpase and xylanases) to assess their deinking efficiency. Three isolates, *Aspergillus* sp. AMA, *Aspergillus terreus* AN1, and *Myceliophthora fergusii* T4I, identified on the basis of morphological and sequencing of amplified ITS1-5.8S-ITS2 rDNA region, showed significant deinking of composite waste paper (70% magazine and 30% Xerox copier/ laser print paper waste) as well as improved properties (brightness, tensile strength, tear index) of recycled paper sheets. The chosen strains *Aspergillus* sp. AMA, *Aspergillus terreus* AN1 and *Myceliophthora fergusii* T4I, showed 53, 52.7, and 40.32% deinking with increase in brightness by 4.32, 3.56, and 3.01 % ISO, respectively. These cultures were found to produce multiple endoglucanases and were characterized to lack a cellulose binding module (CBD), which may be responsible for their better deinking efficiency.

Keywords: Thermophilic fungi; Screening; Cellulases; Deinking; Composite paper waste; EG without CBD

Contact information: Department of Microbiology, Guru Nanak Dev University, Amritsar- India; the first two authors contributed equally. *Corresponding author: chadhabs@yahoo.com

INTRODUCTION

Shortage of forest-based raw materials and problems in processing agro-residues are the major constraints in growth of production from the paper industry. Stringent environmental protection guidelines have also forced paper mills to go for deinking of the waste paper. The waste fiber used to make high-grade recycled paper consists mainly of magazine waste (OMG), mixed office waste (MOW), and old newspaper (ONP). Due to lack of any organized sector for waste paper collection in India, imported paper waste, comprising mainly OMG and MOW, constitutes the main ingredient used for preparing recycled paper pulp (Nichat 2003). These waste furnishes differ in the type of ink formulations and chemical composition. The deinking of composite waste comprising OMG and MOW is suitable for producing newsprint as well as high grade paper because it has longer and brighter fibers when compared to ONP. However, the presence of clay coatings and glue binders in OMG and hard-to-remove thermoplastic copolymer inks in MOW makes the conventional chemical deinking processes expensive and having high potential for environmental damage (Prasad et al 1992; Watson 1988). Therefore, enzymatic deinking is now being considered as a suitable alternate option for replacing some of the deinking chemicals. Workers in the recent past have suggested that microbial enzymes such as cellulase (endoglucanase and β glucosidase), xylanases (Morkbak and

Zimmerman 1998; Elegir et al. 2000; Sreenath et al. 1996; Qin et al. 1998; Viestures and Leitte 1999), esterases, and lipases have important role to play in biological deinking. The enzymatic treatment favors ink detachment from fibers without discharge of pollutants, thus contributing to environmental compatibility. The effect of cellulase in facilitating ink detachment during deinking of xerographic and laser printed-paper has been shown using preparations containing mixed enzyme (endoglucanase, cellobiohydrolase, β -glucosidase and xylanases) and mono-component activities (Prasad et al. 1992; Jeffries et al. 1994). On the other hand, removal of oil-based inks from magazine wastes is facilitated by addition of lipases and esterases. The cellulases bind and alter fiber surface or bonds in vicinity of ink particles resulting in removal of small fibers from the surface of ink particles, thus altering the relative hydrophobicity of the toner particles and reducing the hydrodynamic drag, which facilitate their removal during floatation step (Jeffries et al. 1994).

This study was designed to identify and evaluate novel sources of enzymes from diverse thermophilic/thermotolerant fungal isolates for biological deinking of composite paper furnish comprising of OMG and MOW. An extensive screening of these strains resulted in selection of *Aspergillus* sp. AMA, *Aspergillus terreus* AN₁, and *Myceliophthora fergusii* T4_i as suitable microbial sources of enzymes, for effective deinking.

MATERIAL AND METHODS

Isolation of Fungal Cultures

Twenty thermophilic/thermotolerant strains were isolated from composting materials/ soils collected from different regions of India (Jammu and Kashmir, Amritsar, and Ahmedabad). These cultures were grown at 45°C on yeast starch agar (YpSs, pH 7.0) of the following composition (%; w/v): starch 1.5, yeast extract 0.4, KH₂PO₄ 0.23, K₂HPO₄ 0.2, MgSO₄ · 7H₂O 0.05, citric acid 0.057, and agar 2.0 (Cooney and Emerson 1964) and maintained on the same medium at 4°C. The strains were screened for production of endoglucanase (EG), avicel adsorbable endoglucanase activity (AAEG), β glucosidase, Fpase, and xylanase; in a few selected strains cellobiohydrolase and esterases activities were also assayed. The resultant extracts were used for deinking of composite waste paper. Three strains showing efficient deinking were identified morphologically, microscopically, and on the basis of rDNA sequence of ITS1-5.8 S-ITS2 region.

Extraction of DNA

The DNA was extracted from 40 mg of lyophilized mycelium (ground to fine powder) that was suspended in 550 μ l of extraction buffer (1 M Tris HCl pH 8.0, 4M NaCl, 250mM EDTA, 1% β - Mercaptoethanol, 10% sodium dodecylsulfate, SDS) and 300 μ l of equilibrated phenol. Upon homogenization, the tubes were incubated for 15 minutes at 65°C. The DNA in the aqueous phase was purified with repeated extractions using equal volumes of saturated phenol chloroform iso-amyl alcohol (PCI) mixture (25:24:1). The resultant DNA was precipitated with 9 parts of ice-cold isopropyl alcohol

and 1 part of sodium acetate (3M; pH 8.0). The tubes then were kept at -20°C for 2 h, followed by centrifugation for 15 minutes at 10,000 rpm. The resultant DNA pellets were rinsed with 70% ethanol, air dried, suspended in 50 μl of sterilized double distilled water and stored at 4°C until use.

PCR Amplification of ITS and 18S Region

The ITS1, ITS2 and the intervening 5.8S coding rDNA was amplified by PCR using ITS1 (5' TCCGTAGGTGAACCTGCGG 3') and ITS4 (5' TCCTCCGCTTAT-TGATATGC 3') primer pair (White *et al.* 1990). Amplification reactions mixture (50 μl) contained 25 μl of PCR mix (Genei, Bangalore, India), 2.5 μl of DMSO, 100 pmoles of each primer and 100 ng of DNA template. Thermal cycling consisted of initial denaturation of 4 minutes at 95°C , followed by 30 cycles, denaturation step at 94°C for 50 seconds, annealing step at 51°C for 1 minute, and primer extension at 72°C for 1 minute, followed by final extension step for 10 minutes at 72°C . Amplification products were electrophoretically resolved in 1.4% (w/v) agarose gel containing ethidium bromide, using 1X TAE buffer at 70 V.

Solid Substrate Culturing for Enzyme Production

Solid state fermentation was carried out in Erlenmeyer flasks (250 ml) that contained ground rice straw as a carbon source (5 g) and basal medium (15 ml) of the following composition: KH_2PO_4 0.4%, $\text{CH}_3\text{COONH}_4$ 0.45%, and $(\text{NH}_4)_2\text{SO}_4$ 1.3% (pH, 7.0), which was inoculated with spore suspension (2 ml; 10^7 spores/ml), prepared from seven days old culture grown on agar plates. The flasks were incubated for five days at 45°C . The enzyme was harvested by adding 50 ml of sodium citrate buffer (50mM pH 6.0) to the flasks and kept at 45°C for 1h under mild shaking. The resultant slurry was filtered through muslin cloth and centrifuged at 8800 x g for 10 min, and the extracts were used for enzymatic assay.

Enzymatic Assay

Endoglucanase (1, 4- β -glucan-4-glucanohydrolase, EC 3.2.1.4) and xylanase (endol, 4 β -D- xylanase, EC 3.2.1.8) activities were determined using 1% CM-cellulose and 1% Birch wood xylan, prepared in sodium citrate buffer (50 mM, pH 6.0), respectively. The reaction mixture containing equal amounts of suitably diluted enzyme and substrate was incubated at 50°C for 10 min and 5 min, respectively. The reaction was stopped by addition of DNS followed by boiling (Miller 1959); the colour developed was read at 540 nm using Novaspec II spectrophotometer (Pharmacia). The amounts of released sugar were quantified using glucose and xylose standards, respectively.

The avicel absorbable activity (AAEG) was assayed as described by Arifoglu and Ogel. (2000). The reaction mixture containing 0.5 ml of sodium acetate buffer (25 mM, pH 5.0), 0.5 ml of culture supernatant and 100 mg of avicel was kept at 4°C for 1 h. After centrifugation, the residual EG activity in the supernatant was measured by using CM-cellulose (1%). AAEG was measured indirectly by subtracting avicel non-adsorb able EG activity from total EG activity. Total cellulose activity (Fpase) was measured by using a Whatman No. 1 filter paper strip (1x 6 cm) as substrate (Wood and Bhat 1998).

β -Glucosidase (β -D-glucosido-glucanohydrolase, EC 3.2.1.21) and cellobiohydrolase (EC 3.2.1.91) were assayed using *p*-nitro phenyl- β -D-glucopyranoside (pNPG) and *p*-nitro phenyl- β -D-cellobioside, respectively, in a micro-titre plate based method (Parry et al. 2001). Appropriately diluted enzyme (25 μ l) was mixed with 50 μ l of sodium acetate buffer (50 mM, pH 5.0). The reaction was initiated by adding 25 μ l of pNPG/pNPC (10mM) and incubated at 50 °C for 30 min; the reaction was terminated by adding 100 μ l of NaOH-glycine buffer (0.4 M, pH 10.8), and the developed yellow color was read at 405 nm using an ELISA Reader (MULTISKAN; Lab system). One unit of β -glucosidase/ cellobiohydrolase activity was expressed as the amount of enzyme required to release 1 μ mole of pNP per minute under assay conditions. For assay of esterase activity the above method was used, except that pNP acetate (1 mM) was used as substrate (Ghatora et al. 2006). The enzyme activities were expressed as units per gram dry weight substrate.

Characterization of Crude Endoglucanase

Endoglucanase of the selected strains *Aspergillus* sp. AMA, *Aspergillus terreus* AN₁ and *Myceliophthora fergusii* T4_i was characterized for temperature and pH optima and thermostability. The effect of temperature on the endoglucanase activity was analyzed between 30°C and 90°C at pH 5.0. The optimum pH for enzyme activity was determined using 0.05M buffers ranging from pH 3.0 to 10.0 (citrate buffer (pH 3-6), sodium phosphate buffer (pH 7-8) and glycine- NaOH buffer (pH 9-10)) at optimal temperature previously determined for each enzyme. The stability of endoglucanase was monitored at optimal pH and temperature for 1h and residual activities were assayed.

Strains selected on the basis of efficient deinking of waste paper were further characterized for presence of multiple endoglucanase by developing zymogram. Native polyacrylamide gel electrophoresis (PAGE) 10% with 1% resolving gel was used to resolve the desalted and concentrated enzyme samples (70 μ g). After electrophoresis the gels were incubated for 15 min in 0.05 M sodium acetate buffer (pH 5.0) and overlaid on polyacrylamide gel containing CMC (0.5%,w/v) for 2 h at 50°C. The overlay gel was removed and stained with 0.2% Congo Red. Bands corresponding to EG appeared as clear zone against a dark background after de-staining with 1M NaCl followed by treatment with 10% (v/v) acetic acid solution.

Deinking Experiments

Composite paper waste comprising of 70% OMG waste and 30% MOW was disintegrated in laboratory pulper (Universal) for 10 min at 4% consistency using tap water. The disintegrated pulp was recovered by dewatering through 200 – mesh wire and oven dried. The resultant pulp was suspended in sodium citrate buffer pH 6.0 (10% consistency), and enzymatic treatment was carried out using an enzyme dose of 50 units/100 g of oven dried pulp at 50 °C. To inactivate the enzyme, the pulp suspension was boiled for 10 min. Finally the pulp was washed with tap water through 200-mesh wire and subjected to flotation (Lamort type original Kowaleshowski Flootation cell; capacity 25 Litres equipped with aerator operating at speed of 2500 rpm (model UEC-2026) by Universal Engineering Corporation, Saharanpur, India) for 20 min in presence of surfactant (0.1% Tween 80) and (0.1% CaCl₂) as flotation aids. Control assays without

enzyme treatment were carried out under identical conditions. After flotation, handsheets were prepared (TAPPI method T 205 sp-02) from enzyme-treated, as well as control pulp, using a semi-automatic handsheet maker (Universal Engineering Corporation, Saharanpur, India). The resultant handsheets were analyzed using an ELREPHO 70 image analyzer (Lorentzen and Wettre- Elrepho, Sweden). The brightness (TAPPI, T 452 om-02) and percent residual ink count in the handsheets was measured using the image analyzer at six different places on each handsheet, and results were expressed as mean values. The handsheets were also analyzed for properties like breaking strength, burst index, and tear index according to standard TAPPI methods (Marques et al. 2003).

RESULTS

Screening of Fungal Isolates for Production of Cellulases and Xylanase

Twenty fungal strains were isolated from soil collected from different regions of North India (Jammu and Kashmir, Amritsar, and Ahmedabad). These isolates, on the basis of morphological and microscopic examination of spore arrangements, were identified as *Myceliophthora* sp. strains, (V2A2, MYC and T4I), *Corynascus* sp. (JHG), *Humicola insolens* (J), *Malbranchea flava* (MF), *Melanocarpus* sp. (MEL), *Aspergillus* sp. (LC11, AMA, A6 and AN1), *Torula* sp. (ASS2, T22, T32 and AN6), *Emericella nidulans* (F), *Penicillium* sp. (CD2W3), *Chaetomium* sp. (1CHP), and an unidentified strain CS12. The molecular characterization of the strains showed that *Myceliophthora* sp. (MYC), *Corynascus* sp. (JHG), and *Myceliophthora fergusii* (T4I) formed a distinct clade, whereas, *Malbranchea flava* (MF) had a distinct phylogenetic origin. The strains of *Aspergillus* sp. (AMA) and *A. terreus*, though, belonging to the same genus, were phylogenetically distinct and were supported by lower bootstrap values (Fig. 1). The strains were grown on solidified rice straw based culture medium at 45°C and studied for production of different enzymatic activities which included, endoglucanase (EG), avicel absorbable endoglucanase (AAEG), Fpase, β -glucosidase, and xylanase.

The results in Table 1 show that of the strains included in study, *Melanocarpus* sp. (MEL), produced maximal amount of endoglucanase (115 units/g DW substrate), followed by *Aspergillus* sp. strain AMA (98.5 units/g DW substrate) and *A. terreus* AN1 (77.0 units/g DW substrate). The culture filtrates of *Aspergillus* sp. (AMA), *A. terreus* (AN1), and *M. fergusii* (T4I), did not show any AAEG activity under the given culture conditions. On the other hand *H. insolens* (J) showed maximal AAEG activity corresponding to 76.8 % of the total EG activity. Similarly higher fractions of AAEG activity was also observed for *Corynascus* sp. (JHG) and *Torula* sp.(AN6).

The strain of *Melanocarpus* sp. (MEL) also produced high levels of FPase (11.65 units/g DW substrate) followed by *Aspergillus* sp. (AMA) which produced 4.5 units/g DW substrate of activity in addition to high levels of β -glucosidase activity (250 units/g DW substrate). However, the highest β -glucosidase activity was recorded in *A. terreus* AN1 (500 units/g DW substrate), followed by *Penicillium* sp. CD2W3 (110 units/g) and *Aspergillus* sp. LC11 (108.2 units/g). High level of xylanase was achieved in *Malbranchea* sp. (9000 units/g DW substrate) followed by *Penicillium* sp. CD2W3 that showed (6011 U/g DW substrate). The titers of xylanase in *Aspergillus* sp. AMA (2782

units/ g DW substrate) and *A. terreus* (2580 units/ g DW substrate) were also high. In addition the observed levels of esterase activity in *Aspergillus* sp. (AMA), *Aspergillus terreus* (AN1) and *Myceliophthora fergusii* (T4I) were 86.7, 78.7, and 72.1 (units/ g DW substrate), respectively.

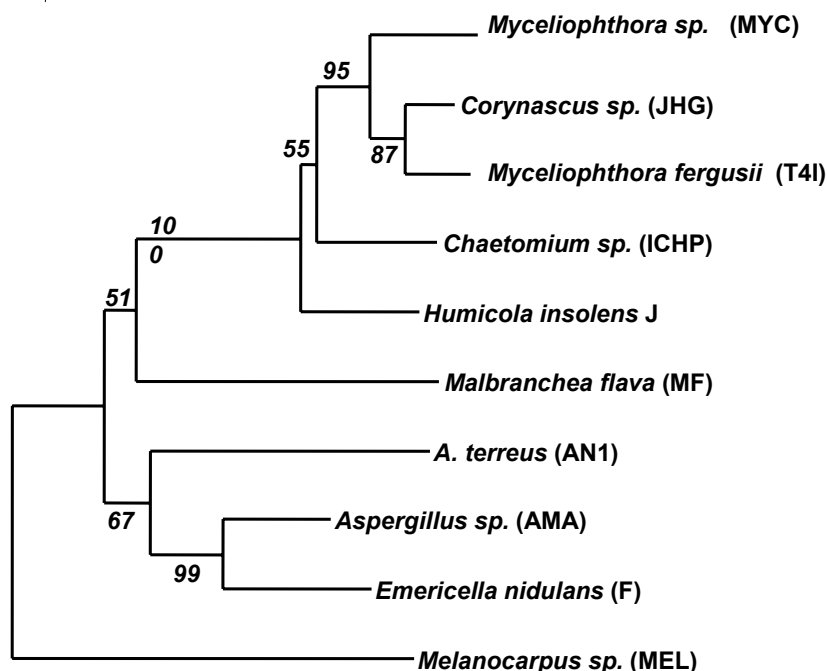


Fig 1. Diagram showing the dendrogram of fungal strains used in the deinking experiment. The strains were characterized on the basis of their ITS1-5.8S-ITS2 sequences and identified, in addition to morphology, on the basis of the alignment of the sequences from NCBI databases. The values at the nodes are bootstrap values.

Deinking Experiments

Table 2 shows results of deinking composite waste comprised of 70% OMG and 30% MOW. The handsheets were prepared with the composite pulp treated with different multi-component enzymes at a dosage of 0.5 units CMCase (EG)/ g pulp. Two parameters i.e., percent residual ink and brightness (ISO), were considered during screening of the potential of these enzymes for biodeinking. The results (Table 2) showed that treatment of pulp with enzyme preparations from *Corynascus* sp. (JHG), *A. terreus* (AN1), *Torula* sp. (AN6), *Myceliophthora* sp. (V2A2), *M. fergusii* (T4i), *Aspergillus* sp. AMA, and *Malbranchea flava* (MF), yielded improvements in brightness. However, all the other preparations resulted in decrease in percent ISO brightness as compared to the control. All enzymes included in study, however, resulted in decrease in percent residual ink ranging between 5 to 53 %, when compared to the control. Maximal deinking efficiency was observed in *Aspergillus* sp. AMA, which showed up to 53% reduction in ink, followed by *A. terreus* AN1 (52.7%) and *M. fergusii* (T4I), showing 40.5 % reduction, with improved brightness of the resultant hand sheets by 4.32, 3.56 and 3.01 % ISO, respectively.

Table 1. Production of Cellulases and Xylanase by Thermophilic / Thermotolerant Fungal Isolates

Location	Strains	CMC-ase (Units/g)	Fpase (Units/g)	β -glucosidase (Units/g)	Avicel adsorbable activity (Units/g)	Xylanase (Units/g)
Jammu	<i>Aspergillus</i> sp. (LC11)	48.0	1.99	108.2	3.7	192
	<i>Corynascus</i> sp. (JHG)	51.2	0.56	11.4	24.8	358
	<i>Aspergillus terreus</i> (AN1)	77.0	4.65	500	0	2580
	<i>Torula</i> sp. (AN6)	28.0	0.142	22.0	12.9	82.0
	<i>Myceliophthora</i> sp (V2A2)	31.3	0.627	20.13	9.2	590.2
	<i>Torula</i> sp. (T22)	11.4	0.20	41.0	2.9	170
	<i>Torula</i> sp. (T32)	26.0	0.96	9.8	2.5	206
Amritsar	<i>Torula</i> sp. (ASS2)	42.5	0.99	63.3	14.3	260.9
	<i>Myceliophthora fergusii</i> (T4I)	36.7	2.29	53.5	0	884.7
	<i>Aspergillus</i> sp. (AMA)	98.5	4.0	250	0	2782
	<i>Melanocarpus</i> (MEL)	115	11.65	27.4	23	1990
	<i>Aspergillus</i> sp. (A6)	47.9	0.85	24.8	18.6	225
	<i>Emericella nidulans</i> . (F)	21.5	2.4	77.0	10.2	329.5
	<i>Myceliophthora</i> sp. (MYC)	35.0	2.44	7.48	5.0	900.2
	<i>Penicillium</i> sp. (CD2W3)	42.0	2.33	110	1.0	6100
	<i>Malbranchea flava</i> (MF)	21.4	2.16	22.3	ND	9000
	<i>Penicillium</i> sp. (T4K)	18.0	.72	24.0		43.0
	Ahmed-abad	Unidentified (CS12)	54.0	1.9	1.82	ND
<i>Chaetomium</i> sp.(1 CHP)		54.5	1.3	3.6	ND	285
<i>Humicola insolens</i> (J)		33.3	1.99	55.8	25.6	271.9

Activities expressed as units/g DW substrate; ND Not Determined

The handsheets prepared from pulp treated with selected enzyme extracts of *Aspergillus* sp. AMA, *Aspergillus terreus* AN₁, and *Myceliophthora fergusii* T4I were evaluated for optical as well as physical and mechanical strength in order to measure the influence of enzyme on deinking (Table 3). The results showed an appreciable increase in burst index and tensile strength of the handsheets prepared after enzymatic treatment. When compared to the control, maximal increases in burst index (74%) and tensile index (52%) were observed in the recycled fibre treated with the enzyme of *A. terreus*. On the other hand, a marked improvement in tear index (9.7%) was observed in the handsheets prepared of enzyme from *M. fergusii* (T4I). A negligible improvement in tear index was observed in hand sheets prepared with fibre treated with *A. terreus* (AN1) and *Aspergillus* sp. (AMA) enzymes.

Table 2. Effect of Enzymatic Treatment on Residual Ink and Brightness

Sr. No.	Organism	Residual ink		Brightness	
1.	Control	63.62	+1.34	81.96	+0.84
2.	Chemical deinking*	30.77	+ 2.80	81.13	+ 0.42
3.	<i>Aspergillus</i> sp. (LC11)	45.96	+0.28	78.98	+0.12
4.	<i>Corynascus</i> sp. JHG	60.29	+0.72	84.30	+0.20
5.	<i>Aspergillus</i> sp (AN1)	30.08	+0.33	85.52	+0.05
6.	<i>Torula</i> sp. (AN6)	57.37	+0.002	80.00	+0.005
7.	<i>Myceliophthora</i> sp (V2A2)	56.32	+1.51	84.97	+0.24
8.	<i>Torula</i> sp. (T22)	54.24	+0.300	77.76	+0.13
9.	<i>Torula</i> sp. (T32)	66.39	+0.49	76.05	+0.20
10.	<i>Torula</i> sp. (ASS2)	45.84	+0.36	79.46	+0.10
11.	<i>Myceliophthora fergusii</i> (T4I)	37.84	+0.54	82.69	+0.08
12.	<i>Aspergillus</i> sp. (AMA)	29.89	+0.23	86.28	+0.05
13.	<i>Melanocarpus</i> (MEL)	60.63	+0.58	78.90	+0.18
14.	<i>Aspergillus</i> sp. (A6)	60.65	+0.43	77.02	+0.19
15.	<i>Emericella nidulans</i> . (F)	63.33	+4.94	79.11	+0.36
16.	<i>Myceliophthora</i> sp. (MYC)	56.43	+3.39	79.34	+0.45
17.	<i>Penicillium</i> sp. (Cd2W3)	59.25	+2.62	81.90	+0.025
18.	<i>Malbranchea flava</i> (MF)	58.30	+0.59	82.22	+0.36
19.	<i>Penicillium</i> sp. (T4K)	58.04	+0.02	80.04	+0.01
20.	Unidentified (CS12)	66.14	+0.73	78.61	+0.22
21.	<i>Chaetomium</i> sp. (IHP)	52.96	+0.93	78.80	+0.09
22.	<i>Humicola insolens</i> (J)	66.57	+1.5	78.24	+0.15

*Chemical deinking was carried out with Sodium silicate 2%; Sodium hydroxide 2% & H₂O₂ 1% instead of enzyme.

Table 3. Effect of the Enzymatic Treatment on Physical and Mechanical Strength Properties

	Deinking efficiency (%)	Brightness (% ISO)	Burst index (KPa m ² /g)	Tensile index (Nm/g)	Tear index (mNm ² /g)
Control pulp	-	81.91	2.34	38.5	9.3
<i>Aspergillus</i> sp. (AMA)	53	86.28	3.99	56.3	9.5
<i>A. terreus</i>	52.7	85.52	4.09	58.80	9.84
<i>M. fergusii</i>	40.5	82.69	3.99	58.57	10.21

Composite paper waste used for preparing recycled sheets

Endoglucanases of Selected Isolates

The selected strains of *Aspergillus* sp. (AMA), *A. terreus* (AN1), and *M. fergusii* (T4I) were further characterized for multiplicity of the endoglucanases (EG). The enzyme extracts were resolved on PAGE, and zymogram for EG were developed. The results in Fig. 2 showed the presence of 4 endoglucanases of different electrophoretic mobility in *A. terreus* (AN1) and three isoforms in extracts of *Aspergillus* sp. (AMA) and *M. fergusii* (T4I). The EG of strains of *Aspergillus* sp. (AMA) and *A. terreus* (AN1) exhibited optimal activity in range at 50°C, whereas, *M. fergusii* (T4I) was optimally active at 60°C. The enzymes from all three strains retained 100% activity up to pH 6.0 (Fig. 3).

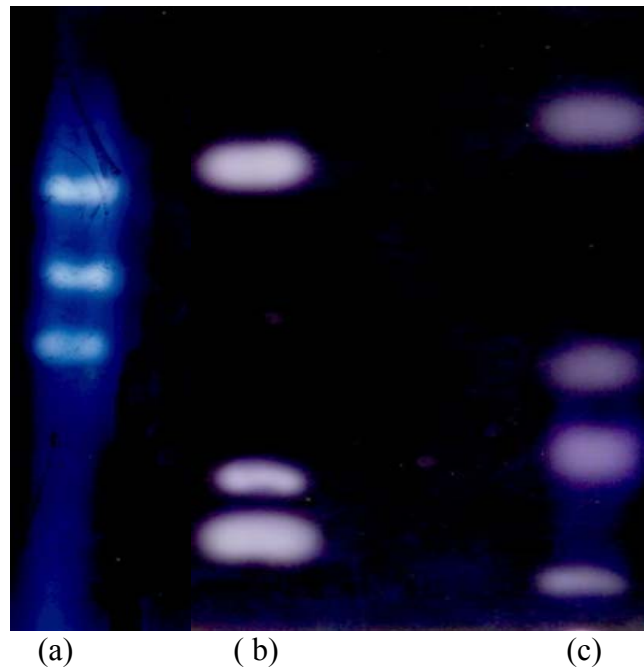


Figure 2. Zymogram showing multiplicity of endoglucanase in (a) *M. fergusii* (T41) b) *Aspergillus* sp. (AMA) c) *A. terreus* (AN1) resolved by PAGE.

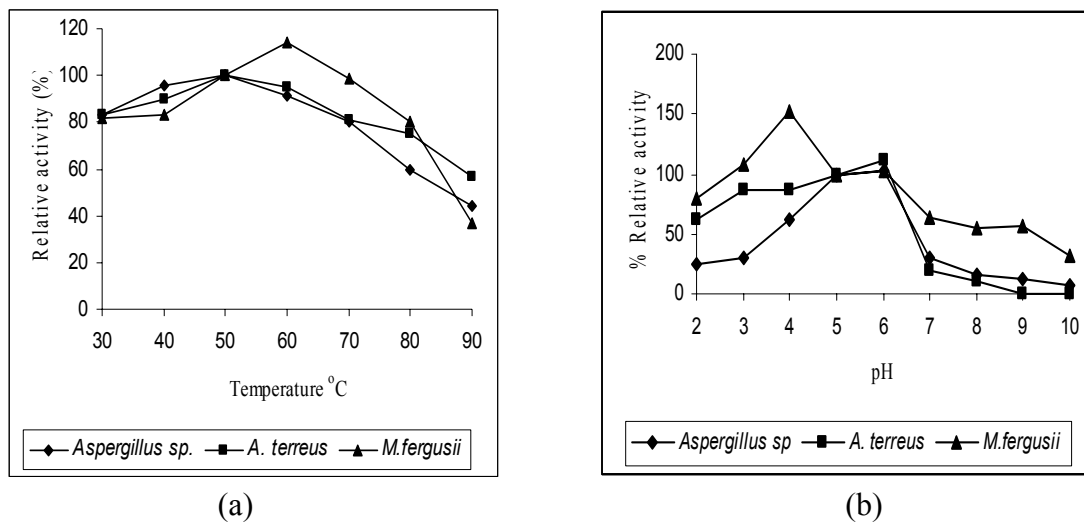


Figure 3. Effect of temperature (a) and pH (b) on the cellulase activity of *Aspergillus* sp. AMA, *Aspergillus terreus* AN1 and *Myceliophthora fergusii* T41.

DISCUSSION

The biological option, using cellulases and esterases, is now a well-documented approach for deinking and recycling of waste paper. Many research papers and a few patents in recent past have been published in this regard. Most of the initial studies on deinking have been carried out with a view to replace chemicals with enzymes. The

cellulases that have mainly been tested are the commercially available sources of multi/mono-component enzyme preparations of *Trichoderma reesei*, *H. insolens* supplied by Novo-Nordisk, IOGEN, Genencor, etc (Pala *et al.*, 2004; Jefferies *et al.* 1994). In addition a few of the recent studies have also tested cellulases (with xylanase activities) from the wild type isolates of *A. terreus*, *Aspergillus* L22, *Trichoderma pseudokoningii*, *Gleophyllum* sp. , *Orpinomyces* sp. , *Fusarium* sp., etc. (Marques *et al.* 2003; Gubitz *et al.* 1998; Geng and Li 2003; Vyas and Lachke 2003).

These enzyme preparations contain mixtures of cell wall degrading enzymes, with endoglucanase (EG) as an important component that randomly chops off the pulp fiber on which ink is sticking. However, most of the cellulase preparations contain multiple forms of EG, which may be classified in the same or different cellulase families. The endoglucanase on the basis of amino acid sequence/hydrophobic cluster analysis can be classified into different families (Henrissat *et al.* 1988). These EG on the basis of affinity for crystalline cellulose, can be further subdivided into those that contain Cellulose Binding Module (CBM) and have specific mechanism of action that is different from those that lack CBM. EG with CBM containing a catalytic domain that is joined to CBD by a linker rich in threonine, serine, and proline (Harrison *et al.* 1998) have been reported both in endoglucanases and cellobiohydrolases of *Trichoderma reesei*, *Hemicolac insolens*, etc. On the other hand, a few of the cellulases classified in families 5, 7, and 12 are reported to lack CBD (Lonsky and Negri 2003). Family 5 endoglucanases from *Bacillus* sp. strain KSM-64, and *A. aceulatus*, family 7 cellulase from *H. insolens* and *M. thermophila* as well as family 12 cellulase from *T. reesei*, which lack CBD are preferred endoglucanases for deinking and textile industry (Lonsky and Negri 2003). Similarly, cellulases Cel B and Cel E from anaerobic fungus *Orpinomyces* sp. that lack CBD have been found suitable for deinking of MOW (Geng and Li 2003). During extensive screening we identified *Aspergillus* sp. (AMA), *A. terreus* (AN1), and *M. fergusii* (T4I) as the strains that produced multiple isoforms of EG and did not show avicel adsorbable endoglucanase activity (AAEG), indicating an apparent lack of CBD. Furthermore, enzymatic deinking with these strains was found to be most efficient, as compared to other sources. Moreover, during purification we found that the endoglucanases bound tightly to the phenyl sepharose column, indicating the hydrophobic nature of enzyme. It has been suggested that removal of fibrous material from toners particles would increase hydrophobicity and thereby facilitate separation during flotation (Jefferies *et al.* 1994).

The next important thing considered in this paper was to isolate enzymatic sources that exhibit high enzyme titres in the culture extracts for process economics. The screening of fungal isolates for production, of cellulases, and hemicellulase, by Solid Substrate Fermentation (SSF), using rice straw as a carbon source, was employed. We have previously shown that rice straw, owing to its heterogeneity of composition, is a suitable source of carbon for producing plant cell wall degrading enzymes by *Myceliophthora* sp., *Melanocarpus* sp. and *Scytalidium thermophilum* (Badhan *et al.* 2007; Jatinder *et al.* 2006 a & b). The screening showed *Aspergillus* sp. and *A. terreus*, produced high titres of EG, the observed FPase and β glucosidase activities were also appreciably higher, and the ratio of FPase: β glucosidase was around 70 to 100. The enzyme preparations also contained good levels of xylanases and esterases. It has been shown in a recent patent (Yang *et al.* 2004) that enzymes with FPase to β glucosidase in

ratio of 1: 100 are efficient for deinking of MOW. In a previous study the positive role of xylanases from *T. lanuginosus* as an additive to endoglucanases was shown to enhance removal of toners from laser printed ink (Gübitz et al. 1998).

The observed enzyme titres in selected isolate of *A. terreus* AN1 in the present study was appreciably higher than that reported in the *A. terreus* isolate CCMI 498 by Marques and co-workers (2003), which may be attributed to the fact that geographically distinct strains show marked variations in the enzyme titres and hence there is need to isolate and screen geographically distinct strains (Sonia et al. 2005).

Following the enzymatic deinking protocol as suggested by Pala and co-workers (2004), we found that deinking of the composite waste by selected enzymes from *A. terreus* (AN1), and *Aspergillus* sp. (AMA) were efficient for deinking. The observed percent deinking were apparently higher as compared to those observed for different commercial enzymes for deinking of non-impact ink printed paper (Pala et al. 2004), however, it may be noted that ink removal from non-impact printing is considered more difficult as compared to other printed paper types. The reason for the observed efficient removal by selected enzymes in this study may be ascribed to either reduction in ink particle size or modification of the ink/surface properties by these enzymes. Moreover, it has also been observed that the removal of the toners with EG without CBD is more efficient in presence of surfactant, as compared to the one with CBD, as these cellulases bind tightly to the cellulose fibre and their removal by non-ionic surfactants is relatively difficult (Lonsky and Negri 2003). The observed reduction in the residual ink also correlated well with the improved brightness of the handsheets. The observed improvement in percent ISO brightness of paper furnishes treated with *Aspergillus* sp. AMA enzyme is among one of the highest reported (Vyas and Lachke 2003). However, no such correlation between deinking and brightness was observed as reported previously (Jefferies et al. 1994). The presence of the pigments in the crude enzyme preparations may some time hinder the improvement in brightness of the paper, and therefore use of partially purified enzymes is the suggested approach.

An appreciable improvement in physical properties of the handsheets prepared with selected enzymes in this study was observed. In fact the observed levels of improvement were much higher as compared to those reported by Pala et al. (2004). However, the observed increases in tensile index and burst index may be attributed to inter-fiber bonding that are characteristic of furnishes from OMG, as used in the present study. A recent patent reported enzymatically deinked paper with 50 to 150% increased tensile index (Lonsky and Negri 2003). Our study showed that rigorous and systematic screening of suitable microbial sources of enzymes can be useful in developing efficient deinking technologies. Further work on the purification of mono-component enzymes and their role in deinking from *Aspergillus terreus* AN₁ and *Aspergillus* sp, AMA, as well as improvement of strains by protoplast fusion, cloning and over expression, etc. for achieving higher enzyme titres, is in progress.

ACKNOWLEDGEMENT

The funding of this research project to BSC by the Department of Biotechnology, Ministry of Science & Technology, Government of India, is duly acknowledged.

REFERENCES CITED

- Arifoglu, N., and Ogel, Z. B. (2000). "Avicel adsorbable endoglucanases production by thermophilic fungus *Scytalidium thermophilum* type culture *torula thermophila*," *Enz. Microb. Technol.* 27, 560-569.
- Badhan, A. K., Chadha, B. S., Kaur, J., Saini, H. S., and Bhat, M. K. (2007). "Production of xylanolytic and cellulolytic enzymes by thermophilic fungus *Myceleophthora* sp. IMI387099," *Biores Technol.* 98, 504-510.
- Cooney, D. C., and Emerson, R. (1964). In: *Thermophilic fungus: An Account of their Biology, Activities and classification*. W. H. Freeman and Co., San Francisco, pp-1-88.
- Elegir, G., Panizza, E., and Canetti, M. (2000). "Neutral enzyme assisted deinking of xerographic office waste with cellulose/amalase mixture," *Tappi. J.* 83, 11-71.
- Geng, X., and Li, K. (2003). "Deinking of recycled mixed office paper using two endoglucanases, Cel B and Cel E, from the anaerobic fungus *Orpinomyces* PC-2," *Tappi. J.* 2, 29-32.
- Ghatora, S. K., Chadha, B. S., Saini, H. S., Bhat, M. K., and Craig, F. (2006). "Diversity of plant cell wall esterases in thermophilic and thermotolerant fungi," *J. Biotechnol.* 125, 434-445.
- Gubitz, G. M., Mansfield, S. D., Bohm, D., and Saddler, J. N. (1998). "Effect of endoglucanases and hemicellulases in magnetic and flotation deinking of xerographic and laser-printed paper," *J. Biotechnol.* 65, 209-215.
- Harrison, M., Nouvenes, A., Jardine, D., Zachara, N., Googly, A., Nevalainen, H., and Packer, N. (1998). "Modified glycosylation of cellobiohydrolase I from a high cellulase-producing mutant strain of *Trichoderma reesi*," *Eur. J. Biochem.* 256, 119-127.
- Henrissat, B., Clarysens, M., Tomme, P., Lemesla, L., and McRhan, J. P. (1988). "Cellulase families revealed by hydrophobic cluster analysis," *Gene* 81, 83-95.
- Jatinder, K., Chadha, B. S., and Saini, H. S. (2006 b). "Optimization of medium components for production of cellulases by *Melanocarpus* sp. MTCC 3922 under solid-state fermentation," *World. J. Microbiol. Biotechnol.* 22, 15-22.
- Jatinder, K., Chadha, B. S., and Saini, H. S. (2006a). "Optimization of culture conditions for production of cellulases and xylanases by *Scytalidium thermophilum* using response surface methodology," *World. J. Microbiol. Biotechnol.* 22, 169-176.
- Jeffries, T. W., Klungness, J. H., Sykes, M. S., and Rutledge, C. K. R. (1994). "Comparison of enzyme-enhanced with conventional deinking of xerographic and laser-printed paper," *Tappi J.* 77, 173-179.
- Lonsky, W. F., and Negri, A. R. (2003). "Enzymatic treatment of pulp to increase strength using truncated hydrolytic enzymes," *US Patent* 6635146.

- Marques, S., Pala, H., Alves, L., Amaral-Collaco, M. T., Gama, F. M., and Gino, F. M. (2003). "Characterization and application of glycanases secreted by *Aspergillus terreus* CCM 1498 and *Trichoderma viride* CCM 184 for enzymatic deinking of mixed office waste paper," *J. Biotechnol.* 100, 2009-2019.
- Miller, G. L. (1959). "Use of dinotrosalicylic acid reagent for determination of reducing sugar," *Anal. Chem.* 31, 420-428.
- Morkbak, A. L., and Zimmermann, W. (1998). "Deinking of mixed office wastepaper, old newspaper and vegetable oil based ink printed paper using cellulases, xylanases and lipases," *Prog. Paper Recycling* 7, 14-21.
- Nichat, B. M. (2003). "Deinking-An environment friendly process," *TCE World*, 1-31.
- Pala, H., Mota, M., and Gama, F. M. (2004). "Enzymatic versus chemical deinking of non-impact ink printed paper," *J. Biotechnol.* 108, 79-89.
- Parry, N. J., Beever, D. E., Owen, E., Vandenbergbe, I., Beeumen, J. V., and Bhat, M. K. (2001). "Biochemical characterization and mechanism of action of thermophilic β -glucosidase purified from *Thermoascus aurantiacus*," *J. Biochem.* 353, 117-127.
- Prasad, D. Y., Heitmann, J. A., and Joyce, T. W. (1992). "Enzyme deinking of laser and xerographic office wastes," *Appita J.* 46, 289-292.
- Qin, M., Gao, P., Yinbo, Q., Fu, Y., Shao, Z., and Quan, W. (1998). "Physical characteristics of enzymatically modified fibers from old newsprint," In: *Proc. Int. Symp. Emerging Technol. in Pulping Papermaking Fast-Grow Wood*, pp. 462-473.
- Sonia, K. G., Chadha, B. S., and Saini, H. S. (2005) "Sorghum straw for xylanase hyper-production by *Thermomyces lanuginosus* (D₂W₃) under solid-state fermentation," *Biores. Technol.* 96, 1561-1569.
- Sreenath, H. K., Yang, V. W., Burdsall, H., and Jefferies, T.W. (1996). "Toner removal by alkaline active cellulases from desert *Basidiomycetes*," In: *Enzymes for pulp and paper Processing. American Chemical Society*, pp. 207-219.
- Viestures, U., and Leitte, M. (1999). "Pulp and waste paper bleaching using xylanases and other enzymatic complexes," In: *Latvian State Institute of Wood Chemistry Year Book*, pp 49-50.
- Vyas, S., and Lachke, A. (2003). "Biodeinking of mixed office waste paper by alkaline active cellulases from alkalotolerant *Fusarium* sp.," *Enz. Microb. Technol.* 32, 236-245.
- Watson, T. (1988). "Magazine waste paper may have future as newsprint," *Resource and Recycling* pp.18-19.
- White, T. J., Bruns, T., Lee, S., and Taylor, J. (1990). "Amplification and direct sequencing of fungal ribosomal RNA genes for phylogenetics," In: M. Innis (ed), *PCR Protocols: A Guide to Methods and Applications*. Academic Press. San Diego, pp. 315-322.
- Wood, T. M., and Bhat, K. M. (1988). "Methods for measuring cellulase activities," *Methods Enzymol.* 160, 87-112.
- Yang, J. L., Ma, J., Pierce, J. M., and Eriksson, K. L. (2004). "Composition for enzymatic deinking of waste paper," *US Patent* 6,767,728.

Article submitted: Dec. 12, 2008; Peer-review completed: Jan. 24, 2008; Revision received and accepted: Feb. 4, 2008; Published: Feb. 6, 2008.

PREPARATION OF MACROPOROUS CELLULOSE-BASED SUPERABSORBENT POLYMER THROUGH THE PRECIPITATION METHOD

Yu Chen,* Yun-fei Liu, and Hui-min Tan

Superabsorbent polymer was prepared by graft polymerization of acrylic acid onto the chain of carboxymethyl cellulose. This superabsorbent polymer was further treated by the solvent precipitation method. We found that the water absorption rate of the treated polymer was greatly increased and the microstructure of the treated polymer was changed from close-grained structures to loose macropores. The swelling processes of the polymers before and after modification fit first-order dynamic processes. The amount of the residual acrylic acid was detected through high performance liquid chromatography (HPLC) with aqueous solution of MOPS of 0.02mol/L (pH=5.70) as the mobile phase. It was found that the amount of the residual acrylic acid decreased from $83.8 \times 10^{-4} \%$ to $6.7 \times 10^{-4} \%$ after treatments.

Keywords: Carboxymethyl cellulose; Superabsorbent polymer; Macropores; Precipitation method

Contact information: School of Material Science and Engineering, Beijing Institute of Technology, Beijing 100081 P. R. China *Corresponding author: cylvy@163.com

INTRODUCTION

Superabsorbent polymers can be described as having a network structure and a moderate degree of crosslinking (Omidian et al. 2005). They can absorb a large amount of water, considerably more than their dry mass. The amount of the absorbed water can range from hundreds of times to thousands of times that of the polymer. These polymers have been extensively used as absorbents in personal care products, such as infant diapers, feminine hygiene products, and incontinence products (Li et al. 2007; Suo et al. 2007; Zhang et al. 2006; Peng et al. 2008). They have also received considerable attention for a variety of more specialized applications, including matrices for enzyme immobilization, bioabsorbents in preparative chromatography, materials for agricultural mulches, and matrices for controlled release devices (Hany 2007; Marcos et al. 2005).

Some natural polymers, such as cellulose or starches, can be prepared as superabsorbent polymers through radical graft polymerization with vinyl monomers and proper crosslinking (Li et al. 2007; Suo et al. 2007; Zhang et al. 2006; Peng et al. 2008). Our research group also has reported the preparation of a superabsorbent polymer by graft copolymerization of sodium acrylate and acrylamide along the chain of carboxymethyl cellulose (Li and Tan 2003; Li et al. 2006). Because of their very good biocompatibility, superabsorbent polymers based on natural polymers are expected to be widely used in many applications such as medical materials, sanitary products, controlled release devices, and matrices for enzyme immobilization (Sannino et al. 2003; Lionetto et al. 2005).

For superabsorbent polymers used as medical and sanitation materials, they must have high absorption rates and low residual levels of toxic chemicals. Usually, the porous superabsorbent polymers are prepared by adding chemical reagents to produce bubbles in

the polymer. Although high water absorption rates have been observed (Chen et al. 1999; Park et al. 1998) in those superabsorbent polymers, toxic chemicals are introduced during this process. In this study, the superabsorbent polymer was modified through novel physical methods, based on the solvent precipitation method. The processes were simple and the results were dramatic. The absorption rate of the polymer was increased greatly, and the amount of residual monomer was decreased markedly. These modification methods have not been reported before. They are likely useful in the preparation of high quality superabsorbent polymers.

EXPERIMENTAL

Materials

Carboxymethyl cellulose (CMC) was supplied by Hebei Maoyuan Chemical Industry Co., Ltd (China). It has a viscosity at 25 °C of 140 ± 60 mPa·s as a 2% aqueous solution, and at a degree of substitution of 0.82. Acrylic acid (AA, Analytical Reagent) was purchased from Tianjin Chemical Reagent Institute (China) and purified by reduced pressure distillation before the polymerization. Ammonium persulfate (APS, Analytical Reagent) was used as the initiator and N, N'-methylene diacrylamide (MBAM, Analytical Reagent) was used as the crosslinking agent. Ethanol and sodium hydroxide are analytical reagents and used as received.

Preparation of the Superabsorbent Polymer

Carboxymethyl cellulose (1.2 g) was dissolved in a specified amount of water and then added into a three-necked flask, which was equipped with a stirring apparatus and a reflux condenser. The solution was stirred for 30 min under the protection of nitrogen and then heated by a water bath of 60 °C. A certain amount of APS (0.3 g) dissolved in a moderate amount of deionized water was slowly added into the flask to initiate the graft polymerization. 12 g acrylic acid neutralized to 50% and 0.45g MBAM were added 30 min later. The total volume of water in the system was controlled at a certain level, whereas the stirring speed was fixed. After reacting for 5h, air was introduced into the reactor to cool down the flask and stop the reaction. The product was precipitated by pouring alcohol into the reaction mixture. The precipitate was filtered, washed thoroughly with the ethanol/water mixture (4:1, v/v) for several times under high-speed stirring, and then soaked with the ethanol/water mixture (4:1, v/v) for 24 h. The product was collected by filtration and dried under vacuum. (Found: $v_{\max}(\text{KBr})$ 3430, 2931, 2560, 1720, 1589, 1450, 1421, 1170, 1040, and 819 cm^{-1})

Treatment of the Superabsorbent Polymer by the Precipitation Method

The superabsorbent polymer (1.0 g) of 80 mesh size was added into 150 ml distilled water. It was allowed to swell during agitation in a water bath at the constant temperature of 25 °C for 48 h. The polymer was recovered by precipitation with ethanol. The precipitate was filtered and dried under vacuum at 60 °C.

Characterization

Test of the water absorption capability

To test the water absorption capability, 0.100 g of the superabsorbent polymer was placed into a sieve pouch. The pouch was then immersed into the distilled water to swell. After a suitable period, the sample was taken out from the water. After removing

the excess water, the weight of the swollen polymer was measured. The swelling ratio (Q , g/g) is calculated by:

$$Q = (m_2 - m_1) / m_1 \quad (1)$$

where m_1 is the weight of the dry superabsorbent polymer, and m_2 is the weight of the swollen superabsorbent polymer.

Determination of the residual acrylic acid

Acrylic acid was detected by HPLC. The Agilent 1100 series HPLC instrument (Agilent Technologies, USA) equipped with a wavelength adjustable UV detector and the chemical workstation software was used. The column was the Diamonsil™ (Diamond)-C18 (5 μ , 250 \times 4.6mm). MOPS aqueous solution of 0.02 M with pH= 5.70 was used as the mobile phase, and the flow rate was 0.8 ml/min. The detection wavelength was 210 nm and the injection volume was 20 μ l.

Dried superabsorbent polymer (0.100 g) was accurately weighed and added to 10 ml 0.9% normal saline. The mixture was agitated on an oscillator at room temperature for 2 h. Then it was filtered with a filter paper. The filtrate liquid was collected and used for HPLC analysis.

Scanning electron microscopy (SEM) examination

The surface structure of the superabsorbent polymer before and after the processing was viewed with a scanning electron microscope (QUANTA200, Philips—FEI Co., Netherlands). The samples were coated with Au prior to SEM observation.

RESULTS AND DISCUSSION

Effect of the Treatments on the Water Absorption Rate of the Polymers

The water absorption rates of the polymers were increased greatly after further treatments by the solvent precipitation method. It can be seen from Fig. 1 that it took about 45 min to reach the steady state of absorption before treatments. For the polymer treated with solvent precipitation method, the water absorption rate reached steady state in just 10 min.

On the assumption that the swelling of the polymer fits a first-order process (Liu et al. 1996), the swelling rate at a given temperature is:

$$dQ_t / dt = k(Q_e - Q_t) \quad (2)$$

where t is the swelling time, Q_t is the swelling ratio at that time, and Q_e is the equilibrium swelling ratio. Eq. 1 can be integrated to:

$$\int_{Q_0}^{Q_t} dQ_t / (Q_e - Q_t) = \int_0^t k dt \quad (3)$$

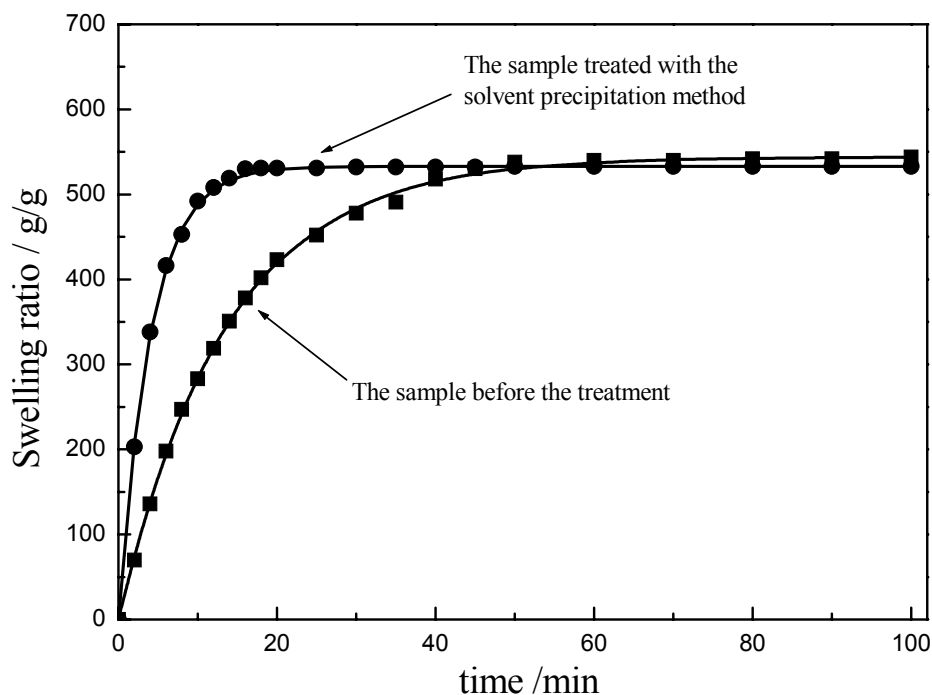


Fig. 1. Water absorption rates before and after treatments

The result is:

$$\ln[(Q_e - Q_0)/(Q_e - Q_t)] = kt \quad (4)$$

then the following equation is gained:

$$Q_t = Q_e - (Q_e - Q_0)/e^{kt} \quad (5)$$

The curve between $\ln[(Q_e - Q_0)/(Q_e - Q_t)]$ and t (the diagonal part of the water absorption curve) was drawn, and the slope was the swelling rate constant (k). The k value of the untreated sample was 0.074; the k values were 0.247 for the samples treated with the solvent precipitation method. The k values also indicated that the water absorption rates of the polymer were increased dramatically after treatments. The theoretical swelling curves of the polymer were obtained by introducing the k values into Equation 5 (the solid line in Fig. 1). The results of theoretical calculation and experiment data agreed well, indicating that the assumption of a first-order process was valid.

The microstructures of the polymers before and after treatments were examined by SEM (Fig. 2). The SEM photographs showed that the microstructures of the polymer were changed from the close-grained structure to loose macropores as the polymers underwent treatments. During the first step of the solvent precipitation method, the polymer was extensively swollen in water. When the organic solvent that is miscible with water was added, water was displaced from the network by the organic solvent. During this displacement process, the polymer retained its expanded porous structure. In

addition, the residual organic solvent left in the precipitated polymer was easily removed by vacuum drying, and the porous structure remained.

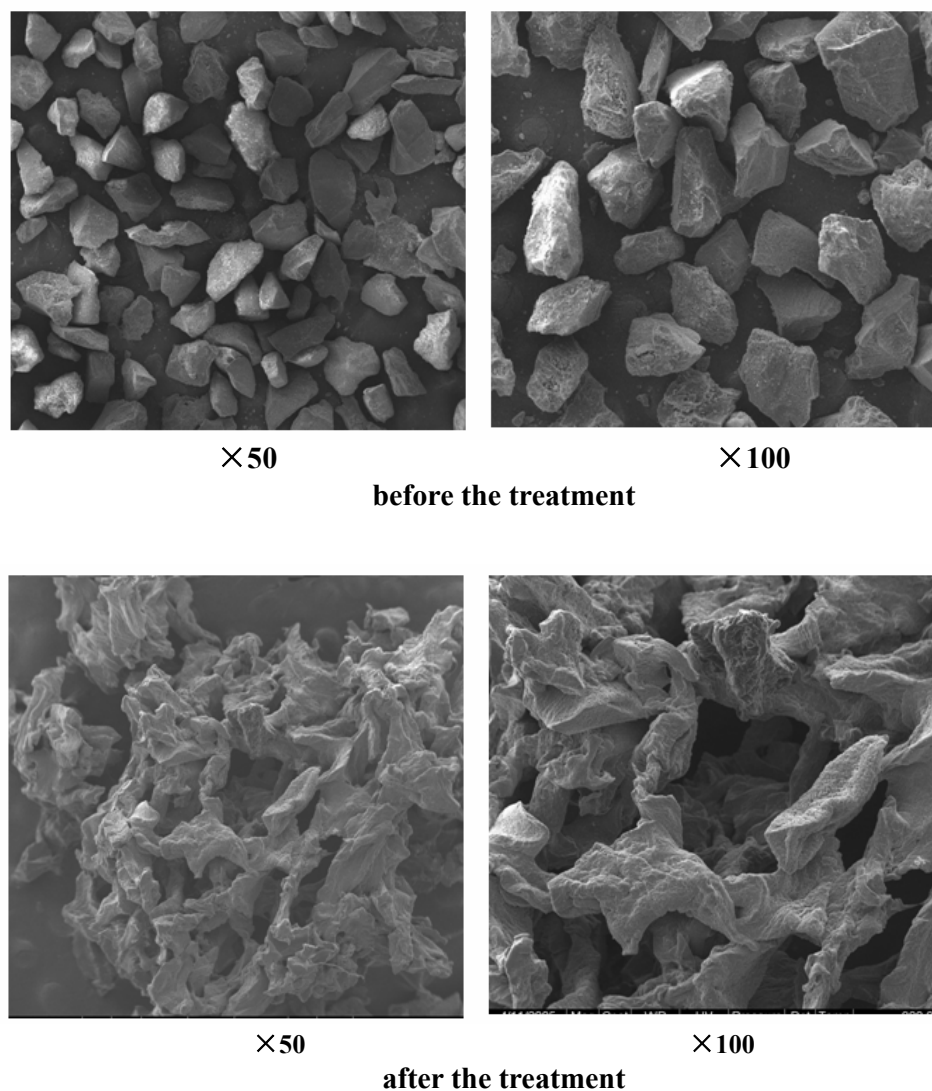


Fig. 2. SEM pictures of the polymer before and after treatments

With the increase of the mean pore size, The Na^+ ions move to the outside of the polymer more easily, and the hydrophilic $-\text{COO}^-$ groups attract more water molecules. Therefore, the water absorption rate of the polymer was enhanced greatly. Moreover, the distance between the polymer chains was increased, and the contractibility of the polymer was decreased, leading to an ultimate increase in the water absorption rate.

Effects of the Treatments on the Amount of the Residual Acrylic Acid Monomer

A standard calibration curve between the concentration of acrylic acid and the area of the chromatographic peak was generated by analyzing a series acrylic acid aqueous solutions at 20, 10, 5, 2, 1, 0.5, 0.2, 0.1, and 0.05 $\mu\text{g/ml}$ by HPLC (Fig. 3). The

relationship between them was expressed as,

$$y = 24.62057 + 152.87579 x \quad (6)$$

where y is the area of the chromatographic peak, x is the concentration ($\mu\text{g/ml}$) of the acrylic acid, and $R=0.99981$.

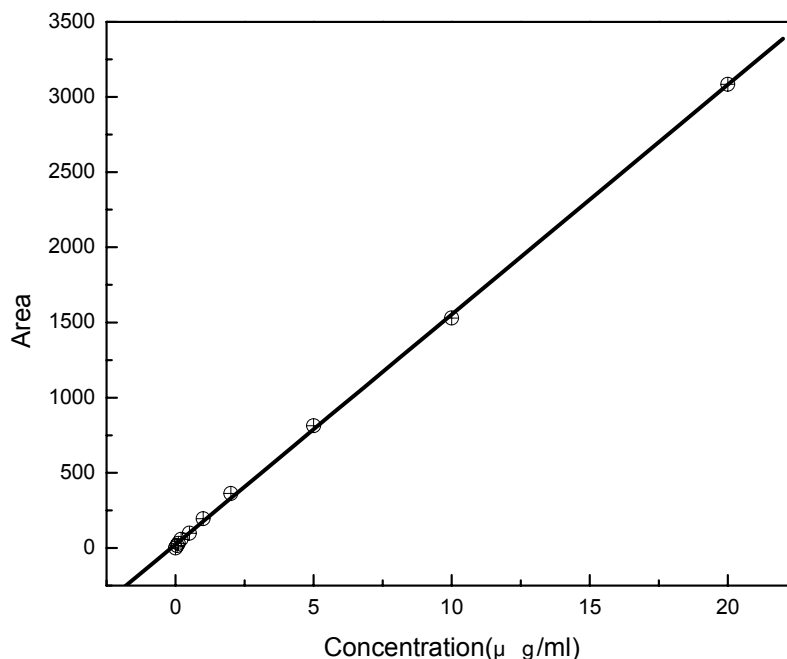


Fig. 3. The standard curve between concentrations of acrylic acid and areas of the chromatographic peak.

Because of the special network structure of the superabsorbent polymers, acrylic acid monomers are easily trapped inside the polymer. To be used as medical materials and sanitarian materials, the amount of the residual monomer must be kept as low as possible. We used solvent precipitation to remove the residual acrylic acid and HPLC to detect it.

It can be seen from the Fig. 4 that the amount of the residual acrylic acid was decreased markedly after treatments with the solvent precipitation method (the amount was decreased from $83.8 \times 10^{-4} \%$ to $6.7 \times 10^{-4} \%$). This dramatic decrease was because, during the process of treatment, the network of the polymer was swollen fully, and the residual hydrophilic acrylic acid monomer was diffused from the network to the water. Moreover, because a large excess of water was added to swell the polymer, even after organic solvent precipitation, few monomers were trapped in the polymer.

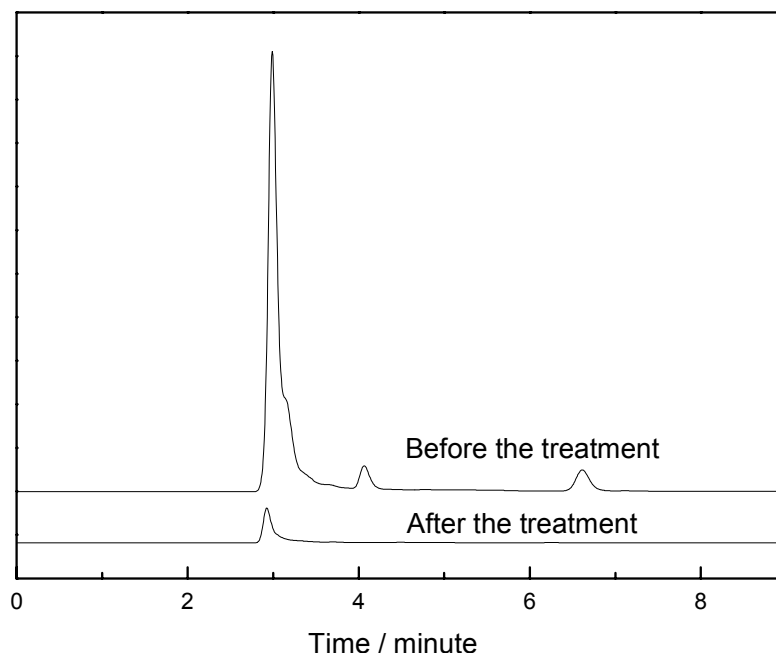


Fig. 4. HPLC diagrams of residual acrylic acid in polymers before and after treatments

CONCLUSIONS

1. A novel superabsorbent polymer was prepared by graft copolymerization of sodium acrylate onto the chain of carboxymethyl cellulose. The superabsorbent polymer was further treated with the solvent precipitation method.
2. The water absorption rate of the polymer was increased greatly as the microstructure of the polymer was changed from a close-grained structure to a loose macroporous structure after the treatments. The water absorption process of the polymers with and without treatments fit a first-order dynamic process.
3. The amount of the residual acrylic acid was detected through high performance liquid chromatography (HPLC) with the aqueous solution of MOPS of 0.02mol/L (pH=5.70) as the mobile phase. It was found that the amount of the residual acrylic acid decreased from $83.8 \times 10^{-4} \%$ to $6.7 \times 10^{-4} \%$ after treatments.
4. The process of this method is simple and the results are very obvious. Moreover, the procedure and results have not previously been reported. The superabsorbent polymers prepared through this method appear to be suitable for medical applications, in which high water absorption rate and low amount of harmful residual monomer are expected to be important.

ACKNOWLEDGMENTS

The authors are grateful for the support of the Natural Science Foundation of China (No. 50773005) and the basic study program of Beijing Institute of Technology (20060442004).

REFERENCES CITED

- Chen, J., Park, H., and Park, K. (1999). "Synthesis of superporous hydrogels: Hydrogels with fast swelling and superabsorbent properties," *Journal of Biomedical Materials Research* 44(1), 53-62.
- Li, J., Ma, F. G., and Tan, H. M. (2003). "Preparation and characterization of super absorbent resin from natural cellulose," *Journal of Beijing Institute of Technology*, 12(3), 312-315.
- Li, J., Wu, H. Y., and Tan, H. M. (2006). "Cytocompatibility evaluation of materials from cellulose," *Transaction of Beijing Institute of Technology* 26(3), 276-278.
- Hany, E. H. (2007). "Synthesis and water sorption studies of pH sensitive poly(acrylamide-co-itaconic acid) hydrogels," *European Polymer Journal* 43(11), 4830-4838.
- Marcos, R. G., Adriano, V. R., and Edvani, C. M., et al. (2005). "Synthesis of a novel superabsorbent hydrogel by copolymerization of acrylamide and cashew gum modified with glycidyl methacrylate," *Carbohydrate Polymers* 61(4), 464-471.
- Omidian, H., Rocca, J. G., and Park, K. (2005). "Advances in superporous hydrogels," *Journal of Controlled Release* 102(1), 3-12.
- Park, K., Chen, J., and Park, H. (1998). "Superporous hydrogel composites: Synthesis, characterization, and application," *American Chemical Society, Polymer Preprints, Division of Polymer Chemistry*, 39(2), 192-193.
- Peng, G., Xu, S. M., and Peng, Y., et al. (2008). "A new amphoteric superabsorbent hydrogel based on sodium starch sulfate," *Bioresource Technology* 99(2), 444-447.
- Sannino, A., Esposito, A., De Rosa, A., et al. (2003). "Biomedical application of a superabsorbent hydrogel for body water elimination in the treatment of edemas," *Journal of Biomedical Materials Research - Part A* 67(3), 1016-1024.
- Suo, A. L., Qian, J. M., and Yao, Y., et al. (2007). "Synthesis and properties of carboxymethyl cellulose-graft-Poly(acrylic acid-co-acrylamide) as a novel cellulose-based superabsorbent," *Journal of Applied Polymer Science* 103(3), 1382-1388.
- Li, A., Zhang, J. P., and Wang, A. Q. (2007). "Utilization of starch and clay for the preparation of superabsorbent composite," *Bioresource Technology* 98, 327-332.
- Lionetto, F., Sannino, A., and Maffezzoli, A. (2005). "Ultrasonic monitoring of the network formation in superabsorbent cellulose based hydrogels," *Polymer* 46(6), 1796-1803.
- Liu, M. Z., Cheng, R. S., and Qian, R. Y. (1996). "Investigation of swelling property of poly(vinyl alcohol) hydrogel," *Acta Polymer Sinica* 2, 234-239.
- Zhang, J. P., Li, A., and Wang, A. Q. (2006). "Study on superabsorbent composite. VI. Preparation, characterization and swelling behaviors of starch phosphate-graft-acrylamide/attapulgite superabsorbent composite," *Carbohydrate Polymers* 65(2), 150-158.

Article submitted: Jan. 8, 2008; Peer review completed: Feb. 1, 2008; Revised version received and accepted: Feb. 4, 2008; Published: Feb. 5, 2008.

SOUTH AMERICA: INDUSTRIAL ROUNDWOOD SUPPLY POTENTIAL

Ronalds W. Gonzalez,^{a*} Daniel Saloni,^a Sudipta Dasmohapatra,^a and Frederick Cubbage^b

South America has substantial potential to expand its forest plantations and raw material supply. From 1997 to 2005, South America had a high annual growth rate in the production of industrial roundwood, with Brazil and Chile being the most important countries. In the same period, Asia had the only negative regional production growth rate in the world, and China became the largest round wood importer in the world. This paper summarizes the status of production, consumption, imports, and exports of industrial roundwood and forest products in South America. Production and exports from South America have continually increased at annual growth rates exceeding the forestry sector in general and the U.S. in particular. Based on timber growing investments to date, a strong timber production and forest products manufacturing sector has developed in the Southern Cone countries of Chile, Brazil, Argentina, and Uruguay, and is increasing in other countries in Latin America. There will be continued opportunities for forest plantations and new manufacturing facilities throughout South America, tempered somewhat by perceived country financial and political risks. These opportunities will allow South America to increase its share of world production and increase imports to North America and to Asia.

Keywords: Roundwood; Wood Trade; South America; China; India; Emerging Markets

Contact information: a: Forest Biomaterials Science and Engineering, North Carolina State University, P. O. Box 8005, Raleigh, NC 27695, USA; b: Department of Forestry and Environmental Resources, North Carolina State University, P. O. Box 8008, Raleigh, NC 27695, USA; *Corresponding author: ronalds@ureach.com

INTRODUCTION

The market of forest products world-wide is always dynamic, but is currently experiencing considerable changes due to the role that the emerging economies are playing. The imports of forest products by China grew from US\$ 5 billion to US\$ 20 billion (annually) in 16 years (1990-2005) (FAO 2007a). In addition, India's forest products imports grew from US\$ 0.8 billion to US\$ 2.3 billion in just seven years (1999-2005) (FAO 2007a). The message is clear that "there will be a need for more raw material and plantations to supply the increasing forest products world demand." It was estimated that around 50 to 100 million hectares of new forest plantations are needed to meet the world industrial wood demand by the year 2010 (Boyle 1999).

South America, comprising Argentina, Bolivia, Brazil, Chile, Colombia, Ecuador, French Guiana, Guyana, Peru, Paraguay, Uruguay, Suriname, and Venezuela, possesses considerable potential for the establishment of new plantations and for increasing its roundwood supply to support its domestic forest products manufacturing and exports.

Latin America had the highest annual increase in the world in industrial roundwood production from 1997 to 2005. Commodity industrial roundwood includes: saw logs or veneer logs, pulpwood, other industrial roundwood, and, in the case of trade, wood chips, wood particles, and residues as noted by FAO (FAO 2007 a).

Brazil and Chile are the largest forest product exporters in South America. Both generally have a positive balance in the trade of forest products, with exports greater than imports. On the other hand, Uruguay, while being the largest exporter of roundwood, ranks fourth in total exports of forest products commodities (FAO 2007a).

South America has a comparative advantage in developing new plantations and forest product industries based on fast growing exotic species, which have the greatest rates of returns in the Americas (Cubbage et al. 2007). Sedjo (1999) summarized how these plantations can help to meet the increasing timber demand, and the favorable situation has continued.

This paper analyzes existing secondary data of forest plantations and production in South America, assesses political and financial risks, and draws conclusions about the potential of South America to provide roundwood and manufactured products to North America and emerging economies in Asia. We synthesize literature from various UN FAO reports and summarize data collected from other industry trade sources from Latin America in order to analyze region-wide opportunities and the merits of individual countries in South America.

DEMAND, PRODUCTION, AND EXPORTS

The emerging economies in Asia are changing the face of the world forest products market. The shortage of available fiber and timber resources, the expanding middle-income economy, and the potential for export manufacturing has led to significant imports of raw materials by China and India. The growing imports of the two countries are creating extremely large structural shifts in the forest products trade; however, the effects on raw material availability and prices of the commodities are still unknown.

Industrial Roundwood Demand of the Emerging Markets

China leads the world in roundwood imports (with Japan in the second place) and the furniture exports. China imports roundwood and sawn wood from the UNECE region (United Nations Economic Commission for Europe), and production from China competes strongly with furniture manufacturers in Europe (FAO 2007(b)). China's imports of industrial roundwood grew from 6 million m³ in 1995 to 30.4 million m³ in 2005 (Fig. 1). Moreover, its imports of pulp for paper increased by 6.4 million tons during the same period. In addition, India imports of industrial roundwood in 2005 (ca. 4.6 million m³) were thirteen times the quantities imported in 1995, although this compared to a relatively low base (FAO 2007a).

The population of Asia is estimated to grow by nearly 2 billion people by 2050. The increase in population alone will mean a 148% increase in production of wood and paper products necessary by 2050 (Juslin and Hansen 2003). The growing demand coupled with the raw material deficit in this region is likely to continue to create

pressures on wood import increases. These increases, in fact, dominate world roundwood production, increasing from 40 million m³ in 1995 to 56 million m³ in 2005 (FAO 2007a). Exports in the rest of the world have changed much less, so China and India will continue to drive much of the new trade in roundwood and pulp in the future.

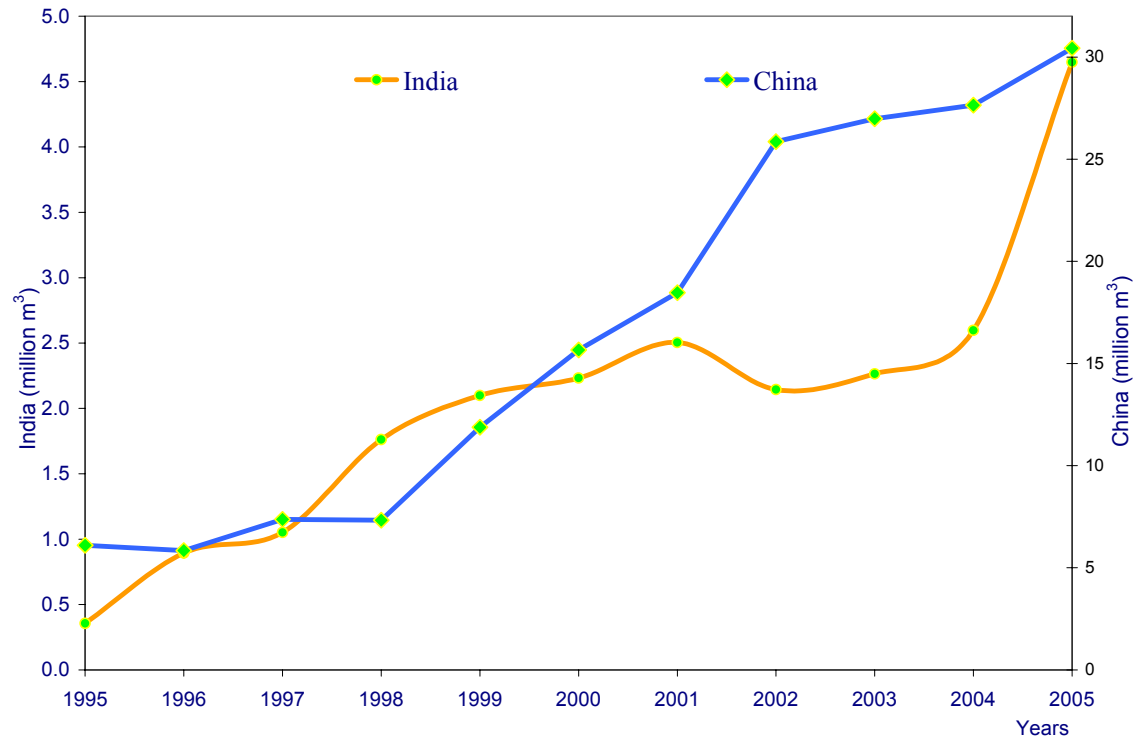


Figure 1. Imports of industrial roundwood-China and India (1995-2005)

Source: FAO, 2007a.

Production and Consumption of Industrial Roundwood in South America: Methodology

A database for South America with information on consumption of industrial roundwood for Argentina, Bolivia, Brazil, Chile, Colombia, Ecuador, Guyana, Peru, Paraguay, Uruguay, Suriname, and Venezuela was developed for different periods. The consumption was estimated as follows:

$$AC = NP + IMP - EXP \quad (1)$$

where:

AC = Apparent Consumption (m³)

NP = National Production (m³)

IMP = Imports (m³)

EXP = Exports (m³)

In addition, the database includes relevant information such as population, gross domestic product (GDP in US\$) and the trade of some commodities between the U.S. and

South American countries. For these, the per capita value was calculated, by dividing each one of them by the size of the population for the corresponding year and country. The database was built by processing and combining online information from the Food and Agriculture Organization of the United Nations (FAO 2007a), the United States International Trade Commission, and the reports of national forestry associations in selected South American countries (BRACELPA 2007; CORMA 2007; INFOR 2007).

The average annual change in the data over time is inherently an exponential function. Accordingly, it was estimated using the price indices method as described by Cubbage and Davis (1986). A log-linear least square regression was performed in order to obtain the slope of the exponential function. The general formula is as follows:

$$\text{Log } (P_n) = \text{Log } (P_o) + n \log (1+i) \quad (2)$$

$\text{Log } (P_o)$ and $\log (1+i)$ are constants, so this equation is of the form:

$$y = a + bx \quad (3)$$

where:

$y = \log (P_n)$ is the dependent variable

$x = n$ is the independent variable

$b = \log (1+i)$ is the slope

$a = \log (P_o)$ is the intercept

To find the annual increase rate the antilog of the slope is calculated and subtracted from (1).

Trends in Production and Consumption

Analyzing the trends from the data reveals several key points. Figure 2 illustrates the South American production and its world share; both variables show a steady growing trend. In 2005, the world production of industrial roundwood was about 1.7 billion m^3 , of which 10% (174.8 million m^3) was accounted for by South America (FAO, 2007a). In the same year, the world share of production for North and Central America, Europe, Asia, Africa, and Oceania were 37%, 32%, 14%, 4%, and 3%, respectively.

As calculated using equation 2, the annual increase in production (%) in the period from 1961 to 2005 was 4.5%, indicating that in 20 years South America has almost doubled its share of world production. During the period from 1997 to 2005, the region showed the highest interannual growing rate in the globe, followed by Europe. The region with the lowest increase in production was Africa, and the only region that experienced a decrease was Asia, at 1.17% percent per year (Fig. 3).

Figure 3 indicates that among countries in South America, Brazil and Chile accounted for up to 95% of the increase in production of industrial roundwood. Certainly, the production of industrial roundwood, sawnwood, wood-based panels, and fiberboard is expected to increase at a consistent rate until 2020 in Brazil and Chile as well as other countries in South America as result of significant planned investments in plantations by both governments, and by local and international companies in the region

(Zhang 2007). This increase in wood production in the region, combined with investments in new and expansion in existing facilities, have led South America to increase paper production by 27% in just 6 years, 2000-2005 (Gonzalez and Rojas 2007; Rojas and Gonzalez 2007).

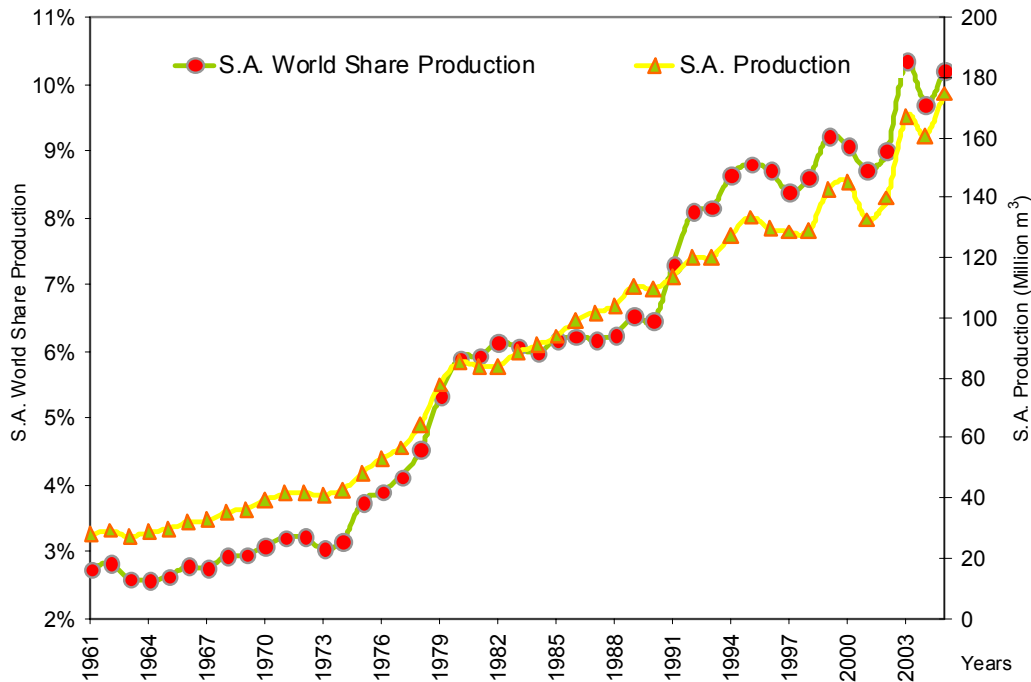


Figure 2. Production of industrial roundwood in South America (1961-2005). Source: FAO, 2007a

Figure 4 shows the consumption and production of industrial roundwood by country in South America. Brazil has about 68% of the total production and consumption in the region, followed by Chile and Argentina. These three countries account for about 92% of the total share of industrial roundwood production in the region. On average, most of the countries consume what they produce, with the exception of Uruguay, where the production is 34% more than its consumption. Uruguay, therefore, is the leading exporter of roundwood, mostly hardwood, in the region. A comparison of the proportion of softwood vs. hardwood for the major producer countries in South America shows that softwoods dominate in Chile (79%) and Argentina (62%), and hardwood production is the highest in Brazil (63%) (Fig. 4).

Chile has the highest annual per capita consumption (2.2 m³ per person) of industrial roundwood among all countries in South America (Fig. 5). The country houses the two largest (by sales in 2006) forest products companies in South America (Arauco and CMPC, respectively). Investments in modern production technologies by these and other forest products businesses, high levels of infrastructure development, plantation development, and extensive domestic and export markets have contributed to the high consumption. Chile is the second largest exporter of forest products in South America (Table 1), with cellulose as the largest export commodity, followed by wood products

(CORMA 2007). As shown in Fig. 5, Uruguay, Paraguay, and Brazil rank next to Chile in annual per capita consumption levels (between 0.66 and 0.63 m³).

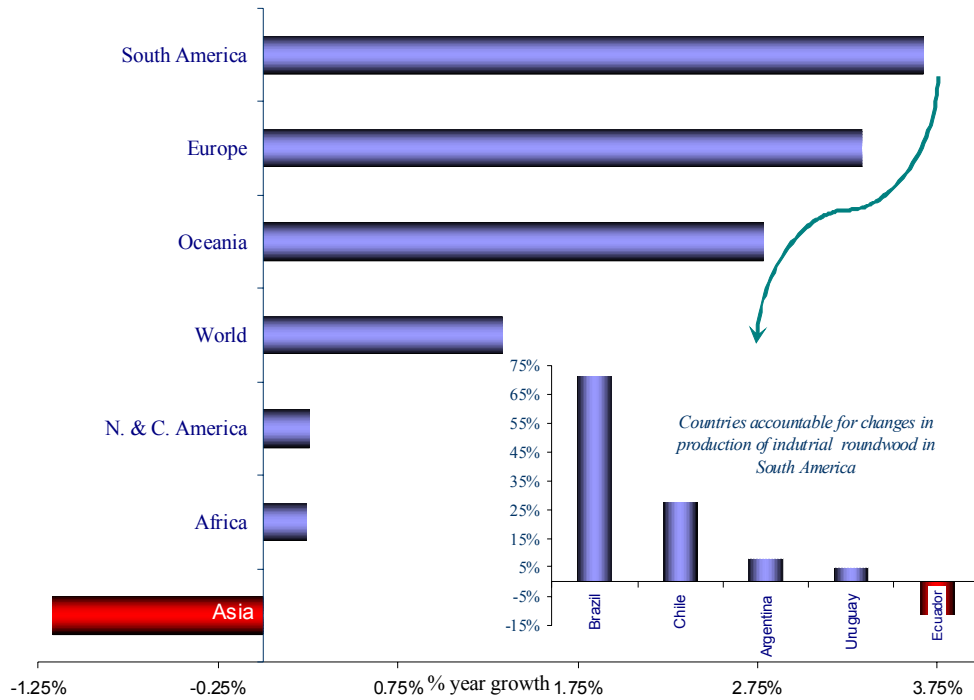


Figure 3. Annual production increase by region (1997-2005)
Source: Data from FAO, 2007a.

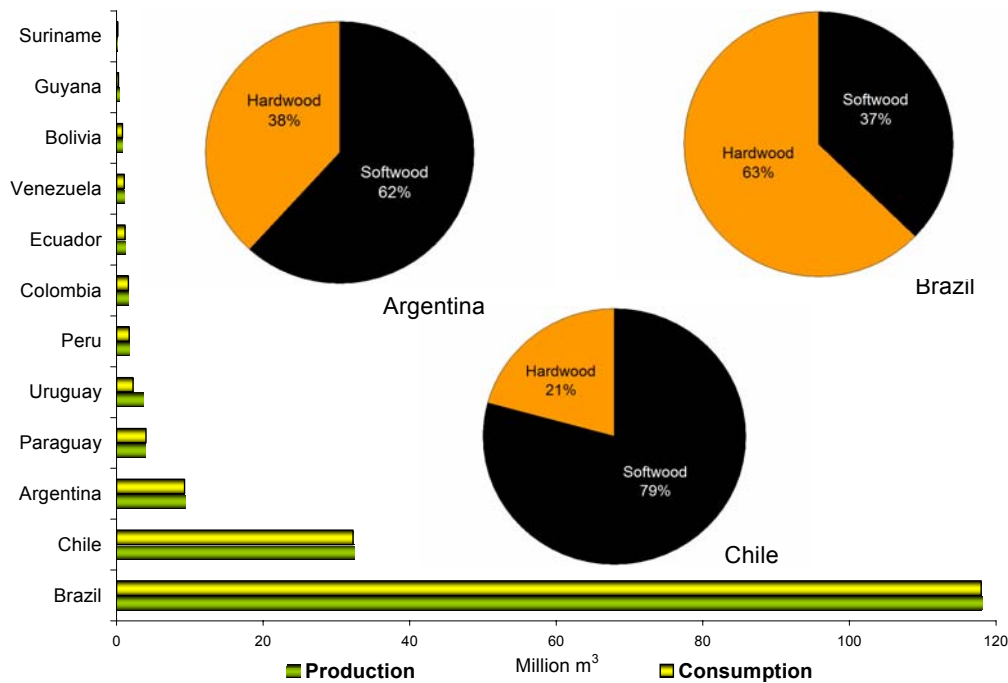


Figure 4. Production and consumption of industrial roundwood by country in South America (2003). Source: FAO, 2007a.

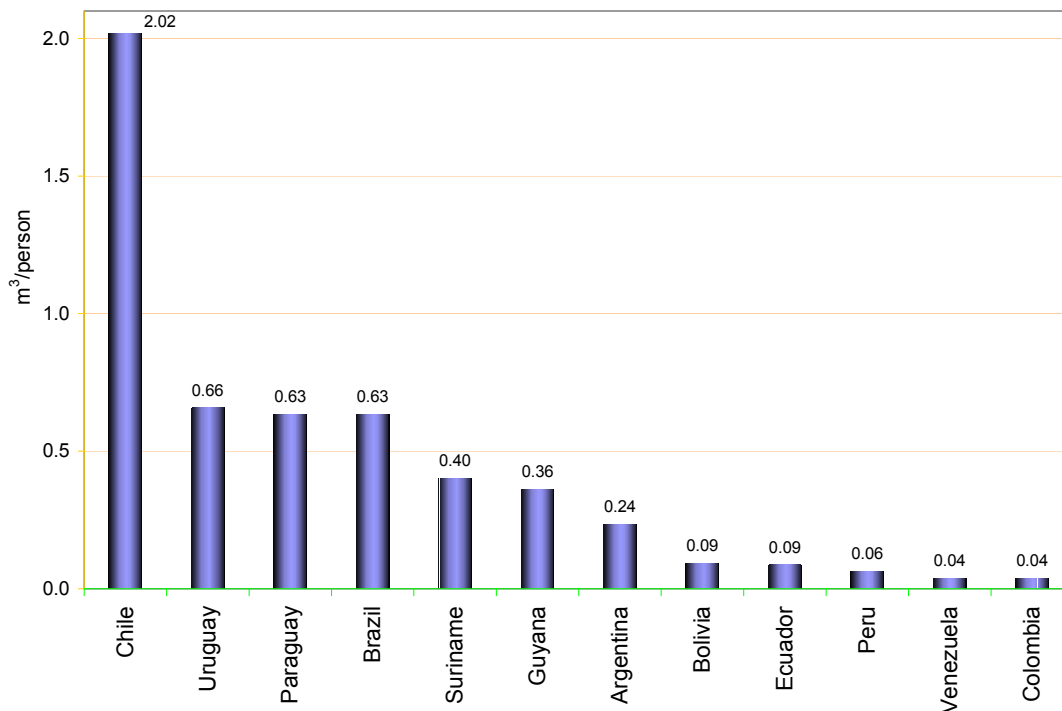


Figure 5. Per capita consumption of industrial roundwood by country in South America (2005)
Source: FAO, 2007a.

Industrial Roundwood and Forest Products Trade

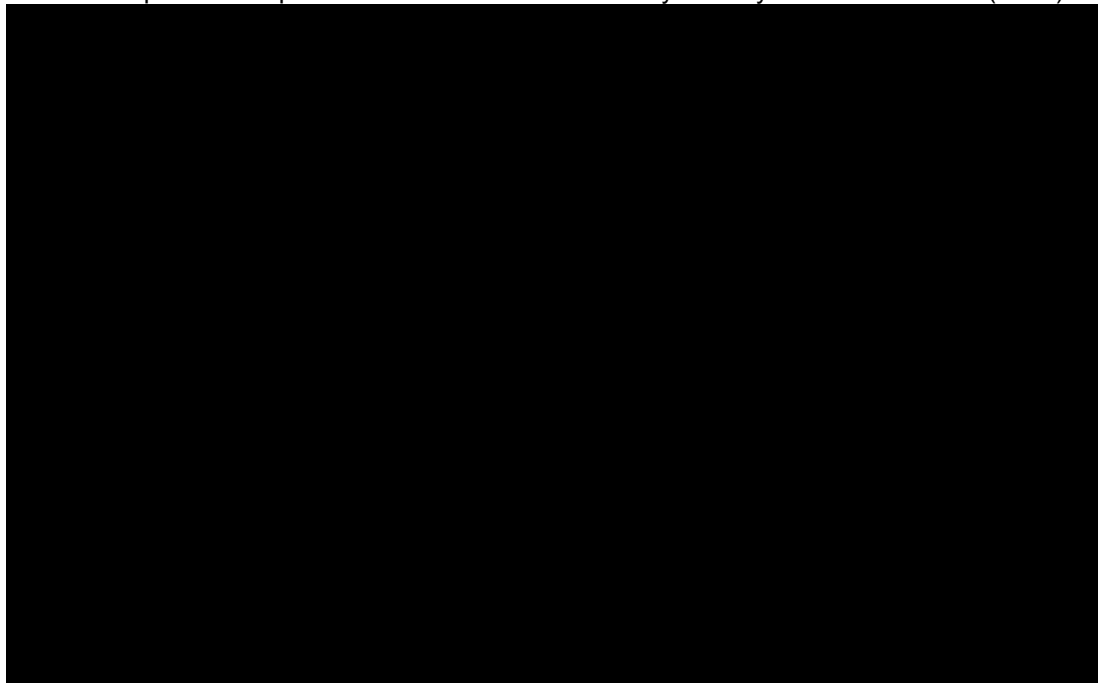
Over the last two decades, South America has increased its trade of forest products as a result of the abundantly available fiber from its maturing plantations and reduced trade barriers.

Uruguay is the largest exporter of industrial roundwood in the region, with about 1.5 million m³ per year (Table 1). Uruguay's roundwood exports currently constitute mostly hardwood timber (*Eucalyptus* sp.), but there are large areas of softwood plantations (*Pinus taeda*) that will mature in the next few years as well. The availability of the Eucalyptus timber and fiber in Uruguay is the basis for the recent announcement for the development of three pulp mill plants in this region, with a combined production of about 3 million tones per year of commercial pulp (Various sources including newspaper articles and personal communication with companies, June 2007). Of these proposed constructions, at least one pulp mill is receiving strong opposition (including a challenge in the world court) from Argentina for environmental and other reasons. If the capacity from the three new mills is realized, Uruguay will rank third among the countries in pulp exports in South America.

Table 1 also illustrates the exports and imports (in US dollar) of forest products by country in South America. Brazil and Chile account for about 87% of the exports from South America. In addition, these are the only two countries that show a positive balance in the trade of forest products. Brazil is one of the major suppliers of hardwood chips to the U.S. The total import values of Brazilian wood chips into the U.S. (hardwood-Eucalyptus) rose from almost none in 2002 to more than US\$ 25 million in

2004 (USITC 2007). The surge in chip imports was an expected response to domestic price increases resulting from local scarcity of hardwoods in the United States. In addition, *Eucalyptus sp.* chips are a highly preferred fiber source for some paper grades over native hardwood chips. The extent of hardwood chip imports to the U.S. from South America is unknown in the future; however, the price ceiling by the chip imports from South America will play an important role in defining the U.S. Southern hardwood stumpage price in the future (Wear et al. 2007). Argentina, Uruguay, Columbia are the third, fourth, and fifth largest countries in terms of their exports of forest products. Among forest products exports, wood pulp accounted for approximately US\$ 3.5 billion in 2005. The Southern U.S. was the most important market for the wood pulp. Other forest products exports include sawnwood and panels that find markets in Europe, North America and Asia. The U.S. import of lumber from South America has been relatively minimal between 1994 and 2005, albeit, increasing steadily. The U.S. imported approximately 1.8 million m³ of softwood lumber in 2005 from South America (Wear et al. 2007).

Table 1. Export and Import Values of Forest Products by country in South America (2005)



Source: FAO, 2007 (a).

Brazil, Argentina, and Columbia account for the largest imports of forest products in the region. These three countries account for 71% of the total amount imported by South America. Paper and paper products such as newsprint, coated paper, and magazine paper account for a substantial amount of imports into this region because of the immaturity in the consumer markets in this region.

FOREST PLANTATIONS

The forest industry in South America is based largely on growth and harvest of forest plantations, consisting mostly of exotic hardwood and softwood species. Natural advantages offered by deep and fertile soils, adequate to plentiful rainfall, almost year-long growing seasons, and advanced silvicultural practices have contributed to South America's leadership in commercial plantation forestry. This region has continued opportunities for establishment of new forest plantations. These opportunities are fueled by the aforementioned factors, coupled with a better ability of the region to establish very well known fast growing exotic species (such as *Eucalyptus* sp, *Gmelina* sp, *Pinus* sp, etc.), moderate land and forest management costs, enhanced research and development, and increasing political stability in most countries. These factors have helped to attract timberland investors such as Timber Investment Management Organizations (TIMOs) and associated industries in the region.

Forest investments have attracted tens of millions of dollars of capital in the last decade, and investors world-wide are continuing to seek safe investments with reasonable rates of return. Uruguay and Brazil with plantations of *Eucalyptus grandis* have had the highest rates of return of all exotic and native forest plantations in the Americas (Cubbage et al. 2007). Moreover, forestry companies in Brazil are the leaders in managing Eucalyptus plantations. Years of research in tree improvement and silviculture have resulted in very fast growth and yields. For example, plantations of *Eucalyptus dunii* are harvested at 7 years old with a mean annual increment of 43 m³/ha/year. For comparison, in the 1980s, the average productivity of eucalyptus plantations in Brazil was about 24 m³/ha/year. Twenty five years later in 2005 the average productivity of *Eucalyptus* sp increased 63 percent to about 39 m³/ha/year (BRACELPA, 2007). Table 2 shows the rotation ages, growth, timberland costs, and rate of return for selected native and exotics plantation in the Americas (Cubbage et al. 2007). The highest rates of return are from plantations of *E. dunii* in Brazil and *E. grandis* in Uruguay (22.9 and 21.9 percent respectively). Plantations of *Pinus taeda* in Brazil produce 1.5 times more than the average production of the same species in the U.S. in a little over half of the time. The higher mean annual increments (MAI) in hardwoods occur in *Eucalyptus* sp. plantations in Brazil and Argentina (43 and 40 m³/ha/year), while the higher MAI in softwood are from *Pinus taeda* plantations in Argentina (35 m³/ha/year).

Brazil has perhaps taken the most advantage of exotic species. These plantations have allowed Brazil to expand its forest products industry rapidly, mostly with short fibers from Eucalyptus plantations. These species and *pinus* sp., to a lesser extent, also form the basis for the rapid growth of the forest products industry in Uruguay, Argentina, Colombia and Venezuela.

Table 3 shows the area under forest plantations in each country in South America in 2005. There are almost 12 million ha of plantations in South America. Most of the planted forest area is concentrated in Brazil, Chile and Argentina. Brazil ranks the highest with more than 5.3 million hectares of planted forest area, which is approximately twice that of Chile, which ranks second. Paraguay and Bolivia are at the end of the list with relatively smaller area under planted forests. The cost of forestland, which affects the returns greatly, varies considerably in the Americas. Values range from US\$ 800-1000/ha

in Argentina, Uruguay, and Venezuela to approximately US\$ 1500-2500/ha in Chile and Brazil.

Table 2. Growth, Timberland Cost and IRR% for Selected Exotic Plantations and Native Species in the Americas

Country	Species	Rotation (years)	Growth (m ³ /ha·yr)	Total yield per rotation (m ³)	Timberland cost (US\$/ha)	Internal rate of return * (%)
Argentina	<i>Pinus taeda</i> -Misiones	20	35	700	800	12.9
	<i>Eucalyptus grandis</i>	14	40	560		13.8
Brazil	<i>Pinus taeda</i>	18	30	540	2,500	16.0
	<i>Eucalyptus dunii</i>	7	43	301		22.9
Chile	<i>Pinus radiata</i>	22	22	484	1,500	16.9
	<i>Nethofagus dombayi</i>	30	18	540		13.6
Uruguay	<i>Pinus taeda</i>	22	20	440	1,000	15.1
	<i>Eucalyptus grandis</i>	16	30	480		21.9
Venezuela ¹	<i>Eucalyptus sp.</i>	6	28	168	1,000	19.0
USA	<i>Pinus taeda</i> planted	30	12	360	1,500	9.5
	<i>Pinus taeda</i> natural	40	7.4	300		7.8
	<i>Pinus palustris</i>	80	4	320		4.3
	Hardwood sp.	80	4	320		3.6

* Discount rate = 8%

Source: Cubbage et al., 2007; Venezuela, estimated by authors.

Table 3. Planted Area by Country in South America (2005)

Country	Planted Forest Area (000 ha)
Brazil	5,384
Chile	2,661
Argentina	1,229
Uruguay	766
Peru	754
Venezuela*	627
Colombia	328
Ecuador	164
Paraguay	43
Bolivia	20
Total	11,976

Source: FAO, 2006. * Asoplant 2007

FINANCIAL AND POLITICAL ENVIRONMENT FOR INVESTMENTS

Perceived and actual financial and political risks are perhaps the most important factors affecting timber and forest products investments. Various data sources estimate financial and political risk (financial, regulatory or political events that contribute to a company's operational risks) in South America by country, as discussed below.

Global Edge (2007) ranks political risk in each country as follows from the most risky (lowest numbers) to least risky (largest numbers): Argentina 1, Venezuela 4, Peru 19, Colombia 20, Brazil 28, and Chile 57. Compared to other countries in this region, Argentina and Venezuela contribute to the highest risk on investments, while Brazil and Chile have the lowest risk in the region.

The COFAC international risk assessments for 2006 provide a country risk rating, using letter grades ranging from A1 (steady political and economic environment with a good payment record of companies and little default probability) to D (a high risk economic and political environment that will further worsen a very bad payment record) (COFAC, 2007). Most developed countries such as Canada, the U.S., and Europe receive an A1 classification. Chile received an A2 (default probability is still weak), and Brazil and Colombia received A4 (an already patchy payment record could be worsened by a deteriorating political and economic environment, but the probability of default is still acceptable). Uruguay and Peru received a B (an unsteady political and economic environment is likely to affect further an already poor payment record). Argentina, Paraguay, Ecuador, and Venezuela received a C rating (a very unsteady political and economic environment could deteriorate an already bad payment record).

The Organisation for Economic Cooperation and Development also rates countries for their political risk related to export transactions and for direct investment, on a scale ranging from 1 (very safe) to 7 (very dangerous). It ranks risk for seven criteria, and six are summarized in Table 4 for each country in South America, as well as the three large North American countries for comparison. As of 2007, the short-term political risk for export transactions in each country was modest, at 4 or less. Long-term political risks in several countries, which are most relevant for forestry investments, were much greater, including a 7 in Argentina, Bolivia, Ecuador, Guyana, Suriname, and a 6 in Venezuela. Chile and Uruguay had the best commercial risk ratings in South America, with an A grade. Seven countries had a commercial risk rating of C, including Argentina, Colombia, and Venezuela. For direct investments, Bolivia, Venezuela, and Ecuador were the most risky for risk of expropriation and government action, and Chile and Uruguay were safest. For the major countries, the transfer risk was greatest in Argentina, Bolivia, and Venezuela. Overall, Chile, Brazil, and Uruguay were ranked as the least risky for export transactions and direct investments in South America.

In addition to risk factors, there are several parameters to consider in the viability and feasibility of investments in these countries, such as the availability of specialized intermediary firms and different types of outsourcing (Khanna et al. 2005).

The organizational environment found in the developing countries can be somewhat frustrating, and bureaucracy is just one of the major problems. The ability to establish businesses rapidly with a minimum amount of red tape and government bureaucracy is another measure of business climate. Figure 6 shows that the number of

days and procedures that are needed to start a business are the greatest in Brazil and Venezuela, followed by Peru and Paraguay (World Bank, 2007). Chile has the lowest number of days and procedures required to establish a business. For comparison, Canada required only 2 days and 3 procedures to establish a business, and the U.S. was 5 days and 5 procedures (World Bank 2007).

Table 4. Risk Assessment for Selected Factors and Countries by the OECD 2007

Country	Export Transactions			Direct Investments		
	Political Risk Short Term	Political Risk Medium/ Long Term	Commercial Risk	War Risk	Risk of Expropriation and Government Action	Transfer Risk
Argentina	3	7	C	2	3	6
Bolivia	3	7	C	4	7	6
Brazil	1	3	B	2	2	3
Canada	1	1	A	1	1	1
Chile	1	2	A	1	1	2
Colombia	2	4	C	5	3	4
Ecuador	4	7	C	5	3	4
French Guiana	1	2	B	2	Na	2
Gayana Mexico	1	2	B	2	1	2
Paraguay	3	6	C	4	4	5
Peru	1	4	B	3	3	3
Suriname	4	7	C	3	5	7
United States	1	1	A	1	1	1
Uruguay	3	4	A	2	2	4
Venezuela	4	6	C	4	7	5

Source: OECD, 2007.

CONCLUSIONS

The emerging economies in Asia and in Latin America are increasing the consumption of forest products and other consumer goods rapidly, which will require increased world production. This growth in consumption will continue, and the greater demand will prompt price increases. The increased demand and prices will allow more opportunities for wood fiber production and secondary manufacturing in South America. Forest products fiber can be supplied in shorter time in South America with the use of fast growing species in appropriate locations. Biological growth factors and economic advantages of low costs of production and high rates of return will favor investment growth in Latin America versus sources in North America.

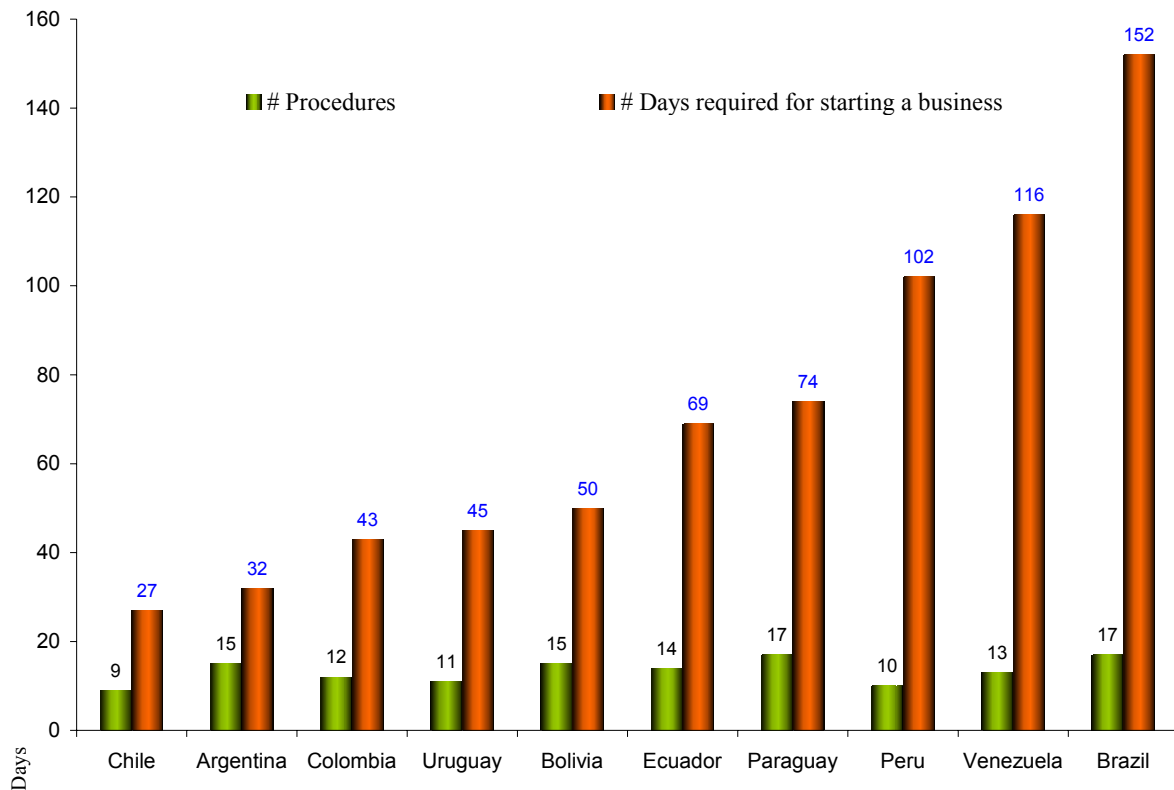


Figure 6. Number of days and procedures required to establish a new business by country in South America (2005); Source: Data from World Bank (2007).

In the last nine years, South America has had rapid annual increases in plantation area and productivity, as well as in secondary forest products. Brazil and Chile are the most important countries accounting for such changes. The largest exporter of industrial roundwood in the region is Uruguay, with 1.5 million m³/year; nevertheless it is placed fourth in total forest product exports. This situation is expected to change with the entry in production of three pulp mills that are being planned or under construction. One of these mills is under construction and should be completed soon. The other has been delayed due to major demonstrations and protests from Argentina, and the third is announced but not yet begun. If realized, the three new pulp mills would make Uruguay the third largest forest product market exporter.

The four Southern Cone countries of Chile, Brazil, Argentina, and Uruguay have the most obvious potential for increased investments in forest plantations and forest products manufacturing in the Americas. They have good biological plantation growth, high rates of return for plantation investments, rapidly increasing domestic economies, relatively stable political conditions, and improving qualities of life.

In addition, Brazil, Chile, and Argentina are able to generate significant amounts of capital for internal investments from internal sources, which allows expansion of their relatively attractive and competitive forestry sectors. Uruguay relies more on foreign

direct investment, but has been the most successful country in all of South Americas in this regard recently. The Coface and OECD rankings class Chile, Brazil, and Uruguay as the countries with the least export and direct investment risks, followed somewhat by Colombia. The other South American countries are classed as having moderate to major country risks, export risks, or direct investment risks. They still may have significant investments made by internal investors, or by other investors in Latin America or Asia, but are less likely to be attractive to North American or perhaps European firms.

Perceived political and financial risk may limit Argentina, Bolivia, and Ecuador more, but the overall attractiveness of at least Argentina remains substantial. It still has attracted major investments from the other Latin America countries such as Chile and Brazil, as well as some from Europe. Other countries such as Colombia, Venezuela, and Paraguay seem to offer significant biological opportunities for forest plantations, and are seeking foreign direct investments. At the moment, Colombia is seeking forestry investments most aggressively, and could achieve some success if their political and personal risk remains low.

In conclusion, South America will be able to supply increasing amounts of raw and processed wood fiber to world markets. Internal and external capital will drive these investments and growth in the forest products sector. The attractive timber-based investments and increasing world demand, especially from Asia, will continue to attract proportionately more investments to the southern hemisphere, and South America still has a large amount of land and reasonable business climates in most countries. Other more developed northern and southern hemisphere countries have much less opportunity for growth in the forestry sector, so South America has a comparative advantage. It will increase its share of the exports to emerging markets and capture more markets in North America and Europe.

REFERENCES CITED

- Asoplant (2007). Surface of forest plantations in Venezuela. Personal communication with Mrs. Beatriz Periche.
- Associacao Brasileira de Celulose e Papel (BRACELPA). (2007). "Desempenho do Setor em 2006 e projecao para 2007," www.bracelpa.org.br. Accessed on 11/19/2007.
- Boyle, J. (1999). "Planted forests: Views and viewpoints," *New Forests*. 17 (1), 5–9.
- Coface. (2007). "Country risk outlook 2006," <http://www.coface-usa.com/>. Accessed on 11/19/2007.
- CORMA. (2007). "Industria forestall," www.corma.cl. Accessed on 05/05/2007.
- Cubbage, F. and Davis, J. (1986). "Historical and regional stumpage price trends in Georgia," *Forest Product Journal*. 36(9), 33-39.
- Cubbage, F., Mac Donagh, P., Sawinski Júnior, J., Rubilar, R., Donoso, P., Ferreira, A., Hoeflich, V., Morales Olmos, V., Ferreira, G., Balmelli, G., Siry, J., Noemi Báez, M., and Alvarez, J. (2007). "Timber investment returns for selected plantation and native forests in South America and the Southern United States," *New Forests*. 33(3):237-255.

- FAO. (1994). *The Road From Rio: Moving Forward in Forestry*, UN-FAO/SARD, Food and Agriculture Organization of the United Nations, Rome. 30 pp. ISBN 92-5-103587-3.
- FAO. (2006). "Global forest resources assessment," In: Cubbage, F. et al. 2007. Timber investment returns for selected plantations and native forests in South America and the Southern United States. *New Forests*. 33(3), 327-355.
- FAO. (2007a). Statistical information. www.fao.org. Accessed on 06/05/2007.
- FAO. (2007b). *Forest Products Annual Market Review 2006-2007*. United Nations Economic Commission for Europe/Food and Agriculture Organization of the United Nations. ECE/TIM/SP/22. United Nations, New York, and Geneva.
- GlobalEdge. (2006). "Market potential indicators for emerging markets-2007," www.globaledge.msu.edu. Accessed on 05/05/2007.
- Gonzalez, R., and Rojas, O. J. (2007). "Paper," in *Forests and Forestry in the Americas: An Encyclopedia*. <http://forestryencyclopedia.jot.com/WikiHome>. Accessed on 11/07/2007.
- INFOR. (2007). "Mercado forestal," <http://www.infor.cl/>. Accessed on 05/05/2007.
- Juslin, H., and Hansen, E. (2003). *Strategic Marketing in the Global Forest Industries*, Authors Academic Press, Corvallis, OR. 610 pp.
- Khanna, T., Palepu, K., and Sinha, J. (2005). "Strategies that fit emerging markets," *Harvard Business Review*. *HBR Spotlight*, 63-76.
- OECD. (2007). "OND/NDD – Country risks synthesizing chart," Organization for Economic Co-operation and Development. <http://www.oecd.org/>. Accessed on 19 November 2007. Last update: 11/15/2007.
- Rojas, O. J., and Gonzalez, R. (2007). "Pulp," in *Forests and Forestry in the Americas: An Encyclopedia*, <http://forestryencyclopedia.jot.com/WikiHome>. Accessed on 11/07/2007.
- Sedjo, R. (1999). "The potential of high-yield plantation forestry for meeting timber needs. Recent performance, future potentials, and environmental implications," *New Forests*. 17(3), 339-359.
- U.S.I.T.C. (2007). "Statistical information," www.usitc.gov. Accessed on 05/05/2007.
- Wear, D., Carter, D. and Prestemon, J. (2007). "The U.S. South's timber sector in 2005: A prospective analysis of recent changes," Southern Research Station, Asheville, NC. http://www.srs.fs.usda.gov/pubs/gtr/gtr_srs099.pdf Accessed on 06/29/2007.
- Zhang, W. (2007). "Overview and forecast on forestry productions worldwide," *Environ. Monitoring and Assessment*. 125(3), 301-312.
- World Bank. (2007). World Development Indicator. www.devdata.worldbank.org. Accessed on 07/27/2007.

Article submitted: December 13, 2007; Peer-review completed: Jan. 31, 2008; Revision received and accepted: Feb. 10, 2008; Published: Feb. 11, 2008.

FEEDSTOCK PRETREATMENT STRATEGIES FOR PRODUCING ETHANOL FROM WOOD, BARK, AND FOREST RESIDUES

Gang Hu, John A. Heitmann,* and Orlando J. Rojas

Energy and environmental issues are among the major concerns facing the global community today. Transportation fuel represents a large proportion of energy consumption, not only in the US, but also world-wide. As fossil fuel is being depleted, new substitutes are needed to provide energy. Ethanol, which has been produced mainly from the fermentation of corn starch in the US, has been regarded as one of the main liquid transportation fuels that can take the place of fossil fuel. However, limitations in the supply of starch are creating a need for different substrates. Forest biomass is believed to be one of the most abundant sources of sugars, although much research has been reported on herbaceous grass, agricultural residue, and municipal waste. The use of biomass sugars entails pretreatment to disrupt the lignin-carbohydrate complex and expose carbohydrates to enzymes. This paper reviews pretreatment technologies from the perspective of their potential use with wood, bark, and forest residues. Acetic acid catalysis is suggested for the first time to be used in steam explosion pretreatment. Its pretreatment economics, as well as that for ammonia fiber explosion pretreatment, is estimated. This analysis suggests that both are promising techniques worthy of further exploration or optimization for commercialization.

Keywords: Energy; Biomass; Pretreatment; Ethanol; Saccharification; Biorefinery; Steam explosion; Ammonia fiber explosion

Contact Information: Department of Wood and Paper Science, North Carolina State University. Campus Box 8005, Raleigh, NC 27695-8005, USA; *Corresponding author: heitmann@ncsu.edu

INTRODUCTION

Energy security and climate change imperatives require large-scale replacement of petroleum-based fuels, as well as improvement of vehicle efficiency (Farrell et al. 2006; Hahn-Hagerdal et al. 2006). Renewable fuels, such as bioethanol, are becoming increasingly important as a consequence of heightened concern for the greenhouse effect, depleting oil reserves, and rising oil prices (Ohgren et al. 2007). Fuel ethanol is mainly used as an oxygenated fuel additive. The higher octane number of the fuel mixture, when it contains ethanol, reduces the need for toxic, octane-enhancing additives such as methyl tertiary butyl ether. Due to the oxygen in ethanol molecules, there is also a reduction of carbon monoxide emission and non-combusted hydrocarbons. It is believed that ethanol is 15% more efficient than gasoline in optimized spark-ignition engines, while it has about the same overall transport efficiency as diesel in compression-ignition engines (Bailey 1996). It is also believed that a given volume of ethanol could provide energy enough to drive about 75~80% of the distance as the same amount of gasoline, although it has the only about two-thirds of the energy content (Galbe and Zacchi 2002). Table 1

shows the densities and low heating values of gasoline, diesel, and ethanol, respectively (US Department of Energy).

Table 1. Energy Content Comparison between Gasoline, Diesel and Ethanol (Data excerpted from the website of US department of energy: Anonymous)

	Density @ 60 °F (lb/gal)	Energy(BTU/Gallon) LHV@60 °F
Gasoline	6.0~6.5	116,090
No. 2 Diesel	7.079	129,050
Ethanol	6.61	76,330

Note: LHV=Low Heating Value

Most ethanol is currently produced by fermentation of either corn starch or sucrose. The United States, Brazil and China are in the top of countries that produce the largest quantities of fuel ethanol. If the oil crisis continues to develop, ethanol is one of the most promising biofuels that can be used to replace gasoline for tomorrow's transportation vehicles. Until recently, the high cost of ethanol production has been a factor retarding commercial use of ethanol and requiring subsidies to promote development. Reduction of the production cost would lead to a faster commercialization of economically feasible processes and would increase the competitiveness of ethanol with fossil fuels. The raw materials account for 40~70% of the total ethanol production costs based on current sugar- or starch-containing feedstocks, such as sugarcane and corn. Commercial feasibility is also dependent on production of animal feed as a by-product (Claassen et al. 1999; Sun and Cheng 2002b). Lignocellulosic biomass is believed to be less expensive and more plentiful than either starch- or sucrose-containing feedstocks. Lignocellulosic-based biofuels could replace about 30% of the petroleum currently consumed by the USA, if materials such as forest residues (e.g. sawdust, wood bark), agricultural residues (e.g. corn stover), and herbaceous grass (e.g. Switchgrass), as well as municipal waste, etc., are used (Galbe and Zacchi 2002; Gray et al. 2006; Mosier et al. 2005; Wyman et al. 2005). It has been estimated that more than one billion tons of such biomass can be made available annually in the USA (Perlack 2005). From the harvest and life cycle points of view, forest materials provide considerable advantages as an input to a biorefinery that might make fuels and chemicals. Extensive research has been exploring substrates from these different categories. Figure 1 summarizes some of the major lignocellulosics that have been investigated for bioethanol production.

Corn stover, wheat straw, and sugar bagasse are among the agricultural residues that have attracted the most interest of research. Other agricultural residues that have been explored include rice straw, rice hull, corncob, oat hull, and corn fiber, among others; these can be classified into a group derived from food crops. Research has also been performed on substrates such as cotton stalk and cotton gin; these can be classified as a group deriving its source from nonfood crops, as shown in Fig. 1 (Chang et al. 2001; Chen and Liu, 2007; Esteghlalian et al. 1997; Moniruzzaman et al. 1997; Rubio et al. 1998; Saha 2003; Saha et al. 2005; Sun and Chen 2007; van Walsum and Shi 2004). Switch grass and Bermuda grass have been the intensive substrates explored in the herbaceous grass category, while other substrates such as reed canarygrass and alfalfa

fiber have also been studied in the same category (Chang et al. 2001; Dien et al. 2006). Some research has utilized municipal wastes as substrates and researched the conversion of these substrates into ethanol (Li et al. 2007; Lissens et al. 2004). A lot of work has been carried out to explore woody substrate to produce ethanol (Ballesteros et al. 2000; Berlin et al. 2007; Demirbas 2004, 2005, 2007, 2008). The woody substrates can be roughly classified into two classes, one is wood or wood chips while the other forest residues. In this review article, the substrates will be majorly focused on woody biomass as long as the discussion of pretreatment and economics are concerned.

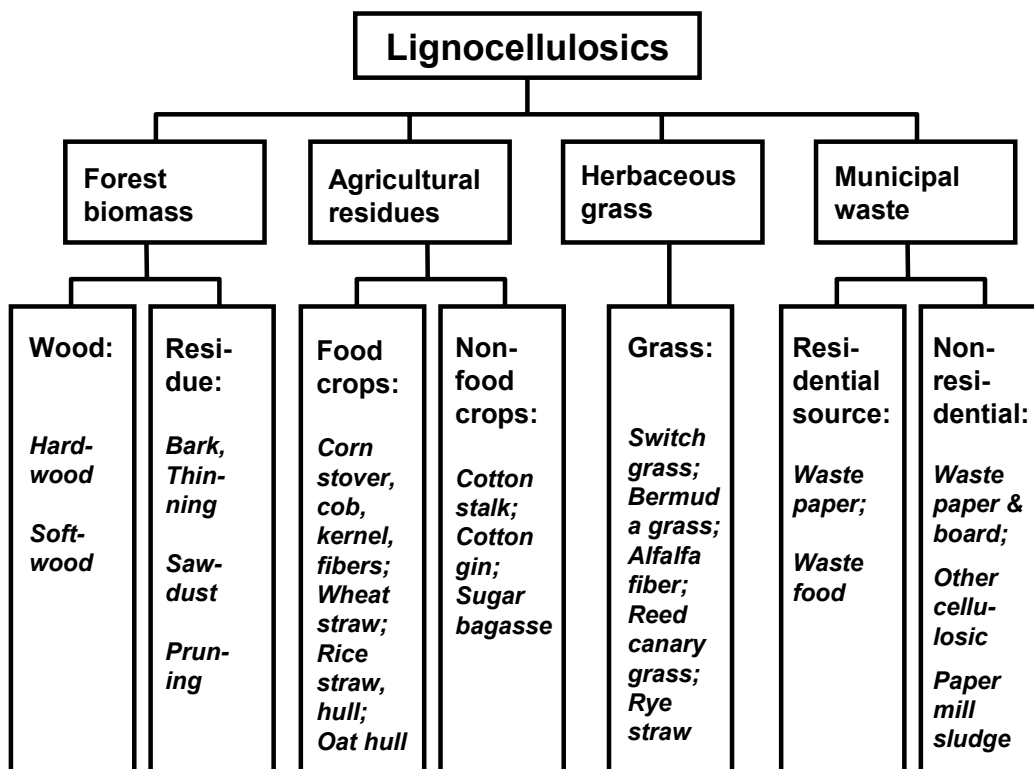


Fig. 1. Major lignocellulosics that have been explored for bioethanol production

Chemical Composition and Role of Pretreatment

Woody materials, including wood, bark, and mixtures of forest residues are composed of cellulose, hemicelluloses, lignin, and small amounts of other species (Fig. 2). Cellulose is composed of anhydro-glucopyranose, or glucose residue, which can be converted to glucose and provides the major source for hexose in woody biomass (Fig. 3). Cellulose is believed to have a highly crystallized structure due to the existence of hydrogen bonds. In contrast to its amorphous region, the crystalline region of cellulose make it hard to hydrolyze (Fig. 4). Hemicellulose is composed of both six-carbon sugars and five-carbon sugars, which include glucose, mannose, arabinose, xylose, and other species (Fig. 5). Xylose is believed to be present in the largest amount in hemicellulose. Unlike cellulose, hemicellulose has a random and amorphous structure, which makes it easily be hydrolyzed by dilute acid or base. Lignin is the third major component in wood

and comprises the glue that protects woody biomass from foreign invasion. It is mainly composed of phenolic units and represents the part of biopolymer that cannot be converted into ethanol directly or indirectly using the current technology. With the exclusion of lignin, the optimistic situation is to preserve and utilize all the carbohydrates and convert them into ethanol fuels. Pretreatments constitute the means to separate carbohydrates and lignin and disrupt the crystalline region of these materials; it should also downgrade carbohydrates as little as possible. Different pretreatment methods have been explored in order to achieve the optimistic situation.

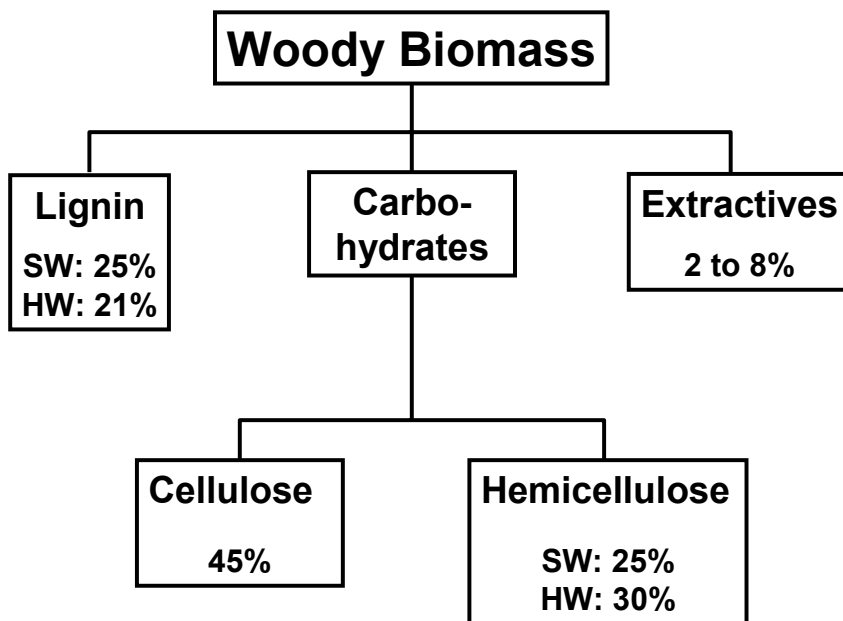


Fig. 2. Chemical composition of woody biomass

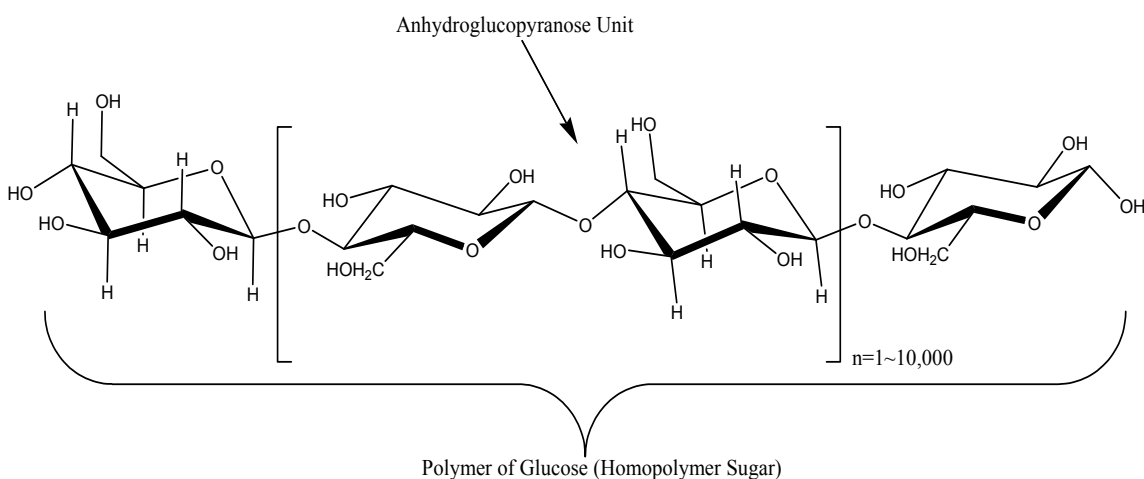


Fig. 3. Chemical structure of cellulose

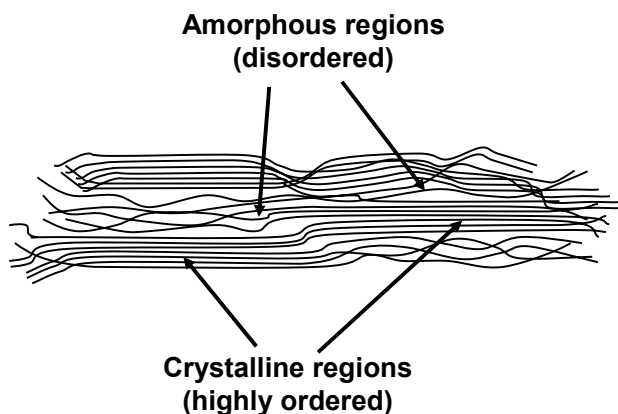


Fig. 4. Schematic drawing of cellulose microfibril

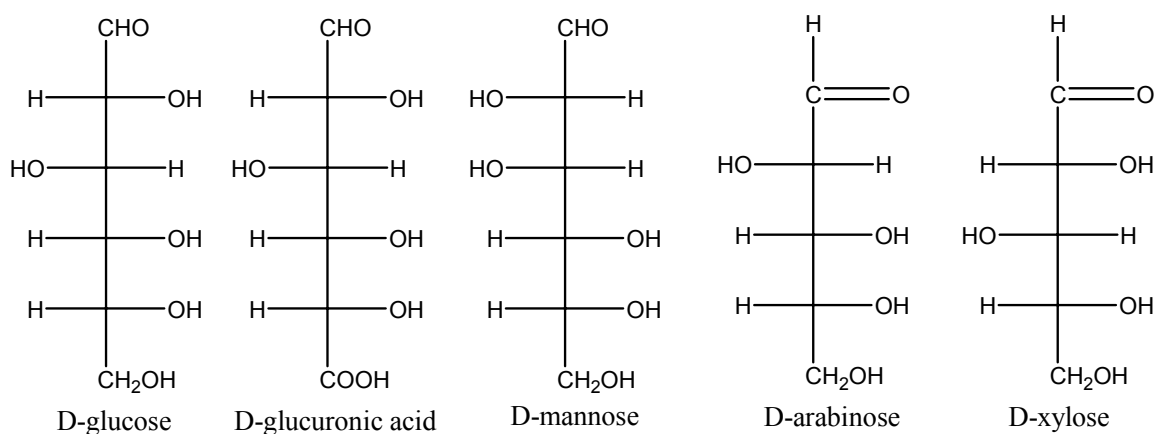


Fig. 5. Chemical compositions of hemicelluloses

In principle, the sugar chains can be hydrolyzed to monomeric sugars, most of which can be fermented to alcohol using yeast. Research is being done to improve the efficiency of transforming these sugars to ethanol. Two recent review articles have summarized in detail acid-based hydrolysis processes and enzyme based hydrolysis processes for ethanol from lignocellulosic materials (Taherzadeh and Karimi 2007a,b). The general approaches for the conversion of biomass to ethanol include the hydrolysis of the hemicellulose and the cellulose to monomer sugars, fermentation of these sugars, and product recovery and concentration by distillation. Figure 6 summarizes these steps.

The main difference between process alternatives in Fig. 6 is the hydrolysis, which can be acid hydrolysis, either dilute or concentrated, or enzymatic hydrolysis (Galbe and Zacchi 2002). Enzymatic hydrolysis has been thought to have the potential for higher yields and reduced formation of toxic compounds so that biomass ethanol is competitive when compared to other liquid fuels on a large scale (Wyman 1999). However, the enzymatic conversion of cellulose to sugar is extremely slow based on current technology. Part of the reason is that the cellulose is well protected by hemicellulose and lignin. It therefore entails pretreatment processes that expose cellulose

in such materials or modify the pore structures so that enzymes can penetrate into fibers and hydrolyze cellulose more readily. After pretreatment, the hydrolysis of the carbohydrate fraction to monomeric sugars can be achieved faster and with greater yields.

PRETREATMENT CATEGORIES

In general, pretreatment can be classified into biological pretreatment, physical pretreatment, and chemical pretreatment according to the different force or energy consumed in the pretreatment process. Some pretreatment combines any two or all of these pretreatment and can produce subcategories. Table 2 summarizes some of the broadly explored pretreatment methods according to this classification (Sun and Cheng 2002b; Taherzadeh and Karimi 2007b).

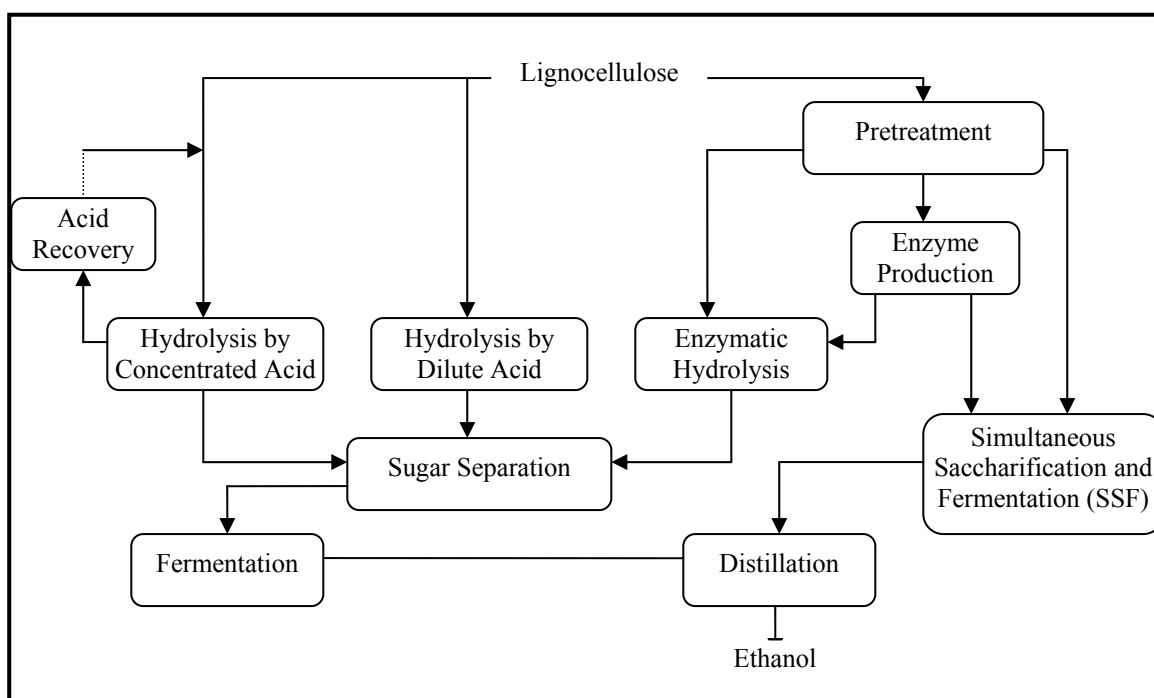


Fig. 6. Production of ethanol from lignocellulosic materials (Galbe et al. 2002)

Some methods that incorporate the combination of or more unit processes (McMillan 1994) have not been included in Table 2. Biological pretreatment has not attracted much attention, probably because of kinetic and economic considerations, although there has been various research showing biological pretreatment can be an effective way to recover sugars from different species of biomass (Kurakake et al. 2007; Taniguchi et al. 2005; Zhang et al. 2007). Physical and chemical pretreatments have been the subject of intensive research. Steam and water are usually excluded from being considered as chemical agents for pretreatment, since no extra chemicals are added to the biomass. Physical pretreatments include comminution, in which the particle sizes of the biomass are reduced with mechanical forces, steam explosion, and hydrothermolysis.

Comminution, including dry, wet, and vibratory ball milling (Millett et al. 1979; Rivers and Emert 1987; Sidiras and Koukios 1989), and compression milling (Tassinari et al. 1980, 1982), is sometimes needed to make material handling easier for the subsequent processing steps (Mosier et al. 2005). Electron beam pretreatment of used newsprint, pulp as well as pulp recovered from clarifier sludge and paper mill sludge has been explored for exploiting the cellulosic substance to make ethanol (Khan et al. 1986, 1987). It has also been used to pretreat softwood to enhance its enzymatic hydrolysis (Khan et al. 1986). Gamma-ray and microwave attracted some interest as well; research has shown their effects on the pretreatment of agricultural waste and other cellulose-containing waste (Kim et al. 2007; Magara et al. 1989). In terms of the practicality and commercialization of physical pretreatment, steam pretreatment and hot water pretreatment have broader prospects. Publications have shown that these pretreatment methods have been attracting much more effort (Brandes and Graff 1985; Broglin 1996; Chandra et al. 2007; Galbe and Zacchi 2007; Saddler et al. 1993; Singh et al. 2004). Their effect on pretreated wood will be summarized later.

Acids or bases promote hydrolysis and improve sugar recovery yields from cellulose by removing hemicellulose or lignin during pretreatment. Sulfuric acid and sodium hydroxide are the most commonly used acid and base, respectively (Mosier et al. 2005). Another approach for pretreatment is to use liquid formulations capable of acting as solvents for cellulose. Work with cellulose solvent systems has shown that enzymatic hydrolysis could be greatly improved, but the work mainly has been restricted to agricultural residues and herbaceous grass. Little has been reported about the use of cellulose solvents in pretreating forest biomass such as wood, bark, or mixtures of such residues. A broad range of chemical pretreatments, such as alkaline peroxide, ozone, and organosolv, which uses Lewis acids such as FeCl_3 , alum etc. in aqueous alcohols, as well as glycerol, dioxane, phenol, or ethylene glycol, have been suggested to disrupt the cellulose structure and promote its hydrolysis. Concentrated mineral acids (H_2SO_4 , HCl), ammonia-based solvents (NH_3 , hydrazine), aprotic solvents such as DMSO, metal complexes (ferric sodium tartrate, codexen, and cuoxan), as well as wet oxidation also reduce cellulose crystallinity, disrupt the association of lignin with cellulose, and dissolve cellulose. However, the economics of these methods do not permit any practical application when compared to the value of glucose (Mosier et al. 2005). Lime pretreatment and ammonia pretreatment have seemed to be the most attractive alkaline pretreatment, while most attention in acid pretreatment has been concentrated on the use of sulfur dioxide and sulfuric acid. These two acid pretreatments have also been combined to the steam pretreatment.

Research on the development of pretreatment technology applicable to ethanol production from woody biomass represents somewhat a different direction. The broadly explored pretreatment methods used in wood are summarized in Table 3. Table 3 lists the pretreatment methods and the mechanistic effect occurred as well. These methods, including steam explosion, liquid hot water, dilute acid, lime and ammonia pretreatment, are considered potentially cost-effective and could be used on a large scale in the future (Mosier et al. 2005). A deeper review of these methods follows, and the authors also propose acetic acid be used as catalyst for further alternatives for combining application of steam explosion pretreatment.

Table 2. Pretreatment Methods of Lignocellulosics for Enzymatic Hydrolysis

Pretreatment	Energy		Effect
	Source	Means	
Biological Pretreatment	Microbe	Fungi	Reduce DP of cellulose and hemicellulose
		Actinomycetes	Remove Lignin
Physical Pretreatment	Comminution	Ball Milling	Decrease particle size, cellulose crystallinity & DP
		Colloid Milling	
		Hammer Milling	
		Compression Milling	
	Irradiation	Electron Beam	Increase surface area and pore sizes
		Gamma-ray	Soften and partially depolymerize lignin
		Microwave	
	Hydrothermolysis	Liquid Hot Water	Partially hydrolyze hemicellulose
	Steam Explosion	High Pressure Steam	
	Other Mechanical Energy	Expansion Extrusion	
Chemical Pretreatment	Acid	carbonic acid	Decrease Crystallinity of Cellulose and its DP Partial or complete hydrolysis of hemicellulose Delignification
		hydrochloric acid	
		hydrofluoric acid	
		nitric acid	
		peracetic acid	
		phosphoric acid	
		sulfur dioxide	
		sulfuric acid	
	Alkaline	lime	
		sodium hydroxide	
		sodium carbonate	
		ammonia	
		ammonium sulfite	
	Gas	Chlorine dioxide	
		Nitrogen Dioxide	
	Oxidant	Hydrogen Peroxide	
		Ozone	
		Wet Oxidation	
	Cellulose Solvent	Cadoxen	
		CMCS	
		DMSO	
	Extraction of Lignin	Hydrozine	
		Ethanol-Water	
Benzene-Water			
Ethylen Glycol			
Butanol-Water			
Swelling Agent			

Table 3. Effect of Pretreatments on the Chemical Composition and Chemical/Physical Structure of Lignocellulosic Biomass (Mosier et al. 2005)

Pretreatment Method	Accessible surface area increases	Cellulose Decrystallization	Hemicellulose Removal	Lignin Removal	Lignin Structure Alteration
Uncatalyzed steam explosion	●		●		○
Liquid hot water	●	ND	●		○
pH controlled hot water	●	ND	●		ND
Flow-through liquid hot water	●	ND	●	○	○
Dilute acid	●		●		●
Flow-through acid	●		●	○	●
Lime	●	ND	○	●	●
Ammonia freeze explosion(AFEX)	●	●	○	●	●
Ammonia recycled percolation(ARP)	●	●	○	●	●

●: Major Effect

○: Minor Effect

ND: Not Determined

Uncatalyzed Steam Explosion

Uncatalyzed steam explosion has been applied commercially to hydrolyze hemicellulose in the Masonite process, in which high-pressure steam is applied on wood chips in a large vessel without chemicals for several minutes, and then some steam is rapidly vented to reduce the pressure while the biomass is discharged into a large vessel for flash cooling. In this process, steam is used to promote hydrolysis of hemicellulose, and the process is terminated by explosive decompression (Avellar and Glasser 1998; Brownell and Saddler 1984; Glasser and Wright 1998; Heitz et al. 1991; Ramos et al. 1993). It is believed that the acetic acids and other acids released in the pretreatment hydrolyze the hemicellulose. Water itself may also act as an acid at high temperature. The expansion at the end of pretreatment terminates the reaction and opens up the particulate structure of wood. The removal of hemicellulose improves the accessibility of cellulose fibrils to enzymes, while the reduction in particle size and increased pore volume in this process is less important in improving the digestibility of the pretreated biomass.

Hot Water Pretreatment

Liquid hot water pretreatment uses pressure to keep water in a liquid state at elevated temperatures. Flow-through processes pass the liquid water at elevated temperatures through the cellulosic material. This method has been termed hydrothermolysis (Bobleter et al. 1981), aqueous or steam/aqueous fractionation (Bouchard et al. 1991), uncatalyzed solvolysis (Mok and Antal 1992), and aquasolv (Allen et al. 1996). This pretreatment usually has involved temperatures of 200-230 °C for up to 15 minutes. Around 40-60% of the total mass is dissolved with 4-22% of the cellulose, 35-60% of the lignin, and all of the hemicellulose being removed (Mok and Antal 1992). It was found that temperature and time had little effect on the pretreatment results, while variability in results was attributed to different biomass types. Co-current, countercurrent, and flow-

through are the major three types of liquid reactor configurations. The generation of acetic acids and other organic acids by cleaving O-acetyl and uronic acid substitutions from hemicellulose can both help and impede hot water pretreatment. The released acids help to catalyze formation and removal of oligosaccharides. On the other hand, released monomeric sugars could be further degraded to aldehydes if acid is used. These aldehydes, principally furfural from pentose and 5-hydroxymethyl furfural from hexose, are inhibitors to enzymes in fermentation (Palmqvist and Hahn-Hägerdal 2000a). The pH of pure water at 200 °C is about 5.0. Water has an unusually high dielectric constant that enables ionic substances to dissociate. All hemicellulose can be dissolved by water; one half to two-thirds of the lignin also dissolves from most biomass when it is treated at 220 °C for 2 min (Antal et al. 1996). Hemiacetal linkages are cleaved, and the released acids subsequently facilitate the breakage of such ether linkages. However, softwoods are less vulnerable to solubilization for reasons that are not well understood. There appears to have been no work showing successful pretreatment of softwood by hot water.

Acid Pretreatment

Work aimed at obtaining lignin from wood has proven that dilute acids are a good choice to disrupt the complex between lignin and carbohydrate (Guerra et al. 2006a,b; Wu and Argyropoulos 2003). Dilute acid pretreatment with sulfuric acid has been extensively researched because it is inexpensive and effective (Nguyen et al. 2000; Tengborg et al., 1998; Torget et al. 1990, 1991), although other acids such as nitric acid, hydrochloric acid and phosphoric acid have also been tested (Brink et al. 1999; Goldstein 1983; Goldstein and Easter 1992; Israilides et al. 1978). Dilute sulfuric acid is mixed with biomass to hydrolyze hemicellulose to xylose and other sugars, and then it can continue breaking xylose down to furfural (Fig. 7). The volatile fraction contains furfural, which can be recovered by distillation. The temperature for this pretreatment is usually at 150-220 °C for seconds to minutes.

It is believed that acid hydrolysis releases oligomers and monosaccharides. It has been modeled as a homogeneous reaction in which the acid catalyzes breakdown of cellulose to glucose, followed by the breakdown of glucose to form 5-hydroxymethylfurfural and other degradation products. Different kinetic models have been adopted to describe the hydrolysis of hemicellulose and formation of furfural and other decomposition products (Converse et al. 1989; Esteghlalian et al. 1997; Kwarteng 1983; Lee et al. 1999). Carbohydrates are easily degraded to furfural and 5-hydroxymethylfurfural in acidic environments (Fig. 7). The further decomposition of these furan derivatives will result in the production of organic acids such as levulinic acid, formic acid, etc. (Fig. 7). These acids, as well as the furan derivatives, are inhibitors to the yeast used in the fermentation process. Meanwhile, the use of acid also imposes concerns related to the corrosion of equipment. The cost involved in pretreatment using only acid also hampers any practicality-oriented research and possible commercial application compared to the other pretreatments such as steam explosion or ammonia fiber explosion, which will be discussed hereafter.

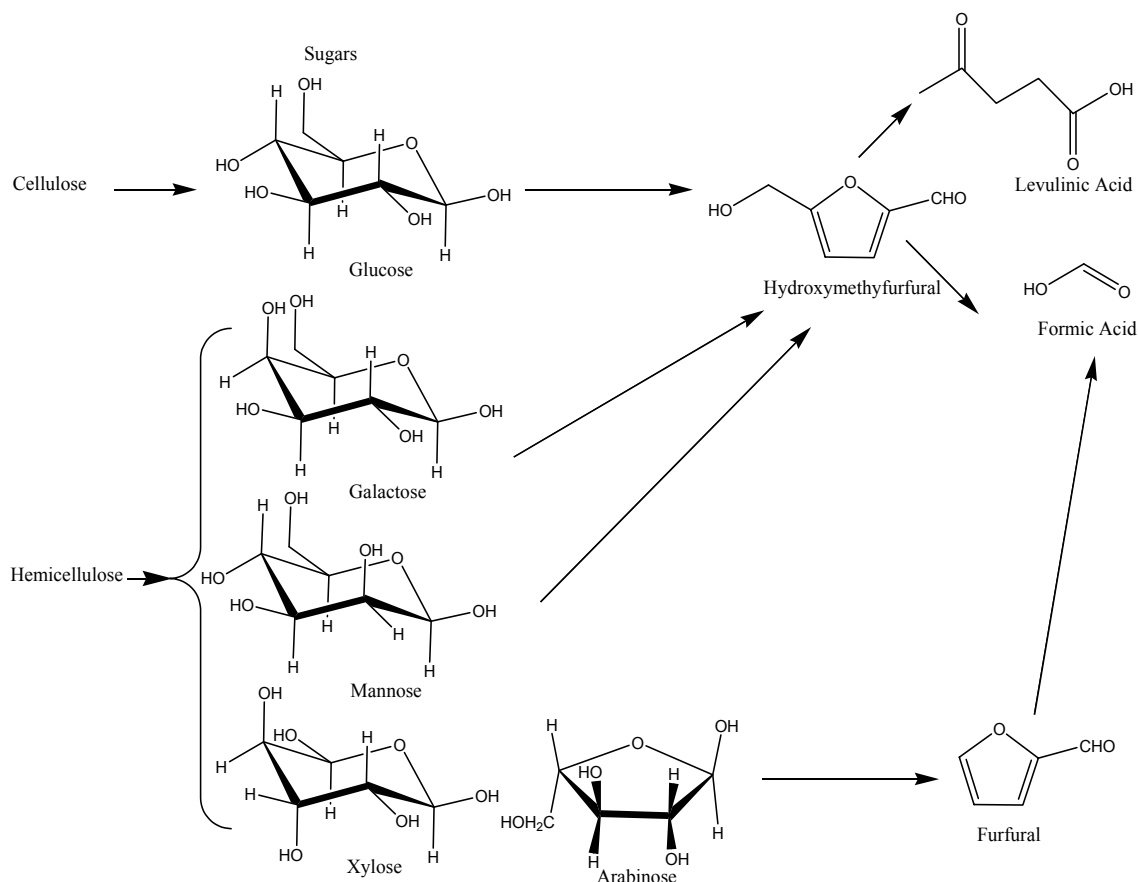


Fig. 7. Reactions occurring to carbohydrates during hydrolysis of lignocellulosic materials. The furan derivatives will react further to form levulinic acid and formic acid.

Steam Pretreatment with Acid Catalyst

Steam explosion using an acid catalyst has been under extensive investigation in recent years. It has been considered to be one of the most promising techniques for commercialization. Ongoing research is still aimed at optimization of its conditions or using different catalysts to fully exploit its advantages, as well as to improve the yield of overall sugars. Steam pretreatment with a sulfuric acid catalyst has been believed to be one of the most likely approaches that could be used commercially in the future. This combines the effect of both acids and steam. Pretreatment with SO_2 has also been thoroughly studied in combination with steam. However, SO_2 is probably less attractive, because of its high toxicity, which may pose safety and health risks. Its advantages lie in its lower corrosiveness and faster and easier penetration during the pretreatment process. The highest yield that has been achieved was about 82%, which was obtained through a two-stage pretreatment, in which the first one used comparatively low temperature, while the second one used a higher temperature. Among all of the one-stage steam pretreatment processes, the highest yield came with a lower dosage of sulfuric acid, which may testify to the hydrolytic effect of acid on carbohydrates (Galbe and Zacchi 2002). Table 4 summarizes some of the pretreatment conditions for acid-catalyzed steam pretreatment of softwood.

Since yield has been one of the important factors that determine the success of commercial production of ethanol from lignocellulosic biomass, further exploration of yield increase of sugars is worthwhile as long as it does not cause any significant increase in pretreatment cost.

Table 4. Pretreatment Conditions for Acid-Catalyzed Steam-Pretreated Softwoods (Galbe et al. 2005)

Substrate	Pretreatment Conditions			Yield* (%)
	Catalyst	Temperature	Time	
Pine	4.44% SO ₂	200 °C	10 min	—
Spruce + Pine	2.0-2.6% SO ₂	180-204 °C	2min	—
Pine	0.5-12% SO ₂	182-248 °C	0.5-18min	—
Pine	2.0-2.6% SO ₂	150-208 °C	2-20min	—
Spruce	0.5-5% H ₂ SO ₄	190-220 °C	50-250s	—
Spruce	0.35% H ₂ SO ₄	215 °C	140s	—
Fir + Pine	0.4% H ₂ SO ₄	200-230 °C	125-305s	—
Spruce + Pine	1-6% SO ₂	190-230 °C	2-15min	66
Spruce	0.5-4% H ₂ SO ₄	180-240 °C	1-20min	67
Fir + Pine ^a	0.6-2.4% H ₂ SO ₄	180-215 °C	100-240s	75~82
	2.5% H ₂ SO ₄	210 °C	100-120s	
Spruce ^a	0.5% H ₂ SO ₄	180 °C	10min	77~80
	1-2% H ₂ SO ₄	180-220 °C	2-10min	

^a Two-stage pretreatment

* yield of sugar as of percent of the theoretical in raw material

Alkaline Pretreatment

Alkaline pretreatment uses low temperature and pressure. It even may be carried out under atmospheric conditions, but the pretreatment time could be hours or even days rather than seconds or minutes. In lime pretreatment, some calcium is converted to irrecoverable salts or incorporated into the biomass. This pretreatment method has also been evaluated with addition of oxygen or air. Chang et al. (2001) used this method to treat poplar wood at 150 °C for 6h with 14-atm oxygen. Other alkali pretreatment formulations include sodium, potassium, calcium, and ammonium hydroxide as reactants. Sodium hydroxide receives the most attention, but lime has the advantage of being a low cost and safe agent, as well as being easily recoverable from water as insoluble CaCO₃ by reaction with CO₂. Then the CaCO₃ can be converted to lime, using lime kiln technology. Addition of air/oxygen improves the delignification of biomass.

Alkaline pretreatment is similar to Kraft pulping, in which lignin is removed, thus improving the reactivity of the remaining polysaccharides. Meanwhile, acetyl groups and the various uronic substitutions on hemicellulose are also removed so that there is less hindrance for enzymes to access the surface of hemicellulose and cellulose.

Ammonia Pretreatment

Ammonia treatment is also, in a strict sense, alkaline treatment. However, it is often considered separately due to its effectiveness and potential benefits in treating agricultural residues and herbaceous materials. Ammonia fiber/freeze explosion (AFEX) pretreatment has been the most frequently evaluated pretreatment of all alkaline pretreatments. Ammonia fiber/freeze pretreatment uses anhydrous liquid ammonia to

treat cellulosic materials in a pressure vessel in the weight ratio of about one to one at ambient or room temperature, and under the vapor pressure of liquid ammonia at said ambient temperature. The mixture is stirred for a certain period of time sufficient for the ammonia to wet and swell the cellulose or cellulose-containing material. At the end of this treatment, the pressure is rapidly reduced to atmospheric, which allows the ammonia to boil. Contact of the material with the ammonia is maintained at the boiling point of the ammonia, which essentially freezes the cellulose-containing material. When treatment is completed, the treated material is separated from the liquid and gaseous ammonia, which is recovered for recycling (Dale 1986). The ammonia freeze explosion pretreatment simultaneously reduces lignin content and removes some hemicellulose, while decrystallizing cellulose. Thus it affects both micro- and macro-accessibility of cellulases to cellulose (Mosier et al. 2005). Liquid ammonia pretreatment may cause mercerization, which spurs cellulose swelling and a phase change from cellulose I to cellulose II. Ammonolysis of glucuronic cross-links makes the carbohydrate more accessible by cellulases (Schwertassek and Hochman 1974).

Pretreatment with aqueous ammonia in a flow-through mode involves putting 5-15% ammonia solution through a column reactor that has been packed with the biomass. Operating conditions of 160-180 °C and 14 min of residence time can be used (Iyer et al. 1996; Yoon et al. 1995). Under these conditions, aqueous ammonia cleaves lignin-carbohydrate linkages and depolymerizes lignin. Due to the reaction between ammonia and water, the resultant species include the hydroxyl ion, whose existence makes this process somewhat similar to an alkaline pulping process. Pretreatment with aqueous ammonia is also known as the ammonia recycled percolation process (ARP). Although it has been reported that a large and adjustable degree of delignification results from tests with hardwood (Yoon et al. 1995) and agricultural residues (Iyer et al. 1996) at 160-180 °C for 14min, it was less efficient in pretreating softwood-based pulp mill sludge (Kim et al. 2000).

AFEX pretreatment yields optimal hydrolysis rates for pretreated lignocellulosics, with close to theoretical yields at low enzyme loadings. It has some unique features that distinguish it from other biomass treatments (Teymouri et al. 2005):

- Nearly all of the ammonia can be recovered and reused, while the remaining portion serves as a nitrogen source for microbes, in downstream processes.
- There is no wash stream in the process. Dry matter recovery following the AFEX treatment is essentially 100%. AFEX is basically a dry-to-dry process. Treated biomass is stable for long periods and can be fed at very high solids loadings in enzymatic hydrolysis or fermentation processes.
- Cellulose and hemicellulose are well preserved in the AFEX process, with little or no degradation. There is no need for neutralization prior to the enzymatic hydrolysis of AFEX-treated biomass.
- Enzymatic hydrolysis of AFEX-treated biomass produces clean sugar streams for subsequent fermentation process.

AFEX is well suited for agricultural and herbaceous residues, but it works only moderately well on hardwoods and is not well suited for softwoods (Mosier et al. 2005). Possible reasons for this could be directly related to the anatomical properties of different cells, since softwood fibers' lumens are thinner and its cell walls are thicker, which might

make the mass transport of ammonia much slower. From a chemical viewpoint, the lignin-carbohydrate complex might be harder to disrupt, while the higher lignin content could make lignin itself harder to degrade. The mass transport of degraded species might be much slower due to the combination of these effects.

The cost of ammonia and especially of ammonia recovery determines the cost of this pretreatment (Holtzaple 1992). Nevertheless, total sugar yield affects the overall economics more strongly. This depends on the loss in yield as well as sugar degradation, which could produce inhibitory products impacting the downstream fermentation. Fortunately, the moderate temperatures (<90 °C) and pH values (<12.0) of the AFEX treatment minimize formation of sugar degradation products, while giving high yields. AFEX is among the more promising pretreatment methods for application with lignocellulosic biomass of lower lignin content.

PERSPECTIVES FOR FUTURE RESEARCH ON WOOD BARK AND FOREST RESIDUES

Currently available pretreatment techniques have provided a broad range of choices that improve the conversion of carbohydrates from lignocellulosic biomass to ethanol. In general, these techniques focus on disrupting the protection of cellulose and hemicellulose by lignin, as well as dissociation between cellulose and hemicellulose. Some of these changes occurring to biomass also decrease the crystallinity of cellulose and increase the specific surface area that cellulase enzymes can access. For softwood and bark biomass, the use of steam explosion with an acidic catalyst seems more promising compared to the current technologies due to their high lignin contents. For some wood bark or sawdust biomasses, if they have less lignin content as well as low densities, AFEX could be an alternative that takes advantage of moderate temperature pretreatment. Increase of the treatment time of AFEX might also work effectively in the case of biomass with comparatively high lignin content such as softwood.

Although steam pretreatment with sulfuric acid or sulfur dioxide as a catalyst has been broadly explored and proved to be effective in treatment of softwood, the presence of sulfur could impose potential threats to some enzymes. It could also cause problems in downstream purification and distillation of products. Furthermore, increased content of sulfur in the final product may incur environmental problems, such as increased emission of SO₂ when ethanol produced is used in vehicles once residual sulfur is carried over to the final product. Unfortunately, no work has been performed to evaluate such effects. The authors believe that the evaluation of this effect will be carried out some day when more ethanol is being made by using these techniques. Considering the autocatalysis effect concomitant with the production of acetic acid or uronic acid from pretreatment of hardwood, we think that using acetic acid as a catalyst could be a better choice than either sulfuric acid or SO₂. Meanwhile, we expect that acetic acid should not have any obviously detrimental effect on cellulase enzymes, since most of those enzymes show their optimal enzymatic activity within the pH range of 4.5~5.5. In addition, this would probably not cause extra problems of inhibition to fermentation or contamination of the final product. With appropriate control of the dosage of acetic acid, there should not be

any inhibitory effect on either cellulase or yeast (Taherzadeh et al. 1997). There is potential to develop acid pretreatment using acetic acid as an alternative.

Ammonia fiber explosion (AFEX) is another promising pretreatment that has been thought to have potential benefits that are both economical and environmental. Current research shows it works well on agricultural residues and hardwood but not on softwood. It has not been evaluated on bark and sawdust. It may be possible to modify AFEX, which uses anhydrous liquid ammonia to pretreat biomass, to treat softwood by extending the pretreatment time. Further research should be conducted to facilitate its use on softwoods.

Generally speaking, we think that the criteria set by the National Research Council provide some general rules to aid in exploration of any pretreatment methods (National Research Council 1999):

1. Avoid the need for reducing the size of biomass particles so that less mechanical energy will be consumed.
2. Preserve the pentose (hemicellulose) fractions to completely use the carbohydrates.
3. Limit the formation of degradation products that inhibit growth of fermentative microorganisms in order to improve the efficiency of enzyme and microbe.
4. Minimize energy demands.
5. Limit overall costs.

These criteria, as well as the generation of a higher-value lignin co-product, form a basis of comparison for various pretreatment options.

Evaluation of Pretreatment Effect

A number of screening variables can be used to evaluate pretreatment effects. These variables can be water retention value (WRV), porosity of pretreated biomass, crystallinity of cellulose, specific surface area of pretreated biomass, and degree of polymerization. However, the complexity of the saccharification and fermentation processes makes it difficult to check the overall performance of the pretreatment and evaluate the potential of pretreatment materials to ethanol using any of these simple screening variables. Sugar yield is one of the most direct indexes to determine pretreatment effect as far as the conservation of carbohydrates is concerned. Enzymatic hydrolysis of the pretreated biomass would be the appropriate way to check this. It is a good scientific approach to check their effects on cellulase and yeast to separate chemical species in pretreated biomass. This approach needs to involve separate hydrolysis and fermentation (SHF); it may also need to evaluate different species individually, as has been done by different researchers (Klinke et al. 2001; Palmqvist and Hahn-Hägerdal 2000a, 2000b). In a commercial setting, the biggest advantage for SHF is that both unit operations can be performed at their optimum operating conditions. However, the hydrolysis can be easily inhibited by either cellobiose or glucose, because both the endoglucanase or exoglucanase and β -glucosidase are end-product inhibiting enzymes. The other approach is the so-called simultaneous saccharification and fermentation (SSF). The produced sugar in SSF will be converted into ethanol, which is much less inhibitory to these isozymes. Meanwhile, SSF is a simpler approach from the viewpoints of capital cost and process consideration. SSF will therefore be a more promising strategy

applicable to commercial environments. An experimental simulation of SSF in the laboratory will give a more productive evaluation than other screening process.

Figure 8 illustrates a general approach for ethanol production, which provides information on different stages that should be considered when one considers further exploration of this process. Review articles provide further information on SSF (Sun and Cheng 2002a; Taherzadeh and Karimi 2007b).

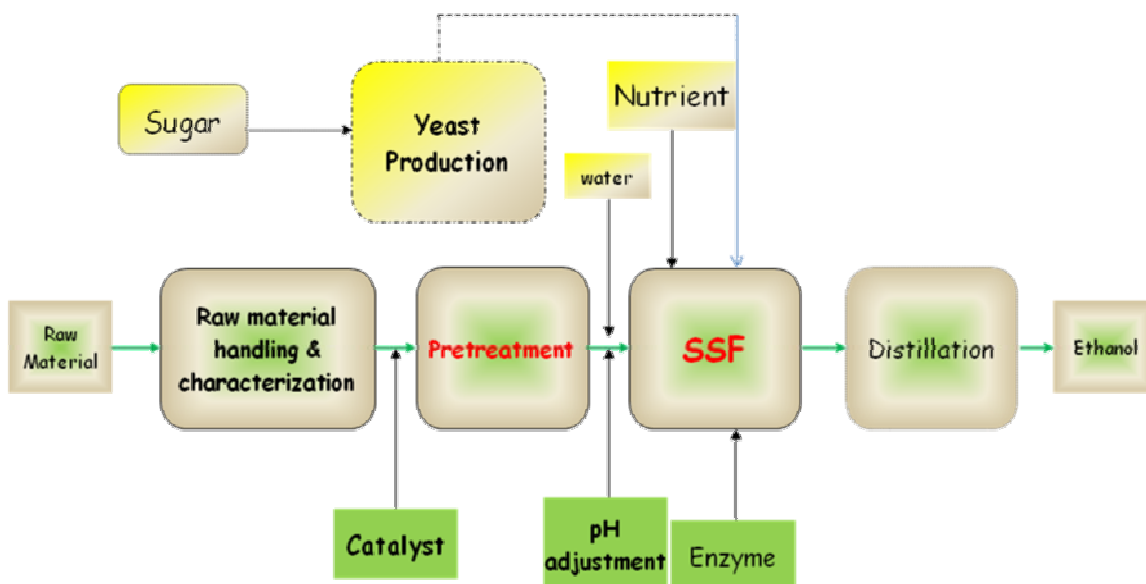


Fig. 8. Basic unit operations for ethanol biorefinery from forest residues

Economic Estimation of Cost Related to Chemicals and Energy in Pretreatment

Economic analysis is less meaningful in a laboratory scale than for a simulated real production situation. It is necessary to point out that assumptions are needed in order to achieve a comparatively credible estimate. In any practical situation, the overall capacity must be at a scale that is large enough to produce economical benefits. Two thousand metric tons per day of biomass would be a reasonable assumption. Two scenarios are considered for our approximation, without the consideration of capital cost, operational cost, etc. One is steam explosion with acetic acid as catalyst, and the other one is ammonia fiber explosion. Elaborations for these two are discussed subsequently, but chemical cost and energy cost are estimated. Capital and operating costs are not included in these estimates.

Pretreatment Cost for Steam Explosion with Acetic Acid as Catalyst

In the case of steam explosion with acetic acid as catalyst, the assumptions are as follows: Acetic acid impregnates the biomass under room temperature conditions. Considering the acid dissociation constant and effect of temperature, the threshold concentration can be set at about 1 mM for the liquid part, which corresponds to a pH value of about 3.9, and the treatment has a catalytic effect to dissociate the complex between carbohydrates and lignin. The pH value calculations are based on the dissociation constant of $K_a=1.8 \times 10^{-5}$. After impregnation, the biomass is brought into a

steam cooker. The temperature is assumed to remain at 200°C for 10 minutes after heating up from normal temperature, which is assumed to be 25 °C on average. Heating up is assumed to take one minute. The solid concentration is taken as 25%. For the simplification of calculations, the major energy consumption of steam is assumed to be consumed during the heating up process, in which the temperature change is 175°C. In order for the hypothetical pretreatment to use steam from a pulp or paper mill's recovery boiler, the steam pressure is assumed to have a pressure of 175psig. The specific heat of wood after it is impregnated in dilute acetic acid is assumed to be the same as that of water, although this could be much lower in the case of oven-dry wood. The estimated energy and chemical cost for this scenario is around \$18.88 per metric ton of dry mass. If the solid concentration is raised to 33%, then the estimated pretreatment cost will be about \$15.28. The total pretreatment costs in both situations are less than 20 dollars; 95% of the cost will be spent on energy. It can also be seen that higher pretreatment solids content results in lower pretreatment costs. Table 5 summarizes the conditions for steam explosion pretreatment with acetic acid as catalyst, as well as the cost estimates.

Table 5: Hypothetic Conditions for Steam Explosion with Acetic Acid and its Cost Estimation

Pretreatment Conditions					
Acetic acid concentration	pH	Solid concentration	Heat-up time	Pretreatment Time	Pretreatment Temperature
1 mM	3.9	25% (33%)	1 min	9 min	200°C
Cost Estimation					
Chemical		Steam			
¹ Acetic Price	Cost (\$/OD on)	Price	Pressure (psi)	² Latent Heat	Cost (\$/OD Ton)
1.35~1.41\$/kg	0.24	³ \$6 /1000 lb (\$0.132/kg)	175	2000 kJ/kg	15.04 (18.64)
Total Pretreatment Cost (\$/ OD ton biomass)			18.88 (15.28)		

¹ Information from Chemical Economics Handbook(Anonymous)

² (Anonymous)

³ Personal communication with Dr. Hasan Jameel, NCSU

⁴ Specific heat of water: 4.186 kJ/kg

Cost Estimation for Ammonia Fiber Explosion

Estimating the cost for ammonia fiber explosion is different due to the recycling of ammonia if capital cost estimation is involved. But if we only consider the energy and chemical cost, the calculation won't be substantially different for the previous case. In this scenario, the pretreatment is assumed to be carried out at 60% moisture content for biomass; the pretreatment temperature is maintained at 90 °C at a pressure of 250~300 psi for 5 minutes. As in the scenario for steam explosion with acetic acid as catalyst, steam of 175 psi is used to reach the desired temperature. The use of anhydrous liquid ammonia is assumed. A jacketed pretreatment reactor is assumed to be used, so that there is no mixing between steam and ammonia, which would help to reduce extra moisture addition. The recycling ratio of ammonia is assumed to be 99%.

Energy needed to heat up liquid ammonia can be estimated from the enthalpy change of ammonia at different states. The enthalpy of saturated liquid ammonia at 25 °C

is 298.8 kJ/kg.K, while that of the superheated ammonia at 90°C is 1604.94 kJ/kg.K. The difference between these enthalpies is used to determine how much energy is used, as well as similar enthalpy differences for wood and moisture. A simple approach is sketched in Fig. 9 to estimate this energy demand for heating up liquid ammonia.

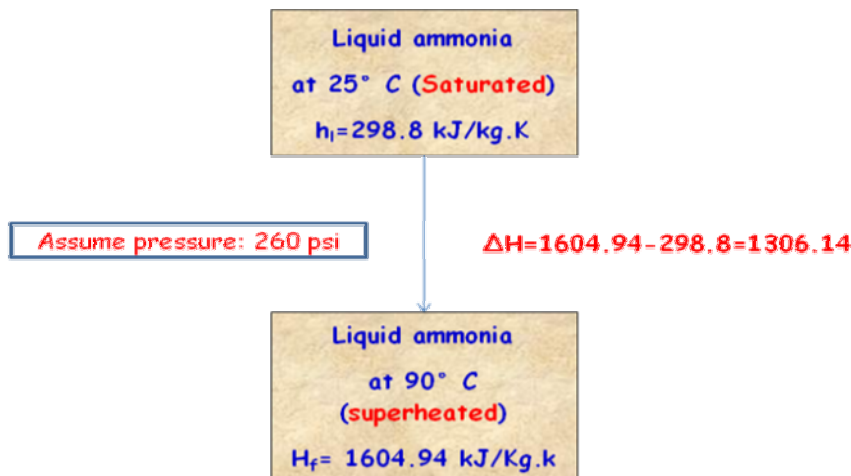


Fig. 9. Enthalpy changes for ammonia used in pretreatment

The energy needed to make this enthalpy change happen is $\Delta H = 1604.94 - 298.8 = 1306.14 \text{ kJ/kg.K}$, which should be included in the calculation of the corresponding steam consumption for pretreatment. With these assumptions the pretreatment cost should be about \$12.28 per metric ton of dry biomass. Table 6 shows the costs for AFEX pretreatment as well as a summary of the corresponding pretreatment conditions. We can see that the total estimated pretreatment cost for AFEX is lower than steam pretreatment with acid catalyst, and so is the cost ratio for energy.

It is necessary to mention that no energy would be needed in the recovery of gaseous ammonia to 25°C after AFEX. Since the boiling point for liquid ammonia is -33.5°C, it has more enthalpy that could be extracted and used in other places in the manufacturing operation, which can make the process more cost-effective if the latent heat of ammonia were used when it is converted back to the liquid state for reuse. However, some extra capital cost would be needed for the installation of recovery equipment, such as a compressor or heat exchanger, as well as equipment for separation of residual water when needed, which is not in the scope of the discussion here. The energy consumption for a compressor is not included here, either.

It can be seen that AFEX is more cost-competitive based on the above cost estimation. Successful breakthrough in application of this method to forest residues can broaden the way through which bioethanol capacity can be increased greatly.

Table 6: Pretreatment Conditions for AFEX and its Cost Estimation

Pretreatment Conditions					
Ammonia Loading	Recycling ratio of Ammonia	Moisture content	Heat-up time	Pretreatment Time	Pretreatment Temperature
1 ton/ ton OD biomass	99%	60%	30s	5 min	90°C
Cost Estimation					
Chemical		Steam for pretreatment			
¹ Anhydrous Liquid Ammonia	Cost (\$/ OD Ton)	Price	Pressure (psi)	² latent heat	Cost (\$/OD Ton)
0.18 \$/kg	1.8	3\$ /1000 lb (0.67\$/kg)	175	2000 kJ/kg	10.48
		⁴ Specific heat (C _p)	1.465 kJ/Kg.K		
Pretreatment Cost (\$/ OD ton biomass)			12.28		

¹ Information for Chemical Economics Handbook(Anonymous)

² <http://www.chemicallogic.com/download/mollier.html>(Anonymous)

³ Specific heat of water: 4.186 kJ/kg

⁴ Specific heat of dry wood is assumed to be 35% of water (McMillin, 1969)

CONCLUSION

Much research has been performed on utilization of biomass to make ethanol; most of this work has been focused on agricultural residues, especially corn stover. Less work has been carried out on using forest residues directly, especially on wood bark, although some work has been directed at wood itself. This paper briefly reviews different pretreatment methods that have been explored. Emphasis was placed on those attracting much interest for the pretreatment of woody biomass. The intention of this review is to shed some light on using whole wood, as well as forest residues, to produce ethanol. The authors are also trying to propose the use of acetic acid as catalyst to pretreat woody biomass.

A simple economic estimation for pretreatment of forest residue shows that AFEX is more promising in terms of operating costs. More important is that this method consumes less energy, while it also maintains a lower total pretreatment cost. However, it must be developed further for use on softwoods and more comprehensive analysis is needed based on experimental data in the future for its application. Estimation of costs involving capital and operation should also be included when it comes to commercial application. The authors hope that this review and the suggestions proposed can expand our insight in understanding pretreatment and provide a reference to facilitate commercialization of bioethanol derived from forest residues.

REFERENCES CITED

Anonymous (2007c). "H₂O Mollier Diagram (Pressure-Enthalpy Diagram)." <http://www.chemicallogic.com/download/mollier/html>

- Anonymous (2007d). "Properties of Fuels":
<http://www.eere.energy.gov/afdc/pdfs/fueltable.pdf>
- Anonymous (2007e). SRI Consulting CEH Report:
<http://www.sriconsulting.com/CEH/Public/Reports/602.5000/>
- Anonymous (2007f). "Thermodynamic property table for superheated vapor of ammonia (NH₃), SI units," 2007:
<http://exergy.sdsu.edu/testhome/Test/solve/basics/tables/tablesPC/superAmmonia-Eng.html>
- Allen, S. G., Spencer, M. J., and Antal, M. J. (1996). "Semi-chemical pulping using the Aquasolv process," *Abstracts of Papers of the American Chemical Society* 211 (Cell), 66.
- Antal, M. J., Jr., Adschiri, T., Ekbom, T., Garcia, A., Matsumura, Y., Minowa, T., et al. (1996). "Hydrogen production from high-moisture content biomass in supercritical water," *Proceedings of the U.S. DOE Hydrogen Program Review, Miami, May 1-2, 1996*, 1, 499-511.
- Avellar, B. K., and Glasser, W. G. (1998). "Steam-assisted biomass fractionation. I. Process considerations and economic evaluation," *Biomass Bioenergy* 14(3), 205-218.
- Bailey, B. K. (1996). "Performance of ethanol as a transportation fuel," In *Handbook on Bioethanol*. C. E. Wyman (ed.), pp. 37-60.
- Ballesteros, I., Oliva, J. M., Navarro, A. A., Gonzalez, A., Carrasco, J., and Ballesteros, M. (2000). "Effect of chip size on steam explosion pretreatment of softwood," *Applied Biochemistry and Biotechnology* 84-6, 97-110.
- Berlin, A., Munoz, C., Gilkes, N., Alamouti, S. M., Chung, P., Kang, K. Y., et al. (2007). "An evaluation of British Columbian beetle-killed hybrid spruce for bioethanol production," *Applied Biochemistry and Biotechnology* 137, 267-280.
- Bobleter, O., Binder, H., Concin, R., and Burtscher, E. (1981). "The conversion of biomass to fuel raw material by hydrothermal treatment," In *Energy from Biomass*, W. Palz, P. Chartier and D.O. Hall (eds.), Applied Science Publ., London 554-562.
- Bouchard, J., Nguyen, T. S., Chornet, E., and Overend, R. P. (1991). "Analytical methodology for biomass pretreatment. Part 2: Characterization of the filtrates and cumulative product distribution as a function of treatment severity," *Bioresource Technology* 36(2), 121-131.
- Brandes, S. D., and Graff, R. A. (1985). "Literature review for steam pretreatment. City Univ. New York, USA., 31 pp.
- Brink, D. L., Lynn, S., and Merriman, M. M. (1999). "Method of treating biomass material," (p. 21 pp). Application: WO: (Regents of the University of California, USA).
- Broglin, J. (1996). "Practical experience with combination processes in woven fabric pad-steam pretreatment," *Melliand Textilberichte* 77, 688,690,692-693,E151-E154.
- Brownell, H. H., and Saddler, J. N. (1984). "Steam-explosion pretreatment for enzymatic hydrolysis," *Biotechnol. Bioeng.*, Suppl. 14, 55-68.
- Chandra, R. P., Bura, R., Mabee, W. E., Berlin, A., Pan, X., and Saddler, J. N. (2007). "Substrate pretreatment: The key to effective enzymatic hydrolysis of lignocellulosics?" In *Biofuels*, pp. 67-93. Springer-Verlag Berlin, Berlin.

- Chang, V. S., Kaar, W. E., Burr, B., and Holtzapple, M. T. (2001). "Simultaneous saccharification and fermentation of lime-treated biomass," *Biotechnology Letters* 23(16), 1327-1333.
- Chen, H. Z., and Liu, L. Y. (2007). "Unpolluted fractionation of wheat straw by steam explosion and ethanol extraction," *Bioresource Technology*, 98(3), 666-676.
- Claassen, P. A. M., Van Lier, J. B., Contreras, A. M. L., Van Niel, E. W. J., Sijtsma, L., Stams, A. J. M., et al. (1999). "Utilisation of biomass for the supply of energy carriers," *Applied Microbiol. Biotech.* 52(6), 741-755.
- Converse, A. O., Kwarteng, I. K., Grethlein, H. E., and Ooshima, H. (1989). "Kinetics of thermochemical pretreatment of lignocellulosic materials," *Applied Biochem. Biotechnol.* 20-21, 63-78.
- Dale, B. E. (1986). "Method for increasing the reactivity and digestibility of cellulose with ammonia," U.S. Patent No. 4600590. Washington, D. C.
- Demirbas, A. (2004). "Ethanol from cellulosic biomass resources," *International Journal of Green Energy* 1(1), 79-87.
- Demirbas, A. (2005). "Bioethanol from cellulosic materials: A renewable motor fuel from biomass." *Energy Sources* 27(4), 327-337.
- Demirbas, A. (2007). "Producing and using bioethanol as an automotive fuel," *Energy Sources Part B-Economics Planning and Policy* 2(4), 391-401.
- Demirbas, A. (2008). "Products from lignocellulosic materials via degradation processes," *Energy Sources Part a-Recovery Utilization and Environmental Effects*, 30(1), 27-37.
- Dien, B. S., Jung, H. J. G., Vogel, K. P., Casler, M. D., Lamb, J. F. S., Iten, L., et al. (2006). "Chemical composition and response to dilute-acid pretreatment and enzymatic saccharification of alfalfa, reed canarygrass, and switchgrass," *Biomass and Bioenergy* 30(10), 880-891.
- Esteghlalian, A., Hashimoto, A. G., Fenske, J. J., and Penner, M. H. (1997). "Modeling and optimization of the dilute-sulfuric-acid pretreatment of corn stover, poplar and switchgrass," *Bioresource Technology* 59(2-3), 129-136.
- Farrell, A. E., Plevin, R. J., Turner, B. T., Jones, A. D., O'Hare, M., and Kammen, D. M. (2006). "Ethanol can contribute to energy and environmental goals," *Science* 311(5760), 506-508.
- Galbe, M., Liden, G., and Zacchi, G. (2005). "Production of ethanol from biomass - Research in Sweden," *Journal of Scientific & Industrial Research* 64(11), 905-919.
- Galbe, M., and Zacchi, G. (2002). "A review of the production of ethanol from softwood," *Applied Microbiol. Biotech.* 59, 618-628.
- Galbe, M., and Zacchi, G. (2007). "Pretreatment of lignocellulosic materials for efficient bioethanol production," In *Biofuels*, pp. 41-65. Springer-Verlag Berlin, Berlin.
- Glasser, W. G., and Wright, R. S. (1998). "Steam-assisted biomass fractionation. II. Fractionation behavior of various biomass resources," *Biomass Bioenergy* 14(3), 219-235.
- Goldstein, I. S. (1983). "Hydrolysis of cellulose by acids," *NATO ASI Series, Series A: Life Sciences*, 67(Biomass Util.), 559-566.
- Goldstein, I. S., and Easter, J. M. (1992). "An improved process for converting cellulose to ethanol," *Tappi J.* 75(8), 135-140.

- Gray, K. A., Zhao, L., and Emptage, M. (2006). "Bioethanol," *Bioinorganic chemistry / Biocatalysis and Biotransformation* 10, 141-146.
- Guerra, A., Filpponen, I., Lucia, L. A., and Argyropoulos, D. S. (2006b). "Comparative evaluation of three lignin isolation protocols for various wood species," *Journal of Agricultural and Food Chemistry* 54(26), 9696-9705.
- Guerra, A., Filpponen, I., Lucia, L. A., Saquing, C., Baumberger, S., and Argyropoulos, D. S. (2006a). "Toward a better understanding of the lignin isolation process from wood," *Journal of Agricultural and Food Chemistry* 54(16), 5939-5947.
- Hahn-Hagerdal, B., Galbe, M., Gorwa-Grauslund, M. F., Liden, G., and Zacchi, G. (2006). "Bio-ethanol - the fuel of tomorrow from the residues of today," *Trends in Biotechnology* 24(12), 549-556.
- Heitz, M., Capek-Menard, E., Koeberle, P. G., Gagne, J., Chornet, E., Overend, R. P., et al. (1991). "Fractionation of *Populus tremuloides* at the pilot plant scale: Optimization of steam pretreatment conditions using the STAKE II technology," *Biores. Technol.* 35(1), 23-32.
- Holtzapple, M. (1992). "Pretreatment of lignocellulosic municipal solid waste by ammonia fiber explosion (AFEX)," In *Applied Biochemistry and Biotechnology*, pp. 5. Humana Press, Clifton, N.J.
- Israilides, C. J., Grant, G. A., and Han, Y. W. (1978). "Sugar level, fermentability, and acceptability of straw treated with different acids," *Applied and Environmental Microbiology* 36(1), 43-46.
- Iyer, P. V., Wu, Z. W., Kim, S. B., and Lee, Y. Y. (1996). "Ammonia recycled percolation process for pretreatment of herbaceous biomass," *Applied Biochemistry and Biotechnology* 57-8, 121-132.
- Khan, A. W., Labrie, J. P., and McKeown, J. (1986). "Effect of electron-beam irradiation pretreatment on the enzymatic hydrolysis of softwood," *Biotechnology and Bioengineering* 28(9), 1449-1453.
- Khan, A. W., Labrie, J. P., and McKeown, J. (1987). "Electron beam irradiation pretreatment and enzymatic saccharification of used newsprint and paper mill wastes," *Radiation Physics and Chemistry* 29(2), 117-120.
- Kim, J. S., Lee, Y. Y., and Park, S. C. (2000). "Pretreatment of wastepaper and pulp mill sludge by aqueous ammonia and hydrogen peroxide," *Applied Biochemistry and Biotechnology* 84-86, 129-139.
- Kim, T.-H., Kim, T.-H., Yu, S., Nam, Y. K., Choi, D.-K., Lee, S. R., et al. (2007). "Solubilization of waste activated sludge with alkaline treatment and gamma ray irradiation." *Journal of Industrial and Engineering Chemistry (Seoul, Republic of Korea)* 13, 1149-1153.
- Klinke, H. B., Thomsen, A. B., and Ahring, B. K. (2001). "Potential inhibitors from wet oxidation of wheat straw and their effect on growth and ethanol production by *Thermoanaerobacter mathranii*," *Applied Microbiology and Biotechnology* 57(5-6), 631-638.
- Kurakake, M., Ide, N., and Komaki, T. (2007). "Biological pretreatment with two bacterial strains for enzymatic hydrolysis of office paper," *Current Microbiology* 54(6), 424-428.
- Kwarteng, I. K. (1983). "Kinetics of acid hydrolysis of hardwood in a continuous plug flow reactor," Dartmouth Coll., Hanover, NH, USA.

- Lee, Y. Y., Iyer, P., and Torget, R. W. (1999). "Dilute-acid hydrolysis of lignocellulosic biomass," *Fermentation and Bioindustrial Chemistry*, 65, 93-115.
- Li, A., Antizar-Ladislao, B., and Khraisheh, M. (2007). "Bioconversion of municipal solid waste to glucose for bio-ethanol production," *Bioprocess and Biosystems Engineering* 30(3), 189-196.
- Lissens, G., Klinke, H., Verstraete, W., Ahring, B., and Thomsen, A. B. (2004). Wet oxidation treatment of organic household waste enriched with wheat straw for simultaneous saccharification and fermentation into ethanol," *Environmental Technology* 25(6), 647-655.
- Magara, K., Azuma, J., and Koshijima, T. (1989). "Microwave-irradiation of lignocellulosic materials. X. Conversion of microwave-irradiated agricultural wastes into ethanol," *Wood Research* 76, 1-9.
- McMillan, J. D. (1994). "Pretreatment of lignocellulosic biomass," In *Enzymatic Conversion of Biomass for Fuels Production* (Washington, Amer Chemical Soc), 292-324.
- Millett, M. A., Effland, M. J., and Caulfield, D. F. (1979). "Influence of fine grinding on the hydrolysis of cellulosic materials - Acid vs. enzymic," *Advances in Chemistry Series* 181, 71-89.
- Mok, W. S. L., and Antal, M. J., Jr. (1992). "Uncatalyzed solvolysis of whole biomass hemicellulose by hot compressed liquid water," *Industrial and Engineering Chemistry Research* 31(4), 1157-1161.
- Moniruzzaman, M., Dale, B. E., Hespell, R. B., and Bothast, R. J. (1997). "Enzymatic hydrolysis of high-moisture corn fiber pretreated by AFEX and recovery and recycling of the enzyme complex," *Applied Biochemistry and Biotechnology* 67(1-2), 113-126.
- Mosier, N., Hendrickson, R., Ho, N., Sedlak, M., and Ladisch, M. R. (2005). "Optimization of pH controlled liquid hot water pretreatment of corn stover," *Bioresource Technology* 96(18), 1986-1993.
- Mosier, N., Wyman, C., Dale, B., Elander, R., Lee, Y. Y., Holtzapple, M., et al. (2005). "Features of promising technologies for pretreatment of lignocellulosic biomass," *Bioresource Technology* 96(6), 673-686.
- Nguyen, Q. A., Tucker, M. P., Keller, F. A., and Eddy, F. P. (2000). "Two-stage dilute-acid pretreatment of softwoods," *Applied Biochemistry and Biotechnology* 84-86, 561-576.
- Ohgren, K., Vehmaanpera, J., Siika-Aho, M., Galbe, M., Viikari, L., and Zacchi, G. (2007). High temperature enzymatic prehydrolysis prior to simultaneous saccharification and fermentation of steam pretreated corn stover for ethanol production," *Enzyme and Microbial Technology* 40(4), 607-613.
- Palmqvist, E., and Hahn-Hägerdal, B. (2000a). "Fermentation of lignocellulosic hydrolysates. I: Inhibition and detoxification," *Bioresource Technology* 74(1), 17-24.
- Palmqvist, E., and Hahn-Hägerdal, B. (2000b). "Fermentation of lignocellulosic hydrolysates. II: Inhibitors and mechanisms of inhibition," *Bioresource Technology*, 74(1), 25-33.
- Perlack, R. D., Wright, L. L., Turhollow, A. F., Graham, R. L., Stokes B. J., and Erbach D. C. (2005). "Biomass as feedstock for a bioenergy and bioproducts industry: The technical feasibility of a billion-ton annual supply," by US DOE, pp. 87.

- Ramos, L. P., Breuil, C., and Saddler, J. N. (1993). "The use of enzyme recycling and the influence of sugar accumulation on cellulose hydrolysis by *Trichoderma* cellulases," *Enzyme and Microbial Technology* 15(1), 19-25.
- Rivers, D. B., and Emert, G. H. (1987). "Lignocellulose pretreatment: A comparison of wet and dry ball attrition," *Biotechnol. Letters* 9(5), 365-368.
- Rubio, M., Tortosa, J. F., Quesada, J., and Gomez, D. (1998). "Fractionation of lignocellulosics. Solubilization of corn stalk hemicelluloses by autohydrolysis in aqueous medium," *Biomass and Bioenergy* 15(6), 483-491.
- Saddler, J. N., Ramos, L. P., and Breuil, C. (1993). "Steam pretreatment of lignocellulosic residues," *Biotechnology in Agriculture Series* 9, 73-91.
- Saha, B. C. (2003). "Hemicellulose bioconversion," *Journal of Industrial Microbiology & Biotechnology* 30(5), 279-291.
- Saha, B. C., Iten, L. B., Cotta, M. A., and Wu, Y. V. (2005). "Dilute acid pretreatment, enzymatic saccharification, and fermentation of rice hulls to ethanol," *Biotechnology Progress* 21(3), 816-822.
- Schwertassek, K., and Hochman, V. (1974). "Determination of the degree of mercerization of cotton mercerized with ammonia," *Melliand Textilberichte International* 55, 544-547.
- Sidiras, D. K., and Koukios, E. G. (1989). "Acid saccharification of ball-milled straw," *Biomass* 19, 289-306.
- Singh, P. N., Robinson, T., and Singh, D. (2004). "Pretreatment of lignocellulosic substrates," *Concise Encyclopedia of Bioresource Technology*, 663-670.
- Sun, F. B., and Chen, H. Z. (2007). "Evaluation of enzymatic hydrolysis of wheat straw pretreated by atmospheric glycerol autocatalysis," *Journal of Chemical Technology and Biotechnology* 82(11), 1039-1044.
- Sun, Y., and Cheng, J. Y. (2002a). "Hydrolysis of lignocellulosic materials for ethanol production: A review," *Bioresource Technology* 83(1), 1-11.
- Taherzadeh, M. J., Eklund, R., Gustafsson, L., Niklasson, C., and Liden, G. (1997). "Characterization and fermentation of dilute-acid hydrolyzates from wood," *Industrial & Engineering Chemistry Research* 36(11), 4659-4665.
- Taherzadeh, M. J., and Karimi, K. (2007a). "Acid-based hydrolysis processes for ethanol from lignocellulosic material: A review," *BioResources* 2(3), 472-499.
- Taherzadeh, M. J., and Karimi, K. (2007b). "Enzyme-based hydrolysis processes for ethanol from lignocellulosic materials: A review," *BioResources* 2(4), 707-738.
- Taniguchi, M., Suzuki, H., Watanabe, D., Sakai, K., Hoshino, K., and Tanaka, T. (2005). "Evaluation of pretreatment with *Pleurotus ostreatus* for enzymatic hydrolysis of rice straw," *Journal of bioscience and bioengineering* 100(6), 637-643.
- Tassinari, T., Macy, C., Spano, L., and Ryu, D. D. Y. (1980). "Energy requirements and process design considerations in compression-milling pretreatment of cellulosic wastes for enzymic hydrolysis," *Biotechnol. Bioeng.* 22, 1689-1705.
- Tassinari, T. H., Macy, C. F., and Spano, L. A. (1982). "Technology advances for continuous compression milling pretreatment of lignocellulosics for enzymic hydrolysis," *Biotechnol. Bioeng.* 24(7), 1495-1505.
- Tengborg, C., Stenberg, K., Galbe, M., Zacchi, G., Larsson, S., Palmqvist, E., et al. (1998). "Comparison of SO₂ and H₂SO₄ impregnation of softwood prior to steam pretreatment on ethanol production," *Applied Biochem. Biotech.* 70-72, 3-15.

- Teymouri, F., Laureano-Perez, L., Alizadeh, H., and Dale, B. E. (2005). "Optimization of the ammonia fiber explosion (AFEX) treatment parameters for enzymatic hydrolysis of corn stover," *Bioresource Technol.* 96(18), 2014-2018.
- Torget, R., Walter, P., Himmel, M., and Grohmann, K. (1991). "Dilute-acid pretreatment of corn residues and short-rotation woody crops," *Applied Biochemistry and Biotechnology* 28-9, 75-86.
- Torget, R., Werdene, P., Himmel, M., and Grohmann, K. (1990). "Dilute acid pretreatment of short rotation woody and herbaceous crops," *Applied Biochem. Biotech.* 24-25, 115-126.
- van Walsum, G. P., and Shi, H. (2004). "Carbonic acid enhancement of hydrolysis in aqueous pretreatment of corn stover," *Bioresource Technology* 93(3), 217-226.
- Wu, S., and Argyropoulos, D. S. (2003). "An improved method for isolating lignin in high yield and purity," *J. Pulp Paper Sci.* 29(7), 235-240.
- Wyman, C. E. (1999). "Biomass ethanol: Technical progress, opportunities, and commercial challenges," *Annual Review of Energy and the Environment* 24, 189-226.
- Wyman, C. E., Dale, B. E., Elander, R. T., Holtzapple, M., Ladisch, M. R., and Lee, Y. Y. (2005). "Coordinated development of leading biomass pretreatment technologies," *Biores. Technol.* 96(18), 1959-1966.
- Yoon, H. H., Wu, Z. W., and Lee, Y. Y. (1995). "Ammonia-recycled percolation process for pretreatment of biomass feedstock," *Applied Biochem. Biotechnol.* 51/52, 5-19.
- Zhang, X., Yu, H., Huang, H., and Liu, Y. (2007). "Evaluation of biological pretreatment with white rot fungi for the enzymatic hydrolysis of bamboo culms," *International Biodeterioration & Biodegradation* 60, 159-164.

Article submitted: Oct. 22, 2007; Peer-review completed: Jan. 14, 2008; Revised version received and accepted: Feb. 11, 2008; Published: Feb. 12, 2008; Erratum: Feb. 25, 2008, Fig. 5 was changed to show the label "D-glucuronic acid" instead of "glucose".